frontiers | Research Topics

Omics in plant-insect interactions

Edited by
Shengli Jing, Guangcun He and Ming-shun Chen

Published in
Frontiers in Plant Science

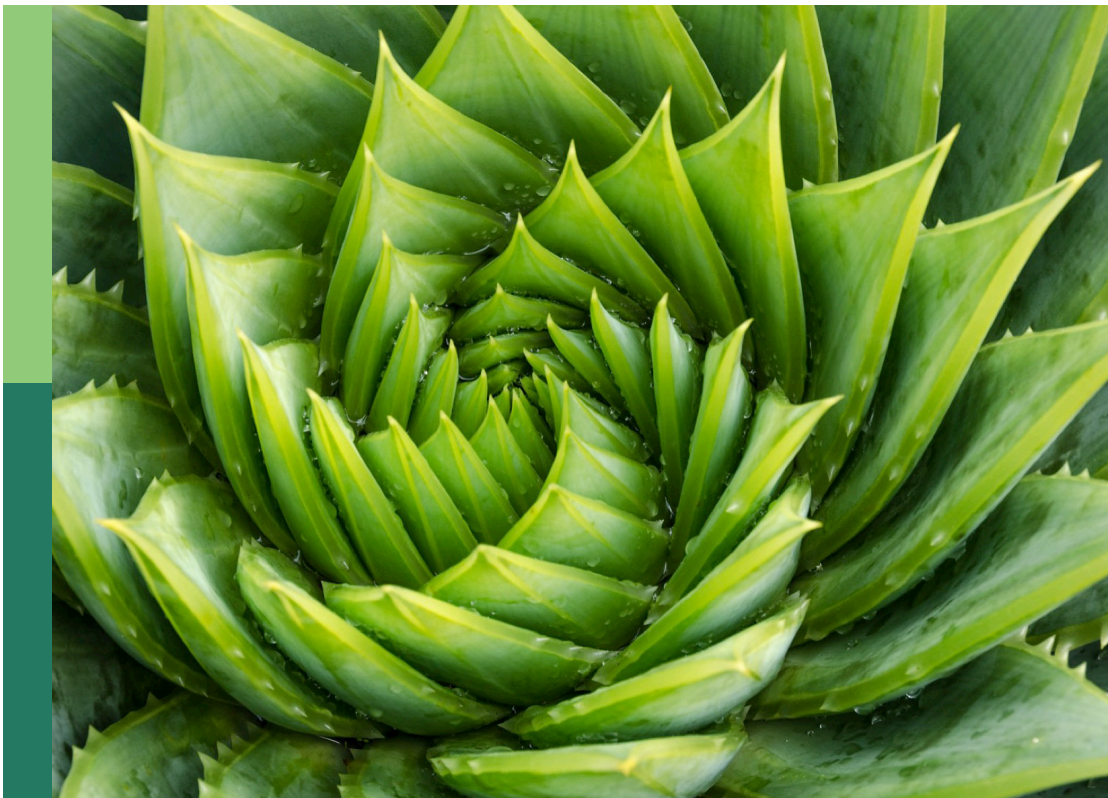

ISSN 1664-8714
ISBN 978-2-8325-5529-3
DOI 10.3389/978-2-8325-5529-3

About Frontiers

Frontiers is more than just an open access publisher of scholarly articles: it is a pioneering approach to the world of academia, radically improving the way scholarly research is managed. The grand vision of Frontiers is a world where all people have an equal opportunity to seek, share and generate knowledge. Frontiers provides immediate and permanent online open access to all its publications, but this alone is not enough to realize our grand goals.

Frontiers journal series

The Frontiers journal series is a multi-tier and interdisciplinary set of open-access, online journals, promising a paradigm shift from the current review, selection and dissemination processes in academic publishing. All Frontiers journals are driven by researchers for researchers; therefore, they constitute a service to the scholarly community. At the same time, the *Frontiers journal series* operates on a revolutionary invention, the tiered publishing system, initially addressing specific communities of scholars, and gradually climbing up to broader public understanding, thus serving the interests of the lay society, too.

Dedication to quality

Each Frontiers article is a landmark of the highest quality, thanks to genuinely collaborative interactions between authors and review editors, who include some of the world's best academicians. Research must be certified by peers before entering a stream of knowledge that may eventually reach the public - and shape society; therefore, Frontiers only applies the most rigorous and unbiased reviews. Frontiers revolutionizes research publishing by freely delivering the most outstanding research, evaluated with no bias from both the academic and social point of view. By applying the most advanced information technologies, Frontiers is catapulting scholarly publishing into a new generation.

What are Frontiers Research Topics?

Frontiers Research Topics are very popular trademarks of the *Frontiers journals series*: they are collections of at least ten articles, all centered on a particular subject. With their unique mix of varied contributions from Original Research to Review Articles, Frontiers Research Topics unify the most influential researchers, the latest key findings and historical advances in a hot research area.

Find out more on how to host your own Frontiers Research Topic or contribute to one as an author by contacting the Frontiers editorial office: frontiersin.org/about/contact

Omics in plant-insect interactions

Topic editors

Shengli Jing — Xinyang Normal University, China

Guangcun He — Wuhan University, China

Ming-shun Chen — United States Department of Agriculture (USDA), United States

Citation

Jing, S., He, G., Chen, M.-s., eds. (2024). *Omics in plant-insect interactions*. Lausanne: Frontiers Media SA. doi: 10.3389/978-2-8325-5529-3

Table of contents

frontiers | Frontiers in Plant Science

TYPE Editorial
PUBLISHED 24 September 2024
DOI 10.3389/fpls.2024.1480678

OPEN ACCESS

EDITED AND REVIEWED BY
Peng Wang,
Jiangsu Province and Chinese Academy of Sciences, China

*CORRESPONDENCE
Shengli Jing
shljing@xynu.edu.cn

RECEIVED 14 August 2024
ACCEPTED 26 August 2024
PUBLISHED 24 September 2024

CITATION
Jing S, He G and Chen M-s (2024) Editorial: Omics in plant-insect interactions.
Front. Plant Sci. 15:1480678.
doi: 10.3389/fpls.2024.1480678

Editorial: Omics in plant-insect interactions

Shengli Jing[1]*, Guangcun He[2] and Ming-shun Chen[3]

[1]College of Life Sciences, Xinyang Normal University, Xinyang, China, [2]State Key Laboratory of Hybrid Rice, College of Life Sciences, Wuhan University, Wuhan, China, [3]Hard Winter Wheat Genetics Research Unit, USDA-ARS, Manhattan, KS, United States

KEYWORDS

plant-insect interactions, multi-omics analysis, resistance mechanism, secondary metabolites, resistance genes

Editorial on the Research Topic
Omics in plant-insect interactions

Insect herbivores and their host plants engage in a dynamic molecular conflict, wherein plants have evolved sophisticated defense mechanisms, while insects have developed strategies to suppress these defenses. These interactions involve intricate molecular processes that are a major focus of research, with the goal of improving pest control strategies.

Herbivorous insects, such as piercing-sucking hemipterans and chewing Lepidopterans, establish close associations with host plants to manipulate plant cellular processes for feeding and reproduction (Erb and Reymond, 2019). In response, plants have evolved complex immune systems composed of signaling pathways, resistance genes, and secondary metabolites. This ongoing molecular arms race between plants and insects is characterized by interactions among a diverse array of molecules from both organisms. Plant secondary metabolites and resistance genes serve as defense mechanisms against insect herbivory, while insects utilize detoxification enzymes and effectors to disrupt plant defenses, enhancing their adaptation.

This Research Topic explores the complex genetic, physical, metabolic, and molecular interactions between plants and insects, examined through advanced omics technologies such as genomics, transcriptomics, and metabolomics. The Research Topic includes 16 original research and review articles focusing on herbivorous insects (e.g., brown planthopper, aphids, psyllids) and their host plants (e.g., rice, maize, cotton), which are summarized below.

Interactions between rice and brown planthopper

Eight articles in this Research Topic (one review and seven research articles) focus on the interaction between rice (*Oryza sativa* L.) and the brown planthopper (*Nilaparvata lugens* Stål, BPH). This interaction serves as a valuable model system for studying the molecular mechanisms underlying plant-insect interactions. The brown planthopper is a major pest that causes significant damage to rice crops (Cheng et al., 2013; Jing et al., 2017), and the deployment of resistant rice varieties has proven effective in managing this pest. To date, over 40 resistance loci and 17 resistance genes for brown planthopper have been identified and functionally characterized (Shar et al., 2023). The molecular mechanisms of

these resistance genes represent a key area of research. This Research Topic includes articles on the molecular mechanisms involving four specific resistance genes: *Bph6*, *Bph14*, *Bph15*, and *Bph30*.

Four articles focus on *Bph15*, examining the specific cells and tissues involved in resistance, the role of *OsWRKY71* in *Bph15*-mediated resistance, the defense mechanisms against BPH populations with varying virulence levels, and transcriptomic analysis to elucidate the mechanisms behind *BPH14*/*BPH15*-conferred resistance. One article investigates how indole-3-acetic acid (IAA) negatively regulates *Bph30*-mediated resistance using combining transcriptomic and metabolomic analyses. Two additional articles (one review and one research) explore the impact of non-coding RNAs on the interaction between rice and brown planthopper, and one article identifies BPH resistance genes using Genome-wide association studies (GWAS) and evaluates the predictive ability of genomic selection for resistance to BPH.

Zha et al. used single-cell sequencing technology to analyze different cell types involved in BPH resistance, comparing the responses of leaf sheaths from susceptible (TN1) and resistant (YHY15) rice varieties 48 hours after infestation. The analysis identified 14,699 cells in TN1 and 16,237 cells in YHY15, which were grouped into nine cell-type clusters using cell-specific marker genes. Significant differences were observed between the two rice varieties in their resistance mechanisms to BPH. Further analysis revealed that different cell types employ distinct molecular mechanisms in response to BPH, enhancing the understanding of the molecular processes underlying rice resistance and accelerating the breeding of insect-resistant rice varieties.

Li et al. discovered that the transcription factor OsWRKY71 is highly responsive to BPH infestation, with early-induced expression in *Bph15* near-isogenic line (NIL) plants. OsWRKY71 localizes in the nucleus of rice protoplasts, and its knockout in the *Bph15*-NIL background using CRISPR-Cas9 technology resulted in compromised *Bph15*-mediated resistance. Transcriptome analysis indicated significant differences in the transcriptional response to BPH infestation between the *wrky71* mutant and the *Bph15*-NIL, affecting the expression of several defense-related genes. The study identified three potential participants (OsSTPS2, OsEXO70J1, and RGA2) in the BPH resistance pathway mediated by OsWRKY71 in *Bph15*-NIL plants, highlighting the crucial role of OsWRKY71 in *Bph15*-mediated resistance.

Yu et al. conducted miRNA and mRNA expression profiling to investigate the differential responses of YHY15 rice to both avirulent (biotype 1) and virulent (biotype Y) BPH. The study found that YHY15 rice exhibited a rapid response to biotype Y BPH infestation, with significant transcriptional changes within 6 hours. The biotype Y-responsive genes were enriched in photosynthetic processes, and biotype Y BPH infestation induced more intense transcriptional responses compared to biotype 1 BPH, affecting miRNA expression, defense-related metabolic pathways, phytohormone signaling, and multiple transcription factors. Callose deposition was also enhanced in biotype Y BPH-infested rice seedlings, indicating a heightened defense response. These findings provide comprehensive insights into the defense mechanisms of resistant rice against virulent BPH populations.

Hu et al. performed transcriptomic analysis to understand the mechanisms behind *Bph14*/*Bph15*-conferred resistance, using near-isogenic lines (NILs) of rice containing *Bph14* (B14), *Bph15* (B15), or both *Bph14* and *Bph15* (B1415), compared to their recurrent parent (RP) variety 'Wushansimiao'. The study identified 14,492 differentially expressed genes (DEGs) across the profiles, with 531 DEGs common to the resistant NILs compared to the RP before and after BPH feeding. The DEGs related to BPH resistance were primarily enriched in defense response and oxidative stress pathways. Twenty-one DEGs were selected as candidate genes for BPH resistance based on their expression patterns and relevance from previous research. OsPOX8.1, one of the candidate genes, was validated in rice protoplasts, showing increased reactive oxygen species (ROS) accumulation, providing insights into the defense mechanisms activated by BPH resistance gene pyramiding in rice.

Shi et al. combined transcriptomic and metabolomic analyses to study *Bph30*-transgenic (Bph30T) rice plants and BPH-susceptible Nipponbare plants. Transcriptomic analysis revealed that many differentially expressed genes (DEGs) in susceptible rice plants were involved in plant hormone signal transduction, particularly in indole-3-acetic acid (IAA) signal transduction. Metabolomic analysis showed that differentially accumulated metabolites (DAMs) in the amino acids and derivatives category were down-regulated, while DAMs in the flavonoids category were up-regulated in resistant plants following BPH feeding. Combined analysis indicated that flavonoid and lignin biosynthesis are involved in resistance, while biosynthesis of various amino acids and IAA are involved in susceptibility. The study confirmed that exogenous IAA application weakened *Bph30*-mediated BPH resistance, demonstrating that IAA negatively regulates *Bph30*-mediated resistance through the shikimate and phenylpropanoid metabolism pathways.

Jing et al. summarized the roles of small RNAs in the rice-BPH interaction. Functional validation experiments indicated that these sRNAs fine-tune plant innate immunity by integrating R gene-mediated resistance, phytohormone signaling, callose deposition, reactive oxygen species (ROS) production, and secondary metabolite biosynthesis. Additionally, sRNAs are involved in key aspects of BPH biology, such as metamorphosis, wing polyphenism, molting, and reproductive development. The study also observed cross-kingdom RNAi in the rice-BPH interaction, suggesting that sRNAs ingested by BPH while feeding on rice may regulate BPH gene expression. These findings highlight the potential of HIGS and SIGS as promising agricultural pest control strategies.

Wu et al. focused on the regulatory roles of non-coding RNAs, specifically long non-coding RNAs (lncRNAs) and circular RNAs (circRNAs), in *Bph6*-transgenic (resistant, BPH6G) and Nipponbare (susceptible, NIP) rice plants infested by brown planthoppers. Genome-wide analysis identified 310 differentially expressed lncRNAs and 129 differentially expressed circRNAs between the resistant and susceptible rice plants. Dual-luciferase reporter assays revealed specific interactions between lncRNAs and microRNAs (miRNAs), such as lncRNA XLOC_042442 targeting miR1846c and lncRNA XLOC_028297 targeting miR530. The study predicted that 39 lncRNAs and 21 circRNAs could interact with 133 common miRNAs and compete for miRNA binding sites with 834

mRNAs, implicating these mRNAs in key biological processes such as cell wall organization, biogenesis, developmental growth, single-organism cellular processes, and stress responses. This study provides a comprehensive identification and characterization of lncRNAs and circRNAs in rice plants infested by BPH, laying a crucial foundation for future research on non-coding RNAs in the rice-BPH interaction.

Zhou et al. present a comprehensive resource on BPH resistance genes and offer practical recommendations for genomic selection in rice breeding programs. Through Genome-Wide Association Studies (GWAS), six loci were significantly associated with BPH resistance across three assessment criteria. Among these, two loci were novel, while others included previously identified BPH-resistant genes such as *Bph6*, *Bph32*, and *Bph37*. The accuracy of genomic prediction (GP) was influenced by the number of SNPs, training population size, and statistical models. To enhance the prediction of BPH resistance, it is recommended to increase SNP numbers beyond 26,000, expand the training population size beyond 737 individuals, and utilize random forest (RF) models. Optimizing these genomic selection strategies will facilitate the development of durable BPH-resistant rice varieties, thereby contributing to sustainable global rice production.

Aphid-mediated tritrophic interactions

Two articles in this Research Topic examine aphids as vectors in tritrophic interactions. Zhao et al. investigate the effects of nitrogen fertilization on the emission of plant volatile organic compounds (VOCs) that mediate interactions among maize, aphids, and ladybirds. Specifically, 1-nonene was identified as a key compound attracting ladybirds, with its release positively correlated with the visitation rates of *Harmonia axyridis*. The study demonstrated that supplying 1-nonene to maize under low-nitrogen conditions increased the attractiveness of plants to ladybirds, highlighting the compound's role in tritrophic interactions. The synthesis of 1-nonene is linked to salicylic acid (SA) and abscisic acid (ABA), indicating complex interactions within plant response mechanisms to nutrient availability and pest infestation. This research enhances our understanding of plant metabolic responses to nutrient levels and offers practical insights for improving pest management and crop production.

Pandey et al. explore the influence of host plants on the gene expression of the cotton aphid (*Aphis gossypii* Glover) when infected with the cotton leafroll dwarf virus (CLRDV). Using four host plants —cotton, hibiscus, okra, and prickly sida—the study revealed significant differences in gene expression among aphids acquiring the virus from different hosts. A total of 2,942 differentially expressed genes (DEGs) were identified, with varying DEG counts across hosts: 750 from cotton, 310 from hibiscus, 1,193 from okra, and 689 from prickly sida. Notably, more genes were overexpressed in aphids from cotton, hibiscus, and prickly sida, while more genes were underexpressed in aphids from okra. These findings underscore the complexity of vector-virus-host interactions and the pivotal role of host plants in influencing disease transmission.

Psyllid-pathogen interactions

Two articles in this Research Topic focus on psyllids as vectors in vector-pathogen interactions. Li et al. examine the biochemical effects of *Candidatus Liberibacter* solanacearum (CLso) infection in potato psyllids (*Bactericera cockerelli*), vectors of diseases such as psyllid yellows, vein-greening (VG), and zebra chip (ZC). Using ultra-performance liquid chromatography tandem mass spectrometry (UPLC-MS/MS), the study identified 34 metabolites related to amino acid, carbohydrate, and lipid metabolism as potential biomarkers of CLso infection. Matrix-assisted Laser Desorption Ionization Mass Spectrometry Imaging (MALDI-MSI) mapped the spatial distribution of these biomarkers, revealing significant down-regulation of 15-keto-Prostaglandin E2 and alpha-D-Glucose in the abdomen of infected psyllids. These findings suggest mechanisms of immune suppression employed by CLso to evade detection and clearance by the psyllid's immune system.

He et al. investigate the interactions between the Asian citrus psyllid (ACP) and *Candidatus Liberibacter* asiaticus (CLas), the causative agent of citrus greening disease. This research explores how different life stages of ACP influence gene expression in response to CLas infection. RNA sequencing (RNA-seq) revealed significant changes in gene expression, particularly in later nymphal stages (4-5) and teneral adults. A large number of genes related to defense mechanisms, developmental processes, and immune responses were found to be highly responsive to CLas infection. Understanding these gene expressions provides insights into how ACP manages the bacterial infection and contributes to disease transmission.

Plant-herbivore interactions

Two articles in this Research Topic focus on interactions between herbivorous insects and their host plants. Liu et al. investigate how insect egg deposition affects plant defenses in willows (*Salix matsudana* 'Zhuliu'). The study found that egg deposition by *Plagiodera versicolora* triggered plant defensive responses and enhanced the plant's ability to cope with subsequent larval feeding. RNA-seq analysis revealed altered expression of genes related to stress responses and metabolic processes. Following larval feeding, increased activity of genes involved in phenylpropanoid biosynthesis and phytohormone signaling was observed, indicating that egg deposition primes the plant for heightened defense. Bioassays demonstrated that larvae feeding on leaves with prior egg deposition exhibited reduced performance, suggesting that the willow's induced defenses effectively decrease larval survivability.

Sun et al. analyze the biochemical and molecular responses of daylilies (*Hemerocallis citrina* 'Datong Huanghua') to feeding by *Thrips palmi*. The study found significant reductions in soluble sugar, amino acid, and free fatty acid levels in daylily leaves after *T. palmi* feeding, alongside increases in secondary metabolites like tannins, flavonoids, and phenols. Key defense enzymes, including

peroxidase (POD), phenylalanine ammonia lyase (PAL), and polyphenol oxidase (PPO), were significantly enhanced. RNA sequencing identified 1,894 differentially expressed genes (DEGs) associated with *T. palmi* feeding, with 698 predicted as transcription factors involved in stress responses. Weighted Gene Co-expression Network Analysis (WGCNA) highlighted 18 hub genes in key modules, potentially crucial for regulating defense responses.

Review articles on plant-insect interactions

Two review articles summarize plant defenses and key insect proteins involved in interactions with host plants. Li et al. review current knowledge and advances in plant defenses against whiteflies, emphasizing the role of trichomes and acylsugars as physical barriers, and secondary metabolites and jasmonate (JA) signaling in chemical defenses. The review discusses genetic and biotechnological approaches to enhance plant resistance, including plant-mediated RNA interference (RNAi) and ectopic expression of insecticidal proteins. These advancements are critical for developing effective and sustainable solutions for whitefly management.

Wang et al. highlight key areas in the study of plant-insect interactions, focusing on the identification of insect elicitors and effectors and their roles in activating plant defense pathways such as jasmonic acid (JA) and salicylic acid (SA) signaling, calcium flux, reactive oxygen species (ROS) bursts, and mitogen-activated protein kinase (MAPK) activation. Multi-omics approaches, including genomics, transcriptomics, and proteomics, are used to analyze insect saliva and salivary glands. The review provides insights into the complex mechanisms of attack and defense and the roles of various elicitors and effectors in these interactions.

Author contributions

SJ: Conceptualization, Data curation, Formal analysis, Funding acquisition, Investigation, Methodology, Project administration, Supervision, Writing – original draft, Writing – review & editing. GH: Data curation, Investigation, Resources, Validation, Writing – review & editing. M-SC: Formal analysis, Investigation, Validation, Writing – review & editing.

Funding

The author(s) declare financial support was received for the research, authorship, and/or publication of this article. This study was supported by grants from the National Natural Science Foundation of China (U1704111, and 31401732), ZHONGYUAN YINGCAI JIHUA (ZYYCYU202012165), the Open Project Funding of the State Key Laboratory of Crop Stress Adaptation and Improvement (2023KF10).

Acknowledgments

We thank the authors who submitted their research or review articles in this Research Topic for their valuable contributions and the reviewers for their rigorous reviews. We also thank the editorial board of "Omics in Plant-Insect Interactions" and the Frontiers specialists, for their support. This manuscript was assisted by ChatGPT (Version: GPT-4, Model: OpenAI GPT-4, Source of Generative AI Technology: OpenAI).

Conflict of interest

The authors declare that the research was conducted in the absence of any commercial or financial relationships that could be construed as a potential conflict of interest.

Publisher's note

References

Cheng, X. Y., Zhu, L. L., and He, G. C. (2013). Towards understanding of molecular interactions between rice and the brown planthopper. *Mol. Plant* 6, 621–634. doi: 10.1093/mp/sst030

Erb, M., and Reymond, P. (2019). Molecular interactions between plants and insect herbivores. *Annu. Rev. Plant Biol.* 29, 527–557. doi: 10.1146/annurev-arplant-050718-095910

Jing, S. L., Zhao, Y., Du, B., Chen, R. Z., Zhu, L. L., and He, G. C. (2017). Genomics of interaction between the brown planthopper and rice. *Curr. Opin. Insect Sci.* 19, 82–87. doi: 10.1016/j.cois.2017.03.005

Shar, S. B. D., Nguyen, C. D., Sanada-Morimura, S., Yasui, H., Zheng, S. H., and Fujita, D. (2023). Development and characterization of near-isogenic lines for brown planthopper resistance genes in the genetic background of japonica rice 'Sagabiyori'. *Breed. Sci.* 73, 382–392. doi: 10.1270/jsbbs.23017

frontiers | Frontiers in Plant Science

TYPE Original Research
PUBLISHED 19 June 2023
DOI 10.3389/fpls.2023.1200014

OPEN ACCESS

EDITED BY
Shengli Jing,
Xinyang Normal University, China

REVIEWED BY
Peiying Hao,
China Jiliang University, China
Hao Zhou,
Sichuan Agricultural University, China

*CORRESPONDENCE
Deze Xu
dezexu@163.com
Lei Zhou
yutian_zhou83@163.com
Aiqing You
aq_you@163.com

†These authors have contributed equally to this work

RECEIVED 04 April 2023
ACCEPTED 26 April 2023
PUBLISHED 19 June 2023

CITATION
Zha W, Li C, Wu Y, Chen J, Li S, Sun M, Wu B, Shi S, Liu K, Xu H, Li P, Liu K, Yang G, Chen Z, Xu D, Zhou L and You A (2023) Single-Cell RNA sequencing of leaf sheath cells reveals the mechanism of rice resistance to brown planthopper (*Nilaparvata lugens*). *Front. Plant Sci.* 14:1200014. doi: 10.3389/fpls.2023.1200014

Single-Cell RNA sequencing of leaf sheath cells reveals the mechanism of rice resistance to brown planthopper (*Nilaparvata lugens*)

Wenjun Zha[1,2†], Changyan Li[1†], Yan Wu[1†], Junxiao Chen[1†], Sanhe Li[1], Minshan Sun[3], Bian Wu[1], Shaojie Shi[1], Kai Liu[1], Huashan Xu[1], Peide Li[1], Kai Liu[1], Guocai Yang[1], Zhijun Chen[1], Deze Xu[1,2*], Lei Zhou[1,2*] and Aiqing You[1,2*]

[1]Key Laboratory of Crop Molecular Breeding, Ministry of Agriculture and Rural Affairs, Hubei Key Laboratory of Food Crop Germplasm and Genetic Improvement, Food Crops Institute, Hubei Academy of Agricultural Sciences, Wuhan, China, [2]Hubei Hongshan Laboratory, Wuhan, China, [3]Henan Assist Research Biotechnology Co., Ltd., Zhengzhou, China

The brown planthopper (BPH) (*Nilaparvata lugens*) sucks rice sap causing leaves to turn yellow and wither, often leading to reduced or zero yields. Rice co-evolved to resist damage by BPH. However, the molecular mechanisms, including the cells and tissues, involved in the resistance are still rarely reported. Single-cell sequencing technology allows us to analyze different cell types involved in BPH resistance. Here, using single-cell sequencing technology, we compared the response offered by the leaf sheaths of the susceptible (TN1) and resistant (YHY15) rice varieties to BPH (48 hours after infestation). We found that the 14,699 and 16,237 cells (identified *via* transcriptomics) in TN1 and YHY15 could be annotated using cell-specific marker genes into nine cell-type clusters. The two rice varieties showed significant differences in cell types (such as mestome sheath cells, guard cells, mesophyll cells, xylem cells, bulliform cells, and phloem cells) in the rice resistance mechanism to BPH. Further analysis revealed that although mesophyll, xylem, and phloem cells are involved in the BPH resistance response, the molecular mechanism used by each cell type is different. Mesophyll cell may regulate the expression of genes related to vanillin, capsaicin, and ROS production, phloem cell may regulate the cell wall extension related genes, and xylem cell may be involved in BPH resistance response by controlling the expression of chitin and pectin related genes. Thus, rice resistance to BPH is a complicated process involving multiple insect resistance factors. The results presented here will significantly promote the investigation of the molecular mechanisms underlying the resistance of rice to insects and accelerate the breeding of insect-resistant rice varieties.

KEYWORDS

single-cell, RNA-seq, leaf sheath cells, resistant, *Nilaparvata lugens*, rice

Introduction

Rice (*Oryza sativa* L.) is one of the most important cereal crops and has been domesticated for approximately 7,500 years (Zong et al., 2007). Stored and unharvested rice can be attacked by >800 species of insect pests (Ghaffar et al., 2011). The brown planthopper (BPH), *Nilaparvata lugens* (Stål), is one of the most economically important insects which can cause huge destruction of rice plants (Xue et al., 2014). BPH can damage rice growth by spreading plant viruses (such as rice grassy and rice-ragged stunt viruses) (Cabauatan et al., 2009) and sucking plant sap.

BPH has co-evolved to adapt strongly to its host, rice (Sezer and Butlin, 1998; Zheng et al., 2021). The widely used insecticides could effectively protect from the BPH and other pests-caused damages. However, overuse of insecticides not only promotes BPH obtaining the adaptability and resistance to insecticides but also causes serious environmental pollution (Senthil-Nathan et al., 2009). However, a complex defense system against BPH also exists in rice. Therefore, developing rice varieties resistant to insects using their insect-resistance genes could be an ideal complement and alternative to existing insect-control measures. Since the first BPH-resistant rice variety was discovered, >40 genes associated with BPH resistance (Akanksha et al., 2019; Li et al., 2019), such as *bph1-40*, have been identified. Some of these BPH-resistant genes, such as *bph1-4*, have been successfully used in breeding BPH-resistant rice varieties (Athwal et al., 1971; Laksminarayana and Khush, 1977). These BPH-resistance genes not only promote rice BPH-resistance but also decrease BPH reproduction and prolong the period of BPH development (Du et al., 2009; Senthil-Nathan et al., 2009; Nguyen et al., 2019). The interaction between BPH and rice is a complex and dynamic process. Currently, it is understood that BPH sucks phloem sap by inserting the stylet bundle with an accompanying salivary sheath into the plant (Spiller, 1990). On its way to the phloem, the mouth stylet bundle pierces through various cells, such as the epidermis, mesophyll, phloem, etc. Thus, multiple resistant mechanisms may interrupt the BPH feeding process at several cellular locations. Moreover, the different cells encountered by the stylet may mount different resistant functions depending on the rice variety. Presently, the identity of the cells involved in insect resistance in rice and the underlying molecular mechanisms remain unknown.

Single-cell RNA sequencing (scRNA-seq) provides a method to examine the expression of all genes in each cell at the transcriptional level (Brennecke et al., 2013; Islam et al., 2014). Recently, scRNA-seq was applied in many fields to explore the heterogeneity of cells (Luecken and Theis, 2019). In addition, studies on heterogeneity in animal cells have been abundantly reported (Butler et al., 2018; Aran et al., 2019; Zhang et al., 2019). However, because of the presence of plant cell walls, the application of scRNA-seq is limited in plants. Currently, several single-cell studies in plants focusing on tissue and cellular functional differentiation–such as differentiation of roots and stems in *Arabidopsis* (Zhang et al., 2021b), stomatal lineage and developing leaf (Lopez-Anido et al., 2021), ploidy-dependence in *Arabidopsis* female gametophytes (Song et al., 2020), leaf and root differentiation in rice (Liu Q. et al., 2021; Wang et al., 2021; Zhang et al., 2021a), differentiation of maize ears facilitates (Xu et al., 2021b), poplar xylem formation (Xie et al., 2022), *Nicotiana attenuate* corolla cells formation (Kang et al., 2022)–have been reported. However, studies on the molecular mechanisms underlying the response of different plant cells to biotic stresses are rarely reported.

Here, we used scRNA-seq to explore the differences in the molecular responses mounted by the various cell types to BPH biotic stress (to BPH infestation) in two rice varieties differing in their resistance to BPH. This study's results will be a reference for future studies revealing the molecular mechanisms of rice insect resistance and provide a theoretical basis for better breeding of varieties resistant to BPH.

Materials and methods

Rice plants cultivation and infesting rice plants with brown planthopper

For this study, seedlings of the rice varieties TN1 (susceptible to BPH) and YHY15 (moderately resistant to BPH) were cultivated in a climate chamber under a 12-h light/12-h dark cycle at 30 ± 1°C and 70% relative humidity. Then, the 2- to 3-instar hopper nymphs were used to infest the seedlings at the third-leaf stage (13 or 14 days old) at a density of eight insects per seedling under the conditions of 70% relative humidity, 25 ± 1°C, and 16-h light/8-h dark cycle. And we covered the stems of each seedling with breathable plastic tubes to prevent the brown planthoppers from escaping. After 48 hours, the leaf sheaths, including herbivore-exposed local (damaged) parts of TN1 and YHY15, were collected for further study. Three seedlings were sampled for each rice variety.

Rice protoplast isolation

The rice protoplast was isolated using the previous methods (Jabnoune et al., 2015; Wang et al., 2021). Briefly, the finely cut rice seedling leaf sheaths were immediately incubated in an enzymes solution containing 10 mM MES, 0.6 M mannitol, 0.75% macerozyme R-10, and 1.5% cellulase RS (pH 5.7) for 3 h (shaking at 70 rpm) at 28°C. After incubation, the enzyme solution was filtered out. The digested protoplasts were washed with the W5 solution (154 mM NaCl, 125 mM $CaCl_2$, 5 mM KCl, and 2 mM MES at pH 5.7) and collected by centrifugation at 300 × g. The protoplasts were resuspended in a solution containing 0.6 M D-Mannitol, 15 mM $MgCl_2$, and 4 mM MES (pH 5.7). A small amount of the single-cell suspension was added to an equal volume of 0.4% trypan blue dye. The concentration of viable cells was adjusted to the desired concentration (1000 to 2000 cells/μL) by counting the cells using Countess® II Automated Cell Counter.

Single-cell RNA sequencing

To generate the single-cell Gel Bead-In-Emulsions (GEMs) from cellular suspensions, a GemCode Single-cell instrument (10x Genomics, Pleasanton, CA, USA) was used. The Chromium Next

GEM Single Cell 3' Reagent Kits v3.1 (CG000183, RevC, 10x Genomics) was used to prepare the library and for sequencing. To construct the library, the barcoded, reverse-transcribed, and full-length cDNAs were amplified using PCR assay. Next, the PCR products were ligated to the adapters for sequencing, followed by PCR amplification according to the DNA template concentrations. Then a paired-end sequencing was conducted using the Illumina platform (Illumina Inc., San Diego, USA) for sequencing libraries.

Preprocessing and cell clustering analysis

To generate counts quantification, alignment, and FASTQ files from raw Illumina BCL files, the Cell Ranger software (version 3.1.0, 10x Genomics) was used. (Lun et al., 2019). To align the sequencing, reads of rice scRNA-seq samples were aligned to the rice reference genome (Kawahara et al., 2013). The Seurat software (V3.1.1, Satija Lab, New York, USA) was used for the analysis of the downstream genes through importing the gene matrices cell for each sample individually (Butler et al., 2018; Stuart et al., 2019). Using DoubletFinder (v2.0.3), we filtered out the cells with doublet GEMs, no less than 8000 UMIs and no less than 10% mitochondrial genes (McGinnis et al., 2019). After normalizing the data, the harmony algorithm was used to correct the batch effect (Korsunsky et al., 2019). Principal component analysis dimensional reduction was applied as a reference according to the previous report (Chung and Storey, 2015). Cells clustering was analyzed using the Louvain method to maximize modularity (Rotta and Noack, 2011). The combination of cell type annotation with these previously reported cell type marker genes was conducted using the R packages SingleR (Aran et al., 2019) and Cellassign (Zhang et al., 2019).

Differentially expressed genes analysis

The Wilcoxon rank sum test was used to compare difference in expression of every detected gene between the given cluster and other cells (Camp et al., 2017). We identified the significantly upregulated genes using the following criteria–genes had to be at least 1.28-fold overexpressed in a target cluster having >25% of same type of cells, and have a p value < 0.01. Subsequently, Kyoto Encyclopedia of Genes and Genomes (KEGG) pathways enrichment analyses and Gene Ontology (GO) functional annotation were conducted to analyze these DEGs (Boyle et al., 2004; Kanehisa and Goto, 2000; Kanehisa et al., 2008).

Gene set variation analysis and cell cycle analysis

GSVA was performed using a collection of gene sets from Molecular Signatures Database (MSigDB) (Liberzon et al., 2015) to identify pathways and cellular processes enriched in different clusters. GSVA was performed as implemented in the GSVA R package version 1.26 (Hanzelmann et al., 2013) based on the cluster-averaged log-transformed expression matrix. According to the expression of the genes associated with G1/S phase (n = 100), S phase (n = 113), G2/M phase (n = 133), M phase (n = 106), and M/G1 phase (n = 106), the cell cycle score was assigned using the package "Seurat" (Macosko et al., 2015). Cells with the highest score <0.3 were defined as non-cycling cells (Neftel et al., 2019). In addition, the Plant Transcription Factor Database (PlantTFDB) was used in the transcript factors annotation (Jin et al., 2017).

RNA *in situ* hybridization assay

The situ hybridization assay was conducted based on the previously published protocol (Umeda et al., 1999). Briefly, hydration and paraffin embedding of the fresh rice seedling leaf sheaths were performed after 12 h fixation with FAA solution (3.7% formaldehyde, 5% acetic acid, and 50% ethanol). Subsequently, the paraffin-embedded rice seedling leaf sheaths were sectioned into 10 μm thick sections and treated for 2 h at 62°C (KD-P, Zhejiang Jinhua Kedi Instrumental Equipment Co., Ltd, China) and xylene (twice for 15 min) to remove paraffin and serially rehydrated using different concentrations of ethanol. Then, the leaf sheath sections were hybridized with RNA probes following a 15-minute Proteinase K (20 μg/ml) (G1234, Nanjing Zoonbio Biotechnology, Ltd., China) digestion (at 37°C) and serial dehydration using different concentrations of ethanol. Next, the probes were transcribed *in vitro* using a Digoxigenin RNA labeling kit (Roche, USA). The transcribed probes were then incubated with the leaf sheath tissue sections. Finally, they were washed and incubated with an anti-digoxigenin-AP (200-052-156, Jackson ImmunoResearch Inc., PA, USA). The RNA hybridization signals were detected at room temperature by staining with a nitro-blue tetrazolium/5-bromo-4-chloro-30-indolyphosphate stock solution (NBT/BCIP solution; Boster Bio, CA, USA). Images were taken in the bright field mode using a microscope (Nikon Eclipse ci, Nikon Instruments Inc., NY, USA).

Results

Characteristics of the constructed single-cell transcriptome library of the leaf sheaths of BPH-resistant rice variety

We isolated protoplasts from rice leaf sheaths after a 48 h infestation with the BPH to generate a single-cell transcriptome of the rice resistant to BPH. The 10x Genomics Chromium and the Illumina sequencing platforms were used to generate scRNA-Seq libraries (Figure 1A). For TN1 and YHY15 samples, we obtained 23,346 and 19,775 reads per cell, respectively. 1,670 expressed genes and 4,600 unique molecular identifiers (UMI) were generated for each cell. In TN1 and YHY15, we also detected 27,740 and 26,710 genes, respectively (Supplementary Tables 1–3). Using t-distributed stochastic neighbor embedding (tSNE) projection, the single-cell transcriptomes were plotted, and largely overlapping distributions between TN1 and YHY15 were observed, suggesting a high reproducibility (Figure 1B). To categorize the single cells, the

10.3389/fpls.2023.1200014

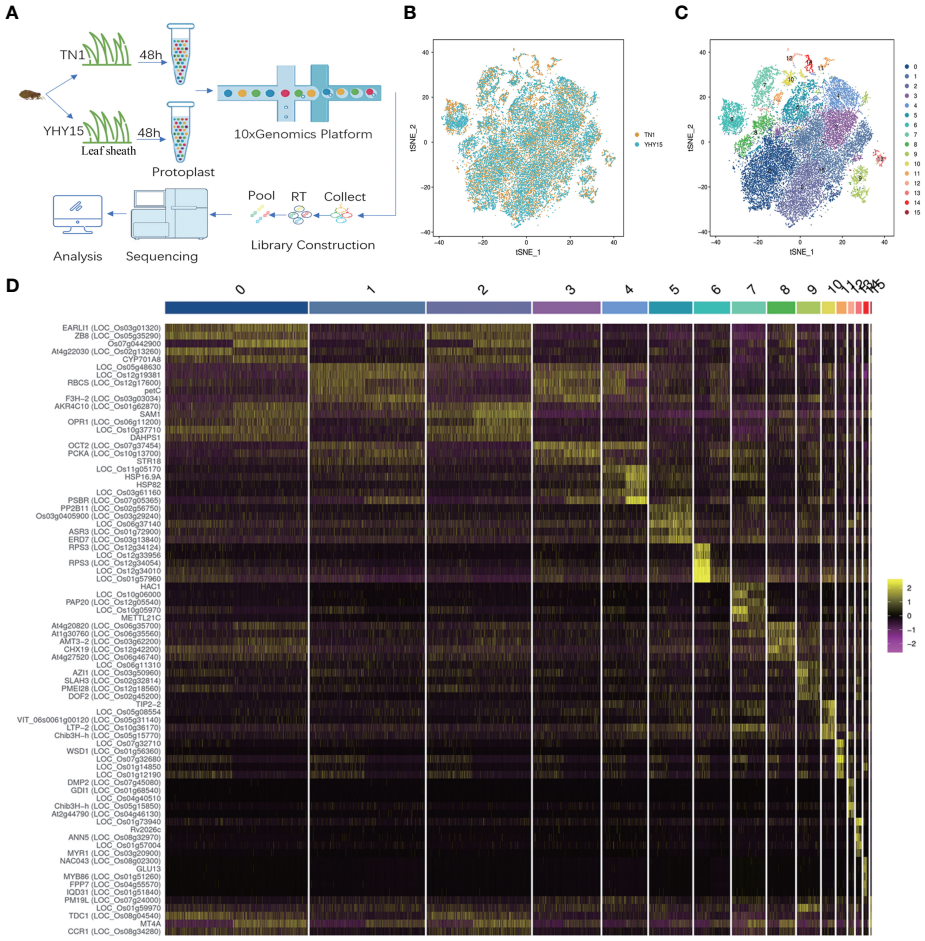

FIGURE 1
Quality control of the rice seedlings scRNA-seq analysis. **(A)** Representative schematic graph showing the workflow of scRNA-seq; **(B)** Representative plot of dimensional reduction of TN1 and YHY15; [Orange- TN1, Blue- YHY15] **(C)** Representative plot of the 16 major clusters of the TN1 and YHY15 cell transcriptomes; **(D)** Top 5 genes exhibiting upregulated expression in 16 clusters. [Yellow- high expression, Purple- low expression].

package "Seurat" was applied. The results showed 16 major clusters of cell transcriptomes in two-dimensional space (Figure 1C). The total cells for TN1 and YHY15 were 14699 and 16237, respectively. Among these 16 clusters, the proportion of cells in most clusters was not significantly different, but the proportion of YHY15 cells was relatively low in clusters 11–14. In contrast, in cluster 15, the cell ratio of YHY15 was higher (Supplementary Table 4). Next, we examined the genes significantly upregulated in the 16 clusters, and the top 5 highly expressed genes were selected in each cluster (Supplementary Table 5); the expression pattern of these genes showed apparent cluster specificity (Figure 1D).

Tissue-specific marker gene analysis of the BPH-inoculated rice leaf sheath transcriptome library revealed nine cell/tissue types

For the assignment of tissue/cell type to clusters, the accumulated transcripts in our single-cell population were analyzed for significant expression of 52 marker genes in leaf sheath tissue/cell types (Supplementary Table 6). Nine major cell-type clusters were observed in both TN1 and YHY15 (Figure 2A) transcriptomes. Through comparing the changes in cell proportions for each cell type, we found that the proportions of mesophyll did not change much, but the proportions of procambium, guard cell, mestome sheath cell, and phloem were quite different (Figure 2B). The expression distribution of some existing marker genes, such as—1) Mesophyll marker genes (*LOC_Os07g38960* (*CAB7*), *LOC_Os01g41710* (*CAB2R*), *LOC_Os12g19470* (*RBCS*), and LOC_*Os12g19381* (*RBCS*)); 2) Procambium marker genes (*LOC_Os02g08100* (*4CL3*), *LOC_Os12g04080* (*TBT1*), and *LOC_Os11g42290* (*TBT1*)); 3) Bulliform marker genes (*LOC_Os06g14540* (*GLU13*)); 4) Phloem marker genes (*LOC_Os06g41090* (*FTIP1*), *LOC_Os01g06500* (*PP2A1*), and *LOC_Os03g07480* (*SUT1*)); 5) Guard cell marker genes (*LOC_Os03g41460* (*SPARK10*) and *LOC_Os04g48530* (*SLAC1*)); and 6) Mestome sheath marker genes (*LOC_Os01g68540* (*GDI1*))—were analyzed in each cell-type cluster. The expression of these genes was consistent with previously reported (Figures 2C–P). Therefore, we focused on detecting expression patterns of three selected genes, viz.,

10.3389/fpls.2023.1200014

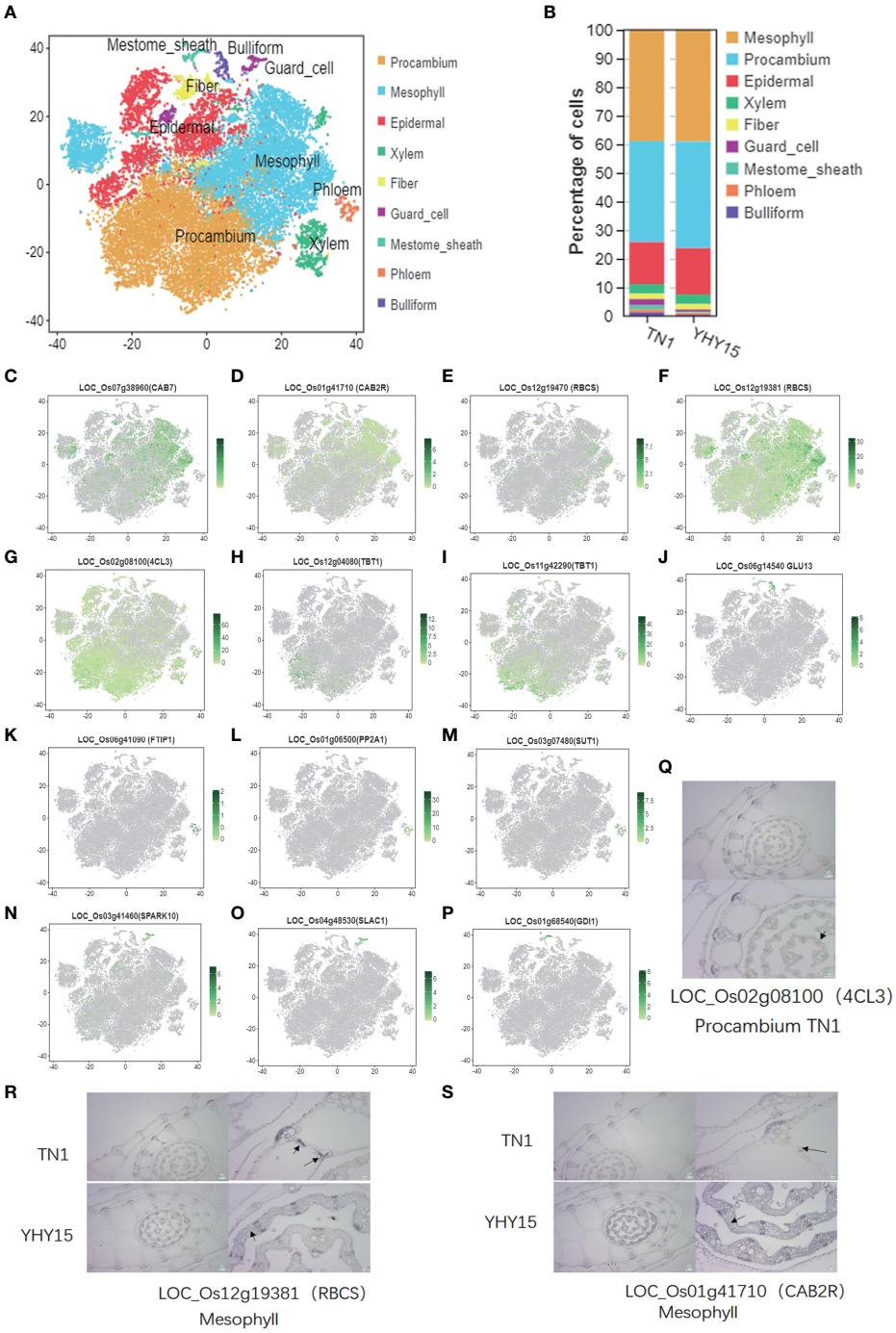

FIGURE 2
Single-cell transcriptome atlas for the rice leaf. **(A)** Representative plot of the combined accumulation of transcript from the tested marker genes (listed in Supplemental Table S1); **(B)** The percentage of cells in cell-type clusters; **(C–P)** tSNE plots of marker genes predicting the identities of clusters [The color scale indicates normalized expression level]; **(C–F)** Mesophyll maker genes, *LOC_Os07g38960* (*CAB7*), *LOC_Os01g41710* (*CAB2R*), *LOC_Os12g19470* (*RBCS*), and *LOC_Os12g19381* (*RBCS*); **(G–I)** Procambium maker genes, *LOC_Os02g08100* (*4CL3*), *LOC_Os12g04080* (*TBT1*), and *LOC_Os11g42290* (*TBT1*); **(J)** Bulliform maker gene, *LOC_Os06g14540* (*GLU13*); **(K–M)** Phloem maker genes, *LOC_Os06g41090* (*FTIP1*), *LOC_Os01g06500* (*PP2A1*), and *LOC_Os03g07480* (*SUT1*); **(N, O)** Guard cell maker genes, *LOC_Os03g41460* (*SPARK10*), *LOC_Os04g48530* (*SLAC1*); **(P)** Mestome sheath maker gene, *LOC_Os01g68540* (*GDI1*); **(Q–S)** Representative images showing the results of *in situ* hybridization. [Black triangles- the identified cell types and gene ID; the scale bare is shown in images].

LOC_Os02g08100 (*4CL3*), *LOC_Os01g41710* (*CAB2R*), and *LOC_Os12g19381* (*RBCS*). The RNA *in situ* hybridization results confirmed the marker gene *LOC_Os02g08100* (*4CL3*) expression in procambium cells at the center of immature young leaf sheath (Figure 2Q). In mesophyll cells, a high RNA abundance of the mesophyll marker genes–*LOC_Os12g19381* (*RBCS*) and *LOC_Os01g41710* (*CAB2R*)–was seen, indicating that the annotation of cell types was reliable (Figures 2R, S).

Functional enrichment of each cluster

The DEGs upregulated in each cluster were identified to obtain the cell types' basic information in all clusters; 3,780 upregulated genes were screened (Supplementary Tables 7, 8). In all, 208 to 856 DEGs were identified. Procambium cells, followed by mesophyll and epidermal cells, had the highest number of DEGs; the least number of DEGs were found in fiber cells (Supplementary Table 7). Next, the potential enriched pathways and functions were determined by KEGG and GO analyses. GO analysis revealed that all eight cell-type clusters (except the phloem cluster) were significantly enriched in the "response to stimulus" biological process. The guard cell, mesophyll, and procambium clusters were significantly enriched in the "metabolic process." Bulliform, epidermal, fiber, guard cell, mesophyll, and procambium clusters were significantly enriched in the "cellular process" (Figure 3A). The molecular function results showed bulliform and mestome sheath were significantly enriched in the "binding" terms. Epidermal and procambium clusters were significantly enriched in "catalytic activity" and "transporter activity" (Figure 3A).

KEGG analysis revealed that the bulliform cluster was significantly enriched in "ribosome," "protein processing in the endoplasmic reticulum," and "phagosome" pathways. The epidermal cluster was significantly enriched in "endocytosis," "glycerolipid-," and "glycerophospholipid-" metabolism pathways. Fiber cluster was significantly enriched in "ubiquitin-mediated proteolysis," "ribosome," "oxidative phosphorylation," "β-Alanine metabolism," "fatty acid degradation," "valine, leucine, and isoleucine degradation," and "histidine metabolism" pathways. Guard cell cluster was significantly enriched in "plant-pathogen interaction" and "MAPK signaling" pathways. Mesophyll cluster was significantly enriched in "ribosome," "photosynthesis," "carbon fixation in photosynthetic organisms," "glycolysis/gluconeogenesis," "oxidative phosphorylation," "carbon metabolism," "mannose and fructose metabolism," 'photosynthesis-antenna proteins," and "valine, leucine, and isoleucine degradation" pathways. Procambium cluster was significantly enriched in "citrate cycle (TCA cycle)," "phenylalanine metabolism," "proteasome," "tryptophan, tyrosine, and phenylalanine biosynthesis," "α-linolenic acid metabolism," "biosynthesis of amino acids," "carbon metabolism," "biosynthesis of secondary metabolites," "glutathione metabolism," "pentose phosphate pathway," "oxidative phosphorylation," and "stilbenoid, diarylheptanoid, and gingerol biosynthesis" pathways (Figure 3B).

The bulliform cluster was similar to the mestome sheath, and the epidermal cluster was similar to the procambium in the Go enrichment profiles.

Susceptible and resistant rice varieties mounted different responses to BPH feeding, which also differed based on cell type

The pseudotime trajectory analysis of all cell-type clusters was conducted to evaluate the responses of the rice cells to BPH infestation (Figure 4A). The development and response processes to BPH feeding could be divided into nine differentiation states (states 1–9) (Figure 4B). Pseudotime path clustering of DEGs revealed branching in the gene expression pattern of the differentiation states (Figure 4C, Supplementary Table 9). Susceptible and resistant rice varieties can mount different gene expression responses to BPH infestation. By comparing the differences in each cell type in TN1 and YHY15, we found that the procambium, epidermal, and fiber cells are similar across all differentiation states. Between TN1 and YHY15, significant differences in differentiation states were observed as follows–a) mestome sheath cells-states 1, 4, 6, and 8; b) guard cells-states 4, 6, 8, 9; c) mesophyll cells-state 8; d) xylem cells-states 1, 6, 8, 9; e)

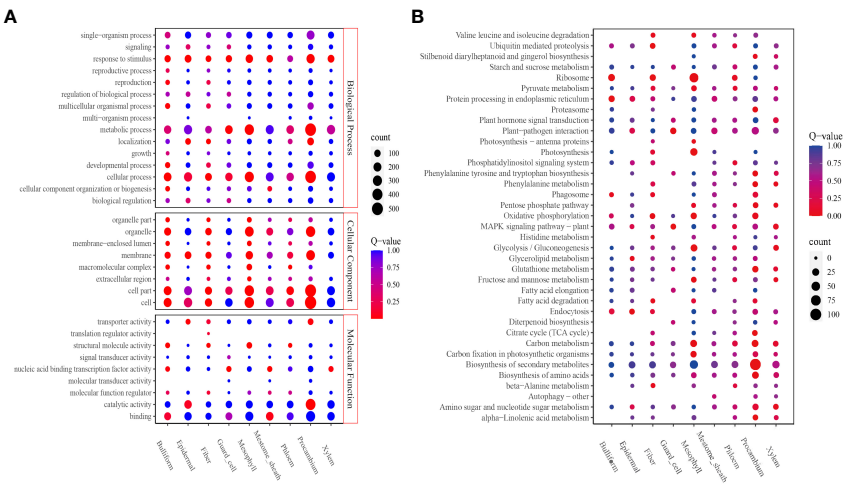

FIGURE 3
Function enrichment analyses. **(A)** GO analysis of all clusters; **(B)** KEGG analysis of all clusters. The level 2 GO terms, such as biological process, molecular function, cellular components, and the top 5 Go pathways and terms, are shown. The number of enriched genes was represented as the size of the circle. The significant enrichments were presented in red, and the insignificant enrichments were presented in blue.

10.3389/fpls.2023.1200014

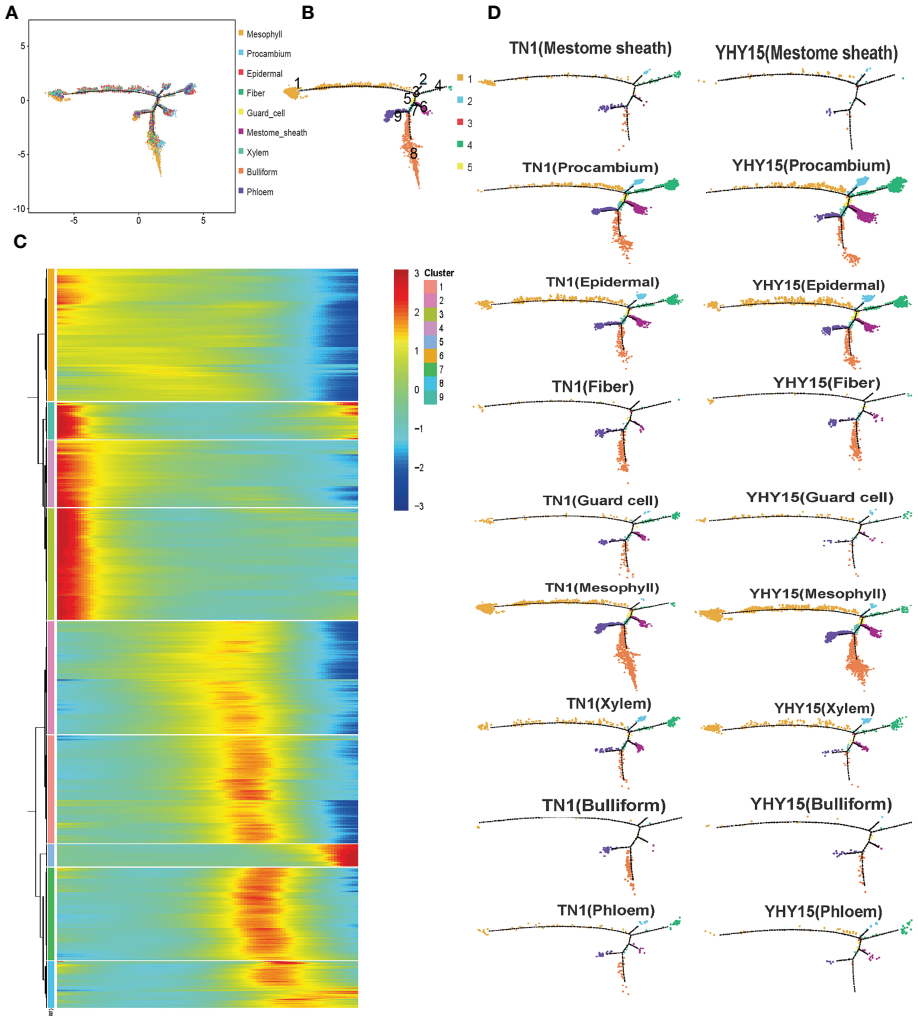

FIGURE 4
Pseudotime trajectory of all cluster's cells. **(A)** Pseudotime analysis using Monocle for cell transcriptomes; **(B)** The state information of differentiation; **(C)** Gene expression heatmap for all cluster genes; **(D)** Expression profile in differentiation state of all subgroup cells.

bulliform cells-states 8, 9; and f) phloem cells-states 1, 4, 6, 8, 9 (Figure 4D).

Expression of genes related to vanillin, capsaicin, and ROS production in the mesophyll cluster depends on BPH-susceptibility

Although epidermal cells are the primary barrier of plants when BPH suck the phloem sap, their stylet bundle mainly pierces mesophyll cells; thus, mesophyll cells form a secondary barrier against further BPH feeding. The pseudotime trajectory analysis results of the mesophyll cells showed that the mesophyll cells were mainly divided into five states (Figure 5A). Comparing the gene expression in TN1 and YHY15 showed that the differences were primarily concentrated in branch 5 (Figure 5B). The overall expression level in cluster 5 was increased compared to that in other branches (Figure 5C). KEGG enrichment analysis of cluster 5 showed that these genes were significantly enriched in "phenylalanine, tyrosine, and tryptophan biosynthesis," "biosynthesis of amino acid," "MAPK signaling," and "phenylalanine metabolism" pathways (Figure 5D, Supplementary Table 10). Phenylalanine metabolism is one of the downstream regulatory pathways of phenylalanine, tyrosine, and tryptophan biosynthesis. In this pathway, the phenylalanine ammonia-lyase (PAL) gene expression–viz. (*LOC_Os02g41670*, *LOC_Os02g41680*), *CYP73A* (*LOC_Os02g26810*, *LOC_Os05g25640*) and *4CL* (*LOC_Os08g34790*)–were mainly affected. These are part of gene regulatory pathways that affect the 4-Coumaroyl-CoA levels and, consequently, the levels of vanillin or capsaicin. The GO enrichment analysis of cluster 5 genes showed that the main enriched GO terms include "response to stimulus" (GO: 0050896), "response to biotic stimulus" (GO: 0009607), etc. (Figure 5E). Three genes–two PAL homologs, two CYP73A homologs, and a 4CL homolog (Figures 5G–K)–in the phenylalanine and vanillin synthesis pathways were significantly different between the two rice varieties (Figure 5F). Further, cell

10.3389/fpls.2023.1200014

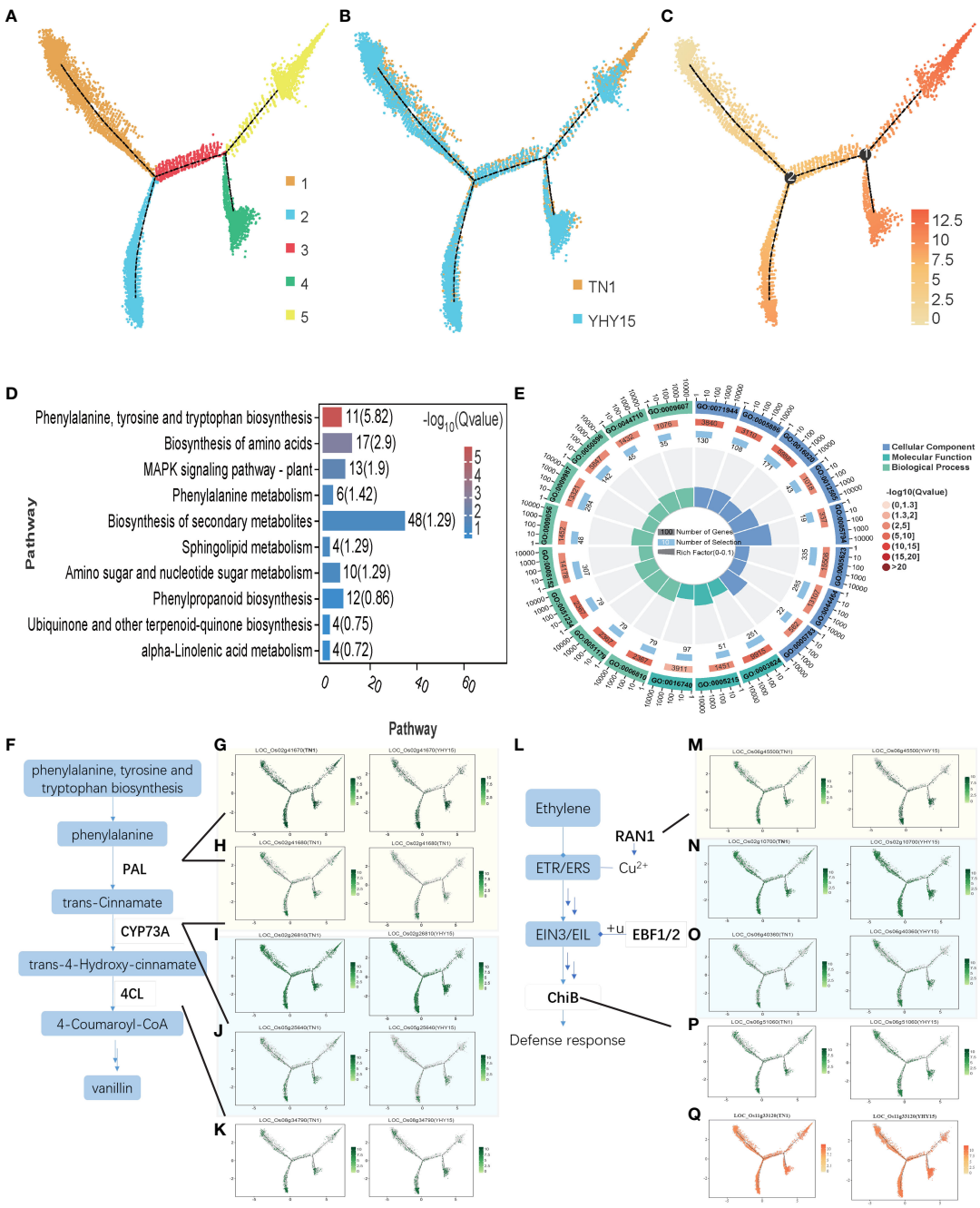

FIGURE 5
Pseudotime trajectory and function analysis of Mesophyll cells. **(A)** The state information of Mesophyll cells differentiation; **(B)** Samples information of Mesophyll cells; **(C)** Pseudotime trajectory of Mesophyll cells; **(D)** KEGG enrichment analysis of cluster 5 of Mesophyll cells; **(E)** GO enrichment analysis of cluster 5 of Mesophyll cells; **(F)** The schematic diagram of phenylalanine pathway; **(G–K)** The expression profiles of genes *LOC_Os02g41670* (*PAL*) **(G)**; *LOC_Os02g41680* (*PAL*) **(H)**; *LOC_Os02g26810* (*CYP73A*) **(I)**; *LOC_Os05g25640* (*CYP73A*) **(J)**, and *LOC_Os08g34790* (*4CL*) **(K)** in TN1 and YHY15 samples; **(L)** The schematic diagram of ethylene response pathway; **(M–Q)** The expression profiles of genes *LOC_Os06g45500* (*RAN1*) **(M)**; *LOC_Os02g10700* (*EBF1/2*) **(N)**; *LOC_Os06g40360* (*EBF1/2*) **(O)**; *LOC_Os06g51060* (*ChiB*) **(P)** and *LOC_Os11g33120* (*ChiB*) **(Q)** in TN1 and YHY15 samples.

number and expression of five genes in cluster 5 were quite different between TN1 and YHY15 varieties. Furthermore, the ethylene response pathway genes–*RAN1*, *EBF1/2*, and *ChiB*–under the MAPK signaling pathway had significant differences in expression levels (Figures 5L–P); thus, they may be involved in the trauma response of rice to BPH feeding. In addition, the expression of cluster 5 gene *LOC_Os11g33120* (encoding a *ROBH* gene involved in reactive oxygen species (ROS) production) was significantly higher in TN1 than in YHY15. Thus, BPH feeding may have triggered differences in ROS production (Figure 5Q).

Phloem cell

Since BPH sucks phloem sap, the feedback of phloem cells to stress is inextricably linked to rice BPH resistance. The pseudotime trajectory analysis showed that the phloem cells were mainly divided into three clusters (Figure 6A). The gene expression level was lowest in cluster 1 and up-regulated in clusters 2 and 3 (Figure 6B). Cluster 1 mainly consists of TN1 cells, while clusters 2 and 3 have more YHY15 cells (Figure 6C). The gene expression level of cluster 1 gradually decreased along pseudotime, while clusters 2 and 3 showed an increasing trend (Figure 6D). The main GO enrichment terms for these genes include "response to stress," "response to abiotic stimulus," and "response to stimulus" (Figure 6E). Cluster 1 has multiple genes closely related to cell wall extension, such as *LOC_Os06g48160* (*XTH22*, xyloglucan endotransglucosylase/hydrolase protein 22) (Figure 6F), *LOC_Os08g40690* (*RIXI*, xylanase inhibitor protein 1) (Figure 6G). It also has energy production genes *LOC_Os11g10480* (*ADH1*, alcohol dehydrogenase I) (Figure 6H). Multiple ABC transporter G family members in cluster 3–such as *LOC_Os09g29660* (*ABCG11*) (Figure 6I), *LOC_Os08g29570* (*ABCG44*) (Figure 6J), *LOC_Os07g33780* (*ABCG43*) (Figure 6K), *LOC_Os01g42410* (*ABCG37*) (Figure 6L), *LOC_Os01g261460* (*ESK1*, promotes xylan acetylation) (Figure 6M), *LOC_Os08g21040* (*ASPG1*, aspartic protease in guard cell) (Figure 6N)–exhibited significantly elevated expression.

Xylem cells

BPH also sucks xylem sap (Seo et al., 2009). The xylem cells were divided into 3 clusters (Figure 7A). The overall expression level was lowest in cluster 1 and higher in clusters 2 and 3 (Figure 7B). Among the three clusters, the main difference between the two varieties was found in cluster 2 (Figures 7C, D). The gene expression level in cluster 1 gradually decreased; it was enriched in genes associated with GO terms "response to stress." On the other hand, the gene expression level in clusters 2 and 3 showed a gradual increase; they were enriched

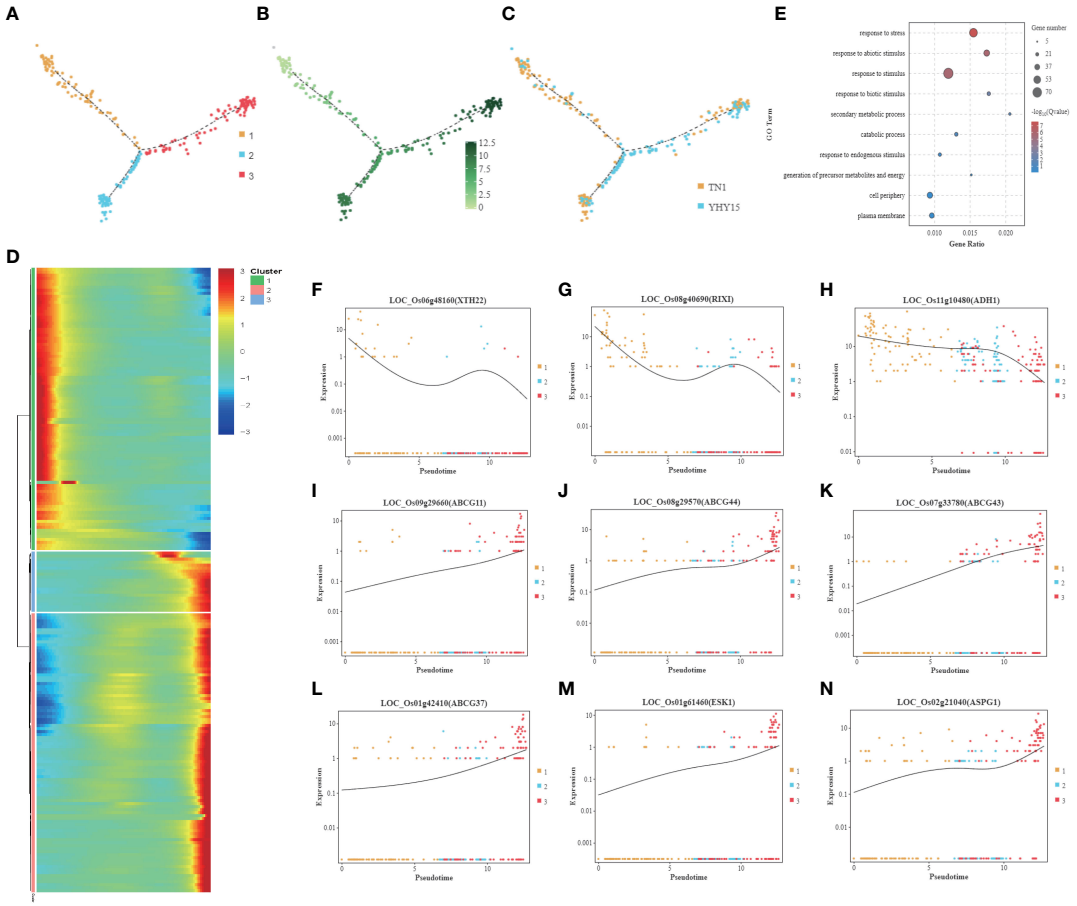

FIGURE 6
Pseudotime trajectory and function analysis of Phloem cells. **(A)** Pseudotime trajectory of Phloem cells; **(B)** The state information of Phloem cells differentiation; **(C)** Samples information of Phloem cells; **(D)** Gene expression heatmap for all cluster genes of Phloem cells; **(E)** GO enrichment analysis of Phloem cells; **(F–N)** Representative graph showing the trend of the selected DEGs expression along pseudotime trajectory during differentiation for each cell type- **(F)** *LOC_Os06g48160* (*XTH22*); **(G)** *LOC_Os08g40690* (*RIXI*); **(H)** *LOC_Os11g10480* (*ADH1*); **(I)** *LOC_Os09g29660* (*ABCG11*); **(J)** *LOC_Os08g29570* (*ABCG44*); **(K)** *LOC_Os07g33780* (*ABCG43*); **(L)** *LOC_Os01g42410* (*ABCG37*); **(M)** *LOC_Os01g261460* (*ESK1*); **(N)** *LOC_Os08g21040* (*ASPG1*). [One single cell was represented as one point. The entire X-axis was defined as "Pseudotime," entire Y-axis was defined as "Relative expression"].

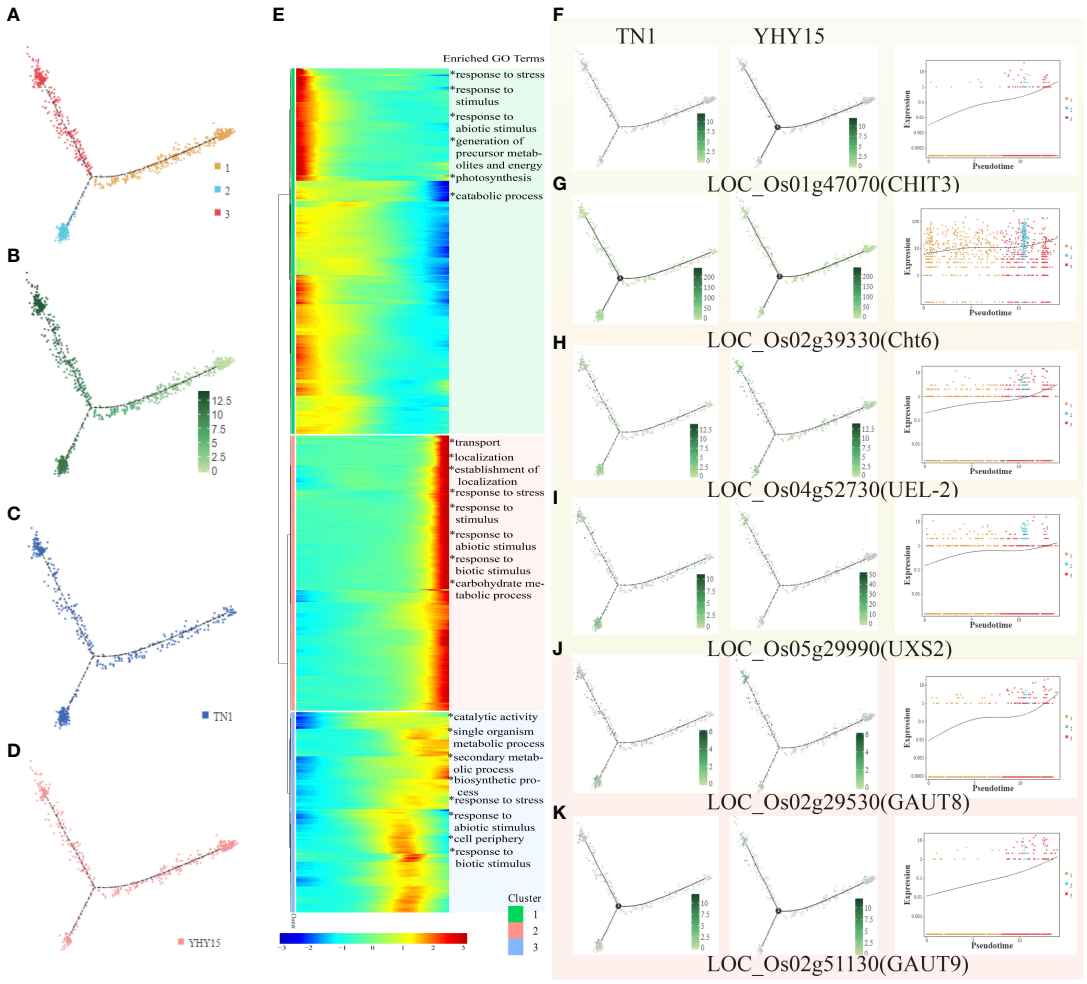

FIGURE 7
Pseudotime trajectory and function analysis of Xylem cells. **(A)** The state information of Xylem cells differentiation; **(B)** Pseudotime trajectory of Xylem cells; **(C)** The expression pattern of Xylem cells in TN1; **(D)** The expression pattern of Xylem cells in YHY15; **(E)** Gene expression heatmap and GO enrichment analysis for all cluster genes of Xylem cells; **(F–K)** Representative graphs showing the profiles of the selected DEGs expression and trend- **(F)** *LOC_Os01g47070* (*CHIT3*); **(G)** *LOC_Os02g39330* (*Cht6*); **(H)** *LOC_Os04g562730* (*UEL-2*); **(I)** *LOC_Os05g29990* (*UXS2*); **(J)** *LOC_Os02g29530* (*GAUT8*); **(K)** *LOC_Os02g51130* (*GAUT9*). [One single cell was represented as one point. The entire X-axis was defined as "Pseudotime," entire Y-axis was defined as "Relative expression"].

in genes associated with GO terms, including "transport," "localization," "response to stress," etc. Cluster 3 was enriched with genes associated with GO terms, such as "catalytic activity," "secondary metabolic process," "biosynthetic process," and "response to stress" (Figure 7E). However, enrichment of KEGG pathways for the three clusters showed that cluster 1 was mainly enriched in pathways associated with "glycolysis/gluconeogenesis," cluster 2 was enriched primarily in pathways such as "phenylalanine, tyrosine, and tryptophan biosynthesis," including "amino sugar and nucleotide sugar metabolism," especially chitin related genes, such as *LOC_Os01g47070* (*CHIT3*), *LOC_Os02g39330* (*Cht6*), *LOC_Os04g52730* (*UEL-2*), *LOC_Os05g29990* (*UXS2*), and so on. In addition, some pectin-related genes (such as *LOC_Os02g29530* (*GAUT8*), *LOC_Os02g51130* (*GAUT9*), etc.) showed significant changes (Figures 7F–K). The major KEGG pathways enriched in cluster 3 are "phenylpropanoid biosynthesis," "phenylalanine metabolism," and "phenylalanine, tyrosine, and tryptophan biosynthesis."

Discussion

BPH is one of the most damaging rice pests, causing substantial economic losses. Breeding BPH-resistant rice varieties has been a successful strategy, but BPH can eventually co-evolve and adapt to the resistance mechanisms of rice plants. BPH has a stylet bundle mouthpart that can pierce and suck the phloem sap of rice. However, when feeding on resistant rice varieties, BPH may fail to reach the phloem and stop feeding due to the presence of repellent substances in any cell type along the way. Therefore, analyzing the BPH-feeding stimulated cell expression patterns of different rice plant tissues will help identify the cells that mediate rice resistance to BPH and reveal the underlying molecular mechanisms. Through enabling transcriptomic analysis at single-cell resolution, the application of scRNA-seq has significantly revolutionized the study of cell and molecular biology. Moreover, it has dramatically enhanced our ability to characterize cell states and gene expression responses to BPH feeding. Here, we first

constructed a single-cell atlas of rice leaf sheath response to BPH infestation.

Previous studies have used scRNA-seq technology to investigate tissue and organ development and differentiation in rice, thus, identifying marker genes that served as important references for our research (Xu et al., 2021b; Zhang et al., 2021a; Zong et al., 2022). However, reports on how different cell types respond–either by producing resistance chemicals or activating other molecular processes –to BPH feeding are lacking. Therefore, we selected 48 h post-infestation time for this study based on previous results that show significant changes in gene expression occurring between 24–48 hours of BPH infestation of rice leaves (Liu Y. et al., 2021; Xu et al., 2021a; Xue et al., 2023).

Here, we found that mainly mestome sheath cells, guard cells, mesophyll cells, xylem cells, bulliform cells, and phloem cells showed differential gene expression in resistant (YHY15) and susceptible (TN1) rice varieties after BPH infestation (Figure 4). This suggests that the factors imparting resistance to BPH may originate from multiple sources; different cells may contribute to insect resistance. Thus, the combined effects of numerous resistance factors may confer insect-resistance properties on plants. Previous studies using electrical penetration graphs and honeydew clocks have shown that rice resistance to BPH is determined by differences in sustained phloem ingestion, not by phloem location (Ghaffar et al., 2011). However, in the susceptible TN1 variety, BPH ingests phloem sap continuously without interruption (Ghaffar et al., 2011). Our results further support that rice resistance to BPH does not arise from a single resistance factor in the phloem but from a combination of resistance factors present in multiple locations in the rice plant.

Here, we found that the cell numbers were higher for mesophyll, procambium, and epidermal cells, with a significant difference in the proportion of mesophyll cells (cluster 4 in Figure 1, Supplementary Table 4) and procambium cells (cluster 2 in Figure 1, Supplementary Table 4). In contrast, the proportion of epidermal cells was less different in TN1 and YHY15 rice varieties (clusters 5, 7, and 8 in Figure 1, Supplementary Table 4). In addition, although the proportion of guard, mestome sheath, and bulliform cells differed approximately by 1% between TN1 and YHY15 rice varieties, the number of these cell types was relatively small. Moreover, procambium cells are the precursors of differentiated mature cells. Further, BPH feeding may mainly involve xylem and phloem sap ingestion (Sōgawa, 1982; Seo et al., 2009). Therefore, we focused on mesophyll, xylem, and phloem cells in this study.

Basal resistance is present in both susceptible and resistant rice varieties. The release of green leaf volatiles, which can prevent BPH infestation, is promoted by BPH feeding (Qi et al., 2011). Additionally, MAPKs, ethylene, and salicylic acid (SA) related signaling pathways were also activated by BPH feeding (Du et al., 2009; Hu et al., 2011; Lu et al., 2011). Here, the DEGs of mesophyll cells in TN1 and YHY15 varieties were mainly related to "phenylalanine, tyrosine, and tryptophan biosynthesis," "MAPK signaling pathway," and "phenylalanine metabolism." PALs is a crucial enzyme that mediates the resistance to BPH by regulating the biosynthesis and accumulation of SA and lignin (He et al., 2020). We found that the downstream genes of the PAL pathway (*CYP73A* and *4CL*), which may mainly induce the synthesis of vanillin and other compounds, were significantly differentially expressed in the two varieties. Vanillin-containing plants have vigorous insecticidal and insect-repellent activities (Kim et al., 2012; Songkro et al., 2012; Kletskova et al., 2017). MAPK signaling pathway is an essential part of the ethylene signaling transduction, which also plays a crucial role in plant defense response to insects (Hu et al., 2011; Hettenhausen et al., 2015; Zhou et al., 2019). The copper-transporting ATPase RAN1 is essential for the biogenesis of ethylene receptors (Binder et al., 2010). F-box proteins EBF1/EBF2 can form SCF complex to degrade EIN3 protein and regulate the expression level of downstream gene *ChiB* which is involved in the rice defense response to BPH (Zhu and Guo, 2008).

In phloem cells, the functions associated with DEGs in the two varieties mainly include cell wall extension, energy production, etc. However, cells of the susceptible variety TN1 were mainly concentrated in cluster 1, primarily associated with cell wall extension function. While clusters 2 and 3 had more cells of the BPH-resistant YHY15 variety, whose function was mainly related to "response to biotic stimulus" (Figure 6). Clusters 2 and 3 were also enriched in "phenylpropanoid biosynthesis pathway genes" such as *LOC_Os02g41670* (*PAL*), *LOC_Os05g35290* (*PAL*), *LOC_Os08g34790* (*4CL5*), *LOC_Os02g08100* (*4CL3*), *LOC_Os09g04050* (*CCR1*), and *LOC_Os01g73200* (*PRDX6*); these genes may promote lignin biosynthesis.

In xylem cells, we found that although DEGs were mainly enriched with genes significantly associated with stress response, their mainly enriched KEGG pathways were practically different, especially cluster 2 (Figure 7), which contained multiple genes related to chitin and pectin metabolism. In plants, chitin oligosaccharides induce various defense responses across multiple plant cells (Kaku et al., 2006). Pectin is a critical component of the cell wall. Therefore, pectin metabolism may be crucial in cell wall integrity and mediate plant defense responses (Wang et al., 2023).

In summary, the differences in immune responses stimulated by BPH infestation–such as MAPK signaling pathway and lignin biosynthesis for preventing callose and cell wall degradations that restrict BPH feeding and disrupt BPH digestion–are caused by the existing differences in TN1 and YHY15 varieties. Compared to the susceptible rice variety, the amplified and accelerated responses of the resistant rice variety may protect the plant from further BPH attack, allowing them to survive. The results of scRNA-seq suggest that multiple resistive factors may work together to make rice plants resistant to BPH, and different cell types may have other molecular mechanisms underlying BPH resistance.

In this study, we successfully—1) mapped a single cell transcriptome atlas of rice leaf sheath affected by BPH infestation; 2) observed the relationship of differentiation among the cell clusters; and 3) identified multiple cell types that may be involved in BPH-defense response mounted by rice. However, further experimental evidence is needed to elucidate the role of multiple cells and genes in BPH resistance. Nevertheless, our investigation provides a basis for mining insect-resistance genes and deciphering the molecular mechanism underlying insect-resistance and importantly guides insect-resistant plant molecular breeding.

Data availability statement

The raw sequence data reported in this paper have been deposited in the Genome Sequence Archive in National Genomics Data Center (https://ngdc.cncb.ac.cn/), China National Center for Bioinformation/Beijing Institute of Genomics, Chinese Academy of Sciences, under project number: PRJCA014345, accession number CRA009555 that are publicly accessible at https://ngdc.cncb.ac.cn/gsa.

Author contributions

WZ, DX, LZ, and AY conceived and designed the experiments. WZ performed most of the experiments. CL, JC, and YW analyzed the data, authored or reviewed article drafts, and approved the final draft. MS analyzed the data. SL and BW provided help with the Q16 RNA *in situ* hybridization experiments. SS, KL, and HX prepared figures and/or tables. PL and KL helped to collect the samples. Finally, GY and ZC helped to revise the manuscript. All authors contributed to the article and approved the submitted version.

Funding

This work was supported by the National Key Research and Development Program of China (No.2021YFD1401100) and the National Natural Science Foundation of China (No.31501654).

Acknowledgments

We are grateful to Dr. Minshan Sun and Henan Assist Research Biotechnology Co., Ltd. (Zhengzhou, China) for assisting in bioinformatics analysis. And we would like to thank TopEdit for the English language editing of this manuscript. We show our appreciation to Guangzhou Gene Denovo Biotechnology Co., Ltd. for support with single-cell sequencing.

Conflict of interest

Author MS is employed by Henan Assist Research Biotechnology Co., Ltd. The remaining authors declare that the research was conducted in the absence of any commercial or financial relationships that could be construed as a potential conflict of interest.

Publisher's note

Supplementary material

The Supplementary Material for this article can be found online at: https://www.frontiersin.org/articles/10.3389/fpls.2023.1200014/full#supplementary-material

References

Akanksha, S., Lakshmi, V. J., Singh, A. K., Deepthi, Y., and Ram, T. (2019). Genetics of novel brown planthopper *Nilaparvata lugens* (Stål) resistance genes in derived introgression lines from the interspecific cross *O. sativa* var. swarna ×. *O. nivara. J. Genet.* 98, 113. doi: 10.1007/s12041-019-1158-2

Aran, D., Looney, A. P., Liu, L., Wu, E., Fong, V., Hsu, A., et al. (2019). Reference-based analysis of lung single-cell sequencing reveals a transitional profibrotic macrophage. *Nat. Immunol.* 20, 163–172. doi: 10.1038/s41590-018-0276-y

Athwal, D. S., Pathak, M. D., Bacalangco, E. H., and Pura, C. D. (1971). Genetics of resistance to brown planthoppers and green leafhoppers *in oryza sativa* l. *Crop Sci.* 11, 47–750. doi: 10.2135/cropsci1971.0011183X001100050043x

Binder, B. M., Rodríguez, F. I., and Bleecker, A. B. (2010). The copper transporter RAN1 is essential for biogenesis of ethylene receptors in *Arabidopsis. J. Biol. Chem.* 285, 37263–37270. doi: 10.1074/jbc.M110.170027

Boyle, E. I., Weng, S., Gollub, J., Jin, H., Botstein, D., Cherry, J. M., et al. (2004). GO:: TermFinder–open source software for accessing gene ontology information and finding significantly enriched gene ontology terms associated with a list of genes. *Bioinformatics* 20, 3710–3715. doi: 10.1093/bioinformatics/bth456

Brennecke, P., Anders, S., Kim, J. K., Kołodziejczyk, A. A., Zhang, X., Proserpio, V., et al. (2013). Accounting for technical noise in single-cell RNA-seq experiments. *Nat. Methods* 10, 1093–1095. doi: 10.1038/nmeth.2645

Butler, A., Hoffman, P., Smibert, P., Papalexi, E., and Satija, R. (2018). Integrating single-cell transcriptomic data across different conditions, technologies, and species. *Nat. Biotechnol.* 36, 411–420. doi: 10.1038/nbt.4096

Cabauatan, P. Q., Cabunagan, R. C., and Choi, I. R. (2009). *Rice viruses transmitted by the brown planthopper Nilaparvata lugens stål* (International Rice Research Institute: Los Baños, Philippines: Planthoppers: new threats to the sustainability to of intensive rice production systems in Asia), 357–368.

Camp, J. G., Sekine, K., Gerber, T., Loeffler-Wirth, H., Binder, H., Gac, M., et al. (2017). Multilineage communication regulates human liver bud development from pluripotency. *Nature* 546, 533–538. doi: 10.1038/nature22796

Chung, N. C., and Storey, J. D. (2015). Statistical significance of variables driving systematic variation in high-dimensional data. *Bioinformatics* 31, 545–554. doi: 10.1093/bioinformatics/btu674

Du, B., Zhang, W., Liu, B., Hu, J., Wei, Z., Shi, Z., et al. (2009). Identification and characterization of *Bph14*, a gene conferring resistance to brown planthopper in rice. *Proc. Natl. Acad. Sci. U.S.A.* 106, 22163–22168. doi: 10.1073/pnas.0912139106

Ghaffar, M. B., Pritchard, J., and Ford-Lloyd, B. (2011). Brown planthopper (*N. lugens* stal) feeding behaviour on rice germplasm as an indicator of resistance. *PloS One* 6, e22137. doi: 10.1371/journal.pone.0022137

Hanzelmann, S., Castelo, R., and Guinney, J. (2013). GSVA: gene set variation analysis for microarray and RNA-seq data. *BMC Bioinf.* 14, 7. doi: 10.1186/1471-2105-14-7

He, J., Liu, Y., Yuan, D., Duan, M., Liu, Y., Shen, Z., et al. (2020). An R2R3 MYB transcription factor confers brown planthopper resistance by regulating the phenylalanine ammonia-lyase pathway in rice. *Proc. Natl. Acad. Sci.* 117, 271–277. doi: 10.1073/pnas.1902771116

Hettenhausen, C., Schuman, M. C., and Wu, J. (2015). MAPK signaling: a key element in plant defense response to insects. *Insect Sci.* 22, 157–164. doi: 10.1111/1744-7917.12128

Hu, J., Zhou, J., Peng, X., Xu, H., Liu, C., Du, B., et al. (2011). The *Bphi008a* gene interacts with the ethylene pathway and transcriptionally regulates *MAPK* genes in the response of rice to brown planthopper feeding. *Plant Physiol.* 156, 856–872. doi: 10.1104/pp.111.174334

Islam, S., Zeisel, A., Joost, S., La Manno, G., Zajac, P., Kasper, M., et al. (2014). Quantitative single-cell RNA-seq with unique molecular identifiers. *Nat. Methods* 11, 163–166. doi: 10.1038/nmeth.2772

Jabnoune, M., Secco, D., Lecampion, C., Robaglia, C., Shu, Q. Y., and Poirier, Y. (2015). An efficient procedure for protoplast isolation from mesophyll cells and nuclear fractionation in rice. *BIO-PROTOCOL* 5, e1412. doi: 10.21769/BioProtoc.1412

Jin, J., Tian, F., Yang, D. C., Meng, Y. Q., Kong, L., Luo, J., et al. (2017). PlantTFDB 4.0: toward a central hub for transcription factors and regulatory interactions in plants. *Nucleic Acids Res.* 45, D1040–D1045. doi: 10.1093/nar/gkw982

Kaku, H., Nishizawa, Y., Ishii-Minami, N., Akimoto-Tomiyama, C., Dohmae, N., Takio, K., et al. (2006). Plant cells recognize chitin fragments for defense signaling through a plasma membrane receptor. *Proc. Natl. Acad. Sci.* 103, 11086–11091. doi: 10.1073/pnas.0508882103

Kanehisa, M., Araki, M., Goto, S., Hattori, M., Hirakawa, M., Itoh, M., et al. (2008). KEGG for linking genomes to life and the environment. *Nucleic Acids Res.* 36, D480–D484. doi: 10.1093/nar/gkm882

Kanehisa, M., and Goto, S. (2000). KEGG: kyoto encyclopedia of genes and genomes. *Nucleic Acids Res.* 28, 27–30. doi: 10.1093/nar/28.1.27

Kang, M., Choi, Y., Kim, H., and Kim, S. G. (2022). Single-cell RNA-sequencing of *Nicotiana attenuata* corolla cells reveals the biosynthetic pathway of a floral scent. *New Phytol.* 234, 527–544. doi: 10.1111/nph.17992

Kawahara, Y., de la Bastide, M., Hamilton, J. P., Kanamori, H., Mccombie, W. R., Ouyang, S., et al. (2013). Improvement of the *Oryza sativa* nipponbare reference genome using next generation sequence and optical map data. *Rice (N Y)* 6, 4. doi: 10.1186/1939-8433-6-4

Kim, S. I., Yoon, J. S., Baeck, S. J., Lee, S. H., Ahn, Y. J., and Kwon, H. W. (2012). Toxicity and synergic repellency of plant essential oil mixtures with vanillin against *Aedes aegypti* (Diptera: culicidae). *J. Med. Entomol* 49, 876–885. doi: 10.1603/me11127

Kletskova, A. V., Potkin, V. I., Dikusar, E. A., and Zolotar, R. M. (2017). New data on vanillin-based isothiazolic insecticide synergists. *Nat. Prod Commun.* 12, 105–106. doi: 10.1177/1934578X1701200130

Korsunsky, I., Millard, N., Fan, J., Slowikowski, K., Zhang, F., Wei, K., et al. (2019). Fast, sensitive and accurate integration of single-cell data with harmony. *Nat. Methods* 16, 1289–1296. doi: 10.1038/s41592-019-0619-0

Laksminarayana, A., and Khush, G. S. (1977). New genes for resistance to the brown planthopper in rice. *Crop Sci.* 17, 96–100. doi: 10.2135/cropsci1977.0011183X001700010028x

Li, Z., Xue, Y., Zhou, H., Li, Y., Usman, B., Jiao, X., et al. (2019). High-resolution mapping and breeding application of a novel brown planthopper resistance gene derived from wild rice (*Oryza. rufipogon* griff). *Rice (N Y)* 12, 41. doi: 10.1186/s12284-019-0289-7

Liberzon, A., Birger, C., Thorvaldsdottir, H., Ghandi, M., Mesirov, J. P., and Tamayo, P. (2015). The molecular signatures database (MSigDB) hallmark gene set collection. *Cell Syst.* 1, 417–425. doi: 10.1016/j.cels.2015.12.004

Liu, Q., Liang, Z., Feng, D., Jiang, S., Wang, Y., Du, Z., et al. (2021). Transcriptional landscape of rice roots at the single-cell resolution. *Mol. Plant* 14, 384–394. doi: 10.1016/j.molp.2020.12.014

Liu, Y., Wang, W., Li, Y., Liu, F., Han, W., and Li, J. (2021). Transcriptomic and proteomic responses to brown plant hopper (*Nilaparvata lugens*) in cultivated and bt-transgenic rice (*Oryza sativa*) and wild rice (*O. rufipogon*). *J. Proteomics* 232, 104051. doi: 10.1016/j.jprot.2020.104051

Lopez-Anido, C. B., Vaten, A., Smoot, N. K., Sharma, N., Guo, V., Gong, Y., et al. (2021). Single-cell resolution of lineage trajectories in the *Arabidopsis* stomatal lineage and developing leaf. *Dev. Cell* 56, 1043–1055 e1044. doi: 10.1016/j.devcel.2021.03.014

Lu, J., Ju, H., Zhou, G., Zhu, C., Erb, M., Wang, X., et al. (2011). An EAR-motif-containing ERF transcription factor affects herbivore-induced signaling, defense and resistance in rice. *Plant J.* 68, 583–596. doi: 10.1111/j.1365-313X.2011.04709.x

Luecken, M. D., and Theis, F. J. (2019). Current best practices in single-cell RNA-seq analysis: a tutorial. *Mol. Syst. Biol.* 15, e8746. doi: 10.15252/msb.20188746

Lun, A. T. L., Riesenfeld, S., Andrews, T., Dao, T. P., Gomes, T.Participants in the 1st Human Cell Atlas, J, et al. (2019). EmptyDrops: distinguishing cells from empty droplets in droplet-based single-cell RNA sequencing data. *Genome Biol.* 20, 63. doi: 10.1186/s13059-019-1662-y

Macosko, E. Z., Basu, A., Satija, R., Nemesh, J., Shekhar, K., Goldman, M., et al. (2015). Highly parallel genome-wide expression profiling of individual cells using nanoliter droplets. *Cell* 161, 1202–1214. doi: 10.1016/j.cell.2015.05.002

McGinnis, C. S., Murrow, L. M., and Gartner, Z. J. (2019). DoubletFinder: doublet detection in single-cell RNA sequencing data using artificial nearest neighbors. *Cell Syst.* 8, 329–337 e324. doi: 10.1016/j.cels.2019.03.003

Neftel, C., Laffy, J., Filbin, M. G., Hara, T., Shore, M. E., Rahme, G. J., et al. (2019). An integrative model of cellular states, plasticity, and genetics for glioblastoma. *Cell* 178, 835–849 e821. doi: 10.1016/j.cell.2019.06.024

Nguyen, C. D., Verdeprado, H., Zita, D., Sanada-Morimura, S., Matsumura, M., Virk, P. S., et al. (2019). The development and characterization of near-isogenic and pyramided lines carrying resistance genes to brown planthopper with the genetic background of japonica rice (*Oryza sativa* l.). *Plants (Basel)* 8, 498. doi: 10.3390/plants8110498

Qi, J., Zhou, G., Yang, L., Erb, M., Lu, Y., Sun, X., et al. (2011). The chloroplast-localized phospholipases d alpha4 and alpha5 regulate herbivore-induced direct and indirect defenses in rice. *Plant Physiol.* 157, 1987–1999. doi: 10.1104/pp.111.183749

Rotta, R., and Noack, A. (2011). Multilevel local search algorithms for modularity clustering. *ACM J. Exp. Algorithmics* 16. doi: 10.1145/1963190.1970376

Senthil-Nathan, S., Choi, M. Y., Paik, C. H., Seo, H. Y., and Kalaivani, K. (2009). Toxicity and physiological effects of neem pesticides applied to rice on the *Nilaparvata lugens* stal, the brown planthopper. *Ecotoxicol Environ. Saf.* 72, 1707–1713. doi: 10.1016/j.ecoenv.2009.04.024

Seo, B. Y., Kwon, Y.-H., Jung, J. K., and Kim, G.-H. (2009). Electrical penetration graphic waveforms in relation to the actual positions of the stylet tips of *Nilaparvata lugens* in rice tissue. *J. Asia-Pacific Entomology* 12, 89–95. doi: 10.1016/j.aspen.2009.02.002

Sezer, M., and Butlin, R. K. (1998). The genetic basis of host plant adaptation in the brown planthopper (*Nilaparvata lugens*). *Heredity* 80, 499–508. doi: 10.1046/j.1365-2540.1998.00316.x

Sōgawa, K. (1982). The rice brown planthopper: feeding physiology and host plant interactions. *Annu. Rev. Entomology* 27, 49–73. doi: 10.1146/annurev.en.27.010182.000405

Song, Q., Ando, A., Jiang, N., Ikeda, Y., and Chen, Z. J. (2020). Single-cell RNA-seq analysis reveals ploidy-dependent and cell-specific transcriptome changes in *Arabidopsis* female gametophytes. *Genome Biol.* 21, 178. doi: 10.1186/s13059-020-02094-0

Songkro, S., Jenboonlap, M., Boonprasertpon, M., Maneenuan, D., Bouking, K., and Kaewnopparat, N. (2012). Effects of glucam p-20, vanillin, and fixolide on mosquito repellency of citronella oil lotions. *J. Med. Entomol* 49, 672–677. doi: 10.1603/me11141

Spiller, N. J. (1990). An ultrastructural study of the stylet pathway of the brown planthopper *Nilaparvata lugens*. *Entomologia Experimentalis Applicata* 54, 191–193. doi: 10.1111/j.1570-7458.1990.tb01329.x

Stuart, T., Butler, A., Hoffman, P., Hafemeister, C., Papalexi, E., Mauck, W. M.3rd, et al. (2019). Comprehensive integration of single-cell data. *Cell* 177, 1888–1902 e1821. doi: 10.1016/j.cell.2019.05.031

Umeda, M., Umeda-Hara, C., Yamaguchi, M., Hashimoto, J., and Uchimiya, H. (1999). Differential expression of genes for cyclin-dependent protein kinases in rice plants. *Plant Physiol.* 119, 31–40. doi: 10.1104/pp.119.1.31

Wang, Y., Huan, Q., Li, K., and Qian, W. (2021). Single-cell transcriptome atlas of the leaf and root of rice seedlings. *J. Genet. Genomics* 48, 881–898. doi: 10.1016/j.jgg.2021.06.001

Wang, D., Kanyuka, K., and Papp-Rupar, M. (2023). Pectin: a critical component in cell-wall-mediated immunity. *Trends Plant Sci.* 28, 10–13. doi: 10.1016/j.tplants.2022.09.003

Xie, J., Li, M., Zeng, J., Li, X., and Zhang, D. (2022). Single-cell RNA sequencing profiles of stem-differentiating xylem in poplar. *Plant Biotechnol. J.* 20, 417–419. doi: 10.1111/pbi.13763

Xu, X., Crow, M., Rice, B. R., Li, F., Harris, B., Liu, L., et al. (2021b). Single-cell RNA sequencing of developing maize ears facilitates functional analysis and trait candidate gene discovery. *Dev. Cell* 56, 557–568 e556. doi: 10.1016/j.devcel.2020.12.015

Xu, N., Wei, S. F., and Xu, H. J. (2021a). Transcriptome analysis of the regulatory mechanism of FoxO on wing dimorphism in the brown planthopper, *Nilaparvata lugens* (Hemiptera: delphacidae). *Insects* 12, 413. doi: 10.3390/insects12050413

Xue, Y., Muhammad, S., Yang, J., Wang, X., Zhao, N., Qin, B., et al. (2023). Comparative transcriptome-wide identification and differential expression of genes and lncRNAs in rice near-isogenic line (KW-*Bph36*-NIL) in response to BPH feeding. *Front. Plant Sci.* 13. doi: 10.3389/fpls.2022.1095602

Xue, J., Zhou, X., Zhang, C. X., Yu, L. L., Fan, H. W., Wang, Z., et al. (2014). Genomes of the rice pest brown planthopper and its endosymbionts reveal complex complementary contributions for host adaptation. *Genome Biol.* 15, 521. doi: 10.1186/s13059-014-0521-0

Zhang, T. Q., Chen, Y., Liu, Y., Lin, W. H., and Wang, J. W. (2021a). Single-cell transcriptome atlas and chromatin accessibility landscape reveal differentiation trajectories in the rice root. *Nat. Commun.* 12, 2053. doi: 10.1038/s41467-021-22352-4

Zhang, T. Q., Chen, Y., and Wang, J. W. (2021b). A single-cell analysis of the *Arabidopsis* vegetative shoot apex. *Dev. Cell* 56, 1056–1074 e1058. doi: 10.1016/j.devcel.2021.02.021

Zhang, A. W., O'flanagan, C., Chavez, E. A., Lim, J. L. P., Ceglia, N., Mcpherson, A., et al. (2019). Probabilistic cell-type assignment of single-cell RNA-seq for tumor microenvironment profiling. *Nat. Methods* 16, 1007–1015. doi: 10.1038/s41592-019-0529-1

Zheng, X., Zhu, L., and He, G. (2021). Genetic and molecular understanding of host rice resistance and *Nilaparvata lugens* adaptation. *Curr. Opin. Insect Sci.* 45, 14–20. doi: 10.1016/j.cois.2020.11.005

Zhou, S., Chen, M., Zhang, Y., Gao, Q., Noman, A., Wang, Q., et al. (2019). *OsMKK3*, a stress-responsive protein kinase, positively regulates rice resistance to Nilaparvata lugens *via* phytohormone dynamics. *Int. J. Mol. Sci.* 20, 3023. doi: 10.3390/ijms20123023

Zhu, Z., and Guo, H. (2008). Genetic basis of ethylene perception and signal transduction in *Arabidopsis*. *J. Integr. Plant Biol.* 50, 808–815. doi: 10.1111/j.1744-7909.2008.00710.x

Zong, Y., Chen, Z., Innes, J. B., Chen, C., Wang, Z., and Wang, H. (2007). Fire and flood management of coastal swamp enabled first rice paddy cultivation in east China. *Nature* 449, 459–462. doi: 10.1038/nature06135

Zong, J., Wang, L., Zhu, L., Bian, L., Zhang, B., Chen, X., et al. (2022). A rice single cell transcriptomic atlas defines the developmental trajectories of rice floret and inflorescence meristems. *New Phytol.* 234, 494–512. doi: 10.1111/nph.18008

frontiers | Frontiers in Plant Science

TYPE Review
PUBLISHED 19 June 2023
DOI 10.3389/fpls.2023.1176048

OPEN ACCESS

EDITED BY
Shengli Jing,
Xinyang Normal University, China

REVIEWED BY
Zhenying Shi,
Center for Excellence in Molecular Plant Sciences (CAS), China
Yan Zhao,
Hunan Hybrid Rice Research Center, China

*CORRESPONDENCE
Wei Hua
huawei@oilcrops.cn

†These authors have contributed equally to this work

RECEIVED 28 February 2023
ACCEPTED 31 March 2023
PUBLISHED 19 June 2023

CITATION
Wang H, Shi S and Hua W (2023) Advances of herbivore-secreted elicitors and effectors in plant-insect interactions. *Front. Plant Sci.* 14:1176048. doi: 10.3389/fpls.2023.1176048

Advances of herbivore-secreted elicitors and effectors in plant-insect interactions

Huiying Wang[1†], Shaojie Shi[2,3†] and Wei Hua[1,2*]

[1]Key Laboratory of Biology and Genetic Improvement of Oil Crops, Ministry of Agriculture and Rural Affairs, Oil Crops Research Institute of the Chinese Academy of Agricultural Sciences, Wuhan, China, [2]Hubei Hongshan Laboratory, Wuhan, China, [3]Hubei Key Laboratory of Food Crop Germplasm and Genetic Improvement, Key Laboratory of Crop Molecular Breeding, Ministry of Agriculture and Rural Affairs, Institute of Food Crops, Hubei Academy of Agricultural Sciences, Wuhan, China

Diverse molecular processes regulate the interactions between insect herbivores and their host plants. When plants are exposed to insects, elicitors induce plant defenses, and complex physiological and biochemical processes are triggered, such as the activation of the jasmonic acid (JA) and salicylic acid (SA) pathways, Ca^{2+} flux, reactive oxygen species (ROS) burst, mitogen-activated protein kinase (MAPK) activation, and other responses. For better adaptation, insects secrete a large number of effectors to interfere with plant defenses on multiple levels. In plants, resistance (R) proteins have evolved to recognize effectors and trigger stronger defense responses. However, only a few effectors recognized by R proteins have been identified until now. Multi-omics approaches for high-throughput elicitor/effector identification and functional characterization have been developed. In this review, we mainly highlight the recent advances in the identification of the elicitors and effectors secreted by insects and their target proteins in plants and discuss their underlying molecular mechanisms, which will provide new inspiration for controlling these insect pests.

KEYWORDS

elicitors, effectors, defense responses, multi-omics approach, plant-insect interactions

Introduction

Plants are constantly being attacked by various insects. Nearly half a million insect species live on plants (Wu and Baldwin, 2010). The vast majority of herbivorous insects feed on plants from a single taxonomic family or a few closely related plant species specifically, while only 10% of them establish intimacy with multiple plant species (Schoonhoven et al., 2005). In addition to the direct damage caused by feeding, insects can also injure plants indirectly by transmitting viral, bacterial, and fungal pathogens. The main strategy for crop protection against insects over the past several decades was the application of chemical insecticides. However, due to the emergence of insect resistance to pesticides and the negative effect on the environment, the use of such compounds has

declined in recent years (Du et al., 2020). Scientists have begun to unravel the molecular mechanisms underpinning the interactions between plants and insects in order to find better ways to control these pests.

Over the years, evidence has been accumulated during the long-term interaction and evolution of plants and insects, and both host plants and insect herbivores have obtained diverse sophisticated mechanisms to adapt to each other. In general, the perception of insect attack is the first step of plant defenses. Insect elicitors are the biologically active molecules from insects' saliva or gut regurgitant; they are recognized by plants and subsequently induce plant defenses (Chen and Mao, 2020; Snoeck et al., 2022). These elicitors are also called herbivore-associated molecular patterns (HAMPs) (Snoeck et al., 2022). The elicitor-induced defenses include depolarization of the plasma trans-membrane potential, activation of JA and SA pathways, ROS burst, callose deposition, Ca^{2+} influx, MAPK activation, etc. (Erb and Reymond, 2019; Ye et al., 2019; Li et al., 2019a). For successful infestation, insect herbivores secret salivary molecules into plant cells to weaken their defense responses; these active molecules are called effectors (Mutti et al., 2008; Bos et al., 2010; Hogenhout and Bos, 2011; Naessens et al., 2015; Rodriguez et al., 2017). Effectors that suppress the plant's responses can be recognized by their corresponding resistance proteins, inducing a second layer of defense, the effector-triggered immunity (ETI) (Jones and Dangl, 2006; Takken and Tameling, 2009). Notably, the second layer of defense response is much more fierce than the first layer. In summary, the active molecules from insect secretion have a significant impact on plant immunity. The molecules that can trigger plant defense responses are defined as elicitors, while those that weaken plant defenses are called effectors (Chen and Mao, 2020). In this review, we mainly discuss the recent advances in research on elicitors and effectors secreted by insects and their roles in the interactions between insects and their host plants. Dissecting the plant host factors and pathways targeted by these active insect molecules will facilitate the characterization of the molecular mechanisms of plant-insect interactions.

Herbivore feeding behaviors

To obtain nutrients from the hosts, insects employ diverse feeding strategies upon landing. Based on the different mouthparts and feeding habits, herbivorous insects can be divided into two groups: chewing and piercing-sucking insects (Schoonhoven et al., 1998; Walling, 2000). The insect species that cause damage with mouthparts evolved for chewing, snipping, or tearing belong to chewing insects, like leaf-eating beetles, caterpillars, or cotton bollworms. Chewing insects have a chewing type of mouth, which consists of the labrum, mandibles, first maxillae, second maxillae, hypopharynx, and epipharynx. The rectangular flap-like labrum is in the middle. The mandibles are paired and bear toothed edges at their inner surfaces; they masticate food using two sets of muscles transversely. The first maxillae and second maxillae are paired. The first maxillae are responsible for holding food and the second maxillae are responsible for pushing masticated food into the mouth. The hypopharynx has a single median tongue-like process, and the opening of the salivary duct lies under the hypopharynx. The epipharynx with taste buds is a single small membranous piece at the base of the labrum (Kahl, 1982; Felton et al., 1999; Stotz et al., 1999). Oral secretion (OS, consisting of regurgitant and saliva) of chewing insects contains active molecules that have a big impact on plant defense responses that are distinguishable from general mechanical damage (Hogenhout and Bos, 2011; Chen and Mao, 2020).

Piercing-sucking herbivorous insects, such as aphids, whiteflies, and planthoppers feed on plants through specially adapted mouthparts known as stylets, which they use to puncture the plant surface to access the phloem sap. The mouthparts of piercing-sucking insects are composed of the labrum, the labium, and the stylet. Among them, the stylet is used for piercing and sucking phloem sap from plants (Sogawa, 1982; Backus, 1988). The feeding strategies of piercing-sucking insects are mainly divided into three major phases, labial exploration, stylet penetration, and phloem-sap sucking (Spiller, 1990; Hao et al., 2008; Cheng et al., 2013b; Will et al., 2013). During their initial encounter with their host plants, insects walk rapidly and dab repeatedly on the plant's surface to find a suitable feeding site, which is essential for the survival of the insects (Sogawa, 1982; Backus, 1988; Walling, 2008). Rice leaf sheath surface is featured in units and subunit structures, including the silico-phellem block, stomate block, large tubercle block, and vein, which are often covered with tubercle papicles, little papicles, glochids, and tenuous hairs. Recent research has shown that the brown planthopper (*Nilaparvata lugens* Stål, BPH), the most destructive pest of rice, preferentially selects the smooth long-cell block to probe their stylets into the leaf sheaths (Shi et al., 2021). Using an Atomic Force Microscope (AFM), Shi et al. (2021) found that the surface hardness of the long-cell block was much lower than that of the other cells. Sensilla basiconica, arranged symmetrically in two separate areas at the distal segment of the labium, was speculated to have a mechano-receptive function (Sogawa, 1982; Backus, 1988). Thus, we suppose that the labium may guide the stylets to find the suitable feeding site by sensing the mechanical heterogeneity of different structures on the plant surface.

Piercing-sucking insects penetrate plants with their stylet and move the stylet toward the phloem (Will et al., 2013). Along the stylet track, different types of cells are regularly penetrated (Will et al., 2013). Sucrose and pH are suggested to be indicators of phloem penetration (Hewer et al., 2010; Hewer et al., 2011). During the penetration process, piercing-sucking insects secrete both gelling and watery saliva from their salivary glands into the plant cells, and the protein compositions of the two types of saliva were shown to have some overlap (Walling, 2008; Huang et al., 2016). The secreted gelling saliva quickly solidifies and forms a continuous salivary sheath along its stylets for providing mechanical stability and protection (Wang et al., 2008). Some secretary proteins have been proven to be the key factors for forming the salivary sheath (Will and Vilcinskas, 2015; Huang et al., 2016; Huang et al., 2017; Shangguan et al., 2018; Huang et al., 2023). Watery saliva contains many active molecules that are involved in the induction or suppression of defenses against insect attack, i.e., the elicitors and effectors (Kaloshian and Walling, 2016; Chen and Mao, 2020).

Multi-omics approach to identifying elicitors and effectors

Saliva is a complex mixture of biomolecules with potential roles in encounters with plant immune responses (Miles, 1999; Will et al., 2013). Functional approaches such as proteomics and transcriptomics have facilitated the high-throughput identification of elicitors/effectors in regurgitant or saliva from various insect species (Harmel et al., 2008; Bos et al., 2010; Cooper et al., 2011; Nicholson et al., 2012; Ji et al., 2013; Nicholson and Puterka, 2014; Huang et al., 2016; Liu X. et al., 2016; Huang et al., 2018; Rao et al., 2019; Huang et al., 2023). The majority of the reported elicitors or effectors discussed below were identified using multi-omics approaches. Here, we take the salivary proteome and transcriptome of *N. lugens* as examples. Through comparative transcriptome analysis of the salivary glands of TN1 and Mudgo populations, 352 genes were predicted to encode secretory proteins (Ji et al., 2013). Among them, endo-β-1,4-glucanase (NlEG1) and NlSEF1 play important roles in rice-BPH interactions (Ji et al., 2017; Ye et al., 2017). Huang et al. (2016) performed proteomic analyses combined with genomic and transcriptomic analysis and identified 202 secreted salivary proteins in *N. lugens*. RNA interference revealed that salivap-3 is required for forming the salivary sheath, while annexin-like5 and carbonic anhydrase are indispensable for BPH survival (Huang et al., 2016). Recently, 1140 protein-coding genes were predicted in the secretome of *N. lugens* by Rao et al. (2019). Sequence analysis and homology searches revealed the presence of both conserved and rapidly evolving salivary proteins. Furthermore, six *N. lugens* secreted elicitors (Nl12, Nl16, Nl28, Nl32, Nl40, and Nl43) were identified by a series of predictions and functional analysis, as discussed below (Rao et al., 2019). The high-throughput identification of these secreted salivary proteins provides the possibility of understanding some aspects of plant-insect molecular interaction mechanisms and identifying potential targets for pest management.

Insect-associated elicitors

In general, plants can recognize elicitors and produce a complex series of defenses. The first reported elicitor β-glucosidase was isolated from the regurgitant of the white butterfly (*Pieri brassicae*). Leaves treated with β-glucosidase enhanced the emission of volatiles that are highly attractive to the parasitic wasp (Mattiacci et al., 1995). The glucose oxidase (GOX) present in the saliva extracted from Noctuid caterpillars (*Helicoverpa zea*) and European corn borer (*Ostrinia nubilalis*) upregulates the expression of genes related to the JA biosynthesis pathway and the late responding defense, such as *proteinase inhibitor 2* (*Pin2*) in tomato (Tian et al., 2012; Louis et al., 2013). External spraying of phospholipase C (PLC), a salivary protein from fall armyworm (*Spodoptera frugiperda*), activates defense responses in maize and Bermuda grass and reduces caterpillar weight gain (Acevedo et al., 2018).

Except for the elicitors isolated from chewing insects, some elicitors were identified in piercing-sucking insects. Mp10 and Mp42 were two elicitors that were identified using a functional genomics approach in aphids. Aphid fecundity decreased when feeding on plants over-expressing *Mp10* and *Mp42*. In addition, Mp10 specifically induced chlorosis in *N. benthamiana* leaves in a SUPPRESSOR OF G2 ALLELE OF *skp1* (SGT1)-dependent manner (Bos et al., 2010; Rodriguez et al., 2014). Cysteine protease Cathepsin B3 (CathB3) was also recognized as a potential elicitor protein, which suppresses aphid feeding by triggering ROS through interacting with an ENHANCED DISEASE RESISTANCE 1-like (EDR1-like) protein (Guo et al., 2020). The mucin-like salivary protein (NlMLP) is a dual-functional protein both for insects and plants. In BPH, NlMLP is required for the formation of salivary sheath. In plants, NlMLP induces cell death, the expression of defense-related genes, and callose deposition (Shangguan et al., 2018). When BPH feed or oviposit, the small N-terminal subunit of vitellogenins (VgN) induces strong defenses, such as ROS burst and other responses in rice (Zeng et al., 2023). The ectopic expression of six secreted salivary proteins from BPH (Nl12, Nl16, Nl28, Nl32, Nl40, and Nl43) could induce cell death, chlorosis, or a dwarf phenotype, respectively in *N. benthamiana* leaves (Rao et al., 2019). Some salivary proteins from other piercing-sucking insects were also identified as the elicitors, like Tet1, Tet2, disulfide isomerase (TetPDI) from spider mite (*Tetranychus evansi*) (Iida et al., 2019; Cui et al., 2023), and RP309 from Fabricius (*Riptortus pedestris*) (Dong et al., 2022). It is noteworthy that although elicitor-induced plant defenses impair the performance of insects on plants, RNA interference (RNAi) experiments have revealed that elicitors are still essential for the survival of insects (Shangguan et al., 2018; Guo et al., 2020; Cui et al., 2023; Zeng et al., 2023).

In addition to the elicitors coming from insects themselves, some elicitors are generated from the microbes they carry. *Buchnera aphidicola* is the endosymbiont of potato aphids (*Macrosiphum euphorbiae*). Over-expression of *Buchnera GroEL* in Arabidopsis plants induces ROS burst and PTI, which is associated with the BRASSINOSTEROID INSENSITIVE1-ASSOCIATED RECEPTOR KINASE 1 (BAK1), thus reducing the fecundity of the aphid (Chaudhary et al., 2014). A porin-like protein (PLP) from bacteria in oral secretions of *Spodoptera littoralis* larvae induces Ca^{2+} flux *in vitro* and upregulates the calmodulin-like CML42 (Guo et al., 2013).

Some elicitors are relatively conserved in their ability to induce responses across a range of plant species. Both Nl32 in planthopper and MP10 in aphids are chemosensory proteins (CSPs), small water-soluble proteins with an OS-D domain that are conserved among different insects (Pelosi et al., 2005; Bos et al., 2010; Rao et al., 2019). Eleven CSPs (NlCSP-1 to -11) were previously identified in BPH, and six out of the eleven CSPs induced similar effects on *N. benthamiana* to those caused by Nl32 and Mp10 (Bos et al., 2010; Zhou et al., 2015; Rao et al., 2019). Nl12 and TetPDI, deriving from planthopper and spider mite, respectively, are the two members of the conserved disulfide isomerase family in eukaryotic organisms (Rao et al., 2019; Cui et al., 2023). Moreover, PDIs from phylogenetically distinct herbivorous and non-herbivorous arthropods could induce plant immunity in an SGT1/HSP90-dependent way (Cui et al., 2023). GOX was also conserved among caterpillar species (Tian et al., 2012; Louis et al., 2013).

10.3389/fpls.2023.1176048

In Figure 1 and Table 1, we summarize the reported insect-associated elicitors from different species and their respective roles.

Effectors involved in plant-insect interactions

To adapt to their host plants, insects secrete a repertoire of effectors to disturb host plant defense responses (Figure 1 and Table 2). GOX from caterpillar *H. zea* was the first reported insect effector. The nicotine accumulation was suppressed significantly by GOX in tobacco (Musser et al., 2002; Musser et al., 2005). Interestingly, the same GOX was characterized as an elicitor in the 'Insect-associated elicitors' section because it induces plant responses in tomato (Tian et al., 2012; Louis et al., 2013). These results indicate that the same protein can act as the effector or as the elicitor when encountering different host plants. The cotton bollworm (*Helicoverpa armigera*) is a destructive lepidopteran insect widely existing in agriculture. Chen et al. (2019) identified an effector, a venom-like protein termed HARP1, from the OS of *H. armigera*. HARP1 stabilizes JAZ degradation and blocks wound-induced JA signaling transduction by forming a protein complex with JAZ. The weight of *H. armigera* larvae was increased significantly on transgenic plants with high-level *HARP1* (Chen et al., 2019). HAS1 is another effector of *H. armigera*. Plants over-expressing *HAS1* exhibit more susceptibility to insect herbivores accompanied by the suppressed JA pathway due to the interactions between HAS1 and JASMONATE-ZIM-domain repressors MYC3/MYC4 (Chen et al., 2023). These results indicate that interfering with the JA pathway is a common strategy of effectors in chewing insects.

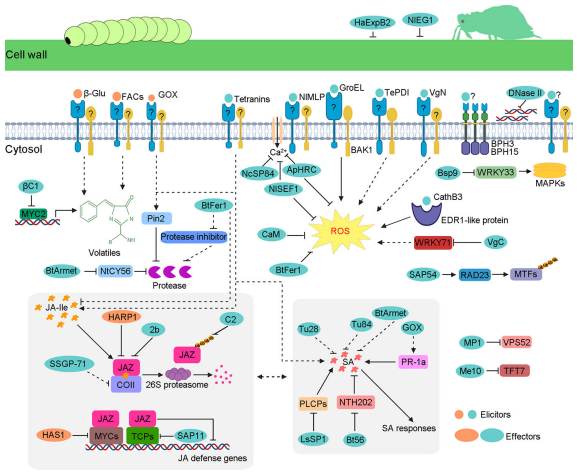

FIGURE 1
Schematic model of insect-secreted elicitors and effectors regulating plant defenses. When insects feed on plants, elicitors induce a complex series of plant defenses, such as ROS burst; upregulation of JA, SA and some volatile; and other unknown responses. However, insects secrete effectors to suppress these defense responses. Some effectors weaken JA pathways, including HARP1, HAS1, 2b, C2, βC1, SAP11, SSGP-71, and BtFer1. Some effectors interfere with SA pathways, such as BtArmet, Bt56, GOX, and LsSP1. The same effector protein can participate in diverse defense pathways. For example, as well as the reduction of the Ca^{2+} influx, ApHRC and NISEF1 also suppress ROS burst. The *B. tabaci* effector BtFer1 not only reduces the accumulation of ROS and JA but also weakens protease inhibitor activity, thus increasing the content of protease to help whitefly feed better. Similar to BtFer1, effector BtArmet interacts with protease inhibitor NtCY56 to block the inhibition of whitefly protease. Mp1 and Me10 target plant proteins VPS52 and TFT7, respectively, which are required for insect resistance. The DNase II targets the extracellular DNA that is released by damaged cells. NIEG1 and HaExPB2 enable the insect's stylet to reach the phloem by degrading celluloses in host plant cell walls.

Like those in chewing insects, effectors in piercing-sucking insects also disturb plant hormone-related defense pathways. Bt56 from the whitefly (*Bemisia tabaci*) increases susceptibility to insects by enhancing the accumulation of SA but not JA. Interaction assays have shown that Bt56 interacts directly with a KNOTTED 1-like homeobox transcription factor NTH202 (Xu et al., 2019). The survival rate and fecundity were significantly lower in insects injected with ds*Bt56* than in those injected with ds*GFP* (Xu et al., 2019). BtArmet, another effector of the *B. tabaci*, increased whitefly performance on tobacco plants by suppressing SA accumulation and binding to the cystatin NtCYS6, a protease inhibitor that prevents insects from continuous ingestion and digestion (Du et al., 2022). BtFer1 is a *B. tabaci* salivary protein with Fe^{2+} binding ability. The results showed that BtFer1 suppressed the JA-mediated signaling pathway, ROS burst, callose deposition, and accumulation of proteinase inhibitors (Su et al., 2019). The small brown planthopper (*Laodelphax striatellus*, SBPH) effector LsSP1 not only binds to sheath protein LsMLP to avoid LsMLP protein being recognized by plants but also interacts with rice papain-like cysteine proteases to inhibit SA biosynthesis and SA-related defenses (Huang et al., 2023).

Moreover, some effectors were reported to target other defense-related pathways in plants. The *L. striatellus* secretes effector protein DNase II to inhibit defense responses by erasing extracellular DNA and reducing hydrogen peroxide (Huang et al., 2019). Interestingly, unlike the VgN, as a reliable elicitor, the C-terminal peptide of vitellogenin (VgC) acts as a novel effector in *L. striatellus*, which attenuates H_2O_2-mediated plant defense by interacting directly with the host transcription factor OsWRKY71 for promoting insect performance (Ji et al., 2021; Zeng et al., 2023). Salivary protein 7 (NlSP7), a salivary protein secreted from the brown planthopper, functions as an effector via mediating tricin metabolism in rice plants (Gong et al., 2022). TFT7, 14-3-3 isoform 7, has been proven to be required for aphid resistance in tomato. *Macrosiphum euphorbiae* saliva-secreted protein Me10 targets the TFT7 as an effective infestation strategy (Chaudhary et al., 2019). Interaction assays have shown that the effector Mp1 from *M. persicae* associates with the host Vacuolar Protein Sorting Associated Protein52 (VPS52), which has a negative impact on insect infestation (Rodriguez et al., 2017). Effector Bsp9 from *B. tabaci* interacts with WRKY33 to interfere with the association between WRKY33 and a central regulator in the MAPK cascade, thus inhibiting plant immunity (Wang et al., 2019). The SSGP-71 (Secreted Salivary Gland Proteins-71) family, which has 426 members, has the greatest representation in the salivary proteome of the Hessian fly. Most SSGP-71 genes encode proteins with a signal peptide and an F box domain, which interacts with an Skp1-like protein (Zhao et al., 2015). The host plant cell wall was the first barrier of defense against

TABLE 1 Insect-associated elicitors.

Name	Origin	Protein characterization	Function	Reference
β-glu	*Pieri brassicae*	β-glucosidase	Release attractive volatiles to parasitic wasps (*Cotesia glomerata*)	Mattiacci et al., 1995
Caeliferins	*Schistocerca americana*	Disulfooxy fatty acids	Induce volatile emissions in corn	Alborn et al., 2007
GOX	*Helicoverpa zea*; European corn borer	Glucose oxidase	Elicit JA pathway and late responding defenses in tomato	Tian et al., 2012; Louis et al., 2013
PLC	*Spodoptera frugiperda*	Phospholipase C	Reduce caterpillar weight gain; Induce defense responses in maize and Bermuda grass	Acevedo et al., 2018
Mp10	*Myzus persicae*	Chemosensory protein	Reduce aphid fecundity in tobacco	Bos et al., 2010
CathB3	*Myzus persicae*	Cysteine protease	Reduce aphid performance; Induce ROS burst in an EDR1-dependent manner in tobacco	Guo et al., 2020
NlMLP	*Nilaparvata lugens*	Mucin-like protein	Salivary sheath formation; Induce plant defense response in rice and tobacco	Shangguan et al., 2018
Nl12	*Nilaparvata lugens*	Disulfide isomerase	Induce cell death, expression of defense-related genes, and callose deposition in tobacco	Rao et al., 2019
Nl16	*Nilaparvata lugens*	Apolipophorin-III protein	Induce cell death, expression of defense-related genes, and callose deposition in tobacco	Rao et al., 2019
Nl28	*Nilaparvata lugens*	Cysteine-rich protein	Induce cell death, expression of defense-related genes, and callose deposition in *Nicotiana benthamiana*	Rao et al., 2019
Nl32	*Nilaparvata lugens*	Chemosensory protein	Induce a dwarf phenotype, expression of defense-related genes, and callose deposition in tobacco	Rao et al., 2019
Nl40	*Nilaparvata lugens*	*N.lugens*-specific salivary protein	Induce chlorosis, expression of defense-related genes, and callose deposition in tobacco	Rao et al., 2019
Nl43	*Nilaparvata lugens*	Uncharacterized protein	Induce cell death, expression of defense-related genes, and callose deposition in tobacco	Rao et al., 2019
VgN	*Nilaparvata lugens*	N-terminal subunit of vitellogenin	Trigger strong defense responses in rice	Zeng et al., 2023
Te1	*Tetranychus evansi*	Tetranins	Induce JA, SA, and ABA biosynthesis in tobacco	Iida et al., 2019
Te2	*Tetranychus evansi*	Tetranins	Induce JA, SA, and ABA biosynthesis in tobacco	Iida et al., 2019
TePDI	*Tetranychus evansi*	Disulfide isomerase	Reduce aphid performance; Induce ROS burst, callose deposition, expression of defense-related genes, and cell death in an SGT1/HSP90-dependent manner in tobacco	Cui et al., 2023
RP309	*Riptortus pedestris*	*R. pedestris*-specific salivary protein	Induce cell death, ROS burst, and the expression of PTI marker genes in tobacco	Dong et al., 2022
PLP	Bacteria *in Spodoptera littoralis*	Porin-like protein	Induce defense-related early events in *Arabidopsis*	Guo et al., 2013
GroEL	*Buchnera aphidicola* in *Macrosiphum euphorbiae*	Chaperonin	Reduce aphid fecundity; Induce ROS burst and expression of PTI marker genes in *Arabidopsis*	Chaudhary et al., 2014

herbivores (Calderón-Cortés et al., 2012). Both nematode (*Heterodera avenae*) expansin-like protein (HaEXPB2) and brown planthopper NlEG1 target the cell wall for promoting insect performance (Liu J. et al., 2016; Ji et al., 2017). Some effectors can suppress elicitor/pathogen-associated molecular pattern (PAMP)-triggered immunity. A macrophage migration inhibitory factor (MIF) is secreted from aphid saliva to promote insect feeding. Further study revealed that over-expressing *MIF* inhibits defense responses caused by the elicitor cryptogein, a 10-kDa protein from the plant pathogen *Phytophthora cryptogea* (Naessens et al., 2015). Transient overexpression of the salivary effector SG2204 from greenbug (*Schizaphis graminum*) and Sm9723 from grain aphid

TABLE 2 Identified insect-associated effector proteins.

Name	Origin	Protein characterization	Function	Reference
GOX	*Helicoverpa zea*	Glucose oxidase	Inhibit the production of nicotine in tobacco	Musser et al., 2002
HARP1	Helicoverpa armigera	Venom R-like protein	Enhance cotton bollworm feeding performance; Block JA pathway by interacting with JAZ in *Arabidopsis*	Chen et al., 2019
HAS1	*Helicoverpa armigera*	Venom R-like protein	Enhance cotton bollworm feeding performance; Block JA pathway by interacting with MYC3/MYC4 in *Arabidopsis*	Chen et al., 2023
C002	*Myzus persicae*	Salivary glands-abundant secretory protein	Promote aphid colonization in tobacco	Pitino and Hogenhout, 2013
Mp55	*Myzus persicae*	Salivary glands-abundant secretory protein	Increase aphid reproduction; Reduce accumulation of 4-methoxyindol-3-ylmethylglucosinolate, callose, and hydrogen peroxide in tobacco	Elzinga et al., 2014
Mp1	*Myzus persicae*	Salivary glands-abundant secretory protein	Increase aphid reproduction; Target trafficking protein VPS52 in tobacco	Rodriguez et al., 2017
MIF	*Acyrthosiphon Pisum*; *Myzus persicae*	Macrophage migration inhibitory factor	Enable aphid survival, fecundity, and feeding; Suppress *Cry*-triggered defenses in tobacco	Naessens et al., 2015
Me10	*Macrosiphum euphorbiae*	Salivary glands-abundant secretory protein	Enhance aphid fecundity; Suppress defenses and interact with tomato TFT7 in tomato	Atamian et al., 2013; Chaudhary et al., 2019
Me23	*Macrosiphum euphorbiae*	Glutathione peroxidase	Suppress plant defenses in tobacco	Atamian et al., 2013
ACE1 and ACE2	*Acyrthosiphon pisum*	Angiotensin-converting enzymes	Enable aphid feeding and survival in tobacco	Wang et al., 2015b
Armet	*Acyrthosiphon pisum*	Arginine-rich, mutated in early stage of tumors	Enable aphid feeding; Elicit SA pathway in tobacco	Wang et al., 2015a; Cui et al., 2019
ApHRC	*Acyrthosiphon pisum*	Histidine-rich Ca^{2+}-binding like protein	Promote aphid colonization; Repress Ca^{2+} elevation and ROS accumulation	Wang et al., 2020
Sg2204	*Schizaphis graminum*	Salivary glands-abundant secretory protein	Enable aphid feeding; Suppress JA, SA pathways, and cell death caused by BAX/INF1 in tobacco	Zhang et al., 2022a
Sm9723	*Sitobion miscanthi*	Salivary glands-abundant secretory protein	Enable aphid feeding; Suppress JA, SA pathways, and BAX/INF1-induced cell death in tobacco	Zhang et al., 2022b
NlEG1	*Nilaparvata lugens*	Endo-β-1,4-Glucanase	Enable BPH feeding; Degrade celluloses in rice	Ji et al., 2017
NlSEF1	*Nilaparvata lugens*	EF-hand calcium-binding protein	Suppress the production of Ca^{2+} and H_2O_2 in rice	Ye et al., 2017
NlugOBP11	*Nilaparvata lugens*	Odorant-binding protein	Enable BPH feeding; Suppress SA pathway in rice	Liu et al., 2021
CaM	*Nilaparvata lugens*; *Laodelphax striatellus*	Calmodulin binding protein	Enable BPH fecundity; Suppress H_2O_2 accumulation, and callose deposition in rice	Fu et al., 2022
NlSP7	*Nilaparvata lugens*	Salivary glands-abundant secretory protein	Enable BPH feeding; Mediate tricin metabolism in rice	Gong et al., 2022
DNase II	*Laodelphax striatellus*	DNase II	Enable SBPH feeding performance; Reduce H_2O_2 and callose accumulation in rice	Huang et al., 2019
VgC	*Laodelphax striatellus*	C-terminal peptide of vitellogenin	Suppress H_2O_2 accumulation by targeting OsWRKY71 in rice	Ji et al., 2021
LsSP1	*Laodelphax striatellus*	Salivary glands-specific protein	Enable SBPH feeding performance; Reduce SA responses by interacting with PLCPs in rice	Huang et al., 2023
LAC1	*Bemisia tabaci*	Laccase	Enable whitefly survival; Upregulated by JA signaling in tomato	Yang et al., 2017
BtFer1	*Bemisia tabaci*	Ferritin	Enable whitefly survival; Suppress JA pathway in tomato	Su et al., 2019
Bsp9	*Bemisia tabaci*	Salivary glands-abundant secretory protein	Promote whitefly performance; Suppress plant defenses by interacting with WRKY33 tobacco	Wang et al., 2019
Bt56	*Bemisia tabaci*	Low molecular weight salivary protein	Promote whitefly performance; Elicit SA pathway by targeting tobacco NTH202	Xu et al., 2019

(Continued)

TABLE 2 Continued

Name	Origin	Protein characterization	Function	Reference
BtArmet	*Bemisia tabaci*	Arginine-rich, mutated in early stage of tumors	Enhance whitefly performance; Target tobacco NtCYS6	Du et al., 2022
Tu28	*Tetranychus urticae*	Protein with Armadillo-type fold domain	Promote spider mite performance; Suppress SA-pathway in tobacco	Villarroel et al., 2016
Tu84/Te84	*Tetranychus urticae*; *Tetranychus evansi*	Salivary glands-abundant secretory protein	Promote spider mite performance; Suppress SA pathway in tobacco	Villarroel et al., 2016
NcSP84	*Nephotettix cincticeps*	EF-hand calcium-binding protein	Bind Ca^{2+} ions and facilitate stylet puncturing in rice	Hattori et al., 2012
NcSP75	*Nephotettix cincticeps*	Salivary glands-specific protein	Enable leafhopper survival and feeding performance in rice	Matsumoto and Hattori, 2018
vH13	*Mayetiola destructor*	*M. destructor*-specific salivary protein	Elicit effector-triggered immunity in resistant wheat containing *H13*	Aggarwal et al., 2014
SSGP-71	*Mayetiola destructor*	E3-ubiquitin-ligase mimic	Target Skp in wheat	Zhao et al., 2015
vH6	*Mayetiola destructor*	E3-ubiquitin-ligase mimic with an F box and 13 LRRs	Elicit effector-triggered immunity in resistant wheat containing *H6*	Zhao et al., 2015
vH9	*Mayetiola destructor*	E3-ubiquitin-ligase mimic without F box	Elicit effector-triggered immunity in resistant wheat containing *H9*	Zhao et al., 2015
SAP11	Aster Yellows phytoplasma *in Macrosteles quadrilineatus*	A 9-kDa protein	Promote leafhopper performance; Bind and destabilize TCP to suppress JA synthesis in *Arabidopsis*	Sugio et al., 2011
SAP54	Aster Yellows phytoplasma *in Macrosteles*	A 10.7-kDa protein	Promote leafhopper colonization; Degrade MTFs by interacting with RAD23 in *Arabidopsis*	MacLean et al., 2011; MacLean et al., 2014
2b	Cucumber mosaic virus in *Myzus persicae*	Virus protein	Interact with JAZ1 to suppress JA signaling in tobacco	Wu et al., 2017
βC1	Tomato yellow leaf curl China virus in *Bemisia tabaci*	Virus protein	Promote whitefly performance; Repress terpenoid synthesis by binding to MYC2	Luan et al., 2013; Li et al., 2014
C2	Tomato yellow leaf curl virus in *Bemisia tabaci*	Virus protein	Promote whitefly survival and reproduction; Suppress plant defenses by interacting with plant ubiquitin	Li et al., 2019b

(*Sitobion miscanthi*) could suppress BAX and PAMP INF1-induced cell death (Zhang et al., 2022a; Zhang et al., 2022b). Furthermore, spider mite effectors Te28 and Te84 could also suppress cell death caused by the elicitor TePDI (Cui et al., 2023). However, as yet, the targets or receptors of many effectors in plants have not been identified.

Like elicitors, some effectors also come from insect-borne microbes. Notable examples are the SAP11 and SAP54 from Aster Yellows phytoplasma strain Witches' Broom (AY-WB). They alter plant development and defense responses by the destabilization of CINCINNATA (CIN)-related TEOSINT BRANCHED1/CYCLOIDEA/PROLIFERATING CELL FACTOR (TCP) and MADS domain transcription factors (MTFs) to enhance insect vector reproduction (MacLean et al., 2011; Sugio et al., 2011; MacLean et al., 2014). Other microbe-derived effectors, such as C2 from tomato yellow leaf curl China virus and 2b from cucumber mosaic virus (CMV), promote insect vector infestation by blocking the JA pathway in the plant (Wu et al., 2017; Li et al., 2019b). Together, these examples illustrate that microbe-derived effectors contribute to facilitating the fitness of their insect vectors as an effective strategy for completing their infection cycles.

R gene-mediated plant resistance to insect herbivores

To fight the secreted effectors, host plants have developed resistance proteins. A set of genes in tomato, melon, and rice conferring resistance against insects has been identified and cloned. Two aphid resistance genes, the *Mi-1.2* gene characterized in the tomato (*Solanum lycopersicum*) and the *Vat* gene characterized in the melon (*Cucumis melo*) confer resistance to the potato aphid (*M. euphorbiae*) and the cotton aphid (*A.gossypii*), respectively (Rossi et al., 1998; Vos et al., 1998; Dogimont et al., 2014). Besides the potato aphid, the *Mi-1.2* gene is also resistant to two whitefly biotypes, a psyllid, and three nematode species, suggesting that the *Mi-1.2* gene confers a broad-spectrum resistance (Vos et al., 1998). With the availability of genome

sequence data and molecular markers in rice, research on BPH-resistance genes has made a spurt of progress. BPH-rice interaction has become an excellent model system for the study of plant-insect interactions and co-evolution (Jing et al., 2017). To date, a total of 17 genes conferring resistance to BPH (*Bph1*, *Bph2*, *Bph3*, *Bph6*, *Bph7*, *Bph9*, *Bph10*, *Bph14*, *Bph15*, *Bph18*, *Bph21*, *Bph26*, *bph29*, *Bph30*, *Bph32*, *Bph37*, *Bph40*) have been cloned and characterized in rice plants (Du et al., 2020; Muduli et al., 2021; Shi et al., 2021; Zhou et al., 2021), which has shed a light on the molecular basis of plant-insect interactions.

Bph14, which encodes a typical NLR protein, was the first isolated BPH-resistance gene (Du et al., 2009). Further research has revealed that BPH14 protein stabilizes WRKY46 and WRKY72 to increase the expression of the receptor-like cytoplasmic kinase gene *RLCK281* in rice (Hu et al., 2017). *Bph9*, a BPH-resistance gene mapped on the long arm of rice chromosome 12 (12L), which is allelic with another seven BPH-resistance genes (*Bph1*, *Bph2*, *Bph7*, *Bph10*, *Bph18*, *Bph21*, and *Bph26*), encodes an unusual NLR protein that confers resistance to BPH by enhancing SA and JA signaling pathways (Zhao et al., 2016). BPH6, an uncharacterized protein that localizes to the exocyst, interacts with the exocyst subunits OsEXO70E1 and OsEXO70H3, increases exocytosis, and participates in cell wall maintenance and reinforcement (Guo et al., 2018; Wu et al., 2022). Recently, a novel dominant BPH-resistance gene, *Bph30*, was isolated from the short arm of rice chromosome 4 (4S) (Wang et al., 2018; Shi et al., 2021). *Bph30* is strongly expressed in sclerenchyma cells and encodes a protein belonging to a novel gene family with two leucine-rich domains (LRDs). A functional study showed that BPH30 enhances cellulose and hemicellulose synthesis, making the cell walls stiffer and sclerenchyma thicker to prevent stylets from penetrating the leaf sheath tissue, thereby conferring broad resistance to BPH and WBPH in rice (Shi et al., 2021). *Bph15* encodes a lectin receptor-like kinase (LecRK), which functions in both innate immunity and seed germination in plants (Cheng et al., 2013a). *Bph3* consists of a cluster of three genes encoding the plasma membrane-localized LecRKs (OsLecRK1, OsLecRK2, and OsLecRK3), which have a cumulative effect on resistance (Liu et al., 2015). These results indicate the diversity in resistance genes and mechanisms.

Based on our knowledge, except for two lectin receptor-like receptors and a few R proteins with unusual structures, such as BPH6 and BPH30, most isolated BPH-resistance proteins belong to nucleotide-binding and leucine-rich repeat (NLR) proteins, suggesting commonality between the perception of phloem-feeding insects and pathogens by plants. *Bph3* and *Bph15* encode the LecRKs, which resemble pattern recognition receptors (PRRs). PRRs are activated in response to microbe/pathogen/herbivore-associated molecular patterns or apoplastic effectors (Kaloshian and Walling, 2016; Ngou et al., 2022). The first layer of resistance to BPH may be BPH3 or BPH15, which is activated by the recognition of elicitors or apoplastic effectors. The second layer of resistance to BPH may be BPH6, BPH14, and BPH9 and their alleles, which can specifically recognize their cognate effectors and trigger defense responses (Jing et al., 2017; Du et al., 2020; Zheng et al., 2021).

Effectors recognized in R protein-mediated resistance

Despite the recent insights into the complex repertoire of R proteins, only a few effectors recognized by R proteins have been identified until now. This may be owing to the genetic intractability of the insects. At least 40 brown planthopper-resistant genes have been discovered, but just four corresponding BPH effector loci (*Qhp7*, *Qgr5*, *Qgr14*, and *vBph1*) were mapped (Jing et al., 2014; Kobayashi et al., 2014). The effectors recognized by R proteins had only been isolated from Hessian fly (*Mayetiola destructor*) until now (Stuart, 2015). The first Hessian fly virulence gene, *virulence to Hessian fly 13* (*vH13*), was isolated using a map-based cloning strategy (Rider et al., 2002; Aggarwal et al., 2009; Aggarwal et al., 2014). Functional assays have shown that *vH13* transcripts are only detected in *H13*-avirulent larvae and are lost in *H13*-virulent larvae. RNAi results revealed that the knockdown of *vH13* helped some *H13*-avirulent larvae to escape the resistance triggered by *H13* in wheat. Furthermore, *vH13* encodes a small modular protein with no sequence similarities to other proteins in the database (Aggarwal et al., 2014).

Two additional Hessian fly effectors, vH6 and vH9, were identified by the completion of the Hessian fly genome sequencing and gene expression analyses. vH6 and vH9 can overcome the resistance mediated by wheat R protein H6 and H9, respectively (Zhao et al., 2015). Both *vH6* and *vH9* encode SSGP-71-like proteins. In H6-virulent Hessian flies, an SSGP-71 gene (*Mdes009086-RA*) is lost, suggesting Mdes009086-RA is the cognate effector of H6. In H9-virulent Hessian flies, two candidate SSGP-71 proteins without F-box domains were perfectly associated with H9 virulence, especially candidate 2 (Mdes015365-RA). These results indicate that the SSGP-71 family may play an essential role in the evolution of Hessian fly biotypes (Zhao et al., 2015). However, no cognate Hessian fly R protein has been cloned successfully, and the recognition mechanism of these Hessian fly effectors by the cognate R protein remains to be explored.

Perspectives and challenges

In recent years, rapid technological progress in the discovery and interrogation of plant and insect genomes, transcriptomes, and proteomes has been made. These developments have provided opportunities for the exploration of molecules delivered by herbivores that activate or suppress plant immunity (Hogenhout and Bos, 2011; Kaloshian and Walling, 2016). Cas9-CRISPR and RNAi technologies can effectively silence host plant/insect genes and, therefore, can help us to reveal the important signal molecules and the key pathways in plant-insect interactions (Ma et al., 2015; Liu et al., 2020; Hough et al., 2022). These discoveries give us an advanced understanding of the plant-insect relationship. In particular, the RNAi tool has made important contributions to the study of the function of insect elicitors and effectors in insect performance and plant immunity. There are several strategies for

the delivery of double-stranded RNA (dsRNA), including external spraying, artificial feeding/micro-injection of synthesized dsRNA, and construction of transgenic plant lines with high levels of endogenous dsRNA (Shangguan et al., 2018; Huang et al., 2020; Zhang et al., 2022a). Over the years, RNAi has been considered an effective strategy for the control of insect pests (Liu et al., 2020; Hough et al., 2022). In addition, great progress has been made in the research of insect resistance proteins, especially the resistance mechanism of BPH-resistant genes (Jing et al., 2017; Du et al., 2020; Zheng et al., 2021).

Despite these advances, major gaps in our understanding of interactions between insect herbivores and host plants remain to be filled. Although a large number of elicitors and effectors have been identified, only a few have revealed corresponding host targets. The plant defense pathways interfered with by the majority of elicitors and effectors are obscure. Additionally, little is known about the relationship between cognate insect effector and cognate R protein. On the one hand, no cognate effector of the cloned R genes has been discovered; on the other hand, while three R protein-recognized effectors in Hessian flies were identified, no corresponding Hessian fly R genes have been cloned. Combining map-based cloning and multi-omics approaches may contribute to overcoming these challenges. We believe that these questions will be the priority of research on plant-insect interactions in the next decade, and the answers to these questions will provide more insight into how to control these pests.

Author contributions

WH proposed the idea. HW and SS drafted the manuscript and designed the figure. WH reviewed and edited the manuscript. All authors contributed to the article and approved the submitted version.

Funding

This review was supported by grants from the Wuhan Science and Technology Major Project on Key techniques of biological breeding and Breeding of new varieties (2022021302024851), the Natural Science Foundation of Hubei Province (2022CFB832), Hubei Academy of Agricultural Science Foundation (2023NKYJJ01), Hubei Key Laboratory of Food Crop Germplasm and Genetic Improvement Foundation (2022lzjj01), and the National Natural Science Foundation of China (32001921).

Acknowledgments

We acknowledge the BioRender tool that we used to create Figure 1.

Conflict of interest

The authors declare that the research was conducted in the absence of any commercial or financial relationships that could be construed as a potential conflict of interest.

Publisher's note

References

Acevedo, F. E., Peiffer, M., Ray, S., Meagher, R., Luthe, D. S., and Felton, G. W. (2018). Intraspecific differences in plant defense induction by fall armyworm strains. *New Phytol.* 218, 310–321. doi: 10.1111/nph.14981

Aggarwal, R., Benatti, T. R., Gill, N., Zhao, C., Chen, M. S., Fellers, J. P., et al. (2009). A BAC-based physical map of the Hessian fly genome anchored to polytene chromosomes. *BMC Genomics* 2, 293. doi: 10.1186/1471-2164-10-293

Aggarwal, R., Subramanyam, S., Zhao, C. Y., Chen, M. S., Harris, M. O., and Stuart, J. J. (2014). Avirulence effector discovery in a plant galling and plant parasitic arthropod, the Hessian fly (*Mayetiola destructor*). *PloS One* 9, e100958. doi: 10.1371/journal.pone.0100958

Alborn, H. T., Hansen, T. V., Jones, T. H., Bennett, D. C., Tumlinson, J. H., Schmelz, E. A., et al. (2007). Disulfooxy fatty acids from the American bird grasshopper *Schistocerca americana*, elicitors of plant volatiles. *Proc. Natl. Acad. Sci. U. S. A.* 104, 12976–12981. doi: 10.1073/pnas.0705947104

Atamian, H. S., Chaudhary, R., Cin, V. D., Bao, E., Girke, T., and Kaloshian, I. (2013). In planta expression or delivery of potato aphid *Macrosiphum euphorbiae* effectors Me10 and Me23 enhances aphid fecundity. *Mol. Plant Microbe In.* 26, 67–74. doi: 10.1094/MPMI-06-12-0144-FI

Backus, E. A. (1988). Sensory systems and behaviours which mediate hemipteran plant-feeding: a taxonomic overview. *J. Insect Physiol.* 34, 151–165. doi: 10.1016/0022-1910(88)90045-5

Bos, J. I., Prince, D., Pitino, M., Maffei, M. E., Win, J., and Hogenhout, S. A. (2010). A functional genomics approach identifies candidate effectors from the aphid species *Myzus persicae* (green peach aphid). *PloS Genet.* 6, e1001216. doi: 10.1371/journal.pgen.1001216

Calderón-Cortés, N., Quesada, M., Watanabe, H., Cano-Camacho, H., and Oyama, K. (2012). Endogenous plant cell wall digestion: a key mechanism in insect evolution. *Annu. Rev. Ecol. Evol. Syst.* 43, 45–71. doi: 10.1146/annurev-ecolsys-110411-160312

Chaudhary, R., Atamian, H. S., Shen, Z., Briggs, S. P., and Kaloshian, I. (2014). GroEL from the endosymbiont *Buchnera aphidicola* betrays the aphid by triggering plant defense. *Proc. Natl. Acad. Sci. U. S. A.* 111, 8919–8924. doi: 10.1073/pnas.1407687111

Chaudhary, R., Peng, H. C., He, J., MacWilliams, J., Teixeira, M., Tsuchiya, T., et al. (2019). Aphid effector Me10 interacts with tomato TFT7, a 14-3-3 isoform involved in aphid resistance. *New Phytol.* 221, 1518–1528. doi: 10.1111/nph.15475

Chen, C., Liu, Y., Song, W., Chen, D., Chen, F., Chen, X., et al. (2019). An effector from cotton bollworm oral secretion impairs host plant defense signaling. *Proc. Natl. Acad. Sci. U. S. A.* 116, 14331–14338. doi: 10.1073/pnas.1905471116

Chen, X., Liu, Y., Wu, M., Yan, L., Chen, C., Mu, Y., et al. (2023). A highly accumulated secretory protein from cotton bollworm interacts with basic helix-loop-helix transcription factors to dampen plant defense. *New Phytol.* 237, 265–278. doi: 10.1111/nph.18507

Chen, C., and Mao, Y. (2020). Research advances in plant-insect molecular interaction. *F1000Res* 19, F1000 Faculty Rev-198. doi: 10.12688/f1000research.21502.1

Cheng, X., Wu, Y., Guo, J., Du, B., Chen, R., Zhu, L., et al. (2013a). A rice lectin receptor-like that is involved in innate immuneresponses also contributes to seed germination. *Plant J.* 76, 687–698. doi: 10.1111/tpj.12328

Cheng, X., Zhu, L., and He, G. (2013b). Towards understanding of molecular interactions between rice and the brown planthopper. *Mol. Plant* 6, 621–634. doi: 10.1093/mp/sst030

Cooper, W. R., Dillwith, J. W., and Puterka, G. J. (2011). Comparisons of salivary proteins from five aphid (Hemiptera: aphididae) species. *Environ. Entomol.* 40, 151–156. doi: 10.1603/EN10153

Cui, J., Bing, X., Tang, Y., Liu, F., Ren, L., Zhou, J., et al. (2023). A conserved protein disulfide isomerase enhances plant resistance against herbivores. *Plant Physiol.* 191, 660–678. doi: 10.1093/plphys/kiac489

Cui, N., Lu, H., Wang, T., Zhang, W., Kang, L., and Cui, F. (2019). Armet, an aphid effector protein, induces pathogen resistance in plants by promoting the accumulation of salicylic acid. *Philos. Trans. R. Soc Lond. B. Biol. Sci.* 4, 20180314. doi: 10.1098/rstb.2018.0314

Dogimont, C., Chovelon, V., Pauquet, J., Boualem, A., and Bendahmane, A. (2014). The *Vat* locus encodes for a CC-NBS-LRR protein that confers resistance to *Aphis gossypii* infestation and *A. gossypii*-mediated virus resistance. *Plant J.* 80, 993–1004. doi: 10.1111/tpj.12690

Dong, Y., Huang, X., Yang, Y., Li, J., Zhang, M., Shen, H., et al. (2022). Characterization of salivary secreted proteins that induce cell death from *Riptortus pedestris* (Fabricius) and their roles in insect-plant interactions. *Front. Plant Sci.* 4. doi: 10.3389/fpls.2022.912603

Du, B., Chen, R., Guo, J., and He, G. (2020). Current understanding of the genomic, genetic, and molecular control of insect resistance in rice. *Mol. Breed.* 40, 24. doi: 10.1007/s11032-020-1103-3

Du, H., Xu, H., Wang, F., Qian, L., Liu, S., and Wang, X. (2022). Armet from whitefly saliva acts as an effector to suppress plant defences by targeting tobacco cystatin. *New Phytol.* 234, 1848–1862. doi: 10.1111/nph.18063

Du, B., Zhang, W., Liu, B., Hu, J., Wei, Z., Shi, Z., et al. (2009). Identification and characterization of *Bph14*, a gene conferring resistance to brown planthopper in rice. *Proc. Natl. Acad. Sci. U. S. A.* 106, 22163–22168. doi: 10.1073/pnas.0912139106

Elzinga, D. A., De Vos, M., and Jander, G. (2014). Suppression of plant defenses by a *Myzus persicae* (green peach aphid) salivary effector protein. *Mol. Plant Microbe In.* 27, 747–756. doi: 10.1094/MPMI-01-14-0018-R

Erb, M., and Reymond, P. (2019). Molecular interactions between plants and insect herbivores. *Annu. Rev. Plant Biol.* 29, 527–557. doi: 10.1146/annurev-arplant-050718-095910

Felton, G. W., Korth, K. L., Bi, J. L., Wesley, S. V., Huhman, D. V., Mathews, M. C., et al. (1999). Inverse relationship between systemic resistance of plants to microorganisms and to insect herbivory. *Curr. Biol.* 9, 317–320. doi: 10.1016/s0960-9822(99)80140-7

Fu, J., Shi, Y., Wang, L., Tian, T., Li, J., Gong, L., et al. (2022). Planthopper-secreted salivary calmodulin acts as an effector for defense responses in rice. *Front. Plant Sci.* 28. doi: 10.3389/fpls.2022.841378

Gong, G., Yuan, L., Li, Y., Xiao, H., Li, Y., Zhang, Y., et al. (2022). Salivary protein 7 of the brown planthopper functions as an effector for mediating tricin metabolism in rice plants. *Sci. Rep.* 25, 3205. doi: 10.1038/s41598-022-07106-6

Guo, H., Wielsch, N., Hafke, J. B., Svatoš, A., Mithöfer, A., and Boland, W. (2013). A porin-like protein from oral secretions of *Spodoptera littoralis* larvae induces defense-related early events in plant leaves. *Insect Biochem. Mol. Biol.* 43, 849–858. doi: 10.1016/j.ibmb.2013.06.005

Guo, J., Xu, C., Wu, D., Zhao, Y., Qiu, Y., Wang, X., et al. (2018). *Bph6* encodes an exocyst-localized protein and confers broad resistance to planthoppers in rice. *Nat. Genet.* 50, 297–306. doi: 10.1038/s41588-018-0039-6

Guo, H., Zhang, Y., Tong, J., Ge, P., Wang, Q., Zhao, Z., et al. (2020). An aphid-secreted salivary protease activates plant defense in phloem. *Curr. Biol.* 30, 4826–4836.e7. doi: 10.1016/j.cub.2020.09.020

Hao, P., Liu, C., Wang, Y., Chen, R., Tang, M., Du, B., et al. (2008). Herbivore-induced callose deposition on the sieve plates of rice: an important mechanism for host resistance. *Plant Physiol.* 146, 1810–1820. doi: 10.1104/pp.107.111484

Harmel, N., Letocart, E., Cherqui, A., Giordanengo, P., Mazzucchelli, G., Guillonneau, F., et al. (2008). Identification of aphid salivary proteins: a proteomic investigation of *Myzus persicae*. *Insect Mol. Biol.* 17, 165–174. doi: 10.1111/j.1365-2583.2008.00790.x

Hattori, M., Nakamura, M., Komatsu, S., Tsuchihara, K., Tamura, Y., and Hasegawa, T. (2012). Molecular cloning of a novel calcium-binding protein in the secreted saliva of the green rice leafhopper *Nephotettix cincticeps*. *Insect Biochem. Mol. Biol.* 42, 1–9. doi: 10.1016/j.ibmb.2011.10.001

Hewer, A., Becker, A., and van Bel, A. J. (2011). An aphid's odyssey–the cortical quest for the vascular bundle. *J. Exp. Biol.* 214, 3868–3879. doi: 10.1242/jeb.060913

Hewer, A., Will, T., and van Bel, A. J. (2010). Plant cues for aphid navigation in vascular tissues. *J. Exp. Biol.* 213, 4030–4042. doi: 10.1242/jeb.046326

Hogenhout, S. A., and Bos, J. I. (2011). Effector proteins that modulate plant-insect interactions. *Curr. Opin. Plant Biol.* 14, 422–428. doi: 10.1016/j.pbi.2011.05.003

Hough, J., Howard, J. D., Brown, S., Portwood, D. E., Kilby, P. M., and Dickma, M. J. (2022). Strategies for the production of dsRNA biocontrols as alternatives to chemical pesticides. *Front. Bioeng Biotechnol.* 10. doi: 10.3389/fbioe.2022.980592

Hu, L., Wu, Y., Wu, D., Rao, W., Guo, J., Ma, Y., et al. (2017). The coiled-coil and nucleotide binding domains of BROWN PLANTHOPPER RESISTANCE14 function in signaling and resistance against planthopper in rice. *Plant Cell* 29, 3157–3185. doi: 10.1105/tpc.17.00263

Huang, H., Cui, J., Xia, X., Chen, J., Ye, Y., Zhang, C., et al. (2019). Salivary DNase II from *Laodelphax striatellus* acts as an effector that suppresses plant defence. *New Phytol.* 224, 860–874. doi: 10.1111/nph.15792

Huang, H., Liu, C., Huang, X., Zhou, X., Zhuo, J., Zhang, C., et al. (2016). Screening and functional analyses of *Nilaparvata lugens* salivary proteome. *J. Proteome Res.* 15, 1883–1896. doi: 10.1021/acs.jproteome.6b00086

Huang, H., Liu, C., Xu, H., Bao, Y., and Zhang, C. (2017). Mucin-like protein, a saliva component involved in brown planthopper virulence and host adaptation. *J. Insect Physiol.* 98, 223–230. doi: 10.1016/j.jinsphys.2017.01.012

Huang, H., Lu, J., Li, Q., Bao, Y., and Zhang, C. (2018). Combined transcriptomic/proteomic analysis of salivary gland and secreted saliva in three planthopper species. *J. Proteomics* 172, 25–35. doi: 10.1016/j.jprot.2017.11.003

Huang, H., Wang, Y., Li, L., Lu, H., Lu, J., Wang, X., et al. (2023). Planthopper salivary sheath protein LsSP1 contributes to manipulation of rice plant defenses. *Nat. Commun.* 14, 737. doi: 10.1038/s41467-023-36403-5

Huang, J., Zhang, N., Shan, J., Peng, Y., Guo, J., Zhou, C., et al. (2020). Salivary protein 1 of brown planthopper is required for survival and induces immunity response in plants. *Front. Plant Sci.* 11. doi: 10.3389/fpls.2020.571280

Iida, J., Desaki, Y., Hata, K., Uemura, T., Yasuno, A., Islam, M., et al. (2019). Tetranins: new putative spider mite elicitors of host plant defense. *New Phytol.* 224, 875–885. doi: 10.1111/nph.15813

Ji, R., Fu, J., Shi, Y., Li, J., Jing, M., Wang, L., et al. (2021). Vitellogenin from planthopper oral secretion acts as a novel effector to impair plant defenses. *New Phytol.* 232, 802–817. doi: 10.1111/nph.17620

Ji, R., Ye, W., Chen, H., Zeng, J., Li, H., Yu, H., et al. (2017). A salivary endo-β-1,4-glucanase acts as an effector that enables the brown planthopper to feed on rice. *Plant Physiol.* 173, 1920–1932. doi: 10.1104/pp.16.01493

Ji, R., Yu, H., Fu, Q., Chen, H., Ye, W., Li, S., et al. (2013). Comparative transcriptome analysis of salivary glands of two populations of rice brown planthopper, *Nilaparvata lugens*, that differ in virulence. *PloS One* 8, e79612. doi: 10.1371/journal.pone.0079612

Jing, S., Zhang, L., Ma, Y., Liu, B., Zhao, Y., Yu, H., et al. (2014). Genome-wide mapping of virulence in brown planthopper identifies loci that break down host plant resistance. *PloS One* 9, e98911. doi: 10.1371/journal.pone.0098911

Jing, S., Zhao, Y., Du, B., Chen, R., Zhu, L., and He, G. (2017). Genomics of interaction between the brown planthopper and rice. *Curr. Opin. Insect Sci.* 19, 82–87. doi: 10.1016/j.cois.2017.03.005

Jones, J. D., and Dangl, J. L. (2006). The plant immune system. *Nature* 444, 323–329. doi: 10.1038/nature05286

Kahl, G. (1982). "Molecular biology of wound healing: the conditioning phenomenon," in *Molecular biology of plant tumors*. Eds. G. Kahl and J. Schell (New York: Academic Press, Inc), 211–267.

Kaloshian, I., and Walling, L. L. (2016). Hemipteran and dipteran pests: effectors and plant host immune regulators. *J. Integr. Plant Biol.* 58, 350–361. doi: 10.1111/jipb.12438

Kobayashi, T., Yamamoto, K., Suetsugu, Y., Kuwazaki, S., Hattori, M., Jairin, J., et al. (2014). Genetic mapping of the rice resistance-breaking gene of the brown planthopper *Nilaparvata lugens*. *Proc. Biol. Sci.* 281, 20140726. doi: 10.1098/rspb.2014.0726

Li, P., Liu, C., Deng, W., Yao, D., Pan, L., Li, Y., et al. (2019b). Plant begomoviruses subvert ubiquitination to suppress plant defenses against insect vectors. *PloS Pathog.* 15, e1007607. doi: 10.1371/journal.ppat.1007607

Li, J., Liu, X., Wang, Q., Huangfu, J., Schuman, M. C., and Lou, Y. (2019a). A group d MAPK protects plants from autotoxicity by suppressing herbivore-induced defense signaling. *Plant Physiol.* 179, 1386–1401. doi: 10.1104/pp.18.01411

Li, R., Weldegergis, B. T., Li, J., Jung, C., Qu, J., Sun, Y., et al. (2014). Virulence factors of geminivirus interact with MYC2 to subvert plant resistance and promote vector performance. *Plant Cell* 26, 4991–5008. doi: 10.1105/tpc.114.133181

Liu, S., Jaouannet, M., Dempsey, D. A., Imani, J., Coustau, C., and Kogel, K. H. (2020). RNA-Based technologies for insect control in plant production. *Biotechnol. Adv.* 39, 107463. doi: 10.1016/j.biotechadv.2019.107463

Liu, J., Peng, H., Cui, J., Huang, W., Kong, L., Clarke, J. L., et al. (2016). Molecular characterization of a novel effector expansin-like protein from *Heterodera avenae* that induces cell death in *Nicotiana benthamiana*. *Sci. Rep.* 6, 35677. doi: 10.1038/srep35677

Liu, H., Wang, C., Qiu, C., Shi, J., Sun, Z., Hu, X., et al. (2021). A salivary odorant-binding protein mediates *Nilaparvata lugens* feeding and host plant phytohormone suppression. *Int. J. Mol. Sci.* 22, 4988. doi: 10.3390/ijms22094988

Liu, Y., Wu, H., Chen, H., Liu, Y., He, J., Kang, H., et al. (2015). A gene cluster encoding lectin receptor kinases confers broad-spectrum and durable insect resistance in rice. *Nat. Biotechnol.* 33, 301–305. doi: 10.1038/nbt.3069

Liu, X., Zhou, H., Zhao, J., Hua, H., and He, Y. (2016). Identification of the secreted watery saliva proteins of the rice brown planthopper, *Nilaparvata lugens* (Stål) by transcriptome and shotgun LC-MS/MS approach. *J. Insect Physiol.* 89, 60–69. doi: 10.1016/j.jinsphys.2016.04.002

Louis, J., Peiffer, M., Ray, S., Luthe, D. S., and Felton, G. W. (2013). Host-specific salivary elicitor(s) of European corn borer induce defenses in tomato and maize. *New Phytol.* 199, 66–73. doi: 10.1111/nph.12308

Luan, J., Yao, D., Zhang, T., Walling, L. L., Yang, M., Wang, Y., et al. (2013). Suppression of terpenoid synthesis in plants by a virus promotes its mutualism with vectors. *Ecol. Lett.* 16, 390–398. doi: 10.1111/ele.12055

Ma, X., Zhang, Q., Zhu, Q., Liu, W., Chen, Y., Qiu, R., et al. (2015). A robust CRISPR/Cas9 system for convenient, high-efficiency multiplex genome editing in monocot and dicot plants. *Mol. Plant* 8, 1274–1284. doi: 10.1016/j.molp.2015.04.007

MacLean, A. M., Orlovskis, Z., Kowitwanich, K., Zdziarska, A. M., Angenent, G. C., Immink, R. G., et al. (2014). Phytoplasma effector SAP54 hijacks plant reproduction by degrading MADS-box proteins and promotes insect colonization in a RAD23-dependent manner. *PloS Biol.* 12, e1001835. doi: 10.1371/journal.pbio.1001835

MacLean, A. M., Sugio, A., Makarova, O. V., Findlay, K. C., Grieve, V. M., Tóth, R., et al. (2011). Phytoplasma effector SAP54 induces indeterminate leaf-like flower development in arabidopsis plants. *Plant Physiol.* 157, 831–841. doi: 10.1104/pp.111.181586

Matsumoto, Y., and Hattori, M. (2018). The green rice leafhopper, *Nephotettix cincticeps* (Hemiptera: cicadellidae), salivary protein NcSP75 is a key effector for successful phloem ingestion. *PloS One* 13, e0202492. doi: 10.1371/journal.pone.0202492

Mattiacci, L., Dicke, M., and Posthumus, M. A. (1995). *beta*-glucosidase: an elicitor of herbivore-induced plant odor that attracts host-searching parasitic wasps. *Proc. Natl. Acad. Sci. U. S. A.* 92, 2036–2040. doi: 10.1073/pnas.92.6.2036

Miles, P. W. (1999). Aphid saliva. *Biol. Rev. Camb. Philos. Soc* 4, 41–85. doi: 10.1111/j.1469-185X.1999.tb00181.x

Muduli, L., Pradhan, S. K., Mishra, A., Bastia, D. N., Samal, K. C., Agrawal, P. K., et al. (2021). Understanding brown planthopper resistance in rice: genetics, biochemical and molecular breeding approaches. *Rice Sci.* 28, 532–546. doi: 10.1016/j.rsci.2021.05.013

Musser, R. O., Cipollini, D. F., Hum-Musser, S. M., Williams, S. A., Brown, J. K., and Felton, G. W. (2005). Evidence that the caterpillar salivary enzyme glucose oxidase provides herbivore offense in solanaceous plants. *Arch. Insect Biochem. Physiol.* 58, 128–137. doi: 10.1002/arch.20039

Musser, R. O., Hum-Musser, S. M., Eichenseer, H., Peiffer, M., Ervin, G., Murphy, J. B., et al. (2002). Herbivory: caterpillar saliva beats plant defences. *Nature* 416, 599–600. doi: 10.1038/416599a

Mutti, N. S., Louis, J., Pappan, L. K., Pappan, K., Begum, K., Chen, M. S., et al. (2008). A protein from the salivary glands of the pea aphid, *Acyrthosiphon pisum*, is essential in feeding on a host plant. *Proc. Natl. Acad. Sci. U. S. A.* 105, 9965–9969. doi: 10.1073/pnas.0708958105

Naessens, E., Dubreuil, G., Giordanengo, P., Baron, O. L., Minet-Kebdani, N., Keller, H., et al. (2015). A secreted MIF cytokine enables aphid feeding and represses plant immune responses. *Curr. Biol.* 25, 1898–1903. doi: 10.1016/j.cub.2015.05.047

Ngou, B. P. M., Ding, P., and Jones, J. D. G. (2022). Thirty years of resistance: zig-zag through the plant immune system. *Plant Cell* 34, 1447–1478. doi: 10.1093/plcell/koac041

Nicholson, S. J., Hartson, S. D., and Puterka, G. J. (2012). Proteomic analysis of secreted saliva from Russian wheat aphid (*Diuraphis noxia* kurd.) biotypes that differ in virulence to wheat. *J. Proteomics* 75, 2252–2268. doi: 10.1016/j.jprot.2012.01.031

Nicholson, S. J., and Puterka, G. J. (2014). Variation in the salivary proteomes of differentially virulent greenbug (*Schizaphis graminum* rondani) biotypes. *J. Proteomics* 105, 186–203. doi: 10.1016/j.jprot.2013.12.005

Pelosi, P., Calvello, M., and Ban, L. (2005). Diversity of odorant-binding proteins and chemosensory proteins in insects. *Chem. Senses* 30, i291–i292. doi: 10.1093/chemse/bjh229

Pitino, M., and Hogenhout, S. A. (2013). Aphid protein effectors promote aphid colonization in a plant species-specific manner. *Mol. Plant Microbe In.* 26, 130–139. doi: 10.1094/MPMI-07-12-0172-FI

Rao, W., Zheng, X., Liu, B., Guo, Q., Guo, J., Wu, Y., et al. (2019). Secretome analysis and *in planta* expression of salivary proteins identify candidate effectors from the brown planthopper *Nilaparvata lugens*. *Mol. Plant Microbe In.* 32, 227–239. doi: 10.1094/MPMI-05-18-0122-R

Rider, S. D.Jr., Sun, W., Ratcliffe, R. H., and Stuart, J. J. (2002). Chromosome landing near avirulence gene *vH13* in the Hessian fly. *Genome* 45, 812–822. doi: 10.1139/g02-047

Rodriguez, P. A., Escudero-Martinez, C., and Bos, J. I. (2017). An aphid effector targets trafficking protein VPS52 in a host-specific manner to promote virulence. *Plant Physiol.* 173, 1892–1903. doi: 10.1104/pp.16.01458

Rodriguez, P. A., Stam, R., Warbroek, T., and Bos, J. I. (2014). Mp10 and Mp42 from the aphid species *Myzus persicae* trigger plant defenses in *Nicotiana benthamiana* through different activities. *Mol. Plant Microbe In.* 27, 30–39. doi: 10.1094/MPMI-05-13-0156-R

Rossi, M., Goggin, F. L., Milligan, S. B., Kaloshian, I., Ullman, D. E., and Williamson, V. M. (1998). The nematode resistance gene *Mi* of tomato confers resistance against the potato aphid. *Proc. Natl. Acad. Sci. U. S. A.* 95, 9750–9754. doi: 10.1073/pnas.95.17.9750

Schoonhoven, L., van Loon, J. J., and Dicke, M. (2005). *Insect–plant biology. 2nd edn* (Oxford: Oxford Univ. Press).

Schulz, A. (1998). The phloem. structure related to function. *Prog. Bot.* 59, 429–475. doi: 10.1007/978-3-642-80446-5_16

Shangguan, X., Zhang, J., Liu, B., Zhao, Y., Wang, H., Wang, Z., et al. (2018). A mucin-like protein of planthopper is required for feeding and induces immunity response in plants. *Plant Physiol.* 176, 552–565. doi: 10.1104/pp.17.00755

Shi, S., Wang, H., Nie, L., Tan, D., Zhou, C., Zhang, Q., et al. (2021). *Bph30* confers resistance to brown planthopper by fortifying sclerenchyma in rice leaf sheaths. *Mol. Plant* 14, 1714–1732. doi: 10.1016/j.molp.2021.07.004

Snoeck, S., Guayazán-Palacios, N., and Steinbrenner, A. D. (2022). Molecular tug-of-war: plant immune recognition of herbivory. *Plant Cell* 34, 1497–1513. doi: 10.1093/plcell/koac009

Sogawa, K. (1982). The rice brown planthopper: feeding physiology and host plant interactions. *Annu. Rev. Entomol.* 27, 49–73. doi: 10.1146/annurev.en.27.010182.000405

Spiller, N. J. (1990). An ultrastructural study of the stylet pathway of the brown planthopper *Nilaparvata lugens*. *Entomol. Exp. Appl.* 54, 191–193. doi: 10.1111/j.1570-7458.1990.tb01329.x

Stotz, H. U., Kroymann, J., and Mitchell-Olds, T. (1999). Plant-insect interactions. *Curr. Opin. Plant Biol.* 2, 268–272. doi: 10.1016/S1369-5266(99)80048-X

Stuart, J. (2015). Insect effectors and gene-for-gene interactions with host plants. *Curr. Opin. Insect Sci.* 9, 56–61. doi: 10.1016/j.cois.2015.02.010

Su, Q., Peng, Z., Tong, H., Xie, W., Wang, S., Wu, Q., et al. (2019). A salivary ferritin in the whitefly suppresses plant defenses and facilitates host exploitation. *J. Exp. Bot.* 70, 3343–3355. doi: 10.1093/jxb/erz152

Sugio, A., Kingdom, H. N., MacLean, A. M., Grieve, V. M., and Hogenhout, S. A. (2011). Phytoplasma protein effector SAP11 enhances insect vector reproduction by manipulating plant development and defense hormone biosynthesis. *Proc. Natl. Acad. Sci. U. S. A.* 108, E1254–E1263. doi: 10.1073/pnas.1105664108

Takken, F. L. W., and Tameling, W. I. L. (2009). To nibble at plant resistance proteins. *Science* 324, 744–746. doi: 10.1126/science.1171666

Tian, D., Peiffer, M., Shoemaker, E., Tooker, J., Haubruge, E., Francis, F., et al. (2012). Salivary glucose oxidase from caterpillars mediates the induction of rapid and delayed-induced defenses in the tomato plant. *PloS One* 7, e36168. doi: 10.1371/journal.pone.0036168

Villarroel, C. A., Jonckheere, W., Alba, J. M., Glas, J. J., Dermauw, W., Haring, M. A., et al. (2016). Salivary proteins of spider mites suppress defenses in *Nicotiana benthamiana* and promote mite reproduction. *Plant J.* 86, 119–131. doi: 10.1111/tpj.13152

Vos, P., Simons, G., Jesse, T., Wijbrandi, J., Heinen, L., Hogers, R., et al. (1998). The tomato *Mi-1* gene confers resistance to both root-knot nematodes and potato aphids. *Nat. Biotech.* 16, 1365–1369. doi: 10.1038/4350

Walling, L. L. (2000). The myriad plant responses to herbivores. *J. Plant Growth Regul.* 19, 195–216. doi: 10.1007/s003440000026

Walling, L. L. (2008). Avoiding effective defenses: strategies employed by phloem-feeding insects. *Plant Physiol.* 146, 859–866. doi: 10.1104/pp.107.113142

Wang, W., Dai, H., Zhang, Y., Chandrasekar, R., Luo, L., Hiromasa, Y., et al. (2015a). Armet is an effector protein mediating aphid-plant interactions. *FASEB J.* 29, 2032–2045. doi: 10.1096/fj.14-266023

Wang, W., Luo, L., Lu, H., Chen, S., Kang, L., and Cui, F. (2015b). Angiotensin-converting enzymes modulate aphid-plant interactions. *Sci. Rep.* 5, 8885. doi: 10.1038/srep08885

Wang, H., Shi, S., Guo, Q., Nie, L., Du, B., Chen, R., et al. (2018). High-resolution mapping of a gene conferring strong antibiosisto brown planthopper and developing resistant near-isogenic lines in 9311 background. *Mol. Breed.* 38, 107. doi: 10.1007/s11032-018-0859-1

Wang, Y., Tang, M., Hao, P., Yang, Z., Zhu, L., and He, G. (2008). Penetration into rice tissues by brown planthopper and fine structure of the salivary sheaths. *Entomol. Exp. Appl.* 129, 295–307. doi: 10.1111/j.1570-7458.2008.00785.x

Wang, Q., Yuan, E., Ling, X., Zhu-Salzman, K., Guo, H., Ge, F., et al. (2020). An aphid facultative symbiont suppresses plant defence by manipulating aphid gene expression in salivary glands. *Plant Cell Environ.* 43, 2311–2322. doi: 10.1111/pce.13836

Wang, N., Zhao, P., Ma, Y., Yao, X., Sun, Y., Huang, X., et al. (2019). A whitefly effector Bsp9 targets host immunity regulator WRKY33 to promote performance. *Philos. Trans. R. Soc Lond. B. Biol. Sci.* 374, 20180313. doi: 10.1098/rstb.2018.0313

Will, T., Furch, A. C., and Zimmermann, M. (2013). How phloem-feeding insects face the challenge of phloem-located defenses. *Front. Plant Sci.* 29. doi: 10.3389/fpls.2013.00336

Will, T., and Vilcinskas, A. (2015). The structural sheath protein of aphids is required for phloem feeding. *Insect Biochem. Mol. Biol.* 57, 34–40. doi: 10.1016/j.ibmb.2014.12.005

Wu, J., and Baldwin, I. T. (2010). New insights into plant responses to the attack from insect herbivores. *Annu. Rev. Genet.* 44, 1–24. doi: 10.1146/annurev-genet-102209-163500

Wu, D., Guo, J., Zhang, Q., Shi, S., Guan, W., Zhou, C., et al. (2022). Necessity of rice resistance to planthoppers for OsEXO70H3 regulating SAMSL excretion and lignin deposition in cell walls. *New Phytol.* 234, 1031–1046. doi: 10.1111/nph.18012

Wu, D., Qi, T., Li, W., Tian, H., Gao, H., Wang, J., et al. (2017). Viral effector protein manipulates host hormone signaling to attract insect vectors. *Cell Res.* 27, 402–415. doi: 10.1038/cr.2017.2

Xu, H., Qian, L., Wang, X., Shao, R., Hong, Y., Liu, S., et al. (2019). A salivary effector enables whitefly to feed on host plants by eliciting salicylic acid-signaling pathway. *Proc. Natl. Acad. Sci. U. S. A.* 116, 490–495. doi: 10.1073/pnas.1714990116

Yang, C., Guo, J., Chu, D., Ding, T., Wei, K., Cheng, D., et al. (2017). Secretory laccase 1 in *Bemisia tabaci* MED is involved in whitefly-plant interaction. *Sci. Rep.* 7, 3623. doi: 10.1038/s41598-017-03765-y

Ye, M., Glauser, G., Lou, Y., Erb, M., and Hu, L. (2019). Molecular dissection of early defense signaling underlying volatile-mediated defense regulation and herbivore resistance in rice. *Plant Cell* 31, 687–698. doi: 10.1105/tpc.18.00569

Ye, W., Yu, H., Jian, Y., Zeng, J., Ji, R., Chen, H., et al. (2017). A salivary EF-hand calcium-binding protein of the brown planthopper *Nilaparvata lugens* functions as an effector for defense responses in rice. *Sci. Rep.* 7, 40498. doi: 10.1038/srep40498

Zeng, J., Ye, W., Hu, W., Jin, X., Kuai, P., Xiao, W., et al. (2023). The N-terminal subunit of vitellogenin in planthopper eggs and saliva acts as a reliable elicitor that induces defenses in rice. *New Phytol.* 238, 1230–1244. doi: 10.1111/nph.18791

Zhang, Y., Liu, X., Francis, F., Xie, H., Fan, J., Wang, Q., et al. (2022a). The salivary effector protein Sg2204 in the greenbug *Schizaphis graminum* suppresses wheat defence and is essential for enabling aphid feeding on host plants. *Plant Biotechnol. J.* 20, 2187–2201. doi: 10.1111/pbi.13900

Zhang, Y., Liu, X., Fu, Y., Crespo-Herrera, L., Liu, H., Wang, Q., et al. (2022b). Salivary effector Sm9723 of grain aphid *Sitobion miscanthi* suppresses plant defense and is essential for aphid survival on wheat. *Int. J. Mol. Sci.* 23, 6909. doi: 10.3390/ijms23136909

Zhao, C., Escalante, L. N., Chen, H., Benatti, T. R., Qu, J., Chellapilla, S., et al. (2015). A massive expansion of effector genes underlies gall-formation in the wheat pest *Mayetiola destructor*. *Curr. Biol.* 25, 613–620. doi: 10.1016/j.cub.2014.12.057

Zhao, Y., Huang, J., Wang, Z., Jing, S., Wang, Y., Ouyang, Y., et al. (2016). Allelic diversity in an NLR gene *BPH9* enables rice to combat planthopper variation. *Proc. Natl. Acad. Sci. U. S. A.* 113, 12850–12855. doi: 10.1073/pnas.1614862113

Zheng, X., Zhu, L., and He, G. (2021). Genetic and molecular understanding of host rice resistance and *Nilaparvata lugens* adaptation. *Curr. Opin. Insect Sci.* 45, 14–20. doi: 10.1016/j.cois.2020.11.005

Zhou, W., Yuan, X., Qian, P., Cheng, J., Zhang, C., Gurr, G., et al. (2015). Identification and expression profiling of putative chemosensory protein genes in two rice planthoppers, *Laodelphax striatellus* (Fallén) and *Sogatella furcifera* (Horváth). *J. Asia Pac. Entomol.* 18, 771–778. doi: 10.1016/j.aspen.2015.09.006

Zhou, C., Zhang, Q., Chen, Y., Huang, J., Guo, Q., Li, Y., et al. (2021). Balancing selection and wild gene pool contribute to resistance in global rice germplasm against planthopper. *J. Integr. Plant Biol.* 63, 1695–1711. doi: 10.1111/jipb.13157

frontiers | Frontiers in Plant Science

TYPE Original Research
PUBLISHED 20 June 2023
DOI 10.3389/fpls.2023.1213257

OPEN ACCESS

EDITED BY
Shengli Jing,
Xinyang Normal University, China

REVIEWED BY
L. Peng,
Guizhou Normal University, China
Koji Miyamoto,
Teikyo University, Japan

*CORRESPONDENCE
Kai Liu
liukrice@163.com
Lei Zhou
yutian_zhou83@163.com
Aiqing You
aq_you@163.com

†These authors have contributed equally to this work and share first authorship

RECEIVED 27 April 2023
ACCEPTED 31 May 2023
PUBLISHED 20 June 2023

CITATION
Shi S, Zha W, Yu X, Wu Y, Li S, Xu H, Li P, Li C, Liu K, Chen J, Yang G, Chen Z, Wu B, Wan B, Liu K, Zhou L and You A (2023) Integrated transcriptomics and metabolomics analysis provide insight into the resistance response of rice against brown planthopper. *Front. Plant Sci.* 14:1213257. doi: 10.3389/fpls.2023.1213257

Integrated transcriptomics and metabolomics analysis provide insight into the resistance response of rice against brown planthopper

Shaojie Shi[1†], Wenjun Zha[1†], Xinying Yu[1], Yan Wu[1], Sanhe Li[1], Huashan Xu[1], Peide Li[1], Changyan Li[1], Kai Liu[1], Junxiao Chen[1], Guocai Yang[1], Zhijun Chen[1], Bian Wu[1], Bingliang Wan[1], Kai Liu[1*], Lei Zhou[1,2*] and Aiqing You[1,2*]

[1]Laboratory of Crop Molecular Breeding, Ministry of Agriculture and Rural Affairs, Hubei Key Laboratory of Food Crop Germplasm and Genetic Improvement, Food Crops Institute, Hubei Academy of Agricultural Sciences, Wuhan, China, [2]Hubei Hongshan Laboratory, Wuhan, China

Introduction: The brown planthopper (Nilaparvata lugens Stål, BPH) is one of the most economically significant pests of rice. The Bph30 gene has been successfully cloned and conferred rice with broad-spectrum resistance to BPH. However, the molecular mechanisms by which Bph30 enhances resistance to BPH remain poorly understood.

Methods: Here, we conducted a transcriptomic and metabolomic analysis of Bph30-transgenic (BPH30T) and BPH-susceptible Nipponbare plants to elucidate the response of Bph30 to BPH infestation.

Results: Transcriptomic analyses revealed that the pathway of plant hormone signal transduction enriched exclusively in Nipponbare, and the greatest number of differentially expressed genes (DEGs) were involved in indole 3-acetic acid (IAA) signal transduction. Analysis of differentially accumulated metabolites (DAMs) revealed that DAMs involved in the amino acids and derivatives category were down-regulated in BPH30T plants following BPH feeding, and the great majority of DAMs in flavonoids category displayed the trend of increasing in BPH30T plants; the opposite pattern was observed in Nipponbare plants. Combined transcriptomics and metabolomics analysis revealed that the pathways of amino acids biosynthesis, plant hormone signal transduction, phenylpropanoid biosynthesis and flavonoid biosynthesis were enriched. The content of IAA significantly decreased in BPH30T plants following BPH feeding, and the content of IAA remained unchanged in Nipponbare. The exogenous application of IAA weakened the BPH resistance conferred by Bph30.

Discussion: Our results indicated that Bph30 might coordinate the movement of primary and secondary metabolites and hormones in plants via the shikimate pathway to enhance the resistance of rice to BPH. Our results have important reference significance for the resistance mechanisms analysis and the efficient utilization of major BPH-resistance genes.

KEYWORDS

rice, brown planthopper, plant-insect interaction, multi-omics analysis, *Bph30*

Introduction

Rice (*Oryza sativa* L.) is the staple food for over 50% of population in the world (Zhang et al., 2018; Tan et al., 2020). BPH is widespread in Asia, Australia and South Pacific Islands and feeds on cultivar and several wild rice varieties (Jing et al., 2017; Zheng et al., 2021). BPHs consume the phloem sap of rice plants specifically, and their feeding activity on susceptible plants leads to the yellowing, browning, and drying of rice plants, eventually resulting in a phenomenon described as 'hopperburn' in the rice paddy (Jing et al., 2017; Tan et al., 2020). BPH can also serve as a vector for the spread of various viruses of rice, such as rice stunt viruses (Cheng et al., 2013; Sarao et al., 2016). The BPH has become the most serious pest that endangers rice production (Tan et al., 2020).

The application of chemical pesticides is one of the main strategies that has been used to control BPH infestation during the past 50 years (Du et al., 2020). However, BPHs have evolved resistance to most insecticides; this, coupled with the environmental pollution associated with insecticide use, has resulted in decreases in the use of chemical pesticides in several countries (Tamura et al., 2014; Du et al., 2020). Much effort is being made to develop the rice varieties resistant to BPH, which is considered an effective and environmentally benign method for the management of BPH (Du et al., 2020). To date, at least 41 resistance loci to brown planthopper have been discovered, and the BPH-resistance function of 17 genes has been experimentally confirmed (Muduli et al., 2021; Shi et al., 2021; Zhou et al., 2021). But, a lack of knowledge of the mechanisms by which these genes confer BPH resistance precludes their effective use for the breeding of rice varieties resistant to BPH. *Bph14* was the first cloned brown planthopper resistance gene in the world; this gene encodes a NLR protein. BPH14 enhances BPH resistance, through the reactive oxygen species (ROS) accumulation, salicylic acid (SA) signaling activation and the promotion of callose deposition in sieve tubes. (Du et al., 2009; Hu et al., 2017). BPH-resistance protein BPH6 mediates the activation of the SA, jasmonic acid (JA) and cytokinin (CK) signaling and promotes the deposition of callose in the phloem following infection of *Bph6*-containing plants with BPHs (Guo et al., 2018). Recently, a study showed that BPH6 interacts with the exocyst subunit OsEXO70H3 and *S*-adenosylmethionine synthase-like protein (SAMSL), promotes SAMSL secretion, increases the content of lignin in the cell wall, and enhances BPH resistance (Wu et al., 2022). The results of the above studies suggest that the BPH resistance conferred by several major BPH-resistance genes in rice is mediated by various resistance pathways.

High-throughput omics approaches have made substantial contributions to the complex mechanisms analysis of key BPH-resistance genes. High-throughput RNA sequencing have revealed that the BPH resistance conferred by *Bph15* is related to plant hormones, transcription factors, receptor kinase, protein post translational modifications, mitogen-activated protein kinase cascades, Ca^{2+} signaling and pathogenesis-related protein. (Lv et al., 2014). A subsequent microRNA sequencing analysis has revealed 23 differentially expressed miRNAs between 9311 and 9311-*Bph15*-NIL following BPH feeding, which targeted to those genes involved in abiotic and biotic stimuli, regulation of plant hormones, cellulose biosynthesis, amino acid synthesis, and protein folding, that mainly related to BPH resistance. (Wu et al., 2017). A total of 24 DEGs have been identified in both the *Bph6*-transgenic plants and Nipponbare plants following BPH infestation, whose expression trends in the two materials were opposite and considered BPH resistance-related (Tan et al., 2020). Multiple differentially accumulated metabolites (DAMs) can be detected in plants using metabolomic approaches (Alamgir et al., 2016; Peng et al., 2016; Liu et al., 2017). DAMs between TN1 rice plants, which are susceptible to BPH, and *Bph15*-containing plants, are involved in the shikimate pathway, and these metabolites are exclusively enriched in *Bph15*-containing plants (Peng et al., 2016). Thus, the *Bph15* gene might enhance BPH resistance through its effects on the shikimate pathway (Peng et al., 2016). Analysis of lipid profiles has revealed that BPH feeding activity promotes phytol and wax metabolism in *Bph6*-transgenic plants, which indicates that these metabolites play key roles in the responses of *Bph6* to BPH infestation (Zhang et al., 2018). Most previous studies examining the mechanisms underlying the BPH resistance conferred by key BPH-resistance genes have used omics approaches to characterize differences in gene expression or changes in metabolites in rice materials following BPH feeding. By contrast, few studies have used combined transcriptome and metabolome analyses to systematically study the mechanisms by which key BPH-resistance genes confer BPH resistance.

Primary and secondary (or specialized) metabolites, as well as plant hormones were the three main groups of metabolites in the

plant kingdom (Erb and Kliebenstein, 2020). Such as amino acids, which belong to primary metabolites, are required for plant growth. Meanwhile primary metabolites are important nutrient sources for invaders as well; these metabolites are thus involved in the responses of plants to biotic stress (Abood and Lösel, 2003; Solomon et al., 2003; Jobic et al., 2007). Secondary metabolites mediate plant-environment interactions (Hartmann, 2007). For example, the production of serotonin is induced by BPH infestation, and the inhibition of serotonin production improved rice's ability to resist BPH (Lu et al., 2018). Flavonoids are the most studied secondary metabolites of crops that are toxic to insects, such as rutin, kaempferol, tricin and quercetin can effectively prevent pests damage to plants (Zhang et al., 2017; Aboshi et al., 2018; Su et al., 2021). Phytohormones also play key roles in plants counteract to external stress. In the early immune response, a complex hormone signaling network is induced by infections caused by invaders (Chen et al., 2021). JA and SA are the two major immune-related phytohormones in plants response to biotic stress (Zhao et al., 2016; Zhang and Li, 2019; He et al., 2020). Other phytohormones, such as CK, ethylene and abscisic acid (ABA) were also reported to be involved in plant defense (Erb et al., 2009; Dervinis et al., 2010; Hu et al., 2011). Primary metabolism, secondary metabolism, and plant hormones are closely linked in plants, and they comprise an efficient defense system for coping with environmental stress (Erb and Kliebenstein, 2020; Chen et al., 2021). However, most previous studies examining the mechanisms of resistance conferred by major BPH-resistance genes have focused on only one aspect of this defense system (Zhao et al., 2016; Lu et al., 2018; Zhang et al., 2018).

Bph30 gene has been cloned from the BPH-resistance rice variety AC-1613 by map-based cloning. BPH30 protein contains two leucine-rich domains (LRDs), enhances the sclerenchyma stiffer and thicker, granting rice resistance to five biotypes of BPH and WBPH (white-backed planthopper). But, the molecular mechanisms by which *Bph30* confers BPH resistance for rice were poorly cleared. Here, we conducted a joint analysis of transcriptome and metabolome to characterize the response of *Bph30* to BPH infestation. Our results revealed that the shikimate pathway, amino acid biosynthesis, phenylpropanoid metabolism, flavonoids, lignin and indole 3-acetic acid (IAA) biosynthesis, and IAA signal transduction were involved in the mechanism of *Bph30*-mediated BPH resistance. We also validated the negative role of IAA in *Bph30*-mediated resistance to brown planthopper. Our results provide a comprehensive overview of the sophisticated mechanism in *Bph30* responses to BPH infestation and will aid the utilization of major BPH-resistance genes in breeding programs aimed at the development of BPH-resistant rice varieties.

Materials and methods

Plants and insects

In this study, we mainly used two types of rice materials. Nipponbare was the BPH-susceptible model variety and the genetically modified background material. BPH30T was *Bph30*-transgenic plants, which was constructed by transforming the *Bph30* genome that cloned from BPH-resistance rice AC-1613 into the Nipponbare background, as previous description (Shi et al., 2021).

The brown planthopper used in this study was a population captured from the rice field in Wuhan, China, and bred on BPH-susceptible TN1 variety for multiple generations. The feeding conditions are 26°C ± 0.5°C, 16-h-light/8-h-dark cycle in Wuhan University (Jing et al., 2012).

BPH resistance evaluation of rice

Evaluation method for phenotypic resistance of rice varieties to brown planthopper was described as previously (Huang et al., 2001; Du et al., 2009). In brief, approximately 15-20 seeds with consistent germination were sown in a circular plastic cup (10-cm-diameter). After 2 weeks of growth, approximately three-leaf stage, infested with BPH according to the standard of 10 insects per seedling. Observed the phenotype of seedlings every day until the susceptible Nipponbare control died (a resistance assay score of 9) or the experimental materials shown the damaged phenotype, each seedling was assigned a resistance score, as described previously (Huang et al., 2001). Three replications were conducted.

Measurement of BPH honeydew excretion and weight gain

The measuring method of BPH honeydew excretion and weight gain was as described previously (Shi et al., 2021). The rice seedlings used in this assay were four-leaf stage. The BPHs used in this assay were the newly emerged short winged female insects. Firstly, the weight of BPHs and parafilm sachets were measured. Then, fixed the pre-weighed parafilm sachet to the base of the rice seedlings, and enclosed one known weight brown planthopper into one parafilm sachet for free feeding for 48 h. Finally, removed the brown planthoppers and the parafilm sachets, and measured the weight of the brown planthopper and the parafilm sachets after feeding. The difference in BPHs weight between before and after feeding was weight gain, and the difference in weight of parafilm sachets before and after BPH feeding was honeydew excretion. 15 replicates were used for analysis in each experiment.

RNA isolation and genes expression analysis

The outermost leaf sheaths of rice seedlings were peeled off and ground into powder in liquid nitrogen immediately. The total RNA was extracted from the tissue powder using TRIzol reagent. Reverse transcription of RNA into cDNA using PrimeScrip RT Reagent Kit (Takara, RR047Q). Application of SYBR Green PCR Master Mix (Applied Biosystems) on CFX96 Real-Time System (Bio-Rad) for

gene expression detection. Each group of samples contained 3 biological replicates. *OsActin1* was selected as the internal reference gene and calculated the expression level of genes using $2^{-\Delta\Delta C(t)}$ method. The rice seedlings used in this experiment were at four-leaf stage. Primer sequences used in this section were listed in Supplementary Table 13.

Construction of the cDNA library and RNA sequencing

The leaf sheaths of Nipponbare and BPH30T at four-leaf stage were used for RNA-sequence. The method of sample preparation: each seedling was fed with 10 brown planthopper nymphs for 48 h as the experimental groups and seedlings not fed by brown planthopper as control groups; the outermost leaf sheaths of seedlings in both the experimental and control groups were simultaneously peeled off and stored in dry ice for subsequent processing. Each treatment contained three biological replicates. The isolation of total RNA, generation of sequencing libraries and RNA sequencing were conducted by Shanghai Personal Biotechnology Co., Ltd.

RNA mapping and differential expression analysis

The low-quality and adaptor sequences were filtered out from raw reads using Trimmomatic and the clean reads were obtained. Then aligned the clean reads to the reference genome Os-Nipponbare version IRGSP-1.0 (annotation version 2022-09-01, https://rapdb.dna.affrc.go.jp/download/irgsp1.html) with Hisat2. The expression level of genes was measured by transcripts per Million (TPM). DESeq2 R package were used for the screening of differentially expressed genes (DEGs), the threshold of screening was $|\log_2$ (Fold Change)$|\geq 1$ and False discovery rate (FDR) ≤ 0.05.

Function analysis of DEGs

DEGs obtained through the above method, were compared to the whole-genome background with hypergeometric test for Gene Ontology (GO) and Kyoto Encyclopedia of Genes and Genomes (KEGG) functional analysis. The hypergeometric test was corrected by Benjamini and Hochberg false discovery rate and the significance threshold is 0.05.

Metabolites analysis

The samples used in metabolomic analysis were the leaf sheaths of Nipponbare and BPH30T at four-leaf stage. The outmost leaf sheath was quickly peeled off and stored in dry ice and sent to Wuhan Maiwei Biotechnology Company for samples pretreatment, metabolites extraction, detection, qualitative, quantitative, and differentially accumulated metabolites (DAMs) analysis. The ultra performance liquid chromatography-tandem mass spectrometry (UPLC-MS/MS) was used to detect the extracted metabolites. The threshold of variable importance in projection (VIP) ≥ 1 and $|\log_2$ (Fold Change)$| \geq 1$ was used for detecting DAMs in two-group analysis.

PCA computational method

In this study, the statistics function prcomp within R (www.r-project.org) was used to conduct principal component analysis (PCA). Before PCA, the data was unit variance scaled.

Metabolites annotation and enrichment analysis

Metabolites identified were annotated by comparing with KEGG compound database (http://www.kegg.jp/kegg/compound/). The metabolic pathways that mapped by annotated metabolites were screened out from KEGG pathway database (http://www.kegg.jp/kegg/pathway.html). Then, the metabolite sets enrichment analysis on metabolic pathways labeled with significantly different metabolites were performed using $p \leq 0.05$ as the significance threshold.

IAA content measurements

The IAA contents of the outermost leaf sheaths of rice seedlings at four-leaf stage were measured. Firstly, the leaf sheaths were peeled off and ground into powder in liquid nitrogen and IAA that in 0.2 g sample powder, was extracted by acetonitrile solution. Then, add 50 mg C18 filler to the acetonitrile solution that dissolved IAA, mix well, centrifuge, take the supernatant, and blow dry with nitrogen gas. Finally, add 200 μl methanol to the sediment for complete dissolution, filtered with 0.22 μm organic phase filter membrane, and the IAA content was detected by HPLC-MS/MS at Nanjing Webiolotech Biotechnology Co., Ltd.

IAA treatment

Prepare the Indole 3-acetic acid (IAA, I2886, Sigma-Aldrich) solution with a concentration of 1μm. Then the BPH30T seedlings were sprayed with IAA solution. After two hours, BPH were released on the seedlings.

Data analysis

All data in this study were statistically analyzed using one-way analysis of variance with PASW Statistics version 18.0.

Results

Evaluation of the resistance of *Bph30*-transgenic (BPH30T) rice plants to BPH infestation

Previous study has indicated that *Bph30* has strong resistance to brown planthopper (Shi et al., 2021). In this study, the phenotype of *Bph30* was verified using *Bph30*-transgenic plants (BPH30T) that with Nipponbare genetic background and contain the genomic fragment of *Bph30* with its native promoter. In the bulk seedling test, when the BPH-susceptible variety Nipponbare all die caused by brown planthopper feeding, the BPH30T plants grow well (Figure 1A). Honeydew excretion and weight gain of BPHs that fed on Nipponbare for 48 h were significantly greater than that fed on BPH30T plants (Figures 1B, C). The survival rate of BPHs after 2 days was significantly higher when they fed on Nipponbare plants than that fed on BPH30T plants (Figure 1D). In addition, host-choice tests revealed that a significantly higher number of BPHs settled on Nipponbare than that settled on BPH30T plants from 3-72 h following the release of BPHs (Figure 1E). These findings suggested that BPH30T plants were highly resistant to BPH.

Previous study has shown that BPH30 enhances the strength of cell wall by promoting the cellulose and hemicellulose biosynthesis (Shi et al., 2021). Cellulose synthesis-related genes, *BC15* (*Os09g0494200*, brittle culm 15), *CESA7* (*Os10g0467800*, cellulose synthase 7), *CSLF4* (*Os07g0553300*, cellulose synthase-like F 4) and hemicellulose synthesis-related gene, *IRX9* (*Os07g0694400*, irregular xylem 9), were selected for expression analysis in Nipponbare and BPH30T plants. Our findings indicated that the expression of cellulose and hemicellulose synthesis-related genes was significantly lower in Nipponbare, before and after BPH feeding, than that in BPH30T plants (Supplementary Figure 1).

Transcriptomic analysis of Nipponbare and BPH30T response to BPH feeding activity

To clarify the mechanism by which *Bph30* confers BPH resistance, RNA sequencing analysis was conducted using leaf sheaths from Nipponbare and BPH30T plants before (S0 and R0) and after BPH feeding for 48 h (S48 and R48). The total number of raw reads generated ranged from 20,579,084 to 28,035,649 for each library. The clean reads ranged from 19,514,119 to 26,954,105, with an average Q30 score of 92.10% to 95.33%, after filtering out adapters, low-quality and uncertain reads. Then, the clean reads were aligned to the genome of Nipponbare (https://rapdb.dna.affrc.go.jp/download/irgsp1.html). The matching rate

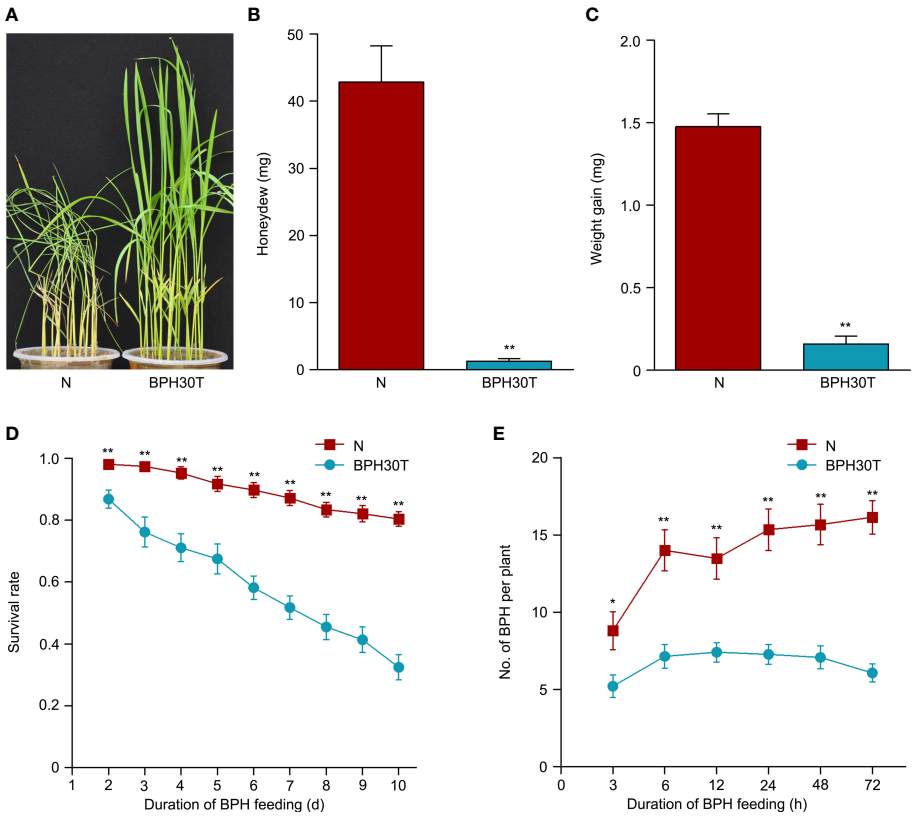

FIGURE 1
BPH resistance evaluation of BPH30T and Nipponbare plants. **(A)** Seedling test identified the phenotype of resistance to BPH of *Bph30*-transgenic plants (BPH30T) and Nipponbare (N). **(B)** The secretion of honeydew by BPH after feeding on BPH30T and N for 48 h. **(C)** BPH weight gain after feeding on BPH30T and N for 48 h. **(D)** Survival rate of BPH feeding on BPH30T and N. **(E)** Selectivity of brown planthopper in BPH30T and N. In **(B–E)**, data represent the means ± SEM. Asterisks indicate significant differences (*represent $p < 0.05$, **represent $p < 0.01$).

ranged from 92.47% to 98.63% for Nipponbare and BPH30T plants (Table 1). Correlation analysis between intra-group samples revealed high correlations among the three replicates within groups, suggesting that the repeatability of the biological replicates and the accuracy of the RNA-seq data were high (Supplementary Figure 2).

To characterize transcriptional-level changes in the two cultivars induced by BPH feeding activity, we conducted an analysis of DEGs, which were identified using the following criteria: $|\log_2 (\text{Fold Change})| \geq 1$ and FDR ≤ 0.05. There were 3,407 DEGs identified in the S0 vs S48 comparison group, including 912 DEGs that up-regulated expression in S48 and 2,495 DEGs that down-regulated in S48 (Supplementary Table 1; Supplementary Figure 3). A total of 4,313 DEGs were detected in the R0 vs R48 comparison group, including 1,264 DEGs that up-regulated expression in R48 and 3,049 DEGs down-regulated in R48 (Supplementary Table 2; Supplementary Figure 3). To elucidate the molecular mechanisms of the DEGs, we carried out the Gene Ontology (GO) and Kyoto Encyclopedia of Genes and Genomes (KEGG) analyses using those DEGs. The results of GO enrichment analysis revealed that the DEGs identified in Nipponbare plants following BPH feeding were mainly enriched in the following GO terms: cellular carbohydrate metabolic process, response to oxidative stress, cellular polysaccharide metabolic process, lignin catabolic and metabolic process, phenylpropanoid catabolic process, phenylpropanoid metabolic process, and so on in the biological process, transferase and peroxidase activity in molecular function and apoplast, extracellular region in cellular component category. However, the DEGs identified in BPH30T plants following BPH infestation were mainly enriched in the following GO terms: single-organism metabolic process, lipid localization, and lipid transport in the biological process; ion and cation binding, oxidoreductase and lyase activity in the molecular function; apoplast, extracellular region and so on in cellular component category (Figure 2; Supplementary Tables 3, 4). KEGG pathway analysis revealed that the DEGs in the two rice varieties following BPH feeding were enriched in phytohormone signal transduction; benzoxazinoid, suberine, cutin, phenylpropanoid and wax biosynthesis; starch, sucrose and cyanoamino acid metabolism. However, the expression of DEGs enriched in biosynthesis of flavonoids were down-regulated in Nipponbare, as well as the DEGs involved in the sesquiterpenoid and triterpenoid biosynthesis, which were involved in the mechanism of indirect defense against BPHs in rice plants, were also down-regulated in Nipponbare (Kamolsukyeunyong et al., 2021). In BPH30T plants, we found that the DEGs enriched in the biosynthesis pathway of amino acid and carbon fixation, which are the sources of the most important nutrients for BPHs, was down-regulated (Figure 3; Supplementary Table 5).

These findings indicated that the responses of Nipponbare plants and BPH30T plants to BPH feeding activity differed. We speculate that the synthesis of toxic and defensive secondary metabolites is reduced in Nipponbare plants following BPH feeding activity, which facilitated the maintenance of normal primary metabolic processes, as well as the success of infection by BPHs. However, the synthesis of primary metabolites is reduced in BPH30T plants, which facilitates the synthesis of toxic and defensive secondary metabolites and impedes BPH infection.

Identification of DEGs involved in BPH resistance

Venn diagrams were made to identify unique and overlapped DEGs in Nipponbare and BPH30T plants to clarify changes in transcription level. A total of 1,677 DEGs, which including 1,067 DEGs were up-regulated and 610 DEGs were down-regulated expression, were detected in Nipponbare following BPH feeding. 2,583 DEGs were identified in BPH30T plants following BPH infestation activity, which contained 1,621 DEGs that were up-regulated and 962 DEGs down-regulated. There were 302 up-regulated and 1,248 down-regulated DEGs overlapped in two varieties during BPH infestation (Figure 4A). In the overlapped

TABLE 1 Statistics of sequencing reads and alignment to the reference genome.

Sample	Raw reads	Clean reads	Q30 (%)	Percentage of alignment (%)
S0-1	26,175,802	24,656,295	93.69	97.35
S0-2	23,155,745	21,869,050	94.12	97.64
S0-3	23,612,057	22,159,036	93.10	97.26
S48-1	20,579,084	19,514,119	94.53	92.47
S48-2	22,683,817	21,301,586	93.30	97.65
S48-3	22,087,338	20,685,803	92.10	92.32
R0-1	23,000,390	21,694,021	94.60	97.77
R0-2	21,083,323	19,928,730	94.19	97.78
R0-3	23,379,633	21,994,210	93.81	97.88
R48-1	22,866,552	21,546,357	93.58	98.49
R48-2	25,583,036	24,136,491	93.93	98.44
R48-3	28,035,649	26,954,105	95.33	98.63

S0, R0, S48 and R48 represent the Nipponbare (S) and BPH30T (R) before (S0 and R0) and after BPH feeding for 48 h (S48 and R48) respectively. 1, 2, 3 represent the three biological repeats.

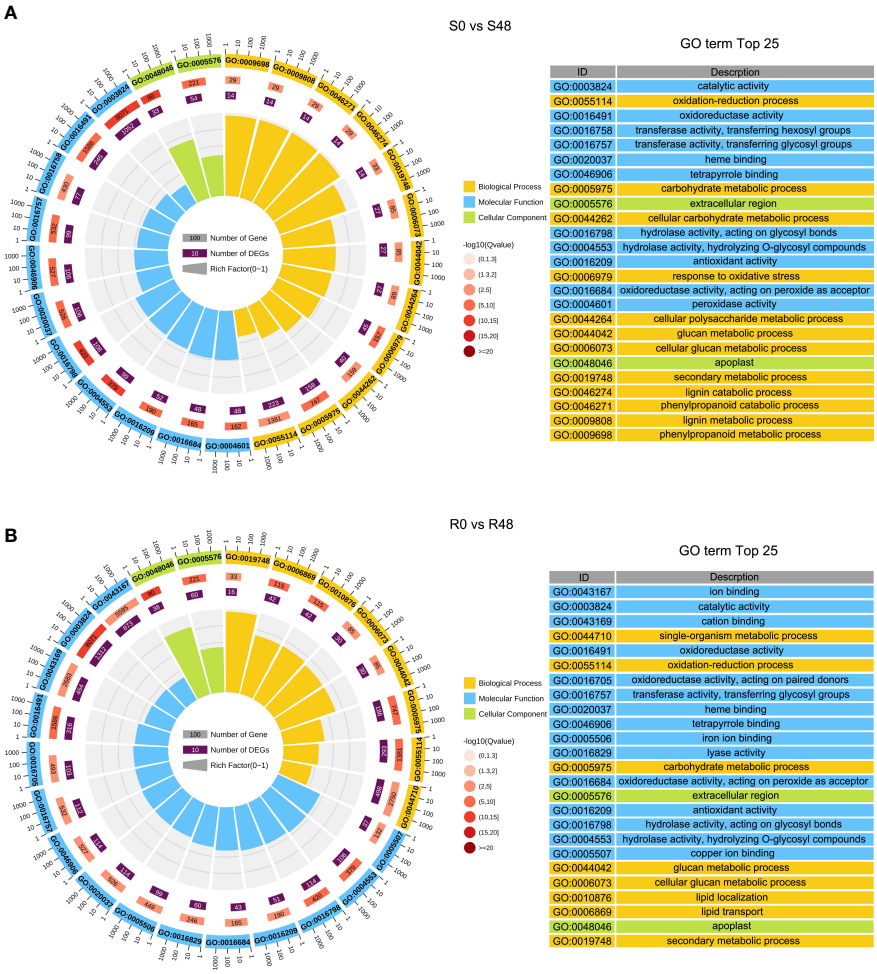

FIGURE 2
GO (Gene Ontology) enrichment analysis of DEGs detected from S0 vs S48 and R0 vs R48 groups. **(A, B)** GO analysis of DEGs in S0 vs S48 **(A)** and R0 vs R48 **(B)**. S0, R0, S48 and R48 represent the Nipponbare (S) and BPH30T (R) before (S0 and R0) and after BPH feeding for 48 h (S48 and R48) respectively. Outer ring, GO terms; second ring, the number of genes enriched into each GO term in the whole genome; third ring, number of genes detected in this study enriched in each GO term; fourth ring, rich factor. The spacing between two lines in the background represents 0.1. .

DEGs sets, we found the expression of several biotic stress related genes exhibited similar changing trend in response to BPH feeding. Such as WRKY transcription factors, *OsWRKY45*, *OsWRKY62*, *OsWRKY65*, *OsWRKY104*, *OsWRKY114*; the gene encoding E3 ligases, *OsBBI1*; NPR1-like gene, *OsNPR3*; all of which were reported involved in plant resistance (Peng et al., 2008; Li et al., 2011; Huangfu et al., 2016; Jiang et al., 2020; Son et al., 2020; Chen et al., 2022; Son et al., 2022). Those findings indicated there may be a common foundational defense mechanism in resistant and susceptible rice varieties to response brown planthopper infestation. But, unique DEGs in Nipponbare and BPH30T plants might affect susceptibility and resistance of *Bph30* to BPHs. KEGG analysis showed these unique DEGs were enriched in different pathways in Nipponbare and BPH30T plants (Supplementary Tables 1, 2). In Nipponbare plants, the unique DEGs were mainly enriched in the following KEGG pathways: flavonoid, phenylpropanoid, cutin, suberine and wax biosynthesis; ABC transporters and plant hormone signal transduction. In BPH30T plants, the unique DEGs were mainly enriched in the metabolic pathways; biosynthesis of amino acids, secondary metabolites, phenylalanine, tyrosine and tryptophan; carbon fixation in photosynthetic organisms (Figure 4B).

Plant hormone signals play key roles in plant-insect interaction, and the pathway of plant hormone signal transduction was only enriched in Nipponbare. To characterize differences in plant hormone signal transduction between Nipponbare and BPH30T plants following BPH feeding activity, a heat map was made using DEGs involved in this pathway. The greatest number of genes were involved in IAA signal transduction (Figure 4C). Most of these DEGs were down-regulated in both Nipponbare and BPH30T, but the extent to which these genes were down-regulated differed in Nipponbare and BPH30T plants, indicating that IAA might play a role in mediating BPH resistance conferred by *Bph30*.

Metabolomic analysis of rice during the response to BPH feeding activity

To further reveal the response of *Bph30* to brown planthopper feeding at the molecular level. We extracted the total metabolites from

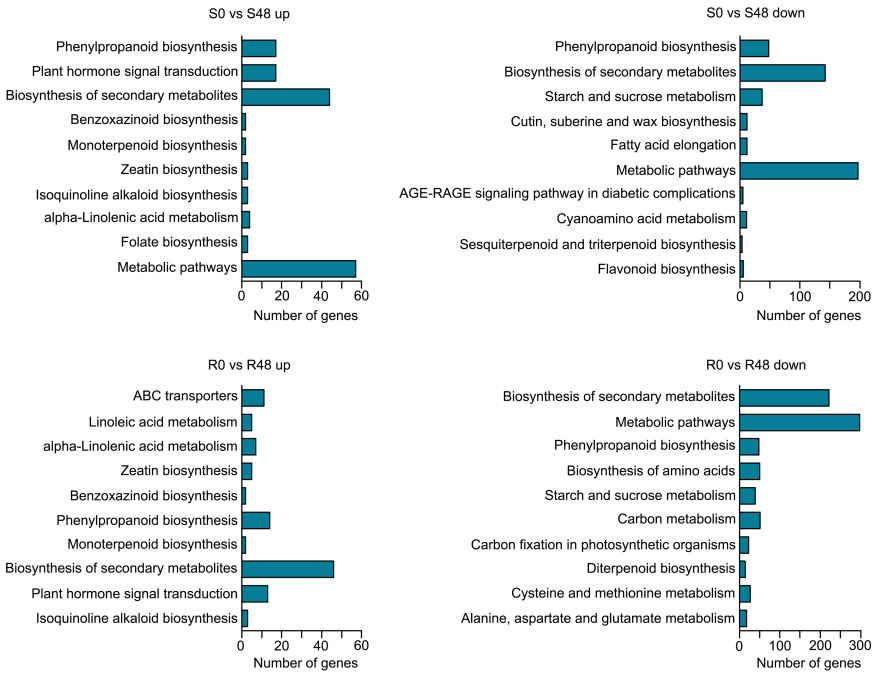

FIGURE 3
KEGG functional analysis of DEGs from the two varieties after BPH feeding compared with unfed control. Enriched KEGG pathways of up-regulated DEGs in Nipponbare and BPH30T (S0 vs S48 up, R0 vs R48 up) and down-regulated DEGs in Nipponbare and BPH30T after BPH feeding for 48 h (S0 vs S48 down, R0 vs R48 down).

Nipponbare and BPH30T plants leaf sheaths before BPH feeding and after BPH infestation for 48 h, and conducted the analysis of metabolite changes in the two rice varieties using UPLC-MS/MS. 1,198 metabolites from 11 different classes were detected (Supplementary Table 6). Coumaroylquinic acid, neochlorogenic acid, eudesmic acid, D-glucopyranoside, D-Glucurono-6,3-lactone, erythorbic acid, 2,4-Dihydroxybenzaldehyde, 4-Hydroxybenzoylmalic acid, apigenin-7-O-glucoside and 3,4-Dimethoxycinnamic acid were the first 10 metabolites that had the largest positive or negative loading values for PC1 in the principal component analysis (PCA). The results of PCA also illustrated differences among groups, biological replicates from the same group were clustered (Figure 5A), suggesting that the metabolite data were reproducible and suitable for subsequent data analyses.

There were 58 DAMs that were detected in Nipponbare plants, in the S0 vs S48 comparison group using $|\log_2$ (Fold Change)$| \geq 1$ and VIP ≥ 1 as the filtering criteria; 24 and 34 of these DAMs were up-regulated and down-regulated, respectively (Figure 5B; Supplementary Table 7). A total of 88 DAMs were detected in BPH30T plants in the R0 vs R48 comparison group, and 43 and 45 of these DAMs were up-regulated and down-regulated, respectively (Figure 5B; Supplementary Table 8). To clarify the functions of DAMs detected from both Nipponbare and BPH30T plants following BPH infestation, we carried out the KEGG enrichment analysis on those DAMs. The DAMs that detected from Nipponbare, were significantly enriched in the KEGG functional pathways of arginine biosynthesis, arachidonic acid metabolism, ABC transporters, glutathione metabolism, biosynthesis of amino acids, and betalain biosynthesis. In BPH30T plants, DAMs were enriched in several KEGG pathways, including glutathione metabolism, nicotinate and nicotinamide metabolism, arginine and proline metabolism, benzoxazinoid biosynthesis, caffeine metabolism, and diterpenoid biosynthesis (Figure 5C; Supplementary Tables 9, 10). These findings indicated that metabolites including primary and secondary metabolites altered greatly in both BPH-susceptible Nipponbare and BPH-resistance BPH30T plants, however, the number of DAMs and the enriched pathways identified in Nipponbare and BPH30T plants were distinct, suggesting that their responses to BPH infestation differed.

Identification of metabolites that mediate BPH resistance

Venn diagrams were made to identify the unique and common DAMs in Nipponbare and BPH30T plants to clarify changes in metabolites. A total of 13 compounds were detected in both Nipponbare and BPH30T plants in the S0 vs S48 and R0 vs R48 comparison groups, including two amino acids and derivatives, one organic acid, four nucleotides and derivatives, four alkaloids, and two other compounds. In Nipponbare plants, 45 unique DAMs were identified, including 16 and 29 DAMs that were up-regulated and down-regulated, respectively. In BPH30T plants, 75 unique DAMs were identified, including 35 and 40 DAMs that were up-regulated and down-regulated, respectively (Figure 6A; Supplementary Table 11).

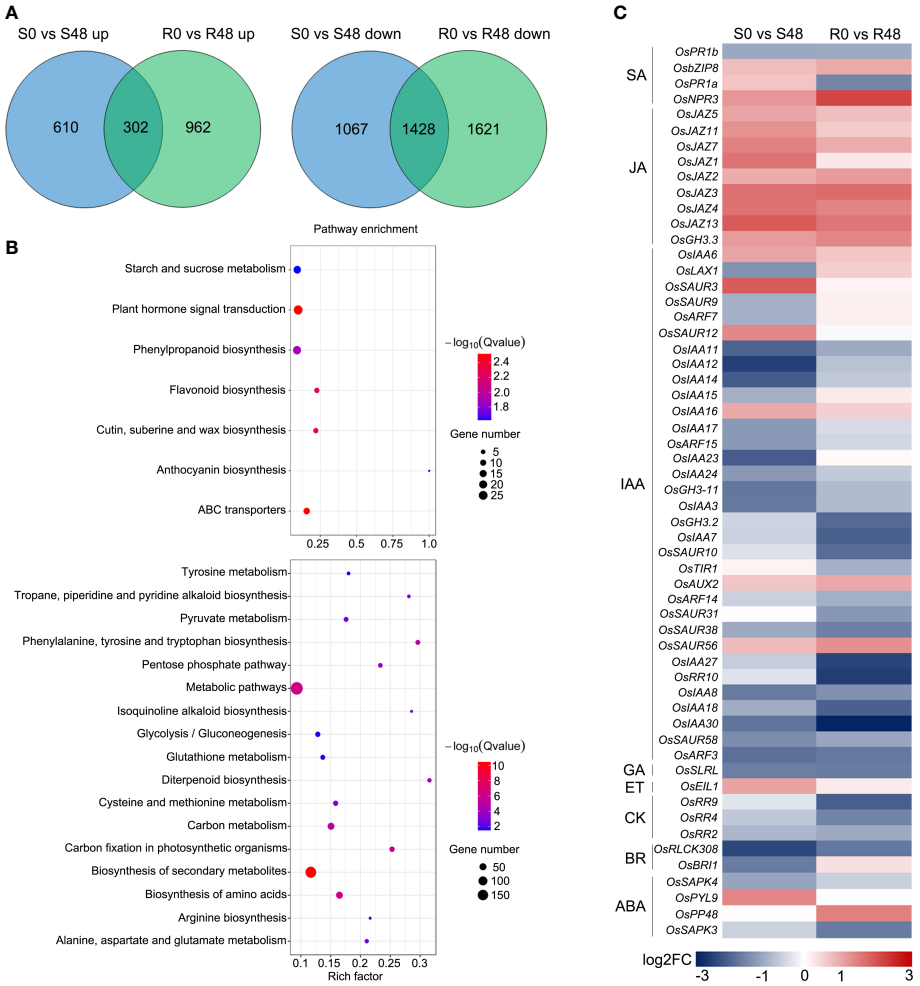

FIGURE 4
Unique DEGs identified from the two rice varieties after BPH infestation. **(A)** Venn diagrams illustrated the unique DEGs in two rice varieties before and after fed by brown planthopper. **(B)** KEGG pathway analysis of the unique DEGs from Nipponbare (up) and BPH30T (down) fed by BPH for 48 h. **(C)** Heat map displayed the unique DEGs related to plant hormone signal transduction in two comparison groups.

A heat map was made to characterize differences and patterns of variation in the 120 DAMs identified in Nipponbare and BPH30T plants. DAMs were identified from the following 11 classes: terpenoids, phenolic acids, flavonoids, nucleotides and derivatives, amino acids and derivatives, organic acids, lipids, others, lignans and coumarins, steroids, and alkaloids. Variation in primary metabolites, including nucleotides and derivatives, organic acids, and lipids, was similar among Nipponbare and BPH30T plants. But DAMs belonged the amino acids and derivatives class were down-regulated in BPH30T plants following BPH infestation. Variation in secondary metabolites such as phenolic acids, terpenoids, steroids, lignans, and coumarins and alkaloids, was not pronounced between Nipponbare and BPH30T plants. However, most DAMs in the flavonoid class showed an upward trend in *Bph30*-transgeneic plants, but down-regulated significantly in Nipponbare (Figure 6B; Supplementary Figure 4). These findings suggested that both amino acid and flavonoid metabolites might be involved in mediating the resistance to BPHs conferred by *Bph30*.

Joint analysis of transcriptome and metabolome

To further characterize the control system of *Bph30* against brown planthopper feeding, we conducted a combined transcriptomic and metabolomic analysis of data from Nipponbare and BPH30T plants. KEGG functional analysis revealed some common functional pathways were enriched in by the two varieties. Such as, cyanoamino acid metabolism and glutathione metabolism, which DEGs and DAMs detected in the both varieties were enriched in. The pathways related in flavonoid biosynthesis, plant hormone signal transduction, ABC transporters, betalain biosynthesis, tyrosine metabolism and isoquinoline alkaloid biosynthesis were only enriched in Nipponbare, while, amino acid biosynthesis, phenylpropanoid biosynthesis, starch and sucrose metabolism, alanine, aspartate and glutamate metabolism, diterpenoid biosynthesis, cysteine and methionine metabolism, and so on, were specifically enriched in BPH30T plants. These findings showed that primary and secondary

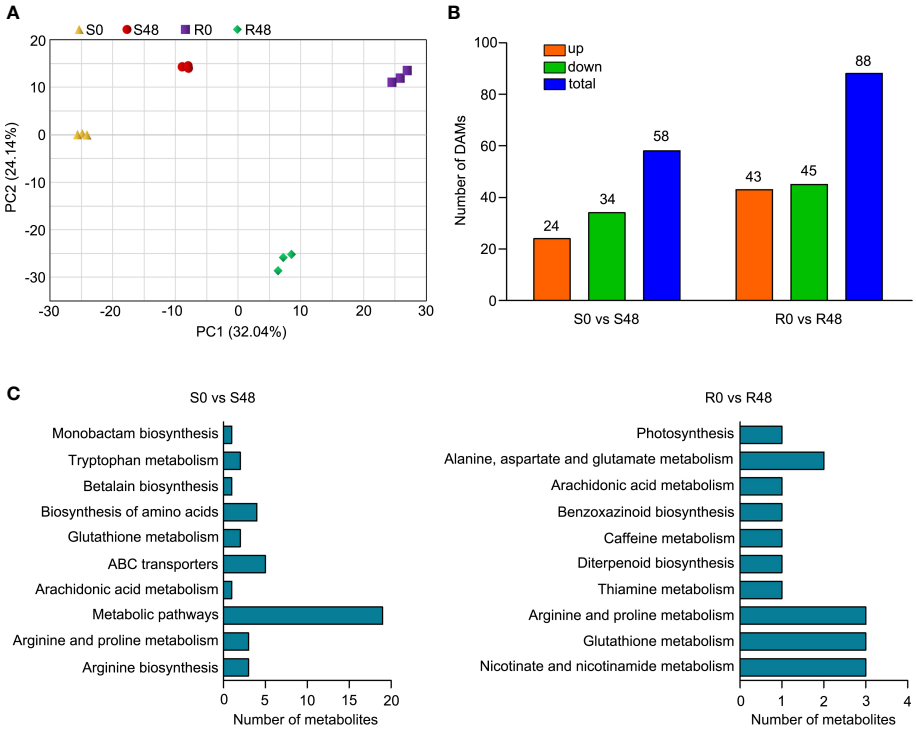

FIGURE 5
Differentially accumulated metabolites (DAMs) identified from the two rice varieties after BPH feeding for 48 h. **(A)** Principal component analysis (PCA) plots of total detected metabolites of S0, S48, R0 and R48. **(B)** The numbers of total, up- and down-regulated DAMs in two comparison groups. **(C)** KEGG pathway analysis of the DAMs in Nipponbare and BPH30T fed by BPH for 48 h.

metabolic processes were activated in both varieties during BPH feeding, but the direction of metabolite transformation were significant different (Figure 7; Supplementary Table 12). The functional analysis also showed that the DEGs and DAMs detected in Nipponbare plants were mainly related to flavonoid biosynthesis and plant hormone signal transduction; by contrast, DEGs and DAMs in BPH30T plants were mainly enriched in amino acid biosynthesis and phenylpropanoid biosynthesis, suggesting those metabolic pathways mentioned above might play a vital role in mediating the BPH resistance conferred by *Bph30*.

The phenylpropanoid metabolism pathway was only enriched in BPH30T plants; this pathway plays key roles in plant growth and development, as well as the interactions between plant and environment (Dong and Lin, 2021). In this pathway, phenylalanine is converted to cinnamic acid by phenylalanine ammonia-lyase (PAL) firstly, then, cinnamic acid is converted to *p*-cinnamic acid by cinnamic acid 4-hydroxylase (C4H), finally, *p*-cinnamic acid is converted into *p*-coumaroyl-CoA by 4-coumarate-CoA ligase (4CL). Next, *p*-coumaroyl-CoA will enter two different metabolic pathways. One of the pathways is the flavonoids biosynthesis, the first step of this pathway is chalcone synthase (CHS) catalyze *p*-coumaroyl-CoA to naringenin chalcone. The other one is hydroxycinnamoyl-CoA shikimate/quinate hydroxycinnamoyl transferase (HCT) catalyze *p*-coumaroyl-CoA convert into *p*-coumaroyl shikimate, entering lignin biosynthetic pathway. In the phenylpropanoid metabolism pathway, up-regulation of one PAL gene (*Os02g0627100*) expression induced by brown planthopper feeding in BPH30T plants specifically. The expression of another PAL gene (*Os04g0518400*) was up-regulated in both Nipponbare and BPH30T plants, but the expression of this gene was up-regulated to a greater degree in the latter than in the former (Figure 8), indicating more initial compound (*p*-coumaroyl-CoA) were provided for the downstream secondary metabolic processes in *Bph30*-transgeneic plants after BPH infestation.

In the flavonoid biosynthesis pathway, the expression of one chalcone isomerase (CHI) gene (*Os12g0115700*) and two flavonoid 3'-hydroxylase (F3'H) genes (*Os03g0367101* and *Os10g0317900*) was down-regulated in Nipponbare plants; however, no changes in the expression of these genes were observed in BPH30T plants (Figure 8). Thus, we speculate that BPHs inhibit flavonoid synthesis, which increases the susceptibility of rice plants to infection when BPHs feed on rice plants lacking *Bph30*; the expression of *Bph30* maintains the normal synthesis of flavonoids under BPH infection in BPH30T plants, which impedes BPH infestation. In lignin biosynthesis, the expression of one cinnamyl alcohol dehydrogenase (CAD) gene (*Os04g0229100*) and one cinnamoyl-CoA reductase (CCR) gene (*Os02g0811600*) was up-regulated exclusively in BPH30T plants (Figure 8), suggesting the lignified cell wall plays a key role in mediating the BPH resistance conferred by *Bph30*; these findings are consistent with the results of our previous study (Shi et al., 2021).

Phenylalanine is one of the products from the shikimate pathway (Dong and Lin, 2021). In this pathway, shikimate is catalyzed by a series of enzymes to synthesize phenylalanine. We found the gene (*Os02g0749300*), which encoded shikimate kinase (SK) that catalyzes

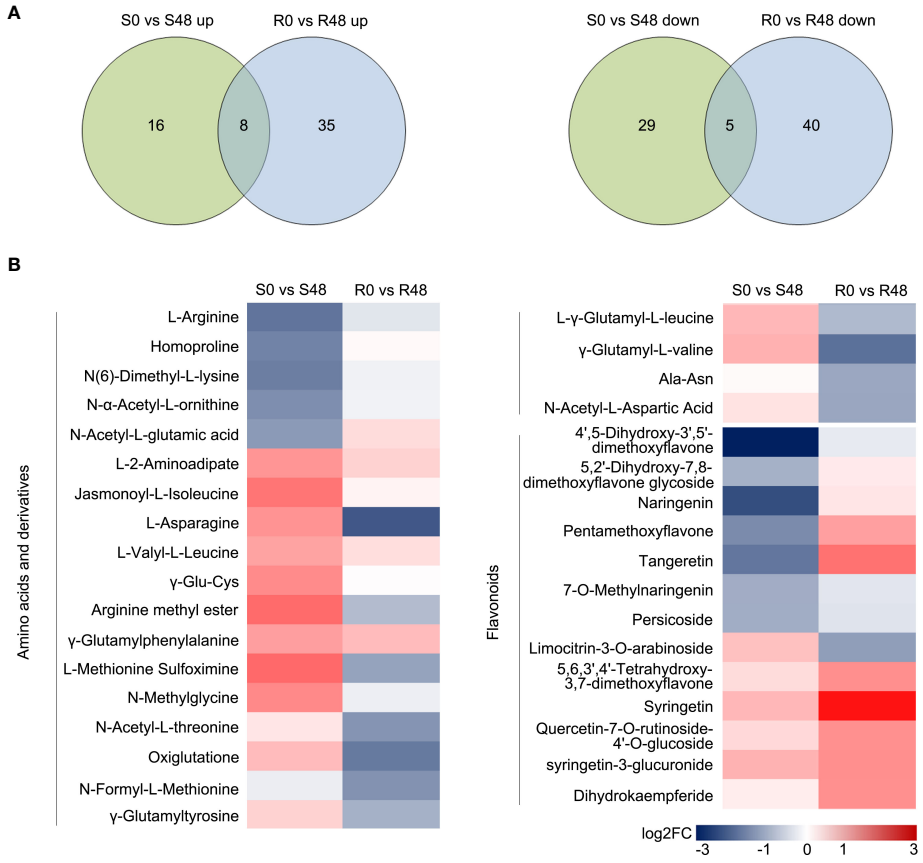

FIGURE 6
Unique DAMs in the two rice varieties after BPH feeding for 48 h. **(A)** Venn diagrams displayed the unique DAMs in two rice varieties before and after fed by brown planthopper. **(B)** Heat map showed the unique DAMs related to amino acids and derivatives and flavonoids in two comparison groups.

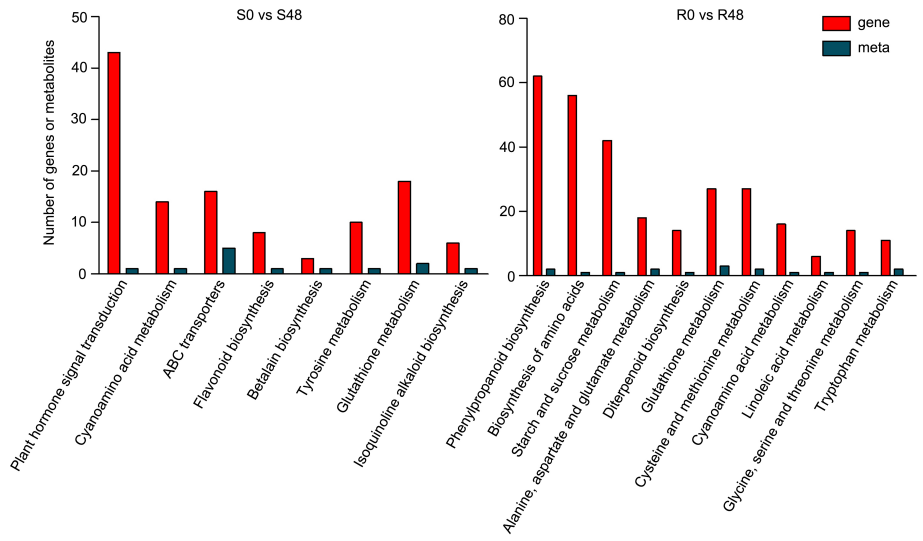

FIGURE 7
Transcriptomic and metabolomic joint analysis of Nipponbare and BPH30T after BPH infestation. KEGG enrichment analysis of the DEGs and DAMs detected from S0 vs S48 and R0 vs R48 groups.

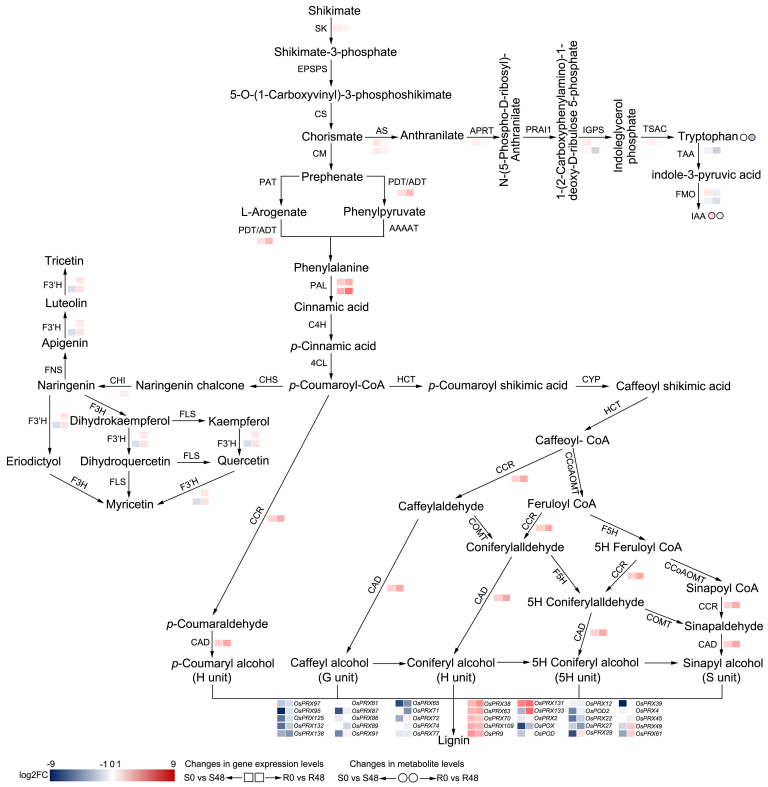

FIGURE 8
Reconstruction of the BPH-resistance related metabolism pathways with the DAMs and DEGs in Nipponbare and BPH30T fed by BPH for 48 h. S0 and S48 indicated Nipponbare fed by BPH for 0 h and 48 h, respectively. R0 and R48 indicated BPH30T fed by BPH for 0 h and 48 h, respectively. The rectangles represent the genes and the circles represent the metabolites. Color change represents the degree of variation.

shikimate to shikimate 3-phosphate, was exclusively down-regulated in BPH30T plants only. The expression of *Os04g0406600*, which encodes the protein (arogenate/prephenate dehydratase, ADT/PDT) that catalyzes the conversion of prephenate to phenylpyruvate and arogenate to phenylalanine, was down-regulated in Nipponbare but up-regulated in BPH30T plants (Figure 8). These findings suggested that *Bph30* regulates the central flux of carbon from primary metabolism to secondary metabolism in BPH30T plants under BPH infection.

Effects of BPH infestation on the IAA synthesis pathway

In rice, IAA is mainly synthesized from tryptophan (Trp). Chorismate, the intermediate product of shikimate pathway, is an initiator substrate for Trp synthesis. In the Trp synthesis pathway, we found that the expression of the anthranilate synthase (AS) genes *Os04g0463500* and *Os03g0826500*, the anthranilate phosphoribosyl transferase (APRT) gene *Os03g0126000*, and the Trp synthase alpha chain (TSAC) gene *Os07g0182100* was down-regulated exclusively in BPH30T plants. The expression of the indole-3-glycerol phosphate synthase (IGPS) gene *Os09g0255400* was down-regulated in both Nipponbare and BPH30T plants; however, the expression of this gene was down-regulated to a greater degree in BPH30T plants than that in Nipponbare; the IGPS gene *Os08g0320400* was specifically down-regulated in BPH30T plants (Figure 8). We also found the Trp content was significantly reduced in BPH30T plants following BPH infestation; however, BPH feeding activity had no effect on the Trp content in Nipponbare.

IAA is synthesized from Trp *via* tryptophan amino transferase (TAA) and flavonoid monooxygenase (FMO). First, Trp is converted to indole-3-pyruvic acid (IPA) by TAA. In the second step, IPA is converted to IAA by FMO (Figure 8). In the DEGs isolated from Nipponbare and BPH30T plants following BPH infestation, we found that the expression of *OsTAA1* (*Os01g0169800*), which encodes TAA, was down-regulated to a greater degree in BPH30T plants than in Nipponbare plants. The expression of *OsYUC5* (*Os12g0512000*), which encodes FMO, was down-regulated in BPH30T plants, and the down-regulation of the expression of *OsYUC9* (*Os01g0273800*) was more pronounced in BPH30T plants than in Nipponbare plants (Figure 8). Analysis of DAMs revealed that the content of IAA was lower in BPH30T plants following BPH feeding activity, but no change in the IAA content was observed in Nipponbare plants under the same conditions (Figure 8). The expression variation of the above genes was verified by qRT-PCR assay (Supplementary Figure 5). These findings indicate that IAA biosynthesis was inhibited by BPH infestation in BPH30T plants.

Overall, these findings suggested that *Bph30* can regulate the primary metabolic pathway (shikimate pathway and Trp

biosynthesis), then affect the secondary metabolic process (phenylpropanoid metabolism, flavonoids and lignin biosynthesis) and IAA biosynthesis, exerting the function of resisting to brown planthopper. Noteworthy, the expression level of the genes that related IAA biosynthesis was lower in BPH30T plants than in Nipponbare and the contents of IAA were lower also in BPH30T plants than that in Nipponbare, suggesting that IAA might negatively regulate *Bph30*-mediated resistance to BPH in rice.

Function of IAA in mediating BPH resistance conferred by *Bph30*

The results of transcriptome, metabolome and combined analysis indicated IAA might play a vital role in *Bph30* against to BPH. To determine the role of IAA in mediating the BPH resistance conferred by *Bph30*, we measured the content of IAA in Nipponbare and BPH30T plants during BPH infestation. The content of IAA decreased significantly in BPH30T plants following BPH feeding activity; however, the content of IAA remained unchanged in Nipponbare plants under the same conditions (Figure 9A). The expression level of IAA-synthesis related genes was tested quantitatively also. The results of qRT-PCR showed the expression of *OsTAA1*, *OsYUC5*, and *OsYUC9* was significantly lower in BPH30T plants than in Nipponbare plants during BPH infestation (Supplementary Figures 6A–C).

Exogenous IAA was applied to BPH30T seedlings to clarify the role of IAA in mediating the BPH resistance conferred by *Bph30*. In bulk seedling test, the leaves of BPH30T plants treated with IAA were curled and yellow caused by BPH fed; by contrast, the leaves of control plants were normal (Figures 9B, C). The weight gain and honeydew excretion of BPHs were significantly higher when they fed on plants treated with IAA than when they fed on control plants (Supplementary Figures 6D, E). The host-choice tests were also performed, and the results showed that a significantly higher number of BPHs settled on the IAA treated plants than that settled on control plants from 3-72 h following the release of BPHs (Figure 9D). Furthermore, the BPH survival rate was significantly higher on IAA treated plants relative to control plants after 3 days (Figure 9E). These findings suggested that IAA negatively regulates BPH resistance conferred by *Bph30*.

Discussion

In plants, resistance to biotic stress is thought to be determined by secondary metabolites. However, primary metabolites can also change when plants experience biotic stress. *Bipolaris oryzae* infection up-regulated the Trp pathway in rice leaves (Ishihara et al., 2008). *Magnaporthe grisea* infestation has been shown to alter the abundance of metabolites involved in the tricarboxylic acid (TCA) cycle and the synthesis of sugar alcohols and aromatic amino acids in barley, rice, and *Brachypodium distachyon* (Parker et al.,

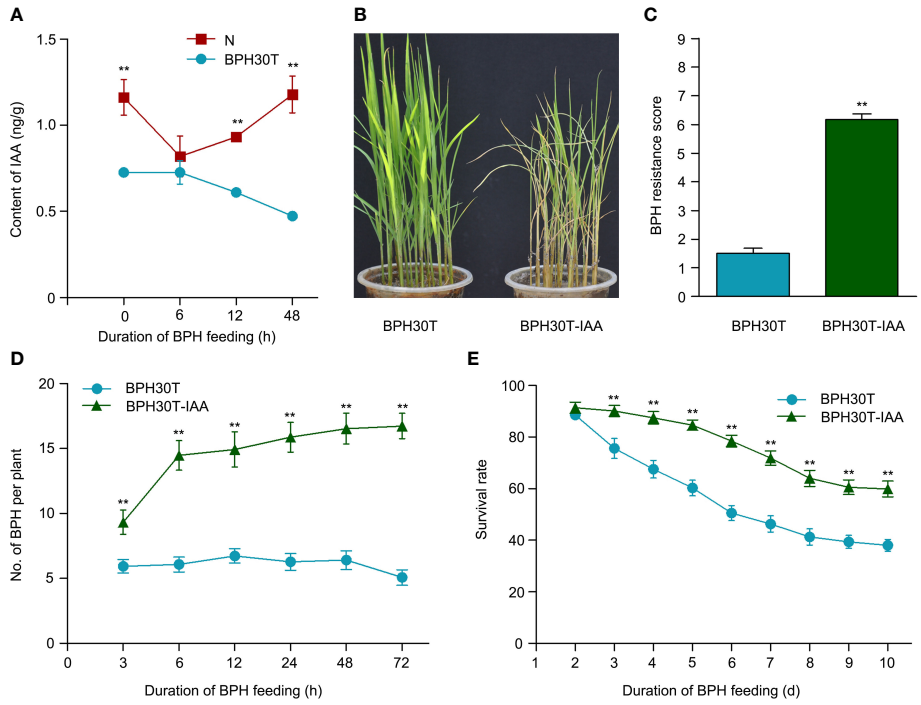

FIGURE 9
The IAA functioned in *Bph30*-mediated resistance to BPH. **(A)** The changes of IAA content in Nipponbare and BPH30T during BPH infestation. Data are means (three individual replicates) ± SEM. N, Nipponbare. **(B, C)** Seedling test identified the phenotype of resistance to BPH **(B)** and resistance score **(C)** of BPH30T treated with 1μm IAA (BPH30T-IAA). Data are means (at least 15 plants) ± SEM. **(D)** Selectivity of brown planthopper on BPH30T and BPH30T-IAA. **(E)** Survival rate of BPH feeding on BPH30T and BPH30T-IAA. In **(D, E)**, data represent the means ± SEM. Asterisks indicate significant differences (*represent $p < 0.01$).

2009). BPH infestation induced changes in the abundances of primary metabolites in rice plants, such as amino acids, sugars, organic acids, lipids, and those metabolites involved in the Trp biosynthetic pathway, TCA cycle, shikimate pathway, GABA shunt, pentose phosphate pathway, wax biosynthesis, sterol biosynthetic pathway (Liu et al., 2010; Uawisetwathana et al., 2015; Peng et al., 2016; Zhang et al., 2018). Amino acids are essential nutrients that BPHs must obtain from the phloem sap of rice plants. When the resistant rice varieties were infected by BPH, the content of amino acids in phloem sap were significantly reduced, and the content of amino acid in BPH honeydew were significantly decreased, suggesting that the amounts of amino acids obtained by BPHs from resistant rice plants was reduced (Peng et al., 2017). We found that the amino acid biosynthesis pathway was down-regulated in BPH30T plants during BPH feeding (Figure 3). The expression of most genes involved in histidine, valine, leucine, isoleucine, serine, cysteine, alanine, glutamine, and homoserine biosynthesis was down-regulated in BPH30T plants but remained unchanged in Nipponbare plants following BPH infestation (Supplementary Figure 7). Thus, we speculate that *Bph30* might induce alterations in primary metabolites to mediate the response to invasion, or modify the composition of phloem sap; for example, *Bph30* reduces the content of amino acids, which makes the phloem sap a suboptimal food source for BPHs; this forces BPHs to colonize from *Bph30*-containing plants to susceptible plants to maximize nutrient acquisition.

Flavonoids play key roles in mediating the interaction between plants and parasites. A previous study showed that *Fusarium graminearum* infection increased the biosynthesis of flavonoid in wheat, and treatment of wheat spikes with exogenous kaempferide and apigenin enhanced the resistance of wheat to *F. graminearum* (Su et al., 2021). Vitexin and vitexin-2”-O-arabinofuranoside are two flavonoid metabolites, which purified from *Basella alba*, significantly inhibit the growth rate of *S. litura* larvae when fed with these two substances (Aboshi et al., 2018). A previous study showed that tricin, which belongs to flavone, is common in gramineous plants, and can significantly improve the resistance of rice to brown planthopper. However, the content of tricin will significantly decrease in rice, when fed by brown planthoppers, indicated may be a protein in BPH regulates the tricin metabolize for feeding (Zhang et al., 2017). Current study showed BPH salivary protein 7 gene (*NlSP7*) was induced by tricin and NlSP7 regulated tricin metabolism in rice plants (Gong et al., 2022). Flavan-3-ols is a type of flavonoids with a high content in Tea (*Camellia sinensis*). Overexpression of Dihydro flavonol 4-reductase gene (*DFR*) and anthocyanidin reductase gene (*ANR*) in *Camellia sinensis* can significantly increase the content of flavan-3-ols and provide protection against feeding by *S. litura* (Kumar and Yadav, 2017). In sum, flavonoids are toxic and defensive secondary metabolites that protect plants from invaders; parasites can regulate the biosynthesis of flavonoids to promote their feeding activity. In our study, the flavonoid biosynthesis pathway was down-regulated exclusively in Nipponbare, and the flavonoid biosynthesis related genes in Nipponbare were also down-regulated (Figure 3; Figure 8), suggested that BPH infestation inhibited the synthesis of flavonoids and increased the susceptibility of rice plants to BPH; however, *Bph30* promoted flavonoid synthesis and increased the resistance of rice to BPHs.

The secondary cell walls of vascular plants are rich in lignin, which provides holding power for terrestrial plants and prevents the harm of invaders (Boerjan et al., 2003; Wang et al., 2017; Yang et al., 2017; Gallego-Giraldo et al., 2018). HCT catalyzes the conversion of *p*-coumarocyl CoA in the lignin biosynthesis. Reducing the expression of *HCT* in plants can reduce the lignin content and alter lignin composition in the second cell wall, and this can facilitate the cell wall degradation by cell wall-degrading enzymes secreted by invaders (Hoffmann et al., 2004). CmMYB19 is a transcription factor isolated from chrysanthemum. In overexpressing *CmMYB19*-transgenic chrysanthemums, the genes involved in lignin synthesis were up-regulated and the content of lignin was increased, which improved the resistance of chrysanthemum to attack by aphids (Wang et al., 2017). A recent report has shown that the BPH-resistance protein BPH6 interacted with the exocyst subunit OsEXO70H3 and SAMSL, and promotes the SAMSL secretion to apoplast, in where it increased lignin sedimentation in the cell wall, which promoted the rice plants resistance to planthoppers (Wu et al., 2022). The results of the above studies suggest that the cell wall can act as a physical barrier that prevents invaders from harming plants. Our previous study has shown that BPH30 enhances the hardness of the cell wall of the sclerenchyma and prevents the stylets of BPHs from impaling the sclerenchyma to reach the phloem for feeding (Shi et al., 2021). In this study, we found the CAD gene (*04g0229100*) and CCR gene (*02g0811600*), which are involved in lignin biosynthesis, were exclusively up-regulated expressed in BPH30T plants (Figure 8), indicating that lignin fulfilled a vital role in BPH30 resistance to brown planthopper, which may be contributed by the reinforcement of the physical barrier.

The biological function of phytohormone auxin is not only to regulate plant growth and development, but also to regulate plant stress resistance (Fu and Wang, 2011; Kidd et al., 2011; Qi et al., 2012; Gomes and Scortecci, 2021). In this study, we found the genes *OsTAA1*, *OsYUC5*, and *OsYUC9*, which related to IAA synthesis, were down-regulated expression in BPH30T plants, after BPH feeding, but unchanged in Nipponbare; the content of IAA in BPH30T plants was significantly lower than that in Nipponbare before and after BPH infestation. We also found IAA can reduce the resistance of *Bph30* to brown planthopper by the assay of exogenous application of IAA (Figure 9). Previous studies have demonstrated the auxin signal transduction is controlled by 3 switch proteins. The first switches are the auxin response factors (ARFs), which are transcription factors that activate the target genes of IAA. The second switches are the transcriptional repressors Aux/IAA, which bind to ARFs in the absence of auxin conditions, inhibiting IAA response genes expression. The third switches are the IAA receptors TIR1/AFB, which are the members of $SCF^{TIR1/AFB}$ ubiquitination E3 complex. As the content of IAA increases, TIR1/AFB receptors bind to Aux/IAA repressor proteins, and mediates the degradation of Aux/IAA repressor proteins through ubiquitination pathway. Therefore, ARF proteins are released, which activates the expression

of IAA response genes (Mockaitis and Estelle, 2008; Weijers and Wagner, 2016). Through analysis of DEGs that detected from the two rice varieties, we found there were seven and two Aux/IAA genes were down-regulated expression in Nipponbare and BPH30T plants, respectively; the expression of one TIR1/AFB gene was inhibited in BPH30T plants, but unchanged in Nipponbare. The ARF genes expression in both Nipponbare and BPH30T plants was inhibited after BPH feeding, but the down-regulated ARF genes in the two varieties differed (Supplementary Figure 8). These results indicated that IAA had a negative effect on BPH30 resistances to BPH, BPH30 altered IAA synthesis and regulated IAA signal transduction, thus improving the rice plants resist to brown planthopper. The target genes of IAA, which might increase susceptibility to BPH, remain unknown. In a future study, we plan to identify these genes.

BPH30 protein contains two LRDs that homologous to leucine-rich repeat domain (LRR) (Shi et al., 2021). Thus we speculated that LRDs may detected the proteins secreted into rice from BPH, transmitting the downstream signals that may involve in regulating endogenous auxin levels and the expression of auxin synthesis genes. But, the protein sequences of BPH30 in Nipponbare and BPH-resistant varieties AC-1613 were significantly different (Shi et al., 2021). So those differences in the protein sequences of BPH30 in Nipponbare from in AC-1613 may result in the loss of the function of recognition the BPH secreted proteins, leading to the failure of regulation of IAA content and biosynthesis genes expressions in rice during BPH infestation. Further researches are needed for the more detailed mechanisms.

Conclusion

In summary, when attacked by BPH, the major BPH-resistance gene *Bph30* enhanced the flow of compounds to flavonoids and lignin biosynthesis through shikimate and phenylpropanoid metabolism pathways, and inhibited the biosynthesis of various amino acids and IAA, indicating BPH30 reprogrammed the direction of metabolite conversion. The results of this study demonstrate that IAA negatively regulates *Bph30*-mediated resistance to BPHs and that IAA signal transduction is involved in *Bph30*-mediated resistance to BPHs. Overall, our work systematically analyzed the molecular mechanism of *Bph30*-mediated resistance to brown planthopper in rice and provided theoretical guidance for rice breeding resistant to BPH.

Data availability statement

All raw RNA sequencing data generated in this study have been deposited under the NCBI SRA database under BioProject PRJNA957551.

Author contributions

LZ and AY conceived and supervised the project. KL (liukrice@163.com) revised the manuscript. SS designed the experiments and performed most of the experiments. XY, YW, SL, HX, PL, CL, KL (liukai11153@126.com), JC, GY, ZC, BW, and BLW performed some of the experiments. SS and WZ analyzed data and wrote the manuscript and contributed equally to this paper. All authors contributed to the article and approved the submitted version.

Funding

This study was supported by grants from the Natural Science Foundation of Hubei Province (2022CFB832), Wuhan Knowledge Innovation Special Dawn Plan Project, Hubei Academy of Agricultural Science Foundation (2023NKYJJ01), Hubei Key Laboratory of Food Crop Germplasm and Genetic Improvement Foundation (2022lzjj01), the Science and Technology Major Program of Hubei Province (2022ABA001, 2021ABA011), and the Wuhan Science and Technology Major Project for Biological Breeding (2022021302024850).

Acknowledgments

We thank Prof. Guangcun He (Wuhan University) for kindly providing the *Bph30*-transgenic plants. No conflict of interest declared.

Conflict of interest

The authors declare that the research was conducted in the absence of any commercial or financial relationships that could be construed as a potential conflict of interest.

Publisher's note

Supplementary material

The Supplementary Material for this article can be found online at: https://www.frontiersin.org/articles/10.3389/fpls.2023.1213257/full#supplementary-material

References

Abood, J. K., and Lösel, D. M. (2003). Changes in carbohydrate composition of cucumber leaves during the development of powdery mildew infection. *Plant Pathol.* 52, 256–265. doi: 10.1046/j.1365-3059.2003.00814.x

Aboshi, T., Ishiguri, S., Shiono, Y., and Murayama, T. (2018). Flavonoid glycosides in malabar spinach *Basella alba* inhibit the growth of *Spodoptera litura* larvae. *Biosci. Biotechnol. Biochem.* 82 (1), 9–14. doi: 10.1080/09168451.2017.1406301

Alamgir, K. M., Hojo, Y., Christeller, J. T., Fukumoto, K., Isshiki, R., Shinya, T., et al. (2016). Systematic analysis of rice (Oryza sativa) metabolic responses to herbivory. *Plant Cell Environ.* 39, 453–466. doi: 10.1111/pce.12640

Boerjan, W., Ralph, J., and Baucher, M. (2003). Lignin biosynthesis. *Annu. Rev. Plant Biol.* 54, 519–546. doi: 10.1146/annurev.arplant.54.031902.134938

Chen, J. Y., Ullah, C., Giddings Vassão, D., Reichelt, M., Gershenzon, J., and Hammerbacher, A. (2021). *Sclerotinia sclerotiorum* infection triggers changes in primary and secondary metabolism in *Arabidopsis thaliana*. *Phytopathology* 111, 559–569. doi: 10.1094/PHYTO-04-20-0146-R

Chen, Y., Wang, J., Nguyen, N. K., Hwang, B. K., and Jwa, N. S. (2022). The NIN-like protein OsNLP2 negatively regulates ferroptotic cell death and immune responses to *Magnaporthe oryzae* in rice. *Antioxidants (Basel)* 11 (9), 1795. doi: 10.3390/antiox11091795

Cheng, X. Y., Zhu, L. L., and He, G. C. (2013). Towards understanding of molecular interactions between rice and the brown planthopper. *Mol. Plant* 6 (3), 621–634. doi: 10.1093/mp/sst030

Dervinis, C., Frost, C. J., Lawrence, S. D., Novak, N. G., and Davis, J. M. (2010). Cytokinin primes plant responses to wounding and reduces insect performance. *J. Plant Growth Regul.* 29, 289–296. doi: 10.1007/s00344-009-9135-2

Dong, N. Q., and Lin, H. X. (2021). Contribution of phenylpropanoid metabolism to plant development and plant-environment interactions. *J. Integr. Plant Biol.* 63 (1), 180–209. doi: 10.1111/jipb.13054

Du, B., Chen, R. Z., Guo, J. P., and He, G. C. (2020). Current understanding of the genomic, genetic, and molecular control of insect resistance in rice. *Mol. Breed.* 40, 24. doi: 10.1007/s11032-020-1103-3

Du, B., Zhang, W. L., Liu, B. F., Hu, J., Wei, Z., Shi, Z. Y., et al. (2009). Identification and characterization of *Bph14*, a gene conferring resistance to brown planthopper in rice. *Proc. Natl. Acad. Sci. USA* 106 (52), 22163–22168. doi: 10.1073/pnas.0912139106

Erb, M., Flors, V., Karlen, D., de Lange, E., Planchamp, C., D'Alessandro, M., et al. (2009). Signal signature of aboveground-induced resistance upon belowground herbivory in maize. *Plant J.* 59 (2), 292–302. doi: 10.1111/j.1365-313X.2009.03868.x

Erb, M., and Kliebenstein, D. J. (2020). Plant secondary metabolites as defenses, regulators, and primary metabolites: the blurred functional trichotomy. *Plant Physiol.* 184 (1), 39–52. doi: 10.1104/pp.20.00433

Fu, J., and Wang, S. P. (2011). Insights into auxin signaling in plant-pathogen interactions. *Front. Plant Sci.* 2. doi: 10.3389/fpls.2011.00074

Gallego-Giraldo, L., Posé, S., Pattathil, S., Peralta, A. G., Hahn, M. G., Ayre, B. G., et al. (2018). Elicitors and defense gene induction in plants with altered lignin compositions. *New Phytol.* 219 (4), 1235–1251. doi: 10.1111/nph.15258

Gomes, G. L. B., and Scortecci, K. C. (2021). Auxin and its role in plant development: structure, signalling, regulation and response mechanisms. *Plant Biol. (Stuttg).* 23 (6), 894–904. doi: 10.1111/plb.13303

Gong, G., Yuan, L. Y., Li, Y. F., Xiao, H. X., Li, Y. F., Zhang, Y., et al. (2022). Salivary protein 7 of the brown planthopper functions as an effector for mediating tricin metabolism in rice plants. *Sci. Rep.* 12 (1), 3205. doi: 10.1038/s41598-022-07106-6

Guo, J. P., Xu, C. X., Wu, D., Zhao, Y., Qiu, Y. F., Wang, X. X., et al. (2018). *Bph6* encodes an exocyst-localized protein and confers broad resistance to planthoppers in rice. *Nat. Genet.* 50 (2), 297–306. doi: 10.1038/s41588-018-0039-6

Hartmann, T. (2007). From waste products to ecochemicals: fifty years research of plant secondary metabolism. *Phytochemistry* 68 (22-24), 2831–2846. doi: 10.1016/j.phytochem.2007.09.017

He, J., Liu, Y. Q., Yuan, D. Y., Duan, M. J., Liu, Y. L., Shen, Z. J., et al. (2020). An R2R3 MYB transcription factor confers brown planthopper resistance by regulating the phenylalanine ammonia-lyase pathway in rice. *Proc. Natl. Acad. Sci. USA* 117 (1), 271–277. doi: 10.1073/pnas

Hoffmann, L., Besseau, S., Geoffroy, P., Ritzenthaler, C., Meyer, D., Lapierre, C., et al. (2004). Silencing of hydroxycinnamoyl-coenzyme a shikimate/quinate hydroxycinnamoyltransferase affects phenylpropanoid biosynthesis. *Plant Cell* 16 (6), 1446–1465. doi: 10.1105/tpc.020297

Hu, L., Wu, Y., Wu, D., Rao, W. W., Guo, J. P., Ma, Y. H., et al. (2017). The coiled-coil and nucleotide binding domains of brown planthopper resistance14 function in signaling and resistance against planthopper in rice. *Plant Cell* 29 (12), 3157–3185. doi: 10.1105/tpc.17.00263

Hu, J., Zhou, J. B., Peng, X. X., Xu, H. H., Liu, C. X., Du, B., et al. (2011). The *Bphi008a* gene interacts with the ethylene pathway and transcriptionally regulates *MAPK* genes in the response of rice to brown planthopper feeding. *Plant Physiol.* 156 (2), 856–872. doi: 10.1104/pp.111.174334

Huang, Z., He, G. C., Shu, L. H., Li, X. H., and Zhang, Q. F. (2001). Identification and mapping of two brown planthopper resistance genes in rice. *Theor. Appl. Genet.* 102, 929–934. doi: 10.1007/s001220000455

Huangfu, J., Li, J., Li, R., Ye, M., Kuai, P., Zhang, T., et al. (2016). The transcription factor OsWRKY45 negatively modulates the resistance of rice to the brown planthopper *Nilaparvata lugens*. *Int. J. Mol. Sci.* 17 (6), 697. doi: 10.3390/ijms17060697

Ishihara, A., Hashimoto, Y., Tanaka, C., Dubouzet, J. G., Nakao, T., Matsuda, F., et al. (2008). The tryptophan pathway is involved in the defense responses of rice against pathogenic infection *via* serotonin production. *Plant J.* 54 (3), 481–495. doi: 10.1111/j.1365-313X.2008.03441.x

Jiang, G., Yin, D., Shi, Y., Zhou, Z., Li, C., Liu, P., et al. (2020). OsNPR3.3-dependent salicylic acid signaling is involved in recessive gene *xa5*-mediated immunity to rice bacterial blight. *Sci. Rep.* 10 (1), 6313. doi: 10.1038/s41598-020-63059-8

Jing, S. L., Liu, B. F., Peng, L., Peng., X. X., Zhu, L. L., Fu, Q., et al. (2012). Development and use of EST-SSR markers for assessing genetic diversity in the brown planthopper (*Nilaparvata lugens* stål). *Bull. Entomol. Res.* 102 (1), 113–122. doi: 10.1017/S0007485311000435

Jing, S. L., Zhao, Y., Du, B., Chen, R. Z., Zhu, L. L., and He, G. C. (2017). Genomics of interaction between the brown planthopper and rice. *Curr. Opin. Insect Sci.* 19, 82–87. doi: 10.1016/j.cois.2017.03.005

Jobic, C., Boisson, A. M., Gout, E., Rascle, C., Fèvre, M., Cotton, P., et al. (2007). Metabolic processes and carbon nutrient exchanges be-tween host and pathogen sustain the disease development during sunflower infection by sclerotinia sclerotiorum. *Planta* 226, 251–265. doi: 10.1007/s00425-006-0470-2

Kamolsukyeunyong, W., Sukhaket, W., Pitija, K., Thorngkham, P., Mahatheeranont, S., Toojinda, T., et al. (2021). Rice sesquiterpene plays important roles in antixenosis against brown planthopper in rice. *Plants (Basel)* 10 (6), 1049. doi: 10.3390/plants10061049

Kidd, B. N., Kadoo, N. Y., Dombrecht, B., Tekeoglu, M., Gardiner, D. M., Thatcher, L. F., et al. (2011). Auxin signaling and transport promote susceptibility to the root-infecting fungal pathogen fusarium oxysporum in arabidopsis. *Mol. Plant Microbe Interact.* 24 (6), 733–748. doi: 10.1094/MPMI-08-10-0194

Kumar, V., and Yadav, S. K. (2017). Pyramiding of tea dihydroflavonol reductase and anthocyanidin reductase increases flavan-3-ols and improves protective ability under stress conditions in tobacco. *3 Biotech.* 7 (3), 177. doi: 10.1007/s13205-017-0819-1

Li, W., Zhong, S., Li, G., Li, Q., Mao, B., Deng, Y., et al. (2011). Rice RING protein OsBBI1 with E3 ligase activity confers broad-spectrum resistance against *Magnaporthe oryzae* by modifying the cell wall defence. *Cell Res.* 21 (5), 835–848. doi: 10.1038/cr.2011.4

Liu, C., Du, B., Hao, F. H., Lei, H. H., Wan, Q. F., He, G. C., et al. (2017). Dynamic metabolic responses of brown planthoppers towards susceptible and resistant rice plants. *Plant Biotechnol. J.* 15, 1346–1357. doi: 10.1111/pbi.12721

Liu, C., Hao, F. H., Hu, J., Zhang, W. L., Wan, L. L., Zhu, L. L., et al. (2010). Revealing different systems responses to brown planthopper infestation for pest susceptible and resistant rice plants with the combined metabonomic and gene-expression analysis. *J. Proteome Res.* 9 (12), 6774–6785. doi: 10.1021/pr100970q

Lu, H. P., Luo, T., Fu, H. W., Wang, L., Tan, Y. Y., Huang, J. Z., et al. (2018). Resistance of rice to insect pests mediated by suppression of serotonin biosynthesis. *Nat. Plants* 4 (6), 338–344. doi: 10.1038/s41477-018-0152-7

Lv, W. T., Du, B., Shangguan, X. X., Zhao, Y., Pan, Y. F., Zhu, L. L., et al. (2014). BAC and RNA sequencing reveal the brown planthopper resistance gene BPH15 in a recombination cold spot that mediates a unique defense mechanism. *BMC Genomics* 15 (1), 674. doi: 10.1186/1471-2164-15-674

Mockaitis, K., and Estelle, M. (2008). Auxin receptors and plant development: a new signaling paradigm. *Annu. Rev. Cell Dev. Biol.* 24, 55–80. doi: 10.1146/annurev.cellbio.23.090506.123214

Muduli, L., Pradhan, S. K., Mishra, A., Bastia, D. N., Samal, K. C., Agrawal, P. K., et al. (2021). Understanding brown planthopper resistance in rice: genetics, biochemical and molecular breeding approaches. *Rice Sci.* 28 (6), 532–546. doi: 10.1016/j.rsci.2021.05.013

Parker, D., Beckmann, M., Zubair, H., Enot, D. P., Caracuel-Rios, Z., Overy, D. P., et al. (2009). Metabolomic analysis reveals a common pattern of metabolic re-programming during invasion of three host plant species by *Magnaporthe grisea*. *Plant J.* 59 (5), 723–737. doi: 10.1111/j.1365-313X.2009.03912.x

Peng, Y., Bartley, L. E., Chen, X., Dardick, C., Chern, M., Ruan, R., et al. (2008). OsWRKY62 is a negative regulator of basal and *Xa21*-mediated defense against *Xanthomonas oryzae* pv. *oryzae* in rice. *Mol. Plant* 1 (3), 446–458. doi: 10.1093/mp/ssn024

Peng, L., Zhao, Y., Wang, H. Y., Song, C. P., Shangguan, X. X., Ma, Y. H., et al. (2017). Functional study of cytochrome P450 enzymes from the brown planthopper (*Nilaparvata lugens* stål) to analyze its adaptation to BPH-resistant rice. *Front. Physiol.* 8. doi: 10.3389/fphys.2017.00972

Peng, L., Zhao, Y., Wang, H. Y., Zhang, J. J., Song, C. P., Shangguan, X. X., et al. (2016). Comparative metabolomics of the interaction between rice and the brown planthopper. *Metabolomics* 12, 132. doi: 10.1007/s11306-016-1077-7

Qi, L. L., Yan, J., Li, Y. N., Jiang, H. L., Sun, J. Q., Chen, Q., et al. (2012). *Arabidopsis thaliana* plants differentially modulate auxin biosynthesis and transport during defense

responses to the necrotrophic pathogen *Alternaria brassicicola*. *New Phytol.* 195 (4), 872–882. doi: 10.1111/j.1469-8137.2012.04208.x

Sarao, P. S., Sahi, G. K., Neelam, K., Mangat, G. S., Patra, B. C., and Singh, K. (2016). Donors for resistance to brown planthopper *Nilaparvata lugens* (Stål) from wild rice species. *Rice Sci.* 23 (4), 219–224. doi: 10.1016/J.RSCI.2016.06.005

Shi, S. J., Wang, H. Y., Nie, L. Y., Tan, D., Zhou, C., Zhang, Q., et al. (2021). *Bph30* confers resistance to brown planthopper by fortifying sclerenchyma in rice leaf sheaths. *Mol. Plant* 14 (10), 1714–1732. doi: 10.1016/j.molp.2021.07.004

Solomon, P. S., Tan, K. C., and Oliver, R. P. (2003). The nutrient supply ofpathogenic fungi; a fertile field for study. *Mol. Plant Pathol.* 4, 203–210. doi: 10.1046/j.1364-3703.2003.00161.x

Son, S., Im, J. H., Song, G., Nam, S., and Park, S. R. (2022). OsWRKY114 inhibits ABA-induced susceptibility to *Xanthomonas oryzae* pv. *oryzae* in rice. *Int. J. Mol. Sci.* 23 (15), 8825. doi: 10.3390/ijms23158825

Son, S., Kim, H., Lee, K. S., Kim, S., and Park, S. R. (2020). Rice glutaredoxin GRXS15 confers broad-spectrum resistance to *Xanthomonas oryzae* pv. *oryzae* and *Fusarium fujikuroi*. *Biochem. Biophys. Res. Commun.* 533 (4), 1385–1392. doi: 10.1016/j.bbrc.2020.10.027

Su, P. S., Zhao, L. F., Li, W., Zhao, J. X., Yan, J., Ma, X., et al. (2021). Integrated metabolo-transcriptomics and functional characterization reveals that the wheat auxin receptor TIR1 negatively regulates defense against *Fusarium graminearum*. *J. Integr. Plant Biol.* 63 (2), 340–352. doi: 10.1111/jipb.12992

Tamura, Y., Hattori, M., Yoshioka, H., Yoshioka, M., Takahashi, A., Wu, J., et al. (2014). Map-based cloning and characterization of a brown planthopper resistance gene BPH26 from oryza sativa l. ssp. indica cultivar ADR52. *Sci. Rep.* 4, 5872. doi: 10.1038/srep05872

Tan, J. Y., Wu, Y., Guo, J. P., Li, H. M., Zhu, L. L., Chen, R. Z., et al. (2020). A combined microRNA and transcriptome analyses illuminates the resistance response of rice against brown planthopper. *BMC Genomics* 21 (1), 144. doi: 10.1186/s12864-020-6556-6

Uawisetwathana, U., Graham, S. F., Kamolsukyunyong, W., Sukhaket, W., Klanchui, A., Toojinda, T., et al. (2015). Quantitative 1H NMR metabolome profiling of Thai jasmine rice (Oryza sativa) reveals primary metabolic response during brown planthopper infestation. *Metabolomics* 11, 1640–1655. doi: 10.1007/s11306-015-0817-4

Wang, Y. J., Sheng, L. P., Zhang, H. R., Du, X. P., An, C., Xia., X. L., et al. (2017). CmMYB19 over-expression improves aphid tolerance in chrysanthemum by promoting lignin synthesis. *Int. J. Mol. Sci.* 18 (3), 619. doi: 10.3390/ijms18030619

Weijers, D., and Wagner, D. (2016). Transcriptional responses to the auxin hormone. *Annu. Rev. Plant Biol.* 67, 539–574. doi: 10.1146/annurev-arplant-043015-112122

Wu, D., Guo, J. P., Zhang, Q., Shi, S. J., Guan, W., Zhou, C., et al. (2022). Necessity of rice resistance to planthoppers for OsEXO70H3 regulating SAMSL excretion and lignin deposition in cell walls. *New Phytol.* 234 (3), 1031–1046. doi: 10.1111/nph.18012

Wu, Y., Lv, W. T., Hu, L., Rao, W. W., Zeng, Y., Zhu, L. L., et al. (2017). Identification and analysis of brown planthopper-responsive microRNAs in resistant and susceptible rice plants. *Sci. Rep.* 7 (1), 8712. doi: 10.1038/s41598-017-09143-y

Yang, Q., He, Y. J., Kabahuma, M., Chaya, T., Kelly, A., Borrego, E., et al. (2017). A gene encoding maize caffeoyl-CoA O-methyltransferase confers quantitative resistance to multiple pathogens. *Nat. Genet.* 49 (9), 1364–1372. doi: 10.1038/ng.3919

Zhang, Z., Cui, B., Yan, S., Li, Y., Xiao, H., Li, Y., et al. (2017). Evaluation of tricin, a stylet probing stimulant of brown planthopper, in infested and non-infested rice plants. *J. Appl. Entomol.* 141, 393–401. doi: 10.1111/jen.12353

Zhang, Y. L., and Li, X. (2019). Salicylic acid: biosynthesis, perception, and contributions to plant immunity. *Curr. Opin. Plant Biol.* 50, 29–36. doi: 10.1016/j.pbi.2019.02.004

Zhang, J. J., Li, Y., Guo, J. P., Du, B., He, G. C., Zhang, Y. J., et al. (2018). Lipid profiles reveal different responses to brown planthopper infestation for pest susceptible and resistant rice plants. *Metabolomics* 14 (9), 120. doi: 10.1007/s11306-018-1422-0

Zhao, Y., Huang, J., Wang, Z. Z., Jing, S. L., Wang, Y., Ouyang, Y. D., et al. (2016). Allelic diversity in an NLR gene BPH9 enables rice to combat planthopper variation. *Proc. Natl. Acad. Sci. USA* 113 (45), 12850–12855. doi: 10.1073/pnas.1614862113

Zheng, X. H., Zhu, L. L., and He, G. C. (2021). Genetic and molecular understanding of host rice resistance and nilaparvata lugens adaptation. *Curr. Opin. Insect Sci.* 45, 14–20. doi: 10.1016/j.cois.2020.11.005

Zhou, C., Zhang, Q., Chen, Y., Huang, J., Guo, Q., Li, Y., et al. (2021). Balancing selection and wild gene pool contribute to resistance in global rice germplasm against planthopper. *J. Integr. Plant Biol.* 63, 1695–1711. doi: 10.1111/jipb.13157

frontiers | Frontiers in Plant Science

TYPE Original Research
PUBLISHED 19 July 2023
DOI 10.3389/fpls.2023.1226641

OPEN ACCESS

EDITED BY
Shengli Jing,
Xinyang Normal University, China

REVIEWED BY
Sudeshna Mazumdar-Leighton,
University of Delhi, India
Christian Paetz,
Max Planck Institute for Chemical Ecology, Germany

*CORRESPONDENCE
Min Lu
lumin@hubu.edu.cn

RECEIVED 22 May 2023
ACCEPTED 26 June 2023
PUBLISHED 19 July 2023

CITATION
Liu F, Li B, Liu C, Liu Y, Liu X and Lu M (2023) Oviposition by *Plagiodera versicolora* on *Salix matsudana* cv. 'Zhuliu' alters the leaf transcriptome and impairs larval performance. *Front. Plant Sci.* 14:1226641. doi: 10.3389/fpls.2023.1226641

Oviposition by *Plagiodera versicolora* on *Salix matsudana* cv. 'Zhuliu' alters the leaf transcriptome and impairs larval performance

Fengjie Liu, Bin Li, Chenghu Liu, Yipeng Liu, Xiaolong Liu and Min Lu*

State Key Laboratory of Biocatalysis and Enzyme Engineering, School of Life Sciences, Hubei University, Wuhan, China

Insect egg deposition can induce plant defenses against their larvae. Previous studies have primarily focused on herbaceous plant defenses; however, little is known about how the *Salicaceae* respond to insect egg deposition and defend themselves against herbivores. By combining plant defense gene studies and bioassays, we investigated the effect of the coleoptera *Plagiodera versicolora* egg deposition on willow (*Salix matsudana* cv. 'Zhuliu') and examined the interactions at the plant resistance and transcriptome levels. RNA-seq data were utilized to analyze changes in the leaf transcriptome with and without oviposition, and also the changes in the leaf transcriptome of feeding-damaged leaves with and without prior oviposition. *P. versicolora* oviposition on willow leaves resulted in altered expression levels of transcripts associated with plant stress and metabolic responses. Compared with leaves with no oviposition, leaves with egg deposition showed a slight increase in phenylpropanoid biosynthesis and phytohormone signaling genes after larval feeding. The RNA-seq analysis revealed alterations in willow transcripts in response to leaf beetle infestations. Bioassays indicated that oviposition by *P. versicolora* on willows reduced subsequent larvae performance, suggesting that prior oviposition by *P. versicolora* could increase willows' resistance to larvae. This study advances our knowledge of how oviposition by coleoptera insects induces changes in the resistance of leaves to herbivory in the *Salicaceae* family.

KEYWORDS

oviposition, RNA sequencing, differentially expressed genes, bioassays, *Plagiodera versicolora*, *Salix matsudana* cv. Zhuliu

1 Introduction

Trees dominate terrestrial ecosystems and provide habitats for many insects (Basset et al., 2012). Over time, trees have evolved various mechanisms to defend themselves against herbivores (Eyles et al., 2010; Caldwell et al., 2016). Multiple studies have demonstrated that plants are capable of responding to imminent stress cues, enhancing their induced stress resistance, and preparing them for potential damage (Mauch-Mani et al., 2017). These cues include insect feeding, leaf volatile emissions by damaged neighboring plants (Heil and Silva Bueno, 2007; Pashalidou et al., 2020), insect sex pheromones (Bittner et al., 2019), and insect egg deposition (Hilker and Fatouros, 2016).

Insect egg deposition triggers plant defense mechanisms that can not only directly affect egg survival but also indirectly increase the defense response against their larvae (Hilker and Fatouros, 2015; Hilker and Fatouros, 2016). Plant defense strategies induced by egg deposition specifically target the eggs themselves rather than the ovipositing female. These strategies include plant-mediated egg desiccation, dropping, crushing, and killing (Yamasaki et al., 2003; Desurmont and Weston, 2011; Petzold-Maxwell et al., 2011). In addition, plants can utilize egg deposition as a reliable signal to predict and prepare for a subsequent larval attack. Prior egg deposition can induce alterations in the quality of feeding-damaged leaves, resulting in impaired larval performance (Pashalidou et al., 2013; Austel et al., 2016; Bandoly et al., 2016; Bertea et al., 2020). For example, when *Spodoptera exigua* fed on *Nicotiana attenuata* leaves with prior egg deposition, larvae suffered higher mortality than those that fed on plants without prior egg deposition (Bandoly et al., 2015).

Molecular analyses revealed that plants exhibit substantial transcriptome changes in response to oviposition cues (Reymond, 2013; Bonnet et al., 2017; Ojeda-Martinez et al., 2022). Several studies have demonstrated that oviposition induces the expression of various defense-related genes in plants. These genes encompass those encoding pathogenesis-related (PR) proteins, responding to biotic and abiotic stresses, regulators of cell death, and innate immunity, and also stressors associated with the production of secondary metabolites, among other things (Little et al., 2007; Büchel et al., 2012). Furthermore, plants with prior oviposition showed stronger defense gene expressions after larval feeding, such as *Arabidopsis*, tobacco, tomato, and elm (Kim et al., 2012; Bandoly et al., 2016; Altmann et al., 2018; Lortzing et al., 2020). Moreover, several studies have shown that the increased efficiency of defense against larvae caused by oviposition is associated with changes in phytohormone levels. For instance, *S. exigua* larvae feeding on *N. attenuata* leaves with prior oviposition could increase the proteinase inhibitor activity in plants (Bandoly et al., 2015). Similarly, when the elm beetle *Xanthogaleruca luteola* fed on elm leaves with prior egg deposition, the plant was able to increase leaf gene expression levels of phenylpropanoid derivatives (Lortzing et al., 2019).

Plagiodera versicolora Laicharting (Coleoptera, Chrysomelidae) is a worldwide forest pest (Utsumi et al., 2009) whose larval and adult stages feed primarily on *Salicaceae* trees such as willows and poplars (Li et al., 2022). Female *P. versicolora* lay eggs almost daily while feeding on young leaves (Ma et al., 2021). The eggs are neatly arranged, usually sticking vertically to the back of the leaf. Studies have shown that crude extracts obtained from the surface of *P. versicolora* egg masses using organic solvents can attract females to lay eggs, while aqueous extracts have been found to repel females (Yang et al., 2005). Willow is a widespread tree throughout the world and is consumed extensively by various herbivores (Tahvanainen et al., 1985; Hallgren, 2003). Recent studies have shown that the egg deposition of *Nematus oligospilus* Förster (Hymenoptera, Tenthredinidae) on willow could increase the plant's jasmonic acid levels, alter its volatile profile, and reduce neonate larval growth (Dávila et al., 2023). However, the effect of coleoptera egg deposition on willow trees and newborn larvae has not been reported. Hence, we used bamboo willow (*Salix matsudana* cv. 'Zhuliu') and *P. versicolora* as a model, and used *de novo* assembled RNA-seq data analysis and bioassays to investigate the willow trees' response to *P. versicolora* egg deposition and larvae. Our results showed that oviposition by *P. versicolora* on willow alters the leaf transcriptome and impairs larval performance.

2 Materials and methods

2.1 Plants and insects

One-year-old bamboo willows (*Salix matsudana* cv. 'Zhuliu') were purchased from Xuanyu Flower Garden, Wuhan, China. The trees were planted in 7-L pots with a 3:1:1 mix of nutrient soil, pearlite, and vermiculite and transferred to a greenhouse (26°C ± 1° C, 60% ± 5% Relative Humidity (RH), Light 16h: Dark 8h (L16:D8). The willow plants were grown for a period of 6 weeks before they were used for the experiments.

P. versicolora adults were collected from the surrounding Sha Lake Park in Hubei Province, Wuhan, China, and reared in ventilated plastic boxes measuring 20 cm × 10 cm × 8 cm, in which they were fed fresh willow leaves. The rearing conditions were maintained in a greenhouse (26°C ± 1°C, 60% ± 5% RH, L16:D8).

2.2 Plant treatments

For all experiments conducted, willows of the same genotype and similar size were carefully selected to ensure that the plants used in each replicate block were comparable. In the experiment, the willows were subjected to the following treatments: (i) *P. versicolora* egg deposition (E), (ii) feeding-damaged leaves without prior egg deposition (CF), (iii) feeding-damaged leaves with prior egg deposition (EF), and (iv) control (C). Experiments were conducted using intact leaves (attached to the plants). Three replicate plants were harvested for each time point and treatment.

To obtain egg deposition plants (E), mated *P. versicolora* females were used to lay eggs on the surface of the willow leaves.

After 3 days, when the eggs were about to hatch, we carefully removed the eggs from the leaves with forceps, and the leaves were collected immediately. In the feeding-damaged leaves treatments (CF and EF), the leaves were exposed to a specific number of newly hatched larvae. In this case, 10 newly hatched larvae were placed on feeding-damaged leaves of each plant. Larvae were removed after 24 h and leaf samples were collected.

2.3 RNA extraction, cDNA library construction, and Illumina sequencing

Approximately 100 mg of each leaf sample was collected and promptly frozen in liquid nitrogen for storage. Three biological replicates were used for each treatment or condition.

Total RNA was extracted using TRIzol reagent (Invitrogen, Carlsbad, CA, USA) following the manufacturer's instructions. One percent agarose gels were used to visualize the integrity of the RNA samples and check for any signs of degradation or contamination. RNA integrity and purity were further assessed using the 2100 Bioanalyzer (Agilent Technologies). The concentration was quantified using the ND-2000 spectrophotometer (NanoDrop Technologies).

Approximately 2 μg of total RNA per sample was used for cDNA library construction. The cDNA libraries were prepared following Illumina® Stranded mRNA Prep, Ligation from Illumina (San Diego, CA), and then subjected to sequencing using the Illumina Novaseq 6000 platform. Sequencing was performed by Shanghai Majorbio Bio-pharm Technology Co., Ltd.

2.4 *De novo* assembly and gene annotation

Raw paired-end reads obtained from the sequencing were subjected to trimming and quality control using fastp (Chen et al., 2018), with default parameters. Clean data of the samples were then assembled *de novo* using Trinity (Grabherr et al., 2011). After assembly, they were further evaluated and optimized using BUSCO (Benchmarking Universal Single-Copy Orthologs) (Manni et al., 2021), TransRate (Smith-Unna et al., 2016), and CD-HIT (Fu et al., 2012). The assembled transcripts were searched again using the NR (NCBI protein non-redundant), Swiss-Prot, Pfam (Protein families), eggNOG (evolutionary genealogy of genes: Non-supervised Orthologous Groups), GO (Gene Ontology), and KEGG (Kyoto Encyclopedia of Genes and Genomes) databases using BLASTX to identify the proteins that had the highest sequence similarity. During the annotation process, a typical cut-off E-value of less than 1.0×10^{-5} was set to determine significant matches between the transcripts and the annotated proteins.

2.5 Differential expression analysis and functional enrichment

To calculate the transcript expression levels of differential expression genes (DEGs), the transcripts per million reads (TPM) method was employed. RNA-Seq by Expectation-Maximization (RSEM) (Li and Dewey, 2011) and Differential Expression analysis for Sequence Count data 2 (DESeq2) (Love et al., 2014) were used to quantify gene abundance and perform differential expression analysis, respectively. DEGs with $|\log2FC| \geq 1$ and False Discovery Rates (FDR) ≤ 0.05 (DESeq2) were considered as significantly different expressions.

Functional enrichment analyses including GO and KEGG were conducted to identify the significantly enriched GO terms and metabolic pathways among the DEGs. A Bonferroni-corrected *P*-value ≤ 0.05 was used to determine significant enrichment. Goatools and KOBAS were used for GO functional enrichment and KEGG pathway analysis, respectively (Xie et al., 2011).

2.6 Quantitative real-time PCR analysis

The cDNA was reverse transcribed using HiScript® III RT SuperMix for qPCR (Vazyme, Nanjing, China). The specific primers for qPCR analysis were provided in Supplementary Table 1. The reference gene used in this study was *ACT7* (Li et al., 2016). A qRT-PCR analysis was performed on the CFX Connect Real-Time System (Bio-Rad, Hercules, CA, USA). The ChamQTM Universal SYBR® qRT-PCR Master Mix (Vazyme, Nanjing, China) was used for reactions, following the manufacturer's instructions. The qRT-PCR reaction programs were as follows: 95°C for 30 s, 40 cycles of 95°C for 5 s, and 60°C for 30 s. Gene expression profiles were analyzed using the $2^{-\Delta\Delta CT}$ method (Livak and Schmittgen, 2001); three replicates were used for each gene.

2.7 Insect performance

To count the number of eggs laid by *P. versicolora* and the hatching rate, only one mated female was allowed to oviposit on the leaves of each plant. A total of seven willows and seven mated females were used. The number of eggs on each leaf was counted at the end of oviposition by the female. After 3 days, the number of larvae hatched on the plants was recorded.

To clarify the effect of prior egg deposition on willows on *P. versicolora* larval growth, we measured larval performance after feeding on willow leaves with and without egg deposition. Using egg deposition and control plants, the eggs were removed after 3 days of

oviposition. Ten newly hatched larvae were placed in the same position on the plant to allow the larvae to feed freely. Four replicates were used in each group. We compared the larval survival rate and body weight of willows with and without prior *P. versicolora* egg deposition. Larval mortality was recorded daily. Body weight was recorded every 2 days with an electronic balance (BT1251, Sartorius Scientific Instruments, China).

2.8 Statistical analysis

R software, version 4.2.2 (R Core Team, 2022), was used for all statistical analyses. Normal distribution and variance homogeneity were assessed using Shapiro–Wilk and Levene's tests, respectively, or visually inspected through Q–Q plots.

We conducted an analysis to examine the impact of prior egg deposition on larval mortality in willows. Survival curves were compared using the logrank (Mantel–Cox) test. To compare the larval body weight between willows with and without prior *P. versicolora* egg deposition, linear mixed models (LMMs) were employed for the analysis. The LMMs included the replicate block as a random factor to account for potential variability.

For evaluating the qRT-PCR data and testing gene expression values, we utilized a one-way analysis of variance (ANOVA). Subsequently, Tukey's HSD test was applied for *post-hoc* comparisons between different groups.

3 Results

3.1 RNA sequencing and *de novo* assembling of transcriptome

To investigate willow response to *P. versicolora* egg deposition and the subsequent larval feeding, we conducted transcriptome sequencing of leaves that had been subjected to various treatments. We obtained 110.47 Gb of raw sequence data, and 92.31% of the bases had a sequence quality score of >Q30. About 132,452 unigenes, with a total length of 95,157,991 and an N50 length of 1,050 bp, were identified (Table 1). Length distribution analysis showed that 42.47% (55,171) of all unigenes were longer than 500 bp in size (Figure 1).

Following the assembly of the transcriptome, annotations for the assembled unigenes were performed using BLAST in six public databases, namely NR, Swiss-Prot, Pfam, eggNOG, GO, and KEGG (Table 2). In the GO analysis, the unigenes were categorized into three main functional categories: biological process (96,417), cellular component (104,536), and molecular function (83,283) (Figure 2A). In the KEGG pathway database, the unigenes were classified into five main categories: the largest category was metabolism (11,423), followed by genetic information processing (6,005), environmental information processing (1,708), cellular processes (1,583), and organismal systems (758) (Figure 2B).

3.2 Transcriptional profiling of willow responses to *P. versicolora* egg deposition

To assess the impact of *P. versicolora* oviposition on the transcription level of willow leaves, we compared the gene expression between leaves exposed to egg deposition (E) and untreated leaf samples (C) after a 3-day period (E vs. C). A total of 3,795 genes were significantly differentially expressed after *P.*

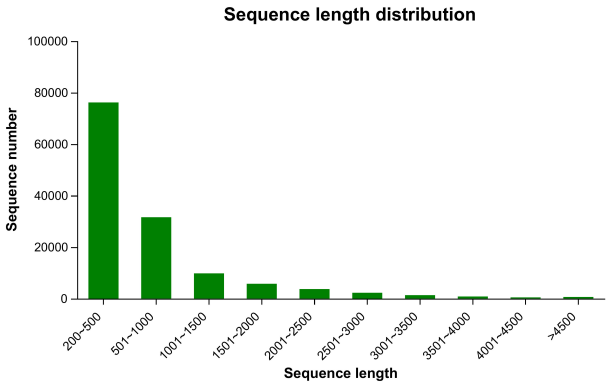

FIGURE 1
Length (bp) distribution of unigenes in the willow leaf transcriptome.

TABLE 1 Result of the *de novo* transcriptome assembly performed with Trinity.

Type	Unigene	Transcript
Total sequence number	132,452	266,041
Total sequence base	95,157,991	230,466,949
Largest length	16,793	16,793
Smallest length	201	201
Average length	718.43	866.28
N50 length	1,050	1,323
E90N50 length	2,138	1,779
Percent GC	39.97	40.66

TABLE 2 Functional annotation of unigenes.

Database	Number of unigenes	Percentage
NR	82,476	62.50%
Swiss-prot	50,359	38.16%
Pfam	36,123	27.37%
eggNOG	70,967	53.78%
GO	69,142	52.39%
KEGG	32,361	24.52%
Total	85,676	64.92%

NR, NCBI protein non-redundant; evolutionary genealogy of genes: Non-supervised Orthologous Groups; GO, Gene Ontology; KEGG, Kyoto Encyclopedia of Genes and Genomes.

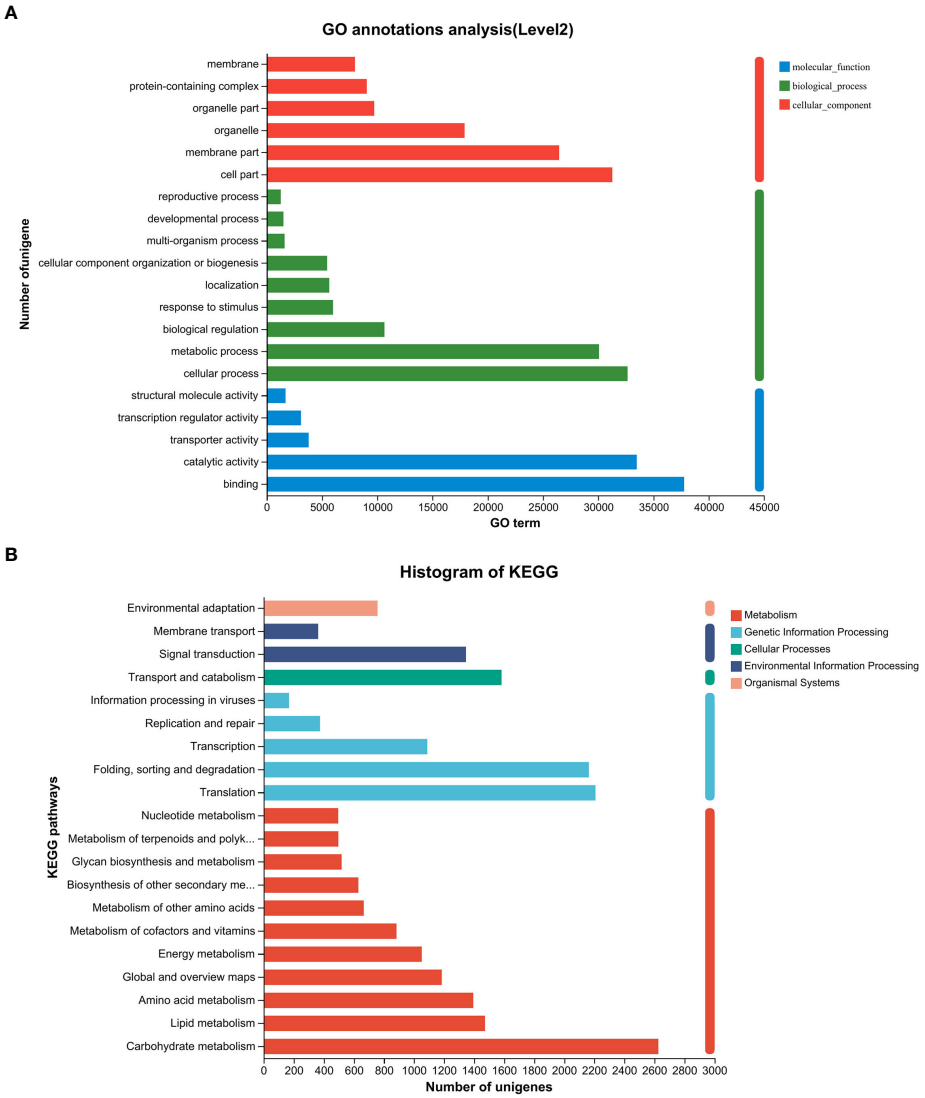

FIGURE 2
Gene function classification of unigenes in the willow leaf transcriptome. **(A)** Main GO categories of unigene. **(B)** KEGG metabolic pathway of unigenes.

versicolora egg deposition (2,239 up-regulated and 1,456 down-regulated) (Figure 3A).

In the GO functional analysis, the DEGs were successfully classified into 46 categories (E vs. C) (Figure 3B). Among these categories, the biological processes categories with the highest number of transcripts were "cellular and metabolic processes" and "biological regulation and stimulus-response" (Figure 3B). KEGG enrichment analysis was mapped to 118 KEGG pathways (Figure 3C). The pathways with the highest unigene representations were ribosome, followed by phenylpropanoid biosynthesis, and starch and sucrose metabolism (Figure 3C). These results suggest that the *P. versicolora* egg deposition could induce changes in the expression levels of transcripts associated with plant stress and metabolic responses.

3.3 Differentially expressed in feeding-damaged leaves with and without prior egg deposition

To study transcriptomic changes in willows induced by *P. versicolora* larval feeding on leaves with prior egg deposition, this treatment was compared with feeding-damaged leaves without prior egg deposition. Results indicate that in the feeding-damaged plants with egg deposition treatment (EF vs. CF) a total of 2,338 genes were significantly differentially expressed (1,385 up-regulated and 953 down-regulated) (Figure 4A).

In the GO functional analysis, the DEGs were successfully classified into 44 categories (EF vs. CF) (Figure 4B). Among these categories, the biological processes categories with the highest number of transcripts

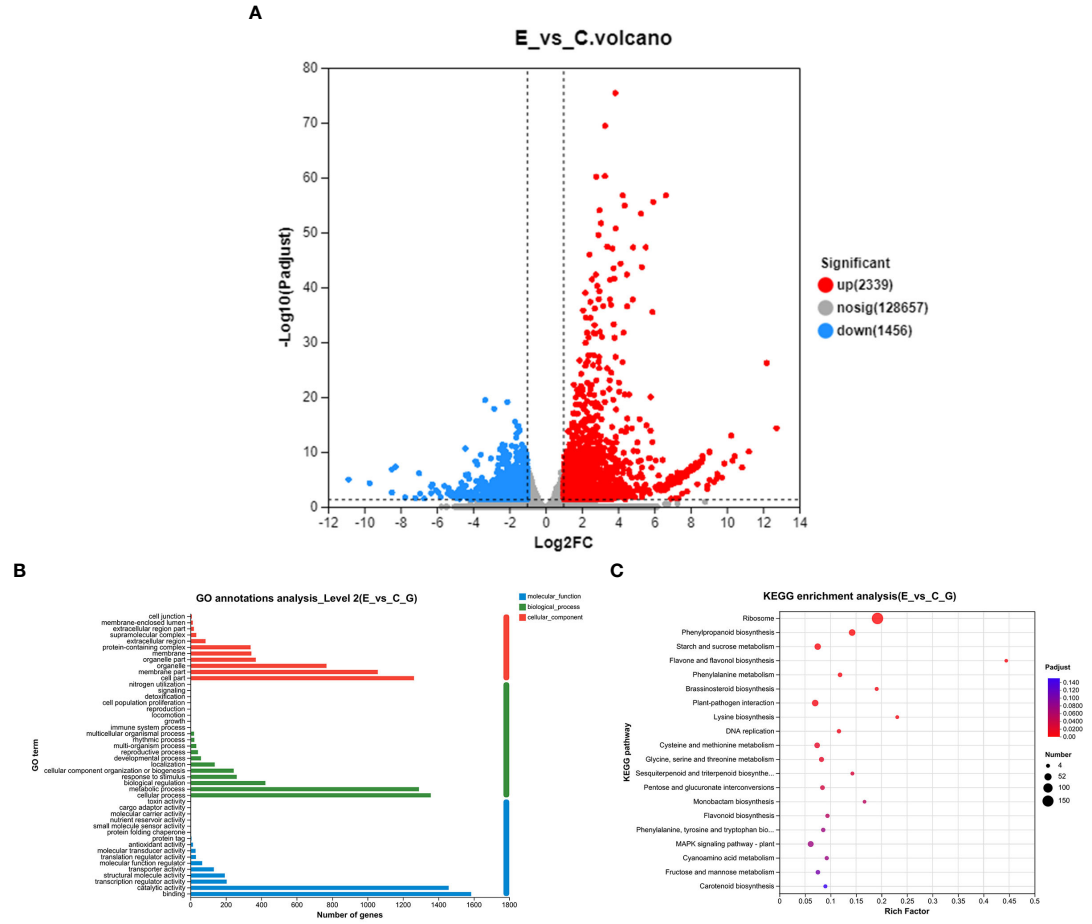

FIGURE 3
With and without prior *P. versicolora* egg deposition induces changes of DEGs (differential expression genes) in the transcriptome. **(A)** Volcano map analysis of DEGs. **(B)** GO annotation analysis of DEGs. **(C)** The top 20 enriched KEGG pathways of DEGs. G refers to unigene.

were "cellular and metabolic processes" and "biological regulation and stimulus-response" (Figure 4B). The KEGG enrichment analysis was mapped to 117 KEGG pathways (Figure 4C). The pathways with the highest unigene representation were ribosome, followed by flavonoid biosynthesis and phenylpropanoid biosynthesis (Figure 4C). Comparison of transcriptome changes in feeding-damaged leaves with and without prior *P. versicolora* egg deposition revealed EF group enrichment of transcripts associated with the plant secondary metabolism pathway, such as flavonoid biosynthesis, phenylpropanoid biosynthesis, Lavone and flavonol biosynthesis, and phenylalanine metabolism (Figure 4C). Thus, egg deposition of *P. versicolora* on willows potentially increases the regulation of plant defense responses to larvae.

3.4 qRT-PCR validation of the candidate genes

To analyze gene expression patterns associated with *P. versicolora* egg deposition, feeding-damaged leaves with and without prior egg deposition on leaves were validated by qRT-PCR. We selected 12 unigenes with high significance levels in GO and KEGG in the "response to wounding," "defense response," "hormone metabolic process," and "Phenylpropanoid biosynthesis" categories. Compared with the control, the gene expression of pathogenesis-related protein 1 (PR 1), chitinases, disease resistance response protein (DRRP), and MLO-like protein increased after 3 days of egg deposition on plants (E), and there was a significant difference in chitinases. Cysteine proteinase inhibitor (CPIN) and the H2O2-related gene WRKY22 expression levels were significantly increased in leaves damaged by feeding with prior egg deposition (EF). The phytohormone salicylic acid (SA)-related gene NIM1 was significantly increased in egg deposition plants (E). Jasmonic acid (JA)-related gene AOS, ethylene-related genes mitogen-activated protein kinases (MAPKs), and oxidative signal inducible 1 (OXI1) significantly increased in EF plants. Phenylalanine ammonialyase (PAL) and cinnamyl alcohol dehydrogenase (CAD), which are related to the phenylpropanoid pathway, increased in plants treated with prior egg deposition (Figure 5).

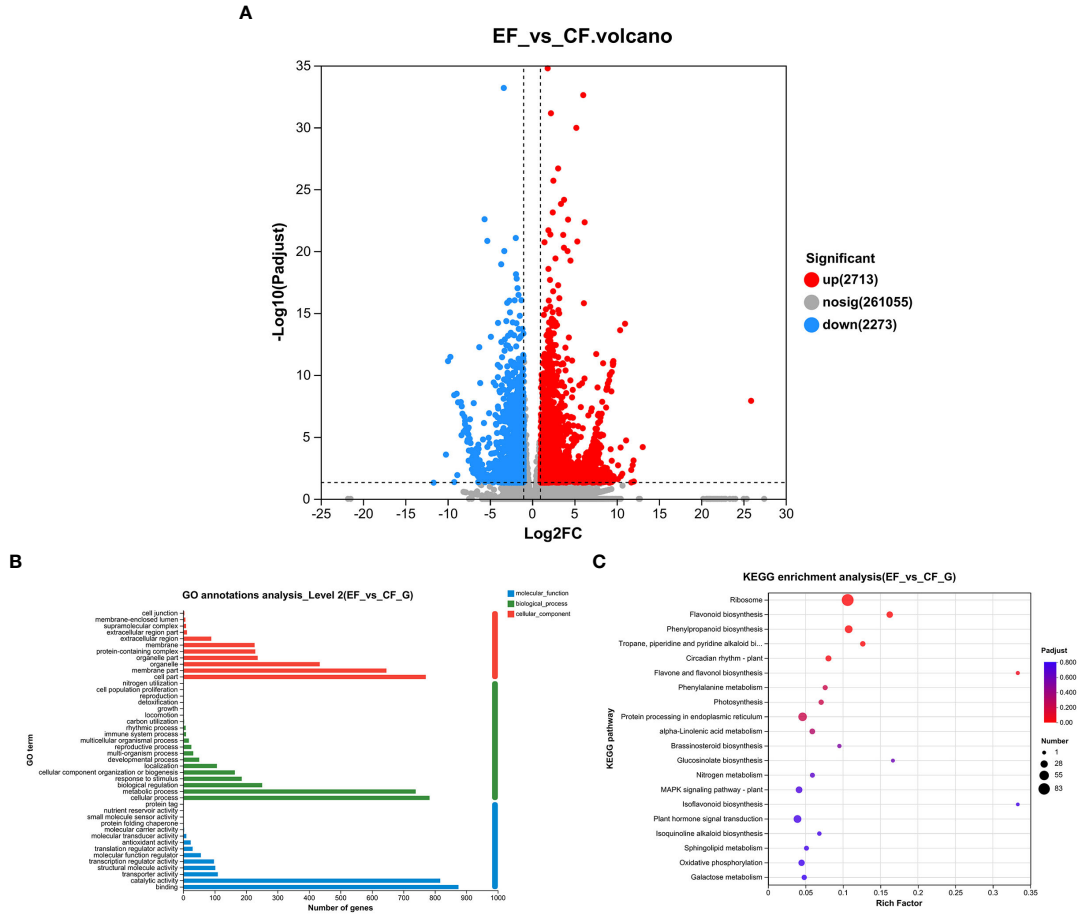

FIGURE 4
Feeding-damaged leaves with and without prior *P. versicolora* egg depositions showed induced changes in DEGs (differential expression genes) in the transcriptome. **(A)** Volcano map analysis of DEGs. **(B)** GO annotation analysis of DEGs. **(C)** The top 20 enriched KEGG pathways of DEGs. G refers to Unigene.

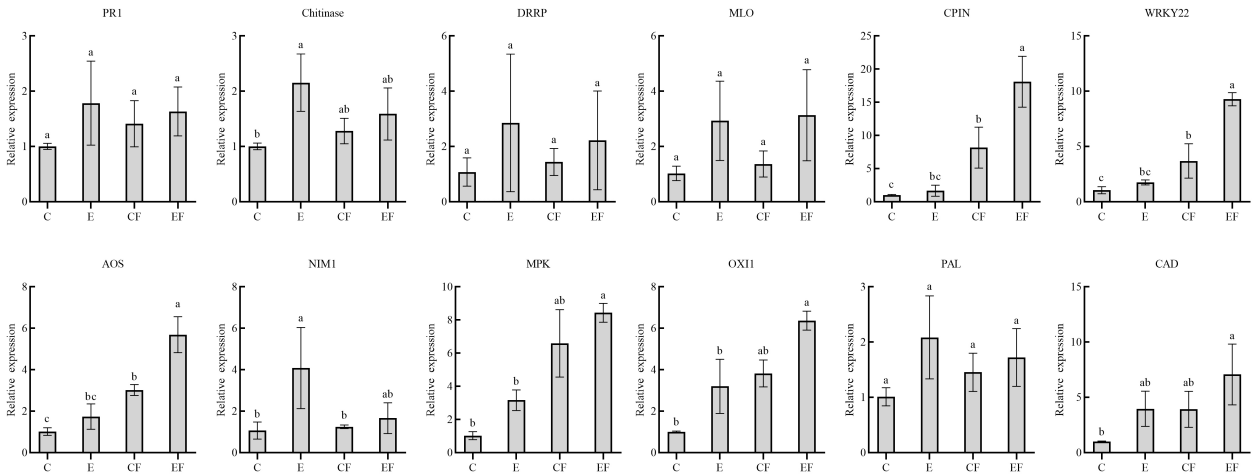

FIGURE 5
Expression analysis of 12 candidate genes in four treatments by qRT-PCR. (i) *P. versicolora* egg deposition (E), (ii) feeding-damaged leaves without prior egg deposition (CF), (iii) feeding-damaged leaves with prior egg deposition (EF), and (iv) control (C). The columns represent averages with vertical lines indicating standard error (SE). The differences in lowercase letters above each bar indicate significant differences ($P < 0.05$).

3.5 *P. versicolora* egg deposition on willow could impair larvae performance

We measured the egg hatching rate and larval performance of *P. versicolora* on willows with prior egg deposition. The number of *P. versicolora* eggs on leaves was 22.14 ± 1.77, and the eggs hatched in about 3 days, with a hatching rate of 99.35%. Larval performance was measured in terms of survival and weight on willows with and without prior *P. versicolora* egg deposition. Larval mortality on leaves with prior egg deposition was significantly higher than on leaves without prior egg deposition (Mantel–Cox test, χ^2 = 3.94, *P*=0.047, Figure 6A). Similarly, the weight of larvae fed on leaves with prior egg deposition was lower than that of those fed on leaves without prior egg deposition (Supplementary Table 2). In particular, on the 4th and 6th days, the body weight was significantly reduced (Figure 6B; Supplementary Table 2). Overall, these results demonstrate the negative impact of *P. versicolora* egg deposition on willow leaves on the subsequent life stages of the larvae.

4 Discussion

4.1 *P. versicolora* egg deposition alters willow leaf transcriptome

This study was particularly focused on the expression of plant defense-related genes. Similarly, changes in defense-related genes were observed in the leaves of *Pieris brassicae* (Little et al., 2007) and *Xanthogaleruca luteola* (Büchel et al., 2012). In willows that were subjected to egg deposition, we observed gene expression levels increase, such as those of pathogenesis-related protein 1 (PR 1), chitinases, disease resistance response protein (DRRP), MLO-like protein, and NPR1/NIM1-interacting protein; this was verified by qRT-PCR, in which chitinases had significant differences. Our findings indicate that the expression of PR proteins by willows plays a potentially significant role in the response to *P. versicolora* egg deposition. PR proteins have been widely recognized for their involvement in defense responses following herbivore attacks (Van Loon et al., 2006). Chitinases, on the other hand, directly contribute to plant defenses by breaking down components of microbial cell walls (Veluthakkal and Dasgupta, 2010). In the case of *Arabidopsis thaliana*, chitinases are induced at and in the vicinity of the site where pierid eggs are laid, suggesting a potential defensive role against newly hatched larvae (Little et al., 2007). In *A. thaliana*, NPR1/NIM1 has been identified as a pivotal regulator of systemic acquired resistance (SAR) (Weigel et al., 2001). NPR1 governs the activation of PR genes involved in the synthesis of SA and plays a critical role in bridging the JA and SA signaling pathways (Spoel et al., 2003).

Oxidative signal inducible 1 (OXI1) plays a critical role in the signaling pathway that links oxidative burst signals to various downstream responses. OXI1 is necessary for the complete activation of MAPKs following exposure to reactive oxygen species (ROS) and elicitors (Rentel et al., 2004). Interestingly, our study demonstrated an elevation in the gene expression levels of both OXI1 and MAPKs in willow trees that were subjected to *P. versicolora* egg deposition (Figure 5). Previous research has indicated that the Hypersensitive Response (HR)-like response to pierid butterfly eggs on *A. thaliana* is associated with ROS accumulation, including hydrogen peroxide (Little et al., 2007; Bruessow et al., 2010; Gouhier-Darimont et al., 2013). However, *P. versicolora* egg deposition did not result in direct physical damage to the leaves, which is similar to the results of pierid butterflies laying eggs on *Arabidopsis*. Whether the deposition of *P. versicolora* eggs on willow leaves causes an HR-like response and what substances cause willow defense may be the focus of our future research.

Additionally, our observations show that the gene expression levels of the phenylalanine pathway are up-regulated in leaves of the willow plants with *P. versicolora* egg deposition. This suggests that insect oviposition could potentially increase the production of plant secondary metabolites, as has been documented in elms (Schott et al., 2021). Phenylalanine ammonia lyase (PAL) plays a critical

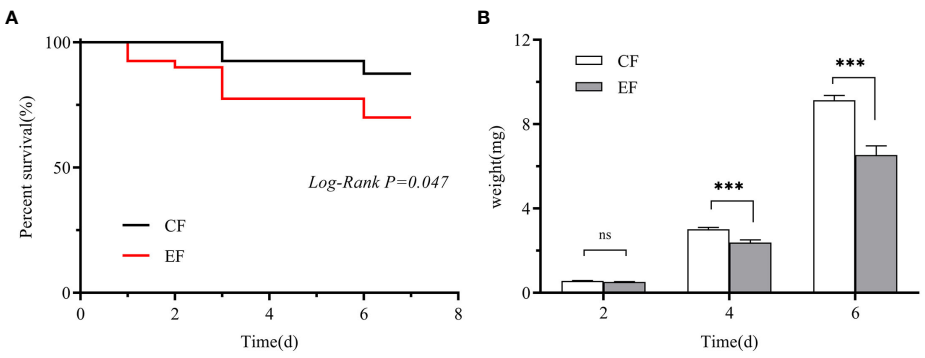

FIGURE 6
Performance of *P. versicolora* larvae feeding on leaves with and without prior egg deposition. CF: feeding-damaged leaves without prior egg deposition; EF: feeding-damaged leaves with prior egg deposition. **(A)** Survival curves for larvae feeding on plants with and without egg deposition. **(B)** Body weights of larvae at days 2, 4, and 6 on plants that were egg-free and plants with egg deposition, respectively. White bars indicate CF and gray bars indicate EF. Values are the means ± SE of four biological replicates. Asterisks indicate significant differences according to linear mixed models and significance levels: n.s: $P > 0.05$, ***: $P < 0.001$).

role in initiating the phenylpropanoid pathway by catalyzing the deamination of phenylalanine (Tohge et al., 2017). The upregulation of this pathway and the activity of PAL highlight the involvement of phenylpropanoid metabolites in the defense response of willows against *P. versicolora* egg deposition. The exact phenylpropanoid-derived secondary metabolites will be studied in the future through metabolomics and HPLC analysis that has been successfully applied in other plant systems to uncover the composition and changing nature of their secondary metabolites.

4.2 *P. versicolora* egg deposition altered willow transcriptome response to larval feeding

Willow leaves damaged by *P. versicolora* feeding with prior egg deposition showed more transcript changes than leaves without egg deposition. This indicates that the initial egg deposition can prime the plant's defense responses, leading to a more coordinated and effective defense against the subsequent feeding stages of the herbivore (Geuss et al., 2017).

Studies have shown that plant exposure to biotic or abiotic stress can influence their transcriptomic responses to subsequent stress (Conrath et al., 2015; Crisp et al., 2016). The transcriptional changes induced by insect eggs in plants can trigger an "alert" state, prompting the plants to reinforce their defenses against herbivores. Our results show that genes related to PR proteins and the cysteine proteinase inhibitor (CPIN) were also up-regulated. Additionally, the induction of lectins and protease inhibitors is known to possess anti-insect properties. Plant proteinase inhibitors have been shown to enhance defenses against insects and pathogens (Delaney et al., 1994). Studies have shown that anti-digestive proteins can impede the feeding of insects by inhibiting the activity of serine proteases in their digestive tracts (Mosolov and Valueva, 2005). *Tribolium castaneum* Herbst (Coleoptera, Tenebrionidae) guts usually show changes in digestive enzymes related to cysteine proteases and serine proteases when the larvae are treated with dietary cysteine peptidase inhibitors (Oppert et al., 2003; Oppert et al., 2010).

The enrichment of willow transcripts from GO categories associated with the phenylpropanoid pathway during larval feeding resulting from *P. versicolora* egg deposition suggests significant alterations in phenylpropanoid patterns. In tobacco leaves infested by moth larvae, prior egg deposition leads to enhanced levels of caffeoylputrescine (Bandoly et al., 2015); *A. thaliana* infested with butterfly eggs and larvae shows elevated levels of kaempferol derivatives (Lortzing et al., 2019); and elm exhibits enhanced phenylpropanoid transcriptional and metabolic responses to larvae (Schott et al., 2021). Thus, willow leaves that previously experienced *P. versicolora* egg deposition may be more effective in limiting herbivores due to the altered metabolite patterns induced by egg-mediated feeding. Using targeted and non-targeted metabolomics analyses and insect detoxification genes to explore the interaction between egg deposition-mediated phytochemical defenses and insects is important for future research.

4.3 Effects of egg deposition on insect performance

Our study shows that *P. versicolora* oviposition on willows could increase tree resistance to larvae. Specifically, when the *P. versicolora* larvae fed on plants with prior egg deposition, they experienced higher mortality and gained less weight (Figure 6). In general, these findings align with previous studies that have reported negative effects on the performance of herbivores when they feed on plants with prior egg deposition (Bandoly et al., 2015; Pashalidou et al., 2015). For example, the larvae of the pine sawfly *Diprion pini* (L.) experienced reduced weight gain and significantly higher mortality when they fed on pine twigs that had been previously laden with eggs (Beyaert et al., 2012).

However, these results were different from the effect of oviposition by a specialist hymenoptera, *Nematus oligospilus*, on *Salix babylonica* foliage (Dávila et al., 2023). Prior *N. oligospilus* egg depositions on *S. babylonica* did not have a significant impact on larval survival. While there was a slight difference in the average mass of mature larvae at 13 days between the egg-free treatment and the control foliage treatment, the difference was not statistically significant. In contrast, *N. oligospilus* experienced a significant increase in prepupal development time when feeding on foliage that had been previously subjected to egg deposition (Dávila et al., 2023). From current experiments, whether it is feeding-damaged leaves with or without prior *P. versicolora* egg deposition, they pupate in about 7 days. The effects of *P. versicolora* egg deposition were mainly concentrated in the larval stage, and the timing of pupae rearing may be similar to *X. luteola* and unaffected (Austel et al., 2016).

5 Conclusion

The present study confirms previous observations made in other plant species, demonstrating that oviposition by *P. versicolora* on willow (*Salix matsudana* cv. 'Zhuliu') increases the plant's resistance to larvae. RNA-seq data analysis revealed changes in the transcriptome of willows with *P. versicolora* egg deposition. Similarly, there was a slight increase in the number of transcriptome changes in leaves with egg deposition after larval feeding damage compared with leaves without egg deposition. These findings suggest that willow not only has the ability to respond directly to *P. versicolora* egg deposition but can also enhance this response when encountering feeding larvae. Therefore, we provide evidence here that insect egg deposition causes transcriptome changes in plants and reduces larval performance, which will be important for further studies of other woody plants, deciduous trees, and insects.

Data availability statement

The datasets presented in this study can be found in online repositories. The names of the repository/repositories and accession number(s) can be found below: https://www.ncbi.nlm.nih.gov/, PRJNA962771.

Author contributions

FL and ML conceived and designed the experiment. FL, BL, and CL performed the experiment. FL and YL analyzed data and wrote the manuscript. XL and ML revised the manuscript. All authors contributed to the article and approved the submitted version.

Funding

This project is supported by the Hubei University National talent project (1070017364).

Conflict of interest

The authors declare that the research was conducted in the absence of any commercial or financial relationships that could be construed as a potential conflict of interest.

Publisher's note

All claims expressed in this article are solely those of the authors and do not necessarily represent those of their affiliated organizations, or those of the publisher, the editors and the reviewers. Any product that may be evaluated in this article, or claim that may be made by its manufacturer, is not guaranteed or endorsed by the publisher.

Supplementary material

The Supplementary Material for this article can be found online at: https://www.frontiersin.org/articles/10.3389/fpls.2023.1226641/full#supplementary-material

References

Altmann, S., Muino, J. M., Lortzing, V., Brandt, R., Himmelbach, A., Altschmied, L., et al. (2018). Transcriptomic basis for reinforcement of elm antiherbivore defence mediated by insect egg deposition. *Mol. Ecol.* 27 (23), 4901–4915. doi: 10.1111/mec.14900

Austel, N., Eilers, E. J., Meiners, T., and Hilker, M. (2016). Elm leaves 'warned' by insect egg deposition reduce survival of hatching larvae by a shift in their quantitative leaf metabolite pattern. *Plant Cell Environ.* 39 (2), 366–376. doi: 10.1111/pce.12619

Bandoly, M., Grichnik, R., Hilker, M., and Steppuhn, A. (2016). Priming of anti-herbivore defence in *Nicotiana attenuata* by insect oviposition: herbivore-specific effects. *Plant Cell Environ.* 39 (4), 848–859. doi: 10.1111/pce.12677

Bandoly, M., Hilker, M., and Steppuhn, A. (2015). Oviposition by *Spodoptera exigua* on *Nicotiana attenuata* primes induced plant defence against larval herbivory. *Plant J.* 83 (4), 661–672. doi: 10.1111/tpj.12918

Basset, Y., Cizek, L., Cuénoud, P., Didham, R. K., Guilhaumon, F., Missa, O., et al. (2012). Arthropod diversity in a tropical forest. *Science* 338 (6113), 1481–1484. doi: 10.1126/science.1226727

Bertea, C. M., Casacci, L. P., Bonelli, S., Zampollo, A., and Barbero, F. (2020). Chemical, physiological and molecular responses of host plants to lepidopteran egg-laying. *Front. Plant Sci.* 10. doi: 10.3389/fpls.2019.01768

Beyaert, I., Köpke, D., Stiller, J., Hammerbacher, A., Yoneya, K., Schmidt, A., et al. (2012). Can insect egg deposition 'warn' a plant of future feeding damage by herbivorous larvae? *Proc. Biol. Sci.* 279 (1726), 101–108. doi: 10.1098/rspb.2011.0468

Bittner, N., Hundacker, J., Achotegui-Castells, A., Anderbrant, O., and Hilker, M. (2019). Defense of scots pine against sawfly eggs (*Diprion pini*) is primed by exposure to sawfly sex pheromones. *Proc. Natl. Acad. Sci. U. S. A.* 116 (49), 24668–24675. doi: 10.1073/pnas.1910991116

Bonnet, C., Lassueur, S., Ponzio, C., Gols, R., Dicke, M., and Reymond, P. (2017). Combined biotic stresses trigger similar transcriptomic responses but contrasting resistance against a chewing herbivore in *Brassica nigra*. *BMC Plant Biol.* 17 (1), 127. doi: 10.1186/s12870-017-1074-7

Bruessow, F., Gouhier-Darimont, C., Buchala, A., Metraux, J. P., and Reymond, P. (2010). Insect eggs suppress plant defence against chewing herbivores. *Plant J.* 62 (5), 876–885. doi: 10.1111/j.1365-313X.2010.04200.x

Büchel, K., McDowell, E., Nelson, W., Descour, A., Gershenzon, J., Hilker, M., et al. (2012). An elm EST database for identifying leaf beetle egg-induced defense genes. *BMC Genom.* 13, 242. doi: 10.1186/1471-2164-13-242

Caldwell, E., Read, J., and Sanson, G. D. (2016). Which leaf mechanical traits correlate with insect herbivory among feeding guilds? *Ann. Bot.* 117 (2), 349–361. doi: 10.1093/aob/mcv178

Chen, S., Zhou, Y., Chen, Y., and Gu, J. (2018). Fastp: an ultra-fast all-in-one FASTQ preprocessor. *Bioinformatics.* 34 (17), i884–i890. doi: 10.1093/bioinformatics/bty560

Conrath, U., Beckers, G. J., Langenbach, C. J., and Jaskiewicz, M. R. (2015). Priming for enhanced defence. *Annu. Rev. Phytopathol.* 53, 97–119. doi: 10.1146/annurev-phyto-080614-120132

Crisp, P. A., Ganguly, D., Eichten, S. R., Borevitz, J. O., and Pogson, B. J. (2016). Reconsidering plant memory: intersections between stress recovery, RNA turnover, and epigenetics. *Sci. Adv.* 2 (2), e1501340. doi: 10.1126/sciadv.1501340

Dávila, C., Fiorenza, J. E., Gershenzon, J., Reichelt, M., Zavala, J. A., and Fernández, P. C. (2023). Sawfly egg deposition extends the insect life cycle and alters hormone and volatile emission profiles. *Front. Ecol. Evol.* 11. doi: 10.3389/fevo.2023.1084063

Delaney, T. P., Uknes, S., Vernooij, B., Friedrich, L., Weymann, K., Negrotto, D., et al. (1994). A central role of salicylic acid in plant disease resistance. *Science* 266, 1247–1250. doi: 10.1126/science.266.5188.1247

Desurmont, G. A., and Weston, P. A. (2011). Aggregative oviposition of a phytophagous beetle overcomes egg crushing plant defences. *Ecol. Entomol.* 36 (3), 335–343. doi: 10.1111/j.1365-2311.2011.01277.x

Eyles, A., Bonello, P., Ganley, R., and Mohammed, C. (2010). Induced resistance to pests and pathogens in trees. *New Phytol.* 185 (4), 893–908. doi: 10.1111/j.1469-8137.2009.03127.x

Fu, L., Niu, B., Zhu, Z., Wu, S., and Li, W. (2012). CD-HIT: accelerated for clustering the next-generation sequencing data. *Bioinformatics* 28 (23), 3150–3152. doi: 10.1093/bioinformatics/bts565

Geuss, D., Stelzer, S., Lortzing, T., and Steppuhn, A. (2017). *Solanum dulcamara*'s response to eggs of an insect herbivore comprises ovicidal hydrogen peroxide production. *Plant Cell Environ.* 40 (11), 2663–2677. doi: 10.1111/pce.13015

Gouhier-Darimont, C., Schmiesing, A., Bonnet, C., Lassueur, S., and Reymond, P. (2013). Signalling of *Arabidopsis thaliana* response to *Pieris brassicae* eggs shares similarities with PAMP-triggered immunity. *J. Exp. Bot.* 64 (2), 665–674. doi: 10.1093/jxb/ers362

Grabherr, M. G., Haas, B. J., Yassour, M., Levin, J. Z., Thompson, D. A., Amit, I., et al. (2011). Full-length transcriptome assembly from RNA-seq data without a reference genome. *Nat. Biotechnol.* 29 (7), 644–652. doi: 10.1038/nbt.1883

Hallgren, P. (2003). Effects of willow hybridisation and simulated browsing on the development and survival of the leaf beetle *Phratora vitellinae*. *BMC Ecol.* 3, 5. doi: 10.1186/1472-6785-3-5

Heil, M., and Silva Bueno, J. C. (2007). Within-plant signaling by volatiles leads to induction and priming of an indirect plant defense in nature. *Proc. Natl. Acad. Sci. U. S. A.* 104 (13), 5467–5472. doi: 10.1073/pnas.0610266104

Hilker, M., and Fatouros, N. E. (2015). Plant responses to insect egg deposition. *Annu. Rev. Entomol.* 60, 493–515. doi: 10.1146/annurev-ento-010814-020620

Hilker, M., and Fatouros, N. E. (2016). Resisting the onset of herbivore attack: plants perceive and respond to insect eggs. *Curr. Opin. Plant Biol.* 32, 9–16. doi: 10.1016/j.pbi.2016.05.003

Kim, J., Tooker, J. F., Luthe, D. S., De Moraes, C. M., and Felton, G. W. (2012). Insect eggs can enhance wound response in plants: a study system of tomato *Solanum lycopersicum* L. and *Helicoverpa zea* boddie. *PloS One* 7 (5), e37420. doi: 10.1371/journal.pone.0037420

Li, B., and Dewey, C. N. (2011). RSEM: accurate transcript quantification from RNA-seq data with or without a reference genome. *BMC Bioinf.* 12, 323. doi: 10.1186/1471-2105-12-323

Li, J., Jia, H., Han, X., Zhang, J., Sun, P., Lu, M., et al. (2016). Selection of reliable reference genes for gene expression analysis under abiotic stresses in the desert biomass willow, *Salix psammophila*. *Front. Plant Sci.* 7. doi: 10.3389/fpls.2016.01505

Li, Y., Ze, L. J., Liu, F. J., Liao, W., Lu, M., and Liu, X. L. (2022). RNA Interference of vATPase subunits a and e affects survival of larvae and adults in *Plagiodera versicolora* (Coleoptera: chrysomelidae). *Pestic Biochem. Physiol.* 188, 105275. doi: 10.1016/j.pestbp.2022.105275

Little, D., Gouhier-Darimont, C., Bruessow, F., and Reymond, P. (2007). Oviposition by *pierid butterflies* triggers defense responses in arabidopsis. *Plant Physiol.* 143 (2), 784–800. doi: 10.1104/pp.106.090837

Livak, K. J., and Schmittgen, T. D. (2001). Analysis of relative gene expression data using real-time quantitative PCR and the 2(-delta delta C(T)) method. *Methods* 25 (4), 402–408. doi: 10.1006/meth.2001.1262

Lortzing, T., Kunze, R., Steppuhn, A., Hilker, M., and Lortzing, V. (2020). Arabidopsis, tobacco, nightshade and elm take insect eggs as herbivore alarm and show similar transcriptomic alarm responses. *Sci. Rep.* 10 (1), 16281. doi: 10.1038/s41598-020-72955-y

Lortzing, V., Oberländer, J., Lortzing, T., Tohge, T., Steppuhn, A., Kunze, R., et al. (2019). Insect egg deposition renders plant defence against hatching larvae more effective in a salicylic acid-dependent manner. *Plant Cell Environ.* 42 (3), 1019–1032. doi: 10.1111/pce.13447

Love, M. I., Huber, W., and Anders, S. (2014). Moderated estimation of fold change and dispersion for RNA-seq data with DESeq2. *Genome Biol.* 15 (12), 550. doi: 10.1186/s13059-014-0550-8

Ma, M., Tu, C., Luo, J., Lu, M., Zhang, S., and Xu, L. (2021). Metabolic and immunological effects of gut microbiota in leaf beetles at the local and systemic levels. *Integr. Zool.* 16 (3), 313–323. doi: 10.1111/1749-4877.12528

Manni, M., Berkeley, M. R., Seppey, M., Simão, F. A., and Zdobnov, E. M. (2021). BUSCO update: novel and streamlined workflows along with broader and deeper phylogenetic coverage for scoring of eukaryotic, prokaryotic, and viral genomes. *Mol. Biol. Evol.* 38 (10), 4647–4654. doi: 10.1093/molbev/msab199

Mauch-Mani, B., Baccelli, I., Luna, E., and Flors, V. (2017). Defense priming: an adaptive part of induced resistance. *Annu. Rev. Plant Biol.* 68, 485–512. doi: 10.1146/annurev-arplant-042916-041132

Mosolov, V. V., and Valueva, T. A. (2005). Proteinase inhibitors and their function in plants: a review. *Appl. Biochem. Microbiol.* 41, 227–261. doi: 10.1007/s10438-005-0040-6

Ojeda-Martinez, D., Diaz, I., and Santamaria, M. E. (2022). Transcriptomic landscape of herbivore oviposition in arabidopsis: a systematic review. *Front. Plant Sci.* 12. doi: 10.3389/fpls.2021.772492

Oppert, B., Elpidina, E. N., Toutges, M., and Mazumdar-Leighton, S. (2010). Microarray analysis reveals strategies of *Tribolium castaneum* larvae to compensate for cysteine and serine protease inhibitors. *Comp. Biochem. Physiol. Part D Genomics Proteomics.* 5 (4), 280–287. doi: 10.1016/j.cbd.2010.08.001

Oppert, B., Morgan, T. D., Hartzer, K., Lenarcic, B., Galesa, K., Brzin, J., et al. (2003). Effects of proteinase inhibitors on digestive proteinases and growth of the red flour beetle, *Tribolium castaneum* (Herbst) (Coleoptera: tenebrionidae). *Comp. Biochem. Physiol. C Toxicol. Pharmacol.* 134 (4), 481–490. doi: 10.1016/s1532-0456(03)00042-5

Pashalidou, F. G., Eyman, L., Sims, J., Buckley, J., Fatouros, N. E., De Moraes, C. M., et al. (2020). Plant volatiles induced by herbivore eggs prime defences and mediate shifts in the reproductive strategy of receiving plants. *Ecol. Lett.* 23 (7), 1097–1106. doi: 10.1111/ele.13509

Pashalidou, F. G., Fatouros, N. E., van Loon, J. J. A., Dicke, M., and Gols, R. (2015). Plant-mediated effects of butterfly egg deposition on subsequent caterpillar and pupal development, across different species of wild Brassicaceae. *Ecol. Entomol.* 40, 444–450. doi: 10.1111/een.12208

Pashalidou, F. G., Lucas-Barbosa, D., van Loon, J. J., Dicke, M., and Fatouros, N. E. (2013). Phenotypic plasticity of plant response to herbivore eggs: effects on resistance to caterpillars and plant development. *Ecology* 94 (3), 702–713. doi: 10.1890/12-1561.1

Petzold-Maxwell, J., Wong, S., Arellano, C., and Gould, F. (2011). Host plant direct defence against eggs of its specialist herbivore, *Heliothis subflexa*. *Ecol. Entomol.* 36 (6), 700–708. doi: 10.1111/j.1365-2311.2011.01315.x

R Core Team. (2022). R: A language and environment for statistical computing. *R Foundation for Statistical Computing* (Vienna, Austria). Available at: https://www.R-project.org/.12c.

Rentel, M. C., Lecourieux, D., Ouaked, F., Usher, S. L., Petersen, L., Okamoto, H., et al. (2004). OXI1 kinase is necessary for oxidative burst-mediated signalling in arabidopsis. *Nature* 27 (6977), 858–861. doi: 10.1038/nature02353

Reymond, P. (2013). Perception, signaling and molecular basis of oviposition-mediated plant responses. *Planta* 238 (2), 247–258. doi: 10.1007/s00425-013-1908-y

Schott, J., Fuchs, B., Böttcher, C., and Hilker, M. (2021). Responses to larval herbivory in the phenylpropanoid pathway of ulmus minor are boosted by prior insect egg deposition. *Planta* 255 (1), 16. doi: 10.1007/s00425-021-03803-0

Smith-Unna, R., Boursnell, C., Patro, R., Hibberd, J. M., and Kelly, S. (2016). TransRate: reference-free quality assessment of *de novo* transcriptome assemblies. *Genome Res.* 26 (8), 1134–1144. doi: 10.1101/gr.196469.115

Spoel, S. H., Koornneef, A., Claessens, S. M., Korzelius, J. P., Van Pelt, J. A., Mueller, M. J., et al. (2003). NPR1 modulates cross-talk between salicylate- and jasmonate-dependent defense pathways through a novel function in the cytosol. *Plant Cell.* 15 (3), 760–770. doi: 10.1105/tpc.009159

Tahvanainen, J., Julkunen-Tiitto, R., and Kettunen, J. (1985). Phenolic glycosides govern the food selection pattern of willow feeding leaf beetles. *Oecologia* 67 (1), 52–56. doi: 10.1007/BF00378451

Tohge, T., de Souza, L. P., and Fernie, A. R. (2017). Current understanding of the pathways of flavonoid biosynthesis in model and crop plants. *J. Exp. Bot.* 68 (15), 4013–4028. doi: 10.1093/jxb/erx177

Utsumi, S., Ando, Y., and Ohgushi, T. (2009). Evolution of feeding preference in a leaf beetle: the importance of phenotypic plasticity of a host plant. *Ecol. Lett.* 12 (9), 920–929. doi: 10.1111/j.1461-0248.2009.01349.x

Van Loon, L. C., Rep, M., and Pieterse, C. M. (2006). Significance of inducible defense-related proteins in infected plants. *Annu. Rev. Phytopathol.* 44, 135–162. doi: 10.1146/annurev.phyto.44.070505.143425

Veluthakkal, R., and Dasgupta, M. G. (2010). Pathogenesis-related genes and proteins in forest tree species. *Trees.* 24, 993–1006. doi: 10.1007/s00468-010-0489-7

Weigel, R. R., Bäuscher, C., Pfitzner, A. J., and Pfitzner, U. M. (2001). NIMIN-1, NIMIN-2 and NIMIN-3, members of a novel family of proteins from arabidopsis that interact with NPR1/NIM1, a key regulator of systemic acquired resistance in plants. *Plant Mol. Biol.* 46 (2), 143–160. doi: 10.1023/a:1010652620115

Xie, C., Mao, X., Huang, J., Ding, Y., Wu, J., Dong, S., et al. (2011). KOBAS 2.0: a web server for annotation and identification of enriched pathways and diseases. *Nucleic Acids Res.* 39 (Web Server issue), W316–W322. doi: 10.1093/nar/gkr483

Yamasaki, M., Yoshimura, A., and Yasui, H. (2003). Genetic basis of ovicidal response to whitebacked planthopper (*Sogatella furcifera* horváth) in rice (*Oryza sativa* L.). *Mol. Breeding* 12, 133–143. doi: 10.1023/A:1026018821472

Yang, Z. D., Zhu, L., Zhao, B. G., and Fang, J. (2005). Bionomics of *Plagiodera versicolora* in the laboratory. *Entomological Knowledge.* 42 (6), 647–650. Available at: https://kns.cnki.net/kcms2/article/abstract?v=F6gKQ3F1NefeecABELnpHlvCrQilO7kGvSxMrE-2fbkp1anGJ3H-a1a_UkXKnMfhjV1IfTXKJ1T9psHvOKLcNbzCFdSI6xnJk5WNBeTKU5ZY1SbxRbFohv4cYbDOmUOI&uniplatform=NZKPT&language=CHS.

frontiers | Frontiers in Plant Science

TYPE Original Research
PUBLISHED 19 July 2023
DOI 10.3389/fpls.2023.1204305

OPEN ACCESS

EDITED BY
Shengli Jing,
Xinyang Normal University, China

REVIEWED BY
Guoxing Wu,
Yunnan Agricultural University, China
Cuixiang Wan,
Nanchang University, China

*CORRESPONDENCE
Xiaolan Wang
wxl1972@gzhu.edu.cn
Liping Hou
houliping7710@163.com

RECEIVED 12 April 2023
ACCEPTED 03 July 2023
PUBLISHED 19 July 2023

CITATION
Li Y, Tan Z, Wang X and Hou L (2023) Metabolic changes and potential biomarkers in "*Candidatus* Liberibacter solanacearum"-infected potato psyllids: implications for psyllid-pathogen interactions. *Front. Plant Sci.* 14:1204305. doi: 10.3389/fpls.2023.1204305

Metabolic changes and potential biomarkers in "*Candidatus* Liberibacter solanacearum"-infected potato psyllids: implications for psyllid-pathogen interactions

Yelin Li[1], Zhiqing Tan[1,2], Xiaolan Wang[1,3]* and Liping Hou[1]*

[1]School of Life Sciences, Guangzhou University, Guangzhou, China, [2]School of Life Sciences, Zhaoqing University, Zhaoqing, China, [3]Guangdong Provincial Key Laboratory of Plant Adaptation and Molecular Design, Guangzhou University, Guangzhou, China

Psyllid yellows, vein-greening (VG), and zebra chip (ZC) diseases, which are primarily transmitted by potato psyllid (PoP) carrying *Candidatus* Liberibacter solanacearum (*C*Lso), have caused significant losses in solanaceous crop production worldwide. Pathogens interact with their vectors at the organic and cellular levels, while the potential changes that may occur at the biochemical level are less well reported. In this study, the impact of *C*Lso on the metabolism of PoP and the identification of biomarkers from infected psyllids were examined. Using ultra-performance liquid chromatography tandem mass spectrometry (UPLC-MS/MS) analysis, metabolomic changes in *C*Lso-infected psyllids were compared to uninfected ones. A total of 34 metabolites were identified as potential biomarkers of *C*Lso infection, which were primarily related to amino acid, carbohydrate, and lipid metabolism. The significant increase in glycerophospholipids is thought to be associated with *C*Lso evading the insect vector's immune defense. Matrix-assisted Laser Desorption Ionization Mass Spectrometry Imaging (MALDI-MSI) was used to map the spatial distribution of these biomarkers, revealing that 15-keto-Prostaglandin E2 and alpha-D-Glucose were highly expressed in the abdomen of uninfected psyllids but down-regulated in infected psyllids. It is speculated that this down-regulation may be due to *C*Lso evading surveillance by immune suppression in the PoP midgut. Overall, valuable biochemical information was provided, a theoretical basis for a better understanding of psyllid-pathogen interactions was offered, and the findings may aid in breaking the transmission cycle of these diseases.

KEYWORDS

infection, psyllid, metabolism, pathogen, interaction, potential biomarkers

Introduction

The potato psyllid (PoP), *Bactericera cockerelli* (Sulc) (Hemiptera : Triozidae), is a phloem-feeding member of the Hemiptera family commonly found on plant species of the Convolvulaceae and Solanaceae families (Baumann, 2005; Fisher et al., 2014). As the vector of the unculturable gram-negative *C*Lso, once it feeds on potato or tomato plants, the psyllid transmits *C*Lso through its saliva, causing psyllid yellows, vein-greening (VG) and zebra chip (ZC) diseases to occur (Alvarado et al., 2012; Mishra and Ghanim, 2022). The common symptoms of psyllid yellows include yellowing of leaves, aerial tubers, shortened and thickened internodes, stunted plant growth, and in extreme cases caused plant death (Munyaneza et al., 2007; Goolsby et al., 2012). It has been reported to cause a decrease in potato crop yield and quality, and ZC disease could result in potato yield losses up to 94% (Greenway, 2014). *C*Lso-infected psyllids can also lead to severe economic losses, in Texas, ca. 33 million dollars annually in potato production due to ZC disease (Prager et al., 2022).

PoP is the only known carrier of the *C*Lso that causes ZC disease (Rondon et al., 2022). Due to the lack of effective integrated management approach for ZC, currently, controlling the spread of ZC and VG diseases caused by *C*Lso is achieved managing the psyllid vector by the use of chemical pesticides, which is costly and poses risks to the environment and human health (Mora et al., 2021). One potential solution to this problem is identifying and deploying *C*Lso-resistant varieties. This is an effective long-term pest management strategy, but it can take a significant amount of time to develop these varieties, and there is the possibility that the pressure of evolution may lead to the development of resistant PoP varieties. Therefore, a more comprehensive and sustainable management plan is needed that not only incorporates genetic tools but also a deeper understanding of the interactions between *C*Lso, its plant hosts, and its insect vector.

Multiple studies have investigated the interactions between psyllids and the bacteria they transmit. For instance, research on the Asian citrus psyllid (ACP) has revealed that infection with *Candidatus* Liberibacter asiaticus (*C*Las) leads to a down-regulation of the phenoloxidase enzyme. Phenoloxidase is associated with the melanization defense response, suggesting that *C*Las suppresses the immune system of the ACP (Eleftherianos and Revenis, 2011). Additionally, the expression of the hexamine protein was found to be suppressed in *C*Las-infected adults, which could indicate that *C*Las may regulate the availability of free amino acids by interfering with hexamerin storage pathways (Burmester et al., 1998).

Transcriptome analysis of infected psyllids has also shown that *C*Lso greatly affects genes involved in metabolic processes, while having a lesser effect on genes associated with immune and stress response (Nachappa et al., 2012). Furthermore, studies of genes related to metabolism and nutrition of adult PoP have revealed that *C*Lso infection alters purine, carbon, pyrimidine, glycerophospholipid, and choline metabolism (Vyas et al., 2015). These studies demonstrate that the bacteria transmitted by psyllids has significant impacts on the physiology, biochemistry, and immunity of the psyllids themselves as well.

Recent studies have also lucubrated the metabolic changes of the ACP when it is infected with the bacteria *C*Las. Research has found that the levels of adenosine triphosphate (ATP) in *C*Las-infected psyllids were higher than in uninfected psyllids, indicating that *C*Las altered the energy metabolism, which means *C*Las took up ATP by using ATP translocase of its psyllid vector (Killiny et al., 2017). Additionally, it has been reported that *C*Las infection can elicit a response to biotic stress or cell damage, and induce nutrient and energetic stress in the host insect (Killiny et al., 2017). These studies have provided a deeper understanding of the metabolic changes that occur in this important insect pest and disease vector at the metabolomic level. As *Liberibacter* species act as intracellular parasites, understanding the metabolic connections between the bacteria and their hosts is a crucial aspect of disease management.

However, the metabolic effects of *C*Lso-infection on its host, the potato or tomato psyllid, have not yet been fully explored. Understanding how metabolic pathways within the potato psyllid host are affected or respond to infection by *Liberibacter* species is crucial for identifying more effective disease management strategies (Pratavieira et al., 2014; Cicalini et al., 2019; Yang et al., 2020).

UPLC-MS/MS, as a high-throughput assay for the rapid detection and identification of metabolites, has been applied to several insect models, such as *Drosophila* (Tuthill et al., 2020), Africanized honey bees (*Apis mellifera* L.) (Barbosa-Medina et al., 2022) and *Aedes* mosquitoes (Chen et al., 2020). Matrix-assisted Laser Desorption Ionization Mass Spectrometry Imaging (MALDI-MSI) not only highly sensitive, but also enables visualization and localization of metabolites in tissues and insect organisms (Susniak et al., 2020; Tuck et al., 2022). The use of MALDI-MSI in combination with ultra performance liquid chromatography (UPLC) has been shown to be effective technique, such as identification of lipid species and tissue-specific analysis in high-sugar-fed *Drosophila* (Tuthill et al., 2020).

In this study, the goal was to use this technology to investigate the changes in PoP metabolites upon infection with the bacterium *C*Lso, with the aim of identifying biomarkers for quick identification of infected psyllids. The changes in these metabolites, whether an increase or decrease, may have influenced the interaction between *C*Lso and the psyllid host and may have facilitated further psyllid transmission to plants. Therefore, the analysis of metabonomic changes between *C*Lso-infected and uninfected psyllids may provides more information about how PoPs respond to and cope with *C*Lso infection.

Materials and methods

Chemicals

Acetonitrile and formic acid (Fisher Scientific, Loughborough, UK) of HPLC-grade were used. Ultrapure water was produced using a Milli-Q plus (Milford, MA, USA) water purification system. Methanol was supplied by Merck (Darmstadt, Germany). Leucine enkephalin was obtained from Waters (Milford, USA). Organic matrix compound, 2,5-dihydroxybenzoic acid (DHB, 98%) was

purchased from Sigma-Aldrich (St. Louis, MO, USA). Gelatin from porcine skin (300 bloom) was purchased from Electron Microscopy Sciences (Hatfield, PA, USA).

Insect source

Live adult psyllids (*Bactericera cockerelli*) (Sulc) that were infected or uninfected with *C*Lso were collected from the potato/tomato psyllid colony maintained by Dr. Brown's lab at the University of Arizona as described (Fisher et al., 2014). The cytochrome oxidase I gene as a molecular marker to haplotype psyllid as "central type", and primers were used to amplify 16S rRNA gene to routinely detect the presence of *C*Lso in colonies by PCR. The collected live psyllids were flash frozen in liquid nitrogen and stored at -80°C until further processed. A total of 100 *C*Lso-infected and 100 uninfected PoP mature adults were selected and divided into 5 sets per treatment type evenly, with 20 PoP in each set. Each set comprised a separate biological replicate.

Metabolite extraction

The extraction of metabolites for UPLC-MS/MS analysis was conducted as described in Overgaard et al. (Overgaard et al., 2007) with minor modifications. In brief, 20 psyllids were randomly selected from each of the infected and uninfected groups. The samples were pulverized using a TissueLyser II (Qiagen) in precooled (liquid nitrogen) 1.5 mL microfuge tubes using a steel ball mill by operating the instrument as follows: running for 30 seconds, stopping for 30 seconds, and repeating this cycle three times at 30 Hz. Next, 400 µL 50% methonal was added and the samples were vortexed briefly, followed by sonication for 5 minutes with the tubes partially submerged in a water bath at room temperature (5200 Bransonic, Danbury, CT, USA). After centrifugation at 20,000 × g (22,000 *rpm*) for 5 minutes, the methonal was transferred to a fresh microfuge tube. The pellet was resuspended in an additional 400 µL of 50% methonal, sonicated, and centrifuged again for 5 min, respectively, and the methonal was combined with the first sample extraction. The pellets were then extracted in the same manner, but using ethyl acetate as solvent. The three ethyl acetate fractions for each sample were combined with the mixture. After three sequential extractions, a centrifugal evaporator (CentriVap Cold Traps, Labconco) was used for solvent removal and sample dryness. Then, the dried extracts were dissolved in 100 µL of methanol/water solution (1:1) and centrifuged at 20,000 × g for 15 min at 4°C. 90 µL supernatants were analyzed *via* LC-MS. All samples of the same volume to be measured were mixed as quality control (QC) samples to monitor the stability of the analysis.

UPLC-MS/MS analysis

Samples were analyzed using a Waters ACQUITY UPLC system (Waters Corporation in Milford, USA) that was coupled with a Waters Synapt G2-S HDMS ion mobility quadrupole time-of-flight mass spectrometry (IM-Q-TOF-MS). The injection volume for each sample was 2 µL. Chromatographic separations were achieved using an ACQUITY BEH C18 column ((100 mm × 2.1 mm, particle size1.7 µm; Waters). The column was eluted at a flow rate of 400 µL·min^{-1}, using mobile phase A consisting of 0.1% formic acid in HPLC-grade water, and mobile phase B consisting of 0.1% formic acid in methanol. An elution gradient system was used, starting with 85% of mobile phase A and 15% of mobile phase B for 1.5 minutes, before it was gradually changed over 6 minutes to 65% A and 35% B, then another 2 minutes to 50% A and 50% B, then in 1 minute to 20% A and 80% B, and maintained at this level for another 1 minute before returning to the initial conditions of 85% A and 15% B over 0.5 minutes. The column was then re-equilibrated at 85% A for 4 minutes. The total analysis time for each sample was 14 minutes. Five biological replicates were performed for each of the two treatment types.

The separated components were analyzed using a Waters Synapt G2-S HDMS ion mobility quadrupole time-of-flight mass spectrometry (IM-Q-TOF-MS) equipped with an ESI-ion mode. The detection parameters were set as follows: capillary voltage of 3 kV, cone voltage of 30 V, calibration with sodium formate, and high resolution mode for the TOF resolution. A lock-mass of leucine encephalin (200 pg/mL) was employed as a lock spray, and a blank was analyzed between every two samples to clean the column. The mass spectrometric profiles were acquired from a scan mass range of 100 to 1000 *m/z* in positive and negative ionization mode.

Data analysis

We performed peak picking, alignment, and normalization of the mass spectral data obtained by UPLC-MS/MS using the ProgenesisQI software program (Waters Corporation, Milford, USA). Based on the retention time [RT], mass-to-charge ratio [*m/z*], and peak intensity from the untargeted analysis, data were exported to Ezinfo and Metlin to identify specific ions that differed significantly in abundance between uninfected and infected insects. The resulting UPLC-MS/MS data, including peak numbers, sample names, and normalized peak areas, were inputted into the SIMCA 14.1 software package (Umetrics, Umea, Sweden) for principal component analysis (PCA) and supervised orthogonal projection to latent structures discriminate analysis (OPLS-DA) models, which were used to evaluate the relationships between the *C*Lso-infected and uninfected samples. The differential metabolites were identified according to the variable importance in projection (VIP) values >1.0 obtained from the OPLS-DA model and p-values <0.05 obtained by Student's t-test, then Kyoto Encyclopedia of Genes and Genomes (KEGG) and LIPID MAPS Structure Database (LMSD) were used for further screening of differential metabolites. KEGG (https://www.genome.jp/kegg/) was used to analyze the enrichment of metabolites, and the enriched metabolic pathways were subjected to a heatmap analysis of multiple change. The KEGG pathways analysis and visualization were done using the free web-based tools, MetaboAnalyst 5.0 (https://www.metaboanalyst.ca/).

Tissue section preparation

Frozen psyllids were placed in a 30% w/v sucrose solution for 1 hour of sucrose infiltration. The insects were then embedded in a 10% w/v gelatin block by laying them out in the same orientation on a pre-made gelatin block and covering them with molten gelatin cooled just before it re-sets. The finished block was trimmed to remove excess gelatin, mounted on a sample holder using molten gelatin, and then frozen. The solidified sample blocks were cut into 20 µm thick sections using a -23°C Leica CM1950 cryostat (Leica Biosystems GmbH, Nussloch, Germany). The frozen tissue slices (serial sections) were then thaw-mounted on standard non-coated histological glass slides (76 mm × 26 mm × 1.2 mm) for MALDI-MSI analysis. About 10 sections were placed on a single sample slide and were desiccated before the matrix application.

MALDI-MSI

Insect samples for MALDI-MSI analysis were prepared using a method similar to the one previously described by Niehoff et al. (Niehoff et al., 2014), with some modifications. 2,5-DHB (20 $mg{\cdot}mL^{-1}$) dissolved in 50% methanol was chosen as the matrix material and was sprayed onto the tissue slices using an automated sprayer (TM-Sprayer^{TM}, HTX Technologies, Carrboro, NC, USA) at a pressure of 80 bar (N) and 16 cycles. After matrix application, the slides were dried at room temperature for 1 hour and then mounted on a sample plate designed for glass slides.

MSI analysis was conducted in positive ion mode using a MALDI-solariX 9.4T FTICR-MS System (Bruker Daltonics Inc, Billerica, USA) equipped with a Smartbeam II laser. The FTMS Control 3.0 and FlexImaging 3.2 software packages (Bruker Daltonics, Bremen, Germany) were used to control the mass spectrometer and set imaging parameters (1 kHz laser, medium spot size laser, 350 ns pulsed ion extraction, mass range of *m/z* 100-2,000, 300 laser shots per spot) and data analyzed by FlexImaging and ClinproTools software (Bruker Daltonics Inc).

For images shown, the *C*Lso infected and uninfected sections were imaged on one plate. Total ion current normalization calculates the normalized peak intensity for each spectral feature (peak) by dividing its intensity by the total ion current in each mass spectrum across an entire imaging data set, in this case across four lens images. Ion intensities are then displayed across the image by assigning the largest normalized signal for each *m/z* to a value of 100% and the lowest normalized signal as 0%. Therefore, each ion image is calculated independently from other ion images. For display purposes, data were interpolated and pixel intensities were rescaled using "brightness optimization" in FlexImaging software. This feature optimizes the brightness of each individual signal to use the entire dynamic range, as indicated by the color scale bars. The integrated intensity for each *m/z* signal (± 0.001% *m/z* units) was plotted as a normalized TIC value. A total of three technical replicates were run to ensure reproducibility of molecular patterns.

Results

Overall changes in metabolites of PoP after *C*Lso infection

Metabolomic analyses were conducted using a UPLC-MS-based method. To classify groups suspected of showing metabolic differences, PCA and OPLS-DA approaches, which are commonly used in metabolomics, were employed. PCA shown a separation between infected and uninfected PoP (Figure 1A). The separated different clusters indicated that *C*Lso-infection changed the metabolic profiles of PoP. To further differentiate the metabolite features and identify potential marker metabolites, a supervised multivariate data analysis approach, OPLS-DA, was performed. As shown in Figure 1B, the infected group was clearly separated from the uninfected group. To ensure the model's quality, the permutation testing of OPLS-DA model was performed. The cumulative values of R^2Y and Q^2 is 0.997 and 0.786, respectively, suggesting that the OPLS-DA model had good fitting and high predictability (Figure 1C) and could be used for further analysis. The S-plot was used to show the differentially accumulated metabolites (DAMs) between infected and uninfected groups (Figure 1D), which may be regarded as potential biomarkers.

Identification of potential biomarkers

Based on the goal for exploring potential biomarkers, so VIP ≥ 1 and $p < 0.05$ as a screened criteria, a total of 142 metabolites were identified (Supplementary Table S1). To further target markers associated with pathogen infection, KEGG database and LMSD database were used. Among 142 metabolites, 34 metabolites were matched to the known substances. They included 19 lipids and lipid-like molecules, 9 organic acids and derivatives, 3 other organic compounds, 1 phenylpropanoids and polyketides, and 2 other compounds (Supplementary Table S2). To clearly visualize the variation trends in metabolite between infected and uninfected groups, a heat map was drawn (Figure 2A). Compared to the control group, 22 metabolites were up-regulated (shown in red) and 12 metabolites were down-regulated (shown in blue) in the infected group (Supplementary Table S3).

Metabolic pathway analysis of infected and uninfected PoP

To identify the most relevant metabolic pathways involved in *C*Lso infection, KEGG enrichment analysis was employed. The x axis indicates that the proportion and numbers of metabolites annotated to the pathway, and the y axis indicates the name of KEGG metabolic pathway. The P-value calculated from the pathway topology analysis was set to 0.05. *C*Lso infection significantly affected arginine biosynthesis, alanine, aspartate, and glutamate metabolism, glutathione metabolism and galactose metabolism as shown in Figure 2B.

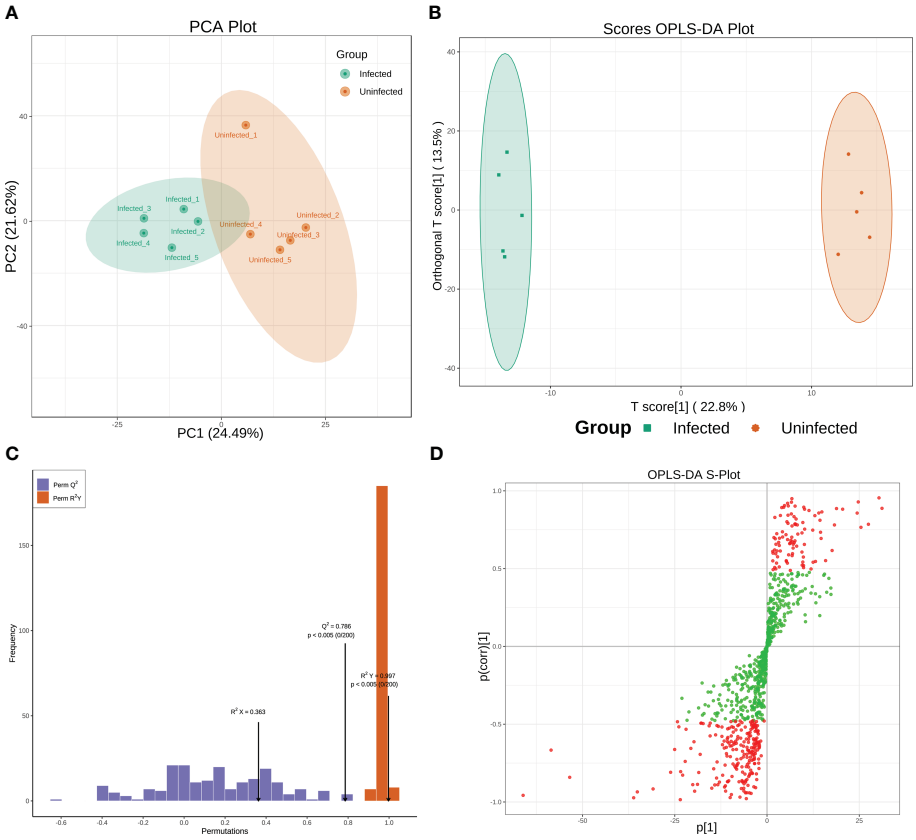

FIGURE 1
(A, B) Principal Component Analysis (PCA) score plot and OPLS-DA scores plot of infected and uninfected group. Each point in the figure represents a sample, and the same set of samples was represented using the same color. **(C)** Permutation tests of the OPLS-DA model. **(D)** S-plot of the OPLS-DA model. Red dots indicated that the VIP values of the metabolites ≥ 1 and green dots indicated that the VIP values of the metabolites ≤ 1.

The metabolic framework based on the DAMs in the infected PoP compared to the uninfected was shown in Figure 3. In infected psyllids, the content of sucrose was up-regulated but the α-D-Glucose was down-regulated, suggesting that *C*Lso affected the galactose metabolism of PoP. The reduction of α-D-Glucose, which is the source of pentose phosphate pathway, leaded to a decrease of its metabolite Ribose-5P. L-aspartic acid, which can enter arginine biosynthesis and affect the content of ornithine, is increased by fumarate through the alanine-aspartate-glutamate metabolism. It indicated that L-aspartic acid as a key metabolite affected the metabolism of *C*Lso-infected PoP. Although there was little effect on most of intermediates in glutathione metabolism, the content of glutamate increased significantly after *C*Lso-infection.

MALDI-MSI analysis

To identify the spatial location of potential biomarkers in PoP tissues, the distribution of these potential biomarkers was examined in psyllid using MALDI-MSI. In a single slice of psyllid, the spatial location images of 30 potential biomarkers were obtained, but 4 of them were not detected in this slice (Table 1). Among them, CE (18:1), 15-keto-Prostaglandin E2, Ornithine, PA(O-18:0/18:3 (6Z,9Z,12Z)), PC(16:1(9E)/0:0), Dopaquinone, D-Ribose 5P, Octadecyl trichloroacetate, and α-D-Glucose were mainly expressed in the head and abdomen of uninfected PoP, but not in infected (Figure 4, 7, 8, 14, 15, 16, 22, 23, 26); Ferulic acid, TG (12:0/12:0/20:5(5Z,8Z,11Z,14Z,17Z)), PC(12:0/18:1(9Z)), PA(O-18:0/17:2(9Z,12Z)), and Sucrose were clearly visible behind the abdomen in infected (Figure 4, 1, 17, 18, 24, 25). This result indicated that MALDI-MS Imaging and LC-MS analysis provide complementary data sets for biomarkers identification. Interestingly, the metabolites 15-keto-Prostaglandin E2 and alpha D-Glucose were significantly down-regulated in the adbomen of infected psyllids. Combining these results, it can be concluded that the metabolites 15-keto-Prostaglandin E2 and α-D-Glucose can potentially act as candidate biomarkers for *C*Lso infection.

Discussion

*C*Lso infection has a significant impact on its host plants and insects, resulting in diseases such as psyllid yellows, vein-greening (VG), and zebra chip (ZC) (Cevallos-Cevallos et al., 2012;

10.3389/fpls.2023.1204305

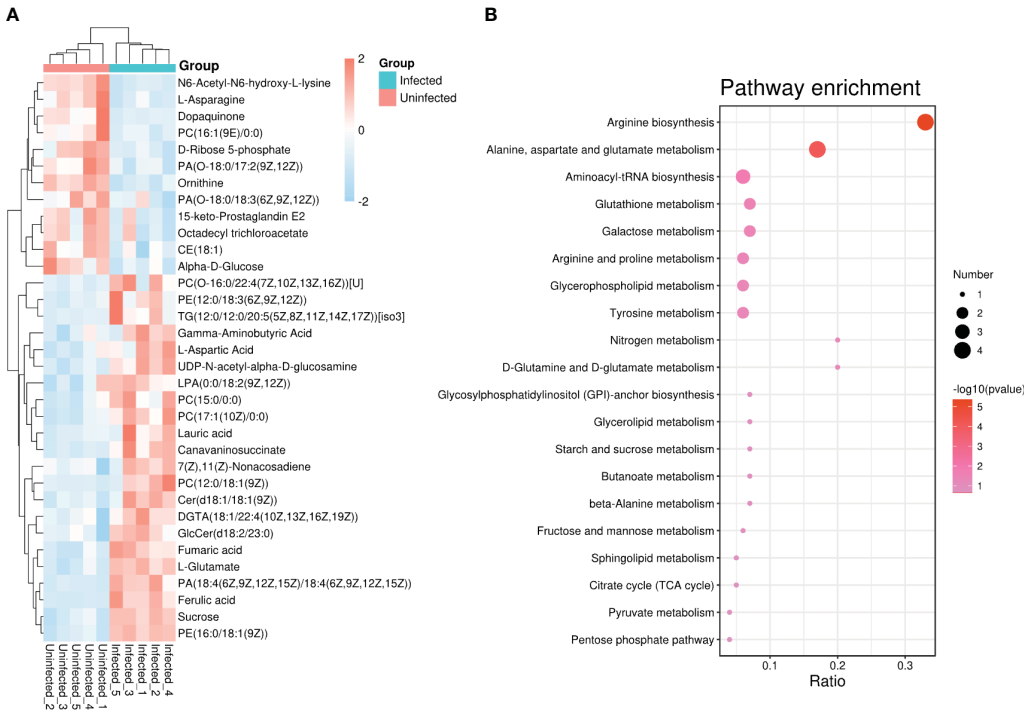

FIGURE 2

(A) Heat map analysis of 34 differential metabolites between infected and uninfected psyllids. The values of differential metabolites were shown as a color scale; **(B)** Results of KEGG pathway enrichment analysis of differential metabolites. The x axis indicates that the proportion and numbers of metabolites annotated to the pathway, and the y axis indicates the name of KEGG metabolic pathway. Dot color and dot size represent the P-value and the number of DAMs respectively.

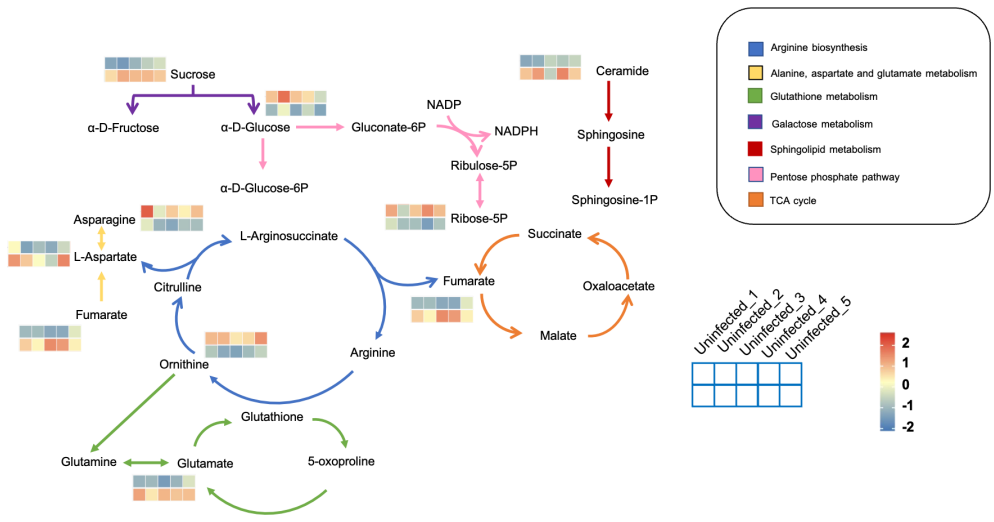

FIGURE 3

The metabolic framework based on the DAMs. Different metabolic pathways were marked with arrows of different colors and the corresponding color of each metabolic pathway is shown in the legend. For example, the arginine synthesis pathway was marked in blue. The changes in metabolites were represented by 10-small-squares heat map, with the top five squares representing the five biological replicates from uninfected groups and the bottom five squares representing the five biological replicates from infected groups. Colors correspond to the significance of accumulated changes of DAMs. Blue: down-regulated compared with uninfected groups. Red: up-regulated compared with uninfected groups.

10.3389/fpls.2023.1204305

TABLE 1 30 potential biomarkers.

No.	VIP	Average Mz	Average RT(min)	identified results	FC
1	1.95	416.14	0.323	Ferulic acid	9.21
2	1.41	433.23	6.6	LPA(0:0/18:2(9Z,12Z))	1.52
3	1.47	685.57	10.926	CE(18:1)	0.48
4	1.48	132.03	0.338	L-Aspartic Acid	1.80
5	1.94	146.04	0.338	L-Glutamate	1.65
6	1.40	102.05	0.336	γ -Aminobutyric Acid	1.55
7	1.39	385.18	5.144	15-keto-Prostaglandin E2(PGE2)	0.56
8	1.96	131.08	0.313	Ornithine	0.54
9	1.93	723.37	2.787	PA(18:4(6Z,9Z,12Z,15Z)/18:4(6Z,9Z,12Z,15Z))	13.61
10	1.85	644.03	0.375	UDP-N-acetyl-alpha-D-glucosamine	3.06
11	1.92	241.09	0.311	N6-Acetyl-N6-hydroxy-L-lysine	0.53
12	1.99	719.20	0.34	PE(16:0/18:1(9Z))	2.72
13	1.84	115.00	0.352	Fumaric acid	2.71
14	1.36	719.48	11.224	PA(O-18:0/18:3(6Z,9Z,12Z))	0.54
15	1.42	492.31	7.22	PC(16:1(9E)/0:0)	0.47
16	1.51	230.02	0.35	Dopaquinone	0.17
17	1.46	775.57	11.184	TG(12:0/12:0/20:5(5Z,8Z,11Z,14Z,17Z))[iso3]	10.18
18	1.58	738.50	9.867	PC(12:0/18:1(9Z))	6.04
19	1.46	693.31	1.62	PE(12:0/18:3(6Z,9Z,12Z))	3.60
20	1.40	830.59	11.225	PC(O-16:0/22:4(7Z,10Z,13Z,16Z))[U]	3.14
21	1.69	601.14	0.352	Cer(d18:1/18:1(9Z))	2.39
22	1.71	264.99	0.356	D-Ribose 5-phosphate	0.48
23	1.39	449.15	5.413	Octadecyl trichloroacetate	0.54
24	1.60	672.99	0.379	PA(O-18:0/17:2(9Z,12Z))	0.50
25	1.94	377.08	0.338	Sucrose	1.87
26	1.62	215.03	0.334	α-D-Glucose	0.51
27	1.55	480.30	7.795	PC(15:0/0:0)	1.59
28	1.69	167.02	0.352	L-Asparagine	0.58
29	1.36	439.41	10.66	7(Z),11(Z)-Nonacosadiene	1.85
30	1.61	830.63	11.191	GlcCer(d18:2/23:0)	2.00

Tamborindeguy et al., 2017). Additionally, the *C*Lso pathogen significantly alters the primary and secondary metabolites in its host insects.

Compared to uninfected insects, the contents of α-D-Glucose and Ribose-5P were significantly decreased, but sucrose was increased in infected insects (Figure 3). When PoP is infected, the *C*Lso competes with it for carbohydrates and uses the energy produced by the host plant to meet its own metabolic needs, such as growth and reproduction. The decrease in glucose content may result from its consumption by *C*Lso. It has been reported that the ATP level of *C*Las-infected psyllids *in vivo* is significantly higher than that of healthy psyllids, and the salivation time is reduced, indicating that the *C*Las-infected psyllids experience a higher level of hunger and have a tendency to forage more. The increase in feeding activity reflects the energy stress caused by *C*Lso infection (Killiny et al., 2017). On the other hand, during infection, the activation of cellular immunity leads to a metabolic switch within the immune cells, which become dependent on a massive supply of glucose and glutamine (Dolezal et al., 2019). Generally, the *C*Lso manipulates the energy metabolism of its insect vectors to ensure its need for high-energy nucleotides. As a result, the glucose requirement of the host plant increases sharply, and the psyllid balances its carbohydrate requirement by sucking more sucrose from the phloem of its host plant. The levels of many amino acids

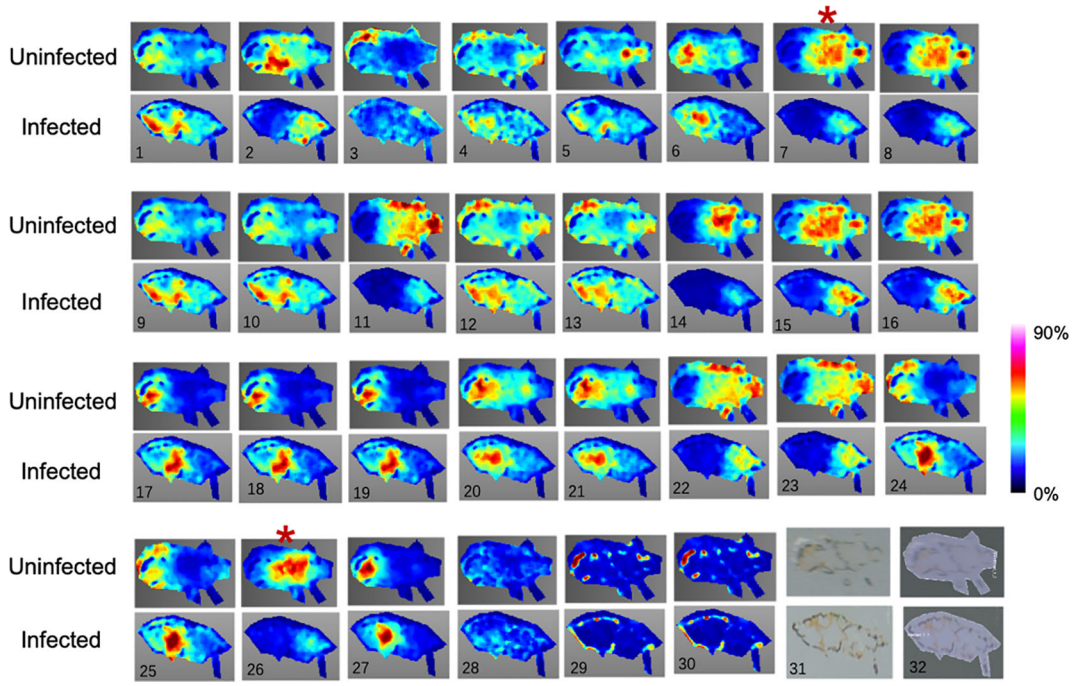

FIGURE 4
The MALDI-MSI and LC-MS analysis of the 30 metabolites differentially expressed between uninfected and infected psyllid. No.31 is the photograph of insects under a light microscope, and No.32 is the photomirror image of insects with DHB matrix. The 30 metabolites in the image correspond to the order in Table 1.

were also altered in the host plant by *C*Lso infection. For example, L-aspartic acid, L-glutamate, and fumarate were significantly increased. It has been reported that amino acids act as the main energy source and help organisms synthesize immune effectors to participate in the immune priming response (Wu et al., 2022).

In addition, the level of GABA in *C*Lso-infected PoP was higher than that of the controls. GABA is a free amino acid that plays an important role as a signaling molecule during plant stress. Previous studies have shown that when plants are subjected to abiotic stress such as salt, drought, and high temperature, as well as biological stress such as pathogen infection and insect feeding, GABA levels increase sharply to defend against such stress. Additionally, GABA is also necessary for the growth of pests (Ramesh et al., 2017). Our hypothesis is that the increased GABA content in psyllid may be related to feeding on infected host plants. On the other hand, the level of GABA was also higher in PoP after *C*Lso infection, probably because of the increased glutamate content. Glutamic acid can be converted to GABA through the action of GAD (glutamic acid decarboxylase), and the increase of L-glutamic acid in our results supports this idea.

Our results also showed that Dopaquinone was significantly reduced in *C*Lso-infected PoP compared to the control. Dopaquinone is an oxidation product of dopamine under the action of tyrosinase (a phenol oxidase), which can be re-oxidized and deposited as melanin. Previous research has found that phenol oxidase (PO) plays an important role in the insect's melanization defense response to invaders (Marmaras et al., 1996). Therefore, we concluded that the significant reduction of Dopaquinone is related to a reduced insect defense response, which facilitates the spread of psyllids to plants.

Ferulic acid (FA) is a type of active ingredient of phenolic acid that is derived from the dehydrogenation of ferulic acid glucoside and is involved in the formation and stabilization of plant lignin (Wang Y. L. et al., 2022). It also acts as an antioxidant, showing significant protective effects during cellular or tissue damage by neutralizing free radicals and reducing the formation of reactive oxygen species (ROS) (Liu et al., 2019). It has been reported that invasive pathogenic bacteria can cause systemic resistance in plants by increasing lignin and the antioxidant function of superoxide dismutase (SOD) to resist invasion (Ahmadifar et al., 2019). FA can inhibit the growth of microbes such as bacteria, protozoa, and fungi (Zuhainis Saad et al., 2008). However, some microbes have the ability to detoxify FA or even use FA as a single carbon source. For example, Zymomonas mobilis ZM4 can detoxify phenolic aldehydes (Yi et al., 2015).

In this study, increased levels of ferulic acid (FA) were found in *C*Lso-infected PoP. However, the presence of FA in insects or bacteria has yet to be identified, even though bacteria plays an important role in the release of FA. The successful colonization of plants by pathogens require an efficient utilization of nutrient resources present in host tissues; therefore, it is not surprising that hosts and pathogens have evolved distinct strategies to compete for this essential element. It can be speculated that the detected FA in PoP comes from the host, triggered by the *C*Lso pathogens transmitted when *C*Lso-infected psyllids feed on potatoes. Whether the FA can inhibit the growth of microbes or whether *C*Lso can use FA as a carbon source requires further research.

Prostaglandins (PGs) are effective immune mediators that can activate the immune response of insects to reject harmful pathogen infections. The effects of eicosanoids in the intimate relationship between host and pathogen have been observed in entomopathogenic nematodes (*Steinernema feltiae*) in lepidopteran insects and in a pathogenic bacterium, *Serratia marcescens*, in mosquitoes (Ahmed et al., 2022; Roy et al., 2022).

Prostaglandin E2 (PGE2) is produced through the oxidation reaction of arachidonic acid (AA) and other polyunsaturated fatty acids, catalyzed by phospholipase A2 (PLA2) through biomembrane phospholipids under various physiological and pathological stimuli (Stanley, 2006; Burke and Dennis, 2009; Stanley and Kim, 2014). During bacterial infections, PGE2 is an extremely active lipid mediator in the immune response, helping the host through various mechanisms. However, it has also been reported that PGE2 can potentiate the survival of intracellular pathogens in the host. The down-regulation of PGE2 metabolites in psyllid midguts suggests that certain pathogens may escape immune surveillance by suppressing the host's immune system and using its biological machinery to spread (Figure 5).

As prokaryotes, bacteria needs to acquire substrates such as cholesterol and sphingolipids from their eukaryotic hosts due to the lack of cellular synthesis tools. Not only are host lipids hijacked, but their metabolism is also altered during infection. Lipids play important roles in the interaction between hosts and pathogenic microorganisms. For example, they can serve as a potential carbon source for oxidative metabolism to restructure complex lipids (Poudyal and Paul, 2022), as mediators to regulate immune and inflammatory responses (Barletta et al., 2016), and as inhibitors of host immune defenses to promote self-colonization and development (Koga et al., 2010). Notably, pathogenic bacteria can inhibit host defense responses to colonization by increasing the lipid content of host macrophages (Koga et al., 2010).

For example, *Mycobacterium bovis* (MTB) infection mainly induces an increase in glycerophospholipids and polyketoic acid in macrophages, leading to the absorption of a large amount of lipids and the formation of foam cells. This in turn inhibits the defense function of macrophages and promotes their colonization and development (Gao et al., 2022). Phosphatidylcholine (PC) (16:1(9E)/0:0) is one of the biomarkers that causes changes in lipid metabolism. In this study, PC (16:1(9E)/0:0) was significantly decreased in CLso-infected PoP. In addition, there was a significant increase in glycerophospholipids in CLso-infected psyllids, such as PA(18:4(6Z,9Z,12Z,15Z)/18:4 (6Z,9Z,12Z,15Z)), TG(12:0/12:0/20:5(5Z,8Z,11Z,14Z,17Z)), PC(12:0/18:1(9Z)), PE(12:0/18:3(6Z,9Z,12Z)), PC(O-16:0/22:4 (7Z,10Z,13Z,16Z)), PE(16:0/18:1(9Z)). It is hypothesized that the changes in lipid metabolism in psyllids were caused by CLso infection. CLso secretes glycerophospholipids in psyllids to inhibit phagocytosis and clearance by the host insect, thus escaping the host's immune defense response and achieving colonization. This study shows that pathogens can use specific strategies to modulate host lipid metabolism and homeostasis in order to maintain fluidity, survival, and dissemination.

The data generated by UPLC-MS can reveal small changes in the metabolic level of a sample and provide insight into the overall metabolic state of the organism. Meanwhile, MALDI-MSI is a reflection of spatial information, and can detect not only the molecules of interest, but also a large number of other analytes simultaneously. We found several organ-specific quality signals in psyllids. For example, a strong signal at *m/z* 416.138 (Ferulic acid), 723.365 (PA(18:4(6Z,9Z,12Z,15Z)/18:4(6Z,9Z,12Z,15Z))), and 644.030 (UDP-N-acetyl-alpha-D-glucosamine) was detected only below the abdomen of infected PoP (Figure 4, 1, 9, 10). 15-keto-Prostaglandin E2, Ornithine, PA(O-18:0/18:3(6Z,9Z,12Z)), PC(16:1 (9E)/0:0), Dopaquinone, D-Ribose 5P, Octadecyl trichloroacetate, and α-D-Glucose were mainly expressed in the head and abdomen of uninfected PoP (Figure 4, 7, 8, 14, 15, 16, 22, 23, 26). The concentrations of these substances significantly differ in the insect.

The disadvantage of conventional metabolic analysis is that it is not achievable to explore the cell-to-cell heterogeneity in the context of an organ or tissue, while the emergence of MALDI-MSI overcomes this problem (Wang G. et al., 2022). MALDI-MSI as a method to measure

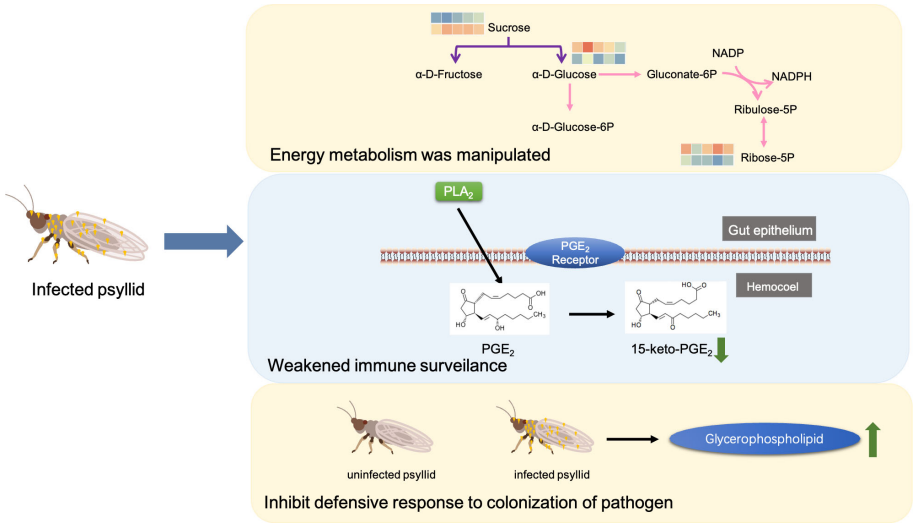

FIGURE 5
Schematic of possible mechanisms of CLso infection in PoP.

the spatial distribution of metabolites at single-cell resolution, provides the possibility to understand the tissue-type-specific metabolic diversity of infected psyllid. According to recent studies, Benkacimi et al. successfully identified two species of bed bugs to the species level using MALDI-TOF/MS (Benkacimi et al., 2020). Tuthill et al. used a combination of HPLC-MS/MS and MALDI-MSI to spatially and temporally localize lipids in the heart and hemolymph of *Drosophila*, identifying potential endocrine mechanisms involved in lipotoxicity and metabolic diseases (Tuthill et al., 2020). These studies give us confidence and experience in studying the smaller insect in question. In this study, we first identified 34 different ions using untargeted UPLC-MS, and then examined the distribution of these candidate markers in PoP using MALDI-MSI imaging of insect tissues. These potential biomarkers can be used to quickly track *C*Lso and further understand the interaction mechanism between the psyllid and *C*Lso pathogens. This study may provides new insights into metabolic changes following *C*Lso infection of potato psyllids.

In conclusion, our results suggested that *C*Lso infection induces nutrient and energy stress, causing changes in the lipid metabolism of psyllids. This weakening of the insect vector's immune defense response promotes colonization and transmission, which will help us better understand the interaction between psyllid and *C*Lso.

Data availability statement

The original contributions presented in the study are included in the article/Supplementary Material. Further inquiries can be directed to the corresponding authors.

Ethics statement

The animal study was reviewed and approved by The Special Committee of Science Ethics of Guangzhou University.

Author contributions

YL: Provided data visualization, validation and wrote the manuscript. ZT: Data Analysis. LH: Provided data visualization, critically reviewed and revised the paper. XW: Formal Analysis, wrote original draft, writing-review and editing. All authors contributed to the article and approved the submitted version.

Funding

This work was supported by grants from Research and development program in key areas of Guangdong Province (2021B0707010010), the National Natural Science Foundation of China (42177262).

Acknowledgments

We would like to express our gratitude to Dr. David Roger and Ruifeng He from the Department of Chemistry at Washington State University for their assistance in obtaining the image mass spectrometric data.

Conflict of interest

The authors declare that the research was conducted in the absence of any commercial or financial relationships that could be construed as a potential conflict of interest.

Publisher's note

Supplementary material

The Supplementary Material for this article can be found online at: https://www.frontiersin.org/articles/10.3389/fpls.2023.1204305/full#supplementary-material

References

Ahmadifar, E., Moghadam, M. S., Dawood, M. A. O., and Hoseinifar, S. H. (2019). Lactobacillus fermentum and/or ferulic acid improved the immune responses, antioxidative defence and resistance against aeromonas hydrophila in common carp (Cyprinus carpio) fingerlings. *Fish. Shellfish. Immunol.* 94, 916–923. doi: 10.1016/j.fsi.2019.10.019

Ahmed, S., Sajjadian, S. M., and Kim, Y. (2022). HMGB1-like dorsal switch protein 1 triggers a damage signal in mosquito gut to activate dual oxidase *via* eicosanoids. *J. Innate. Immun.* 14 (6), 657–672. doi: 10.1159/000524561

Alvarado, V. Y., Odokonyero, D., Duncan, O., Mirkov, T. E., and Scholthof, H. B. (2012). Molecular and physiological properties associated with zebra complex disease in potatoes and its relation with candidatus liberibacter contents in psyllid vectors. *PloS One* 7 (5), e37345. doi: 10.1371/journal.pone.0037345

Barbosa-Medina, A. M., Maciel, E. V. S., Dos Santos, D. M., Lanças, F. M., and Vieira, E. M. (2022). Neonicotinoids exposure assessment in africanized honey bees (*Apis mellifera* l.) by using an environmentally-friendly sample preparation technique followed by UPLC-MS/MS. *J. Environ. Sci. Health Part. B. Pesticides. Food Contaminants. Agric. Wastes.* 57 (4), 252–262. doi: 10.1080/03601234.2022.2047389

Barletta, A. B., Alves, L. R., Silva, M. C., Sim, S., Dimopoulos, G., Liechocki, S., et al. (2016). Emerging role of lipid droplets in aedes aegypti immune response against bacteria and dengue virus. *Sci. Rep.* 6, 19928. doi: 10.1038/srep19928

Baumann, P. (2005). Biology bacteriocyte-associated endosymbionts of plant sap-sucking insects. *Annu. Rev. Microbiol.* 59, 155–189. doi: 10.1146/annurev.micro.59.030804.121041

Benkacimi, L., Gazelle, G., El Hamzaoui, B., Bérenger, J. M., Parola, P., and Laroche, M. (2020). MALDI-TOF MS identification of cimex lectularius and cimex hemipterus bedbugs. *Infect. Genet. Evol.: J. Mol. Epidemiol. Evol. Genet. Infect. Dis.* 85, 104536. doi: 10.1016/j.meegid.2020.104536

Burke, J. E., and Dennis, E. A. (2009). Phospholipase A2 structure/function, mechanism, and signaling. *J. Lipid Res.* 50 Suppl (Suppl), S237–S242. doi: 10.1194/jlr.R800033-JLR200

Burmester, T., Massey, H. C.Jr, Zakharkin, S. O., and Benes, H. (1998). The evolution of hexamerins and the phylogeny of insects. *J. Mol. Evol.* 47 (1), 93–108. doi: 10.1007/pl00006366

Cevallos-Cevallos, J. M., Futch, D. B., Shilts, T., Folimonova, S. Y., and Reyes-De-Corcuera, J. I. (2012). GC-MS metabolomic differentiation of selected citrus varieties with different sensitivity to citrus huanglongbing. *Plant Physiol. Biochem.: PPB* 53, 69–76. doi: 10.1016/j.plaphy.2012.01.010

Chen, Y. A., Lai, Y. T., Wu, K. C., Yen, T. Y., Chen, C. Y., and Tsai, K. H. (2020). Using UPLC-MS/MS to evaluate the dissemination of pyriproxyfen by *Aedes* mosquitoes to combat cryptic larval habitats after source reduction in kaohsiung in southern Taiwan. *Insects* 11 (4), 251. doi: 10.3390/insects11040251

Cicalini, I., Rossi, C., Pieragostino, D., Agnifili, L., Mastropasqua, L., di Ioia, M., et al. (2019). Integrated lipidomics and metabolomics analysis of tears in multiple sclerosis: an insight into diagnostic potential of lacrimal fluid. *Int. J. Mol. Sci.* 20 (6), 1265. doi: 10.3390/ijms20061265

Dolezal, T., Krejcova, G., Bajgar, A., Nedbalova, P., and Strasser, P. (2019). Molecular regulations of metabolism during immune response in insects. *Insect Biochem. Mol. Biol.* 109, 31–42. doi: 10.1016/j.ibmb.2019.04.005

Eleftherianos, I., and Revenis, C. (2011). Role and importance of phenoloxidase in insect hemostasis. *J. Innate. Immun.* 3 (1), 28–33. doi: 10.1159/000321931

Fisher, T. W., Vyas, M., He, R., Nelson, W., Cicero, J. M., Willer, M., et al. (2014). Comparison of potato and asian citrus psyllid adult and nymph transcriptomes identified vector transcripts with potential involvement in circulative, propagative liberibacter transmission. *Pathog. (Basel. Switzerland).* 3 (4), 875–907. doi: 10.3390/pathogens3040875

Gao, W., Cai, Y., Zhang, G., Wang, X., Wang, J., Li, Y., et al. (2022). Lipidomics revealed the global lipid responses of primary bovine alveolar macrophages to infections of mycobacterium tuberculosis and mycobacterium bovis. *Int. Immunopharmacol.* 104, 108407. doi: 10.1016/j.intimp.2021.108407

Goolsby, J. A., Adamczyk, J. J.Jr, Crosslin, J. M., Troxclair, N. N., Anciso, J. R., Bester, G. G., et al. (2012). Seasonal population dynamics of the potato psyllid (Hemiptera: triozidae) and its associated pathogen "Candidatus liberibacter solanacearum" in potatoes in the southern great plains of north America. *J. Econ. Entomol.* 105 (4), 1268–1276. doi: 10.1603/ec11435

Greenway, G. (2014). Economic impact of zebra chip control costs on grower returns in seven US states. *Am. J. Potato. Res.* 91 (6), 714–719. doi: 10.1007/s12230-014-9404-x

Gu, H., Zhang, J., and Bao, J. (2015). High tolerance and physiological mechanism of zymomonas mobilis to phenolic inhibitors in ethanol fermentation of corncob residue. *Biotechnol. Bioeng.* 112 (9), 1770–1782. doi: 10.1002/bit.25603

Killiny, N., Hijaz, F., Ebert, T. A., and Rogers, M. E. (2017). A plant bacterial pathogen manipulates its insect vector's energy metabolism. *Appl. Environ. Microbiol.* 83 (5), e03005–e03016. doi: 10.1128/AEM.03005-16

Koga, H., Kaushik, S., and Cuervo, A. M. (2010). Altered lipid content inhibits autophagic vesicular fusion. *FASEB J.* 24 (8), 3052–3065. doi: 10.1096/fj.09-144519

Liu, Y., Qi, Y., Chen, X., He, H., Liu, Z., Zhang, Z., et al. (2019). Phenolic compounds and antioxidant activity in red- and in green-fleshed kiwifruits. *Food Res. Int. (Ottawa. Ont.)* 116, 291–301. doi: 10.1016/j.foodres.2018.08.038

Marmaras, V. J., Charalambidis, N. D., and Zervas, C. G. (1996). Immune response in insects: the role of phenoloxidase in defense reactions in relation to melanization and sclerotization. *Arch. Insect Biochem. Physiol.* 31 (2), 119–133. doi: 10.1002/(SICI)1520-6327(1996)31:2<119::AID-ARCH1>3.0.CO;2-V

Mishra, S., and Ghanim, M. (2022). Interactions of *Liberibacter* species with their psyllid vectors: molecular, biological and behavioural mechanisms. *Int. J. Mol. Sci.* 23 (7), 4029. doi: 10.3390/ijms23074029

Mora, V., Ramasamy, M., Damaj, M. B., Irigoyen, S., Ancona, V., Ibanez, F., et al. (2021). Potato zebra chip: an overview of the disease, control strategies, and prospects. *Front. Microbiol.* 12. doi: 10.3389/fmicb.2021.700663\

Munyaneza, J. E., Goolsby, J. A., Crosslin, J. M., and Upton, J. E. (2007). Further evidence that zebra chip potato disease in the lower Rio grande valley of Texas is associated with bactericera cockerelli. *Subtropical. Plant Sci.* 60, 27–37.

Nachappa, P., Levy, J., and Tamborindeguy, C. (2012). Transcriptome analyses of bactericera cockerelli adults in response to "Candidatus liberibacter solanacearum" infection. *Mol. Genet. Genomics.: MGG.* 287 (10), 803–817. doi: 10.1007/s00438-012-0713-9

Niehoff, A. C., Kettling, H., Pirkl, A., Chiang, Y. N., Dreisewerd, K., and Yew, J. Y. (2014). Analysis of drosophila lipids by matrix-assisted laser desorption/ionization mass spectrometric imaging. *Analytical. Chem.* 86 (22), 11086–11092. doi: 10.1021/ac503171f

Overgaard, J., Malmendal, A., Sørensen, J. G., Bundy, J. G., Loeschcke, V., Nielsen, N. C., et al. (2007). Metabolomic profiling of rapid cold hardening and cold shock in drosophila melanogaster. *J. Insect Physiol.* 53 (12), 1218–1232. doi: 10.1016/j.jinsphys.2007.06.012

Poudyal, N. R., and Paul, K. S. (2022). Fatty acid uptake in *Trypanosoma brucei*: host resources and possible mechanisms. *Front. Cell. Infect. Microbiol.* 12. doi: 10.3389/fcimb.2022.949409

Prager, S. M., Cohen, A., Cooper, W. R., Novy, R., Rashed, A., Wenninger, E. J., et al. (2022). A comprehensive review of zebra chip disease in potato and its management through breeding for resistance/tolerance to 'Candidatus liberibacter solanacearum' and its insect vector. *Pest Manag. Sci.* 78 (9), 3731–3745. doi: 10.1002/ps.6913

Pratavieira, M., da Silva Menegasso, A. R., Garcia, A. M., Dos Santos, D. S., Gomes, P. C., Malaspina, O., et al. (2014). MALDI imaging analysis of neuropeptides in the africanized honeybee (Apis mellifera) brain: effect of ontogeny. *J. Proteome Res.* 13 (6), 3054–3064. doi: 10.1021/pr500224b

Ramesh, S. A., Tyerman, S. D., Gilliham, M., and Xu, B. (2017). γ-aminobutyric acid (GABA) signalling in plants. *Cell. Mol. Life Sci.: CMLS.* 74 (9), 1577–1603. doi: 10.1007/s00018-016-2415-7

Rondon, S. I., Carrillo, C. C., Cuesta, H. X., Navarro, P. D., and Acuña, I. (2022). "Latin America Potato production," in *Insect pests of potato*, 317–330. doi: 10.1016/C2019-0-03135-4

Roy, M. C., Ahmed, S., and Kim, Y. (2022). Dorsal switch protein 1 as a damage signal in insect gut immunity to activate dual oxidase *via* an eicosanoid, PGE_2. *Front. Immunol.* 13, 994626. doi: 10.3389/fimmu.2022.994626

Stanley, D. (2006). Prostaglandins and other eicosanoids in insects: biological significance. *Annu. Rev. Entomol.* 51, 25–44. doi: 10.1146/annurev.ento.51.110104.151021

Stanley, D., and Kim, Y. (2014). Eicosanoid signaling in insects: from discovery to plant protection. *Crit. Rev. Plant Sci.* 33 (1), 20–63. doi: 10.1080/07352689.2014.847631

Susniak, K., Krysa, M., Gieroba, B., Komaniecka, I., and Sroka-Bartnicka, A. (2020). Recent developments of MALDI MSI application in plant tissues analysis. *Acta Biochim. Polonica.* 67 (3), 277–281. doi: 10.18388/abp.2020_5394

Tamborindeguy, C., Huot, O. B., Ibanez, F., and Levy, J. (2017). The influence of bacteria on multitrophic interactions among plants, psyllids, and pathogen. *Insect Sci.* 24 (6), 961–974. doi: 10.1111/1744-7917.12474

Tuck, M., Grélard, F., Blanc, L., and Desbenoit, N. (2022). MALDI-MSI towards multimodal imaging: challenges and perspectives. *Front. Chem.* 10. doi: 10.3389/fchem.2022.904688

Tuthill, B. F.2nd, Searcy, L. A., Yost, R. A., and Musselman, L. P. (2020). Tissue-specific analysis of lipid species in *Drosophila* during overnutrition by UHPLC-MS/MS and MALDI-MSI. *J. Lipid Res.* 61 (3), 275–290. doi: 10.1194/jlr.RA119000198

Vyas, M., Fisher, T. W., He, R., Nelson, W., Yin, G., Cicero, J. M., et al. (2015). Asian Citrus psyllid expression profiles suggest candidatus liberibacter asiaticus-mediated alteration of adult nutrition and metabolism, and of nymphal development and immunity. *PloS One* 10 (6), e0130328. doi: 10.1371/journal.pone.0130328

Wang, G., Heijs, B., Kostidis, S., Mahfouz, A., Rietjens, R. G. J., Bijkerk, R., et al. (2022). Analyzing cell-type-specific dynamics of metabolism in kidney repair. *Nat. Metab.* 4 (9), 1109–1118. doi: 10.1038/s42255-022-00615-8

Wang, Y. L., Wang, W. K., Wu, Q. C., and Yang, H. J. (2022). The release and catabolism of ferulic acid in plant cell wall by rumen microbes: a review. *Anim. Nutr. (Zhongguo. Xu. Mu. Shou. Yi. Xue. hui).* 9, 335–344. doi: 10.1016/j.aninu.2022.02.003

Wu, G., Liu, J., Li, M., Xiao, Y., and Yi, Y. (2022). Prior infection of galleria mellonella with sublethal dose of bt elicits immune priming responses but incurs metabolic changes. *J. Insect Physiol.* 139, 104401. doi: 10.1016/j.jinsphys.2022.104401

Yang, H., Chandler, C. E., Jackson, S. N., Woods, A. S., Goodlett, D. R., Ernst, R. K., et al. (2020). On-tissue derivatization of lipopolysaccharide for detection of lipid a using MALDI-MSI. *Analytical. Chem.* 92 (20), 13667–13671. doi: 10.1021/acs.analchem.0c02566

Yi, X., Gu, H., Gao, Q., Liu, Z. L., and Bao, J. (2015). Transcriptome analysis of zymomonas mobilis ZM4 reveals mechanisms of tolerance and detoxification of phenolic aldehyde inhibitors from lignocellulose pretreatment. *Biotechnol. Biofuels* 8, 153. doi: 10.1186/s13068-015-0333-9

Zuhainis Saad, W., Abdullah, N., Alimon, A. R., and Yin Wan, H. (2008). Effects of phenolic monomers on the enzymes activities and volatile fatty acids production of neocallimastix frontalis B9. *Anaerobe* 14 (2), 118–122. doi: 10.1016/j.anaerobe.2007.10.003

frontiers | Frontiers in Plant Science

TYPE Original Research
PUBLISHED 08 August 2023
DOI 10.3389/fpls.2023.1250590

OPEN ACCESS

EDITED BY
Shengli Jing,
Xinyang Normal University, China

REVIEWED BY
Di Wu,
Henan Agricultural University, China
Zhanqi Wang,
Huzhou University, China

*CORRESPONDENCE
Jinbo Li
jinboli0606@163.com
Aiqing You
aq_you@hbaas.com

†These authors have contributed equally to this work

RECEIVED 30 June 2023
ACCEPTED 24 July 2023
PUBLISHED 08 August 2023

CITATION
Hu L, Yang D, Wang H, Du X, Zhang Y, Niu L, Wan B, Xia M, Qi H, Mou T, You A and Li J (2023) Transcriptome analysis revealed differentially expressed genes in rice functionally associated with brown planthopper defense in near isogenic lines pyramiding *BPH14* and *BPH15*. *Front. Plant Sci.* 14:1250590. doi: 10.3389/fpls.2023.1250590

Transcriptome analysis revealed differentially expressed genes in rice functionally associated with brown planthopper defense in near isogenic lines pyramiding *BPH14* and *BPH15*

Liang Hu[1†], Dabing Yang[1,2†], Hongbo Wang[1,2†], Xueshu Du[1], Yanming Zhang[3], Liping Niu[3], Bingliang Wan[1], Mingyuan Xia[1], Huaxiong Qi[1], Tongmin Mou[2], Aiqing You[1,4*] and Jinbo Li[1,4*]

[1]Key Laboratory of Crop Molecular Breeding, Ministry of Agriculture and Rural Affairs, Hubei Key Laboratory of Food Crop Germplasm and Genetic Improvement, Food Crops Institute, Hubei Academy of Agricultural Sciences, Wuhan, China, [2]National Key Laboratory of Crop Genetic Improvement, Huazhong Agricultural University, Wuhan, China, [3]State Key Laboratory of Hybrid Rice, College of Life Sciences, Wuhan University, Wuhan, China, [4]Hubei Hongshan Laboratory, Wuhan, China

Although rice has many pests, brown planthopper (BPH) in particular is known to cause substantial damage. The pyramiding application of BPH-resistance genes *BPH14* and *BPH15* has proven effective in enhancing rice defense against BPH. However, the molecular mechanisms underlying *BPH14*/*BPH15*-conferred resistance remain unexplained. In this investigation, we analyzed the transcriptomes of near isogenic lines (NILs) containing either *BPH14* (B14), *BPH15* (B15), or *BPH14/BPH15* (B1415), as well as their recurrent parent (RP) 'Wushansimiao'. In total, we detected 14,492 differentially expressed genes (DEGs) across 12 mRNA profiles of resistant NILs and RP at different feeding stages. In the transcriptomic analysis, 531 DEGs appeared to be common among the resistant NILs compared to RP before and after BPH feeding. These common DEGs were enriched in defense response, phosphorylation, and salt stress response. In addition, 258 DEGs shared only in resistant NILs were obtained among the different feeding stages, which were enriched in oxidative stress response, karrikin response, and chloroplast organization. Considering the expression patterns and relevant research reports associated with these DEGs, 21 were chosen as BPH resistance candidates. In rice protoplasts, the candidate DEG *OsPOX8.1* was confirmed to increase reactive oxygen species (ROS) accumulation by chemiluminescence measurement. Our results provide valuable information to further explore the defense mechanism of insect-resistant gene pyramiding lines and develop robust strategies for insect control.

KEYWORDS

rice, brown planthopper, RNA-sequencing, *BPH14/BPH15*, resistance

Introduction

Worldwide, more than 3.5 billion people utilize rice (*Oryza sativa* L.) as a dietary staple (Wing et al., 2018). Among all rice pests, one of the most damaging is the brown planthopper (*Nilaparvata lugens* Stål, BPH) (Du et al., 2020). As typical sap-sucking insects, BPHs gather in large numbers at the plant base and feed on phloem sap. This type of herbivory causes the drying, browning, wilting, and dwarfing of host plants. Extensive herbivory by BPH can ultimately lead to reduced or no yields, which seriously threatens food security (Cheng et al., 2013b). In addition, BPH can spread and induce various rice diseases, such as grassy dwarf disease and leaf dwarf disease (Jing et al., 2017). Breeding BPH resistant rice varieties is considered a practical, economical, and sustainable management strategy (Du et al., 2020).

In 1969, the International Rice Research Institute (IRRI) first discovered and mapped the *BPH1* BPH resistance gene, which paved the way for future studies of rice resistance to BPH. So far, 17 BPH resistance genes (*BPH37, BPH40, BPH30*, *BPH6*, *BPH32*, *BPH18*, *BPH21*, *BPH10*, *BPH7*, *BPH1*, *BPH9*, *BPH29*, *BPH3*, *BPH26*, *BPH2*, *BPH15*, and *BPH14*) have been successfully cloned in rice (Guo et al., 2022). Of these cloned genes, the majority represent coiled-coil nucleotide-binding site leucine-rich repeat (CC-NBS-LRR) proteins (e.g., *BPH14*), two encode lectin receptor-like kinases (LecRKs) (*BPH3* and *BPH15*), and the remainder encode other types of proteins (Guo et al., 2022). These BPH resistance proteins have diverse structures and functions, and the study of their varied molecular mechanisms can help us to better utilize them in precision breeding schemes.

The *BPH14* gene was the first to be cloned and encodes a nuclear/cytoplasmic CC-NBS-LRR protein which directly binds BPH-derived effector BISP to activate host plant resistance (Du et al., 2009; Guo et al., 2023). Through forming homologous complexes and interacting with transcription factors, BPH14 mediates BPH resistance by triggering the transcription of downstream defense genes (Hu et al., 2017). Meanwhile, *BPH15* encodes a plasma membrane LecRK which is suggested to serve as either a receptor or receptor-associated protein. As such, *BPH15* confers durable, broad-spectrum protection against BPH, as well as other pathogens, by perceiving either plant-derived damage-associated molecular patterns (DAMPs) or BPH-derived herbivore-associated molecular patterns (HAMPs). Furthermore, *BPH15* knock-down makes rice plants more susceptible to BPH and other pathogens (Cheng et al., 2013a).

Plants carrying only a single insect-resistance gene have the potential to become susceptible within a timeframe as short as a few years due to the adaptation of associated insect populations (Jena and Kim, 2010). One effective strategy to provide durable, broad-spectrum BPH protection in rice is the pyramiding of diverse resistance genes (Muduli et al., 2021). Marker-assisted pyramiding of rice with both *BPH14* and *BPH15* resulted in durable and enhanced resistance compared to rice varieties possessing only one of the two genes (Li et al., 2011; Hu et al., 2012; Jiang et al., 2018). In addition, varieties harboring two BPH resistance genes showed a more than 90% reduction in pest density in the field (Zheng et al., 2021). Using a genomics-based breeding approach, Wang et al. precisely incorporated *BPH14* and *BPH15* into recurrent parent (RP) 'Wushansimiao' rice to augment BPH resistance while leaving other agronomic traits unaffected (Wang et al., 2019). Unfortunately, the precise molecular mechanisms resulting in the enhanced BPH resistance of *BPH14*/*BPH15* pyramiding lines remain largely unknown.

In order to study these defense mechanisms, RNA sequencing (RNA-seq) has been successfully employed to characterize the rice transcriptome at different BPH feeding stages (Chen et al., 2022). For instance, the introgression line 'B5' contains five quantitative trait loci (QTL) and two major resistance genes (*BPH14* and *BPH15*) associated with resistance to BPH (Huang et al., 2001; Ren et al., 2004). Both cDNA macroarray and microarray analyses were performed to explore differential transcription between resistant cultivar 'B5' and susceptible cultivar 'MH63' under both BPH herbivory and insect-free conditions. Herbivory by BPH was found to affect a wide variety of gene functional categories, including pathogen-related proteins, oxidative stress, and signaling pathways, among others, suggesting that the adaptation of BPH-infested rice likely involves many pathways and processes (Zhang et al., 2004; Wang et al., 2008). In another experiment, high-throughput RNA-seq was used to discover nearly 3,000 BPH-responsive differentially expressed genes (DEGs) between a *BPH15* introgression line and recipient line. The identified DEGs were associated with a number of Gene Ontology (GO) terms, including hormone signaling, posttranslational protein modifications, transcription factors, pathogen-related genes, Ca^{2+} signaling, and MAPK cascades (Lv et al., 2014). A number of BPH-responsive miRNAs were identified by analyzing the miRNA profiles of a *BPH15* introgression line and susceptible recipient line, which were suggested to regulate several pathways contributing to both basal and BPH-specific defense (Wu et al., 2017). Furthermore, by combining microRNA and transcriptome analyses, 34 miRNAs associated with 42 target genes were identified as potential miRNA-mRNA pairs regulating *BPH6*-mediated resistance, implying the importance of miRNA-mRNA modules in regulating BPH defense (Tan et al., 2020).

Although *BPH14* and *BPH15* have been pyramided into rice varieties to confer durable and stable BPH resistance (Li et al., 2011; Hu et al., 2012; Wang et al., 2016; Wang et al., 2019; Yang et al., 2022), the precise molecular mechanism underlying the BPH resistance of *BPH14*/*BPH15* pyramiding lines remain largely unknown. Here, we analyzed the transcriptomes of near isogenic lines (NILs) containing either *BPH14*, *BPH15*, or both *BPH14*/*BPH15* genes, as well as their RP, before and after BPH infestation. Upon comparison and integration of these four datasets, a total of 21 DEGs were identified as candidates to functionally associate with rice defense against BPH. The data presented here help clarify the mechanism responsible for durable, broad-spectrum BPH resistance in gene pyramiding rice varieties.

Materials and methods

Experimental materials

The NILs containing either *BPH14* (B14), *BPH15* (B15), or both *BPH14*/*BPH15* (B1415) genes were developed using inbred *indica*

rice variety 'Wushansimiao', as the RP (Wang et al., 2019). Seeds were planted in plastic cups (15 cm high by 9 cm wide) at a density of 15 plants per cup, and greenhouse-grown under a 10 h dark (26 ± 2°C)/14 h light (32 ± 2°C) cycle. The BPHs were maintained at Wuhan University, China, on 'Taichung Native1' (TN1; susceptible cultivar, IRRI Acc. No.00105) under environmental conditions identical to those of the rice plants.

BPH resistance evaluation

BPH nymphs (third instar) were introduced at a rate of 8 BPH per seedling to four-leaf stage B14, B15, B1415, and RP seedlings. As described previously (Huang et al., 2001), seedlings were ascribed a resistance score during examination. The average damage severity score (0, 1, 3, 5, 7, or 9) was calculated for each plant after infestation.

Honeydew excretion measurements

Pre-weighed parafilm sachets were used to confine starved (2 h) third instar BPH nymphs and fastened to the leaf sheathes of one-month-old B14, B15, B1415, and RP plants (Pathak et al., 1982). The sachets were removed and emptied of BPH insects after 2 d of active herbivory. All sachets were weighed post BPH removal, and the weight difference before and after 2 d of herbivory was recorded as the amount of honeydew excretion.

Sample collection

Both BPH treatment and sample collection were accomplished according to the endpoint method (Wu et al., 2017). All treatments ended at the same time, despite beginning at different times. After 0, 3, 6, 12, 24, 48, and 72 h, four-leaf stage B14, B15, B1415, and RP seedlings were infested at a rate of 8 BPH nymphs (third instar) per seedling. Each experiment consisted of three biological replicates per treatment, with each replicate containing 15 seedlings. Leaf sheath samples were designated as either the non-infested group (0 h), early infestation group (3, 6, and 12 h), or late infestation group (24, 48, and 72 h). The experimental sample designations were as follows: B14_0, B14_early, and B14_late for the B14 lines; B15_0, B15_early, and B15_late for the B15 lines; B1415_0, B1415_early, B1415_late for the B1415 lines; and RP_0, RP_early, and RP_late for the RP lines. All samples were frozen with liquid N_2 and stored at -80°C prior to analyses.

RNA collection

Total RNA was collected from leaf sheathes with Trizol (Invitrogen). Quality was established with a Bioanalyzer 2200 (Aligent). All samples were stored at -80°C prior to analyses.

cDNA library preparation

A TruSeq Stranded mRNA Library Prep Kit (Illumina) was utilized for preparation of the cDNA libraries, according to the standard protocol. Briefly, oligo (dT) magnetic beads were utilized to purify poly-A mRNA from 1 μg total RNA, which was then fragmented (200-600 bp) for 6 min with divalent cations (85°C). Both first- and second-strand cDNA synthesis were carried out using the cleaved RNA fragments. dUTP mix was utilized for second-strand cDNA synthesis, allowing for second strand separation. The cDNA fragments were then ligated with indexed adapters, A-tailed, and end-repaired. To remove the second-strand cDNA, the ligated cDNA was purified and subjected to uracil DNA glycosylase. The cDNA libraries were created by using PCR to enrich the purified first-strand cDNA. An Agilent 2200 was used for library quality control, and the libraries were sequenced using NovaSeq 6000 on a 150 bp paired-end run.

RNA sequence mapping

Adapter sequences and low-quality reads were removed in order to acquire clean reads. Hisat2 was utilized to align the clean reads with the reference genome (IRGSP1.0, Ensembl) (Kim et al., 2015). Gene counts were acquired with HTseq. Gene expression was quantified according to the fragments per kilo base of exon per million fragments mapped (FPKM) (Anders et al., 2015).

Differential gene expression analysis

DEGs were filtered using the DESeq2 algorithm (Love et al., 2014). Statistically significant DEGs were determined according to *P*-value (< 0.05), fold change (FC; $\log_2$FC > 1 or $\log_2$FC < -1), and FDR (< 0.05) (Benjamini et al., 2001). Here, DEGs are defined as transcripts exhibiting a P-value < 0.05 and at least a 2-fold change in FPKM ($\log_2$FC > 1 or $\log_2$FC < -1).

Gene Ontology (GO) evaluation

GO evaluation was carried out to elucidate the biological importance of the identified DEGs (Ashburner et al., 2000), using GO annotations downloaded from the Gene Ontology (http://www.geneontology.org/), UniProt (http://www.uniprot.org/), and NCBI (http://www.ncbi.nlm.nih.gov/) databases. Statistically significant GO categories were determined with the Fisher's exact test (*P*-value < 0.05).

Kyoto Encyclopedia of Genes and Genomes (KEGG) pathway evaluation

KEGG pathway evaluation was carried out to determine the biological pathways associated with the identified DEGs according to the KEGG database. Statistically significant KEGG pathways

were determined with the Fisher's exact test (P-value < 0.05) (Draghici et al., 2007).

Quantitative real-time PCR (qRT-PCR) assay

A PrimeScript RT Reagent Kit containing gDNA Eraser (RR047A, TaKaRa) was used to convert total RNA into first-strand cDNA. qRT-PCR was accomplished on a CFX96 real-time system (Bio-Rad) with SYBR Green Real-Time PCR Master Mix (QPK-201, Toyobo). All primers are listed in Supplementary Table 1. Gene expression was evaluated by relative quantification, with *TBP* as the endogenous reference (Livak and Schmittgen, 2001).

Gene constructs and transformation

The *NB* domain of *BPH14* and the *OsPOX8.1* coding sequence were amplified from 'B5' and 'Wushansimiao' cDNAs, and then respectively cloned into the ZeBaTA-based pCXUN expression vector with a Myc tag at the c-terminus (Chen et al., 2009). All primers are listed in Supplementary Table 1. The aforementioned constructs were transiently transfected into 10-day old rice stem protoplasts as described previously (Chen et al., 2006).

Protein collection and protein gel blot assay

Transfected protoplasts were extracted using a protein extraction buffer containing 5 mM $MgCl_2$, 100 mM Tris-HCl (pH 7.5), 0.5% (w/v) Triton X-100, and 1 mM EDTA, with 1 mM PMSF and 2 mM DTT included just prior to the assay. Total soluble proteins were collected from rice protoplasts (5×10^6 cells per sample) using 200 µL of extraction buffer. SDS-PAGE was carried out to separate 10 µL of the extract. The extract was diluted (1:1000) with dilution buffer (3% [w/v] BSA, 150 mM NaCl, 0.1% [w/v] Tween 20, 20 mM Tris-HCl [pH 7.4]) and used for anti-Myc antibody (M192-3, MBL) immunoblotting, and subsequently incubated with 5% (w/v) skim milk-diluted (1:10,000) secondary antibody conjugated to horseradish peroxidase (115-035-003, Jackson). Detection was carried out using Tanon high-sig ECL protein gel blotting substrate.

Statistical analyses and reproducibility

All experiments consisted of three biological replicates, except where stated otherwise. Equivalent results were obtained using three independent biological experiments. Statistically significant differences were identified using Student's t-tests at P value < 0.05.

Reactive oxygen species (ROS) assay

Evaluation of ROS production in rice protoplasts (as shown in Figure 1C) was carried out with a modified chemiluminescence method (Zhang et al., 2007). Briefly, the protoplasts were transfected for 16-22 h and then quantified and diluted to 1×10^5 cells/200 µL with W5. To the diluted protoplasts was added 20 µM of the luminol derivative 8-amino-5-chloro-7-phenylpyrido [3,4-d] pyridazine-1,4 (2H,3H) dione (L-012) (Wako) and 20 µg/mL horseradish peroxidase (Sigma-Aldrich). Luminescence was captured using a SpectraMax iD5 multi-mode microplate reader (Molecular Devices).

Results

Performance of *BPH14*/*BPH15* pyramiding NILs against BPH

In this study, four-leaf stage NILs containing either the *BPH14* (B14), *BPH15* (B15), or *BPH14/BPH15* genes (B1415), as well as their RP, were infested with BPH. RP plants began to wither after 4 d of BPH herbivory (average score of 4.7), and wilted completely after 7 d (average score of 8.2). However, the B14, B15 and B1415 plants showed no visible damage (average scores of 3.3, 2.0, and 1.5, respectively) and survived until the end of the experiment (average scores of 4.6, 5.6, and 3.3, respectively) (Figures 2A–D).

To investigate the antibiosis effects of the NIL and RP plants, we measured the quantity of BPH-secreted honeydew. Overall, BPH feeding on RP and NIL plants produced very little honeydew from 3 to 6 h after infestation. Interestingly, the most significant differences in honeydew production were observed at 12 h after infestation, with the amount of honeydew production remaining relatively constant on NIL plants (from a minimum of 0.16 mg at 6 h to a maximum of 0.36 mg at 12 h) and increasing sharply on RP plants (from a minimum of 0.21 mg at 6 h to a maximum of 14.4 mg at 12 h). After 12 h, honeydew production increased on both NIL and RP plants, and remained high from 24 to 72 h after infestation (Figure 2E).

To identify DEGs functionally associated with defense against BPH in NILs pyramiding the BPH14 and BPH15 genes, RNA was extracted from the leaf sheaths of B14, B15, B1415, and RP plants after infestation (0-72 h). Samples were grouped as non-infested (0 h), early feeding stage (3, 6 and 12 h), or late feeding stage (24, 48 and 72 h) for RNA-seq.

Overview of the RNA-Seq results

Differences in BPH-responsive gene expression were analyzed using mRNA libraries. From 36 mRNA libraries, a total of 31,739,768 to 50,072,060 reads were sequenced. After removing low quality sequences, 82.38%-89.76%, 82.96%-90.53%, 81.69%-90.48%, and 87.83%-90.93% of the reads were mapped to

10.3389/fpls.2023.1250590

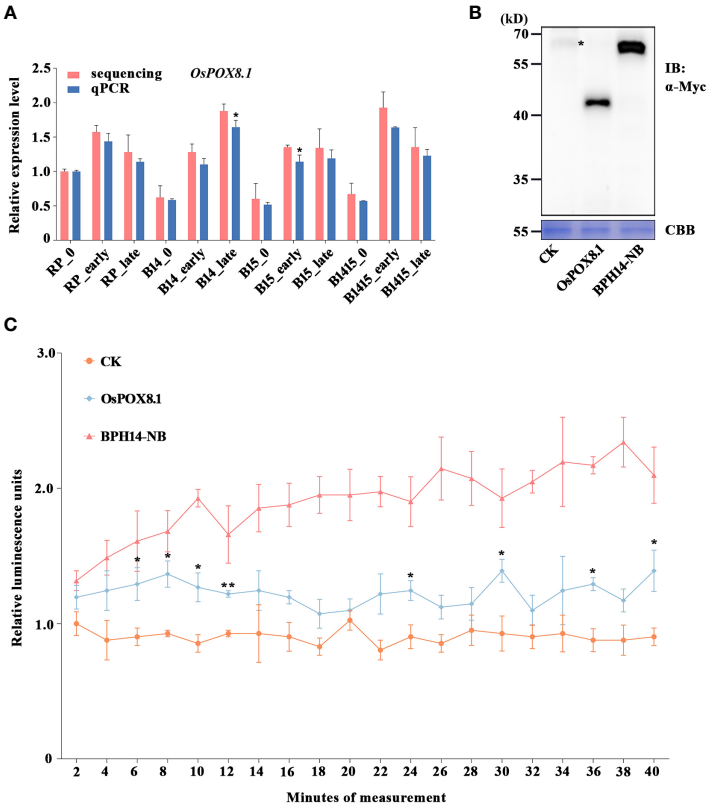

FIGURE 1
Verification of candidate DEG *OsPOX8.1* related to defense response. **(A)** qRT-PCR was used to verify the mRNA expression pattern of *OsPOX8.1* in the RP, B14, B15, and B1415 plants. The rice *TBP* gene was used as a reference control. Gene expression was quantified relative to the value obtained from non-infested RP samples. Data represent the means of three biologically independent experiments for gene expression ± SD. Data were subjected to Student's t-test, and asterisks indicate significant differences between RNA-seq data and qRT-PCR data at the indicated group (**P* < 0.05; ***P* < 0.01). **(B)** Protein immunoblotting of empty vector (CK), *OsPOX8.1*, and NB domain of BPH14 (BPH14-NB) expressed in rice protoplasts. Asterisks indicate nonspecific signals. Coomassie brilliant blue (CBB) staining served as the loading control. Molecular masses (in kilodaltons) are indicated. **(C)** ROS generation in *OsPOX8.1*-overexpressing rice protoplast line. Relative luminescence units indicate relative amounts of ROS production in rice protoplasts at the indicated time points. Protoplast lines transformed with the empty vector and NB domain of BPH14 were used as negative control (CK) and positive control (BPH14-NB), respectively. Data represent the means of three technical replicates from one biological replicate ± SE. Three biologically independent experiments yielded similar results. Data were subjected to Student's t-test, and ROS generation in the BPH14-NB protoplast line significantly differs from that in CK from the first time point onwards. Asterisks indicate significant differences between the OsPOX8.1 protoplast line and CK protoplast line at the indicated time point (**P* < 0.05; ***P* < 0.01).

25,781,469-42,511,732 (RP), 32,708,227-43,047,757 (B14), 29,297,676-41,357,463 (B15), and 33,097,294-44,922,512 (B1415) rice genes, respectively (Supplementary Table 2).

Subsequent to normalization, the average normalized reads from three independent biological replicates were selected for further studies. In total, 14,492 DEGs were identified among 17 comparisons, including nine comparisons among the different varieties (B14_0/RP_0, B14_early/RP_early, B14_late/RP_late, B15_0/RP_0, B15_early/RP_early, B15_late/RP_late, B1415_0/RP_0, B1415_early/RP_early, B1415_late/RP_late) and eight comparisons among the different feeding stages (RP_early/RP_0, RP_late/RP_0, B14_early/B14_0, B14_late/B14_0, B15_early/B15_0, B15_late/B15_0, B1415_early/B1415_0, B1415_late/B1415_0) (Figure 3 and Supplementary Table 3).

A total of 690, 1,388, and 1,400 DEGs were identified in the B14_0/RP_0, B14_early/RP_early, and B14_late/RP_late comparisons, respectively; a total of 6,150, 3,235, and 709 DEGs were identified in the B15_0/RP_0, B15_early/RP_early, and B15_late/RP_late comparisons, respectively; and a total of 960, 1,247, and 520 DEGs were identified in the B1415_0/RP_0, B1415_early/RP_early, and B1415_late/RP_late comparisons, respectively (Figure 3). In addition, 6,165 DEGs were identified in RP plants (1,644 in RP_early/RP_0 and 4,521 in RP_late/RP_0), 7,959 DEGs were identified in B14 plants (889 in B14_early/B14_0 and 7,070 in B14_late/B14_0), 7,784 DEGs were identified in B15 plants (941 in B15_early/B15_0 and 6,843 in B15_late/B15_0), and 4,234 DEGs were identified in B1415 plants (1,224 in B1415_early/B1415_0 and 3,010 in B1415_late/B1415_0). These results illustrate that the DEGs were responsive to BPH feeding, with a higher response in B14 and B15 plants compared to RP, and a lower response in B1415 plants than in RP plants (Figure 3). These results suggest the presence of different modes of regulation at the early and late herbivory stages among the different rice plants.

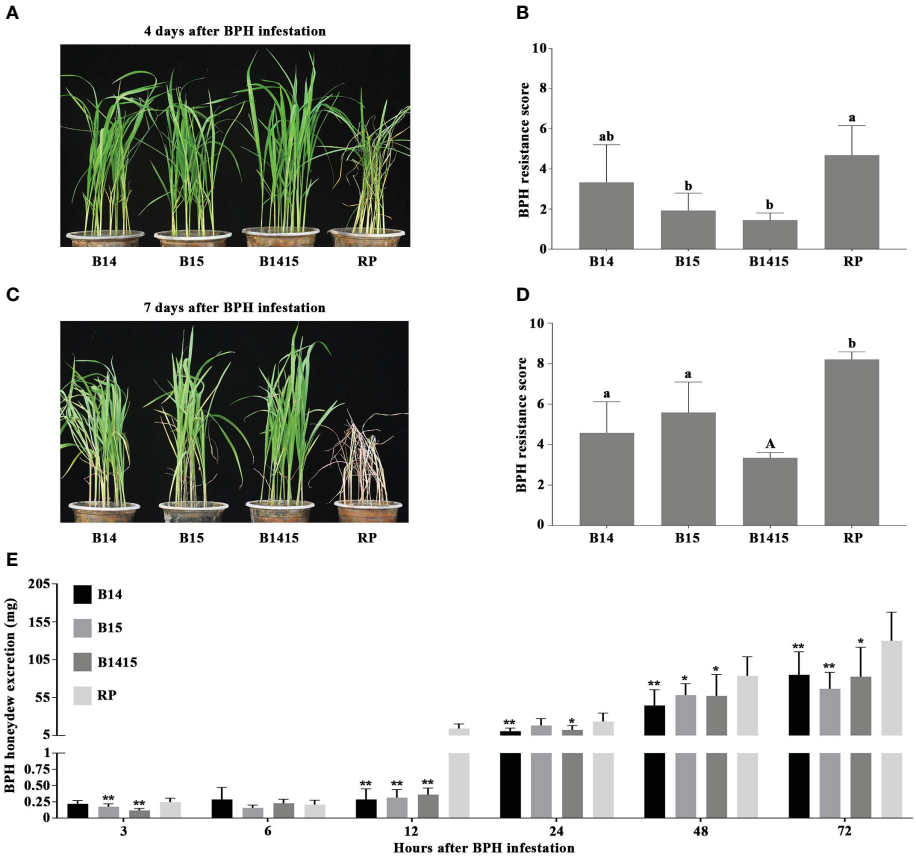

FIGURE 2
Evaluation of BPH resistance of the B14, B15, B1415, and RP plants. **(A)** BPH resistance phenotypes of the B14, B15, B1415, and RP plants after 4 days of BPH feeding. The image shows that the RP plants began to wither while the B14, B15, and B1415 plants showed no visible damage. RP: recurrent parent 'Wushansimiao' for NILs; B14, B15, and B1415: the NILs containing the *BPH14*, *BPH15*, and both *BPH14/BPH15* genes, respectively. **(B)** BPH resistance scores of the B14, B15, B1415, and RP plants after 4 days of BPH feeding. The resistance scores of B14, B15, B1415, and RP were 3.3, 2.0, 1.5, and 4.7, respectively. Lower scores correspond to higher levels of insect resistance. Data represent the means of three biologically independent experiments (with each experiment having 15 seedlings per rice line) ± SD. **(C)** BPH resistance phenotypes of the B14, B15, B1415, and RP plants after 7 days of BPH feeding. The image shows that the RP plants died while the B14, B15, and B1415 plants began to wither. **(D)** BPH resistance scores of the B14, B15, B1415, and RP plants after 7 days of BPH feeding. The resistance scores of B14, B15, B1415, and RP were 4.6, 5.6, 3.3, and 8.2, respectively. **(E)** Honeydew excretion of BPH insects on B14, B15, B1415, and RP plants after 2 days of feeding. Data represent the means of 10 replicates (with each replicate having one BPH insect per plant) ± SD. All data were subjected to Student's t-test, different letters above the bars indicate significant differences between each line of plants **(B, D)** (uppercase letter $P < 0.05$; lowercase letter $P < 0.01$), and asterisks indicate significant differences between NIL and RP plants **(E)** (*$P < 0.05$; **$P < 0.01$).

Reference gene selection and validation of DEGs

During interactions between host plants and herbivores, reference gene expression is often suppressed (Hu et al., 2011). Normalization candidates were chosen after identifying which of the following common rice reference genes were the most stably-expressed: *RPS27α* (Os01g0328400), *ACTIN1* (Os03g0718100), *β-tubulin* (Os03g0780600), *eEF1α* (Os03g0177500), *GAPDH* (Os02g0601300), *SDHA* (Os07g0134800), *HSP* (Os03g0426900), LSD1 (Os12g0611000), *TBP* (Os03g0657000), and *Ubiquitin* (Os03g0131300). Each was evaluated using FPKM values extracted from the RNA-seq data. Overall, both *RPS27α* and *ACTIN1* expressions were significantly reduced after BPH herbivory in all groups. Compared with other candidates, *TBP* exhibited the most stable and appropriate expression level and was chosen as the endogenous reference gene for qRT-PCR validation assays (Figure 4A). The expression levels of eight DEGs were determined by qRT-PCR utilizing gene-specific primers (Supplementary Table 1) for RNA-seq verification, and we found that the data were in agreement (Figure 4B).

Identification of BPH resistance DEGs among the different varieties

To discover BPH resistance-associated genes, DEGs appearing in the comparisons of the resistant NIL vs. RP plants were analyzed by Venn diagrams, respectively (Figures 5A–C). We identified 150 overlapping DEGs in the B14_0/RP_0, B15_0/RP_0, and B1415_0/RP_0 comparisons (Figure 5A); 267 overlapping DEGs in the B14_early/RP_early, B15_early/RP_early, and B1415_early/RP_early comparisons (Figure 5B); and 218 overlapping DEGs in the B14_late/RP_late, B15_late/RP_late, and B1415_late/RP_late

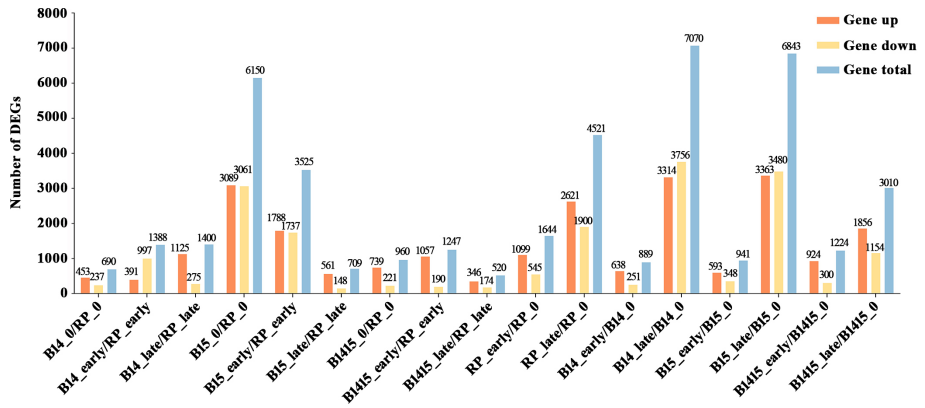

FIGURE 3
Contrast between up-regulated and down-regulated DEGs in all comparisons. "Gene up" represents the number of DEGs that were up-regulated in the compared group. "Gene down" represents the number of DEGs that were down-regulated in the compared group. "Gene total" represents the total number of DEGs in the compared group ($log_2FC > 1$ or $log_2FC < -1$; $P < 0.05$).

comparisons (Figure 5C). By combining these overlapping results, we obtained 531 DEGs common to B14, B15, and B1415 plants before and after BPH feeding, which may be involved in BPH resistance (Supplementary Table 4).

To functionally categorize these 531 DEGs, we analyzed their associated GO terms and KEGG pathways. The DEGs were mainly enriched in the defense response, phosphorylation, and salt stress response GO biological processes; in the ATP binding, nucleotide binding, and kinase activity GO molecular functions; and the integral component of membrane, vacuole, and vacuolar membrane GO cellular components (Figure 5D). For KEGG analysis, the BPH-responsive DEGs were found to be primarily enriched in alpha-linolenic acid metabolism, amino sugar and nucleotide sugar metabolism, fatty acid metabolism, fatty acid degradation, and monoterpenoid biosynthesis. (Figure 5E).

Finally, we comprehensively evaluated both the expression patterns of and the relevant research reports pertaining to the identified DEGs, and ultimately landed on 11 BPH resistance-related genes. Among these, nine were significantly up-regulated in the resistant NIL plants compared with RP plants before and after BPH herbivory, while two (Os02g0599500 and Os10g0180800) were down-regulated in the resistant NIL plants compared with RP plants before and after BPH herbivory (Figure 5F).

Identification of BPH resistance DEGs among the different feeding stages

The DEGs of both resistant NIL and RP plants at the early and late stages of herbivory were compared with those at the non-infested stage using Venn diagrams (Figures 6A, B). A total of 31 DEGs were specifically expressed in B14_early/B14_0, B15_early/B15_0, and B1415_early/B1415_0, while a total of 228 DEGs were specifically expressed in B14_late/B14_0, B15_late/B15_0, and B1415_late/B1415_0 (Figures 6A, B). The common DEGs were further pooled, and 258 DEGs were found to be shared only in resistant NILs during the early or late stages of BPH feeding (Supplementary Table 5).

To functionally categorize these 258 DEGs, we analyzed their associated GO and KEGG pathways. The DEGs were mainly enriched in the response to oxidative stress, chloroplast organization, and response to karrikin GO biological processes; the metal ion binding, transferase activity, and glucosyltransferase activity GO molecular functions; and the cytosol, cell wall, and extracellular region GO cellular components (Figure 6C). For KEGG analysis, the BPH-responsive DEGs were found to be primarily enriched in betalain biosynthesis, biosynthesis of secondary metabolites, metabolic pathways, phagosome, and phenylpropanoid biosynthesis (Figure 6D).

Finally, we comprehensively evaluated both the expression patterns of and the relevant research reports pertaining to the identified DEGs, and ultimately landed on 10 BPH resistance-related genes. Most of these candidates, excluding Os06g0341300, were rapidly up- or down-regulated during the early BPH feeding stage, specifically in resistant NIL plants, with significant differences remaining during the late herbivory stages (Figure 6E).

Verification of candidate DEGs related to BPH resistance

Defense against BPH and other pathogens often involves the generation of ROS (Hu et al., 2017). Specifically, the rapid accumulation of ROS serves as a signal that coordinates an astonishing diversity of defense processes, while also being directly toxic to intruders (Gechev et al., 2006). The *OsPOX8.1* gene, encoding a class III peroxidase, is highly up-regulated in response to blast and bacterial blight, where it is involved in the generation of ROS (Yin et al., 2000; Xiao et al., 2015). Here, the BPH-responsive candidate gene *OsPOX8.1* was found to belong to the GO category "response to oxidative stress" (Figure 6C). Through qRT-PCR validation, we found that *OsPOX8.1* was significantly up-regulated by BPH herbivory only in B14, B15,

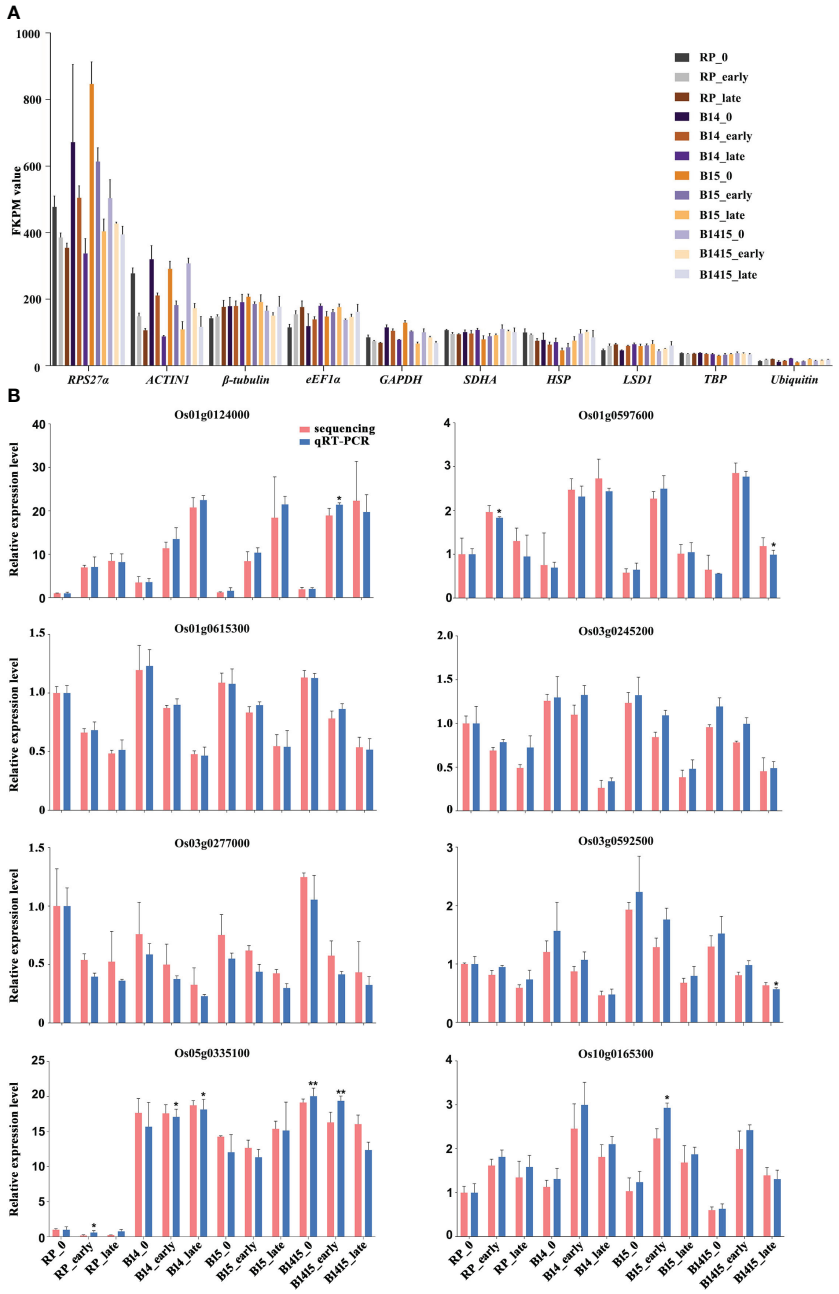

FIGURE 4
Expression profiles of mRNAs. **(A)** FKPM values of *RPS27α*, *ACTIN1*, *β-tubulin*, *eEF1α*, *GAPDH*, *SDHA*, *HSP*, *LSD1*, *TBP*, and *Ubiquitin* from RNA-seq data. **(B)** qRT-PCR was used to verify mRNA expression patterns in the RP, B14, B15, and B1415 plants. The rice *TBP* gene was used as a reference control. Gene expression was quantified relative to the value obtained from non-infested RP samples. Data represent the means of three biologically independent experiments for gene expression ± SD. All data were subjected to Student's t-test, and asterisks indicate significant differences between RNA-seq data and qRT-PCR data for the indicated group (**P* < 0.05; ***P* < 0.01).

and B1415 plants, and the degree of up-regulation was higher in B1415 plants than in B14 or B15 plants. Consistent with the RNA-seq results, *OsPOX8.1* expression was responsive from the early through the late feeding stages (Figure 1A).

To verify whether *OsPOX8.1* regulates ROS levels, rice protoplasts were first transformed with *OsPOX8.1*. An empty vector construct (control, CK) and an auto-activated construct of the NB domain of BPH14 (BPH14-NB) were utilized as negative and positive controls, respectively (Hu et al., 2017). According to the immunoblotting experiments, each of the transformed proteins exhibited expected expression patterns (Figure 1B). ROS production in the protoplast lines was measured histochemically using the chemiluminescence method. The protoplasts transformed with *OsPOX8.1* exhibited ROS accumulation, which was significantly stronger than that of protoplasts transformed with CK, but weaker than that of the protoplasts transformed with BPH14-NB (Figure 1C). These results indicated that *OsPOX8.1* enhanced ROS production in rice protoplasts.

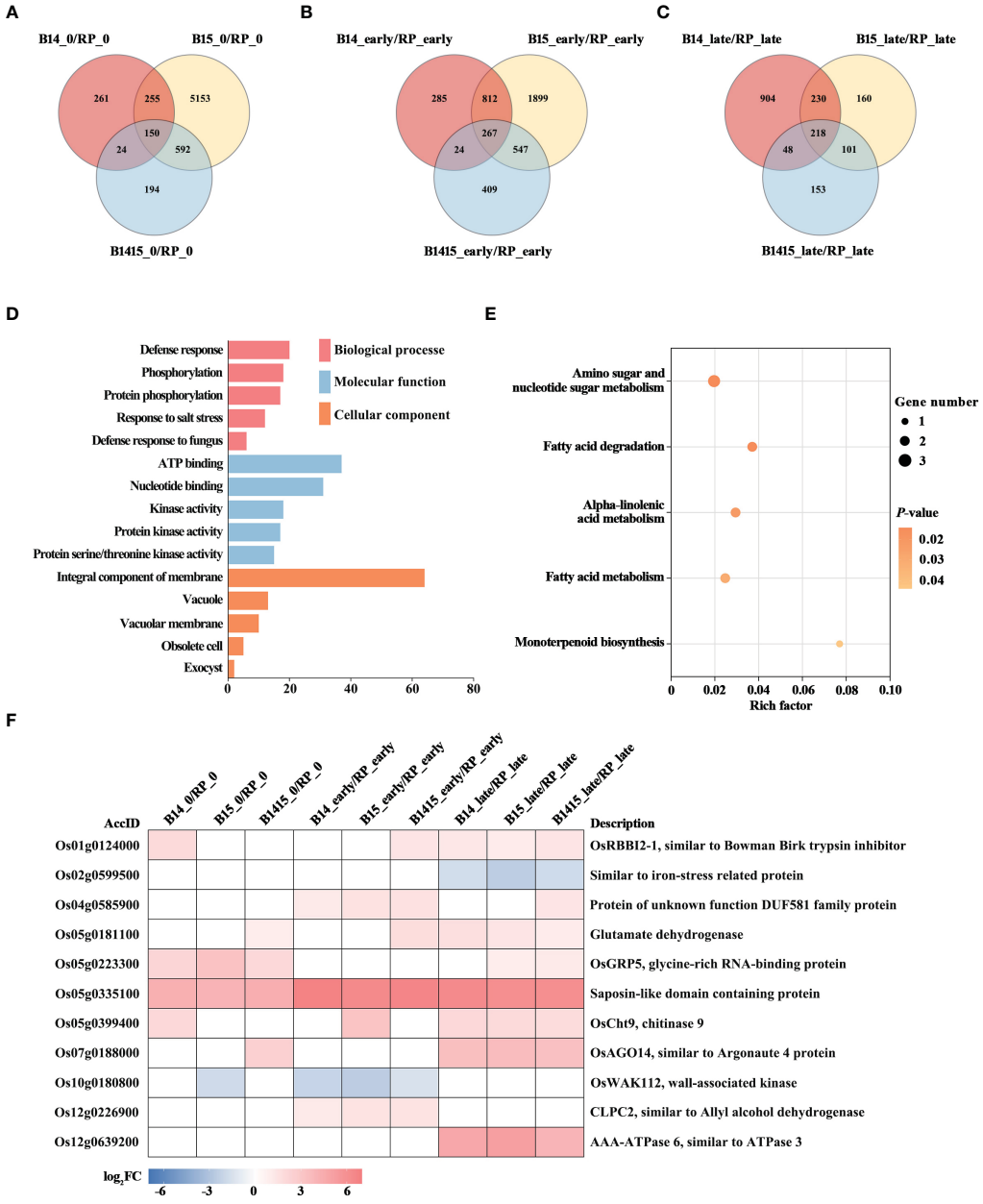

FIGURE 5
Analysis of DEGs related to BPH resistance among the different varieties. **(A-C)** Venn diagrams of the unique and shared DEGs among the different varieties. Venn diagram of the number of DEGs of the resistant NILs compared to RP at the non-infested stage **(A)**, early feeding stage **(B)**, and late feeding stage **(C)**. **(D)** Gene ontology (GO) analysis. Biological processes, molecular functions, and cellular components of the 531 common DEGs among the resistant NILs compared to RP before and after BPH feeding ($P < 0.05$). The x- and y-axes indicate the number of genes in a category and the names of the clusters, respectively. **(E)** Kyoto encyclopedia of genes and genomes (KEGG) analysis. KEGG pathway enrichment analysis of the 531 common DEGs among the resistant NILs compared to RP before and after BPH feeding ($P < 0.05$). The x- and y-axes indicate the rich factor of each pathway and the pathway name, respectively. The bubble size indicates the number of genes. The color bar indicates the *P*-value. **(F)** Hierarchical clustering analysis of 11 potential candidate DEGs related to BPH resistance among the different varieties. The color bar represents fold-change values shown in the $\log_2$ scale based on FPKM values.

Discussion

Pyramiding lines containing both *BPH14* and *BPH15* exhibit more durable and effective protection than lines containing only *BPH14* or *BPH15* (Li et al., 2011; Hu et al., 2012; Jiang et al., 2018). However, the molecular mechanisms of BPH resistance underlying *BPH14*/*BPH15* pyramiding lines are poorly understood. This study is the first to perform an RNA-seq analysis of NILs containing either *BPH14* or *BPH15*, or both, as well as their RP. The data presented here aid our understanding of the regulatory mechanisms of BPH resistance gene pyramiding lines upon BPH attack.

Consistent with the previous study (Wang et al., 2019), performance and evaluation of *BPH14*/*BPH15* pyramiding NILs against BPH showed that pyramiding *BPH14* and *BPH15* in

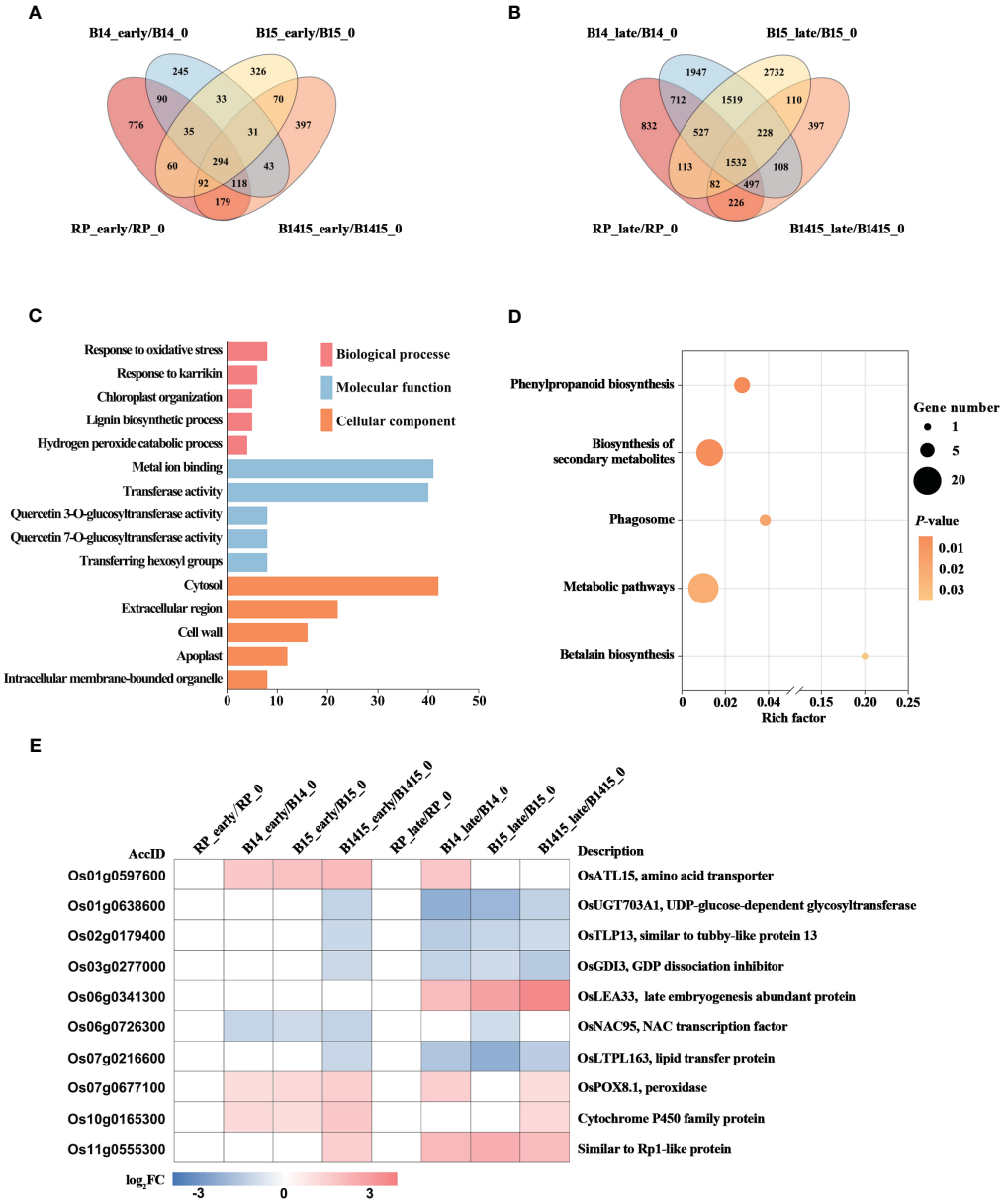

FIGURE 6
Analysis of DEGs related to BPH resistance among the different feeding stages. **(A, B)** Venn diagrams of the unique and shared DEGs among the different feeding stages. Venn diagram of the number of DEGs in early feeding stage **(A)** and late feeding stage **(B)** of the resistant NILs and RP compared to themselves at the non-infested stage. **(C)** Gene ontology (GO) analysis. Biological processes, molecular functions, and cellular components of the 258 DEGs which were shared only in resistant NILs obtained among the different feeding stages ($P < 0.05$). The x- and y-axes indicate the number of genes in a category and the names of the clusters, respectively. **(D)** Kyoto encyclopedia of genes and genomes (KEGG) analysis. KEGG pathway enrichment analysis of the 258 DEGs which were shared only in resistant NILs at the early or late stages of BPH feeding ($P < 0.05$). The x- and y-axes indicate the rich factor in each pathway and the pathway name, respectively. The bubble size indicates the number of DEGs. The color bar indicates the *P*-value. **(E)** Hierarchical clustering analysis of ten potential candidate DEGs related to BPH resistance among the different feeding stages. The color bar represents fold-change values shown in the $\log_2$ scale based on FPKM values.

'Wushansimiao' resulted in significantly enhanced resistance to BPH, with the B1415 plants exhibiting much stronger BPH resistance than the B14 or B15 plants (Figure 2). In addition, there were significant differences in honeydew production on the resistant NIL and RP plants 12 h after infestation (Figure 2E), these results suggested that stronger resistance factors (e.g. callose deposits on sieve plates) might exist to prevent the phloem sap ingestion by BPH from resistant NIL plants than from RP plants (Hao et al., 2008). Therefore, the RNA samples from the NIL and RP plants were categorized as either early feeding stage (before 12 h), late feeding stage (after 12 h), or non-infested.

By comparing mRNA expression between the B14, B15, B1415, and RP plants before and after BPH infestation, a total of 14,492 DEGs were identified among 17 comparisons (Figure 3). Although a comparison of the RNA-seq results between B1415 and RP plants was sufficient to identify BPH resistance-associated DEGs, studying

the RNA-seq results of B14 and B15 plants may provide more details about the mechanism of rice resistance to BPH, and may also more accurately and reliably identify DEGs related to BPH resistance. There were fewer DEGs detected in the B1415_early/RP_early and B1415_late/RP_late comparisons than in the B14_early/RP_early and B14_late/RP_late comparisons or the B15_early/RP_early and B15_late/RP_late comparisons during the early and late feeding stages. These results indicate that the B1415 plants experienced less damage and had a relatively normal physiological status compared to the other plants due to their strong BPH resistance (Figure 3). Meanwhile, the B1415 plants had more up-regulated than down-regulated DEGs, implying that the expression of BPH resistance-related genes might be up-regulated in B1415 plants (Figure 3).

The selection of an appropriate reference gene which exhibits minimal changes in expression during a particular experiment is critical to the accuracy of qRT-PCR analyses. Various housekeeping genes show a certain degree of variability during plant-pathogen and plant-herbivore interactions (Hu et al., 2011). The expressions of some novel candidate reference genes were modified due to metabolic alterations and organ-specific gene expression reprogramming in response to invasion (Mascia et al., 2010). For instance, the conventional reference gene *ACTIN1* exhibits greater dynamic changes in infected plants due to its involvement in the transport of defense-related compounds (Henty-Ridilla et al., 2014). We compared the stability of ten novel reference gene candidates: *RPS27α*, *ACTIN1*, *β-tubulin*, *eEF1α*, *GAPDH*, *SDHA*, *HSP*, *LSD1*, *TBP*, and *Ubiquitin*. Upon comparison of the FPKM values extracted from the RNA-seq data, identical rankings were observed for the most stable reference gene *TBP*, which is in accordance with prior reports (Hu et al., 2011; Guo et al., 2018; Tan et al., 2020). In contrast, *RPS27α* and *ACTIN1* were ranked among the least stable, suggesting that these genes experience highly variable expression during BPH infestation.

A total of 531 DEGs appeared in B14, B15, and B1415 plants, compared to RP plants, before and after BPH infestation. In addition, a greater number of overlapping DEGs were identified in comparisons of different varieties during BPH feeding (267 and 218 overlapping DEGs, as shown in Figures 5B, C, respectively) than before BPH feeding (150 overlapping DEGs, as shown in Figure 5A), suggesting that many DEGs were activated to defend against BPH infestation. These DEGs were most enriched in defense response (GO), which is consistent with the above conclusion (Figure 5D). In addition, KEGG pathway analysis suggested that the responses of resistant NILs against BPH were compensatory or tolerance-enhancing in nature. Specifically, these DEGs were found to be related to alpha-linolenic acid metabolism, amino sugar and nucleotide sugar metabolism, fatty acid metabolism, fatty acid degradation, and monoterpenoid biosynthesis (Figure 5E). Based on the expression patterns of, and relevant references pertaining to, the above DEGs, 11 genes were chosen as potential BPH resistance candidates (Figure 5F). The Bowman-Birk trypsin inhibitor plays a role in the plant biotic stress response by inhibiting trypsin activity (Pang et al., 2013). Iron stress can activate the immune response, and plants may recognize pathogens by way of iron depletion (Herlihy et al., 2020). In *Arabidopsis*, *increased resistance to myzus persicae 1* (*IRM1*) (encoding DUF581 domain-containing protein) overexpression confers aphid resistance (Chen et al., 2013). Furthermore, *glycine-rich RNA-binding protein* (*GRP*) gene knock-out *Arabidopsis* lines are less resistant to *Pseudomonas* (Fu et al., 2007). Egg production and embryonic development of *Meloidogyne incognita* is reduced by chitinase gene expression (Chan et al., 2010). In response to herbivory, Argonautes (AGOs) modulate several defense regulation nodes (Pradhan et al., 2017). In rice, the wall-associated kinases (WAKs) act as both negative and positive regulators of fungal defense (Delteil et al., 2016). Disease susceptibility, the hypersensitive response, and pathogen growth are activated by co-suppression of *CLPC1* and *CLPC2* (Ali et al., 2019). In addition, glutamate dehydrogenase (GDH), saposin-like domain containing protein, and OsAAA-ATPase are importance in pathogen defense (Pageau et al., 2006; Muñoz et al., 2010; Liu et al., 2020b).

The BPH resistance DEGs were then compared between the different feeding stages. There were 258 DEGs shared only among resistant NILs during either the early or late stages of BPH feeding. Interestingly, there were fewer overlapping DEGs (31 of 258 DEGs) specifically expressed in resistant NILs at the early feeding stage and many more overlapping DEGs (228 of 258 DEGs) specifically expressed in resistant NILs are the late feeding stage. These results imply that certain central signal genes rapidly responded to BPH herbivory at the early stage while many more functional DEGs responded to the signal and were activated to defend against the damage caused by BPH invasion (Figures 6A, B). The results of the GO analysis further supported our assumption, as these DEGs were enriched in response to oxidative stress, chloroplast organization, and response to karrikin, all of which are associated with the biotic stress response (Figure 6C). Meanwhile, the DEGs were also enriched in secondary metabolite biosynthesis and phenylpropanoid biosynthesis (KEGG) (Figure 6D). Ten DEGs were selected as potential BPH resistance candidates, which are associated with either pathogen or herbivore resistance (Figure 6E). In rice, the gene *OsATL15* was found to facilitate thiamethoxam accumulation and increase the efficacy of thiamethoxam against BPH (Xiao et al., 2022). In maize, the recessive resistance gene *dissociation inhibitor alpha* (*ZmGDIα*) was found to provide quantitative recessive resistance to maize rough dwarf disease (MRDD) (Liu et al., 2020a). The NAC transcription factors are both negative and positive regulators of downstream defense genes during plant-pathogen interactions. For example, the NAC transcription factor *RIM1* is a negative regulator of rice dwarf virus resistance (Bian et al., 2020). The *lipid transfer protein* (*LTP*) gene coordinates plant resistance to insects and fungi by redirecting metabolic flux (Chen et al., 2021). The peroxidase gene *OsPOX8.1* is strongly induced after pathogen infection, likely through accumulation of ROS (Sun et al., 2014). Here, we confirmed that *OsPOX8.1* could be rapidly and stably induced by BPH infestation, and that overexpression of *OsPOX8.1* in rice protoplasts could increase ROS production (Figure 1). Overexpression of *Oryza sativa Rp1-like 1* (*OsRP1L1*) increased resistance to *Xanthomonas* strains *PXO341* and *PXO86* (Wang et al., 2013). In addition, UDP-glucose-dependent glycosyltransferase, late embryogenesis abundant proteins, tubby-

like proteins, and cytochrome P450 family proteins are all involved in pathogen defense (Cai et al., 2008; Park et al., 2011; Liu et al., 2013; Wang et al., 2022).

Conclusion

This was the first endeavor to precisely identify DEGs functionally associated with BPH resistance in NILs pyramiding *BPH14* and *BPH15*. For this purpose, RNA-seq data were generated from 36 mRNA libraries constructed from NILs containing either *BPH14*, *BPH15*, or both *BPH14*/*BPH15*, as well as their RP, before and after BPH herbivory. The DEGs related to BPH resistance were mainly enriched in defense response and oxidative stress. Additionally, 21 DEGs were chosen as probable BPH resistance candidates by analyzing their expression in different varieties at different feeding stages. One of them, *OsPOX8.1*, was validated in rice protoplasts to increase the accumulation of ROS. Our study not only enhances our understanding of plant-insect interactions in resistance gene pyramiding lines, but will also be foundational for comprehensive functional analyses of the identified candidate DEGs to aid in the improvement of BPH-resistant rice.

Data availability statement

The datasets presented in this study can be found in online repositories. The names of the repository/repositories and accession number(s) can be found below: https://www.ncbi.nlm.nih.gov/, GSE232449.

Author contributions

JL, AY, and LH conceived and designed the research. LH, DY, HW, XD, YZ, LN, BW, MX, HQ, and TM participated in the experiments. LH and DY analyzed the data. HW provided the NILs containing *BPH14*, *BPH15*, and *BPH14*/*BPH15*, as well as their recurrent parent. LH, AY, and JL wrote the manuscript. DY and HW helped to edit the manuscript. All authors read and approved the final manuscript.

Funding

This work was supported by grants from the Hubei Key Laboratory of Food Crop Germplasm and Genetic Improvement Foundation (grant no. 2021lzjj01), Hubei Academy of Agricultural Science Foundation (grant no. 2023NKYJJ02), Natural Science Foundation of Hubei Province (grant no. 2022CFB830), and the Open Research Fund of State Key Laboratory of Hybrid Rice (Wuhan University) (grant no. KF202209).

Acknowledgments

We sincerely thank Wuhan Evergreen Rice Biotechnology Co., Ltd. (unified Social Credit Code: 91420100MA4KQPW30T) for providing brown planthopper resistance identification technology services. Finally, we would like to thank TopEdit for the English language editing of this manuscript.

Conflict of interest

The authors declare that the research was conducted in the absence of any commercial or financial relationships that could be construed as a potential conflict of interest.

Publisher's note

Supplementary material

The Supplementary Material for this article can be found online at: https://www.frontiersin.org/articles/10.3389/fpls.2023.1250590/full#supplementary-material

References

Ali, M. S., Choi, J., Yun, H. K., Choi, S. J., and Baek, K. H. (2019). Co-suppression of *NbClpC1* and *NbClpC2*, chaperone subunits in the Clp protease complex, accelerates hypersensitive response and increases disease susceptibility in *Nicotiana benthamiana*. *J. Plant Pathol.* 101, 1099–1105. doi: 10.1007/s42161-019-00345-z

Anders, S., Pyl, P. T., and Huber, W. (2015). HTSeq-a Python framework to work with high-throughput sequencing data. *Bioinformatics* 31 (2), 166–169. doi: 10.1093/bioinformatics/btu638

Ashburner, M., Ball, C. A., Blake, J. A., Botstein, D., Butler, H., Cherry, J. M., et al. (2000). Gene ontology: tool for the unification of biology. *Nat. Genet.* 25 (1), 25–29. doi: 10.1038/75556

Benjamini, Y., Drai, D., Elmer, G., Kafkafi, N., and Golani, I. (2001). Controlling the false discovery rate in behavior genetics research. *Behav. Brain Res.* 125 (1-2), 279–284. doi: 10.1016/S0166-4328(01)00297-2

Bian, Z., Gao, H., and Wang, C. (2020). NAC transcription factors as positive or negative regulators during ongoing battle between pathogens and our food crops. *Int. J. Mol. Sci.* 22 (1), 81. doi: 10.3390/ijms22010081

Cai, M., Qiu, D., Yuan, T., Ding, X., Li, H., Duan, L., et al. (2008). Identification of novel pathogen-responsive *cis*-elements and their binding proteins in the promoter of *OsWRKY13*, a gene regulating rice disease resistance. *Plant Cell Environ.* 31 (1), 86–96. doi: 10.1111/j.1365-3040.2007.01739.x

Chan, Y. L., Cai, D., Taylor, P. W. J., Chan, M. T., and Yeh, K. W. (2010). Adverse effect of the chitinolytic enzyme PjCHI-1 in transgenic tomato on egg mass production and embryonic development of *Meloidogyne incognita*. *Plant Pathol.* 59 (5), 922–930. doi: 10.1111/j.1365-3059.2010.02314.x

Chen, R., Deng, Y., Ding, Y., Guo, J., Qiu, J., Wang, B., et al. (2022). Rice functional genomics: decades' efforts and roads ahead. *Sci. China Life Sci.* 65, 33–92. doi: 10.1007/s11427-021-2024-0

Chen, S., Songkumarn, P., Liu, J., and Wang, G. L. (2009). A versatile zero background T-vector system for gene cloning and functional genomics. *Plant Physiol.* 150 (3), 1111–1121. doi: 10.1104/pp.109.137125

Chen, S., Tao, L., Zeng, L., Vega-sanchez, M. E., Umemura, K., and Wang, G. L. (2006). A highly efficient transient protoplast system for analyzing defence gene expression and protein-protein interactions in rice. *Mol. Plant Pathol.* 7 (5), 417–427. doi: 10.1111/j.1364-3703.2006.00346.x

Chen, B., Zhang, Y., Sun, Z., Liu, Z., Zhang, D., Yang, J., et al. (2021). Tissue-specific expression of *GhnsLTPs* identified *via* GWAS sophisticatedly coordinates disease and insect resistance by regulating metabolic flux redirection in cotton. *Plant J.* 107 (3), 831–846. doi: 10.1111/tpj.15349

Chen, X., Zhang, Z., Visser, R. G., Broekgaarden, C., and Vosman, B. (2013). Overexpression of *IRM1* enhances resistance to aphids in *Arabidopsis thaliana*. *PloS One* 8 (8), e70914. doi: 10.1371/journal.pone.0070914

Cheng, X., Wu, Y., Guo, J., Du, B., Chen, R., Zhu, L., et al. (2013a). A rice lectin receptor-like kinase that is involved in innate immune responses also contributes to seed germination. *Plant J.* 76 (4), 687–698. doi: 10.1111/tpj.12328

Cheng, X., Zhu, L., and He, G. (2013b). Towards understanding of molecular interactions between rice and the brown planthopper. *Mol. Plant* 6 (3), 621–634. doi: 10.1093/mp/sst030

Delteil, A., Gobbato, E., Cayrol, B., Estevan, J., Michel-Romiti, C., Dievart, A., et al. (2016). Several wall-associated kinases participate positively and negatively in basal defense against rice blast fungus. *BMC Plant Biol.* 16 (1), 1–10. doi: 10.1186/s12870-016-0711-x

Draghici, S., Khatri, P., Tarca, A. L., Amin, K., Done, A., Voichita, C., et al. (2007). A systems biology approach for pathway level analysis. *Genome Res.* 17 (10), 1537–1545. doi: 10.1101/gr.6202607

Du, B., Chen, R., Guo, J., and He, G. (2020). Current understanding of the genomic, genetic, and molecular control of insect resistance in rice. *Mol. Breed.* 40, 1–25. doi: 10.1007/s11032-020-1103-3

Du, B., Zhang, W., Liu, B., Hu, J., Wei, Z., Shi, Z., et al. (2009). Identification and characterization of *Bph14*, a gene conferring resistance to brown planthopper in rice. *Proc. Natl. Acad. Sci. U.S.A.* 106 (52), 22163–22168. doi: 10.1073/pnas.0912139106

Fu, Z. Q., Guo, M., Jeong, B. R., Tian, F., Elthon, T. E., Cerny, R. L., et al. (2007). A type III effector ADP-ribosylates RNA-binding proteins and quells plant immunity. *Nature* 447 (7142), 284–288. doi: 10.1038/nature05737

Gechev, T. S., Van Breusegem, F., Stone, J. M., Denev, I., and Laloi, C. (2006). Reactive oxygen species as signals that modulate plant stress responses and programmed cell death. *Bioessays* 28 (11), 1091–1101. doi: 10.1002/bies.20493

Guo, J., Chen, R., Du, B., Zhu, L., and He, G. (2022). Progress in exploitation and utilization of brown planthopper resistance gene in rice (in Chinese). *Sci. Sin. Vitae* 52, 1326–1334. doi: 10.1360/SSV-2022-0044

Guo, J., Wang, H., Guan, W., Guo, Q., Wang, J., Yang, J., et al. (2023). A tripartite rheostat controls self-regulated host plant resistance to insects. *Nature* 618, 799–807. doi: 10.1038/s41586-023-06197-z

Guo, J., Xu, C., Wu, D., Zhao, Y., Qiu, Y., Wang, X., et al. (2018). *Bph6* encodes an exocyst-localized protein and confers broad resistance to planthoppers in rice. *Nat. Genet.* 50 (2), 297–306. doi: 10.1038/s41588-018-0039-6

Hao, P., Liu, C., Wang, Y., Chen, R., Tang, M., Du, B., et al. (2008). Herbivore-induced callose deposition on the sieve plates of rice: an important mechanism for host resistance. *Plant Physiol.* 146 (4), 1810–1820. doi: 10.1104/pp.107.111484

Henty-Ridilla, J. L., Li, J., Day, B., and Staiger, C. J. (2014). ACTIN DEPOLYMERIZING FACTOR4 regulates actin dynamics during innate immune signaling in *Arabidopsis*. *Plant Cell* 26 (1), 340–352. doi: 10.1105/tpc.113.122499

Herlihy, J. H., Long, T. A., and McDowell, J. M. (2020). Iron homeostasis and plant immune responses: recent insights and translational implications. *J. Biol. Chem.* 295 (39), 13444–13457. doi: 10.1074/jbc.REV120.010856

Hu, J., Li, X., Wu, C., Yang, C., Hua, H., Gao, G., et al. (2012). Pyramiding and evaluation of the brown planthopper resistance genes *Bph14* and *Bph15* in hybrid rice. *Mol. Breed.* 29, 61–69. doi: 10.1007/s11032-010-9526-x

Hu, L., Wu, Y., Wu, D., Rao, W., Guo, J., Ma, Y., et al. (2017). The coiled-coil and nucleotide binding domains of BROWN PLANTHOPPER RESISTANCE14 function in signaling and resistance against planthopper in rice. *Plant Cell* 29 (12), 3157–3185. doi: 10.1105/tpc.17.00263

Hu, J., Zhou, J., Peng, X., Xu, H., Liu, C., Du, B., et al. (2011). The *Bphi008a* gene interacts with the ethylene pathway and transcriptionally regulates *MAPK* genes in the response of rice to brown planthopper feeding. *Plant Physiol.* 156 (2), 856–872. doi: 10.1104/pp.111.174334

Huang, Z., He, G., Shu, L. H., Li, X., and Zhang, Q. (2001). Identification and mapping of two brown planthopper resistance genes in rice. *Theor. Appl. Genet.* 102, 929–934. doi: 10.1007/s001220000455

Jena, K. K., and Kim, S. M. (2010). Current status of brown planthopper (BPH) resistance and genetics. *Rice* 3 (2), 161–171. doi: 10.1007/s12284-010-9050-y

Jiang, H., Hu, J., Li, Z., Liu, J., Gao, G., Zhang, Q., et al. (2018). Evaluation and breeding application of six brown planthopper resistance genes in rice maintainer line Jin 23B. *Rice* 11 (1), 1–11. doi: 10.1186/s12284-018-0215-4

Jing, S., Zhao, Y., Du, B., Chen, R., Zhu, L., and He, G. (2017). Genomics of interaction between the brown planthopper and rice. *Curr. Opin. Insect Sci.* 19, 82–87. doi: 10.1016/j.cois.2017.03.005

Kim, D., Langmead, B., and Salzberg, S. L. (2015). HISAT. A fast spliced aligner with low memory requirements. *Nat. Methods* 12 (4), 357–360. doi: 10.1038/nmeth.3317

Li, J., Chen, Q., Wang, L., Liu, J., Shang, K., and Hua, H. (2011). Biological effects of rice harbouring *Bph14* and *Bph15* on brown planthopper, *Nilaparvata lugens*. *Pest. Manage. Sci.* 67 (5), 528–534. doi: 10.1002/ps.2089

Liu, Q., Deng, S., Liu, B., Tao, Y., Ai, H., Liu, J., et al. (2020a). A *helitron*-induced RabGDIα variant causes quantitative recessive resistance to maize rough dwarf disease. *Nat. Commun.* 11 (1), 495. doi: 10.1038/s41467-020-14372-3

Liu, X., Inoue, H., Tang, X., Tan, Y., Xu, X., Wang, C., et al. (2020b). Rice *OsAAA-ATPase1* is induced during blast infection in a salicylic acid-dependent manner, and promotes blast fungus resistance. *Int. J. Mol. Sci.* 21 (4), 1443. doi: 10.3390/ijms21041443

Liu, Y., Wang, L., Xing, X., Sun, L., Pan, J., Kong, X., et al. (2013). ZmLEA3, a multifunctional group 3 LEA protein from maize (*Zea mays* L.), is involved in biotic and abiotic stresses. *Plant Cell Physiol.* 54 (6), 944–959. doi: 10.1093/pcp/pct047

Livak, K. J., and Schmittgen, T. D. (2001). Analysis of relative gene expression data using real-time quantitative PCR and the $2^{-\Delta\Delta CT}$ method. *Methods* 25 (4), 402–408. doi: 10.1006/meth.2001.1262

Love, M. I., Huber, W., and Anders, S. (2014). Moderated estimation of fold change and dispersion for RNA-seq data with DESeq2. *Genome Biol.* 15 (12), 1–21. doi: 10.1186/s13059-014-0550-8

Lv, W., Du, B., Shangguan, X., Zhao, Y., Pan, Y., Zhu, L., et al. (2014). BAC and RNA sequencing reveal the brown planthopper resistance gene *BPH15* in a recombination cold spot that mediates a unique defense mechanism. *BMC Genomics* 15 (1), 1–16. doi: 10.1186/1471-2164-15-674

Mascia, T., Santovito, E., Gallitelli, D., and Cillo, F. (2010). Evaluation of reference genes for quantitative reverse-transcription polymerase chain reaction norMalization in infected tomato plants. *Mol. Plant Pathol.* 11 (6), 805–816. doi: 10.1111/j.1364-3703.2010.00646.x

Muduli, L., Pradhan, S. K., Mishra, A., Bastia, D. N., Samal, K. C., Agrawal, P. K., et al. (2021). Understanding brown planthopper resistance in Rice: Genetics, biochemical and molecular breeding approaches. *Rice Sci.* 28 (6), 532–546. doi: 10.1016/j.rsci.2021.05.013

Muñoz, F. F., Mendieta, J. R., Pagano, M. R., Paggi, R. A., Daleo, G. R., and Guevara, M. G. (2010). The swaposin-like domain of potato aspartic protease (*St*Asp-PSI) exerts antimicrobial activity on plant and human pathogens. *Peptides* 31 (5), 777–785. doi: 10.1016/j.peptides.2010.02.001

Pageau, K., Reisdorf-Cren, M., Morot-Gaudry, J. F., and Masclaux-Daubresse, C. (2006). The two senescence-related markers, *GS1* (cytosolic glutamine synthetase) and *GDH* (glutamate dehydrogenase), involved in nitrogen mobilization, are differentially regulated during pathogen attack and by stress hormones and reactive oxygen species in *Nicotiana tabacum* L. leaves. *J. Exp. Bot.* 57 (3), 547–557. doi: 10.1093/jxb/erj035

Pang, Z., Zhou, Z., Yin, D., Lv, Q., Wang, L., Xu, X., et al. (2013). Transgenic rice plants overexpressing BBTI4 confer partial but broad-spectrum bacterial blight resistance. *J. Plant Biol.* 56, 383–390. doi: 10.1007/s12374-013-0277-1

Park, H. J., Kwon, C. S., Woo, J. Y., Lee, G. J., Kim, Y. J., and Paek, K. H. (2011). Suppression of UDP-glycosyltransferase-coding *Arabidopsis thaliana UGT74E2* gene expression leads to increased resistance to *Psuedomonas syringae* pv. *Tomato* DC3000 infection. *Plant Pathol. J.* 27 (2), 170–182. doi: 10.5423/PPJ.2011.27.2.170

Pathak, P. K., Saxena, R. C., and Heinrichs, E. A. (1982). Parafilm sachet for measuring honeydew excretion by *Nilaparvata lugens* on rice. *J. Econ. Entomol.* 75 (2), 194–195. doi: 10.1093/jee/75.2.194

Pradhan, M., Pandey, P., Gase, K., Sharaff, M., Singh, R. K., Sethi, A., et al. (2017). Argonaute 8 (AGO8) mediates the elicitation of direct defenses against herbivory. *Plant Physiol.* 175 (2), 927–946. doi: 10.1104/pp.17.00702

Ren, X., Weng, Q., Zhu, L., and He, G. (2004). Dynamic mapping of quantitative trait loci for brown planthopper resistance in rice. *Cereal Res. Commun.* 32, 31–38. doi: 10.1007/BF03543277

Sun, L., Yang, D. L., Kong, Y., Chen, Y., Li, X. Z., Zeng, L. J., et al. (2014). Sugar homeostasis mediated by cell wall invertase GRAIN INCOMPLETE FILLING 1 (GIF1) plays a role in pre-existing and induced defence in rice. *Mol. Plant Pathol.* 15 (2), 161–173. doi: 10.1111/mpp.12078

Tan, J., Wu, Y., Guo, J., Li, H., Zhu, L., Chen, R., et al. (2020). A combined microRNA and transcriptome analyses illuminates the resistance response of rice against brown planthopper. *BMC Genomics* 21 (1), 1–17. doi: 10.1186/s12864-020-6556-6

Wang, X., Chen, J., Yang, Y., Zhou, J., Qiu, Y., Yu, C., et al. (2013). Characterization of a novel NBS-LRR gene involved in bacterial blight resistance in rice. *Plant Mol. Biol. Rep.* 31, 649–656. doi: 10.1007/s11105-012-0537-0

Wang, H., Gao, Y., Mao, F., Xiong, L., and Mou, T. (2019). Directional upgrading of brown planthopper resistance in an elite rice cultivar by precise introgression of two resistance genes using genomics-based breeding. *Plant Sci.* 288, 110211. doi: 10.1016/j.plantsci.2019.110211

Wang, A., Ma, L., Shu, X., Jiang, Y., Liang, J., and Zheng, A. (2022). Rice (*Oryza sativa* L.) cytochrome P450 protein 716A subfamily CYP716A16 regulates disease resistance. *BMC Genomics* 23 (1), 1–13. doi: 10.1186/s12864-022-08568-8

Wang, Y., Wang, X., Yuan, H., Chen, R., Zhu, L., He, R., et al. (2008). Responses of two contrasting genotypes of rice to brown planthopper. *Mol. Plant-Microbe Interact.* 21 (1), 122–132. doi: 10.1094/MPMI-21-1-0122

Wang, H., Ye, S., and Mou, T. (2016). Molecular breeding of rice restorer lines and hybrids for brown planthopper (BPH) resistance using the *Bph14* and *Bph15* genes. *Rice* 9, 1–9. doi: 10.1186/s12284-016-0126-1

Wing, R. A., Purugganan, M. D., and Zhang, Q. (2018). The rice genome revolution: from an ancient grain to Green Super Rice. *Nat. Rev. Genet.* 19 (8), 505–517. doi: 10.1038/s41576-018-0024-z

Wu, Y., Lv, W., Hu, L., Rao, W., Zeng, Y., Zhu, L., et al. (2017). Identification and analysis of brown planthopper-responsive microRNAs in resistant and susceptible rice plants. *Sci. Rep.* 7 (1), 8712. doi: 10.1038/s41598-017-09143-y

Xiao, Y., Zhang, H., Li, Z., Huang, T., Akihiro, T., Xu, J., et al. (2022). An amino acid transporter-like protein (OsATL15) facilitates the systematic distribution of thiamethoxam in rice for controlling the brown planthopper. *Plant Biotechnol. J.* 20 (10), 1888–1901. doi: 10.1111/pbi.13869

Xiao, G. Q., Zhang, H. W., Lu, X. Y., and Huang, R. F. (2015). Characterization and mapping of a novel light-dependent lesion mimic mutant *lmm6* in rice (*Oryza sativa* L.). *J. Integr. Agric.* 14 (9), 1687–1696. doi: 10.1016/S2095-3119(14)60975-8

Yang, D., Xiong, L., Mou, T., and Mi, J. (2022). Improving the resistance of the rice PTGMS line Feng39S by pyramiding blast, bacterial blight, and brown planthopper resistance genes. *Crop J.* 10 (4), 1187–1197. doi: 10.1016/j.cj.2021.11.005

Yin, Z., Chen, J., Zeng, L., Goh, M., Leung, H., Khush, G. S., et al. (2000). Characterizing rice lesion mimic mutants and identifying a mutant with broad-spectrum resistance to rice blast and bacterial blight. *Mol. Plant-Microbe Interact.* 13 (8), 869–876. doi: 10.1094/MPMI.2000.13.8.869

Zhang, J., Shao, F., Li, Y., Cui, H., Chen, L., Li, H., et al. (2007). A *Pseudomonas syringae* effector inactivates MAPKs to suppress PAMP-induced immunity in plants. *Cell Host Microbe* 1 (3), 175–185. doi: 10.1016/j.chom.2007.03.006

Zhang, F., Zhu, L., and He, G. (2004). Differential gene expression in response to brown planthopper feeding in rice. *J. Plant Physiol.* 161 (1), 53–62. doi: 10.1078/0176-1617-01179

Zheng, X., Zhu, L., and He, G. (2021). Genetic and molecular understanding of host rice resistance and *Nilaparvata lugens* adaptation. *Curr. Opin. Insect Sci.* 45, 14–20. doi: 10.1016/j.cois.2020.11.005

frontiers | Frontiers in Plant Science

TYPE Original Research
PUBLISHED 10 August 2023
DOI 10.3389/fpls.2023.1242089

OPEN ACCESS

EDITED BY
Shengli Jing,
Xinyang Normal University, China

REVIEWED BY
Yogesh Vikal,
Punjab Agricultural University, India
Zhenying Shi,
Chinese Academy of Sciences (CAS), China

*CORRESPONDENCE
Bo Du
bodu@whu.edu.cn
Aiqing You
aq_you@163.com

†These authors have contributed equally to this work

RECEIVED 18 June 2023
ACCEPTED 24 July 2023
PUBLISHED 10 August 2023

CITATION
Wu Y, Zha W, Qiu D, Guo J, Liu G, Li C, Wu B, Li S, Chen J, Hu L, Shi S, Zhou L, Zhang Z, Du B and You A (2023) Comprehensive identification and characterization of lncRNAs and circRNAs reveal potential brown planthopper-responsive ceRNA networks in rice. *Front. Plant Sci.* 14:1242089. doi: 10.3389/fpls.2023.1242089

Comprehensive identification and characterization of lncRNAs and circRNAs reveal potential brown planthopper-responsive ceRNA networks in rice

Yan Wu[1,2†], Wenjun Zha[1,2†], Dongfeng Qiu[1†], Jianping Guo[3], Gang Liu[1], Changyan Li[1], Bian Wu[1], Sanhe Li[1], Junxiao Chen[1], Liang Hu[1], Shaojie Shi[1], Lei Zhou[1,2], Zaijun Zhang[1], Bo Du[3]* and Aiqing You[1,2]*

[1]Key Laboratory of Crop Molecular Breeding, Ministry of Agriculture and Rural Affairs, Hubei Key Laboratory of Food Crop Germplasm and Genetic Improvement, Institute of Food Crops, Hubei Academy of Agricultural Sciences, Wuhan, China, [2]Hubei Hongshan Laboratory, Wuhan, China, [3]State Key Laboratory of Hybrid Rice, College of Life Sciences, Wuhan University, Wuhan, China

Brown planthopper (*Nilaparvata lugens* Stål, BPH) is one of the most destructive pests of rice. Non-coding RNA plays an important regulatory role in various biological processes. However, comprehensive identification and characterization of long non-coding RNAs (lncRNAs) and circular RNAs (circRNAs) in BPH-infested rice have not been performed. Here, we performed a genome-wide analysis of lncRNAs and circRNAs in *BPH6*-transgenic (resistant, BPH6G) and Nipponbare (susceptible, NIP) rice plants before and after BPH feeding (early and late stage) via deep RNA-sequencing. A total of 310 lncRNAs and 129 circRNAs were found to be differentially expressed. To reveal the different responses of resistant and susceptible rice to BPH herbivory, the potential functions of these lncRNAs and circRNAs as competitive endogenous RNAs (ceRNAs) were predicted and investigated using Gene Ontology and Kyoto Encyclopedia of Genes and Genomes analyses. Dual-luciferase reporter assays revealed that miR1846c and miR530 were targeted by the lncRNAs XLOC_042442 and XLOC_028297, respectively. In responsive to BPH infestation, 39 lncRNAs and 21 circRNAs were predicted to combine with 133 common miRNAs and compete for miRNA binding sites with 834 mRNAs. These mRNAs predictably participated in cell wall organization or biogenesis, developmental growth, single-organism cellular process, and the response to stress. This study comprehensively identified and characterized lncRNAs and circRNAs, and integrated their potential ceRNA functions, to reveal the rice BPH-resistance network. These results lay a foundation for further study on the functions of lncRNAs and circRNAs in the rice-BPH interaction, and enriched our understanding of the BPH-resistance response in rice.

KEYWORDS

rice, brown planthopper, long non-coding RNA, circular RNA, competitive endogenous RNA

Introduction

Rice, one of the most important food crops worldwide, is host to more than 200 insect pests at different stages of its life cycle. Among these, the brown planthopper (*Nilaparvata lugens* Stål, BPH) is one of the most destructive. Recent surveys suggest that BPH damages rice production severely, accounting for 29.5% of the total rice crop loss due to insects and diseases and making BPH the number one pest of Chinese rice (Du et al., 2020). Therefore, the development and production of BPH-resistant rice varieties is an economical, effective, safe, and environmentally-friendly strategy to control BPH damage (Yu et al., 2022).

In order to improve the resistance of rice to BPH, the genes and signaling pathways pivotal to BPH resistance must be identified and characterized. Over the last five decades, around 40 BPH resistance genes (*R* genes) have been identified, and the mechanisms of rice resistance to BPH have been explored through genetic and biochemical analyses (Chen et al., 2022; Guo et al., 2023). Recently, the novel BPH *R* gene *BPH6*, encoding an exocyst-localized protein, was cloned and found to confer broad-spectrum resistance to planthoppers (Guo et al., 2018). Specifically, the *BPH6* gene promotes exocytosis and participates in the maintenance and reinforcement of plant cell wall (Wu et al., 2022). Further functional characterization of *BPH6* will more precisely illuminate the exact mechanism underpinning *BPH6*-mediated herbivory resistance.

microRNAs (miRNAs) have been demonstrated to regulate rice resistance to various pathogens and herbivores by modulating the expression of target genes at the post-transcriptional level (Kar and Raichaudhuri, 2021). For example, both miR159 and miR160 regulate the defense response against blast disease (Li et al., 2014; Chen et al., 2021), and miR159b, miR164a, and miR167d-5p are involved in the plant immune response to bacterial blight (Jia et al., 2020). These miRNAs fine-tune plant innate immunity through the integration of *R* gene expression, phytohormone signaling, callose deposition, and reactive oxygen species (ROS) production (Kumar et al., 2022). Two miRNAs (miR156 and miR396) have been reported to regulate rice resistance to BPH. Specifically, miR156 regulates jasmonic acid (JA) and jasmonoyl-isoleucine (JA-Ile) biosynthesis through the "miR156-*OsMPK3/6-OsWRKY70*" module, thus negatively regulating BPH resistance (Ge et al., 2018). miR396 also negatively regulates BPH resistance through the "miR396-*OsGRF8-OsF3H*-flavonoid" module (Dai et al., 2019).

Recent studies revealed that long non-coding RNAs (lncRNAs) and circular RNAs (circRNAs) may serve as competing endogenous RNAs (ceRNAs), which could be essential for regulating the circuitry of miRNAs and their target genes (Salmena et al., 2011). Specifically, lncRNAs and circRNAs can modulate the balance between miRNAs and target genes. lncRNAs are eukaryotic non-coding RNAs greater than 200 nucleotides (nt) in length (Kapranov et al., 2007; Ponjavic et al., 2007). They have been found to regulate both biotic and abiotic stress tolerance, as well as various growth and developmental processes in rice (Gao et al., 2020). Non-coding endogenous circRNA molecules are covalently closed continuous loops without 5'-3' polarity or a polyadenylated tail and have been found to respond to abiotic and biotic stimuli and growth processes (Jeck et al., 2013). However, the specific regulatory mechanism underlying lncRNA- and circRNA-mediated BPH resistance in rice remains to be elucidated.

In this study, we performed a genome-wide analysis of lncRNAs and circRNAs in *BPH6*-transgenic (resistant, BPH6G) and Nipponbare (susceptible, NIP) rice plants before and after BPH herbivory via deep RNA-sequencing. We also conducted an integrated analysis of the expression profiles of circRNAs, lncRNAs, and previously identified miRNAs and mRNAs (Tan et al., 2020). lncRNA/circRNA-miRNA-mRNA ceRNA networks were generated by combining the identified and annotated target mRNAs. Our results demonstrated that lncRNAs and circRNAs act as ceRNAs to regulate BPH resistance in rice. This study provides a foundation for further research into the molecular mechanisms underlying *BPH6*-conferred herbivory resistance in rice.

Materials and methods

Plant and BPH materials

Two rice lines were used in this study: Nipponbare (NIP) and *BPH6*-transgenic plants (BPH6G). NIP is a susceptible *japonica* line. BPH6G is a *BPH6*-transgenic line containing the *BPH6* gene with its native Swarnalata promoter (IRRI Acc. No. 33964) in NIP background. The rice plants were grown in plastic cups (9 cm in diameter and 15 cm in height), in a greenhouse with 32 ± 2°C/14 h light and 26 ± 2°C/10 h dark periods. The BPH population was maintained on the susceptible rice cv. Taichung Native1 (IRRI Acc. No.00105) under controlled environmental conditions (as described above) at Wuhan University (Hu et al., 2017).

Evaluation of rice resistance to BPH

Seeds of either NIP or BPH6G were sown in plastic pots covered with nylon mesh. At the four-leaf stage, the rice seedlings were infested with third instar BPH nymphs at a rate of 10 nymphs per plant. Observation continued until susceptible control plants died, and then the rice plants were subsequently photographed and scored. At least three independent biological replicates were performed.

Measurements of honeydew excretion and BPH weight gain were performed following the method of Zheng et al. (Zheng et al., 2021). Twenty female BPH adults, which had been starved for 2 h, were weighed and introduced into a pre-weighed parafilm sachet (1.5 cm × 2.5 cm) fixed on the leaf sheath of each five-leaf stage NIP or BPH6G plant at a height of 2-3 cm above the soil. After 48 h of feeding, the surviving insects and the parafilm sachet were weighed again. The change in the insects' weight was recorded as BPH weight gain, and the change in the sachets' weight was recorded as honeydew excretion.

Sample collection

The endpoint method was utilized for sample collection throughout BPH treatment (Wu et al., 2017). Each treatment began at an individual time point and stopped at the same time.

Seedlings at the four-leaf stage were infested with eight BPHs per seedling and collected after 0, 6, 12, 24, 48, 60, and 72 hours of infestation. Each treatment consisted of three biological replicates, with 15 seedlings per replicate. Leaf sheaths were mixed for non-infested controls (0 h), early infestation stage (6, 12, and 24 h), and late infestation stage (48, 60, and 72 h). BPH6G samples were annotated as R0, R_early, and R_late, and NIP samples were annotated as S0, S_early, and S_late. Leaf sheathes were excised, frozen in liquid nitrogen, and stored at -80°C until use.

Total RNA extraction and high-throughput sequencing

RNA was isolated using an RNAiso Plus kit (TaKaRa), according to the manufacturer's instructions. RNA quality was estimated using a NanoDrop 2000 spectrophotometer (Thermo Fisher Scientific). An Illumina HiSeq 2500 was used for total RNA sequencing. The raw reads were first quality-controlled with FAST-QC by filtering low-quality reads (http://www.bioinformatics.babraham.ac.uk/projects/fastqc/). Afterward, clean reads were aligned to the rice genome using Hisat2 software (Kim et al., 2015).

Identification of lncRNAs and differential expression analysis

The mapped reads were assembled using StringTie (Pertea et al., 2015). All transcriptomes were merged to reconstruct a comprehensive transcriptome using Cuffmerge. Transcripts overlapping with known mRNAs and transcripts shorter than 200 bp were discarded. To identify lncRNAs, we utilized CPAT to predict coding transcripts, and transcripts with coding-prob score > 0.3 were removed (Wang et al., 2013). Transcript expression levels were quantified as fragments per kilobase of exon per million fragments mapped (FPKM). Differential expression *P*-values were calculated using the Bioconductor edgeR package (Robinson et al., 2010). We used the absolute value of $\log_2$FC ≥ 1 and $P < 0.05$ as thresholds to judge the statistical significance of each differential expression result.

Identification of circRNAs and differential expression analysis

The sequencing data was used to predict circRNAs with the ACFS circRNA prediction pipeline (You and Conrad, 2016). Unmapped reads were obtained with BWA-MEM for circRNA identification. The head-to-tail junction was identified and the highest splicing strength score was calculated using MaxEntScan33, with a filtering criterion greater than or equal to 10. Based on the re-alignment of the unmapped reads to the circRNA candidates, reads which mapped to the circRNA back splicing junction (with an overhang of at least 6 nucleotides) were counted for each circRNA. Transcript expression levels were quantified as FPKM. Differential expression *P*-values were calculated using the Bioconductor edgeR package (Robinson et al., 2010). We used the absolute value of $\log_2$FC ≥ 1 and $P < 0.05$ as thresholds to judge the statistical significance of each differential expression result.

Construction and analysis of the ceRNA regulatory network

Based on ceRNA theory (Salmena et al., 2011), we predicted the miRNA-mRNA, miRNA-lncRNA, and miRNA-circRNA interaction pairs using the PsTarget platform, with the standard E = 5 and UPE = 25 (http://plantgrn.noble.org/psRNATarget/analysis). Subsequently, through a combined analysis of miRNA and mRNA expression, lncRNA/circRNA-miRNA-mRNA pathways exhibiting either up-down-up or down-up-down expression modes were selected for further study. Cytoscape3.9.1 was used to display the networks (Shannon et al., 2003).

Analysis of Gene Ontology and Kyoto Encyclopedia of Genes and Genomes pathways

GO annotations from Gene Ontology (http://www.geneontology.org/) were downloaded (Ashburner et al., 2000). Pathway annotations were downloaded from KEGG (http://www.genome.jp/Kegg/). To identify significant GO and pathway categories, Fisher's exact tests were applied under absolute values of $P < 0.05$ and FDR < 0.05 (Draghici et al., 2007).

Quantitative real-time PCR assay

First-strand cDNA was synthesized with a PrimeScript RT reagent kit (TaKaRa, AK2802) using 1 μg of total RNA. The cDNA was amplified by qRT-PCR using SYBR green supermix (Bio-Rad) and a CFX96 real-time system, according to the manufacturer's instructions. All qRT-PCR primers used in this work are listed in Supplementary Table 1. Three biological replicates were performed for each experiment. Normalized expression levels were calculated using the $2^{-\Delta\Delta C\ (t)}$ method, with *TBP* as the internal reference gene.

Luciferase reporter assays

The wild type (WT) and mutated (MUT) lncRNAs containing target miRNA binding sites were synthesized and cloned into the pGreenII 0800-miRNA reporter vector, yielding the lncRNA-WT and lncRNA-MUT vectors, respectively. The miRNA was amplified and cloned into the pCXUN overexpression vector, yielding the miRNA-OE vector. The miRNA-OE/lncRNA-WT, miRNA-OE/lncRNA-MUT, empty vector (PCXUN)/lncRNA-WT, and empty vector (PCXUN)/lncRNA-MUT pairs were co-transfected into rice protoplast cells, which were prepared following the method of Wu

et al. (Wu et al., 2017). After 16 h of transfection, luciferase activities were evaluated with a dual-luciferase reporter assay system (Promega) and a SpectraMax iD5 multi-mode microplate reader (Molecular Devices). In this study, two lncRNA-miRNA interaction pairs (XLOC_042442-miR1846c and XLOC_028297-miR530) were selected to perform the assay (Supplementary Table 1).

Results

lncRNA and circRNA expression in BPH6G and NIP before and after BPH feeding

We evaluated the resistance of *BPH6*-transgenic plants (BPH6G) and susceptible Nipponbare plants (NIP) to BPH at the seedling stage, and the average damage severity score was calculated for each plant after infestation. By the 7th day of BPH infestation, the NIP plants died (average score of 9.0), while the BPH6G plants were still vigorously growing (average score of 2.8) (Figures 1A, B). To confirm these results, we measured the honeydew excretion and weight gain of BPHs allowed to feed on NIP and BPH6G plants for 48 h. BPHs on BPH6G plants excreted less honeydew and had a lower growth rate than BPHs on NIP plants (Figures 1C, D). These results demonstrate that BPH6G confers resistance to BPH infestation, while NIP remained susceptible.

To identify BPH-responsive non-coding RNAs in BPH6G (R) and NIP (S) plants, we obtained the FPKM values of lncRNAs and circRNAs from the whole-transcriptome RNA sequencing data after 0, 6, 12, 24, 48, 60, and 72 h of BPH infestation. The 0 h samples were taken as the non-infested controls, while the mixtures of 6, 12, and 24 h samples were taken as early-stage profiles and the mixtures of 48, 60, and 72 h samples were taken as late-stage profiles. In total, 6 treatment groups were analyzed: R0, R_early, R_late, S0, S_early, and S_late.

Analysis of lncRNA characteristics and response to BPH invasion

The raw reads from 18 rice transcriptomes were combined and filtered, resulting in the identification of 1219 lncRNAs. Most lncRNAs were less than 2,000 nt in length (Figure 2A), with the

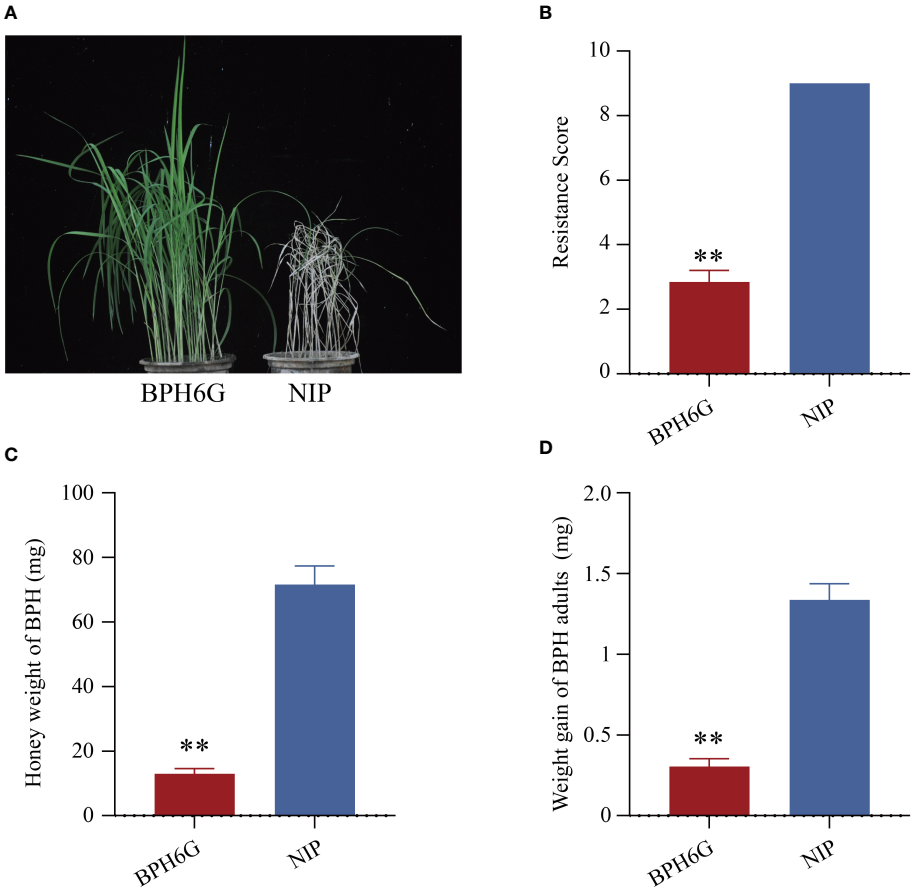

FIGURE 1
Evaluation of BPH resistance in BPH6G and NIP plants. **(A)** BPH resistance phenotypes of BPH6G and NIP plants. **(B)** BPH resistance scores of BPH6G and NIP plants. Lower scores correspond to greater resistance. Data represent the means ± SE of 3 biologically independent experiments. **(C)** Honeydew excretion of BPHs on BPH6G and NIP plants after 2 d of feeding. Data represent the means ± SE of 10 replicates. **(D)** Weight gain of BPHs after 2 d of feeding on BPH6G and NIP plants. Data represent the means ± SE of 10 replicates. Data were analyzed by ANOVA and asterisks indicate statistically significant differences. $^{**}P < 0.01$.

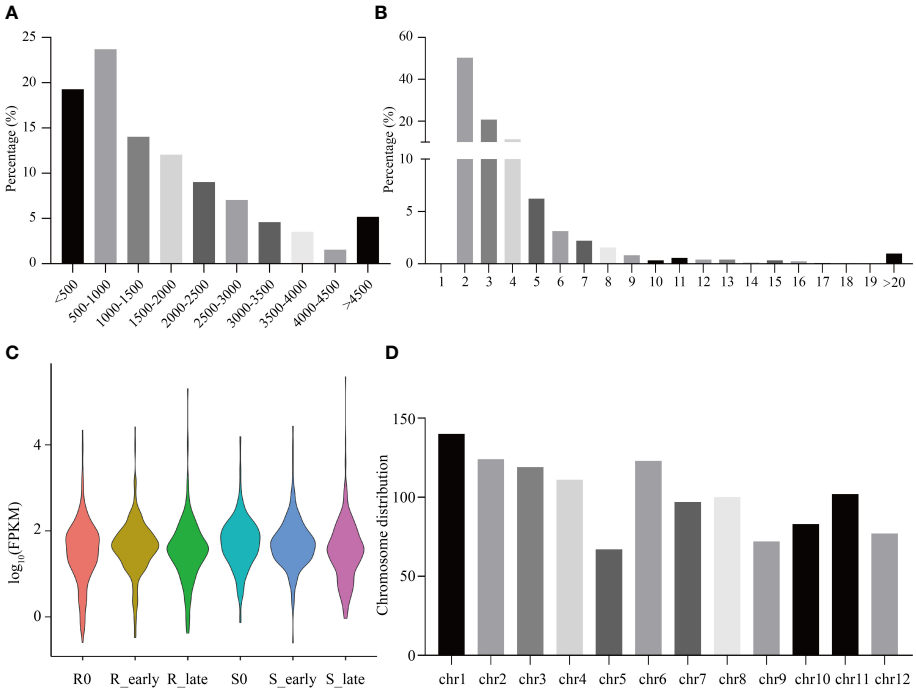

FIGURE 2
Identification and distribution of all lncRNAs. **(A)** Lengths of lncRNAs. **(B)** Number of exons. **(C)** FPKM distribution of lncRNAs in six groups. **(D)** Chromosomal distribution of all lncRNAs.

majority containing 2-4 exons, and 50.29% containing two exons (Figure 2B). The six treatment groups (R0, R_early, R_late, S0, S_early, and S_late) exhibited different lncRNA expression profiles (Figure 2C). The chromosomal distribution of the identified lncRNAs is shown in Figure 2D. Different chromosomes contained different numbers of lncRNAs, with chromosome 1 (Chr 1) containing the greatest number (Figure 2D).

The lncRNA expression levels were compared between treatments, and the differentially expressed lncRNAs (DElncRNAs) exhibiting absolute value of $\log_2$FC ≥ 1 and $P < 0.05$ among the 6 treatment groups are shown in Figure 3A. The total number of DElncRNAs in group S (S_early/S_0 and S_late/S_0, 190) was higher than that of group R (R_early/R_0 and R_late/R_0, 108). During the late stage, the number of DElncRNAs in group S (S_late/S_0, 152) was 4 times greater than during the early stage (S_early/S_0, 38). The number of early and late DElncRNAs in group R was similar (R_early/R_0, 40; R_late/R_0, 68). There were 303 DElncRNAs identified in the three comparison groups among different varieties (R0/S0, R_early/S_early, and R_late/S_late) (Figure 3A), and the chromosomal distribution of the DElncRNAs was evaluated (Figure 3B). In order to identify lncRNAs related to BPH resistance in rice, we analyzed these DElncRNAs with a Venn diagram (Figure 3C). Overall, 60 DElncRNAs exhibited differential expression in R and S after BPH feeding (only in R_early/S_early and R_late/S_late). Thirty-two DElncRNAs were identified in R_early/R_0 which were absent in S_early/S_0 and 32 DElncRNAs were identified in R_late/R_0 which were absent in S_late/S_0. The expression profiles of these DElncRNAs were found for some modules (Figure 3D; Supplementary Tables 2, 3). These results indicate that susceptible and resistant plants contained similar numbers of BPH-responsive lncRNAs during the early stage (38 in S_early/S_0 and 40 in R_early/R_0), although only 8 were identified in both groups (Figure 3C). Conversely, susceptible plants contained a greater number of BPH-responsive lncRNAs than resistant plants during the late stage (Figures 3A, C). That is, the two genotypes responded to BPH herbivory in entirely different manners. Subsequently, qRT-PCR was used to study the expression levels of these 6 DElncRNAs (Figure 4A). The data were consistent with the sequencing results, which confirmed that the results were reliable and could be used for intensive studies. Overall, the results confirmed that the numbers and types of BPH-responsive lncRNAs were different between resistant and susceptible plants, suggesting that lncRNAs are involved in the response of rice to BPH herbivory.

Analysis of DElncRNA function via ceRNA regulatory networks in response to BPH feeding

In plants, lncRNAs indirectly regulate mRNA expression through their regulation of miRNA (Bartel, 2009; Thomas et al., 2010). By combining the psRNA target tool results with the miRNA and mRNA high-throughput sequencing data (Tan et al., 2020), we predicted the presence of 15, 30, 20, and 83 DElncRNAs binding to 15, 35, 35, and 87 differentially expressed miRNAs (DEmiRNAs) in R_early/R0, R_late/R0, S_early/S0, and S_late/S0, respectively (Supplementary Figure 1; Supplementary Tables 4–7). These DElncRNAs may affect the expression of their

10.3389/fpls.2023.1242089

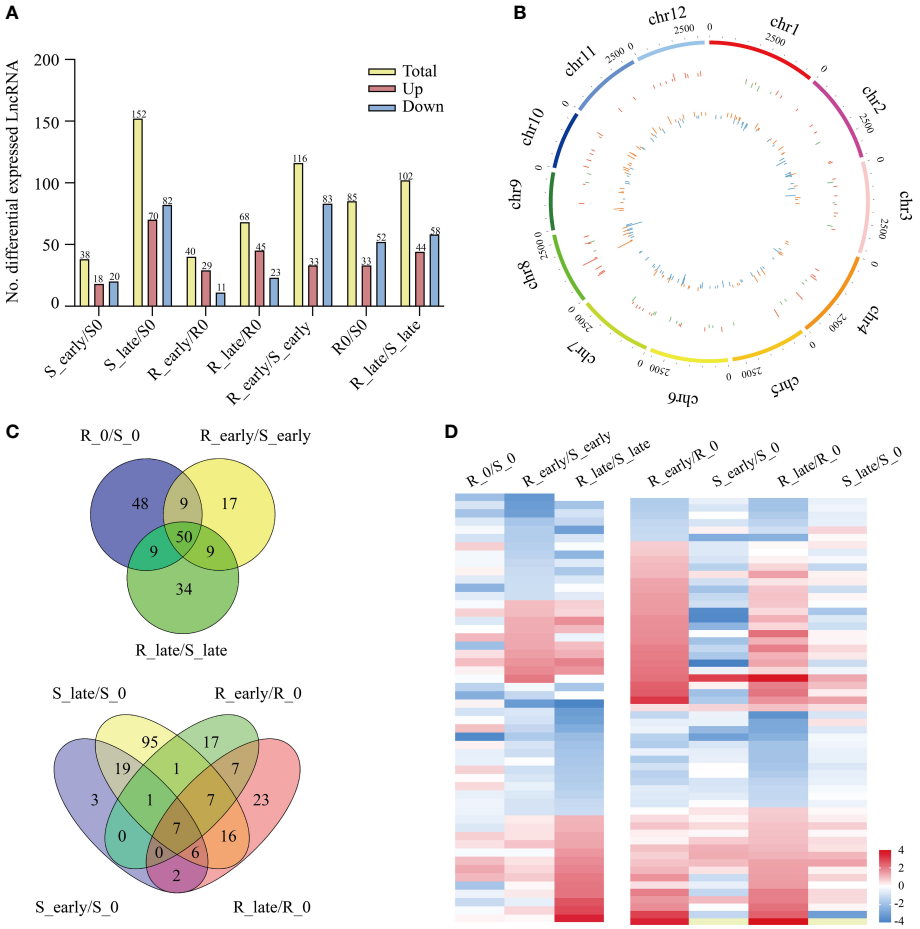

FIGURE 3
Differentially expressed lncRNAs. **(A)** Number of DElncRNAs up- or down-regulated in all comparisons. **(B)** Genomic distribution of all DElncRNAs. The two circles (from outer to inner) represented the expression levels (log_2FC) of DElncRNAs in the resistant plants (red indicates increased expression, and green denotes decreased expression), and in the susceptible plants (orange indicates increased expression, and blue denotes decreased expression), and fold change of the expression levels, respectively. **(C)** Venn diagrams of the unique and shared DElncRNAs. **(D)** Heat map of the DElncRNAs in differential comparisons, yellow indicates N/A.

target differentially expressed mRNAs (DEmRNAs) (105, 242, 295, and 934 in R_early/R0, R_late/R0, S_early/S0, and S_late/S0, respectively) by sponging their corresponding DEmiRNAs (Supplementary Tables 4–7). The DElncRNAs, DEmiRNAs, and DEmRNAs in the ceRNA network were compared using Venn diagrams (Supplementary Figure 1).

To validate whether these DElncRNAs affected the expression of their corresponding DEmiRNAs, two DElncRNAs (XLOC_042442 and XLOC_028297) and their target DEmiRNAs (miR1846c and miR530) were selected for luciferase reporter assay verification. First, we constructed XLOC_042442 and XLOC_028297 WT or MUT (predicted miRNA binding sites) luciferase plasmids in the pGreenII 0800-miRNA dual luciferase reporter vector, and luciferase activity was evaluated after co-transfection of miRNA-containing (miR1846c and miR530, respectively) and luciferase plasmids. In rice protoplasts, we observed that overexpression of miR1846c and miR530 (miR1846c-OE and miR530-OE) reduced the luciferase activity significantly. At the same time, miRNA binding site mutations reversed the luciferase activity, suggesting that XLOC_042442 and XLOC_028297 function as ceRNAs by sponging miR1846c and miR530, respectively (Figure 4B).

The potential regulatory roles of the DElncRNAs via the ceRNA network were predicted by analyzing the functions of their target DEmRNAs through GO and KEGG pathway analysis (Supplementary Figures 2, 3). The GO annotations ($P < 0.05$) of the four groups of target DEmRNAs contained multiple biological processes, cellular components, and molecular functions (Supplementary Figure 2). In BPH6G at the early feeding stage (R_early/R0), these GO terms were most significantly enriched in DNA replication initiation, plastid inner membrane, and syn-pimara-7,15-diene synthase activity. In NIP at the early feeding stage (S_early/S0), these GO terms were most significantly enriched in plant-type cell wall biogenesis, plasma membrane, and cellulose synthase activity. In BPH6G at the late feeding stage (R_late/R0), these GO terms were most significantly enriched in hydrogen peroxide catabolic process, integral component of membrane, and transmembrane transporter activity. In NIP at the late feeding stage (S_late/S0), these GO terms were most significantly enriched in regulation of hormone levels, plasma membrane, and ATP binding.

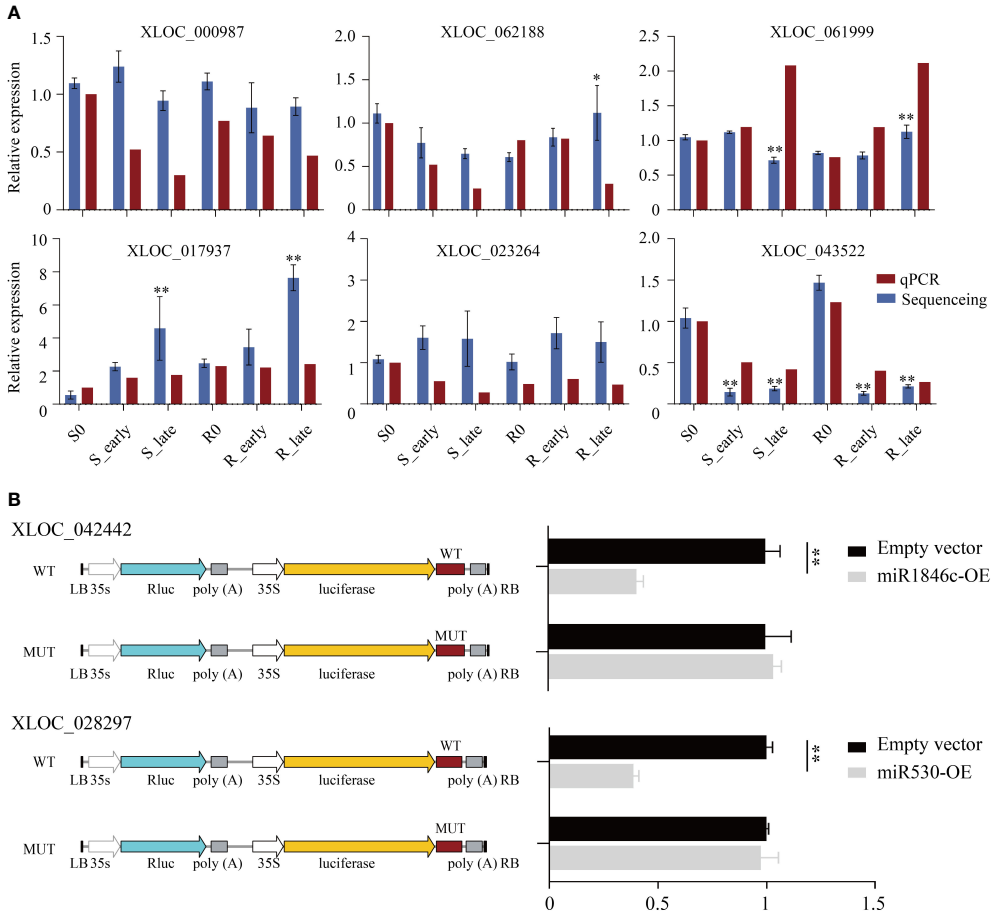

FIGURE 4
Detection of candidate lncRNAs expression levels and validation of target miRNAs. **(A)** DElncRNAs validated by qRT-PCR. **(B)** The luciferase reporter assay illustrates that candidate DElncRNAs could serve as a sponge for predicted target DEmiRNAs. Data are presented as the means ± SE of 3 biologically independent experiments. Data were analyzed by ANOVA and asterisks indicate statistically significant differences. *$P < 0.05$, **$P < 0.01$.

KEGG pathway analysis was performed on the four groups of DEmRNAs, which showed that DNA replication and metabolic pathways were the most significantly enriched pathways (Supplementary Figure 3).

Analysis of circRNA characteristics and response to BPH

In this study, we identified a total of 1914 circRNAs, and the genomic distribution of these circRNAs is shown in Figure 5A. Different chromosomes contained different numbers of circRNAs, with chromosome 1 (Chr 1) containing the greatest number (Figure 5A). In terms of length, the majority of circRNAs were between 300-600 bp (Figure 5B). The circRNA expression levels among the 6 treatment groups were visualized using violin plots (Figure 5C). GO annotation of the circRNA source genes showed that they were enriched in the following biological process terms: cellular component organization, organic substance metabolic process, and nitrogen compound metabolic process; the following cellular component terms: intracellular part, intracellular organelle, and intracellular organelle part; and the following molecular function terms: hydrolase activity, heterocyclic compound binding, and protein binding (Figure 5D). KEGG pathway analysis showed that fatty carbon metabolism, glycolysis/gluconeogenesis, RNA degradation, carbon fixation in photosynthetic organisms, and mRNA surveillance pathway were most significantly enriched (Figure 5E).

The circRNAs expression levels were compared between treatments, and we identified a total of 129 differentially expressed circRNAs (DEcircRNAs) exhibiting absolute value of $\log_2FC \geq 1$ and $P < 0.05$ among the 6 treatment groups (Figure 6A). Group S (S_early/S_0 and S_late/S_0, 110) contained 3 times more DEcircRNAs than group R (R_early/R_0 and R_late/R_0, 31), and the DEcircRNAs in group S were primarily down-regulated. The numbers of DEcircRNAs in the early and late stages of group R were similar (R_early/R_0, 12; R_late/R_0, 19), and less than that in group S (S_early/S_0, 54; S_late/S_0, 56). The numbers of up- and down-regulated DEcircRNAs were similar in group R (7/5 in R_early/R0, 8/11 in R_late/R0). There were 84 DEcircRNAs contained in the three comparison groups among different varieties (R0/S0, R_early/S_early, and R_late/S_late) (Figure 6A). The distribution and expression of DEcircRNAs were also mapped to the chromosomes of the two materials (Figure 6B).

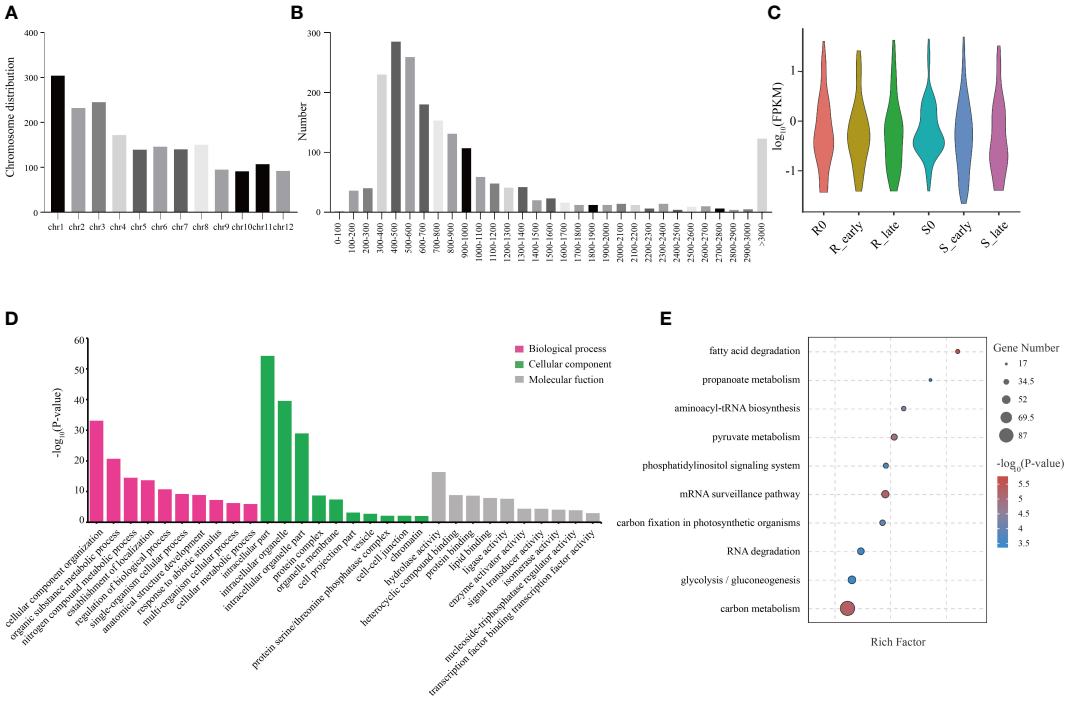

FIGURE 5
Distribution of circRNAs and GO and KEGG analyses of source genes. **(A)** Chromosomal distribution of circRNAs. **(B)** Lengths of circRNAs. **(C)** FPKM distribution of circRNAs in six groups. **(D)** GO enrichment analysis of circRNA source genes. **(E)** KEGG pathway enrichment analysis of circRNA source genes.

In order to identify circRNAs related to BPH resistance in rice, we analyzed the DEcircRNAs between and within groups of resistant and susceptible plants before and after BPH feeding using Venn diagrams (Figures 6C, D). A total of 39 DEcircRNAs exhibited differential expression between R and S after BPH feeding (only in R_early/S_early and R_late/S_late). Ten DEcircRNAs were identified in R_early/R_0 which were absent in S_early/S_0, and 14 DEcircRNAs were identified in R_late/R_0 which were absent in S_late/S_0. The expression patterns of these DEcircRNAs are shown as a heat map (Figure 6E; Supplementary Tables 8, 9). The quantitative detection results were consistent with the sequencing data, which confirmed the reliability of the sequencing results (Figure 6F). Overall, these results confirmed that the numbers and types of BPH-responsive circRNAs were different between resistant and susceptible plants, suggesting that circRNAs are involved in the response of rice to BPH herbivory.

By combining the psRNA target tool results with the miRNA and mRNA high-throughput sequencing data (Tan et al., 2020), we predicted the existence of 8, 10, 19, and 26 DEcircRNAs binding to 42, 61, 29, and 114 DEmiRNAs in the R_early/R0, R_late/R0, S_early/S0, and S_late/S0 comparisons, respectively (Supplementary Tables 10–13). These DEcircRNAs may affect the expression of their target DEmRNAs (187, 401, 222, and 1090 in R_early/R0, R_late/R0, S_early/S0, and S_late/S0, respectively) by sponging their corresponding DEmiRNAs (Supplementary Tables 10–13). The DEcircRNAs, DEmiRNAs, and DEmRNAs in the ceRNA network were compared by Venn diagrams (Supplementary Figure 1).

The potential regulatory roles of the circRNAs via the ceRNA network were predicted by analyzing the functions of all the target DEmRNAs through GO and KEGG pathway analyses (Supplementary Figures 4, 5). The GO annotations ($P < 0.05$) of the four groups of DEmRNAs are listed in Supplementary Figure 3 and Supplementary Tables 10–13, and include a multitude of biological processes, cellular components, and molecular functions. In BPH6G at the early feeding stage (R_early/R0), these GO terms were most significantly enriched in cell wall biogenesis, photosystem II antenna complex, and kinase activity. In NIP at the early feeding stage (S_early/S0), these GO terms were most significantly enriched in plant-type cell wall biogenesis, plasma membrane, and cellulose synthase (UDP-forming) activity. In BPH6G at the late feeding stage (R_late/R0), these GO terms were most significantly enriched in metabolic process, integral component of membrane, and cellulose synthase (UDP-forming) activity. In NIP at the late feeding stage (S_late/S0), these GO terms were most significantly enriched in cell wall organization, plasma membrane, and ATP binding. KEGG pathway analysis was performed on the four groups of DEmRNAs, which showed that DNA replication and metabolic pathways were the most significantly enriched pathways (Supplementary Figure 4).

Analysis of key ceRNA pathways responding to BPH infestation

The lncRNA/circRNA-miRNA-mRNA interaction networks were predicted using psTarget software and consolidated using whole-transcriptome RNA sequencing data (Figure 7A;

10.3389/fpls.2023.1242089

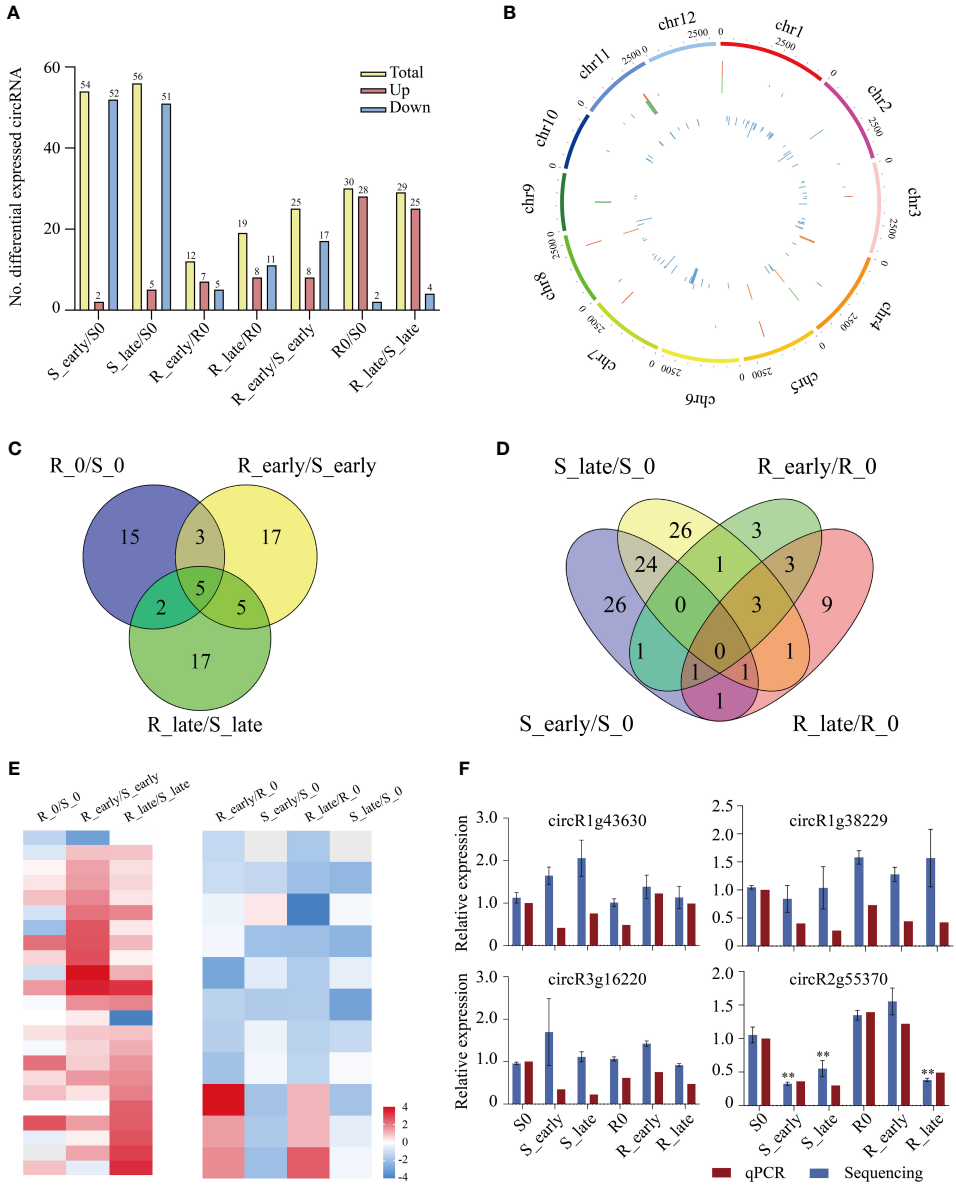

FIGURE 6
Differentially expressed circRNAs. **(A)** Number of DEcircRNAs up- or down-regulated in all comparisons. **(B)** Genomic distribution of all DEcircRNAs. The two circles (from outer to inner) represented the expression levels (log_{10}FPKM) of DEcircRNAs in the resistant plants (red indicates increased expression, and green denotes decreased expression), DEcircRNAs in the susceptible plants (orange indicates increased expression, and blue denotes decreased expression), and fold change of the expression levels, respectively. **(C-D)** Venn diagrams of the unique and shared DEcircRNAs. **(E)** Heat map of the unique DEcircRNAs in differential comparisons. **(F)** Validation of candidate DEcircRNAs expression levels by qRT-PCR. circR1g43630, chr1_25000624_24999798_+826-LOC_Os01g43630; circR1g38229, chr1_21426198_21424262_+1936-LOC_Os01g38229; circR3g16220, chr3_8951244_8940833_-10411-LOC_Os03g16220; circR2G55370, chr2_33928616_33914366_+14250-LOC_Os02g55370. Data were analyzed by ANOVA and asterisks indicate statistically significant differences. $^{**}P < 0.01$.

Supplementary Table 14). Specifically, the interaction network was established based on the relationship between the DElncRNAs/DEcircRNAs and DEmiRNAs and DEmRNAs. A total of 39 DElncRNAs were predicted to bind 50 DEmiRNAs and 381 target DEmRNAs, while 21 DEcircRNAs were predicted to bind 116 DEmiRNAs and 760 target DEmRNAs. The ceRNA network with 39 DElncRNAs, 21 DEcircRNAs, 133 DEmiRNAs, and 834 DEmRNAs is depicted in Figure 7A and Supplementary Table 14.

The potential regulatory roles of the ceRNA networks were analyzed by characterizing the function of 834 target DEmRNAs through GO enrichment and KEGG pathway analyses. GO annotation showed that the network was primarily enriched in the following biological processes: cell wall organization or biogenesis, developmental growth, and single-organism cellular process; the following cellular components: intrinsic component of membrane, external encapsulating structure, and side of membrane; and the following molecular functions: transferase activity, signaling receptor activity, and carbohydrate binding (Figure 7B). In addition, the network was found to be enriched in the following KEGG pathways: metabolic pathways, biosynthesis of

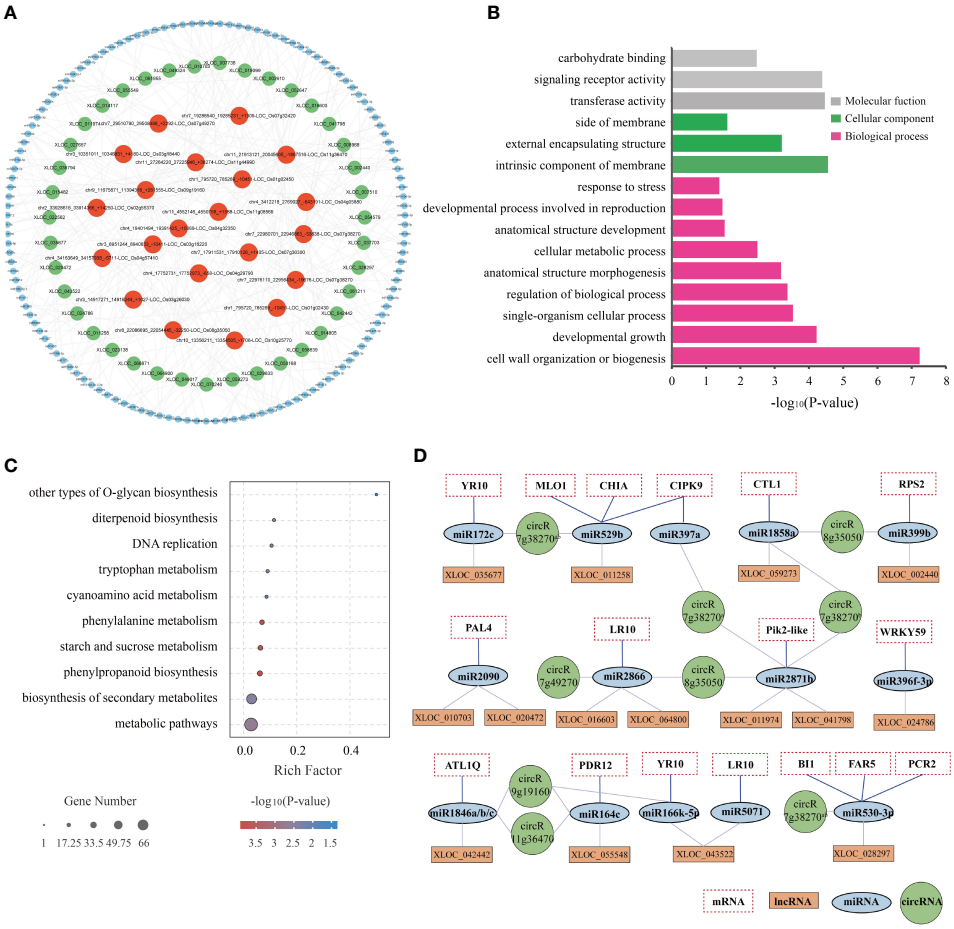

FIGURE 7
Regulatory network of potential BPH resistance-related lncRNAs and circRNAs. **(A)** CeRNA networks of potential BPH resistance-related DElncRNAs/DEcircRNAs-DEmiRNAs. Different colored circles indicate different non-coding RNA types: red represents DEcircRNAs, green represents DElncRNAs, and blue represents DEmiRNAs. **(B)** GO enrichment of 834 target DEmRNAs regulated by the ceRNA network. **(C)** KEGG enrichment of 834 target DEmRNAs regulated by the ceRNA network. **(D)** Core ceRNA networks of lncRNAs/circRNAs-miRNAs-mRNAs were significantly enriched in GO term "response to stimulus" (GO: 0006950). circR7g38270[a], chr7_22980701_22946863_-33838-LOC_Os07g38270; circR7g38270[b], chr7_22976110_22956434_-19676-LOC_Os07g38270; circR8g35050, chr8_22086695_22054445_-32250-LOC_Os08g35050; circR7g49270, chr7_29510790_29508498_+2292-LOC_Os07g49270; circR9g19160, chr9_11675871_11394316_+281555-LOC_Os09g19160; circR11g36470, chr11_21913121_20045605_-1867516-LOC_Os11g36470.

secondary metabolites, phenylpropanoid biosynthesis, starch and sucrose metabolism, and phenylalanine metabolism (Figure 7C). These results illustrated that both metabolism- and response-related genes are regulated by the ceRNA network in both resistant and susceptible plants in response to BPH herbivory.

Notably, the GO term "response to stimulus" (GO: 0006950) was significantly enriched in 80 DEmRNAs (Supplementary Table 14). After consultation of relevant literature, several specific components of the lncRNA/circRNA-miRNA-mRNA interaction network were selected for further study: 6 DEcircRNAs, 15 DElncRNAs, 16 DEmiRNAs, and 17 DEmRNAs (Figure 7D). The lncRNAs XLOC_024786, XLOC_055548, and XLOC_043522, as well as the circRNAs circR9g19160 and circR11g36470, were predicted to combine with miR396f-3p, miR164c, and miR166k-5p. These three miRNA families have been described as regulators of rice innate immunity against fungi and bacteria (Raquel et al., 2018; Wang et al., 2018b; Li et al., 2019). In plants, *R* genes with the NB-ARC structure play vital roles in disease and pathogen resistance by recognizing specific effectors and inducing rapid and robust resistance responses (Jones and Dangl, 2006). In this study, we identified 6 NB-ARC domain-containing *R* proteins (MLO1-like, RPS2-like, RPM1-like, PIK2-like, RGA4-like (YP10), and RGA5-like (LP10)), which were negatively regulated by miR529b, miR399b, miR2886, miR2871b, miR396f-3p, and miR172c/miR166k-5p. These miRNAs were sponged by lncRNAs XLOC_011258, XLOC_002440, XLOC_016603/XLOC_064800, XLOC_011974/XLOC_041798, XLOC_024784, and XLOC_035677/XLOC_043522, respectively. Both *CTL1/BC15* and *CHIA*, which encode membrane-associated chitinase-like proteins, have been reported to be involved in rice resistance (Wu et al., 2012), and are negatively regulated by the XLOC_059273/circR8g35050-miR1858a and XLOC_011258/circR7g38270-miR529b modules, respectively. Additionally, *CIPK9*, *ATL1Q*, and *PDR12* have been reported to be involved in signal transduction and play significant roles in abiotic and biotic stress response (Guzmán, 2012; Kanwar et al., 2014; Nguyen et al., 2014). These genes were

predicted to be the targets of miR397a, miR1846a/b/c, and miR164c, and these miRNAs were predicted to be regulated by circR7g38270, XLOC_042442, circR9g19160, circR11g36470, and XLOC_055548. Finally, *PAL4* has been associated with broad-spectrum disease resistance in rice (Tonnessen et al., 2015), and is negatively regulated by the XLOC_010703-miR2090 and XLOC_020472-miR2090 modules. These examples imply that ceRNAs might play important regulatory roles in the resistance of rice to BPH herbivory.

In a previous study, an integrated analysis of the miRNAs and target mRNA genes related to BPH resistance in *BPH6*-transgenic plants and NIP was performed (Tan et al., 2020). A network of 34 miRNAs corresponding to 42 target genes was identified, which were potentially related to BPH resistance (Tan et al., 2020). Meanwhile, considering our ceRNA results, we obtained a core ceRNA network consisting of 6 lncRNAs, 4 circRNAs, 23 miRNAs, and 24 mRNAs (Figure 8). This core ceRNA network might also play a vital role in the resistance of rice to BPH herbivory.

Discussion

In rice, both lncRNAs and circRNAs have been reported to regulate plant growth and development, as well as the biotic and abiotic stress responses (Sanchita and Asif, 2020; Zhang et al., 2020). To date, several lncRNAs have been functionally characterized in rice. For example, *LDMAR* (*long-day-specific male fertility-associated RNA*) is a 1236bp photoperiod sensitive lncRNA which regulates male sterility in rice. The normal development of plant pollen under long-day conditions requires a high level of *LDMAR* expression (Fan et al., 2016). The expression of the lncRNA *IPS1* (*induced by phosphate starvation 1*) is altered under nitrogen and phosphorus starvation, suggesting that *IPS1* may regulate the balance of these macronutrients (Shin et al., 2018). Overexpression of the lncRNA *LAIR* (*leucine-rich repeat receptor kinase antisense intergenic RNA*) in rice increases grain yield and induces the expression of several leucine-rich repeat receptor kinase-coding genes (Wang et al., 2018a). Although there has been some research into plant circRNAs, currently-reported mechanisms of circRNA formation are largely based on bioinformatics analyses rather than convincing experimental evidence, which is still in the theoretical stage (Zhang et al., 2020). To the best of our knowledge, this is the first study to comprehensively identify and characterize BPH-responsive lncRNAs and circRNAs associated with ceRNA networks in rice. Therefore, the results presented here further our understanding of non-coding RNA regulation of the rice response to BPH infestation.

In this study, we identified BPH-responsive lncRNAs and circRNAs, and their differential expression patterns were analyzed in *BPH6*-transgenic and NIP rice plants. Our genome-wide analysis of lncRNA and circRNA expression showed that susceptible NIP plants contained greater numbers of both DElncRNAs and DEcircRNAs than resistant BPH6-transgenic plants, and that the majority of these DElncRNAs and DEcircRNAs were down-regulated in NIP plants. The functions of these lncRNAs and circRNAs via the ceRNA network were also predicted by GO and KEGG analyses of target mRNAs (Supplementary Figures 2–5). The

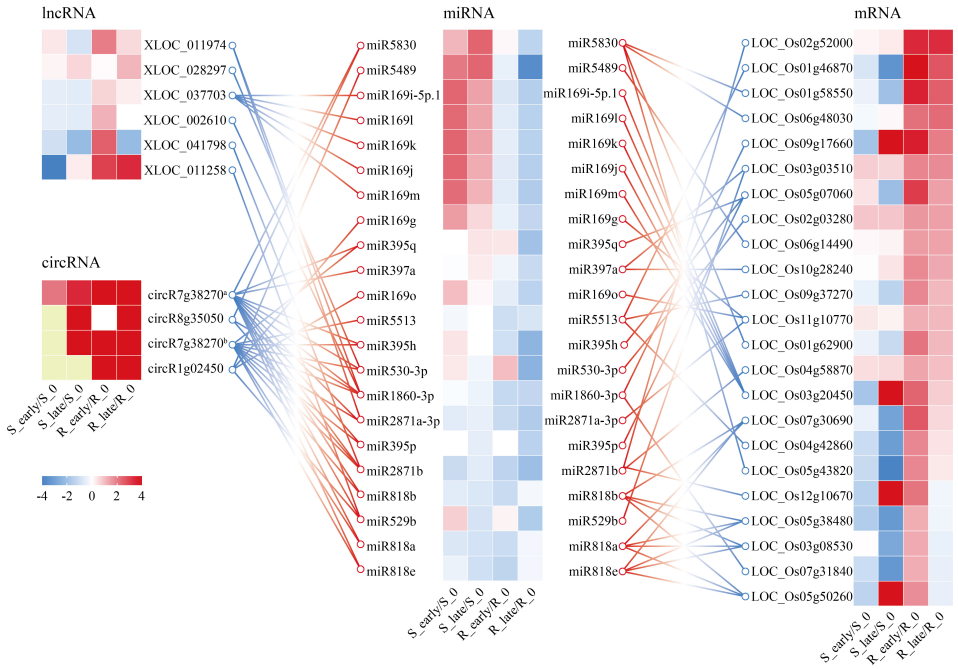

FIGURE 8
CeRNA networks of lncRNA/circRNA-miRNA-mRNA related to plant resistance. Yellow indicates N/A. circR7g38270[a], chr7_22980701_22946863_-33838-LOC_Os07g38270; circR8g35050, chr8_22086695_22054445_-32250-LOC_Os08g35050; circR7g38270[b], chr7_22976110_22956434_-19676-LOC_Os07g38270; circR1g02450, chr1_795720_785269_-10451-LOC_Os01g02450.

GO and KEGG pathway results differed between the resistant and susceptible varieties at both the early and late feeding stages (Supplementary Figures 2–5). Our results suggest that the BPH-responsive lncRNAs and circRNAs in *BPH6G* and NIP were involved in different ceRNA pathways.

The interactions between different RNAs were predicted based on ceRNA theory, and multiple BPH-resistance related networks were identified and included 39 lncRNAs, 21 DEcircRNAs, 133 DEmiRNAs, and 834 DEmRNAs (Figure 7A; Supplementary Table 14). The functions of the ceRNA networks were then explored through GO and KEGG pathway analyses (Figures 7B, C). Among the ceRNA networks, 80 DEmRNAs were predicted to be involved in the response to stress (GO: 0006950) (Supplemental Table 15). A core ceRNA network of these DEmRNAs is shown in Figure 7D. Among them, OsmiR396 has been identified as a negative regulator of rice innate immunity against *Magnaporthe oryzae* by silencing multiple growth-regulating factors (*OsGRFs*) in rice (Chandran et al., 2019). Overexpression of OsmiR396 makes rice susceptible to blast, while suppression of OsmiR396 makes rice resistant to blast and improves yield (Chandran et al., 2019). In addition, overexpression of OsmiR396f resulted in enhanced immunity to *Dickeya zeae* by suppressing the target gene *OsGRF* (Li et al., 2019). A previous study showed that OsmiR396 also acts as a negative regulator of BPH resistance via the OsmiR396-*OsGRF8*-*OsF3H*-flavonoid pathway (Dai et al., 2019). Our results showed that OsmiR396f-3p, which targets the *OsWRKY59* transcription factor, is regulated by lncRNA XLOC_024786. Hence, we speculate that the XLOC_024786-OsmiR396f-3p-*OsWRKY59* module may play a vital role in rice resistance to BPH herbivory (Figure 7D). OsmiR164a has been reported to negatively regulate rice immunity to *M. oryzae* and *Xanthomonas oryzae* pv. *oryzae* by regulating the *OsNAC60* transcription factor (Wang et al., 2018b; Jia et al., 2020). We also found that lncRNA XLOC_055549 could sponge miR164a, suggesting that the XLOC_055549-OsmiR164a module may be a key regulator of BPH resistance (Figure 7D). The miR166 family is highly conserved (Kumar et al., 2022). The miR166 family members OsmiR166k and OsmiR166h have been shown to function as positive regulators of defense against *M. oryzae* and *Fusarium fujikuroi* by targeting the *ethylene insensitive 2* (*EIN 2*) gene via cross-regulation (Raquel et al., 2018). This study demonstrated that lncRNA XLOC_043522 negatively regulates the expression of miR166k-5p, thus up-regulating the expression of the *R* gene *YR10* (Figure 7D). The ceRNA networks identified in this study are likely to play important roles in rice resistance to BPH. By integrating and analyzing the results of our ceRNA study, alongside the results of Tan et al.'s miRNA and target mRNA study, a core ceRNA network containing lncRNAs, circRNAs, miRNAs, and mRNAs was produced (Figure 8) (Tan et al., 2020). These results provide evidence of novel regulatory mechanisms underlying rice BPH resistance. Our future research will focus on elucidating of the BPH-responsive ceRNA network in rice, which will greatly increase our knowledge of plant resistance to insect damage.

The rice-BPH system is considered an excellent model for the study of plant-insect interaction and co-evolution (Jing et al., 2017). Xiao et al. provided evidence that lncRNAs might play important roles in the high fecundity and virulence adaptation of BPH (Xiao et al., 2015). A previous study has reported the differential expression of lncRNAs between two virulent BPH populations, including susceptible (TN1) and resistant (YHY15) rice planthopper varieties (Zha et al., 2022). In total, 157 differentially expressed lncRNAs and 675 differentially expressed mRNAs were found to be involved in BPH adaptation to rice resistance (Zha et al., 2022). Here, we studied the differential expression of lncRNAs and circRNAs in rice before and after BPH herbivory. Our analysis indicated that both lncRNAs and circRNAs play important roles in rice resistance to BPH. These results suggest the presence of mutual regulatory relationships between rice and BPH at the non-coding RNA level, and provide a basis for further studies of the molecular mechanism underlying co-evolution between rice and BPH.

Data availability statement

The datasets presented in this study can be found in online repositories. The names of the repository/repositories and accession number(s) can be found below: https://www.ncbi.nlm.nih.gov/, GSE123148.

Author contributions

AY, BD, and YW conceived and designed the experiments. YW, WZ, and DQ performed the experiments and analyzed the data. YW wrote the paper. JG developed the BPH6G line. GL, CL, BW, SL, JC, LH, and SS contributed reagents, materials, and analysis tools. LH, LZ, and ZZ revised the paper. YW, WZ, and DQ contributed equally to this paper. All authors contributed to the article and approved the submitted version.

Funding

This work was supported by the Science and Technology Major Program of Hubei Province (2022ABA001), the Youth Project of Natural Science Foundation of Hubei Province (2022CFB747), the Youth Science Foundation Project of Hubei Academy of Agricultural Sciences (2023NKYJJ03), and funding from the Hubei Key Laboratory of Food Crop Germplasm and Genetic Improvement (2021lzjj04).

Acknowledgments

We would thank Novel Bioinformatics Ltd., Co. (Shanghai, China) for conducting the whole transcriptome sequencing. And we would also like to thank TopEdit (www.topeditsci.com) for its linguistic assistance during the preparation of this manuscript.

Conflict of interest

The authors declare that the research was conducted in the absence of any commercial or financial relationships that could be construed as a potential conflict of interest.

Publisher's note

Supplementary material

The Supplementary Material for this article can be found online at: https://www.frontiersin.org/articles/10.3389/fpls.2023.1242089/full#supplementary-material

SUPPLEMENTARY FIGURE 1
Venn diagrams of the DElncRNAs, DEcircRNAs, DEmiRNAs, and DEmRNAs in the ceRNA network. **(A–C)**. Venn diagrams of DElncRNAs, DEmiRNAs, and DEmRNAs in the ceRNA network of lncRNA-miRNA-mRNA. **(D–F).** Venn diagrams of DEcircRNAs, DEmiRNAs, and DEmRNAs in the ceRNA network of circRNA-miRNA-mRNA.

SUPPLEMENTARY FIGURE 2
GO enrichment of the target genes of DElncRNAs via the ceRNA network at the early and late feeding stages in susceptible and resistant plants.

SUPPLEMENTARY FIGURE 3
KEGG pathway analysis of the target genes of DElncRNAs via the ceRNA network at the early and late feeding stages in susceptible and resistant plants. The red color represents the pathways with $P < 0.05$.

SUPPLEMENTARY FIGURE 4
GO enrichment of the target genes of DEcircRNAs via the ceRNA network at the early and late feeding stages in susceptible and resistant plants.

SUPPLEMENTARY FIGURE 5
KEGG pathway analysis of the target genes of DEcircRNAs via the ceRNA network at the early and late feeding stages in susceptible and resistant plants. The red color represents the pathways with $P < 0.05$.

References

Ashburner, M., Ball, C. A., Blake, J. A., Botstein, D., Butler, H., Cherry, J. M., et al. (2000). Gene ontology: tool for the unification of biology. *Nat. Genet.* 25 (1), 25–29. doi: 10.1038/75556

Bartel, D. P. (2009). MicroRNAs: target recognition and regulatory functions. *Cell* 136 (2), 215–233. doi: 10.1016/j.cell.2009.01.002

Chandran, V., Wang, H., Gao, F., Cao, X. L., Chen, Y. P., Li, G. B., et al. (2019). miR396-osGRFs module balances growth and rice blast disease-resistance. *Front. Plant Sci.* 9. doi: 10.3389/fpls.2018.01999

Chen, R., Deng, Y., Ding, Y., Guo, J., Qiu, J., Wang, B., et al. (2022). Rice functional genomics: decades' efforts and roads ahead. *Sci. China Life Sci.* 65 (1), 33–92. doi: 10.1007/s11427-021-2024-0

Chen, J. F., Zhao, Z. X., Li, Y., Li, T. T., and Wang, W. M. J. R. (2021). Fine-tuning roles of osa-miR159a in rice immunity against *Magnaporthe oryzae* and development. *Rice* 14 (1), 1–11. doi: 10.1186/s12284-021-00469-w

Dai, Z., Tan, J., Zhou, C., Yang, X., Yang, F., Zhang, S., et al. (2019). The OsmiR396-OsGRF8-OsF3H-flavonoid pathway mediates resistance to the brown planthopper in rice (*Oryza sativa*). *Plant Biotechnol. J.* 17 (8), 1657–1669. doi: 10.1111/pbi.13091

Draghici, S., Khatri, P., Tarca, A. L., Amin, K., Done, A., Voichita, C., et al. (2007). A systems biology approach for pathway level analysis. *Genome Res.* 17 (10), 1537–1545. doi: 10.1101/gr.6202607

Du, B., Chen, R., Guo, J., and He, G. (2020). Current understanding of the genomic, genetic, and molecular control of insect resistance in rice. *Mol. Breed.* 40 (2), 1–25. doi: 10.1007/s11032-020-1103-3

Fan, Y., Yang, J., Mathioni, S. M., Yu, J., Shen, J., Yang, X., et al. (2016). *PMS1T*, producing phased small-interfering RNAs, regulates photoperiod-sensitive male sterility in rice. *Proc. Natl. Acad. Sci. U.S.A.* 113 (52), 15144–15149. doi: 10.1073/pnas.1619159114

Gao, C., Zheng, X., Li, H., Mlekwa, U. A., Yu, G., and Jie, X. (2020). Roles of lncRNAs in rice: advances and challenges. *Rice Sci.* 27 (5), 384–395. doi: 10.1016/j.rsci.2020.03.003

Ge, Y., Han, J., Zhou, G., Xu, Y., Ding, Y., Shi, M., et al. (2018). Silencing of miR156 confers enhanced resistance to brown planthopper in rice. *Planta* 248, 813–826. doi: 10.1007/s00425-018-2942-6

Guo, J., Wang, H., Guan, W., Guo, Q., Wang, J., Yang, J., et al. (2023). A tripartite rheostat controls self-regulated host plant resistance to insects. *Nature* 618, 799–807. doi: 10.1038/s41586-023-06197-z

Guo, J., Xu, C., Wu, D., Zhao, Y., Qiu, Y., Wang, X., et al. (2018). *Bph6* encodes an exocyst-localized protein and confers broad resistance to planthoppers in rice. *Nat. Genet.* 50 (2), 297–306. doi: 10.1038/s41588-018-0039-6

Guzmán, P. (2012). The prolific ATL family of RING-H2 ubiquitin ligases. *Plant Signaling Behav.* 7 (8), 1014–1021. doi: 10.4161/psb.20851

Hu, L., Wu, Y., Wu, D., Rao, W., Guo, J., Ma, Y., et al. (2017). The coiled-coil and nucleotide binding domains of BROWN PLANTHOPPER RESISTANCE14 function in signaling and resistance against planthopper in rice. *Plant Cell* 29 (12), 3157–3185. doi: 10.1105/tpc.17.00263

Jeck, W. R., Sorrentino, J. A., Wang, K., Slevin, M. K., Burd, C. E., Liu, J., et al. (2013). Circular RNAs are abundant, conserved, and associated with ALU repeats. *RNA* 19 (2), 141–157. doi: 10.1261/rna.035667.112

Jia, Y., Li, C., Li, Q., Liu, P., Liu, D., Liu, Z., et al. (2020). Characteristic Dissection of *Xanthomonas oryzae* pv. *oryzae* Responsive MicroRNAs in Rice. *Int. J. Mol. Sci.* 21 (3), 785. doi: 10.3390/ijms21030785

Jing, S., Zhao, Y., Du, B., Chen, R., Zhu, L., and He, G. (2017). Genomics of interaction between the brown planthopper and rice. *Curr. Opin. Insect Sci.* 19, 82–87. doi: 10.1016/j.cois.2017.03.005

Jones, J. D., and Dangl, J. L. (2006). The plant immune system. *Nature* 444 (7117), 323–329. doi: 10.1038/nature05286

Kanwar, P., Sanyal, S. K., Tokas, I., Yadav, A. K., Pandey, A., Kapoor, S., et al. (2014). Comprehensive structural, interaction and expression analysis of CBL and CIPK complement during abiotic stresses and development in rice. *Cell Calcium* 56 (2), 81–95. doi: 10.1016/j.ceca.2014.05.003

Kapranov, P., Cheng, J., Dike, S., Nix, D. A., Duttagupta, R., Willingham, A. T., et al. (2007). RNA maps reveal new RNA classes and a possible function for pervasive transcription. *Science* 316 (5830), 1484–1488. doi: 10.1126/science.113834

Kar, M. M., and Raichaudhuri, A. (2021). Role of microRNAs in mediating biotic and abiotic stress in plants. *Plant Gene* 26, 100277. doi: 10.1016/j.plgene.2021.100277

Kim, D., Langmead, B., and Salzberg, S. L. (2015). HISAT: a fast spliced aligner with low memory requirements. *Nat. Methods* 12 (4), 357–360. doi: 10.1038/nmeth.3317

Kumar, K., Mandal, S. N., Neelam, K., and De Los Reyes, B. G. (2022). MicroRNA-mediated host defense mechanisms against pathogens and herbivores in rice: balancing gains from genetic resistance with trade-offs to productivity potential. *BMC Plant Biol.* 22 (1), 351. doi: 10.1186/s12870-022-03723-5

Li, W., Jia, Y., Liu, F., Wang, F., Fan, F., Wang, J., et al. (2019). Integration analysis of small RNA and degradome sequencing reveals microRNAs responsive to *Dickeya zeae* in resistant rice. *Int. J. Mol. Sci.* 20 (1), 222. doi: 10.3390/ijms20010222

Li, Y., Lu, Y.-G., Shi, Y., Wu, L., Xu, Y.-J., Huang, F., et al. (2014). Multiple rice microRNAs are involved in immunity against the blast fungus *Magnaporthe oryzae*. *Plant Physiol.* 164 (2), 1077–1092. doi: 10.1104/pp.113.230052

Nguyen, V. N. T., Moon, S., and Jung, K. H. (2014). Genome-wide expression analysis of rice ABC transporter family across spatio-temporal samples and in response to abiotic stresses. *J. Plant Physiol.* 171 (14), 1276–1288. doi: 10.1016/j.jplph.2014.05.006

Pertea, M., Pertea, G. M., Antonescu, C. M., Chang, T.-C., Mendell, J. T., and Salzberg, S. L. (2015). StringTie enables improved reconstruction of a transcriptome from RNA-seq reads. *Nat. Biotechnol.* 33 (3), 290–295. doi: 10.1038/nbt.3122

Ponjavic, J., Ponting, C. P., and Lunter, G. (2007). Functionality or transcriptional noise? Evidence for selection within long noncoding RNAs. *Genome Res.* 17 (5), 556–565. doi: 10.1101/gr.6036807

Raquel, S. G., Hsing, Y., and San, S. B. (2018). The Polycistronic miR166k-166h Positively Regulates Rice Immunity via Post-transcriptional Control of *EIN2*. *Front. Plant Sci.* 9, 337. doi: 10.3389/fpls.2018.00337

Robinson, M. D., McCarthy, D. J., and Smyth, G. K. (2010). edgeR: a Bioconductor package for differential expression analysis of digital gene expression data. *Bioinformatics* 26 (1), 139–140. doi: 10.1093/bioinformatics/btp616

Salmena, L., Poliseno, L., Tay, Y., Kats, L., and Pandolfi, P. P. (2011). A ceRNA hypothesis: the Rosetta Stone of a hidden RNA language? *Cell* 146 (3), 353–358. doi: 10.1016/j.cell.2011.07.014

Sanchita, T. P.K., and Asif, M. H. (2020). Updates on plant long non-coding RNAs (lncRNAs): the regulatory components. *Plant Cell Tissue Organ Culture* 140 (2), 259–269. doi: 10.1007/s11240-019-01726-z

Shannon, P., Markiel, A., Ozier, O., Baliga, N. S., Wang, J. T., Ramage, D., et al. (2003). Cytoscape: a software environment for integrated models of biomolecular interaction networks. *Genome Res.* 13 (11), 2498–2504. doi: 10.1101/gr.1239303

Shin, S. Y., Jeong, J. S., Lim, J. Y., Kim, T., Park, J. H., Kim, J. K., et al. (2018). Transcriptomic analyses of rice (*Oryza sativa*) genes and non-coding RNAs under nitrogen starvation using multiple omics technologies. *BMC Genomics* 19 (1), 532. doi: 10.1186/s12864-018-4897-1

Tan, J., Wu, Y., Guo, J., Li, H., Zhu, L., Chen, R., et al. (2020). A combined microRNA and transcriptome analyses illuminates the resistance response of rice against brown planthopper. *BMC Genomics* 21 (1), 144. doi: 10.1186/s12864-020-6556-6

Thomas, M., Lieberman, J., and Lal, A. (2010). Desperately seeking microRNA targets. *Nat. Struct. Mol. Biol.* 17 (10), 1169–1174. doi: 10.1038/nsmb.1921

Tonnessen, B. W., Manosalva, P., Lang, J. M., Baraoidan, M., Bordeos, A., Mauleon, R., et al. (2015). Rice phenylalanine ammonia-lyase gene *OsPAL4* is associated with broad spectrum disease resistance. *Plant Mol. Biol.* 87 (3), 273–286. doi: 10.1007/s11103-014-0275-9

Wang, Y., Luo, X., Sun, F., Hu, J., Zha, X., Su, W., et al. (2018a). Overexpressing lncRNA *LAIR* increases grain yield and regulates neighbouring gene cluster expression in rice. *Nat. Commun.* 9 (1), 3516. doi: 10.1038/s41467-018-05829-7

Wang, L., Park, H. J., Dasari, S., Wang, S., Kocher, J.-P., and Li, W. (2013). CPAT: Coding-Potential Assessment Tool using an alignment-free logistic regression model. *Nucleic Acids Res.* 41 (6), e74–e74. doi: 10.1093/nar/gkt006

Wang, Z., Xia, Y., Lin, S., Wang, Y., Guo, B., Song, X., et al. (2018b). Osa-miR164a targets *OsNAC60* and negatively regulates rice immunity against the blast fungus *Magnaporthe oryzae*. *Plant J.* 95 (4), 584–597. doi: 10.1111/tpj.13972

Wu, D., Guo, J., Zhang, Q., Shi, S., Guan, W., Zhou, C., et al. (2022). Necessity of rice resistance to planthoppers for OsEXO70H3 regulating SAMSL excretion and lignin deposition in cell walls. *New Phytol.* 234 (3), 1031–1046. doi: 10.1111/nph.18012

Wu, Y., Lv, W., Hu, L., Rao, W., Zeng, Y., Zhu, L., et al. (2017). Identification and analysis of brown planthopper-responsive microRNAs in resistant and susceptible rice plants. *Sci. Rep.* 7 (1), 8712. doi: 10.1038/s41598-017-09143-y

Wu, B., Zhang, B., Dai, Y., Zhang, L., Shang-Guan, K., Peng, Y., et al. (2012). *Brittle culm15* encodes a membrane-associated chitinase-like protein required for cellulose biosynthesis in rice. *Plant Physiol.* 159 (4), 1440–1452. doi: 10.1104/pp.112.195529

Xiao, H., Yuan, Z., Guo, D., Hou, B., Yin, C., Zhang, W., et al. (2015). Genome-wide identification of long noncoding RNA genes and their potential association with fecundity and virulence in rice brown planthopper, *Nilaparvata lugens*. *BMC Genomics* 16, 749. doi: 10.1186/s12864-015-1953-y

You, X., and Conrad, T. O. (2016). Acfs: accurate circRNA identification and quantification from RNA-Seq data. *Sci. Rep.* 6 (1), 1–11. doi: 10.1038/srep38820

Yu, S., Ali, J., Zhou, S., Ren, G., Xie, H., Xu, J., et al. (2022). From Green Super Rice to green agriculture: Reaping the promise of functional genomics research. *Mol. Plant* 15 (1), 9–26. doi: 10.1016/j.molp.2021.12.001

Zha, W., Li, S., Xu, H., Chen, J., Liu, K., Li, P., et al. (2022). Genome-wide identification of long non-coding (lncRNA) in *Nilaparvata lugens*'s adaptability to resistant rice. *PeerJ* 10, e13587. doi: 10.7717/peerj.13587

Zhang, P., Li, S., and Chen, M. (2020). Characterization and function of circular RNAs in plants. *Front. Mol. Biosci.* 7, 91. doi: 10.3389/fmolb.2020.00091

Zheng, X., Xin, Y., Peng, Y., Shan, J., Zhang, N., Wu, D., et al. (2021). Lipidomic analyses reveal enhanced lipolysis in planthoppers feeding on resistant host plants. *Sci. China Life Sci.* 64 (9), 1502–1521. doi: 10.1007/s11427-020-1834-9

frontiers | Frontiers in Plant Science

TYPE Original Research
PUBLISHED 17 August 2023
DOI 10.3389/fpls.2023.1229620

OPEN ACCESS

EDITED BY
Shengli Jing,
Xinyang Normal University, China

REVIEWED BY
Sonam Popli,
University of Toledo, United States
Liang Hu,
Hubei Academy of Agricultural Sciences, China

*CORRESPONDENCE
Judith K. Brown
jbrown@ag.arizona.edu

RECEIVED 26 May 2023
ACCEPTED 10 July 2023
PUBLISHED 17 August 2023

CITATION
He R, Fisher TW, Saha S, Peiz-Stelinski K, Willis MA, Gang DR and Brown JK (2023) Differential gene expression of Asian citrus psyllids infected with '*Ca.* Liberibacter asiaticus' reveals hyper-susceptibility to invasion by instar fourth-fifth and teneral adult stages.
Front. Plant Sci. 14:1229620.
doi: 10.3389/fpls.2023.1229620

Differential gene expression of Asian citrus psyllids infected with '*Ca.* Liberibacter asiaticus' reveals hyper-susceptibility to invasion by instar fourth-fifth and teneral adult stages

Ruifeng He[1,2], Tonja W. Fisher[3], Surya Saha[4,5], Kirsten Peiz-Stelinski[6], Mark A. Willis[1], David R. Gang[1] and Judith K. Brown[3]*

[1]Institute of Biological Chemistry, Washington State University, Pullman, WA, United States, [2]Soybean Genomics and Improvement Laboratory, US Department of Agriculture (USDA)-Agricultural Research Service (ARS), Beltsville, MD, United States, [3]School of Plant Sciences, University of Arizona, Tucson, AZ, United States, [4]Sol Genomics Network, Boyce Thompson Institute, Ithaca, NY, United States, [5]School of Animal and Comparative Biomedical Sciences, University of Arizona, Tucson, AZ, United States, [6]Citrus Research and Education Center, Department of Entomology and Nematology, University of Florida, Lake Alfred, FL, United States

The bacterial pathogen *Candidatus* Liberibacter asiaticus (CLas) is the causal agent of citrus greening disease. This unusual plant pathogenic bacterium also infects its psyllid host, the Asian citrus psyllid (ACP). To investigate gene expression profiles with a focus on genes involved in infection and circulation within the psyllid host of CLas, RNA-seq libraries were constructed from CLas-infected and CLas-free ACP representing the five different developmental stages, namely, nymphal instars 1-2, 3, and 4-5, and teneral and mature adults. The Gbp paired-end reads (296) representing the transcriptional landscape of ACP across all life stages and the official gene set (OGSv3) were annotated based on the chromosomal-length v3 reference genome and used for *de novo* transcript discovery resulting in 25,410 genes with 124,177 isoforms. Differential expression analysis across all ACP developmental stages revealed instar-specific responses to CLas infection, with greater overall responses by nymphal instars, compared to mature adults. More genes were over-or under-expressed in the 4-5th nymphal instars and young (teneral) adults than in instars 1-3, or mature adults, indicating that late immature instars and young maturing adults were highly responsive to CLas infection. Genes identified with potential for direct or indirect involvement in the ACP-CLas circulative, propagative transmission pathway were predominantly responsive during early invasion and infection processes and included canonical cytoskeletal remodeling and endo-exocytosis pathway genes. Genes with predicted functions in defense, development, and immunity

exhibited the greatest responsiveness to CLas infection. These results shed new light on ACP-CLas interactions essential for pathogenesis of the psyllid host, some that share striking similarities with effector protein-animal host mechanisms reported for other culturable and/or fastidious bacterial- or viral-host pathosystems.

KEYWORDS

circulative, *Diaphorina citri*, host-pathogen interactions, propagative transmission, psyllidae, RNA-seq analysis

Introduction

The Asian citrus psyllid (ACP), *Diaphorina citri* is a phloem-feeding insect classified in the family, Liviidae (Order Hemiptera; Suborder Homoptera). It is the insect vector of the fastidious, plant phloem-inhabiting, gram-negative pathogen bacterium '*Candidatus* Liberibacter asiaticus' (CLas), causal agent of the now widespread citrus greening disease that has affected the citrus industry, worldwide (Gottwald, 2010). The psyllid-CLas pathosystem has been problematic in other plant hosts in the subfamily, Aurantioideae, family Rutaceae (Grafton-Cardwell et al., 2013; Hall et al, 2013). In the United States, citrus greening has spread throughout all major citrus-growing areas in Florida and is responsible for outbreaks in commercial citrus in California, Texas, and other U.S. citrus-growing states (Stokstad, 2012). Invasions of *D. citri* have been reported in Arizona, but CLas has not been detected there in citrus trees. Since the initial discovery in Florida in 2005, and spread to other production areas in the U.S. the production of oranges has been reduced more than 50% (Ledford, 2017).

The ACP life cycle consists of seven stages, five nymphal instars (1~5), the teneral adult, and the adult. The average developmental time from egg to adult ranges from 14.1 days at 28°C to 49.3 days at 15°C (Hall et al, 2013). The mode of ACP-mediated psyllid transmission is persistent, and CLas is circulative and propagative in the vector. Psyllids ingests CLas while feeding on the phloem of infected plants, and CLas passes from the food canal into the alimentary canal (gut) where it multiplies and forms extensive biofilms (Wang and Trivedi, 2013). From the gut, CLas enters the hemolymph where it becomes motile, circulates to the oral region, and presumably enters the salivary glands. From the salivary glands, CLas cells are inoculated to the plant phloem in salivary contents during psyllid feeding (Ammar et al., 2011).

Extremely low-level transmission of CLas does from parent to offspring (transovarial) has been reported in laboratory studies, however, it may not be biologically relevant (Pelz-Stelinski et al., 2010; Kelley and Pelz-Stelinski, 2019). If viable in nature, transovarial transmission could feasibly provide a fail-safe mechanism to ensure CLas survival in a fraction of the ACP population (Vyas et al., 2015). A very low frequency of sexual transmission between males and females has been documented (Mann et al., 2011). Studies have shown rates of infection in ACP adults harboring detectable CLas, reared from the egg to adult stage on CLas-infected citrus plants, averaged ~40% and ranged from 30%-80% depending on the plant host growth-stage, season, temperature, humidity, and other environmental factors (Gottwald, 2010). No difference in inoculation efficiency has been reported for male and female psyllids (Ammar et al., 2020).

Young ACP nymphal stages acquire CLas and the adults transmit the bacterium and are involved in transmission and tree-to-tree spread (Kelley and Pelz-Stelinski, 2019; Ammar et al., 2020). The ACP nymphal stages acquire CLas at high rates that range from 60 to 100%. By comparison, even after a 5-week acquisition-access period (AAP) on infected plants, only 40% of the adults have acquired the pathogen (Pelz-Stelinski et al., 2010). Thus, CLas is efficiently transmitted by ACP adults only when acquired during the nymphal stage. Infection of adults and nymphal instars by CLas does not cause mortality. In adults, CLas infection has little discernable effect on longevity, and potential negative effects are offset by an increased fecundity (Pelz-Stelinski and Killiny, 2016; Ren et al., 2016). Although CLas multiplies in both the nymphs and adults, it accumulates to higher levels and in shorter periods of time by nymphs than by adults (Ammar El et al., 2016). The specific ACP nymphal stage or stages primarily involved in CLas ingestion that results in adult transmission have not been determined.

Liberibacter-encoded effector proteins have been posited as essential for infection of and systemic circulation within the ACP vector. After ingestion, CLas invades and colonizes the gut. After extensive multiplication, it utilizes exocytosis to exit, enter the hemolymph, and gain entry into the salivary glands where acquisition occurs (Cicero et al., 2017; Kruse et al., 2017). A number of psyllid proteins have been implicated in'*Ca*. Liberibacter' effector interactions during ingestion, adhesion, multiplication, biofilm formation, circulation, and the acquisition phases (Fisher et al., 2014; Vyas et al., 2015). While differentially expressed CLas-responsive proteins have been identified in ACP nymphs and adults of ACP (Ramsey et al., 2017; Ramsey et al., 2022) and the related pathosystem involving the potato psyllid (PoP), *Bactericera cockerelli* and '*Ca*. Liberibacter solanacearum' (CLso) (Vyas et al., 2015), the interactions between ACP and CLas throughout the developmental stages have not been explored in detail to enable characterization of age-related transcriptional dynamics. Previously, CLas-infected and uninfected nymphs and adult differential expression profiles have implicated

developmentally regulated, stage-specific gene expression and/or proteins indicative mechanisms associate with gut invasion and salivary glands acquisition (Fisher et al., 2014; Vyas et al., 2015; Ramsey et al., 2017; Ramsey et al., 2022), and in addition for ACP, adult stage-specific transmission. Evidence of differential expression of defense-, stress-, and nutritionally related genes among the different ACP life history stages are hypothesized to reflect the distinct evolutionary history of ACP-CLas host-parasite interactions. Detailed analysis of the developmental physiology of CLas-infected psyllid and plant hosts could help explain the basis for the observed bimodal immature/adult acquisition/transmission and provide new insights in the unusual dual animal-plant host strategy of "*Ca*. Liberibacter" spp.

Exploiting RNA interference (RNAi) for managing insect pests and pathogens in agricultural crops is of increasing interest (Jain et al., 2021). RNA interference involves naturally occurring biochemical processes associated with organismal defenses that are highly conserved among eukaryotes. Triggering an RNAi response canonically results in gene silencing in which a foreign mRNA is targeted for degradation to impede gene expression or translation by sequence-specific, small interfering RNAs (siRNAs) complementary to the target mRNA (Hannon, 2002; Mito et al., 2011). In insects, exogenous double stranded RNAs (dsRNAs) have been used to induce RNAi pathway activation in a recipient insect to cause mortality or other phenotypes of interest. Silencing ACP genes to cause death or silence genes that impede efficient CLas transmission relies in part on functional genomic studies to gain a deeper understanding of basic ACP biology and of ACP-CLas interactions that facilitate multiplication, invasion, and systemic infection of the psyllid host and vector of this plant pathogen. The feasibility of RNAi in the potato psyllid (Mondal et al., 2022) and ACP has been demonstrated (El-Shesheny et al., 2013; Killiny et al., 2014; Kishk et al., 2017; Yu et al., 2017; Santos-Ortega and Killiny, 2018; Pacheco et al., 2020; Dos Santos Silva et al., 2022; Guo et al., 2022; Paredes-Montero et al., 2022) and functional genomics and proteomics studies have begun to inform effective and specific RNAi targets for PoP and ACP (Fisher et al., 2014; Vyas et al., 2015; Yang et al., 2022).

The objective of this study was to analyze sequence psyllid stage-specific transcriptomes and identify differentially expressed genes in ACP nymphal instars, 1-2, 3, and 4,5, and two developmental adult stages, the teneral stage, which are not yet reproductively mature, and reproductive, mature adults. The goal is to dissect instar-specific ACP responses to CLas invasion, multiplication, and systemic infection of the insect host. Of particular interest were differentially expressed genes (DEGs) predicted to contribute to the early-instar susceptibility to CLas gut invasion and early multiplication and to down-stream processes leading to systemic infection of the older immature (4-5) instars, the teneral (immature) adults. The rationale is that adults, which manifest transmission-competency, are so, only when CLas acquisition occurs during nymphal developmental stages when presumed barriers that impede adult acquisition do not exist and/or may be relaxed.

Materials and methods

Psyllid colonies

The CLas-infected and -uninfected ACP colonies were reared in laboratory cultures maintained on a CLas host (Citrus spp.) (CLas-infected) or a CLas-immune rutaceous plant species (CLas-free). Cultures were established in 2005 from a field population collected in Polk Co., FL (28.0' N, 81.9' W) prior to the establishment of HLB. Cultures were reared continuously and serially transferred periodically to the same host species, 'Valencia' sweet orange (*Citrus sinensis* (L.) plants, at the University of Florida Citrus Research and Education Center (maintained by coauthor Dr. K.S. Pelz-Stelinski, Lake Alfred, FL). The ACP colonies were maintained year-round on caged citrus trees, with ACP+ and ACP- colonies in separate walk-in growth rooms, IFAS Lake Alfred Research Center, FL for more than 10 years. The colonies have been assayed routinely for ACP presence (initially, seasonal CLas load), and in the CLas-free colony, for CLas absence. An established method, qPCR amplification of the CLas 16S rRNA gene, was used for CLas detection in psyllids (Li et al., 2006; Martini et al., 2015).

Five stages of nymphs (1–5 instar) and two stages of adults (teneral adult and mature adult) were collected, with 150 1^{st}-3^{rd} instars and 100 4^{th}-5^{th} instars (I-4,5), teneral adults (TA) and mature adults (MA) (also known as post teneral adults (PTA)) per sample, with 6 replicates for each. Males and females were collected in pairs to achieve nearly equal numbers of both, so that a comprehensive accurate representation of the transcriptome could be generated over the entire range of adult and nymph life stages. Live psyllids were collected from colonies and were frozen in liquid N_2, lightly crushed in 0.5 ml Trizol (Invitrogen, Carlsbad, CA), and shipped overnight on dry ice to Washington State University where they were stored at -80°C until use.

RNA isolation and quality control

For RNA extraction, 0.2 ml chloroform was added to 0.5 ml Trizol homogenate, followed by vigorous sample shaking for 30 s. Samples were allowed to rest for 3 min at room temperature, followed by centrifugation at 12,000 ×g for 15 min at 4°C to separate organic and aqueous phases. The aqueous phase (150-200 µL) was transferred to a sterile RNase-free tube and an equal volume of 100% EtOH was added, with mixing. The RNA was purified using the RNeasy Mini Kit (Qiagen, Valencia, CA), according to the manufacturer's protocol. The Trizol RNA purification protocol that includes a DNase treatment step was implemented., according to the manufacturer's instructions. The quality and quantity of the RNA samples was analyzed with a NanoDrop 2000 Spectrophotometer (Thermo Scientific, Wilmington, DE). The integrity of the RNA preparations was confirmed using an Agilent 2100 Bioanalyzer (Agilent Technologies Inc., Santa Clara, CA).

Library construction and Illumina sequencing

The Illumina libraries were constructed from RNA transcripts purified using the TruSeq RNA Sample Preparation Kit v2, Cat. # RS-122-2002 (Set B) from Illumina. In brief, the poly(A) RNA was isolated from 2 µg of total RNA from each sample using magnetic oligo (dT) beads. Following purification, the mRNA was fragmented by zinc treatment at 94°C for 3 min and reverse-transcribed to synthesize first strand cDNA using SuperScript II reverse transcriptase (Invitrogen, Carlsbad, California) and random primers. Second-strand cDNA synthesis was performed, with the products then being subjected to end-repair and phosphorylation, and addition of an "A" base to the 3′ ends of the blunt phosphorylated DNA fragments. Illumina multiple indexing adapters were ligated to the fragments, as described by Illumina's TruSeq RNA Sample Preparation V2 Guide (Illumina). The cDNA fragments flanked by Illumina PE adapters were selected and purified by AMPure XP beads for downstream enrichment. The cDNA fragments were amplified by PCR Primers PE 1.0 and PE 2.0 (Illumina) that anneal to the ends of the adapters, using the PCR program of 30 s at 98°C followed by 15 cycles of 10 s at 98°C, 30 s at 60° C, 30 s at 72°C and a final elongation step of 5 min at 72°C. The products were purified using AMPure XP beads to create an Illumina paired-end library. Library quality control was performed with a Bioanalyzer DNA 1000 Chip Series II (Agilent). A qPCR method was employed for quantifying libraries in advance of generating clusters. The libraries were diluted to a final concentration of 10 nM. The paired-end libraries were applied for cluster generation at a concentration of 10 pM on a flowcell in a cBOT (Illumina). Sequencing was performed on an Illumina HiSeq2500 platform by Macrogen with one lane for 12 pooled libraries (total 60 libraries in 5 lanes) to generate 2 × 150 bp paired end reads. The base-calling and quality value calculations were performed by the Illumina data processing pipeline CASAVA v1.8.4 and v1.7.0, respectively. Various quality controls including removal of reads containing primer/adaptor sequences, trimming read length and filtering high-quality reads based on the score values, were performed using Illumina CASAVA v1.7.0.

Read mapping and identification of DEGs

The ACP reference genome Version 3 and official gene set version 3 (OGSv3) annotation files (Hosmani et al., 2019) were downloaded from the ACP genome website (https://www.citrusgreening.org/organism/Diaphorina_citri/genome). The raw sequencing reads were assessed using FastQC-v0.11.3 (Andrews) and trimmed for adapters and low quality using Trimmomatic-0.33 (Bolger et al., 2014). All cleaned reads were mapped to the ACP reference genome OGSv3 using HISAT2 (Kim et al., 2019). Mapped files were sorted with samtools rocksort. After sorting, a genome-guided transcriptome assembly described by Saha et al. (Saha et al., 2017) was performed using StringTie (Pertea et al., 2015). The reference genome and gene model annotation files were downloaded from the genome website (https://www.citrusgreening.org/organism/Diaphorina_citri/genome).

Differential expression analysis between the CLas-infected (infected) treatment and CLas-free (uninfected) control in the same stages (intra-stage) or the CLas-infected (infected) treatments between different stages (inter-stage) were performed using the DESeq2 R package. The False Discovery Rate (FDR) of 5% and *P*-value 0.05 were set as the threshold for significant differential expression. The hierarchical cluster analysis of differentially expressed genes (DEGs) was conducted using MeV (multi-experiment viewer) software. The significantly DEGs between the two arbitrary samples were identified based on the following thresholds: $|\log2 \text{ (fold-change (A/B))}| > 1$ and corrected P-value < 0.05. A and B represent the normalized expression of genes in any two samples, respectively.

Annotation, Gene Ontology and KEGG enrichment analysis of DEGs

We supplied the OGSv3 annotation to StringTie during reference-guided transcript assembly so that it preserved the connection between the gene name in OGSv3 and the *de novo* assembled MSTRG transcripts reported by it. This information was used for extracting the functional annotations of the transcripts from OGSv3 genes, which were annotated using protein orthologs and the AHRD pipeline (Hosmani et al., 2019).

Ortholog assignment and pathway mapping were carried out via the KEGG (Kyoto Encyclopedia of Genes and Genomes) Automatic Annotation Server with the BBH (bi-directional best hit) method (http://www.genome.jp/kegg/kaas/) (Moriya et al., 2007; Kanehisa et al., 2016). The differentially expressed (fold-change ≥ 2 and $p<0.05$) genes (DEGs)/genes between uninfected and infected from different stages were mapped to KEGG biochemical pathways by BLAST comparisons against a set of orthologous groups in KEGG EGENES, resulting in the KEGG Orthology (KO) assignments and the Enzyme Commission (EC) distribution in the pathway databases. The following six data sets were submitted to KAAS; for simplicity in naming, the first letter indicates the ACP life stage, followed by a number(s) indicating larval (or nymphal) instar stage(s), with the last letter, being an 'L' (Liberibacter) if infected with CLas: 1) all of the ACP genes, 2) the genes differentially expressed (fold-change ≥ 2 and $p<0.05$) between CLas-free instars 1-2 (I12) and CLas-infected instars 1-2 (I12L) comparisons, 3) the genes differentially expressed ($p<0.05$) between CLas-free instar 3 (I3) and CLas-infected instar 3 (I3L) comparisons, 4) the genes differentially expressed ($p<0.05$) between CLas-free instars 4-5 (I45), and CLas-infected instars 4-5 (I45L) comparisons, 5) the genes differentially expressed ($p<0.05$) between CLas-free teneral adult (TA) and CLas-infected teneral adult (TAL) comparisons, and 6) the genes differentially expressed ($p<0.05$) between CLas-free mature adult (MA) and CLas-infected mature adult (MAL) comparisons. All of the results were obtained using the TCW query and display interface, hence, are reproducible, with one exception. The KEGG results are provided in an additional file as an Appendix that explains how each table and figure was generated.

Illumina data

The Illumina paired end transcript reads from the five stages of nymphs (1–5 instar) and two stages of adults (teneral adult and mature adult) have been uploaded to NCBI SRA under Bioproject PRJNA746599 (https://www.ncbi.nlm.nih.gov/bioproject/?term=PRJNA746599) with accessions: SRX20741680 ~ SRX20741739. To improve the accessibility and usability of this data for the citrus greening research community, data will be incorporated in future versions of the Psyllid Expression Network (https://cgen.citrusgreening.org/). This visualization tool is available to access publicly available transcriptomics data for *D.citri* from multiple tissues, life stages, infection states, and of the citrus host plant, in an expression cube for comparative analyses.

Results and discussion

De novo transcript discovery using a comprehensive sampling of expression data from every ACP life stage

Polyadenylated ACP RNA was isolated and used to construct 60 Illumina paired-end sequencing libraries, from pools of five developmental stages (instar 1-2, instar 3, instar 4-5, teneral adults, and mature adults) of CLas-free and CLas-infected ACP with six replicates each. Sequencing was carried out as described in the *Methods* section and producing 1,960 million paired-end 150 bp sequencing reads consisting of 296 G bp (Additional file 1).

Quality filtering removed approximately 2% low-quality reads found to be present in most of the replicated samples. Most replicates contained 4-7% rRNA and 5-12% mitochondrial RNA reads, which were also removed from downstream analysis. Principal Component Analysis (PCA) was carried out to determine if the sequencing data were representative and of high quality. The evaluation of sequence data and PCA were carried out for all developmental stages/groups. However, the instar 4-5 (I45) group showed the most significant overall differential expression; it was selected and highlighted here to visually represent the overall trend (Figures 1, 2). Importantly, the instar 4-5 (I45) group exhibited the most responsive stage to CLas infection/invasion, based on the extensive number of differentially expressed genes, compared to the other stages/groups, making it the most representative. In addition, one sample (ACP_U3-4 in Figure 1 or Instar4,5 neg4 in Figure 2) failed to pass quality control and so the data were not included. An optimized index was built for the chromosomal length version 3.0 reference assembly with splice junctions based on official gene set (OGSv3) and overall, the alignments were found to be consistent at approximately 85-87%. The transcriptome data were used to extend the OGSv3 beta annotation, which resulted in the *de novo* transcript discovery of a total of 25,410 genes with 124,177 isoforms.

Greater differential gene expression in instars 4-5 and more over-expressed genes compared to under-expressed expression in teneral adults

Among the total of assembled/aligned genes in each stage, 21805 genes were identified as significantly differentially expressed genes in response to CLas infection (with False Discovery Rate (FDR) of 5% and *P*-value < 0.05), including 4768 genes (33%) from instar 1-2 (I-1,2), 4901 genes (35%) from instar 3 (I-3), 6389 genes (44%) from instar 4-5 (I-4,5), 4843 genes (33%) from teneral adult (TA) and 904 genes (6%) from mature adult (MA) (Table 1). In general, there were more over-expressed than under-expressed genes (in total, 11032 over-expressed genes

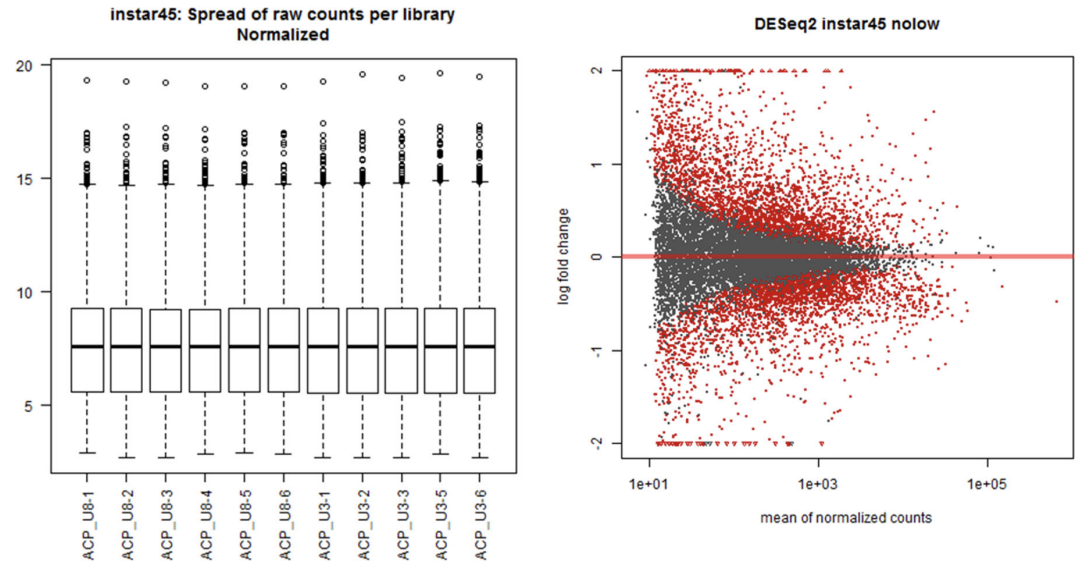

FIGURE 1
Sequencing data distribution and normalization for the Asian citrus psyllid (ACP) immature group consisting of 4th and 5th instars (I4-5).

10.3389/fpls.2023.1229620

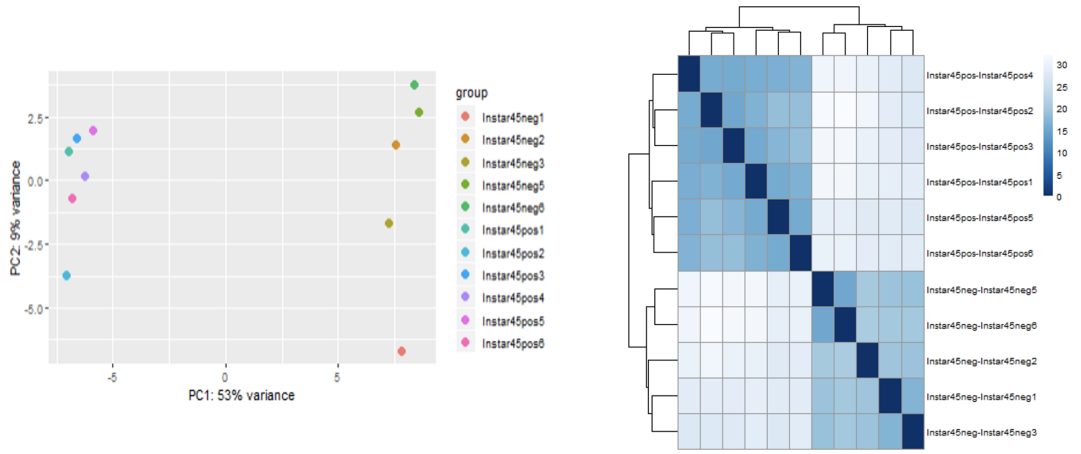

FIGURE 2
Principal component and pairwise correlation analysis of sequencing data for Asian citrus psyllid (ACP) immature group consisting of 4th and 5th instars (I4-5), infected or uninfected with '*Candidatus* Liberibacter asiaticus'.

compared to 10773 under-expressed genes among different stages in response to CLas infection) (Table 1). These results showed more differentially expressed genes were associated with the nymphal instars (including instar 1-2, instar 3 and instar 4-5) compared to adults, indicating that instars are more responsive to CLas infection. In particular, the instar 4-5 stage contained more DEGs (3147 over-expressed and 3242 under-expressed, totaling 6389 genes), indicating instar 4-5 was much more sensitive/responsive than the others to CLas infection. Further, more over-expressed genes among the instar 4-5 and teneral adults than in other stages, with 3147 and 2639 genes over-expressed in immature instars 4-5 and teneral adults, respectively (Table 1).

Differential gene expression in response to CLas infection was also compared among different stages (inter-stages). In total, 2314 DEGs were identified in nymphal instar 4-5 compared to instar 3, including 1248 over-expressed genes, which was much higher than other comparisons (Table 2). Nymphal instars 4-5 and teneral adults showed the largest changes in gene expression in response to CLas infection. Furthermore, there were more over-expressed genes (566 genes) than under-expressed genes (244 genes) in the teneral stage as compared with instar 4-5 (Table 2), indicating that CLas infection mainly causes up-regulation of ACP genes.

The differentially expressed genes identified herein were classified by predicted biological functions using KEGG analysis to obtain an overview of the processes altered by gene differential expression in response to CLas infection. Using KAAS (KEGG Automatic Annotation Server), which provides functional annotation of genes by BLAST comparisons against the manually curated KEGG GENES database to produce KO (KEGG Orthology) assignments and automatically generated KEGG pathways, the genes differentially expressed (FDR of 5% and P-value < 0.05) in the different life stages/groups, in response to CLas infection, were assigned to KEGG biochemical pathways.

The genes assigned to nymphal instar 3, instars 4-5 and teneral adults dominated the pathways (Figure 3), with most being distributed in categories "biosynthesis of secondary metabolites" (127 gens from instar 3, 170 genes from instar 4-5 and 146 genes from teneral adults), "ribosome" (45 genes from instar 3, 84 genes from instar 4-5 and 76 genes from teneral adults), "oxidative phosphorylation" (43 genes from instar 3, 42 genes from instar 4-5 and 57 genes from teneral adults), and "endocytosis" (39 genes from instar 3, 49 genes from instar 4-5 and 53 genes from teneral adults), documenting significant transcriptional changes among the different ACP life stages in response to CLas infection (Figure 3). These observations also suggested that CLas infection resulted in more significant effects on the nymphal instars 4-5 and teneral adults, than to the three youngest immature instars (1,2 and 3) and mature adults.

TABLE 1 Summary of intra-stage differentially expressed genes in response to 'Candidatus Liberibacter asiaticus' (CLas) infection of ACP.

Intra-stages (Clas-infected vs. –uninfected ACP)	Up (%)	Down (%)	Total (%)
Instar 1-2 group	2320 (16%)	2448 (17%)	4768 (33%)
Instar 3	2409 (17%)	2492 (18%)	4901 (35%)
Instar 4-5 group	3147 (22%)	3242 (22%)	6389 (44%)
Teneral adult (TA)	2649 (18%)	2194 (15%)	4843 (33%)
Mature adult (MA)	507 (3.4%)	397 (2.6%)	904 (6%)
Total	11032	10773	21805

TABLE 2 Inter-stage differentially expressed genes in response to '*Candidatus* Liberibacter asiaticus' (CLas) infection of ACP.

Inter-stages (Clas-infected ACP)	Up	Down	Total
Instar 3 vs. instar 1-2 group	584	545	1129
Instar 4-5 group vs. instar 3	1248	1066	2314
Teneral adult (TA) vs. instar 4-5 group	566	244	810
Mature adult (MA) vs. teneral adult (TA)	6	10	16
Total	2404	1865	4269

Unique and shared differentially expressed responsive genes between developmental stages

Cross-development stage comparisons of CLas-responsive genes were performed to determine if bacterium infection had a universal effect on gene function and gene expression levels. Among these DEGs, some were shared by two, three, four, or five stages (Figure 4). For example, a U6 snRNA-associated Sm-like protein gene (MSTRG.13654) was highly over-expressed (more than 2-9-fold in different stages) and shared by all five life stages after CLas infection. This gene is involved in RNA processing and associated with RNA degradation and the spliceosome. In contrast, the H +/sugar cotransporter gene (MSTRG.17346) was under-expressed, a pattern that was shared in common by all four CLas-infected life stage groups examined here, except for the mature adult stage. Among the 609 DEGs with 2-fold differences that were assigned to KEGG pathways, 290 (48%) DEGs were from teneral adults and 140 (23%) DEGs were from instar 4-5, and approximately 64 (10%), 60 (10%), and 55 (9%) DEGs were from instar 1-2, instar 3 and mature adult respectively. Among these, 442 (73%) genes were over-expressed, whereas 167 (27%) genes were under-expressed. Among 290 DEGs from teneral adults and 140 DEGs from instar 4-5, 231 (80%) and 107 (76%) were over-expressed, respectively, whereas among the 60 DEGs from instar 3, 32 (53%) were under-expressed (Figure 4).

The 50 top over-expressed and 50 top under-expressed genes in response to CLas infection in most life stages are shown, highlighted (Additional file 2 and 3). Interestingly, the top 50 over-expressed genes were primarily associated with the teneral adult stage (41/50), while the top 50 under-expressed genes were distributed across different stages, however, the majority were associated with the teneral adult stage. The predominantly over-expressed genes were assigned to sugar metabolism and glycan degradation, signaling pathway, oxidative phosphorylation, ribosome, ubiquitin and collagen pathways. Among these, a calmodulin gene (MSTRG.16314) was overexpressed in three CLas-infected groups: instars 4-5, teneral adults and mature adults), with greater than 60-fold in the teneral adult stage, alone (Additional file 2). Calmodulin (CaM) is a multifunctional intermediate calcium-binding messenger protein and directly or indirectly has a functional role in nearly every physiological process. Calmodulin is involved in the activation of phosphorylase kinase that leads to cleavage of glucose from glycogen-by-glycogen phosphorylase (Nishizawa et al., 1988).

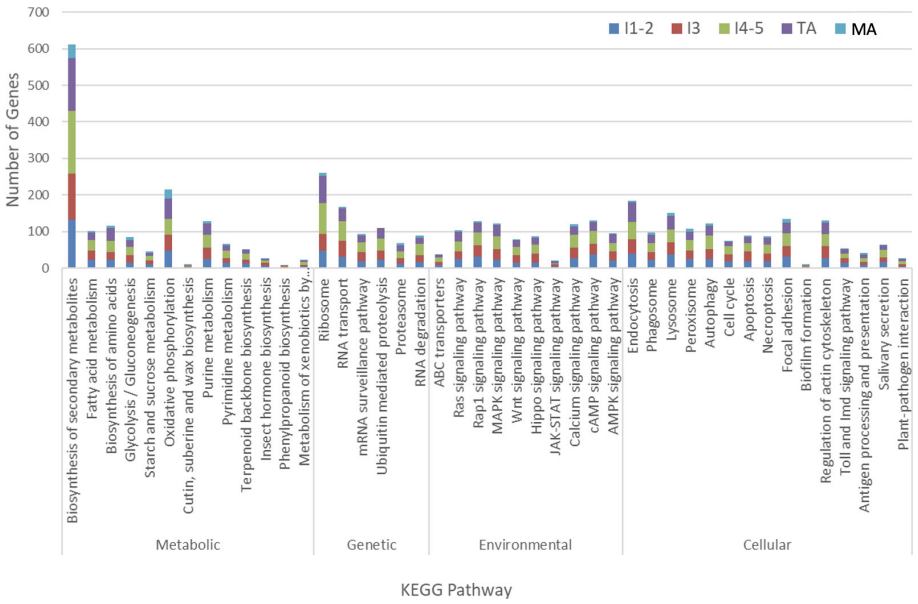

FIGURE 3
KEGG analysis of differentially expressed Asian citrus psyllid genes in response to '*Candidatus* Liberibacter asiaticus' infection.

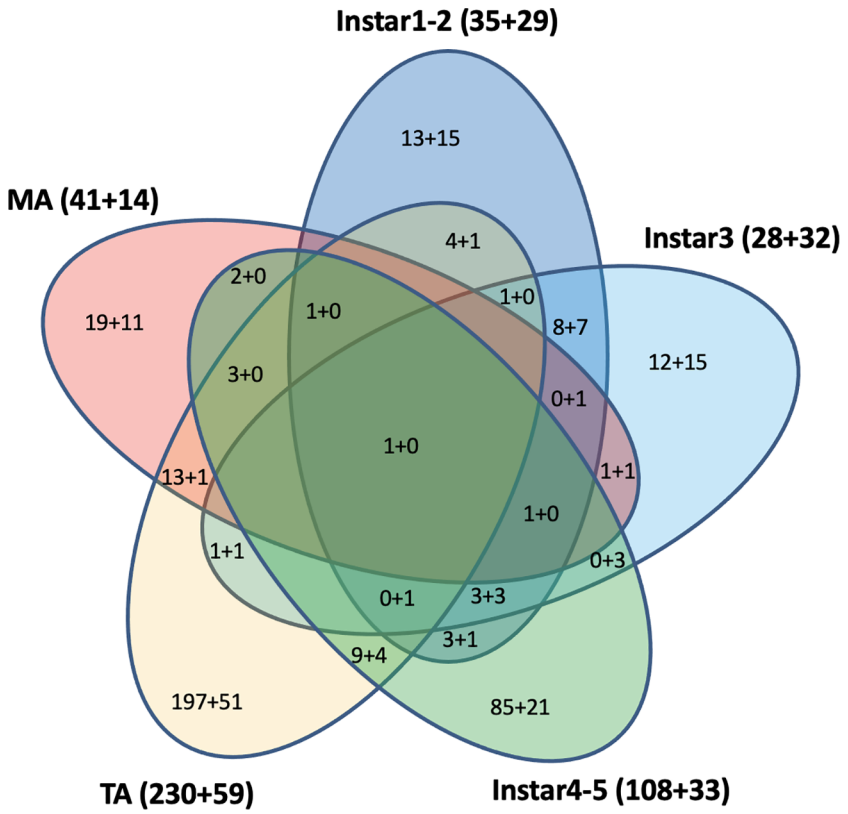

FIGURE 4
Differentially expressed KEGG pathway Asian citrus psyllid genes: up-regulated (indicated, as before '+'), compared to down-regulated (indicated, after '+'). Fold-changes >2, P<0.05.

Also, a number of sugar metabolism- and glycan degradation-related genes were over-expressed in response to CLas infection, strongly implicating pathogen modulation of primary energy-producing molecules. For example, a gene (MSTRG.18384) coding arylsulfatase B was over-expressed in all five stages, at greater than 7-fold in the instar 4-5 stage. This gene is involved in glycosaminoglycan degradation. In contrast, the most under-expressed genes were assigned to cytoskeleton proteins, membrane trafficking and exocytosis, peptidase inhibitors, and biofilm formation categories, suggestive of cytoskeletal remodeling to aid CLas invasion and multiplication, while potentially moderating the advancement of systemic invasion.

Energy metabolism is altered in ACP in response to CLas infection

Many of the top 50 up- and under-expressed genes were mitochondrial and energy metabolism-related genes/proteins. For example, mitochondrial mRNA pseudo uridine synthase TRUB2 (MSTRG.9981) was over-expressed in stages instar 4-5 (I-4,5) and teneral adult (TA) (> 6-fold). In addition, an EMRE (essential MCU regulator, mitochondrial) gene (MSTRG.15478) and a ubiquinol-cytochrome c reductase subunit 9 (MSTRG.22133), which is involved in oxidative phosphorylation and energy metabolism, were also highly over-expressed in the teneral adult stage (TA) (Additional file 2). Also, an ATPase subunit b, mitochondrial (MSTRG.5785), involved in oxidative phosphorylation and energy metabolism, was under-expressed more than 4-fold after CLas infection in stage I45 compared to stage I3. Two ATP synthase genes (MSTRG.23375 and MSTRG.11595) were significantly over-expressed in stage TA (Additional file 5). This increase in the availability of ATP for expensive-energy driven processes is consistent with a previous report (Killiny et al., 2017) reported that the ATP levels were significantly higher in CLas-infected than in CLas-free psyllids. Gene expression analysis showed upregulation of ATP synthase subunits, while ATPase enzyme activity was lower in CLas-infected psyllids. Further, ATP synthase subunit expression was about 5-fold greater in CLas-infected ACP indicating that the CLas alters the energy metabolism of its insect vector. These results suggest such changes are not due solely to changes at the biochemical/metabolic level but rather that they are regulated by specific changes in expression of the genes that control those metabolic processes.

This latter result is consistent with the results of a recent study in which a total of 196 mitochondrial proteins were identified in the ACP gut proteome, and 25 of 26 differentially expressed proteins in CLas-infected ACP guts were downregulated, resulting in widespread depression of mitochondrial function (Kruse et al., 2017). In this study, however, the latter genes, analyzed for whole psyllids (not gut, only) were mostly over-expressed in senior nymphal stages (especially in instar 4-5) and adult stages

(especially in TA), and under-expressed in junior nymphal stages, especially instar 1-2 and instar 3. These observations suggested that CLas infection regulates the ACP energy metabolism of the psyllid host and vector, most likely obtaining direct energy for multiplication and growth in the form of ATP from its host. This observation may further provide insights into requirements for CLas culturing *in vivo*. A recent transcriptome profiling of CLas in citrus and psyllids has also identified genes related to transcription or translation associated with resilience to plant host defense response that were upregulated in citrus. Strikingly, genes involved in energy generation were expressed at higher levels in ACP host, compared to the citrus host plant (De Francesco et al., 2022).

Ubiquitination, cellular stress and apoptosis to CLas infection

Ubiquitin modification or ubiquitination has critical functions in recognition and clearance of certain invading bacteria through autophagy and also exert multiple effects on the host immune system. The ubiquitin-proteasome system (UPS) is a key signaling pathway in host responsiveness to bacterial or viral pathogen infection (Kocaturk and Gozuacik, 2018), and to infect their host, some bacterial effectors interfere with the process, for example, by catalyzing attachment of ubiquitin to host proteins and subvert cell functions (Dupont et al., 2010; Vozandychova et al., 2021) Ubiquitination of proteins regulates protein stability, receptor internalization, enzyme activity, and protein-protein interactions, including receptor-mediated endocytosis, signaling, and membrane protein trafficking (Raiborg and Stenmark, 2009). In this study, a number of ubiquitination- and proteasome-related proteins/genes were identified with predicted involvement in post-translational attachment of ubiquitin to a target proteins that function in cell cycle progression, and cell proliferation, and development. Most of these genes were over-expressed in CLas infected ACP, most notably in immature stages 4 and 5 (I-4,5) and teneral adults (TA) (Additional file 7), and further, some were represented among the top 50 DEGs (Additional file 4).

Interestingly, nearly all top over-expressed genes with greater than 1000-fold that were overexpressed in infected immature instars 4 and 5 (I-4,5), compared to infected immature instar 3 (I-3), were assigned to the ubiquitin-proteasome system (UPS) and membrane trafficking pathways, including SPRY domain-containing SOCS box protein 3 (MSTRG.18581), AN1-type zinc finger and ubiquitin domain-containing protein 1 (MSTRG.15367), dynein light chain roadblock-type (MSTRG.10226), 20S proteasome subunit beta 1 (MSTRG.6586), E3 ubiquitin-protein ligase RNF115/126 (MSTRG.16443). These proteins/genes are involved in bacterial infection, cell stress response, and the host immunological processing of endogenous antigens. These results indicated that the stage 4-5 instar (I-4,5) is a highly important stage or point of switching from somewhat benign interactions with the host, to accelerated CLas invasion, requiring a more robust response to CLas infection, based on the evidence that more DEGs dominated in the instar 4-5 stage. This is consistent with the previous identification of a number of ubiquitination and proteasome-related DEGs in the ACP midgut, in response to CLas infection (Yu et al., 2020) and supports the hypothesis that CLas may activate host ubiquitination to eliminate immune-related proteins.

Heat shock proteins (HSPs) are ubiquitous and conserved chaperones with cytoprotective activities that are known to be particularly prominent under pathological conditions through the initiation of protein folding, repair, and refolding to minimize cellular damage and apoptosis (Ikwegbue et al., 2017). The HSPs have been recognized as important immune-response proteins that combat biological and environmental stresses in well-studied insect systems (Aguilar et al., 2005; Gotz et al., 2012). Consistent with the recent report (Liu et al., 2020), in this study, several heat shock protein genes were among the top 50 under-expressed gene list, with some shared among the different life stages/groups (Additional file 3). This differential regulation of HSPs strongly suggests that CLas infection activates and then depresses the ACP immune system to modulate attack by the host at particular times in the infection process over others, relative to key 'pathogenesis' requirements required during each different host life stage or group (herein).

Apoptosis is a kind of programmed cell death that is important for many processes, among which are immunity, development, and cell homeostasis. Virus-associated apoptosis has been reported in the brown planthopper, *Nilaparvata lugens* (Stål), the vector of *Rice ragged stunt virus* (RRSV), in which RRSV is propagative. The RRSV was shown to induce apoptosis in the salivary gland cells of *N. lugens*, which was regulated in a caspase-dependent manner. The inhibition of expression of *N. lugens caspase-1* genes was found to significantly interfer with virus transmission (Huang et al., 2015). A recent study has reported apoptosis occurs in CLas-exposed ACP guts (Kruse et al., 2017). Significantly more nuclear fragmentation was observed in midgut cells of adults compared to ones of nymph, and protein biomarkers of apoptosis were more abundant in midguts of CLas(+) compared to infected adult insects (Ghanim et al., 2016; Kruse et al., 2017; Mann et al., 2018). Differences in histone cross-links observed between CLas(+) nymphs and adult *D. citri* suggested that while nuclear fragmentation and apoptosis were observed in adult midguts during CLas acquisition, nymph midgut nuclear morphology was largely unaffected by insect exposure to CLas (Ramsey et al., 2022). In this study, of the 90 ACP DEGs identified in this pathway, 20, 25, 24, 17, and 4 were significantly ($p<0.05$) differentially expressed in response to CLas infection of immature instar1-2, instar3, instar4-5, TA and MA stages, respectively (Additional file 8). The 19 up-regulated genes ($p<0.05$) in stage TA found to be most responsive to CLas infection were expressed in the apoptosis pathway diagram (Figure 5).

Adhesion, endocytosis, and cytoskeleton changes potentially involved in entry and systemic invasion

Adhesion molecules are sticky cell-surface molecules that facilitate intercellular binding and communication and govern

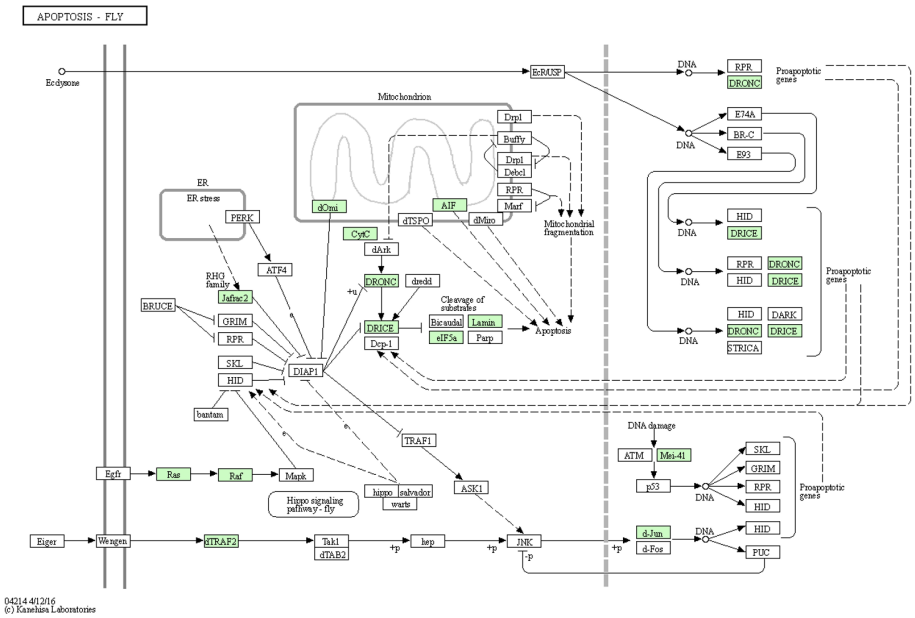

FIGURE 5
Apoptosis pathway diagram showing the 19 up-regulated genes (P<0.05) in the teneral adult stage, responsive to '*Candidatus* Liberibacter asiaticus' infection. Assigned genes are shaded in green.

cell-to-cell interactions necessary for pathogen detection by the host. The plant-pathogenic bacterium *Xylella fastidiosa* adhesins binds to carbohydrates, an interaction essential for the initial cell attachment to the leafhopper vector, the requisite for bacterial transmission to the host plant (Killiny et al., 2012). Among the top-50 over-expressed gene list, a cell adhesion molecule related to protocadherin-15 (MSTRG.4446) was identified in the teneral adult stage. Interestingly, two under-expressed cell adhesion molecule genes (MSTRG.21105, MSTRG.19362), also among the top-50-list of genes, were identified in the youngest two immature instar stages (I12) and in mature ACP adult stage, respectively. Among DEGs, 134 genes assigned to the focal adhesion category were significantly ($p < 0.05$), differentially expressed in all stages, with more over-expressed (n=99) than under-expressed (n=35) genes (Figure 3 and Additional file 8). Most of the over-expressed genes were assigned to cuticle proteins, serine/threonine-protein phosphatase, zinc finger protein, adhesive plaque matrix protein, Ras-related C3 botulinum toxin substrate 1, laminin, talin and vitellogenin, potentially indicative of adhesion leading to active cytoskeletal and endosomal remodeling, and/or endo-exocytosis in the insect vector gut, potentiating hemolymph entry and translocation (systemic spread) and/or salivary glands association and entry.

Endocytosis is known to facilitate host invasion by many viral and bacterial pathogens (Ungewickell and Hinrichsen, 2007; Glebov, 2020). More recently, evidence suggests that the severe acute respiratory syndrome coronavirus 2 (SARS-CoV-2) may employ distinct endocytic pathways for entry of the upper and lower respiratory tract, leading to the consideration of clinically approved drugs as potential candidates for repurposing them as blockers of the different potential routes for SARS-CoV-2 endocytosis (Glebov, 2020). The pathogen *Salmonella enterica* remodels the host cell endosomal system for efficient intravacuolar nutrition (Liss et al., 2017). Both biological adhesion and endocytosis appeared to be extremely important to CLas-ACP interactions, specifically, CLas-cell attachment during entry and later, for biofilm formation, and to facilitate exit from the gut to the lumen. Among 185 identified DEGs in the endocytosis pathway, they are distributed in different stages with more over-expressed in teneral adult stage (TA) (46 up- and 7 under-expressed), with a greater number being under-expressed in immature instars 4 and 5 (I4-5) (19 over-expressed and 30 under-expressed) in response to CLas infection (Additional file 8). The 47 genes that were most significantly up-regulated ($p<0.05$) in the TA stage, in response to CLas infection, were expressed in the endocytosis pathway diagram (Figure 6). Based on these results, it can be posited that the early ACP developmental stages, e.g. instars 1-3, were not as responsive to CLas, as are the late immature stages, instars 4-5, and teneral adults (TA), which is consistent with the results of a previous study (Vyas et al., 2015). Thus, the instars 4-5 exhibited the most actively-responsive stage to CLas infection/invasion processes underway, with many more genes showing differential expression in this stage than in the three (youngest) immature stages (I-1,2 and I-3), the latter stages when CLas is hypothesized to be targeted effectively by ACP host defenses (Fisher et al., 2014; Vyas et al., 2015), compared to the most being under-expressed genes in the two oldest immature instar stages (I-4,5). In the latter two stages (I-4,5), it may be that CLas down-regulates endocytosis-related gene expression to prevent death of ACP before CLas can be transmitted to the plant host.

The cytoskeleton is well-known for its roles in cell division, shape, cell motility and intracellular transport and has important functions in innate immunity and cellular self-defense against

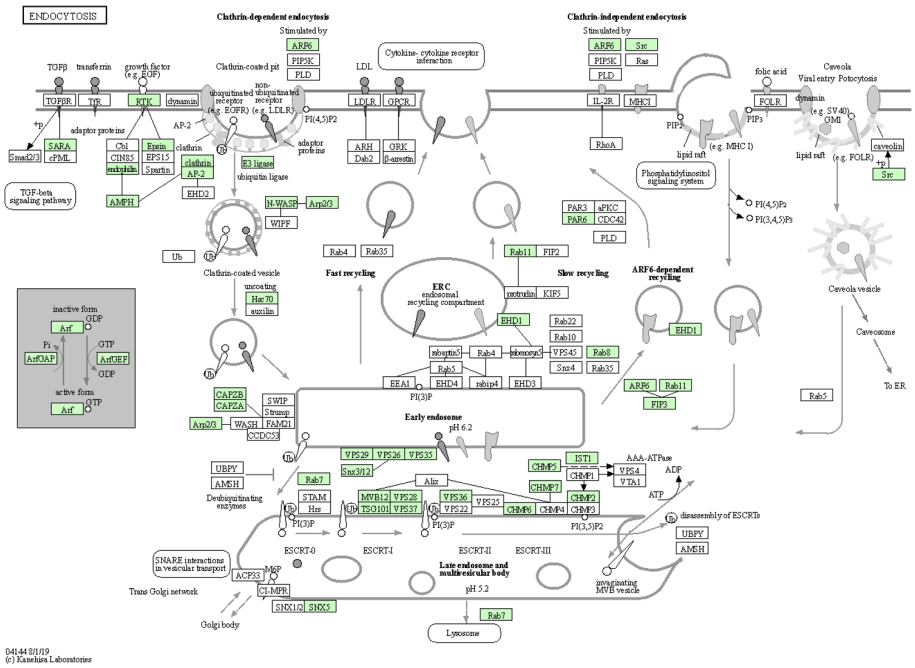

FIGURE 6
Endocytosis pathway diagram showing the 47 up-regulated genes (P<0.05) in the teneral adult stage, responsive to '*Candidatus* Liberibacter asiaticus' infection. Assigned genes are shaded in green.

bacterial and viral pathogens (Mostowy and Shenoy, 2015). Characteristic of the arms race, bacterial pathogens have mechanisms to avoid or exploit the autophagy machinery (which utilizes the cytoskeleton) for intracellular survival (Mostowy, 2014). A recent quantitative analysis of ubiquitylome-proteome crosstalk showed that cytoskeleton proteins were associated with CLas infection of ACP, in that 21 lysine ubiquitinated proteins were associated with the cytoskeleton functions (Zhang et al., 2023). Further, the structure of the cytoskeleton has been shown to undergo modification in the *D. citri* midgut post-CLas infection (Ghanim et al., 2016), an observation that is supported by the previous *in silico* predictions based on comparative transcriptome analysis (Fisher et al., 2014; Vyas et al., 2015). Also, quantitative isotope-labeled cross-linker proteomics investigation revealed developmental variation in protein interactions and post-translational modifications in CLas infection of ACP. The most represented protein category among cross-linking proteins abundant in both ACP nymphs and adults were cytoskeleton/muscle protein complexes which might be expected to represent hallmark morphological and behavioral differences between different ACP life stages, reported in a previous study (Ramsey et al., 2022). These collective observations suggest that CLas differentially alters certain cytoskeletal proteins during invasion and infection processes as CLas pathogen infection of ACP proceeds.

In this study, 130 DEGs associated with regulation of the actin cytoskeleton were identified, and most were upregulated in the CLas-infected groups, compared to the CLas-free groups (Additional file 8). More importantly, some cytoskeleton-related genes (such as actin-binding protein gene MSTRG.12781, tubulin monoglycylase gene MSTRG.9444, katanin p60 ATPase-containing subunit A1 gene MSTRG.20422) were listed in the top-50 DEGs and were highly over-expressed in stages I45 and TA compared to stage I3 in response to CLas infection (Additional file 4). These results indicate that ACP responds strongly to CLas infection at the latter stages of nymphal development in a manner that appears to abate further infection/multiplication of the CLas pathogen, potentially explaining, at least in part, why ACP appears to be much more susceptible to long-term, successful colonization by CLas when infection occurs during early nymphal development stages, e.g. prior to instars 4,5 (I-4,5).

Immune and defense responses

A number of immunity related genes (Kruse et al., 2017) responded at different stages of ACP development to CLas infection, including immune regulating signaling pathways, Toll signaling pathway, JAK/STAT pathway, and ABC transporter activity (Table 3). The Toll signaling pathway plays a key role in the innate immune system. This immune pathway is responsible for activation of antimicrobial peptides involved in the inhibition of dengue virus proliferation in symbiotic *Wolbachia*-infected mosquitoes (Pan et al., 2012). The Janus kinase/signal transducer of activators of transcription (JAK/STAT) pathway is linked to many developmental processes, in addition to a major role in immunity. A number of differentially expressed genes in these pathways were identified with more over-expressed than under-

10.3389/fpls.2023.1229620

TABLE 3 Immune response and transmission pathway-related genes in response to '*Candidatus* Liberibacter asiaticus' (CLas) infection of ACP.

GO Description	GO ID	Assigned Contigs	Up-regulated contigs	UP%	Down-regulated contigs	Down%
Immune regulating signaling pathway	GO: 0002764	617	130	21	18	3
Toll signaling pathway	GO: 0008069	181	9	5	0	0
JAK/STAT pathway	GO: 0007259	88	6	7	0	0
ABC transporter activity	GO: 0043190	69	6	9	2	3
Protease-binding activity	GO: 0002020	258	49	19	5	2
Antimicrobial response	GO: 0019730	244	48	20	10	4
Pathogenesis	GO: 0009405	665	99	15	13	2
Autophagy	GO: 0006914	1174	226	19	31	3
Endocytosis	GO: 0006897	1665	212	13	28	2
Exocytosis	GO: 0006887	798	120	15	2	1

expressed genes (on average, 11% up- compared to 2% under-expressed) (Table 3). Among 244 genes assigned to the antimicrobial response category, 48 (20%) were over-expressed, and 10 (4%) were under-expressed, including, notably, a transferrin gene exhibiting 9-fold and 3-fold upregulation in instars 1-2 and mature adults, respectively. Significant differences between insect and mammalian systems exist with respect to ferritin/transferrin-related iron metabolism (Kosmidis et al., 2011; Meyron-Holtz et al., 2011). Specifically, unlike in mammals, insect transferrins and ferritins have key roles in iron transport, with insect ferritins usually being secreted proteins. In comparative transcriptome studies of CLas-infected ACP and CLso-infected potato psyllid, the importance of iron-chelating functions was suggested based on over-expression of iron- and iron-transport genes, which suggested the exploitation of ACP by CLas for iron nutrition (Fisher et al., 2014; Vyas et al., 2015), Transferrin, on the other hand, is a glycoprotein required for iron transport, is recognized by bacterial outer membrane receptors of transferrin-iron complexes and is also recognized as a virulence determinant for *Wuchereria bancrofti*, causal agent of elephantiasis, which is transmitted by *Aedes aegypti* in a circulative-propagative manner (Magalhaes et al., 2008). It seems likely that this protein functions similarly in the CLas-ACP pathosystem.

Further, a cathepsin L1-like gene was highly over-expressed in all stages after CLas infection, especially in instar1-2 with up to 1000-fold change. Cysteine proteinases, which contain various proteinases, including cathepsins B (cathB), C, F, H, K, and L etc., are involved in multiple functions such as extracellular matrix turnover, antigen presentation, processing events, digestion, immune invasion (Verma et al., 2016). Insect cysteine proteinases play roles in tissue remodeling, molting and metamorphosis during development (Wang et al., 2010). In aphid, gut cathepsin indirectly modulates virus transmission. Host plants indirectly influence plant virus transmission by altering gut cysteine protease activity of aphid vectors. The increased activity of cathB and other cysteine proteases at the cell membrane indirectly decreases virus transmission by aphids, indicating that cathB clearly has important functions in the aphid gut. A similar process may occur in ACP in response to CLas infection, and indeed, has been implicated in a previous comparative transcriptome study (Vyas et al., 2015).

Taken together, these results indicated that CLas infection significantly affects immune response-related genes in different life stages of ACP. These transmission-related genes apparently have different roles based on the differential expression patterns observed among the different ACP life stages, which are expected to harbor a life-stage specific 'physiological environment'. Consistent with a recent study of the CLas-infected ACP by comparative transcriptome analyses, 499 over-expressed DEGs and 279 under-expressed DEGs were identified that were associated with ubiquitination, immune response, the ribosome, endocytosis, cytoskeleton, and detoxification (i.e. insecticide resistant phenotype). The KEGG analysis revealed that most DEGs were involved in endocytosis and the ribosome (Yu et al., 2020). Integrating these new and archived organ-specific transcriptome data, also showed that the top DGEs from each dataset (bacteriome, midgut, and salivary gland) were sorted by major functional groups including ubiquitination, endocytosis, immunity, and ribosomal-related transcripts (Mann et al., 2022).

In summary, these results have shown that gene expression varies significantly among the different CLas-infected ACP developmental and physiologically distinct stages with respect to responsiveness to CLas-pathogenesis. The infection cycle is expected to initiate with the youngest immature instar, and culminates in the mature adult, which serves as the CLas vector to both the plant and psyllid hosts. Inoculated flush leaves serve as the source of CLas inoculum for ingestion and subsequent infection of young ACP offspring that ingest CLas from citrus leaves on which they feed immediately after hatching. The requirement for early-stage CLas infection of the offspring and for efficient acquisition (to salivary glands) that results in efficient transmission by the adult stage suggests that the barrier to further acquisition may be established by the 4-5th immature instar stage. The different ACP gene expression profiles associated with each immature instar group (1,2 and 3,4) or single instar (3), and the teneral and mature adult psyllids reflect a dynamic infection process, and is consistent with a propagative, circulative mode of ACP-mediated CLas transmission. The nymphal instars 4-5 and teneral adults mounted the most striking responses to CLas infection, based on the greatest number of up or down-regulation genes, during the CLas infection cycle, dramatically more-so than the nymphal instars 1-2, instar 3 and mature, or mature adults. Through this global differential analysis of the transcriptome profiles for the CLas-infected and CLas-free ACP host, the five groups (1,2; 3, 4; teneral adult, mature adult) and/or single immature instar-3, which represent distinct developmental stages, distinct life-stage physiological requirements have been revealed in response to CLas infection. Among them are hallmark genes and biological pathways involved in psyllid development, nutrition, immunity in relation to CLas invasion and systemic infection of the ACP host, consistent with and recognizable in well-studied pathosystems and host-parasite interactions. This new knowledge will go far to enhance the understanding of host-pathogen interactions in the numerous psyllid - 'Ca. Liberibacter' pathosystems recently recognized as emergent vector-pathogen complexes in agricultural crops worldwide.

Conclusion

The central hypothesis of this study is that different ACP life stages influence gene expression that reflect differential responsiveness to CLas infection in a manner that is consistent with the circulative, propagative mode of ACP transmission of the CLas pathogen, unusual in its ability to infect both its psyllid and plant host. These results demonstrate that the early psyllid life-stages are critical targets of CLas invasion, multiplication, circulation, and acquisition or entry into the salivary glands and possibly the oral cavity. The CLas pathogen significantly altered the expression of a diverse repertoire of ACP genes, with the nymphal instars 4-5 and teneral adults in particular, exhibiting the greatest changes in gene expression in response to CLas infection, both in magnitude (fold change in expression) and richness (numbers of responsive genes). These observations further suggest that adults, particularly, the teneral and mature adults have evolved some extent of tolerance to CLas infection and/or that CLas may modulate certain ACP physiological processes to slow the accumulation of detrimental pathogenic effects, outcome(s), of which either or both scenarios may be attributable to long-term host-pathogen co-evolution (Fisher et al., 2014; Vyas et al., 2015). Regardless of mechanism, CLas survival is ensured because ACP-mediated CLas transmission occurs before the psyllid host and vector becomes debilitated by the infection and succumbs to death (Cicero et al., 2017).

Age- and lifespan-related factors are known in other insect vector-pathosystems to be determinants of transmission efficiency. Somewhat notable among known plant insect vector-transmitted fastidious bacterial pathosystems, the ACP immature instars or nymphs, rather than adults, are the chief life stages involved in CLas acquisition, albeit this feature has been commonly associated with the circulative, propagative mode of transmission employed by certain plant virus-insect pathosystems. Gene expression patterns, in particular, that were associated with the instar 4–5 group and teneral (immature) adults, revealed that psyllid defenses are most responsive during the transition period between nymph and adult, thereby potentially diminishing the potential for CLas acquisition by ACP during this developmental window. The developmental stage-associated changes in gene expression that reflect direct response to CLas infection and pathogenesis further supports the observation the dynamics between ACP development and CLas infection, acquisition, and transmission (vector) potential are tightly coordinated.

Some or most DEGs identified here represent potential candidate gene targets for further elucidating CLas-ACP interactions involved in transmission through functional genomics studies, and also for translation to RNAi-mediated strategies for ACP/HLB management. The deployment of RNAi as a component of integrated management approaches for ACP-CLas pathosystem has promise as an alternative or complementary strategy to the intensive chemical control of ACP that embodies the primary management strategy advocated for HLB, although that strategy is costly, unsustainable, and has in general, been ineffective in the long-term particularly, once persistent infection of citrus-growing areas has manifested (Hall, 2013).

This study provides the first the evidence for detailed ACP-stage specific differential expression of immature instars 1,2 compared to 3, and 4-5 and the teneral and mature adult stages, and highlights a number of potential candidates for functional genomic, follow-on validation to better understand host-pathogen mechanisms and processes that drive the success of the ACP-CLas pathosystem and has intriguing applications to other insect vector-borne pathogen complexes.

Data availability statement

The datasets presented in this study can be found in online repositories. The names of the repository/repositories and accession number(s) can be found in the article/Supplementary Material.

Author contributions

RH, DG and JB contributed to the conception and design of the study. RH conducted the RNA-seq library construction and sequencing. RH, TF, SS and MW performed the data analysis. KP-S provided insect samples. JB and DG contributed with research grant funding application and management. RH wrote the first draft of the manuscript. RH, DG and JB wrote the final version of the manuscript. All authors contributed to the article and approved the submitted version.

Funding

The authors declare that this study received funding from the Florida Citrus Res. & Dev. Foundation: Citrus psyllid transcriptome and time course differential expression in whole psyllids and psyllid organs. 2010- 2013. Grant #21; and the USDA-NIFA SRCRI. NuPsyllid-Rear and release psyllids as biocontrol for HLB. 2013-2017. Subcontract: Citrus Research and Development Foundation, Inc. 13-005NU-784. The funders were not involved in the study design, collection, analysis, interpretation of data, the writing of this article or the decision to submit it for publication.

Conflict of interest

The authors declare that the research was conducted in the absence of any commercial or financial relationships that could be construed as a potential conflict of interest.

Publisher's note

Supplementary material

The Supplementary Material for this article can be found online at: https://www.frontiersin.org/articles/10.3389/fpls.2023.1229620/full#supplementary-material

References

Aguilar, R., Jedlicka, A. E., Mintz, M., Mahairaki, V., Scott, A. L., and Dimopoulos, G. (2005). Global gene expression analysis of Anopheles Gambiae responses to microbial challenge. *Insect Biochem. Mol. Biol.* 35, 709–719. doi: 10.1016/j.ibmb.2005.02.019

Ammar, E. D., George, J., Sturgeon, K., Stelinski, L. L., and Shatters, R. G. (2020). Asian citrus psyllid adults inoculate huanglongbing bacterium more efficiently than nymphs when this bacterium is acquired by early instar nymphs. *Sci. Rep.* 10, 18244. doi: 10.1038/s41598-020-75249-5

Ammar, E., Shatters, R. G., Lynch, C., and Hall, D. G. (2011). Detection and Relative Titer of Candidatus Liberibacter asiaticus in the Salivary Glands and Alimentary Canal of Diaphorina citri (Hemiptera: Psyllidae) Vector of Citrus Huanglongbing Disease. *Ann. Entomological Soc. America* 104, 526–533. doi: 10.1603/AN10134

Ammar El, D., Ramos, J. E., Hall, D. G., Dawson, W. O., and Shatters, R. G.Jr. (2016). Acquisition, Replication and Inoculation of Candidatus Liberibacter asiaticus following Various Acquisition Periods on Huanglongbing-Infected Citrus by Nymphs and Adults of the Asian Citrus Psyllid. *PloS One* 11, e0159594. doi: 10.1371/journal.pone.0159594

Andrews, S. *FastQC: A quality control tool for high throughput sequence data*. Available at: http://www.bioinformatics.babraham.ac.uk/projects/fastqc/.

Bolger, A. M., Lohse, M., and Usadel, B. (2014). Trimmomatic: a flexible trimmer for Illumina sequence data. *Bioinformatics* 30, 2114–2120. doi: 10.1093/bioinformatics/btu170

Cicero, J. M., Fisher, T. W., Qureshi, J. A., Stansly, P. A., and Brown, J. K. (2017). Colonization and intrusive invasion of potato psyllid by 'Candidatus liberibacter solanacearum'. *Phytopathology* 107, 36–49. doi: 10.1094/PHYTO-03-16-0149-R

De Francesco, A., Lovelace, A. H., Shaw, D., Qiu, M., Wang, Y., Gurung, F., et al. (2022). Transcriptome profiling of 'Candidatus liberibacter asiaticus' in citrus and psyllids. *Phytopathology* 112, 116–130. doi: 10.1094/PHYTO-08-21-0327-FI

Dos Santos Silva, J., De Santana Cerqueira, L. R., Hunter, W. B., and De Andrade, E. C. (2022). RNAi feeding bioassay: A protocol for dsRNA screening against asian citrus psyllid and related hemipteran insects. *Methods Mol. Biol.* 2360, 85–90. doi: 10.1007/978-1-0716-1633-8_8

Dupont, N., Temime-Smaali, N., and Lafont, F. (2010). How ubiquitination and autophagy participate in the regulation of the cell response to bacterial infection. *Biol. Cell* 102, 621–634. doi: 10.1042/BC20100101

El-Shesheny, I., Hajeri, S., El-Hawary, I., Gowda, S., and Killiny, N. (2013). Silencing abnormal wing disc gene of the Asian citrus psyllid, Diaphorina citri disrupts adult wing development and increases nymph mortality. *PloS One* 8, e65392. doi: 10.1371/journal.pone.0065392

Fisher, T. W., Vyas, M., He, R., Nelson, W., Cicero, J. M., Willer, M., et al. (2014). Comparison of potato and asian citrus psyllid adult and nymph transcriptomes identified vector transcripts with potential involvement in circulative, propagative liberibacter transmission. *Pathogens* 3, 875–907. doi: 10.3390/pathogens3040875

Ghanim, M., Fattah-Hosseini, S., Levy, A., and Cilia, M. (2016). Morphological abnorMalities and cell death in the Asian citrus psyllid (Diaphorina citri) midgut associated with Candidatus Liberibacter asiaticus. *Sci. Rep.* 6, 33418. doi: 10.1038/srep33418

Glebov, O. O. (2020). Understanding SARS-CoV-2 endocytosis for COVID-19 drug repurposing. *FEBS J* 287, 3664–3671. doi: 10.1111/febs.15369

Gottwald, T. R. (2010). Current epidemiological understanding of citrus Huanglongbing. *Annu. Rev. Phytopathol.* 48, 119–139. doi: 10.1146/annurev-phyto-073009-114418

Gotz, M., Popovski, S., Kollenberg, M., Gorovits, R., Brown, J. K., Cicero, J. M., et al. (2012). Implication of Bemisia tabaci heat shock protein 70 in Begomovirus-whitefly interactions. *J. Virol.* 86, 13241–13252. doi: 10.1128/JVI.00880-12

Grafton-Cardwell, E. E., Stelinski, L. L., and Stansly, P. A. (2013). Biology and management of Asian citrus psyllid, vector of the huanglongbing pathogens. *Annu. Rev. Entomol* 58, 413–432. doi: 10.1146/annurev-ento-120811-153542

Guo, C. F., Qiu, J. H., Hu, Y. W., Xu, P. P., Deng, Y. Q., Tian, L., et al. (2022). Silencing of V-ATPase-E gene causes midgut apoptosis of Diaphorina citri and affects its acquisition of Huanglongbing pathogen. *Insect Sci* 30, 1022–1034. doi: 10.1111/1744-7917.13146

Hall, D.G.R.,M.L., Ammar, E. D., and Halbert, S. E. (2013). Asian citrus psyllid, Diaphorina citri, vector of citrus huanglongbing disease. *Entomologia Experimentalis Applicata* 146, 207–223. doi: 10.1111/eea.12025

Hannon, G. J. (2002). RNA interference. *Nature* 418, 244–251. doi: 10.1038/418244a

Hosmani, P. S., Flores-Gonzalez, M., Shippy, T., Vosburg, C., Massimino, C., Tank, W., et al. (2019). Chromosomal length reference assembly for Diaphorina citri using single-molecule sequencing and Hi-C proximity ligation with manually curated genes in developmental, structural and immune pathways. *bioRxiv* 1-24. doi: 10.1101/869685

Huang, H. J., Bao, Y. Y., Lao, S. H., Huang, X. H., Ye, Y. Z., Wu, J. X., et al. (2015). Rice ragged stunt virus-induced apoptosis affects virus transmission from its insect vector, the brown planthopper to the rice plant. *Sci. Rep.* 5, 11413. doi: 10.1038/srep11413

Ikwegbue, P. C., Masamba, P., Oyinloye, B. E., and Kappo, A. P. (2017). Roles of heat shock proteins in apoptosis, oxidative stress, human inflammatory diseases, and cancer. *Pharm. (Basel)* 11, 1–18. doi: 10.3390/ph11010002

Jain, R. G., Robinson, K. E., Asgari, S., and Mitter, N. (2021). Current scenario of RNAi-based hemipteran control. *Pest Manag Sci.* 77, 2188–2196. doi: 10.1002/ps.6153

Kanehisa, M., Sato, Y., Kawashima, M., Furumichi, M., and Tanabe, M. (2016). KEGG as a reference resource for gene and protein annotation. *Nucleic Acids Res.* 44, D457–D462. doi: 10.1093/nar/gkv1070

Kelley, A. J., and Pelz-Stelinski, K. S. (2019). Maternal contribution of candidatus liberibacter asiaticus to asian citrus psyllid (Hemiptera: liviidae) nymphs through

oviposition site inoculation and transovarial transmission. *J. Econ Entomol* 112, 2565–2568. doi: 10.1093/jee/toz197

Killiny, N., Hajeri, S., Tiwari, S., Gowda, S., and Stelinski, L. L. (2014). Double-stranded RNA uptake through topical application, mediates silencing of five CYP4 genes and suppresses insecticide resistance in Diaphorina citri. *PloS One* 9, e110536. doi: 10.1371/journal.pone.0110536

Killiny, N., Hijaz, F., Ebert, T. A., and Rogers, M. E. (2017). A plant bacterial pathogen manipulates its insect vector's energy metabolism. *Appl. Environ. Microbiol.* 83, e03005-16. doi: 10.1128/AEM.03005-16

Killiny, N., Rashed, A., and Almeida, R. P. (2012). Disrupting the transmission of a vector-borne plant pathogen. *Appl. Environ. Microbiol.* 78, 638–643. doi: 10.1128/AEM.06996-11

Kim, D., Paggi, J. M., Park, C., Bennett, C., and Salzberg, S. L. (2019). Graph-based genome alignment and genotyping with HISAT2 and HISAT-genotype. *Nat. Biotechnol.* 37, 907–915. doi: 10.1038/s41587-019-0201-4

Kishk, A., Anber, H. A., Abdel-Raof, T. K., El-Sherbeni, A. D., Hamed, S., Gowda, S., et al. (2017). RNA interference of carboxyesterases causes nymph mortality in the Asian citrus psyllid, Diaphorina citri. *Arch. Insect Biochem. Physiol.* 94, 1–13. doi: 10.1002/arch.21377

Kocaturk, N. M., and Gozuacik, D. (2018). Crosstalk between mamMalian autophagy and the ubiquitin-proteasome system. *Front. Cell Dev. Biol.* 6, 128. doi: 10.3389/fcell.2018.00128

Kosmidis, S., Botella, J. A., Mandilaras, K., Schneuwly, S., Skoulakis, E. M. C., Rouault, T. A., et al. (2011). Ferritin overexpression in Drosophila glia leads to iron deposition in the optic lobes and late-onset behavioral defects. *Neurobiol. Dis.* 43, 213–219. doi: 10.1016/j.nbd.2011.03.013

Kruse, A., Fattah-Hosseini, S., Saha, S., Johnson, R., Warwick, E., Sturgeon, K., et al. (2017). Combining 'omics and microscopy to visualize interactions between the Asian citrus psyllid vector and the Huanglongbing pathogen Candidatus Liberibacter asiaticus in the insect gut. *PloS One* 12, e0179531. doi: 10.1371/journal.pone.0179531

Ledford, H. (2017). PLANT PATHOLOGY Engineered virus in line to battle citrus disease. *Nature* 545, 277–278. doi: 10.1038/545277a

Li, W., Hartung, J. S., and Levy, L. (2006). Quantitative real-time PCR for detection and identification of Candidatus Liberibacter species associated with citrus huanglongbing. *J. Microbiol. Methods* 66, 104–115. doi: 10.1016/j.mimet.2005.10.018

Liss, V., Swart, A. L., Kehl, A., Hermanns, N., Zhang, Y., Chikkaballi, D., et al. (2017). Salmonella enterica remodels the host cell endosomal system for efficient intravacuolar nutrition. *Cell Host Microbe* 21, 390–402. doi: 10.1016/j.chom.2017.02.005

Liu, K., He, J., Guan, Z., Zhong, M., Pang, R., and Han, Q. (2020). Transcriptomic and metabolomic analyses of diaphorina citri kuwayama infected and non-infected with candidatus liberibacter asiaticus. *Front. Physiol.* 11, 630037. doi: 10.3389/fphys.2020.630037

Magalhaes, T., Oliveira, I. F., Melo-Santos, M. A., Oliveira, C. M., Lima, C. A., and Ayres, C. F. (2008). Expression of defensin, cecropin, and transferrin in Aedes aEgypti (Diptera: Culicidae) infected with Wuchereria bancrofti (Spirurida: Onchocercidae), and the abnormal development of nematodes in the mosquito. *Exp. Parasitol.* 120, 364–371. doi: 10.1016/j.exppara.2008.09.003

Mann, M., Fattah-Hosseini, S., Ammar, E. D., Stange, R., Warrick, E., Sturgeon, K., et al. (2018). Diaphorina citri Nymphs Are Resistant to Morphological Changes Induced by "Candidatus Liberibacter asiaticus" in Midgut Epithelial Cells. *Infect. Immun.* 86, 1–19. doi: 10.1128/iai.00889-17

Mann, R. S., Pelz-Stelinski, K., Hermann, S. L., Tiwari, S., and Stelinski, L. L. (2011). Sexual transmission of a plant pathogenic bacterium, Candidatus Liberibacter asiaticus, between conspecific insect vectors during mating. *PloS One* 6, e29197. doi: 10.1371/journal.pone.0029197

Mann, M., Saha, S., Cicero, J. M., Pitino, M., Moulton, K., Hunter, W. B., et al. (2022). Lessons learned about the biology and genomics of Diaphorina citri infection with "Candidatus Liberibacter asiaticus" by integrating new and archived organ-specific transcriptome data. *Gigascience* 11, 1–16. doi: 10.1093/gigascience/giac035

Martini, X., Hoffmann, M., Coy, M. R., Stelinski, L. L., and Pelz-Stelinski, K. S. (2015). Infection of an insect vector with a bacterial plant pathogen increases its propensity for dispersal. *PloS One* 10, e0129373. doi: 10.1371/journal.pone.0129373

Meyron-Holtz, E. G., Moshe-Belizowski, S., and Cohen, L. A. (2011). A possible role for secreted ferritin in tissue iron distribution. *J. Neural Transm.* 118, 337–347. doi: 10.1007/s00702-011-0582-0

Mito, T., Nakamura, T., Bando, T., Ohuchi, H., and Noji, S. (2011). The advent of RNA interference in Entomology. *Entomological Sci.* 14, 1–8. doi: 10.1111/j.1479-8298.2010.00408.x

Mondal, M., Carver, M., and Brown, J. K. (2022). Characteristics of environmental RNAi in potato psyllid, Bactericera cockerelli (Sulc) (Hemiptera: Psylloidea: Triozidae). *Front. Physiol.* 13, 931951. doi: 10.3389/fphys.2022.931951

Moriya, Y., Itoh, M., Okuda, S., Yoshizawa, A. C., and Kanehisa, M. (2007). KAAS: an automatic genome annotation and pathway reconstruction server. *Nucleic Acids Res.* 35, W182–W185. doi: 10.1093/nar/gkm321

Mostowy, S. (2014). Multiple roles of the cytoskeleton in bacterial autophagy. *PloS Pathog.* 10, e1004409. doi: 10.1371/journal.ppat.1004409

Mostowy, S., and Shenoy, A. R. (2015). The cytoskeleton in cell-autonomous immunity: structural determinants of host defence. *Nat. Rev. Immunol.* 15, 559–573. doi: 10.1038/nri3877

Nishizawa, Y., Okui, Y., Inaba, M., Okuno, S., Yukioka, K., Miki, T., et al. (1988). Calcium/calmodulin-mediated action of calcitonin on lipid metabolism in rats. *J. Clin. Invest.* 82, 1165–1172. doi: 10.1172/JCI113713

Pacheco, I. S., Galdeano, D. M., Maluta, N. K. P., Lopes, J. R. S., and MaChado, M. A. (2020). Gene silencing of Diaphorina citri candidate effectors promotes changes in feeding behaviors. *Sci. Rep.* 10, 5992. doi: 10.1038/s41598-020-62856-5

Pan, X., Zhou, G., Wu, J., Bian, G., Lu, P., Raikhel, A. S., et al. (2012). Wolbachia induces reactive oxygen species (ROS)-dependent activation of the Toll pathway to control dengue virus in the mosquito Aedes aEgypti. *Proc. Natl. Acad. Sci. United States America* 109, E23–E31. doi: 10.1073/pnas.1116932108

Paredes-Montero, J. R., Arif, U., and Brown, J. K. (2022). Knockdown of ecdysteroid synthesis genes results in impaired molting and high mortality in Bactericera cockerelli (Hemiptera: Triozidae). *Pest Manag Sci.* 78, 2204–2214. doi: 10.1002/ps.6848

Pelz-Stelinski, K. S., Brlansky, R. H., Ebert, T. A., and Rogers, M. E. (2010). Transmission parameters for candidatus liberibacter asiaticus by asian citrus psyllid (Hemiptera: psyllidae). *J. Economic Entomology* 103, 1531–1541. doi: 10.1603/EC10123

Pelz-Stelinski, K. S., and Killiny, N. (2016). Better together: association with 'Candidatus liberibacter asiaticus' Increases the reproductive fitness of its insect vector, diaphorina citri (Hemiptera: liviidae). *Ann. Entomol Soc. Am.* 109, 371–376. doi: 10.1093/aesa/saw007

Pertea, M., Pertea, G. M., Antonescu, C. M., Chang, T. C., Mendell, J. T., and Salzberg, S. L. (2015). StringTie enables improved reconstruction of a transcriptome from RNA-seq reads. *Nat. Biotechnol.* 33, 290–295. doi: 10.1038/nbt.3122

Raiborg, C., and Stenmark, H. (2009). The ESCRT machinery in endosomal sorting of ubiquitylated membrane proteins. *Nature* 458, 445–452. doi: 10.1038/nature07961

Ramsey, J. S., Chavez, J. D., Johnson, R., Hosseinzadeh, S., Mahoney, J. E., Mohr, J. P., et al. (2017). Protein interaction networks at the host-microbe interface in Diaphorina citri, the insect vector of the citrus greening pathogen. *R Soc. Open Sci.* 4, 160545. doi: 10.1098/rsos.160545

Ramsey, J., Zhong, X., Saha, S., Chavez, J., Johnson, R., Mahoney, J., et al. (2022). Quantitative isotope-labeled cross-linker proteomics reveals developmental variation in protein interactions and post-translational modifications in diaphorina citri, the citrus greening insect vector. *ACS Agric. Sci. Technol.* 2, 486–500. doi: 10.1021/acsagscitech.1c00264

Ren, S. L., Li, Y. H., Zhou, Y. T., Xu, W. M., Cuthbertson, A. G., Guo, Y. J., et al. (2016). Effects of Candidatus Liberibacter asiaticus on the fitness of the vector Diaphorina citri. *J. Appl. Microbiol.* 121, 1718–1726. doi: 10.1111/jam.13302

Saha, S., Hosmani, P. S., Villalobos-Ayala, K., Miller, S., Shippy, T., Flores, M., et al. (2017). Improved annotation of the insect vector of citrus greening disease: biocuration by a diverse genomics community. *Database (Oxford)* 2017, 1–20. doi: 10.1093/database/bax032

Santos-Ortega, Y., and Killiny, N. (2018). Silencing of sucrose hydrolase causes nymph mortality and disturbs adult osmotic homeostasis in Diaphorina citri (Hemiptera: Liviidae). *Insect Biochem. Mol. Biol.* 101, 131–143. doi: 10.1016/j.ibmb.2018.09.003

Stokstad, E. (2012). Agriculture. Dread citrus disease turns up in California, Texas. *Science* 336, 283–284. doi: 10.1126/science.336.6079.283

Ungewickell, E. J., and Hinrichsen, L. (2007). Endocytosis: clathrin-mediated membrane budding. *Curr. Opin. Cell Biol.* 19, 417–425. doi: 10.1016/j.ceb.2007.05.003

Verma, S., Dixit, R., and Pandey, K. C. (2016). Cysteine proteases: modes of activation and future prospects as pharmacological targets. *Front. Pharmacol.* 7, 107. doi: 10.3389/fphar.2016.00107

Vozandychova, V., Stojkova, P., Hercik, K., Rehulka, P., and Stulik, J. (2021). The ubiquitination system within bacterial host-pathogen interactions. *Microorganisms* 9, 638. doi: 10.3390/microorganisms9030638

Vyas, M., Fisher, T. W., He, R., Nelson, W., Yin, G., Cicero, J. M., et al. (2015). Asian citrus psyllid expression profiles suggest candidatus liberibacter asiaticus-mediated alteration of adult nutrition and metabolism, and of nymphal development and immunity. *PloS One* 10, e0130328. doi: 10.1371/journal.pone.0130328

Wang, L. F., Chai, L. Q., He, H. J., Wang, Q., Wang, J. X., and Zhao, X. F. (2010). A cathepsin L-like proteinase is involved in moulting and metamorphosis in Helicoverpa armigera. *Insect Mol. Biol.* 19, 99–111. doi: 10.1111/j.1365-2583.2009.00952.x

Wang, N., and Trivedi, P. (2013). Citrus huanglongbing: a newly relevant disease presents unprecedented challenges. *Phytopathology* 103, 652–665. doi: 10.1094/PHYTO-12-12-0331-RVW

Yang, S., Zou, Z., Xin, T., Cai, S., Wang, X., Zhang, H., et al. (2022). Knockdown of hexokinase in Diaphorina citri Kuwayama (Hemiptera: Liviidae) by RNAi inhibits chitin synthesis and leads to abnormal phenotypes. *Pest Manag Sci.* 78, 4303–4313. doi: 10.1002/ps.7049

Yu, X., Gowda, S., and Killiny, N. (2017). Double-stranded RNA delivery through soaking mediates silencing of the muscle protein 20 and increases mortality to the Asian citrus psyllid, Diaphorina citri. *Pest Manag Sci.* 73, 1846–1853. doi: 10.1002/ps.4549

Yu, H. Z., Li, N. Y., Zeng, X. D., Song, J. C., Yu, X. D., Su, H. N., et al. (2020). Transcriptome analyses of diaphorina citri midgut responses to candidatus liberibacter asiaticus infection. *Insects* 11, 171. doi: 10.3390/insects11030171

Zhang, J. B., Zou, X. J., Zhang, Q., Wang, A. Y., Amir, M. B., Du, Y. M., et al. (2023). Quantitative ubiquitylome crosstalk with proteome analysis revealed cytoskeleton proteins influence CLas pathogen infection in Diaphorina citri. *Int. J. Biol. Macromol* 232, 123411. doi: 10.1016/j.ijbiomac.2023.123411

frontiers | Frontiers in Plant Science

TYPE Review
PUBLISHED 30 August 2023
DOI 10.3389/fpls.2023.1232735

OPEN ACCESS

EDITED BY
Shengli Jing,
Xinyang Normal University, China

REVIEWED BY
Qingjun Wu,
Chinese Academy of Agricultural Sciences, China
Ting Chen,
Guangdong Academy of Agricultural Sciences, China
Hai-jian Huang,
Ningbo University, China

*CORRESPONDENCE
Li-Long Pan
panlilong@zju.edu.cn

†These authors share first authorship

RECEIVED 01 June 2023
ACCEPTED 14 August 2023
PUBLISHED 30 August 2023

CITATION
Li D, Li H-Y, Zhang J-R, Wu Y-J, Zhao S-X, Liu S-S and Pan L-L (2023) Plant resistance against whitefly and its engineering. *Front. Plant Sci.* 14:1232735. doi: 10.3389/fpls.2023.1232735

Plant resistance against whitefly and its engineering

Di Li[1†], Heng-Yu Li[1†], Jing-Ru Zhang[1], Yi-Jie Wu[1], Shi-Xing Zhao[1], Shu-Sheng Liu[1] and Li-Long Pan[1,2*]

[1]Ministry of Agriculture Key Laboratory of Molecular Biology of Crop Pathogens and Insects, Key Laboratory of Biology of Crop Pathogens and Insects of Zhejiang Province, Institute of Insect Sciences, Zhejiang University, Hangzhou, China, [2]The Rural Development Academy, Zhejiang University, Hangzhou, China

Plants face constant threats from insect herbivores, which limit plant distribution and abundance in nature and crop productivity in agricultural ecosystems. In recent decades, the whitefly *Bemisia tabaci*, a group of phloem-feeding insects, has emerged as pests of global significance. In this article, we summarize current knowledge on plant defenses against whitefly and approaches to engineer plant resistance to whitefly. Physically, plants deploy trichome and acylsugar-based strategies to restrain nutrient extraction by whitefly. Chemically, toxic secondary metabolites such as terpenoids confer resistance against whitefly in plants. Moreover, the jasmonate (JA) signaling pathway seems to be the major regulator of whitefly resistance in many plants. We next review advances in interfering with whitefly-plant interface by engineering of plant resistance using conventional and biotechnology-based breeding. These breeding programs have yielded many plant lines with high resistance against whitefly, which hold promises for whitefly control in the field. Finally, we conclude with an outlook on several issues of particular relevance to the nature and engineering of plant resistance against whitefly.

KEYWORDS

phloem-feeding insects, *Bemisia tabaci*, plant defense, plant-whitefly interaction, resistance breeding

1 Introduction

Plants, whether wild or cultivated, are constantly confronted with many biotic and abiotic threats (Wilkinson et al., 2019). The biotic threats encompass pathogens such as viruses, bacteria and fungi, as well as herbivores including insects and large animals. Among these biotic factors, insect herbivores are particularly significant due to their remarkable diversity and abundance (Savary et al., 2019; Wilkinson et al., 2019). Extensive research in recent decades has revealed general principles underlying the intimate interactions between insect herbivores and their plant hosts (Erb and Reymond, 2019; Snoeck et al., 2022). Insect herbivores employ a range of behavioral and molecular strategies to facilitate nutrient extraction (Dussourd, 2017; Stahl et al., 2018), while plants deploy various defense responses to deter insect herbivores (Erb and Reymond,

2019; Snoeck et al., 2022). The long-lasting and ongoing arms race between plants and insect herbivores has shaped the ecology and evolution of both groups of organisms in nature (Bergelson et al., 2001; Zust et al., 2012). In agricultural practices, insect herbivores, alongside other pests, pose serious threats to global food security (Savary et al., 2019). Therefore, an improved understanding of plant-insect herbivore interactions is crucial, from both scientific and applied perspectives.

Many insect herbivores such as the whitefly, have specialized in feeding on plant phloem and thus are referred to as phloem-feeding insects. Despite their small size (around 1.0 mm in length for adults), whiteflies are highly prolific, with females each capable of producing dozens to hundreds of eggs depending on environmental conditions (Byrne and Bellows, 1991). Whiteflies cause significant losses to crop through direct sap feeding, inducing plant physiological disorders and promoting the growth of sooty mold (Oliveira et al., 2001; Farina et al., 2022). Moreover, whiteflies can indirectly harm plants by transmitting plant viruses, particularly begomoviruses and criniviruses, resulting in severe viral disease epidemics (Gilbertson et al., 2015; Fiallo-Olivé et al., 2020; Wang and Blanc, 2021). For example, whiteflies are known to vector over 400 viruses belonging to the genus *Begomovirus* through a persistent circulative manner, leading to the occurrence of numerous viral diseases (Gilbertson et al., 2015; Fiallo-Olivé et al., 2020; Wang and Blanc, 2021; Fiallo-Olivé and Navas-Castillo, 2023).

As a group of piercing-sucking insects, the feeding behavior of whitefly differs significantly from that of insects with chewing mouthparts. Correspondingly, the responses of plants to whitefly infestation differ significantly from those mounted against chewing insects (Kaloshian and Walling, 2005; Kempema et al., 2007; Zarate et al., 2007; Walling, 2008; Wang et al., 2017). Additionally, when compared to some other closely-related piercing-sucking insects including aphids, whiteflies are unique in many ways with regard to interactions with plants due to their distinctive size, feeding habits and life history (Walling, 2008; Wang et al., 2017). Therefore, explorations of plant resistance against whitefly may add to our knowledge of insect-plant interactions. More importantly, the distinctiveness of whitefly-plant interactions urges more efforts in resistance engineering as plant cultivars obtained from breeding programs against other groups of insect herbivores may fail to control whitefly. Under this scenario, innovations to specifically augment plant resistance against whitefly are required and will be invaluable in sustaining the production of whitefly-susceptible crops.

The continuous research efforts and rapid development of novel research tools such as omics, have promoted the dissection of plant resistance against whitefly (Zogli et al., 2020). Additionally, in recent years, significant advances have been made in interfering with the whitefly-plant interface through the engineering of plant resistance. In this article, we aim to summarize and review these recent advances. First, we will describe current understanding of plant traits that confer resistance to whitefly. Next, we will summarize the progress made in engineering plant resistance to whitefly using conventional and biotechnology-based breeding. Finally, we will highlight several issues related to the investigation and engineering of plant resistance against whitefly.

2 Plant physical traits that confer resistance to whitefly

Physical traits of resistance impact insect herbivores physically, such as restricting their movement or hindering their feeding. When whiteflies feed on plants (Figure 1A), trichomes and acylsugars serve as major physical traits that confer resistance to whitefly (Figure 1B).

2.1 Trichomes

Trichomes are specialized hairs on the surface of plants that can be epidermal protuberances of different sizes, shapes and arrangements. They can be classified as glandular and non-glandular based on their ability to synthesize, secrete and store substances (Tissier, 2012). The role of trichomes in whitefly-plant interactions has been intensively studied in wild relatives of cultivated tomato, in which trichomes were categorized into seven types with four of them being glandular (types I, IV, VI, and VII) and three being non-glandular (types II, III, and V) (Simmons and Gurr, 2005). Glandular trichomes and their exudates play an important role in plant defense against whitefly (Figure 1B). The entrapment of whitefly on tomato leaves was first reported by Kisha (1981). Further exploration revealed a key role of glandular type IV and VI trichomes in reducing whitefly adult survival and oviposition rate (Channarayappa et al., 1992; Snyder et al., 1998). Detailed profiling of whitefly feeding activities revealed that type IV glandular trichomes disrupted whitefly probing behavior (Narita et al., 2023).

Compounds in the exudates of these trichomes such as acylsugars were identified to be vital in conferring resistance to whitefly in plants including tomato and *Nicotiana benthamiana*. High resistance against whitefly was mechanically transferable by applying the trichome exudates from resistant *S. pennellii* accessions (LA716, LA1340, LA1674 and LA2560) onto the leaves of susceptible tomato plants (Liedl et al., 1995; Muigai et al., 2002). Significant, positive correlations were found between acylsugar content and whitefly resistance when analyzing tomato genotypes with varying acylsugar contents (Dias et al., 2016; Marchant et al., 2020; Dias et al., 2021; de Lima Filho et al., 2022). Furthermore, acylsugar compositions from several *S. pennellii* accessions with high whitefly resistance were characterized, revealing synergistic interactions between different kinds of acylsugars (Leckie et al., 2016). In *N. benthamiana* plants, CRISPR/Cas9 mutagenesis of acylsugar acyltransferase genes significantly decreased acylsugar contents and resistance against whitefly while maintaining the structure and abundance of trichomes on the leaf surface (Feng et al., 2022).

The role of trichomes in other plants has also been explored. Many studies analyzed the correlation between whitefly resistance

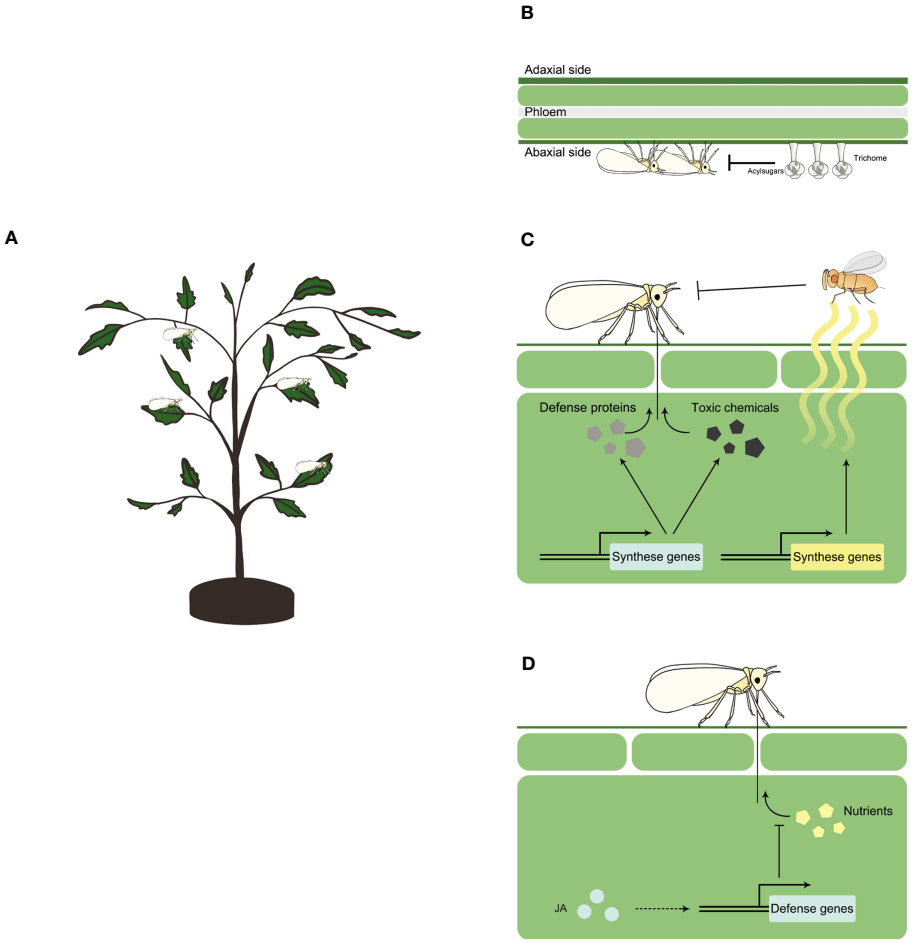

FIGURE 1
Plant resistance against whitefly Schematic representation of whitefly feeding a plant **(A)**, and plant resistance against whitefly at physical **(B)**, chemical **(C)** and signaling **(D)** level. Physically, plants may use trichome and acylsugar to constrain whitefly feeding. Chemically, plants may synthase a repertoire of secondary metabolites such as terpenoids, glucosinolates, phenolic compounds and lignin, and defense proteins such as glucosidase, glucanase and chitinase to inhibit whitefly herbivory. Plants may also synthase and release volatile organic chemicals (VOCs) such as ocimene, myrcene, methyl salicylate and tetradecane, to attract natural enemies of whitefly. At signaling level, jasmonates (JA) controls the expression of defense genes to inhibit the ingestion of plant nutrients by whitefly.

and overall trichome density without classifying trichomes into specific types such as glandular or non-glandular. Results have shown that the role of trichomes varies depending on the plant species, highlighting intrinsic variation between plant species. For example, in tobacco and cassava, negative correlation was observed between whitefly resistance and overall trichome density (Li et al., 2014; Pastório et al., 2023), whereas in black gram a positive correlation was found (Taggar and Gill, 2012). On the other hand, no significant correlation was identified between whitefly resistance and trichome density in cucumber (Novaes et al., 2020). In some cases, the correlation may vary among cultivars of the same plant species. Field trials on cotton cultivars, for example, showed higher whitefly population density on cotton plants with higher trichome density, indicating a negative correlation between trichome density and whitefly resistance (Zia et al., 2011; Prado et al., 2016; Siddiqui et al., 2021; Suthar et al., 2022). However, positive correlations between overall trichome density and whitefly resistance in cotton have also been reported (Thomas et al., 2014; Zhu et al., 2018). Similar variations have been observed in studies on soybean (McAuslane, 1996; Baldin et al., 2017). Furthermore, the contribution of trichome length to plant defenses against whitefly has been investigated, revealing negative correlation between trichome length and plant defenses against whitefly in eggplant and black gram plants (Taggar and Gill, 2012; Hasanuzzaman et al., 2016).

So far, studies conducted on tomato indicate that trichomes exhibiting defenses against whitefly have been observed only in wild relatives of cultivated tomato and tomato cultivars obtained from breeding programs involving wild relatives of tomato. For other plant species, studies have been mostly focused on crop cultivars, and the results generally suggest a lack of contribution of trichomes to plant defense. To clarify the role of trichomes in plant defenses against whitefly in plant species beyond tomato, it is necessary to investigate the trichomes of wild relatives of these crop species. Furthermore, in studies involving non-tomato plants, the correlation between whitefly resistance and overall trichome density is often analyzed. However, this approach may mask the function of specific trichome types, such as glandular trichomes,

which play a significant role in whitefly resistance. Therefore, further empirical studies are needed to gain a better understanding on the role of trichomes in plant defense against whitefly.

2.2 Other physical traits

In addition to trichomes, other physical traits such as leaf shape, color and lamina thickness have been investigated for their potential contribution to plant defenses against whitefly. For example, cotton varieties with okra-shaped leaves exhibited higher whitefly resistance compared to broad-leaved varieties (Chu et al., 2002). Narrow and thinner leaves were associated with increased whitefly resistance in tomato breeding lines (Pal et al., 2021). Leaf color also plays a role, as eggplant varieties with leaves reflecting more green light and exhibiting higher overall brightness displayed higher whitefly resistance (Hasanuzzaman et al., 2016). Conversely, in common bean, luminosity and the intensity of green and yellow colors were negatively correlated with whitefly resistance (Santos et al., 2020). Regarding leaf lamina thickness, field tests involving green gram, cotton, cucumber and eggplant, consistently reported higher whitefly populations on varieties with thicker leaf lamina, indicating a negative correlation between leaf lamina thickness and whitefly resistance (Butter and Vir, 1989; Shibuya et al., 2009; Jindal and Dhaliwal, 2011; Hasanuzzaman et al., 2016). Although these morphological traits have been implicated in contributing to resistance in many studies, their precise roles in whitefly-plant interactions have yet to be determined. Further detailed investigations are necessary to dissect the specific functions of these traits, categorize them and consider them in resistance breeding programs.

3 Plant chemical traits that confer resistance to whitefly

In plant resistance against insect herbivores, plant chemicals play a significant role either directly or indirectly by attracting natural enemies of the herbivores, thereby providing protection to the plants (Yactayo-Chang et al., 2020). In the context of whitefly-plant interactions, several chemicals that contribute to direct or indirect defenses against whitefly have been identified (Figure 1C).

3.1 Direct chemical defense

3.1.1 Secondary metabolites

Secondary metabolites play a major role in plant defense against insect herbivores (Luo et al., 2023), yet only a few have been examined for their contribution to resistance against whitefly. Luan et al. (2013) found that whitefly feeding increased the contents of several terpenoids including cedinene in tobacco plants, and manipulation of cedinene contents through gene silencing or over-expression of *5-epi-aristolochene synthase* indicated that cedinene positively regulated resistance against whitefly. As revealed by metabolites profiling and feeding assays, many phenolic glycosides from tomato plants were identified to contribute to plant defenses against whitefly (Xia et al., 2021). Glucosinolates are a major group of secondary metabolites in crucifers, and are shown to contribute to resistance against whitefly when they accumulated to unnaturally high levels, but not under natural conditions. Elbaz et al. (2012) found that the survival and developmental rate of whitefly nymphs significantly decreased with the accumulation of aliphatic glucosinolate through *AtMYB29* overexpression. Whitefly oviposition preference for *Arabidopsis thaliana* plants was significantly reduced when the contents of aliphatic and total glucosinolates were increased to unnaturally high levels through *AtMYB28* and *AtMYB51* over-expression (Markovich et al., 2013). Using *Brassica* crops that vary in glucosinolate profile and *Arabidopsis* mutants defective in glucosinolate biosynthesis or hydrolysis, Li et al. (2021) revealed that the performance of invasive MEAM1 whiteflies and indigenous Asia II 3 whiteflies was unaffected by glucosinolates when these chemicals were maintained at natural levels in these plants.

Additionally, other secondary metabolites have been implicated in plant defense against whitefly. Studies have reported a positive correlation between the total content of phenolic components and whitefly resistance in eggplant and tomato (Hasanuzzaman et al., 2016; Pal et al., 2021). In tobacco plants, it was observed that certain phenolic compounds, such as chlorogenic acid, catechin, cafeic acid, p-coumaric acid, rutin and ferulic acid, increased in response to whitefly infestations, suggesting their potential role in resistance (Zhang et al., 2017). Similarly, in soybean and cassava, rutin and lignin (along with its derivatives) showed positive association with whitefly resistance (Vieira et al., 2016; Perez-Fons et al., 2019). Furthermore, whitefly infestation has been found to induce callose deposition, which may contribute to plant defense by plugging sieve pores (Kempema et al., 2007; Li et al., 2017).

Many plant secondary metabolites have been shown empirically to contribute to plant defense against insects with chewing mouthparts (Yactayo-Chang et al., 2020; Luo et al., 2023). However, research on the contribution of secondary metabolites to plant defense against whitefly has been limited. There are still many unanswered questions regarding the induction and mechanisms of action of secondary metabolites in whitefly defense. To address these gaps, it would be valuable to draw upon the abundant information available from studies on chewing insects (Yactayo-Chang et al., 2020; Luo et al., 2023). A better understanding of how plant secondary metabolites function in whitefly resistance could have practical implications for the development of novel pesticides.

3.1.2 Defense proteins

Upon infestation by insect herbivores, plants can activate the expression of defense proteins, which can disrupt the normal physiological processes of the insects, including digestion and absorption of nutrients (Howe and Jander, 2008). The role of defense proteins in resistance against whitefly has been extensively studied, particularly focusing on CYS6, a protease

inhibitor in tobacco plants. Genetic manipulation of *CYS6* and feeding assays using purified CYS6 have demonstrated its direct contribution to plant defense against whitefly (Du et al., 2022). Additionally, whitefly infestation has been found to induce the expression of various plant defense proteins. For example, increased local expression of *β-glucosidase* was found in squash plants infested by whitefly (van de Ven et al., 2000). Tomato and cassava plants, when infested by whitefly, showed significant increases in the expression of *β-1,3-glucanase*, *chitinase* and *peroxidase* (Mayer et al., 1996; Antony and Palaniswami, 2006). Furthermore, whitefly infestation led to increased activity of polyphenoloxidase in cucumber and pepper plants, as well as superoxide dismutase, peroxidase and polyphenoloxidase in tomato and soybean plants (Zhang et al., 2008; Latournerie-Moreno et al., 2015; de Lima Toledo et al., 2021; Harish et al., 2023). Additionally, the expression of several pathogenesis-related proteins in tomato was also found to be upregulated in response to whitefly infestation (Puthoff et al., 2010).

The accumulation of defense proteins in response to whitefly infestation is widely acknowledged, but their precious role in plant defenses against whitefly remains largely unknown. To address this knowledge gap, additional case studies, similar to the work of Du et al. (2022) are necessary. Assays involving genetic manipulation of plant genes that encode whitefly infestation-inducible defense proteins and feeding experiment with purified proteins would provide valuable insights into the genuine contribution of these defense proteins to resistance against whitefly.

3.2 Indirect defenses

In addition to direct defense, whitefly feeding can induce the release of plant volatile organic compounds (VOCs) in plants, which attract the natural enemies of whitefly and help protect the plants (Figure 1C). In terms of predators, Nomikou et al. (2005) found that two predatory mites *Typhlodromips swirskii* and *Euseius scutalis* showed a significant preference for whitefly-infested cucumber plants compared to non-infested plants, and this preference was mediated by the volatiles emitted by plants. Silva et al. (2018) showed that the predatory mirid *Macrolophus basicornis* was attracted to tomato plants infested by a mixture of whitefly eggs, nymphs and adults. As for parasitoids, Zhang et al. (2013) demonstrated that whitefly infestation in *Arabidopsis* plants led to the accumulation of ocimene/myrcene, which effectively attracted the whitefly parasitoid *Encarsia formosa*. In response to whitefly herbivory, melon plants released methyl salicylate and tetradecane, which facilitated the attraction of the whitefly parasitoid *E. desantisi* (Silveira et al., 2018). Similarly, whitefly infestation of tomato plants resulted in the emission of β-myrcene and β-caryophyllene, which mediated host location of the parasitic wasp *E. formosa* (Chen et al., 2020).

Due to the differences in feeding behavior, the quantity and quality of VOCs produced by whitefly-infested plants are expected to vary compared to plants attacked by other insects. For example, whitefly may interfere with the indirect plant defense mounted against spider mites in Lima bean (Zhang et al., 2009). It should be noted, however, whitefly-induced VOCs have been identified only in a few case studies (see above). In addition to VOCs, other plant traits such as architecture and glandular trichomes also contribute to indirect defenses against insect herbivores (Pearse et al., 2020). Therefore, further research is required to fully explore the potential of indirect defenses in whitefly control, by investigating plant characteristics that facilitate natural enemy-mediated plant protection.

4 Plant signaling pathway against whitefly

The jasmonate (JA) signaling pathway, as a conserved core pathway regulating plant response to insect herbivory (Erb and Reymond, 2019), plays a major role in plant defense against whitefly (Figure 1D). Studies using *Arabidopsis* mutants with varying levels of JA defense have demonstrated the control of basal defense against whitefly by JA signaling pathway (Zarate et al., 2007). Manipulation of JA signaling pathways in tobacco plants through virus-induced gene silencing or genetic mutation of *MYC2* resulted in increased whitefly survival and fecundity (Zhang et al., 2012; Li et al., 2014). In tomato, when compared to control, whitefly survival and fecundity increased on JA-deficient *spr2* mutant plants and decreased on JA-overexpression 35S-*prosystemin* transgenic plants (Sun et al., 2017). Exogenous application of JA on tomato plants significantly reduced whitefly survival and fecundity (Shi et al., 2017). Additionally, several downstream defense genes involved in JA signaling pathway against whitefly have been identified, including terpenoid synthesis genes, the expression of which is positively modulated by JA treatment (Li et al., 2014).

5 Engineering of plant resistance to whitefly

Both conventional and biotechnology-based breeding approaches have been employed in the engineering of plant resistance against whitefly. These research endeavors have resulted in the development of numerous genetic resources that can be utilized to enhance plant resistance against whitefly.

5.1 Naturally occurring resistances and their utilization in resistance breeding

Whiteflies exhibit variability in their host plant range, with different species showing variations in survival and fecundity on different plant species, as well as cultivars or ecotypes of the same plant species (Zang et al., 2006; Xu et al., 2011). Wild relatives of cultivated crops often exhibit higher resistance to insect pests compared to crop cultivars (Li et al., 2018; Ferrero et al., 2020). The naturally occurring resistance found in these plants, including genes or quantitative trait loci (QTLs) associated with resistance, can be directly utilized in resistance breeding (Broekgaarden et al., 2011). Consequently, significant research efforts have been

dedicated to the identification of plant resistance genes or QTLs and their application in breeding initiatives.

5.1.1 Plant resistance genes or QTLs conferring resistance to whitefly

Tomato has been extensively studied in the context of resistance genes or QTLs due to the significance of whitefly in tomato production. Several whitefly resistance genes or QTLs have been identified in tomato, providing valuable genetic resources for breeding. Among these genes, *Mi-1* has been the focus of extensive research (Nombela and Muñiz, 2010). *Mi-1*, a member of nucleotide-binding, leucine-rich repeat family of resistance genes, was initially identified for conferring resistance to root-knot nematodes (Roberts and Thomason, 1986). It was later found to also impart resistance to phloem-feeding insects like aphids and whiteflies (Rossi et al., 1998; Nombela et al., 2003). Subsequent analysis revealed a series of plant factors that may affect whitefly resistance conferred by *Mi-1*, such as Hsp90, salicylic acid and plant age and size (Rodríguez-Álvarez et al., 2015; Rodríguez-Álvarez et al., 2017; Pascual et al., 2023). Additionally, functional characterization of *Mi-1.2*-like orthologs in cotton demonstrated their potential contribution to plant resistance against whitefly, highlighting the potential of *Mi-1.2*-like genes in whitefly control in cotton plants (Aslam et al., 2023). Furthermore, several other genes or QTLs that may confer whitefly resistance, such as *Wf-1* and *Wf-2*, have been identified in *S. pennellii*, *S. galapagense* and *S. habrochaites* (Leckie et al., 2012; Firdaus et al., 2013; Lucatti et al., 2014; Santegoets et al., 2021). Notably, a major QTL that controls the density of type IV trichomes, a major contributor to whitefly resistance, was identified in *S. pimpinellifolium* (Mata-Nicolás et al., 2021).

In contrast, in other crops and their wild relatives, the identification of QTLs related to whitefly resistance is limited, indicating the need for further research. For example, in melon, only two additive QTLs affecting whitefly fecundity, namely *BtB-VII.1* and *BtB-IX.1*, have been identified (Boissot et al., 2010). In soybean, whitefly resistance was found to be controlled by two major genes as well as polygenes, with the major genes showing an inheritability of over 85% (Xu et al., 2010).

5.1.2 Conventional resistance breeding

Conventional breeding for plant resistance involves incorporating resistance traits from highly resistant plant accessions into target crop cultivars. So far, conventional resistance breeding has been reported only in tomato. In the first attempt, a tomato cultivar carrying the *Mi-1* gene, Motelle, was obtained from the crossing between *S. lycopersicum* Moneymaker and *S. peruvianum*; detailed mapping revealed that Motelle differed from Moneymaker only in the presence of a 650 kb region containing the *Mi-1* gene from *S. peruvianum* (Ho et al., 1992). While Motelle was initially obtained for nematode control, subsequent studies revealed that plants of this cultivar displayed significantly lower susceptibility to whitefly than Moneymaker (Nombela et al., 2000; Jiang et al., 2001). Since then, several more studies have been reported using wild relatives of cultivated tomato as donor of whitefly resistance. For example, plant traits associated with whitefly resistance from the wild tomato *S. pimpinellifolium* accession TO-937 were introgressed into Moneymaker, resulting in lines with increased whitefly resistance (Rodríguez-López et al., 2011; Escobar-Bravo et al., 2016). Several mini tomato lines that displayed high whitefly resistance were obtained through interspecific crossing between *S. lycopersicum* mini tomato cultivars and *S. pennellii* LA-716 (Maciel et al., 2017). Tomato lines obtained from the above attempts were further used in resistance breeding. For example, Gouveia et al. (2018) used two tomato lines that carry the *Mi* gene and differ in acyl-sugar content in a crossing experiment and obtained several tomato lines with high whitefly resistance.

It is important to note that tomato cultivars obtained through conventional resistance breeding, using wild *Solanum* species as donors of whitefly resistance, exhibit only partial resistance against whitefly. This may be attributed to the fact that whiteflies are capable of surviving and reproducing on wild relatives of crops, albeit with reduced performance compared to that on cultivated crops. Moreover, conventional resistance breeding is characterized by its unpredictable nature and time-consuming processes, underscoring the need for biotechnology-based approaches in whitefly resistance breeding.

5.2 Biotechnology-based resistance breeding

Biotechnology-based breeding, which entails targeted manipulation or introduction of genetic materials in crops, represents a promising alternative for crop breeding as it is more targeted and efficient (Barrows et al., 2014). In biotechnology-based resistance breeding against whitefly, plant-mediated RNA interference (RNAi) of whitefly genes and ectopic expression of insecticidal proteins or foreign genes that manipulate the production of insecticidal chemicals in plants, have been explored.

5.2.1 Plant-mediated RNA interference of whitefly genes

RNAi, a specific post-transcriptional gene silencing mechanism triggered by double-stranded RNA (dsRNA) or small interfering RNA (siRNA), has been harnessed in resistance breeding for whitefly management (Table 1). Ghanim et al. (2007) demonstrated that injection of dsRNA into whitefly hemolymph activated RNAi and downregulated of the transcription of target genes, confirming the presence and functionality of the RNAi machinery. Subsequently, the efficacy of orally-delivered dsRNAs/siRNAs was compared, showing that targeting the *V-ATPase A* led to efficient downregulation of the target gene and high whitefly mortality (Upadhyay et al., 2011). Based on these findings, transgenic tobacco plants were generated to produce long dsRNA precursor that would produce siRNAs targeting whitefly *V-ATPase A* mRNA. Bioassay revealed that expressing the dsRNA precursor significantly downregulated *V-ATPase A* transcription, increased whitefly mortality, and protected tobacco plants from heavy

TABLE 1 Resistance engineering in plants that targets whitefly genes using RNA interference.

Target genes in whitefly	Methods of targeting	Test plant	Effects on whitefly	Reference
v-ATPase A	Expression of dsRNA	*Nicotiana tabacum*	Decreased adult survival	Thakur et al., 2014
Acetylcholinesterase and *ecdysone receptor*	Expression of dsRNA	*N. tabacum*	Decreased adult survival	Malik et al., 2016
v-ATPase	Expression of dsRNA	*Lactuca sativa*	Decreased adult survival and fecundity	Ibrahim et al., 2017
F1F0 ATP synthases	Expression of miRNA	*Gossypium hirsutum*	Decreased adult survival	Wamiq and Khan, 2018
Sex lethal, *acetylcholinesterase* and *orcokinin*	Expression of artificial miRNA	*N. tabacum*	Retarded nymph development, decreased population growth	Zubair et al., 2020
v-ATPase	Expression of siRNA	*Phaseolus vulgaris*	Decreased adult survival	Ferreira et al., 2022
Trehalose-6-phosphate synthase 1 and *2*	Expression of dsRNA	*N. tabacum*	Retarded nymph development, decreased adult survival and fecundity	Gong et al., 2022
v-ATPase A	Expression of siRNA	*Solanum lycopersicum*	Decreased adult survival and fecundity	Pizetta et al., 2022
Aquaporin and *alpha glucosidase*	Phloem-specific expression of dsRNA	*N. tabacum*	Decreased adult survival	Raza et al., 2016
Glutathione S-transferase 5	Phloem-specific expression of dsRNA	*Arabidopsis thaliana*	Prolonged nymph development	Eakteiman et al., 2018

whitefly infestation (Thakur et al., 2014). Similarly, the expression of dsRNA in lettuce or siRNA in common beans and tomato targeting a whitefly *V-ATPase* gene, significantly increased resistance to whitefly (Ibrahim et al., 2017; Ferreira et al., 2022; Pizetta et al., 2022). Additional studies have employed RNAi to downregulate whitefly genes, highlighting the promising potential of this approach in whitefly management (Malik et al., 2016; Eakteiman et al., 2018). The expression of dsRNA targeting whitefly *acetylcholinesterase*, *ecdysone receptor* and two *trehalose-6-phosphate synthase genes* in tobacco plants conferred resistance against whitefly (Malik et al., 2016; Gong et al., 2022).

Notably, phloem-specific expression of dsRNA that was achieved through the use of phloem-specific promoters, has shown high effectiveness in combating whiteflies. In tobacco plants, phloem-specific expression of dsRNA targeting two genes responsible for whitefly osmotic pressure maintenance led to a significant increase in whitefly mortality (Raza et al., 2016). Similarly, in *A. thaliana*, phloem-specific expression of dsRNA targeting whitefly detoxification genes extended the developmental period of whitefly nymphs (Eakteiman et al., 2018).

Manipulation of the expression of intrinsic or artificial micro RNAs (miRNAs) that target whitefly genes in plants was also shown to confer plants with whitefly resistance. Using *in silico* prediction, a cotton miRNA ghr-miR166b was found to target several whitefly genes involved in mitochondrial ATP synthase. Overexpression of ghr-miR166b in cotton plants significantly increased whitefly mortality and protected plants from whitefly infestation (Wamiq and Khan, 2018). Overexpression of an engineered artificial miRNA targeting three whitefly genes including *sex lethal*, *acetylcholinesterase* and *orcokinin* conferred high resistance against whitefly in tobacco plants (Zubair et al., 2020).

Furthermore, different strategies to generate transgenic plants that express dsRNA have been explored and compared. Currently, there are two main approaches for transforming, namely nuclear transformation and transplastomics (Zhang et al., 2017). Dong et al. (2020) found that transgenic tobacco plants derived from nuclear transformation were more effective for whitefly management than those derived from transplastomics. Further analysis revealed that the lower effectiveness of transplastomic plants could be attributed to the inability of whitefly to ingest dsRNA from plastids. This study not only highlights the difference between whitefly and insects with chewing mouthparts, but also provides reference information for optimizing RNAi-based resistance breeding against whitefly.

5.2.2 Ectopic expression of foreign genes

The commonly-used Bt toxins are ineffective against hemipteran insects like whitefly due to their mode of action (Palma et al., 2014). Therefore, in resistance breeding against whitefly, insecticidal proteins other than Bt have been identified from various sources and utilized for ectopic expression. For example, ectopic expression of the *Aspergillus niger β-glucosidase* gene in tobacco plants markedly increased resistance against whitefly (Wei et al., 2007). In tobacco plants, expression of *Pinellia ternate* agglutinin, a protein with lectin and insecticidal activity against whitefly, resulted in a reduction of over 90% in whitefly nymphal survival and population size (Jin et al., 2012). Another study screened proteins from ferns, a group of plants

known for their intrinsic resistance to whitefly, and identified Tma12, a protein with chitin-binding and chitinase activity from *Tectaria macrodonta*. Expression of Tma12 in cotton plants resulted in a reduction of over 90% in whitefly population, decreased the incidence of whitefly-borne cotton leaf curl viral diseases, and disrupted whitefly life cycles (Shukla et al., 2016). Additionally, tissue-specific expression of insecticidal proteins has been explored. Phloem-specific expression of a neurotoxin and an onion leaf lectin in tobacco plants resulted in nearly 100% whitefly mortality (Javaid et al., 2016). Moreover, effective resistance against both whitefly and cotton bollworm were achieved in cotton plants by expressing both Bt and *Allium sativum* lectin genes (Din et al., 2021). These studies demonstrate that while classical Bt toxins are not effective against whitefly, other insecticidal proteins from diverse sources may hold significant potential in managing whitefly and can be used in conjunction with Bt toxins to control multiple insect pests.

Another strategy for resistance breeding against whitefly involves manipulating the production of plant chemicals that display insecticidal properties. Some chemicals derived from plants have been found to be highly toxic to whitefly. Manipulating the production of these chemicals in plants can be achieved through the ectopic expression of foreign genes. For example, the over-expression of the *pectin methylesterase* gene from *A. thaliana* and *A. niger* in transgenic tobacco plants substantially increased methanol production, resulting in reduction of the whitefly population (Dixit et al., 2013). Ectopic expression of the *7-epizingiberene synthase* and *Z-Z-farnesyl-diphosphate synthase* genes from *S. habrochaites* in the glandular trichomes of *S. lycopersicum* plants led to the production of 7-epizingiberene, a chemical with toxic and repellent properties against whitefly (Bleeker et al., 2012).

6 Future perspectives

In the study and engineering of plant resistance against whitefly, significant progress has been made, but there are still important issues that require further exploration. One such question is the identification of whitefly-derived factors that trigger plant defense responses during whitefly herbivory. Another key area is the improvement of identification and utilization of plant resistance genes, thereby developing more effective breeding strategies. Additionally, the potential use of whitefly horizontally transferred genes (HTGs) as targets for RNAi in resistance breeding is worth investigating. Utilizing HTGs as RNAi targets could potentially enhance the efficacy and specificity of resistance breeding. These areas of research hold great promises in advancing our understanding of plant resistance to whitefly and developing innovative approaches for whitefly management.

6.1 Whitefly-derived elicitors of plant defenses

While physical traits of plant resistances are often expressed constitutively, chemical traits are often induced by whitefly herbivory. In the research to unravel the induction of chemical defense, mechanical damage and elicitors from saliva and eggs were found to mediate the perception of chewing insects by plants (Bonaventure, 2012). For phloem-feeders, a cysteine protease Cathepsin B3 from the saliva of aphids and a salivary protein NlG14 from the rice brown planthopper were shown to serve as elicitors of plant defense responses (Guo et al., 2020; Gao et al., 2022). Whiteflies exhibit distinct behavior and physiology compared to chewing insects and other phloem-feeding insects (Kempema et al., 2007; Walling, 2008). Consequently, the perception of whitefly feeding by plants may differ from that of the other insect herbivores. So far only one case study reported the activation of plant defenses by factors from whitefly. Whitefly may glycosylate salicylic acid ingested from plants and the secretion of honeydew containing salicylic acid glycoside may induce the accumulation of endogenous free salicylic acid and the expression of downstream genes in the salicylic acid signaling pathway (VanDoorn et al., 2015). Therefore, further investigations are necessary to identify whitefly-derived factors that mediate plant perception of whitefly herbivory. These factors could be metabolites or proteins that come into contact with plants during whitefly feeding, oviposition or honeydew secretion. Additionally, whitefly-derived nucleotides, such as small RNAs, have been shown to be transferred into plants during feeding, and may serve as potential elicitors of plants defenses (van Kleeff et al., 2016). Future studies in this area can draw upon research on the other groups of insect herbivores and harness sophisticated techniques including transgenes and RNAi.

6.2 Identification of genetic resources for resistance breeding

Few resistance genes from crops or their close wild relatives have been identified as possible genetic resources in resistance breeding against whitefly, and many of these genes have shown limited effectiveness (as mentioned earlier). Therefore, further efforts are needed to explore genetic resources from these plants. Additionally, it is worth considering alternative sources of genetic resistance. Resistance genes have already been discovered in unexpected sources. For example, Tma12 identified from fern exhibits high resistance to insect herbivores, including whitefly (Shukla et al., 2016). This suggests that resistance genes may be obtained from non-hosts or poor hosts of whitefly. Identification of these plants is relatively straightforward, and various strategies such as mass spectrum identification of insecticidal proteins, distant hybridization and genome-wide association studies can be utilized to identify key genomic loci associated with resistance. By exploring these diverse genetic resources, we can potentially uncover novel resistance genes for effective whitefly management.

6.3 Horizontally transferred genes as RNAi targets in resistance breeding

HTGs are acquired by organisms from other organisms through means other than reproduction. In whiteflies, dozens of HTGs have been discovered since their initial report in 2020 (Lapadula et al., 2020; Xia et al., 2021; Gilbert and Maumus, 2022; Li et al., 2022).

Many of these HTGs appear to play important roles in the life history of whiteflies. For example, the HTG *BtPMaT1* from plants enables whiteflies to neutralize phenolic glucosides and feed on toxic plants (Xia et al., 2021). HTGs have unique biological importance in whiteflies and the presumably low prevalence of whitefly HTGs in other groups of insects make them ideal targets for RNAi. Recently, two studies targeting whitefly HGTs revealed that they can be used as targets in whitefly control without adverse effects on non-target organisms (Xia et al., 2021; Feng et al., 2023). This progress highlights the need for further exploration of HTGs as RNAi targets in resistance breeding. Additionally, the utilization of phloem-specific promoters can enhance the efficacy and specificity of RNAi technology. By harnessing HTGs and incorporating phloem-specific promoters, researchers can develop more effective and targeted approaches to combat whitefly infestation.

Author contributions

L-LP and S-SL contributed to conception and design of this review. DL, H-YL, and J-RZ collected the references. DL, H-YL, J-RZ, Y-JW, and S-XZ wrote the first of the manuscript, and S-SL and L-LP revised the manuscript. All authors contributed to manuscript revision, read, and approved the submitted version.

Funding

Financial support was provided by the National Key R&D Program of China (2022YFD1401200) and the earmarked fund for China Agriculture Research System (CARS-23-C05).

Conflict of interest

The authors declare that the research was conducted in the absence of any commercial or financial relationships that could be construed as a potential conflict of interest.

Publisher's note

All claims expressed in this article are solely those of the authors and do not necessarily represent those of their affiliated organizations, or those of the publisher, the editors and the reviewers. Any product that may be evaluated in this article, or claim that may be made by its manufacturer, is not guaranteed or endorsed by the publisher.

References

Antony, B., and Palaniswami, M. S. (2006). *Bemisia tabaci* feeding induces pathogenesis-related proteins in cassava (*Manihot esculenta* Crantz). *Indian J. Biochem. Biol.* 43, 182–185.

Aslam, M. Q., Hussain, A., Akram, A., Hussain, S., Naqvi, R. Z., Amin, I., et al. (2023). Cotton *Mi-1.2*-like gene: A potential source of whitefly resistance. *Gene* 851, 146983. doi: 10.1016/j.gene.2022.146983

Baldin, E. L. L., Cruz, P. L., Morando, R., Silva, I. F., Bentivenha, J. P. F., Tozin, L. R. S., et al. (2017). Characterization of antixenosis in soybean genotypes to *Bemisia tabaci* (Hemiptera: Aleyrodidae) biotype B. *J. Econ. Entomol.* 110, 1869–1876. doi: 10.1093/jee/tox143

Barrows, G., Sexton, S., and Zilberman, D. (2014). Agricultural biotechnology: the promise and prospects of genetically modified crops. *J. Econ. Perspect.* 28, 99–120. doi: 10.1257/jep.28.1.99

Bergelson, J., Dwyer, G., and Emerson, J. J. (2001). Models and data on plant-enemy coevolution. *Annu. Rev. Genet.* 35, 469–499. doi: 10.1146/annurev.genet.35.102401.090954

Bleeker, P. M., Mirabella, R., Diergaarde, P. J., VanDoorn, A., Tissier, A., Kant, M. R., et al. (2012). Improved herbivore resistance in cultivated tomato with the sesquiterpene biosynthetic pathway from a wild relative. *Proc. Natl. Acad. Sci. U.S.A.* 109, 20124–20129. doi: 10.1073/pnas.1208756109

Boissot, N., Thomas, S., Sauvion, N., Marchal, C., Pavis, C., and Dogimont, C. (2010). Mapping and validation of QTLs for resistance to aphids and whiteflies in melon. *Theor. Appl. Genet.* 121, 9–20. doi: 10.1007/s00122-010-1287-8

Bonaventure, G. (2012). Perception of insect feeding by plants. *Plant Biol.* 14, 872–880. doi: 10.1111/j.1438-8677.2012.00650.x

Broekgaarden, C., Snoeren, T. A. L., Dicke, M., and Vosman, B. (2011). Exploiting natural variation to identify insect-resistance genes. *Plant Biotchnol. J.* 9, 819–825. doi: 10.1111/j.1467-7652.2011.00635.x

Butter, N. S., and Vir, B. K. (1989). Morphological basis of resistance in cotton to the whitefly Bemisia tabaci. *Phytoparasitica* 17, 251–561. doi: 10.1007/BF02980754

Byrne, D. N., and Bellows, T. S. (1991). Whitefly biology. *Annu. Rev. Entomol.* 36, 431–457. doi: 10.1146/annurev.en.36.010191.002243

Channarayappa, S. G., Muniyappa, V., and Frist, R. H. (1992). Resistance of Lycopersicon species to Bemisia tabaci, a tomato leaf curl virus vector. *Can. J. Bot.* 70, 2184–2192. doi: 10.1139/b92-270

Chen, C. S., Zhao, C., Wu, Z. Y., Liu, G. F., Yu, X. P., and Zhang, P. J. (2020). Whitefly-induced tomato volatiles mediate host habitat location of the parasitic wasp Encarsia formosa, and enhance its efficacy as a bio-control agent. *Pest Manage. Sci.* 77, 749–757. doi: 10.1002/ps.6071

Chu, C. C., Natwick, E. T., and Henneberry, T. J. (2002). Bemisia tabaci (Homoptera: Aleyrodidae) biotype B colonization on okra- and normal-leaf upland cotton strains and cultivars. *J. Econ. Entomol.* 95, 733–738. doi: 10.1603/0022-0493-95.4.733

de Lima Filho, R. B., Resende, J. T. V., de Oliveira, J. R. F., Nardi, C., Silva, P. R., Rech, C., et al. (2022). Relationship between acylsugars and leaf trichomes: mediators of pest resistance in tomato. *Insects* 13, 738. doi: 10.3390/insects13080738

de Lima Toledo, C. A., Ponce, F. D., Oliveira, M. D., Aires, E. S., Junior, S. S., Lima, G. P. P., et al. (2021). Change in the physiological and biochemical aspects of tomato caused by infestation by cryptic species of Bemisia tabaci MED and MEAM1. *Insects* 12, 1105. doi: 10.3390/insects12121105

Dias, D. M., Erpen-Dalla Corte, L., Resende, J. T. V., Zeffa, D. M., Resende, N. C. V., Zanin, D. S., et al. (2021). Acylsugars in tomato varieties confer resistance to the whitefly and reduce the spread of fumagine. *Bragantia* 80, e4421. doi: 10.1590/1678-4499.20210022

Dias, D. M., Resende, J. T., Marodin, J. C., Matos, R., Lustosa, I. F., and Resende, N. C. (2016). Acyl sugars and whitefly (Bemisia tabaci) resistance in segregating populations of tomato genotypes. *Genet. Mol. Res.* 15, gmr.15027788. doi: 10.4238/gmr.15027788

Din, S. U., Azam, S., Rao, A. Q., Shad, M., Ahmed, M., Gul, A., et al. (2021). Development of broad-spectrum and sustainable resistance in cotton against major insects through the combination of Bt and plant lectin genes. *Plant Cell Rep.* 40, 707–721. doi: 10.1007/s00299-021-02669-6

Dixit, S., Upadhyay, S. K., Singh, H., Sidhu, O. P., Verma, P. C., and Chandrashekar, K. (2013). Enhanced methanol production in plants provides broad spectrum insect resistance. *PloS One* 8, e79664. doi: 10.1371/journal.pone.0079664

Dong, Y., Yang, Y., Wang, Z. C., Wu, M. T., Fu, J. Q., Guo, J. Y., et al. (2020). Inaccessibility to double-stranded RNAs in plastids restricts RNA interference in Bemisia tabaci (whitefly). *Pest Manage. Sci.* 76, 3168–3176. doi: 10.1002/ps.5871

Du, H., Xu, H. X., Wang, F., Qian, L. X., Liu, S. S., and Wang, X. W. (2022). Armet from whitefly saliva acts as an effector to suppress plant defences by targeting tobacco cystatin. *New Phytol.* 234, 1848–1862. doi: 10.1111/nph.18063

Dussourd, D. E. (2017). Behavioral sabotage of plant defenses by insect folivores. *Annu. Rev. Entomol.* 62, 15–34. doi: 10.1146/annurev-ento-031616-035030

Eakteiman, G., Moses-Koch, R., Moshitzky, P., Mestre-Rincon, N., Vassão, D. G., Luck, K., et al. (2018). Targeting detoxification genes by phloem-mediated RNAi: a new

approach for controlling phloem-feeding insect pests. *Insect Biochem. Mol. Biol.* 100, 10–21. doi: 10.1016/j.ibmb.2018.05.008

Elbaz, M., Halon, E., Malka, O., Malitsky, S., Blum, E., Aharoni, A., et al. (2012). Asymmetric adaptation to indolic and aliphatic glucosinolates in the B and Q sibling species of Bemisia tabaci (Hemiptera: Aleyrodidae). *Mol. Ecol.* 21, 4533–4546. doi: 10.1111/j.1365-294X.2012.05713.x

Erb, M., and Reymond, P. (2019). Molecular interactions between plants and insect herbivores. *Annu. Rev. Entomol.* 70, 527–557. doi: 10.1146/annurev-arplant-050718-095910

Escobar-Bravo, R., Alba, J. M., Pons, C., Granell, A., Kant, M. R., Moriones, E., et al. (2016). A jasmonate-inducible defense trait transferred from wild into cultivated tomato establishes increased whitefly resistance and reduced viral disease incidence. *Front. Plant Sci.* 7, 1732. doi: 10.3389/fpls.2016.01732

Farina, A., Barbera, A. C., Leonardi, G., Massimino Cocuzza, G. E., Suma, P., and Rapisarda, C. (2022). Bemisia tabaci (Hemiptera: Aleyrodidae): what relationships with and morpho-physiological effects on the plants it develops on? *Insects* 13, 351. doi: 10.3390/insects13040351

Feng, H. L., Acosta–Gamboa, L., Kruse, L. H., Tracy, J. D., Chung, S. H., Fereira, A. R. N., et al. (2022). Acylsugars protect Nicotiana benthamiana against insect herbivory and desiccation. *Plant Mol. Biol.* 109, 505–522. doi: 10.1007/s11103-021-01191-3

Feng, H. L., Chen, W. B., Hussain, S., Shakir, S., Tzin, V., Adegbayi, F., et al. (2023). Horizontally transferred genes as RNA interference targets for aphid and whitefly control. *Plant Biotechnol. J.* 21, 754–768. doi: 10.1111/pbi.13992

Ferreira, A. L., Faria, J. C., Moura, M. C., Zaidem, A. L. M., Pizetta, C. S. R., Freitas, E. O., et al. (2022). Whitefly-tolerant transgenic common bean (Phaseolus vulgaris) line. *Front. Plant Sci.* 13, 984804. doi: 10.3389/fpls.2022.984804

Ferrero, V., Baeten, L., Blanco-Sánchez, L., Planelló, R., Díaz-Pendón, J. A., Rodríguez-Echeverría, S., et al. (2020). Complex patterns in tolerance and resistance to pests and diseases underpin the domestication of tomato. *New Phytol.* 226, 254–266. doi: 10.1111/nph.16353

Fiallo-Olivé, E., and Navas-Castillo, J. (2023). Begomoviruses: what is the secret(s) of their success? *Trends Plant Sci.* 28, 715–727. doi: 10.1016/j.tplants.2023.01.012

Fiallo-Olivé, E., Pan, L. L., Liu, S. S., and Navas-Castillo, J. (2020). Transmission of begomoviruses and other whitefly-borne viruses: dependence on the vector species. *Phytopathology* 110, 10–17. doi: 10.1016/j.tplants.2023.01.012

Firdaus, S., van Heusden, A. W., Hidayati, N., Supena, E. D. J., Mumm, R., de Vos, R. C. H., et al. (2013). Identification and QTL mapping of whitefly resistance components in Solanum galapagense. *Theor. Appl. Genet.* 126, 1487–1501. doi: 10.1007/s00122-013-2067-z

Gao, H. L., Zou, J. Z., Lin, X. M., Zhang, H. H., Yu, N., and Liu, Z. W. (2022). Nilaparvata lugens salivary protein NlG14 triggers defense response in plants. *J. Exp. Bot.* 73, 7477–7487. doi: 10.1093/jxb/erac354

Ghanim, M., Kontsedalov, S., and Czosnek, H. (2007). Tissue-specific gene silencing by RNA interference in the whitefly Bemisia tabaci (Gennadius). *Insect Biochem. Mol. Biol.* 37, 732–738. doi: 10.1016/j.ibmb.2007.04.006

Gilbert, C., and Maumus, F. (2022). Multiple Horizontal acquisitions of plant genes in the whitefly Bemisia tabaci. *Genome Biol. Evol.* 14, evac141. doi: 10.1093/gbe/evac141

Gilbertson, R. L., Batuman, O., Webster, C. G., and Adkins, S. (2015). Role of the insect supervectors Bemisia tabaci and Frankliniella occidentalis, in the emergence and global spread of plant viruses. *Annu. Rev. Virol.* 2, 67–93. doi: 10.1146/annurev-virology-031413-085410

Gong, C., Yang, Z. Z., Hu, Y., Wu, Q. J., Wang, S. L., Guo, Z. J., et al. (2022). Silencing of the BtTPS genes by transgenic plant-mediated RNAi to control Bemisia tabaci MED. *Pest Manage. Sci.* 78, 1128–1137. doi: 10.1002/ps.6727

Gouveia, B. T., de Oliveira, A. M. S., Ribeiro, G. H. M. R., and Maluf, W. R. (2018). Resistance to whitefly (Bemisia argentifolii) and repellency to the two-spotted spider mite (Tetranychus urticae) in tomato plant hybrids with high leaf contents of acylsugar and the Mi gene. *Euphytica* 214, 140. doi: 10.1007/s10681-018-2224-1

Guo, H., Zhang, Y., Tong, J., Ge, P., Wang, Q., Zhao, Z., et al. (2020). An aphid-secreted salivary protease activates plant defense in phloem. *Curr. Biol.* 30, 4826–4836. doi: 10.1016/j.cub.2020.09.020

Harish, G. N., Singh, R., Sharma, S., and Taggar, G. K. (2023). Changes in defense-related antioxidative enzymes amongst the resistant and susceptible soybean genotypes under whitefly, Bemisia tabaci (Hemiptera: Aleyrodidae) stress. *Phytoparasitica* 51, 63–75. doi: 10.1007/s12600-022-01028-9

Hasanuzzaman, A. T. M., Islam, M. N., Zhang, Y., Zhang, C. Y., and Liu, T. X. (2016). Leaf morphological characters can be a factor for intra-varietal preference of whitefly Bemisia tabaci (Hemiptera: Aleyrodidae) among eggplant varieties. *PloS One* 11, e0153880. doi: 10.1371/journal.pone.0153880

Ho, J. Y., Weide, R., Ma, H. M., Vanwordragen, M. F., Lambert, K. N., Koornneef, M., et al. (1992). The root-knot nematode resistance gene (Mi) in tomato-construction of a molecular linkage map and identification of dominant cDNA markers in resistant genotypes. *Plant J.* 2, 971–982. doi: 10.1046/j.1365-313X.1992.t01-8-00999.x

Howe, G. A., and Jander, G. (2008). Plant immunity to insect herbivors. *Annu. Rev. Entomol.* 59, 41–66. doi: 10.1146/annurev.arplant.59.032607.092825

Ibrahim, A. B., Monteiro, T. R., Cabral, G. B., and Aragão, F. J. L. (2017). RNAi-mediated resistance to whitefly (Bemisia tabaci) in genetically engineered lettuce (Lactuca sativa). *Transgenic Res.* 26, 613–624. doi: 10.1007/s11248-017-0035-0

Javaid, S., Amin, I., Jander, G., Mukhtar, Z., Saeed, N. A., and Mansoor, S. (2016). A transgenic approach to control hemipteran insects by expressing insecticidal genes under phloem-specifc promoters. *Sci. Rep.* 6, 34706. doi: 10.1038/srep34706

Jiang, Y. X., Nombela, G., and Muniz, M. (2001). Analysis by DC-EPG of the resistance to Bemisia tabaci on an Mi-tomato line. *Entomol. Exp. Appl.* 99, 295–302. doi: 10.1046/j.1570-7458.2001.00828.x

Jin, S. X., Zhang, X. L., and Daniell, H. (2012). Pinellia ternata agglutinin expression in chloroplasts confers broad spectrum resistance against aphid, whitefly, Lepidopteran insects, bacterial and viral pathogens. *Plant Biotechnol. J.* 10, 313–327. doi: 10.1111/j.1467-7652.2011.00663.x

Jindal, V., and Dhaliwal, G. S. (2011). Mechanisms of resistance in cotton to whitefly (Bemisia tabaci): antixenosis. *Phytoparasitica* 39, 129–136. doi: 10.1007/s12600-011-0144-x

Kaloshian, I., and Walling, L. L. (2005). Hemipterans as plant pathogens. *Annu. Rev. Phytopathol.* 43, 491–521. doi: 10.1146/annurev.phyto.43.040204.135944

Kempema, L. A., Cui, X. P., Holzer, F. M., and Walling, L. L. (2007). Arabidopsis transcriptome changes in response to phloem-feeding silverleaf whitefly nymphs. Similarities and distinctions in responses to aphids. *Plant Physiol.* 143, 849–865. doi: 10.1104/pp.106.090662

Kisha, J. S. (1981). Observation on the trapping of the whitefly Bemisia tabaci by glandular hairs on tomato leaves. *Ann. Appl. Biol.* 97, 123–127. doi: 10.1111/j.1744-7348.1981.tb03004.x

Lapadula, W. J., Mascotti, M. L., and Juri Ayub, M. (2020). Whitefly genomes contain ribotoxin coding genes acquired from plants. *Sci. Rep.* 10, 15503. doi: 10.1038/s41598-020-72267-1

Latournerie-Moreno, L., Ic-Caamal, A., and Ruiz-Sanchez, E. (2015). Survival of Bemisia tabaci and activity of plant defense-related enzymes in genotypes of Capsicum annuum L. *Chil. J. Agr. Res.* 75, 71–77. doi: 10.4067/S0718-58392015000100010

Leckie, B. M., D'Ambrosio, D. A., Chappell, T. M., Halitschke, R., De Jong, D. M., Kessler, A., et al. (2016). Differential and synergistic functionality of acylsugars in suppressing oviposition by insect herbivores. *PloS One* 11, e0153345. doi: 10.1371/journal.pone.0153345

Leckie, B. M., De Jong, D. M., and Mutschler, M. A. (2012). Quantitative trait loci increasing acylsugars in tomato breeding lines and their impacts on silverleaf whiteflies. *Mol. Breed.* 30, 1621–1634. doi: 10.1007/s11032-012-9746-3

Li, X. H., Garvey, M., Kaplan, I., Li, B. P., and Carrillo, J. (2018). Domestication of tomato has reduced the attraction of herbivore natural enemies to pest-damaged plants. *Agr. For. Entomol.* 20, 390–401. doi: 10.1111/afe.12271

Li, Y., Lin, H. F., Jin, P., Chen, D. X., and Li, M. Y. (2014). The selectivity of Q-biotype Bemisia tabaci for different varieties of tobacco, Nicotiana tabacum. *Chin. J. Appl. Entomol.* 51, 1320–1326.

Li, Y., Liu, Z. G., Liu, C., Shi, Z. Y., Pang, L., Chen, C. Z., et al. (2022). HGT is widespread in insects and contributes to male courtship in lepidopterans. *Cell* 185 (16), 2975–2987. doi: 10.1016/j.cell.2022.06.014

Li, J., Qian, H. M., Pan, L. L., Wang, Q. M., and Liu, S. S. (2021). Performance of two species of whiteflies is unaffected by glucosinolate profile in Brassica plants. *Pest Manage. Sci.* 77, 4313–4320. doi: 10.1002/ps.6460

Li, P., Shu, Y. N., Fu, S., Liu, Y. Q., Zhou, X. P., Liu, S. S., et al. (2017). Vector and nonvector insect feeding reduces subsequent plant susceptibility to virus transmission. *New Phytol.* 215, 699–710. doi: 10.1111/nph.14550

Li, R., Weldegergis, B. T., Li, J., Jung, C., Qu, J., Sun, Y., et al. (2014). Virulence factors of geminivirus interact with MYC2 to subvert plant resistance and promote vector performance. *Plant Cell* 26, 4991–5008. doi: 10.1105/tpc.114.133181

Liedl, B. E., Lawson, D. M., White, K. K., Shapiro, J. A., Cohen, D. E., Carson, W. G., et al. (1995). Acylsugars of wild tomato Lycopersicon pennellii alters settling and reduces oviposition of Bemisia argentifolii (Homoptera, Aleyrodidae). *J. Econ. Entomol.* 88, 742–748. doi: 10.1093/jee/88.3.742

Luan, J. B., Yao, D. M., Zhang, T., Walling, L. L., Yang, M., Wang, Y. J., et al. (2013). Suppression of terpenoid synthesis in plants by a virus promotes its mutualism with vectors. *Ecol. Lett.* 16, 390–398. doi: 10.1111/ele.12055

Lucatti, A. F., Meijer-Dekens, F. R. G., Mumm, R., Visser, R. G. F., Vosman, B., and van Heusden, S. (2014). Normal adult survival but reduced Bemisia tabaci oviposition rate on tomato lines carrying an introgression from S. habrochaites. *BMC Genet.* 15, 142. doi: 10.1186/s12863-014-0142-3

Luo, M., Li, B., Jander, G., and Zhou, S. Q. (2023). Non-volatile metabolites mediate plant interactions with insect herbivores. *Plant J.* 114, 1164–1177. doi: 10.1111/tpj.16180

Maciel, G. M., Almeida, R. S., da Rocha, J. P. R., Andaló, V., Marquez, G. R., Santos, N. C., et al. (2017). Mini tomato genotypes resistant to the silverleaf whitefly and to two-spotted spider mites. *Genet. Mol. Res.* 16, gmr16019539. doi: 10.4238/gmr16019539

Malik, H. J., Raza, A., Amin, I., Schefer, J. A., Schefer, B. E., Brown, J. K., et al. (2016). RNAi-mediated mortality of the whitefly through transgenic expression of double-stranded RNA homologous to acetylcholinesterase and ecdysone receptor in tobacco plants. *Sci. Rep.* 6, 38469. doi: 10.1038/srep38469

Marchant, W. G., Legarrea, S., Smeda, J. R., Mutschler, M. A., and Srinivasan, R. (2020). Evaluating acylsugars-mediated resistance in tomato against Bemisia tabaci and

transmission of tomato yellow leaf curl virus. *Insects* 11, 842. doi: 10.3390/insects11120842

Markovich, O., Kafle, D., Elbaz, M., Malitsky, S., Aharoni, A., Schwarzkopf, A., et al. (2013). Arabidopsis thaliana plants with different levels of aliphatic- and indolyl-glucosinolates affect host selection and performance of Bemisia tabaci. *J. Chem. Ecol.* 39, 1361–1372. doi: 10.1007/s10886-013-0358-0

Mata-Nicolás, E., Montero-Pau, J., Gimeno-Paez, E., AGarcía-Pérez, A., Ziarsolo, P., Blanca, J., et al. (2021). Discovery of a major QTL controlling trichome IV density in tomato using K-Seq genotyping. *Genes* 12, 243. doi: 10.3390/genes12020243

Mayer, R. T., McCollum, T. G., and McDonald, R. E. (1996). "Bemisia feeding induces pathogenesis-related proteins in tomato," in *Bemisia 1995: taxonomy, biology, damage, control and management*. Eds. D. Gerling and R. T. Mayer (UK: Intercept), 179–188.

McAuslane, H. J. (1996). Influence of leaf pubescence on ovipositional preference of Bemisia argentifolii (Homoptera: Aleyrodidae) on soybean. *Environ. Entomol.* 25, 834–841. doi: 10.1093/ee/25.4.834

Muigai, S. G., Schuster, D. J., Snyder, J. C., Scott, J. W., Bassett, M. J., and McAuslane, H. J. (2002). Mechanisms of resistance in Lycopersicon germplasm to the whitefly Bemisia argentifolii. *Phytoparasitica* 30, 347–360. doi: 10.1007/BF02979682

Narita, J. P. Z., Fatoretto, M. B., Lopes, J. R. S., and Vendramim, J. D. (2023). Type-IV glandular trichomes disrupt the probing behavior of Bemisia tabaci MEAM1 and Tomato severe rugose virus inoculation in tomato plants. *J. Pest Sci.* 96, 1035–1048. doi: 10.1007/s10340-023-01599-4

Nombela, G., Beitia, F., and Muniz, M. (2000). Variation in tomato host response to Bemisia tabaci (Hemiptera: Aleyrodidae) in relation to acyl sugar content and presence of the nematode and potato aphid resistance gene Mi. *Bull. Entomol. Res.* 90, 161–167. doi: 10.1017/S0007485300000274

Nombela, G., and Muñiz, M. (2010). "Host plant resistance for the management of Bemisia tabaci: a multi-crop survey with emphasis on tomato," in *Bemisia: Bionomics and Management of a Global Pest*. Eds. P. A. Stansly and E. N. Steven (New York: Springer), 357–384.

Nombela, G., Williamson, V. M., and Muñiz, M. (2003). The rootknot nematode resistance gene Mi-1.2 of tomato is responsible for resistance against the whitefly Bemisia tabaci. *Mol. Plant-Microbe Inte.* 16, 645–649. doi: 10.1094/MPMI.2003.16.7.645

Nomikou, M., Meng, R. X., Schraag, R., Sabelis, M. W., and Janssen, A. (2005). How predatory mites find plants with whitefly prey. *Exp. Appl. Acarol.* 36, 263–275. doi: 10.1007/s10493-005-6650-0

Novaes, N. S., Lourencao, A. L., Bentivenha, J. P. F., Baldin, E. L. L., and Melo, A. M. T. (2020). Characterization and potential mechanisms of resistance of cucumber genotypes to Bemisia tabaci (Hemiptera: Aleyrodidae). *Phytoparasitica* 48 (4), 643–657. doi: 10.1007/s12600-020-00826-3

Oliveira, M. R. V., Henneberry, T. J., and Anderson, P. (2001). History, current status, and collaborative research projects for Bemisia tabaci. *Crop Prot* 20, 709–723. doi: 10.1016/S0261-2194(01)00108-9

Pal, S., Karmakar, P., Chattopadhyay, A., and Ghosh, S. K. (2021). Evaluation of tomato genotypes for resistance to whitefly (Bemisia tabaci Gennadius) and tomato leaf curl virus in Eastern India. *J. Asia-Pacific Entomol.* 24, 68–76. doi: 10.1016/j.aspen.2021.04.001

Palma, L., Muñoz, D., Berry, C., Murillo, J., and Caballero, P. (2014). Bacillus thuringiensis toxins: an overview of their biocidal activity. *Toxin* 6, 3296–3325. doi: 10.3390/toxins6123296

Pascual, S., Rodríguez-Álvarez, C. I., Kaloshian, I., and Nombela, G. (2023). Hsp90 gene is required for Mi-1-mediated resistance of tomato to the whitefly Bemisia tabaci. *Plants* 12, 641. doi: 10.3390/plants12030641

Pastório, M. A., Hoshino, A. T., Kitzberger, C. S. G., Bortolotto, O. C., de Oliveira, L. M., dos Santos, A. M., et al. (2023). The leaf color and trichome density influence the whitefly infestation in different cassava cultivars. *Insects* 14, 4. doi: 10.3390/insects14010004

Pearse, I. S., LoPresti, E., Schaeffer, R. N., Wetzel, W. C., Mooney, K. A., Ali, J. G., et al. (2020). Generalising indirect defence and resistance of plants. *Ecol. Lett.* 23, 1137–1152. doi: 10.1111/ele.13512

Perez-Fons, L., Bohorquez-Chaux, A., Irigoyen, M. L., Garceau, D. C., Morreel, K., Boerjan, W., et al. (2019). A metabolomics characterisation of natural variation in the resistance of cassava to whitefly. *BMC Plant Biol.* 19, 518. doi: 10.1186/s12870-019-2107-1

Pizetta, C. S. R., Ribeiro, W. R., Ferreira, A. L., Moura, M. D., Bonfim, K., Pinheiro, P. V., et al. (2022). RNA interference-mediated tolerance to whitefly (Bemisia tabaci) in genetically engineered tomato. *Plant Cell Tissue Organ Culture* 148, 281–291. doi: 10.1007/s11240-021-02185-1

Prado, J. C., Penaflor, M., Cia, E., Vieira, S. S., Silva, K. I., Carlini-Garcia, L. A., et al. (2016). Resistance of cotton genotypes with different leaf colour and trichome density to Bemisia tabaci biotype B. *J. Appl. Entomol.* 140, 405–413. doi: 10.1111/jen.12274

Puthoff, D. P., Holzer, F. M., Perring, T. M., and Walling, L. L. (2010). Tomato pathogenesis-related protein genes are expressed in response to Trialeurodes vaporariorum and Bemisia tabaci biotype B feeding. *J. Chem. Ecol.* 36, 1271–1285. doi: 10.1007/s10886-010-9868-1

Raza, A., Malik, H. J., Shafiq, M., Amin, I., Scheffler, J. A., Scheffler, B. E., et al. (2016). RNA interference based approach to down regulate osmoregulators of whitefly (Bemisia tabaci): potential technology for the control of whitefly. *PloS One* 11, e0153883. doi: 10.1371/journal.pone.0153883

Roberts, P. A., and Thomason, I. J. (1986). Variability in reproduction of isolates of Meloidogyne incognita and M. javanica on resistant tomato genotypes. *Plant Dis.* 70, 547–551. doi: 10.1094/PD-70-547

Rodríguez-Álvarez, C. I., López-Climent, M. F., Gómez-Cadenas, A., Kaloshian, I., and Nombela, G. (2015). Salicylic acid is required for Mi-1-mediated resistance of tomato to whitefly Bemisia tabaci, but not for basal defense to this insect pest. *Bull. Entomol. Res.* 105, 574–582. doi: 10.1017/S0007485315000449

Rodríguez-Álvarez, C. I., Muñiz, M., and Nombela, G. (2017). Effect of plant development (age and size) on the Mi-1-mediated resistance of tomato to whitefly Bemisia tabaci. *Bull. Entomol. Res.* 107, 768–776. doi: 10.1017/S0007485317000281

Rodríguez-López, M. J., Garzo, E., Bonani, J. P., Fereres, A., FernándezMuñoz, R., and Moriones, E. (2011). Whitefly resistance traits derived from the wild tomato Solanum pimpinellifolium affect the preference and feeding behavior of Bemisia tabaci and reduce the spread of tomato yellow leaf curl virus. *Phytopathology* 101, 1191–1201. doi: 10.1094/PHYTO-01-11-0028

Rossi, M., Goggin, F. L., Milligan, S. B., Kaloshian, I., Ullman, D. E., and Williamson, V. M. (1998). The nematode resistance gene Mi of tomato confers resistance against the potato aphid. *Proc. Natl. Acad. Sci. U.S.A.* 95, 9750–9754. doi: 10.1073/pnas.95.17.9750

Santegoets, J., Bovio, M., Westende, W. V., Voorrips, R. E., and Vosman, B. (2021). A novel non-trichome based whitefly resistance qtl in solanum galapagense. *Euphytica* 217, 3. doi:10.1007/s10681-021-02770-7

Santos, T. L. B., Baldin, E. L. L., Ribeiro, L. P., Souza, C. M., Soares, M. C. E., Fanela, T. L. M., et al. (2020). Resistance sources and antixenotic factors in Brazilian bean genotypes against Bemisia tabaci. *Neotropical Entomol.* 50, 129–144. doi: 10.1007/s13744-020-00821-7

Savary, S., Willocquet, L., Pethybridge, S. J., Esker, P., McRoberts, N., and Nelson, A. (2019). The global burden of pathogens and pests on major food crops. *Nat. Ecol. Evol.* 3, 430–439. doi: 10.1038/s41559-018-0793-y

Shi, X. B., Pan, H. P., Xie, W., Wang, S. L., Wu, Q. J., Chen, G., et al. (2017). Different effects of exogenous jasmonic acid on preference and performance of viruliferous Bemisia tabaci B and Q. Entomol. *Exp. Appl.* 165, 148–158. doi: 10.1111/eea.12635

Shibuya, T., Hirai, N., Sakamoto, Y., and Komuro, J. (2009). Effects of morphological characteristics of Cucumis sativus seedlings grown at different vapor pressure deficits on initial colonization of Bemisia tabaci (Hemiptera: Aleyrodidae). *J. Econ. Entomol.* 102, 2265–2267. doi: 10.1603/029.102.0631

Shukla, A. K., Upadhyay, S. K., Mishra, M., Saurabh, S., Singh, R., Singh, H., et al. (2016). Expression of an insecticidal fern protein in cotton protects against whitefly. *Nat. Biotechnol.* 34, 1046–1051. doi: 10.1038/nbt.3665

Siddiqui, S., Abro, G. H., Syed, T. S., Buriro, A. S., Ahmad, S., Majeed, M. Z., et al. (2021). Identification of cotton physio-morphological marker for the development of cotton resistant varieties against sucking insect pests: a biorational approach for insect-pest management. *Pakistan J. Zool.* 53, 1383–1391. doi: 10.17582/journal.pjz/20190703060702

Silva, D. B., Bueno, V. H. P., Van Loon, J. J. A., Peñaflor, M. F. G. V., Bento, J. M. S., and Lenteren, J. C. V. (2018). Attraction of three mirid predators to tomato infested by both the tomato leaf mining moth Tuta absoluta and the whitefly Bemisia tabaci. *J. Chem. Ecol.* 44, 29–39. doi: 10.1007/s10886-017-0909-x

Silveira, T. A., Sanches, P. A., Zazycki, L. C. F., Costa–Lima, T. C., Cabezas–Guerrero, M. F., Favaris, A. P., et al. (2018). Phloem-feeding herbivory on flowering melon plants enhances attraction of parasitoids by shifting floral to defensive volatiles. *Arthropod-plant Inte.* 12, 751–760. doi: 10.1007/s11829-018-9625-x

Simmons, A. M., and Gurr, G. M. (2005). Trichomes of Lycopersicon species and their hybrids: effects on pests and natural enemies. *Agr. For. Entomol.* 7, 265–276. doi: 10.1111/j.1461-9555.2005.00271.x

Snoeck, S., Guayazan-Palacios, N., and Steinbrenner, A. D. (2022). Molecular tug-of-war: Plant immune recognition of herbivory. *Plant Cell* 34, 1497–1513. doi: 10.1093/plcell/koac009

Snyder, J. C., Simmons, A. M., and Thacker, R. R. (1998). Attractancy and ovipositional response of adult Bemisia argentifolii (Homoptera: Aleyrodidae) to type IV trichomes density on leaves of Lycopersicon hirsutum grown in three day-length regimes. *J. Entomol. Sci.* 33, 270–281. doi: 10.18474/0749-8004-33.3.270

Stahl, E., Hilfiker, O., and Reymond, P. (2018). Plant-arthropod interactions: who is the winner? *Plant J.* 93, 703–728. doi: 10.1111/tpj.13773

Sun, Y. C., Pan, L. L., Ying, F. Z., Li, P., Wang, X. W., and Liu, S. S. (2017). Jasmonic acid-related resistance in tomato mediates interactions between whitefly and whitefly transmitted virus. *Sci. Rep.* 7, 566. doi: 10.1038/s41598-017-00692-w

Suthar, T., Gupta, N., Pathak, D., Sharma, S., and Rathore, P. (2022). Morpho-anatomical characterization of interspecific derivatives of Gossypium hirsutum L. x G. armourianum Kearney cross for whitefly tolerance. *Phytoparasitica* 50, 423–441. doi: 10.1007/s12600-021-00963-3

Taggar, G. K., and Gill, R. S. (2012). Preference of whitefly, Bemisia tabaci, towards black gram genotypes: role of morphological leaf characteristics. *Phytoparasitica* 40, 461–474. doi: 10.1007/s12600-012-0247-z

Thakur, N., Upadhyay, S. K., Verma, P. C., Chandrashekar, K., Tuli, R., and Singh, P. K. (2014). Enhanced whitefly resistance in transgenic tobacco plants expressing double stranded RNA of V-ATPase A gene. *PloS One* 9, e87235. doi: 10.1371/journal.pone.0087235

Thomas, A., Kar, A., Rebijith, K. B., Asokan, R., and Ramamurthy, V. V. (2014). Bemisia tabaci (Hemiptera: Aleyrodidae) species complex from cotton cultivars: a comparative study of population density, morphology, and molecular variations. *Ann. Entomol. Soc Am.* 107, 389–398. doi: 10.1603/AN13124

Tissier, A. (2012). Glandular trichomes: what comes after expressed sequence tags? *Plant J.* 70, 51–68. doi: 10.1111/j.1365-313X.2012.04913.x

Upadhyay, S. K., Chandrashekar, K., Thakur, N., Verma, P. C., Borgio, J. F., Singh, P. K., et al. (2011). RNA interference for the control of whiteflies (Bemisia tabaci) by oral route. *J. Biosci.* 36, 153–161. doi: 10.1007/s12038-011-9009-1

van de Ven, W. T. G., LeVesque, C. S., Perring, T. M., and Walling, L. L. (2000). Local and systemic changes in squash gene expression in response to silverleaf whitefly feeding. *Plant Cell* 12, 1409–1423. doi: 10.1105/tpc.12.8.1409

VanDoorn, A., de Vries, M., Kant, M. R., and Schuurink, R. C. (2015). Whiteflies glycosylate salicylic acid and secret the conjugate *via* their honeydew. *J. Chem. Ecol.* 41, 52–58. doi: 10.1007/s10886-014-0543-9

van Kleeff, P. J. M., Galland, M., Schuurink, R. C., and Bleeker, P. M. (2016). Small RNAs from Bemisia tabaci are transferred to Solanum lycopersicum phloem during feeding. *Front. Plant Sci.* 7, 1759. doi: 10.3389/fpls.2016.01759

Vieira, S. S., Lourencao, A. L., Graca, J. P., Janegitz, T., Salvador, M. C., Oliveira, M. C. N., et al. (2016). Biological aspects of Bemisia tabaci biotype B and the chemical causes of resistance in soybean genotypes. *Arthropod-Plant Inte.* 10, 525–534. doi: 10.1007/s11829-016-9458-4

Walling, L. L. (2008). Avoiding effective defenses: strategies employed by phloem-feeding insects. *Plant Physiol.* 146, 859–866. doi: 10.1104/pp.107.113142

Wamiq, G., and Khan, J. A. (2018). Overexpression of ghr–miR166b generates resistance against Bemisia tabaci infestation in Gossypium hirsutum plants. *Planta* 247, 1175–1189. doi: 10.1007/s00425-018-2852-7

Wang, X. W., and Blanc, S. (2021). Insect transmission of plant single-stranded DNA viruses. *Annu. Rev. Entomol.* 66, 389–405. doi: 10.1146/annurev-ento-060920-094531

Wang, X. W., Li, P., and Liu, S. S. (2017). Whitefly interactions with plants. *Curr. Opin. Insect Sci.* 19, 70–75. doi: 10.1016/j.cois.2017.02.001

Wei, S., Semel, Y., Bravdo, B. A., Czosnek, H., and Shoseyov, O. (2007). Expression and subcellular compartmentation of Aspergillus Niger beta-glucosidase in transgenic tobacco result in an increased insecticidal activity on whiteflies (Bemisia tabaci). *Plant Sci.* 172, 1175–1181. doi: 10.1016/j.plantsci.2007.02.018

Wilkinson, S. W., Magerøy, M. H., Lopez Sanchez, A., Smith, L. M., Furci, L., Cotton, T. A., et al. (2019). Surviving in a hostile world: plant strategies to resist pests and diseases. *Annu. Rev. Phytopathol.* 57, 505–529. doi: 10.1146/annurev-phyto-082718-095959

Xia, J. X., Guo, Z. J., Yang, Z. Z., Han, H. L., Wang, S. L., Xu, H. F., et al. (2021). Whitefly hijacks a plant detoxification gene that neutralizes plant toxins. *Cell* 184, 1693–1705. doi: 10.1016/j.cell.2021.02.014

Xu, R., Li, W., Zhang, L. F., Lin, Y. H., Qi, B., and Xing, H. (2010). A study on the inheritance of resistance to whitefly in soybean. *Sci. Agric. Sin.* 43, 80–86.

Xu, J., Lin, K. K., and Liu, S. S. (2011). Performance on different host plants of an alien and an indigenous Bemisia tabaci from China. *J. Appl. Entomol.* 135, 771–779. doi: 10.1111/j.1439-0418.2010.01581.x

Yactayo-Chang, J. P., Tang, H. V., Mendoza, J., Christensen, S. A., and Block, A. K. (2020). Plant defense chemicals against insect pests. *Agronomy* 10, 1156. doi: 10.3390/agronomy10081156

Zang, L. S., Chen, W. Q., and Liu, S. S. (2006). Comparison of performance on different host plants between the B biotype and a non-B biotype of Bemisia tabaci from Zhejiang, China. *Entomol Exp. Appl.* 121, 221–227. doi: 10.1111/j.1570-8703.2006.00482.x

Zarate, S. I., Kempema, L. A., and Walling, L. L. (2007). Silverleaf whitefly induces salicylic acid defenses and suppresses effectual jasmonic acid defenses. *Plant Physiol.* 143, 866–875. doi: 10.1104/pp.106.090035

Zhang, J., Khan, S. A., Heckel, D. G., and Bock, R. (2017). Next-generation insect-resistant plants: RNAi-mediated crop protection. *Trends Biotechnol.* 35, 871–882. doi: 10.1016/j.tibtech.2017.04.009

Zhang, T., Luan, J. B., Qi, J. F., Huang, C. J., Li, M., Zhou, X. P., et al. (2012). Begomovirus-whitefly mutualism is achieved through repression of plant defenses by a virus pathogenicity factor. *Mol. Ecol.* 21, 1294–1304. doi: 10.1111/j.1365-294X.2012.05457.x

Zhang, X., Sun, X., Zhang, H. P., Xue, M., and Wang, D. (2017). Phenolic compounds induced by Bemisia tabaci and Trialeurodes vaporariorum in Nicotiana tabacum L. and their relationship with the salicylic acid signaling pathway. *Arthropod-Plant Inte.* 11, 659–667. doi: 10.1007/s11829-017-9508-6

Zhang, P. J., Xu, C. X., Zhang, J. M., Lu, Y. B., Wei, J. N., Liu, Y. Q., et al. (2013). Phloem-feeding whiteflies can fool their host plants, but not their parasitoids. *Funct. Ecol.* 27, 1304–1312. doi: 10.1111/1365-2435.12132

Zhang, S. Z., Zhang, F., and Hua, B. Z. (2008). Enhancement of phenylalanine ammonia lyase, polyphenoloxidase, and peroxidase in cucumber seedlings by Bemisia tabaci (Gennadius) (Hemiptera: Aleyrodidae) infestation. *Agr Sci. China* 7, 82–87. doi: 10.1016/S1671-2927(08)60025-5

Zhang, P. J., Zheng, S. J., Van Loon, J. J. A., Boland, W., David, A., Mumma, R., et al. (2009). Whiteflies interfere with indirect plant defense against spider mites in Lima bean. *Proc. Natl. Acad. Sci. U.S.A.* 106, 21202–21207. doi: 10.1073/pnas.0907890106

Zhu, L. Z., Li, J. Y., Xu, Z. P., Manghwar, H., Liang, S. J., Li, S. L., et al. (2018). Identification and selection of resistance to Bemisia tabaci among 550 cotton genotypes in the field and greenhouse experiments. *Front. Agr. Sci. Eng.* 5, 236–252. doi: 10.15302/J-FASE-2018223

Zia, K., Ashfaq, M., Arif, M. J., and Sahi, S. T. (2011). Effect of physico-morphic characters on population of whitefly Bemisia tabaci in transgenic cotton. *Pakistan J. Agric. Sci.* 48, 63–69.

Zogli, P., Pingault, L., Grover, S., and Louis, J. (2020). Ento(o)mics: the intersection of 'omic' approaches to decipher plant defense against sap-sucking insect pests. *Curr. Opin. Plant Biol.* 56, 153–161. doi: 10.1016/j.pbi.2020.06.002

Zubair, M., Khan, M. Z., Rauf, I., Raza, A., Shah, A. H., Hassan, I., et al. (2020). Artificial micro RNA (amiRNA)-mediated resistance against whitefly (Bemisia tabaci) targeting three genes. *Crop Prot* 137, 105308. doi: 10.1016/j.cropro.2020.105308

Zust, T., Heichinger, C., Grossniklaus, U., Harrington, R., Kliebenstein, D. J., and Turnbull, L. A. (2012). Natural enemies drive geographic variation in plant defenses. *Science* 338, 116–119. doi: 10.1126/science.1226397

frontiers | Frontiers in Plant Science

TYPE Original Research
PUBLISHED 02 November 2023
DOI 10.3389/fpls.2023.1260526

OPEN ACCESS

EDITED BY
Shengli Jing,
Xinyang Normal University, China

REVIEWED BY
Ruifeng He,
Agricultural Research Service (USDA), United States
Xianjin Qiu,
Yangtze University, China
Hao Zhou,
Sichuan Agricultural University, China

*CORRESPONDENCE
Wentang Lv
lvwentang@whu.edu.cn

†These authors have contributed equally to this work

RECEIVED 18 July 2023
ACCEPTED 09 October 2023
PUBLISHED 02 November 2023

CITATION
Li X, Zhang J, Shangguan X, Yin J, Zhu L, Hu J, Du B and Lv W (2023) Knockout of *OsWRKY71* impairs *Bph15*-mediated resistance against brown planthopper in rice. *Front. Plant Sci.* 14:1260526. doi: 10.3389/fpls.2023.1260526

Knockout of *OsWRKY71* impairs *Bph15*-mediated resistance against brown planthopper in rice

Xiaozun Li[1†], Jian Zhang[1†], Xinxin Shangguan[2,3], Jingjing Yin[1], Lili Zhu[2], Jie Hu[4], Bo Du[2] and Wentang Lv[1*]

[1]Shandong Academy of Agricultural Sciences, Jinan, China, [2]State Key Laboratory of Hybrid Rice, College of Life Sciences, Wuhan University, Wuhan, China, [3]Key Laboratory of Plant Genetics and Molecular Breeding, Zhoukou Normal University, Zhoukou, China, [4]State Key Laboratory of Ecological Pest Control for Fujian and Taiwan Crops, Fujian Agriculture and Forestry University, Fuzhou, China

The *Bph15* gene, known for its ability to confer resistance to the brown planthopper (BPH; *Nilaparvata lugens* Stål), has been extensively employed in rice breeding. However, the molecular mechanism by which *Bph15* provides resistance against BPH in rice remains poorly understood. In this study, we reported that the transcription factor *OsWRKY71* was highly responsive to BPH infestation and exhibited early-induced expression in *Bph15*-NIL (near-isogenic line) plants, and OsWRKY71 was localized in the nucleus of rice protoplasts. The knockout of *OsWRKY71* in the *Bph15*-NIL background by CRISPR-Cas9 technology resulted in an impaired *Bph15*-mediated resistance against BPH. Transcriptome analysis revealed that the transcript profiles responsive to BPH differed between the *wrky71* mutant and *Bph15*-NIL, and the knockout of *OsWRKY71* altered the expression of defense genes. Subsequent quantitative RT-PCR analysis identified three genes, namely sesquiterpene synthase *OsSTPS2*, EXO70 family gene *OsEXO70J1*, and disease resistance gene *RGA2*, which might participate in BPH resistance conferred by *OsWRKY71* in *Bph15*-NIL plants. Our investigation demonstrated the pivotal involvement of *OsWRKY71* in *Bph15*-mediated resistance and provided new insights into the rice defense mechanisms against BPH.

KEYWORDS

rice, brown planthopper, *Bph15*, *OsWRKY71*, defense mechanism, transcriptome

Introduction

The brown planthopper (BPH; *Nilaparvata lugens* Stål) is a major rice (*Oryza sativa*) pest and a representative piercing-sucking insect. The most effective strategy for managing BPH is the cultivation of insect-resistant rice varieties (Zhang, 2007). Research has identified and characterized a total of 34 major BPH resistance genes, with fifteen of them having been isolated (Du et al., 2020; Chen et al., 2022). Among these genes, *Bph14*

encodes a nucleotide-binding and leucine-rich repeat (NLR) protein, which interacts with OsWRKY46 and OsWRKY72, ultimately leading to the activation of downstream defensive genes in rice (Du et al., 2009; Hu et al., 2017). A recent discovery has revealed that Bph14 can directly bind BPH effector BISP, leading to the activation of effector-triggered immunity (ETI) (Guo et al., 2023). *Bph6* encodes a unique leucine-rich repeat (LRR) protein that is specifically localized within the exocyst complex and exhibits interactions with OsEXO70E1 and OsEXO70H3. This interaction promotes protein secretion and strengthens the plant cell wall (Guo et al., 2018; Wu et al., 2022). *Bph30* encodes a novel protein comprising two leucine-rich domains, which is expressed in sclerenchyma cells and enhances the deposition of hemicellulose (Shi et al., 2021). *Bph3*, which was discovered in Rathu Heenati (RH), encodes three lectin receptor kinases (*OsLecRK1-OsLecRK3*) that are located on the plasma membrane and function as receptors in plant immunity (Liu et al., 2014). The *Bph15* locus, derived from *Oryza officinalis*, is a compound locus consisting of two genes. One of these genes is identical to *Bph3* (Cheng et al., 2013a; Xiao et al., 2016), while the other major genetic locus has been localized to the adjacent 580-kb recombination cold-spot region (Lv et al., 2014). The resistance to BPH is mediated through a molecular mechanism that shares similarities with defense mechanisms against pathogens (Cheng et al., 2013b; Du et al., 2020; Chen et al., 2022). *Bph15* and *Bph3* potentially function as receptors for recognizing herbivore-associated molecular patterns (HAMPs), thereby initiating pattern-triggered immunity (PTI). However, the precise molecular mechanisms underlying the functions of *Bph15* and *Bph3* remain poorly elucidated.

In the realm of plants, WRKY transcription factors (TFs) represent a substantial assemblage of TFs, characterized by a discernible affinity for the W-box sequence situated within the promoter regions of their respective target genes (Rushton et al., 2010). The influence of WRKY transcription factors on the immune responses of plants is both significant and extensive (Eulgem and Somssich, 2007). In rice, numerous WRKY TFs have been identified as positive regulators of plant pathogen resistance, exemplified by the enhanced resistance against diverse pathogens observed in *OsWRKY13*, *OsWRKY30*, *OsWRKY45*, and *OsWRKY89* (Qiu et al., 2007; Shimono et al., 2007; Wang et al., 2007; Peng et al., 2012). However, the role of *OsWRKY45* is of significant interest due to its documented importance in providing the rice R protein Pb1 against fungal pathogens, albeit with a negative impact on resistance against the BPH (Inoue et al., 2013; Huangfu et al., 2016). Additionally, another WRKY transcription factor, *OsWRKY53*, has been discovered to act as a positive regulator of plant pathogen and BPH resistance. Moreover, it has been identified as a negative feedback regulator of *MPK3* in response to the herbivorous striped stem borer (SSB) (Chujo et al., 2007; Hu et al., 2015; Hu et al., 2016). The activation of *OsWRKY70* in response to BPH attack has been demonstrated to result in a reduction in gibberellic acid (GA) production in rice, leading to an increased susceptibility to BPH (Li et al., 2015). In general, WRKY TFs play a significant role in regulating plant immune response and can have both positive and negative effects on defense against various pests and pathogens in rice.

Among the members of the OsWRKY IIa subfamily, *OsWRKY28*, *OsWRKY62*, *OsWRKY71*, and *OsWRKY76* are encompassed (Peng et al., 2010). Among these genes, *OsWRKY28* and *OsWRKY76* function as negative regulators of basal defense responses against blast fungus (Chujo et al., 2013; Yokotani et al., 2013). *OsWRKY62* functions as a suppressor of basal and *Xa21*-mediated defense against the bacterial pathogen (Peng et al., 2008). In the absence of *Pi9*, *OsWRKY62* assumes a beneficial role in regulating blast resistance; however, in the presence of *Pi9*, it assumes an adverse role (Shi et al., 2023). The involvement of *OsWRKY71*, which is activated by biotic elicitors and pathogen invasion, plays a significant role in the defense response of rice. Overexpression of *OsWRKY71* enhances rice's resistance to *Xoo*13751, resulting in the constitutive expression of two marker genes, *OsNPR1* and *OsPR1b* (Liu et al., 2007). Furthermore, *OsWRKY71* can interact with the promoter region of the blast resistance gene *GF14b*, thereby influencing its expression (Liu et al., 2016). In addition, *OsWRKY71* also functions as a transcriptional inhibitor (Chujo et al., 2008). Previous studies showed that the overexpression of *OsWRKY71* leads to an increase in H_2O_2 accumulation, resulting in enhanced resistance against the small brown planthopper (*Laodelphax striatellus*, SBPH) in rice (Ji et al., 2021). However, its role in regulating resistance against the BPH remains unclear.

Our previous research indicated that the expression of *OsWRKY71* is up-regulated in the *Bph15* introgression line following BPH feeding (Lv et al., 2014). This study demonstrated that *OsWRKY71* plays a critical role in the *Bph15*-mediated resistance against BPH. The knockout of *OsWRKY71* resulted in an impaired BPH resistance in *Bph15*-NIL. Transcriptome sequencing analysis demonstrated distinct transcript profiles between the *OsWRKY71* knockout plants and *Bph15*-NIL plants, suggesting that *OsWRKY71* is involved in regulating the expression of plant defense genes. Further investigation using qRT-PCR identified three genes, namely sesquiterpene synthase *OsSTPS2*, EXO70 family gene *OsEXO70J1*, and disease resistance gene *RGA2*, which may participate in the BPH resistance conferred by *OsWRKY71* in *Bph15*-NIL plants.

Materials and methods

Plant materials and insects

As previously stated by Lv et al. (2014), the near-isogenic line *Bph15*-NIL (XF07-151) was found to possess the resistance gene *Bph15* in the Taichung Native 1 (TN1) background. This particular line, *Bph15*-NIL, was employed as a control in the study due to its demonstrated resistance. In contrast, the varieties TN1 and Nipponbare (NIP) were selected as susceptible rice controls. The BPH insects, which were reared on the TN1 variety, were utilized for plant feeding during the research conducted at Wuhan University in China.

Development of mutants and overexpression transgenic plants

The *wrky71* mutants were generated using CRISPR-Cas9 technology (Ma et al., 2015). The target sequence of *WRKY71* was designed and used to generate sgRNA expression cassettes driven by the OsU6a promoter. Using an Agrobacterium-mediated technique, the resulting structure was transformed into *Bph15*-NIL plants. The confirmation of T_0 transgenic plants was achieved through genomic targeting by directly sequencing PCR products. The identification of homozygous mutant plants was conducted using PARMS (Penta-primer Amplification Refractory Mutation System) genotyping technology, and these plants were subsequently cultivated for bioassay purposes (Lv et al., 2019).

To construct plasmids for the overexpression of *OsWRKY71*, a 1047 bp coding sequence (CDS) fragment of *OsWRKY71* (accession no. AY676927) was amplified from *Bph15*-NIL (Supplementary Table S1). The PCR product was subsequently introduced into the binary vector pCXUN (accession no. FJ905215). Using an *Agrobacterium*-mediated technique, the resulting structure was transformed into Nipponbare and *Bph15*-NIL plants. The T_2 homozygous plants were grown for the following bioassay.

BPH resistance evaluation

A progeny test was conducted to obtain the rice resistance scores. The seedling stage of rice varieties was evaluated for resistance against BPH, with each cultivar or line being replicated a minimum of three times. Eighteen seeds were collected from individual plants and planted in plastic cups, or fifty seeds were randomly planted in plastic boxes. At the three-leaf stage, eight nymphs of BPH (second- or third-instar) were introduced to infest the seedlings. The plant condition was assessed and assigned a resistance score ranging from 0 to 9, with 9 indicating the highest susceptibility and 0 indicating the highest resistance level, as explained in previous research (Huang et al., 2001).

BPH weight gain assays

The assessment of BPH insect performance on rice encompassed the utilization of assays to quantify BPH weight gain and weight gain rate. BPH was introduced to seedlings at the four-leaf stage after the planting of each line's seeds in a plastic cup with a diameter of 10 cm. Newly emerged female BPH insects were weighed and enclosed in parafilm sachets, which were then affixed to the leaf sheath of a seedling at the four-leaf stage. The BPH instars were allowed to feed on the rice crops for 48 hours. After this feeding period, each insect was removed from the sachet and reweighed. The BPH weight gain was determined by measuring the difference between the initial and final weights of the BPH insect. Furthermore, we computed the weight gain rate, which is determined by dividing the weight gained by the insect's initial weight before feeding. For each cultivar or line, a minimum of three replicates, each containing 10 insects, were utilized.

RNA-seq and data analysis

Stems of three-leaf stage *Bph15*-NIL and *wrky71* mutant *wrky71-5-9* were harvested for 0 (uninfested control), 3, and 24 HAI (hours after BPH infestation). All treatments were terminated at the same time, as previously described (Lv et al., 2014). The *Bph15*-NIL samples were designated as R0, R3, and R24, while the *wrky71-5-9* samples were labeled as S0, S3, and S24. The RNA-seq analysis was conducted using an Illumina Novaseq™ 6000 (LC-Bio Technology CO., Ltd.).

Using the Illumina paired-end RNA-seq technique, transcriptome sequencing was performed, resulting in a total of 305 million paired-end reads with a length of 2×150 bp. Following the application of Cutadapt, the reads underwent filtration and purification, resulting in 42 Gbp of reads with high quality. Subsequently, the cleaned reads were aligned to the rice reference genome using HISAT2. The estimation of transcript expression levels was conducted using the StringTie and Ballgown software, and the expression abundance was determined by calculating the FPKM values. The DESeq2 software was employed for performing differential expression analysis between distinct groups. Genes displaying a p-value below 0.05 and an absolute fold change exceeding 2 were categorized as differentially expressed genes (DGEs). Furthermore, the DGEs underwent subsequent analysis to ascertain the enrichment of functions associated with Gene Ontology (GO) and KEGG pathways. The bioinformatics analysis was carried out utilizing the OmicStudio tools accessible at https://www.omicstudio.cn/tool.

Quantitative RT-PCR

The stems of three-leaf stage *Bph15*-NIL, *wrky71-5-9*, and TN1 were collected after BPH infestation for 0, 3, 6, 12, 24, and 48 HAI. All treatments were terminated simultaneously. The tissue expression profile samples included different rice tissues: stem and leaf of 10 days seedling; stem, sheath, and leaf at the heading stage; stem, sheath, and leaf at 7 days after pollination. The TRIzol reagent (Invitrogen) was employed for the extraction of total RNA. Subsequently, the PrimeScript RT Reagent Kit (Takara) was utilized to perform reverse transcription of 1 μg of total RNA from each sample into cDNA. The qRT-PCR analysis was performed using the QuantStudio™ 5 (Applied Biosystems) and gene-specific primers (Supplementary Table S1) in conjunction with the TB Green (TaKaRa) in the PCR system. The internal control TBP (LOC_Os03g45410) was utilized to standardize the results, and the gene expression levels were determined using the $2^{-\Delta\Delta Ct}$ method. Three biological replicates were conducted for each gene in the qRT-PCR analysis.

Subcellular localization analysis

The coding sequences of *OsWRKY71* were amplified through PCR utilizing the primers OsWRKY71-YFP (Supplementary Table S1). Subsequently, the sequences were cloned downstream of a

ubiquitin promoter, in frame with YFP, within the vector pCAMBIA1300. The resulting construct was designated as OsWRKY71-YFP. To serve as a nucleus marker, a bZIP63-CFP expressing construct was developed and cloned into the pGWB17 vector. The expression constructs were simultaneously introduced into rice protoplasts. The fluorescence was detected using a confocal laser-scanning microscope (FV1000, Olympus).

Statistical analyses

The data were subjected to statistical analysis using a one-way ANOVA in either Microsoft Excel or SPSS software (version 20).

Results

OsWRKY71 is early induced by BPH in *Bph15*-NIL

In our previous study, it was observed that the expression of *OsWRKY71* increased in response to BPH feeding in the *Bph15* introgression line (Lv et al., 2014). To further investigate the role of *OsWRKY71* in the response to BPH, we conducted an analysis of its expression in both the *Bph15*-NIL and TN1 rice plants at various time points following BPH infestation (0, 3, 6, 12, 24, and 48 HAI). The expression level of *OsWRKY71* in the *Bph15*-NIL was significantly higher than in TN1 at 0, 3, and 6 HAI, but this expression pattern was reversed at 12 and 24 HAI (Figure 1A). This suggests that the expression profile of *OsWRKY71* in *Bph15*-NIL differs from that of TN1. Specifically, *OsWRKY71* is early induced by BPH in *Bph15*-NIL. Tissue expression analysis demonstrated that the expression level of *OsWRKY71* is higher in the leaf and sheath tissues at the heading stage compared to other tissues (Figure 1B). Therefore, *OsWRKY71* may play a role in *Bph15*-mediated BPH resistance.

OsWRKY71 is localized in the nucleus

Inconsistent subcellular localization of OsWRKY71 has been reported in previous studies (Liu et al., 2007; Kim et al., 2016; Ji et al., 2021). The present study reveals a significant colocalization between OsWRKY71 and the nucleus marker bZIP63 in rice protoplasts, thereby providing substantial evidence supporting the nuclear localization of OsWRKY71 (Figure 2). This localization pattern is consistent with the well-established role of transcription factors, which primarily function within the nucleus to regulate gene expression.

Knockout of *OsWRKY71* impairs the *Bph15*-mediated resistance against BPH

To further understand the role of *OsWRKY71* in *Bph15*-mediated resistance, we used CRISPR-Cas9 technology to knockout *OsWRKY71* in the *Bph15-NIL* background. Consequently, we achieved the creation of four distinct homozygous mutant plants, denoted as *wrky71-5-9*, *wrky71-2-1*, *wrky71-3-3*, and *wrky71-6-2*, within the T_2 generation. Subsequent DNA sequencing analysis unveiled that each mutant exhibited distinct genetic alterations within the targeted region of the *OsWRKY71* gene. It was observed that *wrky71-5-9* had an insertion of A, *wrky71-2-1* had a deletion of 4 base pairs, *wrky71-3-3* had a deletion of 5 base pairs, and *wrky71-6-2* had a deletion of 13 base pairs (Figure 3A). The BPH resistance scores of the *wrky71* mutants were evaluated, revealing that *wrky71-5-9*, *wrky71-2-1*, *wrky71-3-3*, and *wrky71-6-2* plants were susceptible. Conversely, the *Bph15*-NIL plants, which possessed intact *OsWRKY71*, exhibited resistance and survived the BPH attack (Figure 3B). The mean resistance score for *Bph15*-NIL plants was determined to be 3.27, indicating their resistance to BPH. Conversely, the *wrky71* mutants exhibited significantly higher resistance scores, ranging

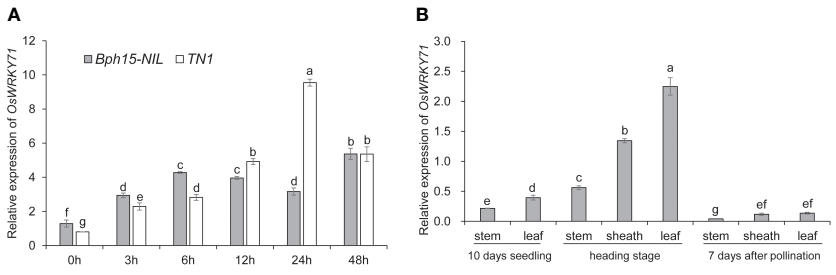

FIGURE 1
The expression profile of *OsWRKY71*. **(A)** Time-dependent expression of *OsWRKY71* in the resistant plant *Bph15*-NIL and susceptible plant TN1 after BPH infestation. **(B)** Tissue expression profile of *OsWRKY71* in various organs. Data represent the means ± SD. The average is determined by calculating the mean of three biological repeats. Significant differences ($p < 0.05$) are indicated by varying letters above the bars, as determined by a one-way ANOVA.

10.3389/fpls.2023.1260526

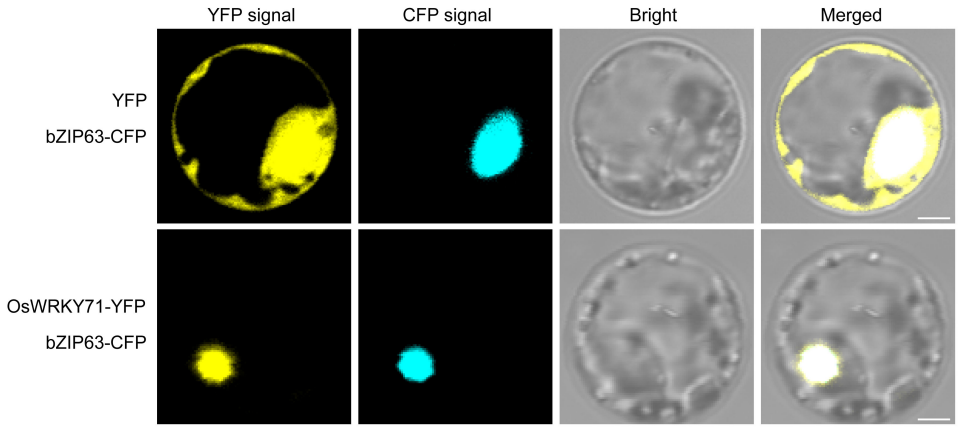

FIGURE 2
OsWRKY71 subcellular localization. The OsWRKY71-YFP and nucleus marker bZIP63-CFP were co-expressed in rice protoplasts. Scale bars, 2.5 μ m.

from 7.42 to 8.51, thereby suggesting their susceptibility to BPH (Figure 3C). Additionally, BPH insects that consumed the *wrky71* mutants displayed a greater increase in weight compared to those that consumed *Bph15*-NIL plants (Figures 3D, E). These findings provide evidence that the knockout of *OsWRKY71* impairs the resistance of *Bph15*-NIL plants to BPH, thereby emphasizing the crucial role of *OsWRKY71* in *Bph15*-mediated resistance.

We also generated overexpression lines of *OsWRKY71* in both the Nipponbare and *Bph15*-NIL backgrounds. However, the overexpression of *OsWRKY71* in both backgrounds did not result in significant differences in BPH resistance compared to the control plants. Specifically, the *Bph15*-NIL-OE plants, which overexpressed *OsWRKY71* in the *Bph15*-NIL background, exhibited BPH resistance scores similar to those of the *Bph15*-NIL control plants. This suggests that the overexpression of *OsWRKY71* did not enhance the resistance provided by *Bph15* (Supplementary Figure S1A). In a similar vein, the NIP-OE plants, characterized by the overexpression of *OsWRKY71* in the Nipponbare background, exhibited susceptibility to BPH and were killed by BPH at the same time as the susceptible Nipponbare plants (Supplementary Figure S1B). These observations imply that increasing the expression of the *OsWRKY71* gene does not exert any discernible influence on BPH resistance, irrespective of the presence or absence of

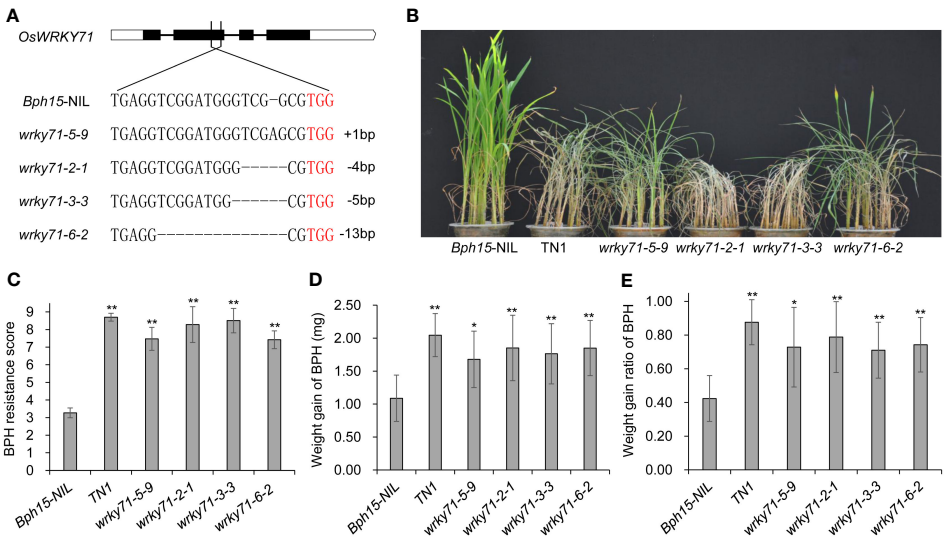

FIGURE 3
BPH resistance test of the *OsWRKY71* knockout plants. **(A)** Four representative homozygous *wrky71* mutants in the *Bph15*-NIL background. TGG (red) is the PAM sequence. **(B)** BPH resistance evaluation of *wrky71* mutants. **(C)** BPH average resistance scores of *wrky71* mutants. Data represent the means ± SD from three separate experiments, each consisting of 15 seedlings per rice line. Significant differences in comparison with *Bph15*-NIL are indicated by asterisks above the bars (**p < 0.01 by one-way ANOVA). **(D, E)** BPH weight gain and weight gain rate assays of *wrky71* mutants. Data represent the means ± SD from three separate experiments, each consisting of 10 BPH insects per replicate. Significant differences in comparison with *Bph15*-NIL are indicated by asterisks above the bars (**p < 0.01, *p < 0.05 by one-way ANOVA).

10.3389/fpls.2023.1260526

Bph15. Consequently, it can be deduced that *OsWRKY71* does not function as a positive regulator of basal resistance in the absence of *Bph15*.

The transcript profiles that respond to BPH are different in the *wrky71* mutant and *Bph15*-NIL

To investigate the potential mechanism underlying the impact of the *wrky71* mutant on *Bph15*-mediated resistance to BPH, we conducted an analysis of the transcriptomes of *wrky71-5-9* and *Bph15*-NIL using RNA-seq. The RNA-seq analysis identified a total of 1387 differentially expressed genes (DEGs) among seven comparisons: R0_S0, R3_S3, R24_S24, R0_R3, R0_R24, S0_S3, and S0_S24 (Supplementary Table S2). Significant disparities in gene expression were observed between the *wrky71* mutant and *Bph15*-NIL. Specifically, in the comparisons of R0_S0, R3_S3, and R24_S24, the *wrky71* mutant displayed significant alterations in 390, 208, and 153 genes, respectively, when compared to *Bph15*-NIL. Moreover, the *wrky71* mutant displayed 248 and 339 DEGs in the S0_S3 and S0_S24 comparisons, respectively. Conversely, in *Bph15*-NIL, there were 607 and 529 DEGs in the R0_R3 and R0_R24 comparisons, respectively. Notably, both the R and S comparisons exhibited a higher abundance of up-regulated genes compared to down-regulated genes (Figure 4A). Subsequent analysis revealed significant disparities in the majority of the up-regulated and down-regulated genes between the *wrky71* mutant and *Bph15*-NIL (Figure 4B). Additionally, hierarchical cluster analysis of 1387 DEGs further confirmed substantial distinctions between the R and S comparisons (Supplementary Figure S2).

The enriched Gene Ontology (GO) terms identified in this study suggest that the response to BPH feeding in both the *wrky71* mutant and *Bph15*-NIL rice involves multiple key biological processes. Specifically, the common GO terms observed in the up-regulated DEGs (Supplementary Figure S3; Table S3_1) in the S0_S3, S0_S24, R0_R3, and R0_R24 comparisons include wounding response, chitin response, fungus defense, and salicylic acid (SA) response. These shared GO terms indicate that both the *wrky71* mutant and *Bph15*-NIL rice employ similar defense mechanisms in response to BPH feeding. Significant disparities in enriched GO terms were observed when comparing gene expression between the *wrky71* mutant and *Bph15*-NIL rice. Specifically, the R0_R3 and R0_R24 comparisons revealed enriched GO terms related to water deprivation response, cell wall, autophagy, and trehalose phosphatase. Conversely, the S0_S3 and S0_S24 comparisons exhibited specifically enriched GO terms associated with ethylene (ET) response, jasmonic acid (JA) response, gibberellin metabolic, bacterium defense, virus defense, and herbivore response (Figure 5; Supplementary Tables S3_2-S3_5). The enriched GO term "sesquiterpene biosynthetic" in both the R0_R24 and S0_S3 comparisons suggests that this biological process may play a crucial role in conferring resistance to BPH in both the *wrky71* mutant and *Bph15*-NIL rice (Figure 5). These results emphasize the potential contribution of diverse biological processes and signaling pathways in the resistance mechanisms of the *wrky71* mutant and *Bph15*-NIL rice, providing valuable insights for future investigations on BPH resistance in rice.

The KEGG pathway enrichment analysis demonstrated significant enrichment in multiple pathways within the transcript profiles of both the *wrky71* mutant and *Bph15*-NIL plants upon exposure to BPH infestation. Notably, these pathways encompassed plant-pathogen interaction, plant hormone signal, autophagy, et al. (Supplementary Figure S4; Table S4_1). Intriguingly, the R0_R3 and R0_R24 comparisons exhibited a higher number of genes involved in these pathways compared to the S0_S3 and S0_S24 comparisons (Supplementary Figure S5; Tables S4_2-S4_5). This observation implies the existence of discrete regulatory mechanisms functioning in the two genotypes in response to BPH infestation. Overall, these findings provide insights into the molecular

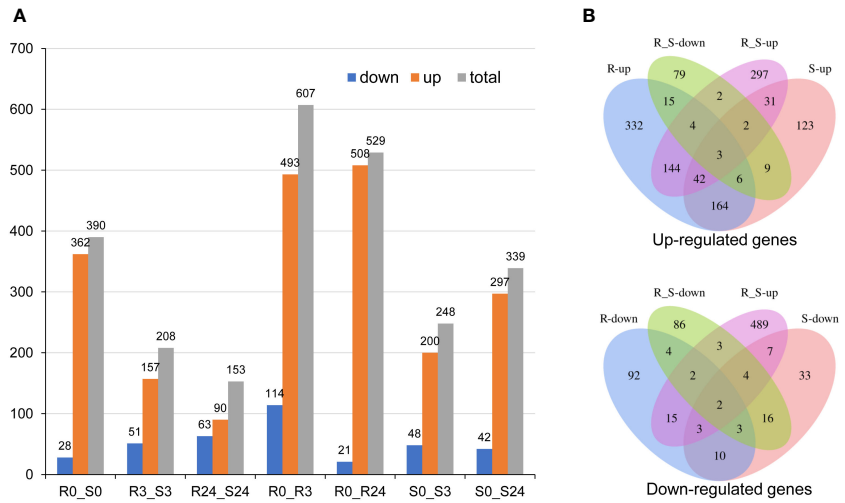

FIGURE 4
DEGs of two rice varieties (*Bph15*-NIL and *wrky71-5-9*). **(A)** The DEGs in all comparisons. **(B)** Venn diagrams of the up-regulated and down-regulated DEGs.

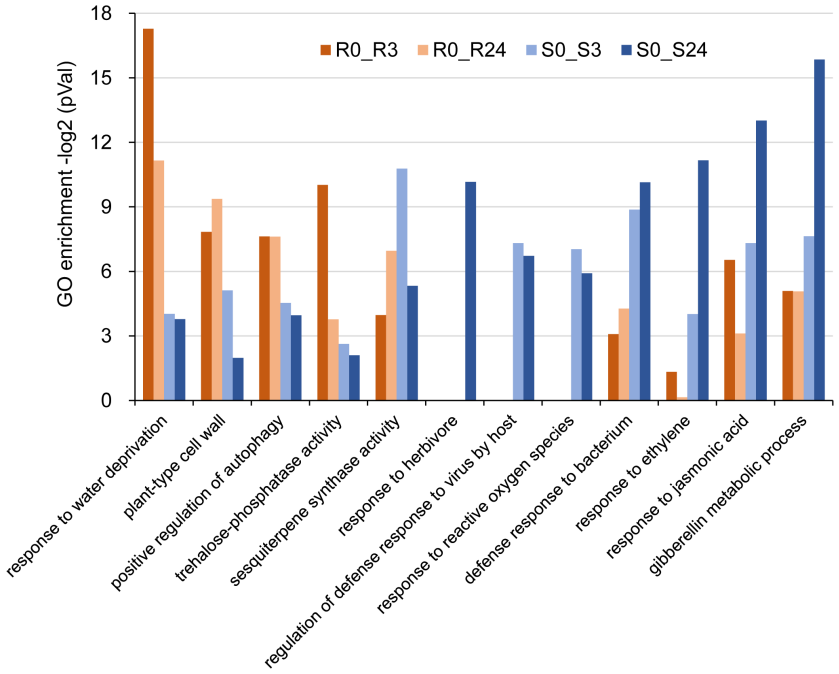

FIGURE 5
Representative GO terms of up-regulated DEGs in R0_R3, R0_R24, S0_S3, and S0_S24 comparisons. vertical coordinate: -log_2(P-value). -log_2(P-value) > 6.64 = $p < 0.01$, -log_2(P-value) > 4.32 = $p < 0.05$.

mechanisms of BPH resistance in rice and underscore the importance of *OsWRKY71* in governing gene expression during BPH infestation.

Knockout of *OsWRKY71* alters the expression of plant defense genes

The study revealed a significant down-regulation of the sesquiterpene synthase gene *OsSTPS2* in the R3_S3 and R24_S24 comparisons (Figure 6). Subsequent analysis using qRT-PCR demonstrated a notable decrease in expression levels of *OsSTPS2* in both the *wrky71* mutant and TN1 compared to *Bph15*-NIL at all five time points (Figure 7). Terpenes, a class of secondary metabolites, possess diverse functions, including defense against herbivores. Previous research has demonstrated the differential expression of *OsSTPS2* in rice cultivars RH (carrying *Bph3*) and KD (sensitive to BPH), and its involvement in BPH antixenosis resistance (Kamolsukyunyong et al., 2013; Kamolsukyeunyong et al., 2021). This suggests that *OsSTPS2* may participate in BPH resistance conferred by *OsWRKY71* in *Bph15*-NIL plants.

The excretion of proteins associated with resistance and the plant's resistance to BPH are influenced by the trafficking pathway that relies on the presence of EXO70. Specifically, the functions of *OsEXO70E1* and *OsEXO70H3* are involved in *Bph6*-mediated BPH resistance (Guo et al., 2018; Wu et al., 2022). Our investigation led to the discovery of the *OsEXO70J1* gene (LOC_Os08g13570), a member of the EXO70 family, which exhibited significant up-regulation in the R0_R3 and R0_R24 comparisons, but down-regulation in the R3_S3 comparison (Figure 6; Supplementary Figure S6). Additionally, the results of qRT-

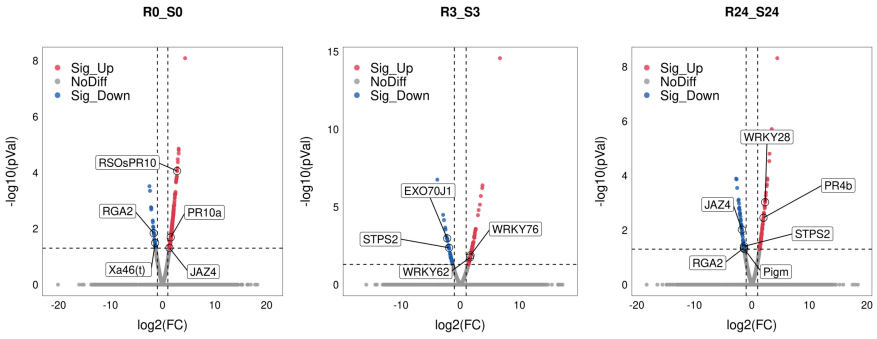

FIGURE 6
Volcano plots of R0_S0, R3_S3, and R24_S24 comparisons. The representative DEGs were marked as boxes.

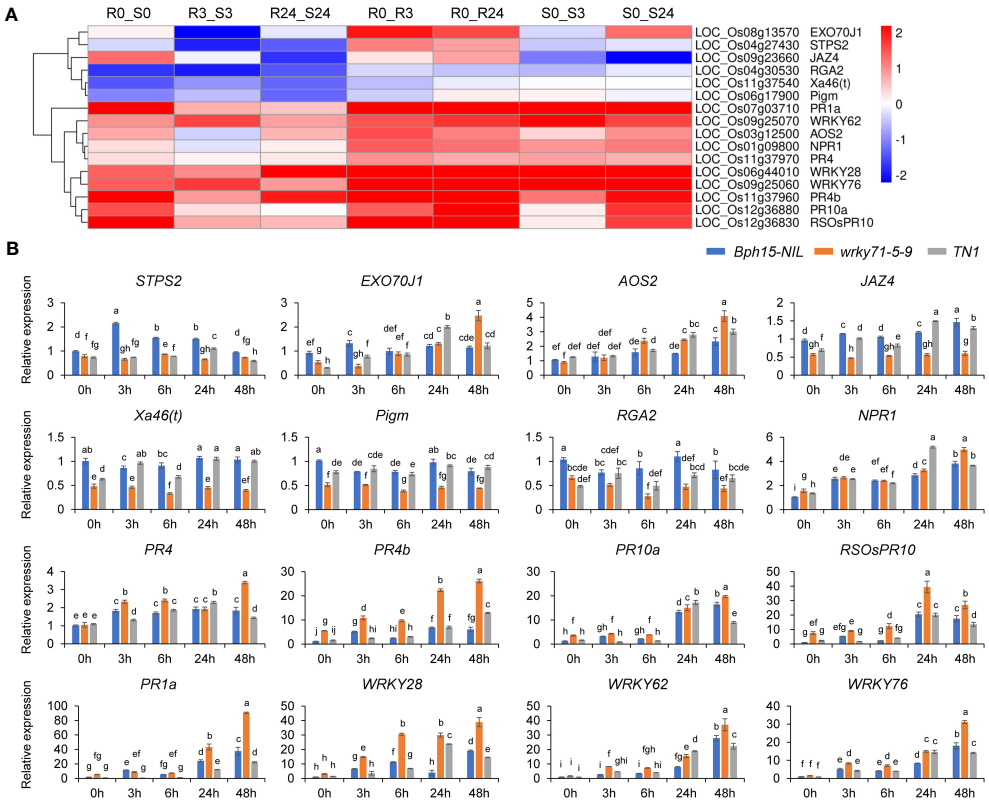

FIGURE 7
Heat map and qRT-PCR analysis of representative DGEs. **(A)** Heat map of representative DGEs studied in this work. **(B)** qRT-PCR analysis of representative DGEs. Data represent the means ± SD. Significant differences ($p < 0.05$) are indicated by varying letters above the bars, as determined by a one-way ANOVA.

PCR analysis showed that the expression levels of *OsEXO70J1* were reduced in both the *wrky71* mutant and TN1 cultivars compared to *Bph15*-NIL at the onset of BPH infestation (Figure 7). This suggests that *OsEXO70J1* may participate in BPH resistance conferred by *OsWRKY71* in *Bph15*-NIL plants.

Interestingly, the down-regulation of three R genes, namely *Xa46(t)* (LOC_Os11g37540), *Pigm* (LOC_Os06g17900), and *RGA2* (LOC_Os04g30530), was observed in the R_S comparisons (Figure 6). It was found that BPH feeding did not induce the up-regulation of these genes in any of the rice lines. However, the expression levels of these genes were significantly reduced in the *wrky71* mutant compared to *Bph15*-NIL. Additionally, the expression level of *RGA2* was also decreased in TN1 when compared to *Bph15*-NIL plants (Figure 7). These findings suggest that *OsWRKY71* may be involved in controlling the expression of these three R genes and contribute to disease resistance in rice. It is also suggested that the R gene *RGA2* may have a dual function in both disease and BPH resistance.

The influence of the SA and JA pathways on plant responses to insects is of significant importance. However, our previous study suggested that the SA signaling pathway may not be triggered in *Bph15*-mediated resistance (Lv et al., 2014). In this current investigation, we focused on the JA pathway and found that the expression levels of the *AOS2* gene, which is involved in JA synthesis, were increased in both the *wrky71* mutant and TN1 compared to *Bph15*-NIL. Furthermore, the transcript levels of the JA repressor *JAZ4* were lower in the *wrky71* mutant compared to *Bph15*-NIL and TN1 (Figure 7). The results indicate that *OsWRKY71* may inhibit the JA pathway in *Bph15*-NIL plants. Hence, the *Bph15*-mediated BPH resistance may not be associated with the SA and JA signaling pathways.

The present study observed an increase in the expression of *NPR1* and five PR genes (*PR1a*, *PR4*, *PR4b*, *PR10a*, and *RSOsPR10*) in all three rice lines. However, the expression levels of these genes were higher in the *wrky71* mutant compared to *Bph15*-NIL plants (Figure 7). This suggests that these genes may be involved in a common defense mechanism in both resistant and susceptible rice varieties. These results are consistent with our previous study (Lv et al., 2014). It was observed that the transcript levels of *OsWRKY28*, *OsWRKY62*, and *OsWRKY76*, members of the OsWRKY IIa subfamily, exhibited a significant increase in all three rice lines. However, in the *wrky71* mutant, their expression levels were even higher compared to *Bph15*-NIL plants (Figure 7). This suggests that in the absence of *Bph15*, these genes may act as promoters of BPH resistance, but in the presence of *Bph15*, they could exert an inhibitory effect. These findings are consistent with the previous studies conducted by Chujo et al. (2013) and Shi et al. (2023).

Discussion

BPH resistance genes *Bph15* and *Bph3* may act as pattern recognition receptors (PRRs) in the activation of PTI for plant immunity (Du et al., 2020; Chen et al., 2022). The present study has revealed the significant contribution of *OsWRKY71* in the *Bph15*-mediated resistance against BPH. The knockout of *OsWRKY71* has been observed to impair the resistance to BPH in *Bph15*-NIL plants, as depicted in Figure 3. These findings underscore the role of *OsWRKY71* in the underlying molecular mechanisms of *Bph15*-mediated resistance against BPH. In our previous studies, we successfully cloned the first BPH resistance gene *Bph14*, and observed the interaction between the BPH14 protein and OsWRKY46 and OsWRKY72 (Du et al., 2009; Hu et al., 2017). Further research about how *OsWRKY71* is induced by *BPH15* and BPH infestation will enhance our comprehension of the signaling pathways implicated in rice defense against BPH.

The study by Liu et al. (2007) and Ji et al. (2021) reported that *OsWRKY71* enhances resistance to bacterial blight and SBPH in the Nipponbare variety of rice. However, our study found that overexpression of *OsWRKY71* did not increase resistance to BPH in both the Nipponbare and *Bph15*-NIL backgrounds. This suggests that *OsWRKY71* may have varying effects on resistance to BPH and other pathogens or piercing-sucking insects. Similar contrasting roles have been observed for another gene, *OsWRKY45*, in rice pathogens and BPH resistance (Huangfu et al., 2016).

Interestingly, the *OsWRKY71* gene displayed an early induced expression pattern in *Bph15*-NIL, while its level of gene expression was comparatively lower than that of the TN1 at 12 and 24 HAI (Figure 1A). However, little is known about the underlying mechanism, and more research needs to be done. The induced expression pattern in TN1 suggests that *OsWRKY71* may potentially contribute to a basal defense in susceptible rice varieties. However, it is important to note that the NIP-OE plants, which overexpress *OsWRKY71*, exhibited susceptibility to BPH infestation (Supplementary Figure S1B). This indicates that *OsWRKY71* does not function as a promoter of basal resistance in the absence of *Bph15*. Previous studies have demonstrated that *OsWRKY62* can play opposite roles depending on the existence or nonexistence of the blast-resistance gene *Pi9* (Shi et al., 2023). Similarly, it is plausible that *OsWRKY71*, akin to *OsWRKY62*, possesses a dual capacity in governing the basal resistance against BPH in rice. Nevertheless, further research is required to ascertain whether *OsWRKY71* acts as a negative modulator of BPH basal defense.

Previous research has provided evidence for the involvement of the plant sesquiterpene synthase *OsSTPS2* in an antixenosis mechanism of BPH resistance mediated by *Bph3* (RH variety) (Kamolsukyunyong et al., 2013; Kamolsukyeunyong et al., 2021). In this study, we observed that the expression of *OsSTPS2* was suppressed in the *wrky71* mutant within the *Bph15*-NIL genetic background (Figure 7). This finding suggests that *OsSTPS2* may play a part in the antixenosis process of BPH resistance regulated by *Bph15*, and its regulation is mediated by the *Bph15-OsWRKY71* pathway. Our future investigations aim to identify the specific plant volatile compounds released by the *wrky71* mutant and *Bph15*-NIL following BPH infestation. Furthermore, our previous research has demonstrated the involvement of *OsEXO70E1* and *OsEXO70H3* in the *Bph6*-mediated resistance against planthoppers, as they facilitate exocytosis and enhance the strength of the cell wall (Guo et al., 2018; Wu et al., 2022). Notably, the analysis revealed a significant enrichment of the GO term "plant-type cell wall" in the R comparison (Figure 5). Moreover, the expression of *OsEXO70J1* was found to be downregulated in both the *wrky71* mutant and TN1 varieties, in contrast to *Bph15*-NIL, during the initial infestation of BPH (Figure 7). This finding suggests that *OsEXO70J1* may contribute to the resistance against BPH conferred by *OsWRKY71* in *Bph15*-NIL plants. Interestingly, the study found that the disease-resistance gene *RGA2* may also participate in BPH resistance conferred by *OsWRKY71* in *Bph15*-NIL plants. This implies that the plant immune system, traditionally recognized for its role in protecting against pathogens, may also be involved in plant-insect interactions. There may be shared downstream signaling mechanisms within the plant immune system that are relevant to these diverse types of interactions.

The SA and JA plant hormone signals are essential for defending rice against insects. However, the effectiveness of SA and JA in regulating rice defense against BPH is dependent on the specific genotype of the rice. The SA pathway is implicated in BPH resistance mediated by *Bph6*, *Bph9*, and *Bph14* (Du et al., 2009; Zhao et al., 2016; Guo et al., 2018). Moreover, the synergistic impact of SA and JA has been observed to enhance BPH resistance in *Bph6* plants, as reported by Guo et al. (2018). However, it has been discovered that *Bph15*-mediated BPH immunity is not influenced by the SA and JA pathways. This suggests the existence of additional mechanisms contributing to *Bph15*-mediated resistance. Additionally, *NPR1*, *PR1a*, *PR4*, *PR4b*, *PR10a*, and *RSOsPR10* are involved in a shared fundamental protective mechanism in both susceptible and resistant varieties of rice, except for *Bph15*-mediated BPH resistance.

Based on the findings of the study, it was observed that BPH insects that fed on the *wrky71* mutants exhibited a slight reduction in weight in comparison to those that fed on TN1 plants (Figures 3C–E). This implies that the *wrky71* mutants possess little resistance against BPH. Thus, it can be inferred that there exist other pathways implicated in *Bph15*-mediated BPH resistance signaling, and *OsWRKY71* does not exclusively regulate this resistance. The *Bph15*-NIL harbors two BPH resistance genes (*Bph3* and *Bph15*) (Lv et al., 2014; Xiao et al., 2016), thereby indicating the presence of multiple mechanisms contributing to BPH resistance. Further research should be undertaken to clone and characterize the resistance gene located in the recombination cold-spot region (Lv et al., 2014) to gain a more comprehensive understanding of their molecular mechanism against BPH. One potential approach involves the reconstruction of the genetic population capable of producing crossover in the recombination cold-spot region. This necessitates the identification of susceptible parents exhibiting a greater degree of chromosomal homology within the specified interval. Additionally, the deficiency in the *Bph15* physical map (Lv et al., 2014) could be addressed through the utilization of third-generation PacBio long-read sequencing to achieve completion.

In summary, the most significant finding to emerge from this study is that *OsWRKY71* plays a critical role in the *Bph15*-mediated BPH resistance in rice. This investigation significantly enhances our comprehension of the molecular mechanisms underlying *Bph15*-mediated BPH resistance. Further investigations should be conducted to successfully clone and identify all resistance genes in the *Bph15* locus.

Data availability statement

The raw sequence files were deposited in the GSA database of the National Genomics Data Center (https://ngdc.cncb.ac.cn) with the accession number CRA011634 (https://ngdc.cncb.ac.cn/gsa/browse/CRA011634).

Author contributions

XL: Investigation, Writing – original draft, Writing – review & editing. JZ: Investigation, Writing – original draft, Writing – review & editing. XS: Investigation, Writing – review & editing. JY: Investigation, Writing – review & editing. LZ: Investigation, Writing – review & editing. JH: Investigation, Writing – review & editing. BD: Investigation, Writing – review & editing. WL: Funding acquisition, Investigation, Project administration, Resources, Supervision, Writing – original draft, Writing – review & editing.

Funding

The author(s) declare financial support was received for the research, authorship, and/or publication of this article. This work was supported by the National Natural Science Foundation of China (Grant No. 31601650 and 32001921), the Young Talents Training Program of Shandong Academy of Agricultural Sciences, the Science and Technology Innovation Project of Shandong Academy of Agricultural Sciences (Grant No. CXGC2018E16), the Open Research Fund of the State Key Laboratory of Hybrid Rice (Wuhan University) (Grant No. KF201902), the Agricultural Variety Improvement Project of Shandong Province (Grant No. 2022LZGC024), and the Key Research and Development Plan of Shandong Province (Grant No. 2022TZXD0040).

Acknowledgments

We thank Prof. Guangcun He (Wuhan University) for providing the *Bph15*-NIL. We also thank Prof. Xianzhi Xie (Shandong Academy of Agricultural Sciences) and Dr. Jianping Guo (Wuhan University) for providing helpful suggestions in this work.

Conflict of interest

The authors declare that the research was conducted in the absence of any commercial or financial relationships that could be construed as a potential conflict of interest.

Publisher's note

Supplementary material

The Supplementary Material for this article can be found online at: https://www.frontiersin.org/articles/10.3389/fpls.2023.1260526/full#supplementary-material

SUPPLEMENTARY FIGURE 1
BPH-resistance scores of the *OsWRKY71* overexpression lines in the *Bph15*-NIL and Nipponbare backgrounds. **(A)** BPH-resistance scores of the *OsWRKY71* overexpression lines in the *Bph15*-NIL backgrounds. Bph15NIL-OE1, -OE2, and -OE3 are homozygous T_2 progeny from independent transformants. **(B)** BPH-resistance scores of the *OsWRKY71* overexpression lines in the Nipponbare backgrounds. NIP-OE1, -OE2, and -OE3 are homozygous T_2 progeny from independent transformants. Data represent the means ± SD from three separate experiments, each consisting of 15 seedlings per rice line. Significant differences ($p < 0.05$) are indicated by varying letters above the bars, as determined by a one-way ANOVA.

SUPPLEMENTARY FIGURE 2
Hierarchical cluster analysis of 1387 DEGs based on the $\log_2$(FC).

SUPPLEMENTARY FIGURE 3
GO enrichment analysis of 1387 DEGs.

SUPPLEMENTARY FIGURE 4
KEGG pathway enrichment analysis of 1387 DEGs.

SUPPLEMENTARY FIGURE 5
Representative KEGG pathway numbers of R0_R3, R0_R24, S0_S3, and S0_S24 comparisons.

SUPPLEMENTARY FIGURE 6
Volcano plots of R0_R3, R0_R24, S0_S3, and S0_S24 comparisons. Horizontal coordinate: $\log_2$(fold change), vertical coordinate: $-\log_{10}$(P-value). The representative DEGs were marked as boxes.

References

Chen, R., Deng, Y., Ding, Y., Guo, J., Qiu, J., Wang, B., et al. (2022). Rice functional genomics: decades' efforts and roads ahead. *Sci. China Life Sci.* 65, 33–92. doi: 10.1007/s11427-021-2024-0

Cheng, X., Wu, Y., Guo, J., Du, B., Chen, R., Zhu, L., et al. (2013a). A rice lectin receptor-like kinase that is involved in innate immune responses also contributes to seed germination. *Plant J.* 76, 687–698. doi: 10.1111/tpj.12328

Cheng, X., Zhu, L., and He, G. (2013b). Towards understanding of molecular interactions between rice and the brown planthopper. *Mol. Plant* 6, 621–634. doi: 10.1093/mp/sst030

Chujo, T., Kato, T., Yamada, K., Takai, R., Akimoto-Tomiyama, C., Minami, E., et al. (2008). Characterization of an elicitor-induced rice WRKY gene, *OsWRKY71*. *Biosci. Biotechol. Biochem.* 72, 240–245. doi: 10.1271/bbb.70553

Chujo, T., Miyamoto, K., Shimogawa, T., Shimizu, T., Otake, Y., Yokotani, N., et al. (2013). *OsWRKY28*, a PAMP-responsive transrepressor, negatively regulates innate immune responses in rice against rice blast fungus. *Plant Mol. Biol.* 82, 23–37. doi: 10.1007/s11103-013-0032-5

Chujo, T., Takai, R., Akimoto-Tomiyama, C., Ando, S., Minami, E., Nagamura, Y., et al. (2007). Involvement of the elicitor-induced gene *OsWRKY53* in the expression of defense-related genes in rice. *Biochim. Biophys. Acta (BBA) - Gene Structure Expression* 1769, 497–505. doi: 10.1016/j.bbaexp.2007.04.006

Du, B., Chen, R., Guo, J., and He, G. (2020). Current understanding of the genomic, genetic, and molecular control of insect resistance in rice. *Mol. Breed.* 40, 24. doi: 10.1007/s11032-020-1103-3

Du, B., Zhang, W., Liu, B., Hu, J., Wei, Z., Shi, Z., et al. (2009). Identification and characterization of *Bph14*, a gene conferring resistance to brown planthopper in rice. *Proc. Natl. Acad. Sci. U.S.A.* 106, 22163–22168. doi: 10.1073/pnas.0912139106

Eulgem, T., and Somssich, I. (2007). Networks of WRKY transcription factors in defense signaling. *Curr. Opin. Plant Biol.* 10, 366–371. doi: 10.1016/j.pbi.2007.04.020

Guo, J., Wang, H., Guan, W., Guo, Q., Wang, J., Yang, J., et al. (2023). A tripartite rheostat controls self-regulated host plant resistance to insects. *Nature* 618, 799-807. doi: 10.1038/s41586-023-06197-z

Guo, J., Xu, C., Wu, D., Zhao, Y., Qiu, Y., Wang, X., et al. (2018). *Bph6* encodes an exocyst-localized protein and confers broad resistance to planthoppers in rice. *Nat. Genet.* 50, 297–306. doi: 10.1038/s41588-018-0039-6

Hu, L., Wu, Y., Wu, D., Rao, W., Guo, J., Ma, Y., et al. (2017). The coiled-coil and nucleotide binding domains of BROWN PLANTHOPPER RESISTANCE14 function in signaling and resistance against planthopper in rice. *Plant Cell* 29, 3157–3185. doi: 10.1105/tpc.17.00263

Hu, L., Ye, M., Li, R., and Lou, Y. (2016). OsWRKY53, a versatile switch in regulating herbivore-induced defense responses in rice. *Plant Signal Behav.* 11, e1169357. doi: 10.1080/15592324.2016.1169357

Hu, L., Ye, M., Li, R., Zhang, T., Zhou, G., Wang, Q., et al. (2015). The rice transcription factor WRKY53 suppresses herbivore-induced defenses by acting as a negative feedback modulator of mitogen-activated protein kinase activity. *Plant Physiol.* 169, 2907–2921. doi: 10.1104/pp.15.01090

Huang, Z., He, G., Shu, L., Li, X., and Zhang, Q. (2001). Identification and mapping of two brown planthopper resistance genes in rice. *Theor. Appl. Genet.* 102, 929–934. doi: 10.1007/s001220000455

Huangfu, J., Li, J., Li, R., Ye, M., Kuai, P., Zhang, T., et al. (2016). The transcription factor *OsWRKY45* negatively modulates the resistance of rice to the brown planthopper *Nilaparvata lugens*. *Int. J. Mol. Sci.* 17, 697. doi: 10.3390/ijms17060697

Inoue, H., Hayashi, N., Matsushita, A., Xinqiong, L., Nakayama, A., Sugano, S., et al. (2013). Blast resistance of CC-NB-LRR protein Pb1 is mediated by WRKY45 through protein-protein interaction. *Proc. Natl. Acad. Sci. U.S.A.* 110, 9577–9582. doi: 10.1073/pnas.1222155110

Ji, R., Fu, J., Shi, Y., Li, J., Jing, M., Wang, L., et al. (2021). Vitellogenin from planthopper oral secretion acts as a novel effector to impair plant defenses. *New Phytol.* 232, 802–817. doi: 10.1111/nph.17620

Kamolsukyeunyong, W., Sukhaket, W., Pitija, K., Thorngkham, P., Mahatheeranont, S., Toojinda, T., et al. (2021). Rice sesquiterpene plays important roles in antixenosis against brown planthopper in rice. *Plants* 10, 1049. doi: 10.3390/plants10061049

Kamolsukyunyong, W., Sukhaket, W., Ruanjaichon, V., Toojinda, T., and Vanavichit, A. (2013). Single-feature polymorphism mapping of isogenic rice lines identifies the influence of terpene synthase on brown planthopper feeding preferences. *Rice* 6, 18. doi: 10.1186/1939-8433-6-18

Kim, C., Vo, K., Nguyen, C., Jeong, D., Lee, S., Kumar, M., et al. (2016). Functional analysis of a cold-responsive rice WRKY gene, *OsWRKY71*. *Plant Biotechnol. Rep.* 10, 13–23. doi: 10.1007/s11816-015-0383-2

Li, R., Zhang, J., Li, J., Zhou, G., Wang, Q., Bian, W., et al. (2015). Prioritizing plant defence over growth through WRKY regulation facilitates infestation by non-target herbivores. *eLife* 4, e04805. doi: 10.7554/eLife.04805

Liu, X., Bai, X., Wang, X., and Chu, C. (2007). *OsWRKY71*, a rice transcription factor, is involved in rice defense response. *J. Plant Physiol.* 164, 969–979. doi: 10.1016/j.jplph.2006.07.006

Liu, Y., Wu, H., Chen, H., Liu, Y., He, J., Kang, H., et al. (2014). A gene cluster encoding lectin receptor kinases confers broad-spectrum and durable insect resistance in rice. *Nat. Biotechnol.* 33, 301. doi: 10.1038/nbt.3069

Liu, Q., Yang, J., Zhang, S., Zhao, J., Feng, A., Yang, T., et al. (2016). *OsGF14b* positively regulates panicle blast resistance but negatively regulates leaf blast resistance in rice. *Mol. Plant Microbe Interact.* 29, 46–56. doi: 10.1094/mpmi-03-15-0047-r

Lv, W., Du, B., Shangguan, X., Zhao, Y., Pan, Y., Zhu, L., et al. (2014). BAC and RNA sequencing reveal the brown planthopper resistance gene *BPH15* in a recombination cold spot that mediates a unique defense mechanism. *BMC Genomics* 15, 674. doi: 10.1186/1471-2164-15-674

Lv, W., Yin, J., Yin, X., Xu, G., Wu, X., Li, X., et al. (2019). Application of PARMS technology in genotyping of rice gene edited progeny. *Shandong Agric. Sci.* 51, 8–13.

Ma, X., Zhang, Q., Zhu, Q., Liu., W., Chen, Y., Qiu, R., et al. (2015). A robust CRISPR/Cas9 system for convenient, high-efficiency multiplex genome editing in monocot and dicot plants. *Mol. Plant* 8, 1274–1284. doi: 10.1016/j.molp.2015.04.007

Peng, Y., Bartley, L., Canlas, P., and Ronald, P. (2010). OsWRKY IIa transcription factors modulate rice innate immunity. *Rice* 3, 36–42. doi: 10.1007/s12284-010-9039-6

Peng, Y., Bartley, L., Chen, X., Dardick, C., Chern, M., Ruan, R., et al. (2008). OsWRKY62 is a negative regulator of basal and *Xa21*-mediated defense against *Xanthomonas oryzae* pv. *oryzae* in rice. *Mol. Plant Microbe Interact.* 1, 446–458. doi: 10.1093/mp/ssn024

Peng, X., Hu, Y., Tang, X., Zhou, P., Deng, X., Wang, H., et al. (2012). Constitutive expression of rice *WRKY30* gene increases the endogenous jasmonic acid accumulation, PR gene expression and resistance to fungal pathogens in rice. *Planta* 236, 1485–1498. doi: 10.1007/s00425-012-1698-7

Qiu, D., Xiao, J., Ding, X., Xiong, M., Cai, M., Cao, Y., et al. (2007). OsWRKY13 mediates rice disease resistance by regulating defense-related genes in salicylate- and jasmonate-dependent signaling. *Mol. Plant Microbe Interact.* 20, 492–499. doi: 10.1094/mpmi-20-5-0492

Rushton, P., Somssich, I., Ringler, P., and Shen, Q. (2010). WRKY transcription factors. *Trends Plant Sci.* 15, 247–258. doi: 10.1016/j.tplants.2010.02.006

Shi, S., Wang, H., Nie, L., Tan, D., Zhou, C., Zhang, Q., et al. (2021). *Bph30* confers resistance to brown planthopper by fortifying sclerenchyma in rice leaf sheaths. *Mol. Plant* 14, 1714–1732. doi: 10.1016/j.molp.2021.07.004

Shi, X., Xiong, Y., Zhang, K., Zhang, Y., Zhang, J., Zhang, L., et al. (2023). The ANIP1-OsWRKY62 module regulates both basal defense and Pi9-mediated immunity against *Magnaporthe oryzae* in rice. *Mol. Plant* 16, 739–755. doi: 10.1016/j.molp.2023.03.001

Shimono, M., Sugano, S., Nakayama, A., Jiang, C., Ono, K., Toki, S., et al. (2007). Rice WRKY45 plays a crucial role in benzothiadiazole-inducible blast resistance. *Plant Cell* 19, 2064–2076. doi: 10.1105/tpc.106.046250

Wang, H., Hao, J., Chen, X., Hao, Z., Wang, X., Lou, Y., et al. (2007). Overexpression of rice WRKY89 enhances ultraviolet B tolerance and disease resistance in rice plants. *Plant Mol. Biol.* 65, 799–815. doi: 10.1007/s11103-007-9244-x

Wu, D., Guo, J., Zhang, Q., Shi, S., Guan, W., Zhou, C., et al. (2022). Necessity of rice resistance to planthoppers for OsEXO70H3 regulating SAMSL excretion and lignin deposition in cell walls. *New Phytol.* 234, 1031–1046. doi: 10.1111/nph.18012

Xiao, C., Hu, J., Ao, Y., Cheng, M., Gao, G., Zhang, Q., et al. (2016). Development and evaluation of near-isogenic lines for brown planthopper resistance in rice cv. 9311. *Sci. Rep.* 6, 38159. doi: 10.1038/srep38159

Yokotani, N., Sato, Y., Tanabe, S., Chujo, T., Shimizu, T., Okada, K., et al. (2013). WRKY76 is a rice transcriptional repressor playing opposite roles in blast disease resistance and cold stress tolerance. *J. Exp. Bot.* 64, 5085–5097. doi: 10.1093/jxb/ert298

Zhang, Q. (2007). Strategies for developing green super rice. *Proc. Natl. Acad. Sci. U.S.A.* 104, 16402–16409. doi: 10.1073/pnas.0708013104

Zhao, Y., Huang, J., Wang, Z., Jing, S., Wang, Y., Ouyang, Y., et al. (2016). Allelic diversity in an NLR gene *BPH9* enables rice to combat planthopper variation. *Proc. Natl. Acad. Sci. U.S.A.* 113, 12850–12855. doi: 10.1073/pnas.1614862113

frontiers | Frontiers in Plant Science

TYPE Mini Review
PUBLISHED 23 November 2023
DOI 10.3389/fpls.2023.1326726

OPEN ACCESS

EDITED BY
Jihong Hu,
Northwest A&F University, China

REVIEWED BY
Hai-jian Huang,
Ningbo University, China
Peiying Hao,
China Jiliang University, China

*CORRESPONDENCE
Bin Yu
yubin_2015@126.com
Qingsong Liu
liuqingsong@xynu.edu.cn

RECEIVED 23 October 2023
ACCEPTED 10 November 2023
PUBLISHED 23 November 2023

CITATION
Jing S, Xu J, Tang H, Li P, Yu B and Liu Q (2023) The roles of small RNAs in rice-brown planthopper interactions. *Front. Plant Sci.* 14:1326726. doi: 10.3389/fpls.2023.1326726

The roles of small RNAs in rice-brown planthopper interactions

Shengli Jing, Jingang Xu, Hengmin Tang, Peng Li, Bin Yu* and Qingsong Liu*

College of Life Sciences, Xinyang Normal University, Xinyang, China

Interactions between rice plants (*Oryza sativa* L.) and brown planthoppers (*Nilaparvata lugens* Stål, BPHs) are used as a model system to study the molecular mechanisms underlying plant-insect interactions. Small RNAs (sRNAs) regulate growth, development, immunity, and environmental responses in eukaryotic organisms, including plants and insects. Recent research suggests that sRNAs play significant roles in rice-BPH interactions by mediating post-transcriptional gene silencing. The focus of this review is to explore the roles of sRNAs in rice-BPH interactions and to highlight recent research progress in unraveling the mechanism of cross-kingdom RNA interference (ckRNAi) between host plants and insects and the application of ckRNAi in pest management of crops including rice. The research summarized here will aid in the development of safe and effective BPH control strategies.

KEYWORDS

sRNAs, *Oryza sativa*, brown planthopper, RNAi, resistance

Introduction

Rice (*Oryza sativa* L.) is a globally-important staple food which is susceptible to damage from hundreds of insect herbivores throughout its lifecycle (Du et al., 2020). One of the most destructive of these insect herbivores is the brown planthopper (*Nilaparvata lugens* Stål, BPH), which is responsible for severely reduced rice yields and substantial economic losses each year (Shi et al., 2021; Shi et al., 2023). Once outbreaks, the insects can completely destroy crops, an effect called "hopperburn" (Backus et al., 2005).

Plants have evolved an intricate, double-layered defense system to effectively resist and respond to herbivorous pests. The first layer is referred to as pathogen-associated molecular pattern (PAMP)-triggered immunity (PTI) (Jing et al., 2017). PTI activates downstream defense-related signaling cascades, such as the phytohormone-mediated defense response pathway (Erb and Reymond, 2019; Wang et al., 2023). The second layer is known as effector-triggered immunity (ETI), which is a robust resistance (R) protein-mediated defense response (Jones and Dangl, 2006; Takken and Tameling, 2009; Rodriguez et al., 2017). Recent research suggests that plants respond to herbivory through a series of defense-related processes, including phytohormone signaling and secondary metabolite biosynthesis, many of which are regulated by small RNAs (sRNAs) (Sattar and Thompson, 2016).

sRNAs are eukaryotic non-coding RNA molecules, approximately 20-30 nucleotides (nt) in length, which regulate gene expression via RNA silencing (Zamore and Haley, 2005; Chapman and Carrington, 2007). According to their precursor structures and associated genetic pathways, plant sRNAs are classified into two major classes: microRNAs (miRNAs) and small interfering RNAs (siRNAs) (Bartel, 2009; Chen, 2009; Katiyar-Agarwal and Jin, 2010). Likewise, insect sRNAs are divided into three major classes: miRNAs, endogenous-siRNAs (endo-siRNAs), and piwi-interacting RNAs (piRNAs) (Golden et al., 2008). In both plants and animals, miRNAs are 20-24 nt single-stranded non-coding RNAs which mediate post-transcriptional gene silencing by binding to mRNAs containing specific complementary base pairs (Zhang et al., 2006; Bartel, 2009; Ghini et al., 2018). Global sRNA sequence profiling of rice and BPH has enabled the identification and characterization of many sRNAs, particularly miRNAs, involved in rice-BPH interactions (Zha et al., 2016; Wu et al., 2017; Nanda et al., 2020). The focus of this review is to explore the roles of sRNAs in rice-BPH interactions and to highlight recent research progress in unraveling the mechanism of cross-kingdom RNA interference (RNAi) between host plants and insects. The research summarized here will aid in the development of safe and effective BPH control strategies.

Rice-derived sRNAs involved in BPH resistance

In plants, sRNAs play significant roles in growth, development, abiotic and biotic stress responses (Khraiwesh et al., 2012; Duan et al., 2015; Yue et al., 2017; Chen et al., 2019; Kryovrysanaki et al., 2022). Several studies have utilized RNA and sRNA profiling to identify sRNAs in rice. Functional validation experiments indicate that these sRNAs fine-tune plant innate immunity by integrating *R* gene-mediated resistance, phytohormone signaling, callose deposition, reactive oxygen species (ROS) production, and secondary metabolite biosynthesis (Wu et al., 2017; Ge et al., 2018; Dai et al., 2019; Tan et al., 2020; Lü et al., 2022; Shen et al., 2023).

To date, approximately 17 BPH-resistance (*R*) genes have been identified in both wild and cultivated rice (Wang et al., 2023). Considerable research has been conducted to characterize the mechanism by which *R* genes confer BPH resistance (Jing et al., 2017; Zheng et al., 2021). Through miRNA sequencing, Wu et al. (2017) identified 23 and 674 differentially expressed miRNAs (DEMs) (including 464 known and 183 novel miRNAs) between resistant (carrying BPH-resistance gene *Bph15*) and susceptible rice varieties before and after BPH infestation, respectively. The identified DEMs were primarily involved in basal defense and BPH-specific resistance. Similarly, an integrated miRNA and mRNA analysis identified 217 DEMs between *Bph6*-carrying transgenic rice lines and wild type plants after BPH infestation (Tan et al., 2020). Of these, nine miRNAs were specifically expressed in transgenic rice lines, suggesting their involvement in *Bph6*-mediated resistance to the BPH. In addition, both Nanda et al. (2020) and Lü et al. (2022) identified an array of BPH-responsive miRNAs between resistant and susceptible rice varieties. Although these findings suggest that miRNAs likely participate in the BPH defense response, the involvement of only a few miRNAs has been experimentally verified (Table 1).

It is well known that the phytohormone signaling plays an important role in rice defense against BPH (Zhou et al., 2009). Recent research suggests that miRNAs regulate rice resistance to BPH by post-transcriptionally regulating the expression of target genes involved in phytohormone signaling. For example, *Osa-miR156* negatively regulates BPH resistance by modulating jasmonic acid (JA) signaling (Ge et al., 2018). *Osa-miR156*-silenced plants (MIM156) exhibited increased resistance to BPH via upregulated expression of *OsMPK3* and *OsMPK6* and downregulated expression of *OsWRKY70*, a transcription factor which positively regulates JA signaling. Furthermore, the expression of the JA biosynthesis gene *OsHI-LOX* and the contents of JA and bioactive jasmonoyl-isoleucine (JA-Ile) were significantly reduced in MIM156 plants. Altogether, it appears that *Osa-miR156* regulates JA biosynthesis and BPH resistance via the MAPK cascade in rice. In addition, *Osa-miR162a* is strongly induced by BPH herbivory in rice seedlings (Chen et al., 2023). Functional verification indicated that *Osa-miR162a* regulates BPH resistance in rice by inhibiting the α-linolenic acid metabolism pathway, which itself regulates JA biosynthesis (Chen et al., 2023).

In rice, secondary metabolites have been shown to inhibit both the feeding and development of BPH. Furthermore, miRNAs can regulate the expression of genes involved in secondary metabolite biosynthesis to modulate BPH resistance. For example, *OsmiR396* was found to negatively regulate BPH resistance via the *OsmiR396–growth-regulating factor 8* (*OsGRF8*)*–OsF3H*–flavonoid module (Dai et al., 2019). Transgenic plants over-expressing *growth-regulating factor 8* (*OsGRF8*), the target gene of *OsmiR396*, exhibit enhanced BPH resistance due to downregulation of *OsmiR396*. Overall, it appears that *OsmiR396-OsGRF8* modulates BPH resistance by regulating the expression of the *flavanone 3-hydroxylase* (*OsF3H*) gene, which is involved in flavonoid biosynthesis (Dai et al., 2019). More recent research indicated that *OsmiR159* negatively regulates BPH resistance through the *OsmiR159–OsGA-MYBL2* module and the *OsmiR159–OsGAMYBL2–GS3* signaling pathway (Shen et al., 2023). Despite these advancements, the molecular mechanism underlying miRNA-mediated BPH resistance in rice is still poorly understood.

The roles of sRNAs in BPH physiology

Advances in genomics have greatly expanded our understanding of the roles sRNAs play in BPH physiology and environmental response (Sattar and Thompson, 2016; Zha et al., 2016). Emerging evidence suggests that sRNAs participate in BPH metamorphosis, wing polyphenism, molting, and reproductive development (Chen et al., 2013; Xu et al., 2013; Chen et al., 2018; Ye et al., 2019; Xu et al., 2020; Li et al., 2021; Wang et al., 2022). Combing transcriptomic and genomic data, Xu et al. (2013) identified key genes involved in the BPH siRNA and miRNA pathways. RNAi knockdown of these genes severely affected BPH

10.3389/fpls.2023.1326726

TABLE 1 The sRNAs involved in rice-BPH interactions.

miRNA	Origin	Target	Acquire method	Reference
Osa-miR156	*Oryza sativa*	*Squamosa promoter binding protein-like gene3/11/12/13/14 (SPL3/SPL11/SPL12/SPL13/SPL14)*	sRNA sequencing and experiment validation	Ge et al., 2018
Osa-miR160f-5p	*Oryza sativa*	*Auxin response factor 16 (ARF16)*	sRNA sequencing	Wu et al., 2017
Osa-miR167a-5p	*Oryza sativa*	*NB-ARC domain containing protein (NB-ARC)*	sRNA sequencing	Wu et al., 2017
OsmiR396	*Oryza sativa*	*Growth regulating factor 8 (OsGRF8)*	sRNA sequencing and experiment validation	Dai et al., 2019
OsmiR159	*Oryza sativa*	*OsGAMYBL2*	Experiment validation	Shen et al., 2023
Osa-miR812s	*Oryza sativa*	*Pectin methylesterase inhibitor (PEMI)*	sRNA sequencing	Nanda et al., 2020
Osa-miR530-5p	*Oryza sativa*	*Allene oxide synthase (AOS)*	sRNA sequencing	Nanda et al., 2020
Osa-miR3980a-5p	*Oryza sativa*	*Squamosa promoter binding protein (SBP)*	sRNA sequencing	Nanda et al., 2020
Osa-miR156l-5p	*Oryza sativa*	*No apical meristem (NAM)*	sRNA sequencing	Nanda et al., 2020
Osa-miR2118g	*Oryza sativa*	*NB-ARC domain containing protein (NB-ARC)*	sRNA sequencing	Nanda et al., 2020
Osa-miR435	*Oryza sativa*	*α/β hydrolase*	sRNA sequencing	Nanda et al., 2020
Osa-miR2871a-3p	*Oryza sativa*	*Glycosyltransferase family protein (GTF)*	sRNA sequencing	Nanda et al., 2020
Osa-miR172a	*Oryza sativa*	*AP2/EREBP family transcription factor (AP2/ERE)*	sRNA sequencing	Nanda et al., 2020
Osa-miR156b-3p	*Oryza sativa*	*GDSL-like lipase (GDSL)*	sRNA sequencing	Tan et al., 2020
Osa-miR169i-5p.2	*Oryza sativa*	*Leucine rich repeat family protein (LRR)*	sRNA sequencing	Tan et al., 2020
Nlu-miR-14-3p	*Nilaparvata lugens*	*NlInR* genes	sRNA sequencing	Xu et al., 2020
Nlu-miR-9a-5p	*Nilaparvata lugens*	*NlInR* genes	sRNA sequencing	Xu et al., 2020
Nlu-miR-315-5p	*Nilaparvata lugens*	*NlInR* genes	sRNA sequencing	Xu et al., 2020
Nlu-miR-1000-1-3p	*Nilaparvata lugens*	*Ultrabithorax (NlUbx)*	sRNA sequencing	Xu et al., 2020
Nlu-mir-9a	*Nilaparvata lugens*	*Ultrabithorax (NlUbx)*	Experiment validation	Li et al., 2021
Nlu-miR-8-5p	*Nilaparvata lugens*	*Membrane-bound trehalase (Tre-2)*	sRNA sequencing	Chen et al., 2013
Nlu-miR-2a-3p	*Nilaparvata lugens*	*Phosphoacetylglucosamine mutase (PAGM)*	sRNA sequencing	Chen et al., 2013
Nlu-miR-4868b	*Nilaparvata lugens*	*N. lugens glutamine synthetase (NlGS)*	sRNA sequencing and experiment validation	Fu et al., 2015
Nlu-miR-173	*Nilaparvata lugens*	*N. lugens Ftz-F1 (NlFtz-F1)*	sRNA sequencing and experiment validation	Chen et al., 2018

(Continued)

TABLE 1 Continued

miRNA	Origin	Target	Acquire method	Reference
Nlu-miR-2703	*Nilaparvata lugens*	*N. lugens chitin synthase gene A*	Experiment validation	Li et al., 2017
Nlu-miR-34-5p	*Nilaparvata lugens*	*Hormone receptor 4 (HR4)/Caspase-1 (Cp-1) and Spermatogenesis-associated protein 20 (SPATA20)*	sRNA sequencing and experiment validation	Wang et al., 2022
Osa-miR162a[a]	*Oryza sativa*	*N. lugens target of rapamycin (NlTOR)*	Conserved miRNA function prediction and experiment validation	Shen et al., 2021; Chen et al., 2023
Osa-miR5795[a]	*Oryza sativa*	*N. lugens vitellogenin (NlVg)*	sRNA sequencing and experiment validation	Lü et al., 2022

a: Rice-derived sRNAs that function with cross-kingdom RNA interference to the brown planthopper.

development and morphology, suggesting that siRNAs and miRNAs may play a crucial role in BPH development and metamorphosis (Xu et al., 2013).

In BPH, wing polyphenism is determined by environmental cues such as the nutritional status of host rice plants, population density, and photoperiod (Xu et al., 2020; Li et al., 2021). These environmental cues affect wing polyphenism by way of several complex regulatory pathways, including insulin/IGF-1 signaling (IIS), juvenile hormone (JH), and 20-hydroxyecdysone (20E) signaling (Xu et al., 2015). Research suggests that these signaling pathways are modulated by an array of miRNAs. For example, RNA sequencing of long wing (LW) and short wing (SW) BPH strains identified a complicated miRNA network which may modulate wing morphological plasticity in a growth-stage dependent manner (Xu et al., 2020). Three miRNAs (*Nlu-miR-14-3p*, *Nlu-miR-9a-5p*, and *Nlu-miR-315-5p*) have been confirmed to interact with *NlInR* genes, which are the part of IIS signaling pathway (Xu et al., 2020). In addition, *Nlu-miR-34* has been shown to modulate wing polyphenism by targeting *NlInR1* and mediating the cross-talk between the IIS, JH, and 20E signaling pathways via a positive autoregulatory feedback loop (Ye et al., 2019). Both Nlu-miR-1000-1-3p (Xu et al., 2020) and *Nlu*-mir-9a (Li et al., 2021) were predicted to target the wing development regulatory gene *Ultrabithorax* (*NlUbx*), and both were found to be differentially expressed between LW and SW BPH. Finally, the *NlInRs/Nlu-mir-9a/NlUbx* regulatory cascade appears to control wing dimorphism by regulating the host's nutritional status (Li et al., 2021).

Molting is crucial to normal insect development, and is at least partially controlled by the chitin biosynthesis pathway and 20E signaling (Chen et al., 2013). Through deep miRNA sequencing of BPH instars at specific stages and during four molting periods, 21 (Chen et al., 2013) and 36 (Chen et al., 2018) specific mature miRNAs were identified, respectively. Among them, *Nlu-miR-8-5p*, *Nlu-miR-2a-3p*, and *Nlu-miR-173* were found to target genes in the chitin biosynthesis pathway, as well as transcription factor *NlFtz-F1*. All three miRNAs appear to regulate molting and chitin biosynthesis through 20E signaling (Chen et al., 2013; Chen et al., 2018). The expression of *chitin synthase gene A* was downregulated when its specific siRNA and its regulated miRNA (*Nlu-miR-2703*) were injected into BPH, reducing both chitin biosynthesis and molting success (Li et al., 2017).

sRNAs have also been found to regulate BPH fecundity by modulating the expression of genes associated with reproductive development. For example, injecting *Nlu-miR-34-5p* mimics can decrease BPH fecundity by reducing *vitellogenin (Vg)* expression (Wang et al., 2022). The biosynthesis of Vg is crucial for oocyte accumulation and successful reproduction (Wang et al., 2022). Glutamine synthetase (NlGS), a protein involved in ovary development which regulates Vg accumulation, has been identified as a target of *Nlu-miR-4868b* (Zhai et al., 2013; Fu et al., 2015). *NlGS* expression was downregulated following injection of the *Nlu-miR-4868b* mimic, but upregulated following injection of the *Nlu-miR-4868b* inhibitor. Additionally, overexpression of *Nlu-miR-4868b* reduced both insect fecundity and *Vg* expression.

Finally, miRNAs play important regulatory roles in environmental responses such as the adaptation to resistant rice varieties. Zha et al. (2016) constructed and sequenced two sRNA libraries using two BPH populations exhibiting different levels of virulence: biotype 1, which only survives on the susceptible rice variety 'Taichung Native 1 (TN1)', and biotype Y, which is able to survive on the resistant rice variety 'YHY15' (carrying BPH-resistance gene *Bph15*). The researchers identified 26 DEMs between these two BPH populations, suggesting that these BPH miRNAs may regulate adaptability to resistant rice varieties. However, the precise functions of these miRNAs require further confirmation.

Cross-kingdom RNAi in the rice-BPH interaction

Research suggests that sRNAs can be transferred between host plants and interacting organisms, thereby inducing gene silencing via a mechanism known as "cross-kingdom RNAi" (Huang et al., 2019). This scenario was first reported in the interaction between plants and fungi. For example, gray mold (*Botrytis cinerea*)-derived sRNAs were found to be able to control the *Arabidopsis thaliana* RNAi system by binding to AGO1, ultimately silencing genes involved in plant immunity (Weiberg et al., 2013). Cross-kingdom RNAi has also been observed in the rice-BPH interaction (Shen et al., 2021; Lü et al., 2022). Rice-derived

sRNAs may be ingested when BPH feed on rice plants, allowing them to regulate BPH gene expression.

Recently, rice-derived *Osa-miR162a*, a conserved plant miRNA, was found to effectively silence *NlTOR* (*Target of rapamycin*) expression in BPH through the cross-kingdom RNAi mechanism (Shen et al., 2021). Both ingestion and injection of *Osa-miR162a* mimics result in reduced female BPH fecundity and Vg activity, which is regulated by the TOR signaling pathway. In addition, allowing BPH adults to feed on *Osa-miR162a*- or *Osa-miR162a-m1* (a modified derivative of *Osa-miR162a*)-overexpressing transgenic rice lines consistently resulted in reduced egg production and hatching success. These results suggest that these miRNAs confer resistance to BPH in rice, and that *Osa-miR162a* may be a potential target for BPH control (Shen et al., 2021; Chen et al., 2023).

Another rice-derived miRNA, *Osa-miR5795*, has also been found to impact BPH fecundity (Lü et al., 2022). By sequencing and analyzing sRNAs from six rice varieties exhibiting variable BPH resistance, 45 resistance-related DEMs were identified between BPH-susceptible and BPH-resistant rice varieties prior to BPH infestation, as well as 144 feeding-induced DEMs. Twenty-five of these DEMs were shared between both groups and were found to be directly involved in the rice-BPH interaction. In addition, seven potential cross-kingdom miRNAs were identified, and their targets were primarily involved in fecundity, feeding, digestion, and detoxification. Based on their predicted binding sites, two of these cross-kingdom miRNAs were selected to verify their function in BPH fecundity. Consequently, BPH oviposition was significantly reduced following injection with *Osa-miR5795* mimics targeting the fecundity marker gene *NlVg* (Lü et al., 2022).

Both of these rice-derived miRNAs (*Osa-miR162a* and *Osa-miR5795*) appear to play an important role in rice-BPH interactions through cross-kingdom regulation of *NlTOR* and *NlVg* expression, both of which regulate fecundity in BPH (Table 1). However, to date no sRNAs, particularly BPH-derived miRNAs, appear to be involved in rice-BPH interactions through cross-kingdom RNAi trafficking.

Application of cross-kingdom RNAi in crop protection

miRNA-mediated gene regulation has emerged as a novel strategy to improve insect resistance in crop plants, including rice. Host-induced gene silencing (HIGS) is a novel concept based on the cross-kingdom RNAi mechanism. HIGS involves overexpressing insect-targeted double-stranded RNAs (dsRNAs) or artificial miRNAs in host plants to specifically block the expression of feeding- and survival-related genes in target pests and pathogens (Huang et al., 2019; Jiang et al., 2023; Mahanty et al., 2023) (Figure 1A). A growing number of studies have demonstrated the successful application of HIGS in crop protection (Escobar et al., 2001; Seemanpillai et al., 2003; Zha et al., 2011; Van et al., 2014; Coleman et al., 2015; Shivakumara et al., 2017; Panwar et al., 2018). In this context, we will use the application of HIGS to manage BPH

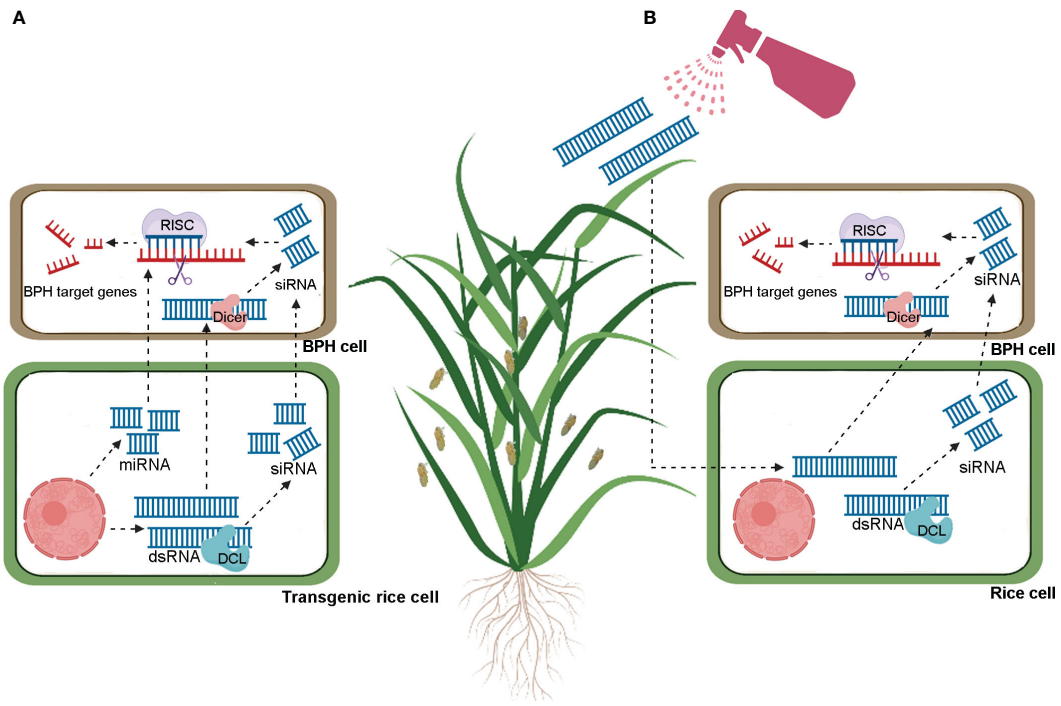

FIGURE 1
Schematic models for brown planthoppers control through host induced gene silencing (HIGS, A) and spray induced gene silencing (SIGS, B). In HIGS **(A)**, transgenic plants produce exogenous dsRNA or miRNA, or external spraying **(B)** delivers exogenous dsRNA. These dsRNA are processed into small interfering RNAs (siRNAs) by rice Dicer-like (DCL) proteins. The siRNAs are then transferred to brown planthopper (BPH) cells and bind to complementary sequences on BPH target mRNA. Through the assistance of the RNA-induced silencing complex (RISC), the target transcripts are silenced. Additionally, exogenous dsRNA and miRNAs produced by transgenic plants can be directly absorbed by BPH, resulting in gene silencing.

as an example. Two salivary proteins secreted by BPH are mucin-like protein (NlMLP) and salivary protein 1 (NlSP1). Ectopic expression of these genes in tobacco (*Nicotiana benthamiana*) leaves induced the expression of defense-related genes and callose deposition, suggesting that these two proteins function as elicitors (Shangguan et al., 2018; Huang et al., 2020). Compared to controls which received no injection or were injected with *dsGFP*, insects injected with *dsNlMLP* or *dsNlSP1* exhibited significantly reduced weight gain and survival rates, suggesting that NlMLP and NlSP1 are essential for BPH survival (Shangguan et al., 2018; Huang et al., 2020). Similarly, BPH feeding on transgenic plants constitutively expressing *dsNlMLP* or *dsNlSP1* also exhibited reduced weight gain and survival rates compared to insects feeding on wild type plants (Shangguan et al., 2018; Huang et al., 2020). Although allowing insects to feed on plants overexpressing exogenous dsRNA was not as effective as injecting insects directly, HIGS remains a promising pest control strategy. However, the implementation of HIGS depends on the generation of transgenic plants, which is both time-intensive and costly (Jiang et al., 2023; Mahanty et al., 2023). These limitations have so far hampered the application of HIGS to BPH control in rice.

Recently, a novel RNAi-based crop protection strategy called "spray-induced gene silencing (SIGS)" has been developed (Jiang et al., 2023; Mahanty et al., 2023). As the name implies, SIGS does not require genetic modification and instead involves simply spraying crop plants with synthesized exogenous dsRNA to selectively knock down insect or pathogen genes (Figure 1B). This technology has been successfully used to control rice blast disease (*Magnaporthe oryzae*) by spraying dsRNA targeting the fungal pathogenicity gene *MoDES1* (Sarkar and Roy-Barman, 2021). Recently, a nanocarrier-dsRNA spray delivery system was developed to control the white-backed planthopper (WBPH) (*Sogatella furcifera*) under laboratory conditions (Guo et al., 2023a, and Guo et al., 2023b). The results demonstrated the efficacy of the nanocarrier spray system for inducing RNAi-mediated knockdown of WBPH genes, including *SfTH*, *SfEGFR*, *Sfzfh-2*, *SfAbd-A*, and *SfAbd-B*. In addition, the treatment resulted in significant phenotypic defects and increased mortality in WBPH (Guo et al., 2023a, and Guo et al., 2023b). These promising results lay a foundation for the further development and application of SIGS to control rice pests, including BPH.

Perspectives and challenges

A growing body of research has revealed the involvement of sRNAs in the interaction between rice and BPH. The majority of these sRNAs have been predicted and/or identified through multi-omics analyses, and their targets have been predicted computationally. However, many of these results still require experimental validation. Moreover, the molecular mechanisms underlying sRNA-mediated rice-BPH interactions remain poorly understood. The pathways of sRNA transfer between rice and BPH should also be comprehensively evaluated. Our growing understanding of cross-kingdom RNAi has paved the way for the development of promising agricultural pest control strategies, including HIGS and SIGS. Nevertheless, HIGS and SIGS face several technical challenges. The stability and uptake efficiency of dsRNA and sRNA need to be strengthened and off-target activities must be avoided. We predict that the development and application of environmentally-friendly RNAi-based technology will become an agronomic research focus, and that the communication of cross-kingdom sRNAs will emerge as a hot research topic.

Author contributions

SJ: Project administration, Writing – original draft, Writing – review & editing. JX: Writing – review & editing. HT: Writing – review & editing. PL: Writing – review & editing. BY: Writing – original draft, Writing – review & editing. QL: Writing – original draft, Writing – review & editing.

Funding

The author(s) declare financial support was received for the research, authorship, and/or publication of this article. This review was supported by grants from the National Natural Science Foundation of China (U1704111 and 31401732), ZHONGYUAN YINGCAI JIHUA (ZYYCYU202012165), and Henan Province Science and Technology Research Project (222102110116).

Acknowledgments

We acknowledge the BioRender tool that we used to create Figure 1. We appreciate the linguistic assistance provided by TopEdit (www.topeditsci.com) during the preparation of this manuscript.

Conflict of interest

The authors declare that the research was conducted in the absence of any commercial or financial relationships that could be construed as a potential conflict of interest.

Publisher's note

References

Backus, E., Serrano, M., and Ranger, C. (2005). Mechanisms of hopperburn: an overview of insect taxonomy, behavior, and physiology. *Annu. Rev. Entomol.* 50, 125–151. doi: 10.1146/annurev.ento.49.061802

Bartel, D. (2009). MicroRNAs: Target recognition and regulatory functions. *Cell* 136, 215–233. doi: 10.1016/j.cell.2009.01.002

Chapman, E., and Carrington, J. (2007). Specialization and evolution of endogenous small RNA pathways. *Nat. Rev. Genet.* 8, 884–896. doi: 10.1038/nrg2179

Chen, X. (2009). Small RNAs and their roles in plant development. *Annu. Rev. Cell Dev. Biol.* 25, 21–44. doi: 10.1146/annurev.cellbio.042308.113417

Chen, X., Jiang, L., Zheng, J., Chen, F., Wang, T., Wang, M., et al. (2019). A missense mutation in *Large Grain Size 1* increases grain size and enhances cold tolerance in rice. *J. Exp. Bot.* 70, 3851–3866. doi: 10.1093/jxb/erz192

Chen, J., Li, T., Pang, R., Yue, X., Hu, J., and Zhang, W. (2018). Genome-wide screening and functional analysis reveal that the specific microRNA nlu-miR-173 regulates molting by targeting *Ftz-F1* in *Nilaparvata lugens*. *Front. Physiol.* 9. doi: 10.3389/fphys.2018.01854

Chen, J., Liang, Z., Liang, Y., Pang, R., and Zhang, W. (2013). Conserved microRNAs miR-8-5p and miR-2a-3p modulate chitin biosynthesis in response to 20-hydroxyecdysone signaling in the brown planthopper, *Nilaparvata lugens*. *Insect Biochem. Mol. Biol.* 43, 839–848. doi: 10.1016/j.ibmb.2013.06.002

Chen, J., Liu, Q., Yuan, L., Shen, W., Shi, Q., Qi, G., et al. (2023). Osa-miR162a enhances the resistance to the brown planthopper via α-linolenic acid metabolism in rice (*Oryza sativa*). *J. Agric. Food Chem.* 71, 11847–11859. doi: 10.1021/acs.jafc.3c02637

Coleman, A., Wouters, R., Mugford, S., and Hogenhout, S. (2015). Persistence and transgenerational effect of plant-mediated RNAi in aphids. *J. Exp. Bot.* 66, 541–548. doi: 10.1093/jxb/eru450

Dai, Z., Tan, J., Zhou, C., Yang, X., Yang, F., Zhang, S., et al. (2019). The OsmiR396-OsGRF8-OsF3H-flavonoid pathway mediates resistance to the brown planthopper in rice (*Oryza sativa*). *Plant Biotechnol. J.* 17, 1657–1669. doi: 10.1111/pbi.13091

Du, B., Chen, R., Guo, J., and He, G. (2020). Current understanding of the genomic, genetic, and molecular control of insect resistance in rice. *Mol. Breed.* 40, 24. doi: 10.1007/s11032-020-1103-3

Duan, P., Ni, S., Wang, J., Zhang, B., Xu, R., Wang, Y., et al. (2015). Regulation of *OsGRF4* by OsmiR396 controls grain size and yield in rice. *Nat. Plants* 2, 15203. doi: 10.1038/nplants.2015.203

Erb, M., and Reymond, P. (2019). Molecular interactions between plants and insect herbivores. *Annu. Rev. Plant Biol.* 29, 527–557. doi: 10.1146/annurev-arplant-050718-095910

Escobar, M., Civerolo, E., Summerfelt, K., and Dandekar, A. (2001). RNAi-mediated oncogene silencing confers resistance to crown gall tumorigenesis. *Proc. Natl. Acad. Sci. U.S.A.* 98, 13437–13442. doi: 10.1073/pnas.241276898

Fu, X., Li, T., Chen, J., Dong, Y., Qiu, J., Kang, K., et al. (2015). Functional screen for microRNAs of *Nilaparvata lugens* reveals that targeting of glutamine synthase by miR-4868b regulates fecundity. *J. Insect Physiol.* 83, 22–29. doi: 10.1016/j.jinsphys.2015.11.003

Ge, Y., Han, J., Zhou, G., Xu, Y., Ding, Y., Shi, M., et al. (2018). Silencing of miR156 confers enhanced resistance to brown planthopper in rice. *Planta* 248, 813–826. doi: 10.1007/s00425-018-2942-6

Ghini, F., Rubolino, C., Climent, M., Simeone, I., Marzi, M., and Nicassio, F. (2018). Endogenous transcripts control miRNA levels and activity in mammalian cells by target-directed miRNA degradation. *Nat. Commun.* 9, 3119. doi: 10.1038/s41467-018-05182-9

Golden, D., Gerbasi, V., and Sontheimer, E. (2008). An inside job for siRNAs. *Mol. Cell* 31, 309–312. doi: 10.1016/j.molcel.2008.07.008

Guo, H., Liu, X. Z., Long, G. J., Gong, L. L., Zhang, M. Q., Ma, Y. F., et al. (2023a). Functional characterization of developmentally critical genes in the white-backed planthopper: Efficacy of nanoparticle-based dsRNA sprays for pest control. *Pest Manage. Sci.* 79, 1048–1061. doi: 10.1002/ps.7271

Guo, H., Lona, G. J., Liu, X. Z., Ma, Y. F., Zhang, M. Q., Gong, L. L., et al. (2023b). Functional characterization of tyrosine melanin genes in the white-backed planthopper and utilization of a spray-based nanoparticle-wrapped dsRNA technique for pest control. *Int. J. Biol. Macromol.* 230, 123123. doi: 10.1016/j.ijbiomac.2022.123123

Huang, C., Wang, H., Hu, P., Hamby, R., and Jin, H. (2019). Small RNAs-big players in plant-microbe interactions. *Cell Host Microbe* 26, 173–182. doi: 10.1016/j.chom.2019.07.021

Huang, J., Zhang, N., Shan, J., Peng, Y., Guo, J., Zhou., C., et al. (2020). Salivary protein 1 of brown planthopper is required for survival and induces immunity response in plants. *Front. Plant Sci.* 11. doi: 10.3389/fpls.2020.571280

Jiang, C., Li, Z., Zheng, L., Yu, Y., and Niu, D. (2023). Small RNAs: Efficient and miraculous effectors that play key roles in plant-microbe interactions. *Mol. Plant Pathol.* 24, 999–1013. doi: 10.1111/mpp.13329

Jing, S., Zhao, Y., Du, B., Chen, R., Zhu, L., and He, G. (2017). Genomics of interaction between the brown planthopper and rice. *Curr. Opin. Insect Sci.* 19, 82–87. doi: 10.1016/j.cois.2017.03.005

Jones, J. D., and Dangl, J. L. (2006). The plant immune system. *Nature* 444, 323–329. doi: 10.1038/nature05286

Katiyar-Agarwal, S., and Jin, H. (2010). Role of small RNAs in host-microbe interactions. *Annu. Rev. Phytopathol.* 48, 225–246. doi: 10.1146/annurev-phyto-073009-114457

Khraiwesh, B., Zhu, J., and Zhu, J. (2012). Role of miRNAs and siRNAs in biotic and abiotic stress responses of plants. *Biochim. Biophys. Acta* 1819, 137–148. doi: 10.1016/j.bbagrm.2011.05.001

Kryovrysanaki, N., James, A., Tselika, M., Bardani, E., and Kalantidis, K. (2022). RNA silencing pathways in plant development and defense. *Int. J. Dev. Biol.* 66, 163–175. doi: 10.1387/ijdb.210189kk

Li, T., Chen, J., Fan, X., Chen, W., and Zhang, W. (2017). MicroRNA and dsRNA targeting chitin synthase A reveal a great potential for pest management of the hemipteran insect *Nilaparvata lugens*. *Pest Manage. Sci.* 73, 1529–1537. doi: 10.1002/ps.4492

Li, X., Zhao, M., Tian, M., Zhao, J., Cai, W., and Hua, H. (2021). An InR/mir-9a/NlUbx regulatory cascade regulates wing diphenism in brown planthoppers. *Insect Sci.* 28, 1300–1313. doi: 10.1111/1744-7917.12872

Lü, J., Liu, J., Chen, L., Sun, J., Su, Q., Li, S., et al. (2022). Screening of brown planthopper resistant miRNAs in rice and their roles in regulation of brown planthopper fecundity. *Rice Sci.* 29, 559–568. doi: 10.1016/j.rsci.2022.05.003

Mahanty, B., Mishra, R., and Joshi, R. K. (2023). Cross-kingdom small RNA communication between plants and fungal phytopathogens-recent updates and prospects for future agriculture. *RNA Biol.* 20, 109–119. doi: 10.1080/15476286.2023.2195731

Nanda, S., Yuan, S., Lai, F., Wang, W., Fu, Q., and Wan, P. (2020). Identification and analysis of miRNAs in IR56 rice in response to BPH infestations of different virulence levels. *Sci. Rep.* 10, 19093. doi: 10.1038/s41598-020-76198-9

Panwar, V., Jordan, M., McCallum, B., and Bakkeren, G. (2018). Host-induced silencing of essential genes in Puccinia triticina through transgenic expression of RNAi sequences reduces severity of leaf rust infection in wheat. *Plant Biotechnol. J.* 16, 1013–1023. doi: 10.1111/pbi.12845

Rodriguez, P. A., Escudero-Martinez, C., and Bos, J. I. (2017). An aphid effector targets trafficking protein VPS52 in a host-specific manner to promote virulence. *Plant Physiol.* 173, 1892–1903. doi: 10.1104/pp.16.01458

Sarkar, A., and Roy-Barman, S. (2021). Spray-induced silencing of pathogenicity gene *MoDES1* via exogenous double-stranded RNA can confer partial resistance against fungal blast in rice. *Front. Plant Sci.* 12. doi: 10.3389/fpls.2021.733129

Sattar, S., and Thompson, G. A. (2016). Small RNA regulators of plant-hemipteran interactions: micromanagers with versatile roles. *Front. Plant Sci.* 7, 1241. doi: 10.3389/fpls.2016.01241

Seemanpillai, M., Dry, I., Randles, J., and Rezaian, A. (2003). Transcriptional silencing of geminiviral promoter-driven transgenes following homologous virus infection. *Mol. Plant Microbe Interact.* 16, 429–438. doi: 10.1094/MPMI.2003.16.5.429

Shangguan, X., Zhang, J., Liu, B., Zhao, Y., Wang, H., Wang, Z., et al. (2018). A mucin-like protein of planthopper is required for feeding and induces immunity response in plants. *Plant Physiol.* 176, 552–565. doi: 10.1104/pp.17.00755

Shen, W., Cao, S., Liu, J., Zhang, W., Chen, J., and Li, J. (2021). Overexpression of an Osa-miR162a derivative in rice confers cross-kingdom RNA interference-mediated brown planthopper resistance without perturbing host development. *Int. J. Mol. Sci.* 22, 12652. doi: 10.3390/ijms222312652

Shen, Y., Yang, G., Miao, X., and Shi, Z. (2023). OsmiR159 modulate BPH resistance through regulating G-protein γ subunit *GS3* gene in rice. *Rice* 16, 30. doi: 10.1186/s12284-023-00646-z

Shi, S., Wang, H., Nie, L., Tan, D., Zhou, C., Zhang, Q., et al. (2021). *Bph30* confers resistance to brown planthopper by fortifying sclerenchyma in rice leaf sheaths. *Mol. Plant* 14, 1714–1732. doi: 10.1016/j.molp.2021.07.004

Shi, S., Zha, W., Yu, X., Wu, Y., Li, S., Xu, H., et al. (2023). Integrated transcriptomics and metabolomics analysis provide insight into the resistance response of rice against brown planthopper. *Front. Plant Sci.* 14. doi: 10.3389/fpls.2023.1213257

Shivakumara, T., Chaudhary, S., Kamaraju, D., Dutta, T., Papolu, P., Banakar, P., et al. (2017). Host-induced silencing of two pharyngeal gland genes conferred transcriptional alteration of cell wall-modifying enzymes of *Meloidogyne incognita* vis-a-vis perturbed nematode infectivity in eggplant. *Front. Plant Sci.* 8. doi: 10.3389/fpls.2017.00473

Takken, F. L. W., and Tameling, W. I. L. (2009). To nibble at plant resistance proteins. *Science* 324, 744–746. doi: 10.1126/science.1171666

Tan, J., Wu, Y., Guo, J., Li, H., Zhu, L., Chen, R., et al. (2020). A combined microRNA and transcriptome analyses illuminates the resistance response of rice against brown planthopper. *BMC Genom.* 21, 144. doi: 10.1186/s12864-020-6556-6

Van, E., Powell, C., Shatters, R., and Borovsky, D. (2014). Control of larval and egg development in *Aedes aegypti* with RNA interference against juvenile hormone acid methyl transferase. *J. Insect Physiol.* 70, 143–150. doi: 10.1016/j.jinsphys.2014.08.001

Wang, H., Shi, S., and Hua, W. (2023). Advances of herbivore-secreted elicitors and effectors in plant-insect interactions. *Front. Plant Sci.* 14. doi: 10.3389/fpls.2023.1176048

Wang, N., Zhang, C., Chen, M., Shi, Z., Zhou, Y., Shi, X., et al. (2022). Characterization of MicroRNAs associated with reproduction in the brown planthopper, *Nilaparvata lugens*. *Int. J. Mol. Sci.* 23, 7808. doi: 10.3390/ijms23147808

Weiberg, A., Wang, M., Lin, F., Zhao, H., Zhang, Z., Kaloshian, I., et al. (2013). Fungal small RNAs suppress plant immunity by hijacking host RNA interference pathways. *Science* 342, 118–123. doi: 10.1126/science.1239705

Wu, Y., Lv, W., Hu, L., Rao, W., Zeng, Y., Zhu, L., et al. (2017). Identification and analysis of brown planthopper-responsive microRNAs in resistant and susceptible rice plants. *Sci. Rep.* 7 (1), 8712. doi: 10.1038/s41598-017-09143-y

Xu, H. J., Chen, T., Ma, X. F., Xue, J., Pan, P. L., Zhang, X. C., et al. (2013). Genome-wide screening for components of small interfering RNA (siRNA) and microRNA (miRNA) pathways in the brown planthopper, *Nilaparvata lugens* (Hemiptera: Delphacidae). *Insect Mol. Biol.* 22, 635–647. doi: 10.1111/imb.12051

Xu, H., Xue, J., Lu, B., Zhang, X., Zhuo, J., He, S., et al. (2015). Two insulin receptors determine alternative wing morphs in planthoppers. *Nature* 519, 464–467. doi: 10.1038/nature14286

Xu, L., Zhang, J., Zhan, A., Wang, Y., Ma, X., Jie, W., et al. (2020). Identification and analysis of microRNAs associated with wing polyphenism in the brown planthopper, *Nilaparvata lugens*. *Int. J. Mol. Sci.* 21, 9754. doi: 10.3390/ijms21249754

Ye, X., Xu, L., Li, X., He, K., Hua, H., Cao, Z., et al. (2019). miR-34 modulates wing polyphenism in planthopper. *PloS Genet.* 15, e1008235. doi: 10.1371/journal.pgen.1008235

Yue, E., Li, C., Li, Y., Liu, Z., and Xu, J. (2017). MiR529a modulates panicle architecture through regulating squamosa promoter binding-like genes in rice (*Oryza sativa*). *Plant Mol. Biol.* 94, 469–480. doi: 10.1007/s11103-017-0618-4

Zamore, P., and Haley, B. (2005). Ribo-gnome: The big world of small RNAs. *Science* 309, 1519–1524. doi: 10.1126/science.1111444

Zha, W., Peng, X., Chen, R., Du, B., Zhu, L., and He, G. (2011). Knockdown of midgut genes by dsRNA-transgenic plant-mediated RNA interference in the hemipteran insect *Nilaparvata lugens*. *PloS One* 6, e20504. doi: 10.1371/journal.pone.0020504

Zha, W., Zhou, L., Li, S., Liu, K., Yang, G., Chen, Z., et al. (2016). Characterization and comparative profiling of the small RNA transcriptomes in the Hemipteran insect *Nilaparvata lugens*. *Gene* 595, 83–91. doi: 10.1016/j.gene.2016.09.042

Zhai, Y., Zhang, J., Sun, Z., Dong, X., He, Y., Kang, K., et al. (2013). Proteomic and transcriptomic analyses of fecundity in the brown planthopper *Nilaparvata lugens* (Stål). *J. Proteome. Res.* 12, 5199–5212. doi: 10.1021/pr400561c

Zhang, B., Pan, X., Cobb, G., and Anderson, T. (2006). Plant microRNA: a small regulatory molecule with big impact. *Dev. Biol.* 289, 3–16. doi: 10.1016/j.ydbio.2005.10.036

Zheng, X., Zhu, L., and He, G. (2021). Genetic and molecular understanding of host rice resistance and *Nilaparvata lugens* adaptation. *Curr. Opin. Insect Sci.* 45, 14–20. doi: 10.1016/j.cois.2020.11.005

Zhou, G., Qi, J., Ren, N., Cheng, J., Erb, M., Mao, B., et al. (2009). Silencing *OsHI-LOX* makes rice more susceptible to chewing herbivores, but enhances resistance to a phloem feeder. *Plant J.* 60, 638–648. doi: 10.1111/j.1365-313X.2009.03988.x

frontiers | Frontiers in Plant Science

TYPE Original Research
PUBLISHED 08 January 2024
DOI 10.3389/fpls.2023.1296915

OPEN ACCESS

EDITED BY
WànkuíGong,
Institute of Cotton Research of Chinese Academy of Agricultural Sciences, China

REVIEWED BY
Yuanchen Zhang,
Anyang Institute of Technology, China
Hongjie Feng,
Institute of Cotton Research (CAAS), China

*CORRESPONDENCE
Shang Wang
shangwang@jlu.edu.cn
Jing-Hui Xi
jhxi1965@jlu.edu.cn

RECEIVED 19 September 2023
ACCEPTED 14 December 2023
PUBLISHED 08 January 2024

CITATION
Zhao S-W, Pan Y, Wang Z, Wang X, Wang S and Xi J-H (2024) 1-nonene plays an important role in the response of maize-aphid-ladybird tritrophic interactions to nitrogen.
Front. Plant Sci. 14:1296915.
doi: 10.3389/fpls.2023.1296915

1-nonene plays an important role in the response of maize-aphid-ladybird tritrophic interactions to nitrogen

Shi-Wen Zhao[1], Yu Pan[1], Zhun Wang[2], Xiao Wang[1], Shang Wang[1]* and Jing-Hui Xi[1]*

[1]College of Plant Science, Jilin University, Changchun, China, [2]Plant Quarantine Laboratory, Changchun Customs Technology Center, Changchun, China

Plant volatile organic compounds (VOCs) are the key distress signals involved in tritrophic interactions, by which plants recruit predators to protect themselves from herbivores. However, the effect of nitrogen fertilization on VOCs that mediate tritrophic interactions remains largely unidentified. In this study, a maize (*Zea mays*)-aphid (*Rhopalosiphum padi)*-ladybird (*Harmonia axyridis)* tritrophic interaction model was constructed under high-nitrogen (HN) and low-nitrogen (LN) regimens. *H. axyridis* had a stronger tendency to be attracted by aphid-infested maize under HN conditions. Then, volatiles were collected and identified from maize leaves on which aphids had fed. All of the HN-induced volatiles (HNIVs) elicited an electroantennogram (EAG) response from *H. axyridis*. Of these HNIVs, 1-nonene was attractive to *H. axyridis* under simulated natural volatilization. Furthermore, our regression showed that the release of 1-nonene was positively correlated with *H. axyridis* visitation rates. Supplying 1-nonene to maize on which aphids had fed under LN enhanced attractiveness to *H. axyridis*. These results supported the conclusion that 1-nonene was the active compound that mediated the response to nitrogen in the tritrophic interaction. In addition, the 1-nonene synthesis pathway was hypothesized, and we found that the release of 1-nonene might be related to the presence of salicylic acid (SA) and abscisic acid (ABA). This research contributes to the development of novel environmentally friendly strategies to optimize nitrogen fertilizer application and to improve pest control in maize crops.

KEYWORDS

nitrogen, tritrophic interactions, maize, 1-nonene, *Rhopalosiphum padi*, *Harmonia axyridis*

1 Introduction

Tritrophic interactions are among the most important components of all terrestrial ecosystems (Turlings and Erb, 2018). When under attack by herbivores, some plants recruit a third trophic level, which increases the plant's attractiveness to the natural enemies of herbivores, and these organisms then provide the plant protection from herbivory and reduce plant damage (Hiltpold et al., 2011; Ali et al., 2023). Since evidence for an active role of herbivore-damaged plants in recruiting natural enemies of herbivores was first reported, an increasing number of different species of plants have been found to attract a range of herbivore enemies after an herbivore attack, including insect predators, parasitoids, predatory mites, nematodes, and birds (Clavijo et al., 2012; Meijer et al., 2023). Thus, tritrophic interactions are being increasingly discussed as an environmentally friendly crop protection strategy (Heil, 2008; Yang et al., 2023).

Volatile organic compounds (VOCs) serve as attractants for predators and parasitoids and play an important role in tritrophic interactions (Hiltpold et al., 2011; Aartsma et al., 2017; Turlings and Erb, 2018). Both green leaf volatiles (GLVs) and terpenoids attract predators or parasitoids of herbivores (Kessler and Baldwin, 2001). For example, (S)-(+)-linalool production was induced in *Oryza sativa* (rice) that had been attacked by *Spodoptera frugiperda* and in *Vicia faba* (broad bean) plants that were fed on by *Acyrthosiphon pisum* (pea aphids), and this compound attracted parasitic wasps. In addition, (L)-(+)-linalool produced by wild tobacco (*Nicotiana attenuata*) mediates a tritrophic interaction that involves *Manduca sexta* and predatory *Geocoris* spp. (big-eyed bugs) (He et al., 2019). In maize, GLVs are released in significant amounts after fresh damage to aboveground tissues (Turlings and Erb, 2018). The blend of volatiles emitted by maize plants attacked by noctuid species attracts parasitic wasps, such as *Cotesia marginiventris*, *Cotesia kariyai* (Turlings et al., 1990; Schnee et al., 2002; Kuramitsu et al., 2019). In underground tissues, β-b-caryophyllene is released in maize roots after damage by *Diabrotica virgifera* larvae to attract the entomopathogenic nematode *Heterorhabditis megidis* (Hiltpold et al., 2011). Thus, VOCs released by maize play important role in mediating interactions between pests and their enemies.

Nitrogen (N), which is one of the most important macronutrients for plants, plays a predominant role in the photosynthesis, growth, and development of plants; this has led to the application of N fertilizers as a key practice for increasing crop production (Chen et al., 2008; Kutyniok and Müller, 2013; Chesnais et al., 2016). In agroecosystems, the nutritional status of plants affects multitrophic plant-insect-predatory interactions (Jamieson et al., 2012). The response of tritrophic interactions between parasitoids and their host insects to nitrogen fertilizers has been researched extensively. Many studies have shown that improvement in N inputs enhances parasitism (Aqueel et al., 2014; Chesnais et al., 2016; Zhu et al., 2020a) and influences the growth and development of both pests and their parasites (Kaneshiro et al., 1996; Aqueel et al., 2014). In addition, nitrogen levels affect the levels of plant hormones and the expression of numerous genes involved in metabolite synthesis, which subsequently results in changes in plant volatiles that might be the key signals used by natural enemies to find pests (Chen et al., 2008; Kutyniok and Müller, 2013). For example, rice plants treated with different nitrogen levels showed changes in the composition of volatiles, which regulated the foraging and searching behavior of *Cyrtorhinus lividipennis* (Lou and Cheng, 2003; Zhu et al., 2020b). Although it has been speculated that a higher N level would increase the attractiveness of plants to natural enemies via plant-based cues (Loader and Damman, 1991; Zhu et al., 2020a), the relative importance of individual compounds in mediating the response of tritrophic interactions to nitrogen is still poorly characterized.

As the most widely grown crop, maize is an excellent subject for studying the effects of nitrogen fertilization on tritrophic interactions (Jagtap et al., 2020). The aphid *Rhopalosiphum padi* (L.) is a major herbivore of maize in many countries (Chirgwin et al., 2022). *Harmonia axyridis* Pallas (Coleoptera: Coccinellidae) is widely reported as a natural enemy of *R. padi* (Kontodimas and Stathas, 2005). Therefore, it is necessary to study the interactions among these three species. In this study, we explored how nitrogen fertilization impacted the ability of maize plants infected with *R. padi* to attract *H. axyridis*. Furthermore, the active compounds mediating the response of the maize-*R. padi*-*H. axyridis* tritrophic interactions with nitrogen were verified. These results might help in the development of novel strategies to optimize nitrogen application, improve yields, and facilitate biological control of pests of the important crop maize.

2 Materials and methods

2.1 Plant materials

The maize cultivar 'B73' was sown in plastic pots (height, 20 cm; diameter, 15 cm) that contained a mixture of sterilized field soil and sand (3:1) (Schnable et al., 2009). The soil was nutrient-poor (organic matter 31.67 g/kg, total nitrogen 0.716 g/kg, total phosphorus 0.135 g/kg, and available nitrogen 5.86 mg/kg). Fertilization was started on day seven of the experiment with a modified Hoagland solution. Depending on the N treatment scheme, the nutrient solution contained 15 mM KNO_3 (for the HN treatment) or 0.15 mM KNO_3 (for the LN treatment) (Schluter et al., 2012). The seedlings were grown in a climate chamber (22 ± 2°C, 70% relative humidity, 16 h:8 h light:dark). Experimentation began 20 d (three leaf stage) after germination.

2.2 Insect rearing

A population of *R. padi* was obtained from a single individual. *R. padi* and *H. axyridis* were reared in a Perspex rearing cabinet under controlled conditions (22 ± 2°C, 70% relative humidity, 16 h:8 h light:dark). *R. padi* and female *H. axyridis* were obtained from the Agricultural Experiment Base of Jilin University (Changchun, Jilin, China) (Qin et al., 2021).

2.3 Collection and identification of maize VOCs

VOCs from leaves of aphid-infested maize under high- and low-nitrogen conditions were collected using a dynamic headspace solid-phase microextraction (SPME) method (Pan et al., 2021). Maize leaves without aphid honeydew were strictly screened out for the experiment to avoid interference from aphid honeydew. Twenty adult aphids were allowed to feed on maize plants for 24 h and later removed before collection. A 0.5 g sample of leaves from each of those two groups was placed into a 50 mL glass bottle. An SPME fibre that was coated with polydimethylsiloxane-divinylbenzene (PDMS-DVB, 65 mm), purchased from Supelco (Bellefonte, PA, U.S.), was conditioned at 250°C for 30 min in a gas chromatograph injection port, according to the manufacturer's guidelines. Plants were kept in a glass container for 1 h before sampling, headspace sample from the empty glass container was collected as controls, and the controls were used to eliminate impure volatiles emitted by the headspace collecting instrument. The SPME fibre was inserted into the opening of the glass container, and the fibre was extended to absorb the plant volatiles. After 1 h, the SPME fibre was inserted directly into a gas chromatograph-mass spectrometer (GCMS-QP2010Ultra, SHIMADZU, Japan) equipped with an Rxi-5MS capillary column (30 m length, 0.32 mm i.d., 0.25 μm film thickness). The fibre was inserted into the injector port at 250°C and desorbed for 5 min. After fibre insertion, the column temperature was maintained at 40°C for 1 min and then increased to 250°C at 10°C min^{-1}, followed by a final stage of 4 min at 250°C. Six replicates were included for each treatment. The volatile compounds were identified by matching their retention times to those of authentic standards, as well as by comparing the MS spectrum fragmentation patterns to the NIST08 Mass Spectral Library (National Institute of Standards and Technology, Washington D.C., U.S.) and authentic standards (Ye et al., 2018; Pan et al., 2021). The Kovats retention index of each volatile component was calculated using the retention time, and the data were matched to previously published data. The peak area of each component of the volatiles, which were tentatively identified, represented the relative quantity (Hiltpold et al., 2011).

The authentic standards benzaldehyde (98%), acetic acid (98%), 1-nonene (95%), and indole (98%) were purchased from Sigma Aldrich (Deisenhofen, Germany) and dissolved in hexane for the subsequent assay. The amount of volatiles emitted in the sample headspace was determined by a semiquantitative method (Erb et al., 2015). One-microlitre samples of the authentic compound standards at five concentrations (10 ng/μL, 25 ng/μL, 50 ng/μL, 100 ng/μL, and 200 ng/μL) were injected into the liquid chromatograph. The standard curve and linear regression equation were calculated by quantifying 1 μL samples of authentic compound standards at various concentrations and measuring the corresponding peak areas from liquid chromatography. The amounts of the of natural volatiles emitted in the headspace sample were calculated using the linear regression equation with the corresponding peak areas.

2.4 *H. axyridis* Y-maize assays

A Y-tube olfactometer was used to determine the behavioral responses of *H. axyridis* to aphid-infested maize under different nitrogen levels. Prior to each experiment, all glassware was washed with distilled water and baked in an oven overnight at 160°C. A 20 W fluorescent light was placed 0.5 m above the olfactometer. Host-related behaviour was examined as follows: to examine the behavioral response of *H. axyridis* to maize fed on by aphids under high/low-nitrogen conditions, two choice tests were performed using a glass Y-tube olfactometer (20 cm×20 cm×20 cm arm length, 4 cm diameter, 75°Y angle). The tests included 1) healthy maize under HN vs. healthy maize under LN, 2) aphid-infested maize under LN vs. healthy maize under LN, 3) aphid-infested maize under HN vs. healthy maize under LN, and 4) aphid-infested maize under HN vs. aphid-infested maize under LN. Plants were kept in a glass container for 1 h before bioassays to eliminate any contaminating volatiles from the system. Aphids were removed prior to the experiment to eliminate the effects of their volatiles. *H. axyridis* was introduced into the main arm of the Y-tube olfactometer. Air was then blown through two glass containers and then into the two side arms at 400 mL/min. *H. axyridis* was considered to have made the first choice when it moved > 3 cm into either arm (visually assessed by a line marked on both arms). The final choice for *H. axyridis* was the arm it was in at the end of the 5-min experimental period. We excluded *H. axyridis* individuals that did not make any choice within 5 min from the data analysis. *H. axyridis* females were placed individually in the Y-tube for the behavioral assay. The experiment had six replicates in total, ten females and new plants were used per replicate For each replicate, 5 females were moved in one direction and the others were moved in the other direction to control for any directional bias in the room. Each insect was used only once (Gouinguené et al., 2005).

The responses of *H. axyridis* to a single compound were also determined using a Y-tube olfactometer as described above. The compounds in the dispensers placed in the treated arm were allowed to evaporate for 1 h before insect placement; the control dispenser was placed in the control arm. As previously described (Pan et al., 2021), the dispensers consisted of 2-mL amber glass vials containing 1 mL of authentic compounds (106.5 ng/μL 1-nonene, 149.9 ng/μL acetic acid, 15.04 ng/μL indole, and 15.13 ng/μL benzaldehyde). The vials were sealed with open screw caps that contained a rubber septum, which was pierced with a 2-μL micropipette tip. Control dispensers were prepared in the same way with 1 mL of hexane. The amounts of compounds that the dispensers released approximately corresponded to those of high nitrogen-induced volatiles (HNIVs) emitted by maize.

2.5 Electroantennogram response of *H. axyridis*

An electroantennogram (EAG) assay was performed to measure the sensitivity of *H. axyridis* to benzaldehyde, 1-nonene, acetic acid, azulene, indole, caryophyllene, and (-)-aristolene. Solutions of

single synthetic compounds were diluted in distilled paraffin oil. The antennae of *H. axyridis* insects were removed carefully at the base, and several terminal segments at the distal end were excised before attaching them to electrodes using Spectra 360 conductive gel (Parker, Fairfield, USA). Test compounds (i.e., 10 µL, 10 µg/µL) were applied to a piece of filter paper, which was inserted into a syringe. The strip was placed in the syringe, which delivered a continuous humidified (60–70%) air flow (500 mL/min) and added a compensatory flow. The duration of the stimulation was 0.1 s, and the signal from each antenna was recorded for 4s. Two minutes intervals were allowed between stimulations to restore EAG sensitivity. At least five individuals were tested, and each individual was tested three times. The response to the reference standard (*z*)-3-hexen-1-ol was measured at the beginning and end of each recording session to correct for the loss of sensitivity in the preparation. For correction, it was assumed that the decrease in sensitivity was linear over time. The data were then normalized to the standard as follows (Jing et al., 2021):

$$\mathrm{rEAG} = \frac{\mathrm{EAG(A)}}{\mathrm{EAG(std1)} + \frac{\mathrm{EAG(std2)}-\mathrm{EAG(std1)}}{\mathrm{RT(std2)}-\mathrm{RT(std1)}} \times (\mathrm{RT(A)} - \mathrm{RT(std1)})},$$

where rEAG is the relative EAG response, EAG(A) is the amplitude (mV) of the EAG response to compound A, EAG(std1) is the EAG response to the standard at the beginning of the recording, EAG(std2) is the EAG response to the standard at the end of the recording, T(A) is the time elapsed before stimulation with compound A, T(std1) is the time of the first stimulation, and T (std2) is the time of the final stimulation.

2.6 *H. axyridis* tent assays

To test the visit number of *H. axyridis*, tent (2 m × 2 m × 1.5 m) assays were conducted. The four treatments in the four corners of the tents were healthy maize under HN, healthy maize under LN, aphid-infested maize under HN, and aphid-infested maize under LN. There were six replicates, and 30 females were used for each replicate. Each replicate was conducted for 15 min. The number of *H. axyridis* individuals that visited each of the four treatments was recorded. The location of four treatments was randomly arranged for each replicate (Zhang et al., 2022).

2.7 Verification of active compounds using repeated bioassays

The tent assays were conducted again to determine the behavioral responses of *H. axyridis* to 1-nonene and acetic acid in the repeated bioassays as described above. The four treatments, including aphid-infested maize under LN, aphid-infested maize under HN, aphid-infested maize under LN supplied with 1-nonene, and aphid-infested maize under LN supplied with acetic acid, were placed at the four corners.

A Perspex four-arm olfactometer was used to determine the behavioral responses of *H. axyridis* to 1-nonene in the repeated bioassays. Four treatments with 0.5 g of leaves or compound dispensers (used to supply 1-nonene and acetic acid) were placed in 50 mL bottles that were connected directly to the four olfactometer chamber arms. The compound dispensers were the same as those described for the Y-tube. The four treatments included aphid-infested maize under LN, aphid-infested maize under HN, aphid-infested maize under LN supplied with 1-nonene, and aphid-infested maize under LN supplied with acetic acid (control) at each of the four sides of the olfactometer. An airstream at 400 mL per min was created by removing air from the center of the chamber with a vacuum pump. A 20 W fluorescent light was placed 0.5 m above the olfactometer. To avoid visual distraction of *H. axyridis*, a white curtain was placed around the olfactometer. Air was passed through a charcoal filter to remove any impurities. Filtered air flowed over the odor source into each of the four arms towards the center of the chamber. A single *H. axyridis* individual was introduced into the center of the chamber and observed for 5 min. If it walked up in the direction of the olfactometer and into one arm, it was recorded and removed. If an *H. axyridis* did not choose an arm within 5 min, it was considered nonresponsive and discarded. The experiment had six replicates, and 30 *H. axyridis* were used for each replicate. The olfactometer was rotated 90° after 5 *H. axyridis* individuals were tested. All equipment was cleaned before use (Ye et al., 2018; Zhang et al., 2022).

2.8 Quantitative RT–PCR

All RNA was extracted from maize-leaves using RNAiso Plus (Takara, Dalian, China) according to the manufacturer's protocol. The PrimeScript™ RT Reagent Kit with gDNA Eraser (RR047A, Takara, Dalian, China) was used for cDNA synthesis. Specific primer pairs for RT–qPCR for selected key genes in the synthesis pathways from the maizeGDP website were designed using Primer Premier 5.0 software (Supplementary Table 1). *Actin* (GenBank accession number: J01238) was used as a candidate reference gene (Manoli et al., 2012). The PCR conditions were as follows: 95°C for 30 s, followed by 40 cycles of 94°C for 5 s, 60°C for 10 s, and 72°C for 34 s. The reaction mixture (final volume of 20 µL) contained 1 µL of cDNA, 10 µL of SYBR Premix Ex Taq, 0.4 µL of 10 µM forward primer, 0.4 µL 10 µM of reverse primer, 0.4 µL of ROX Reference Dye II, and 7.8 µL of double-distilled water. After RT–qPCR, melting curves were evaluated to confirm single peaks and to check amplification specificity. Subsequently, the relative expression level was calculated using the $2^{-\Delta\Delta Ct}$ method (Pfaffl, 2001). The reaction was performed with three biological replicates and three technical replicates (Pan et al., 2021).

2.9 Phytohormone analysis

Maize leaves samples (approximately 100 mg) were harvested and transferred to FastPrep tubes. One milliliter of ethyl acetate spiked with 200 ng of d5-JA, d6-ABA, and d4-SA was added to each

sample (n = 9) and used as the internal standards for JA, ABA, and SA, respectively. Ten-microlitre aliquots of the samples were analyzed using a triple quadrupole liquid chromatography with tandem mass spectrometry (LC–MS/MS) system (Shimadzu LC-20A coupled with an Applied Biosystems API4000 mass spectrometer); this apparatus was equipped with an SB-C18 column (2.1 mm×150 mm, 3.5 μm; Agilent Technologies) and kept in a thermostat-controlled chamber at 35°C. A mobile phase composed of solvent A (0.1% formic acid) and solvent B (acetonitrile) was used in gradient mode for separation at a constant flow rate of 0.2 mL min^{-1}. The compounds were detected in electrospray ionization negative mode. JA, SA, and ABA were quantified by comparing their peak areas with the peak areas of their respective internal standards (Pan et al., 2021).

2.10 Statistical analysis

Statistically significant differences for the volatile were using Student's *t*-test. Y-tube olfactometer bioassays were analyzed with a Shapiro-Wilk test to determine heteroscedasticity of error variance and normality, significance of the linear regressions ($p< 0.10$), the data conform to normal distribution, so Y-tube olfactometer bioassays were analyzed using a paired *t*-test, Multiple comparisons of phytohormone data were performed using Tukey's test. Multiple comparisons of EAG data were performed using Dunnett's test. The averages of the amounts of emitted volatiles and phytohormone from the different treatment groups were used for correlation analysis. The released volatiles and the number of *H. axyridis* visits was conducted using a simple regression. The amounts of VOCs emitted from aphid-infested maize in HN and LN are listed in Table 1, and the amounts of VOCs emitted from healthy maize in HN and LN were obtained from a previous article from our laboratory (Zhao et al., 2022). IBM SPSS statistics version 20 (Chicago, IL, U.S.) was used to conduct above statistical analyses. Principal component analysis (PCA) and random forest analysis were conducted by the online program MetaboAnalyst (https://www.metaboanalyst.ca/). Generalized linear mixed models (GLMM) with Poisson distribution were performed to test difference in the four-arms bioassays and the tent bioassays using R version 4.2.1 (R Core Team, 2022). The GLMM were analyzed with lme-function of lme4 package. For *post hoc* analysis of the above data, the multiple comparisons were performed and the *p*-value were calculated using Holm's tests. The random effect analysis for the replication was conducted, there is no random effects of replication in the assays.

3 Results

3.1 High nitrogen levels enhanced the ability of infected maize to attract *H. axyridis*

The Y-tube olfactory behavior experiment showed that under HN conditions, *H. axyridis* preferred aphid-infested maize to healthy maize (t = 4.464; df = 10; p = 0.001), furthermore, *H. axyridis* was attracted by aphid-infested maize under HN conditions rather than LN conditions (t = 9.19; df = 10; $p<$ 0.0001) (Figure 1). However, nitrogen level did not affect their trend to healthy maize (t = 0.439; df = 10; p = 0.67), besides, aphid infestation did not affect their trend to maize under LN conditions (t = 0.341; df = 10; p = 0.145). That is, we concluded that *H. axyridis* used the VOCs of maize to locate this crop, moreover, aphids infestation had effect on the *H. axyridis* choice to maize under HN conditions and nitrogen level affect the attraction of aphid-infested maize to the *H. axyridis*.

TABLE 1 Volatile organic compounds (VOCs) emitted from aphid-infested-maize leaves under high and low nitrogen conditions.

Compound	High nitrogen condition	Low nitrogen condition	
Farnesol	0.23 ± 0.07	0.16 ± 0.06	NS
1-Nonene	0.37 ± 0.08	0.13 ± 0.01	***
Benzaldehyde	0.79 ± 0.09	0.54 ± 0.10	*
Squalane	0.30 ± 0.09	0.19 ± 0.05	NS
Longifolene	0.22 ± 0.14	0.16 ± 0.04	NS
Eicosane	0.17 ± 0.04	0.18 ± 0.07	NS
Ylangene	0.77 ± 0.14	0.78 ± 0.27	NS
Naphthalene	0.62 ± 0.11	0.90 ± 0.18	NS
Copaene	2.13 ± 0.38	2.08 ± 0.36	NS
Caryophyllene	0.01 ± 0.01	0.57 ± 0.19	***
Azulene	0.44 ± 0.05	0.75 ± 0.08	*
alpha-Cubebene	0.30 ± 0.19	0.28 ± 0.18	NS
(+)-Cycloisosativene	0.25 ± 0.12	0.21 ± 0.11	NS
(-)-Aristolene	0.16 ± 0.1	0.41 ± 0.19	*
Indole	0.49 ± 0.09	0.14 ± 0.04	***
Acetic acid	0.24 ± 0.09	0.01 ± 0.01	***
Hexadecanoic acid	0.28 ± 0.03	0.27 ± 0.04	NS

The relative amounts of volatile compounds (mean Area% ± s.e, n = 6). NS indicates no significant difference. Asterisks indicate statistically significant differences under high nitrogen conditions compared with low nitrogen conditions. The nutrient solution contained 15 mM for the HN treatment or 0.15 mM KNO3 for the LN treatment. (Student's t-test: * p< 0.05; ** p< 0.01; *** p< 0.001).

3.2 Identification of differential VOCs from aphid-infested maize under high- and low-nitrogen conditions

To identify the volatiles emitted by the maize plants that triggered indirect defense, samples of the volatiles were collected from infested plants. GC–MS analysis detected 17 major VOCs from maize under high/low-nitrogen conditions (Table 1). Seven of these volatile compounds showed significant differences between HN and LN conditions. Benzaldehyde (t = 4.464; df = 10; $p< 0.05$),

10.3389/fpls.2023.1296915

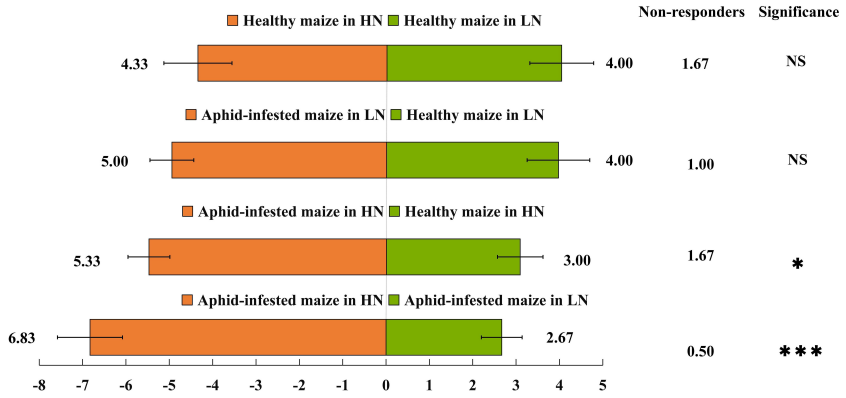

FIGURE 1
Behavioural responses of Harmonia axyridis. A Y-tube olfactometer was used to determine the behavioral responses of H. axyridis to maize under different treatments: healthy maize under high-nitrogen (HN) conditions vs. healthy maize under low-nitrogen (LN) conditions; healthy maize under low-nitrogen conditions vs. aphid-infested maize under low-nitrogen conditions; healthy maize under high-nitrogen conditions vs. aphid-infested maize under high-nitrogen conditions; and aphid-infested maize under high-nitrogen conditions vs. aphid-infested maize under low-nitrogen conditions. There are six replicates in the Y-tube olfactometer assays, 10 H. axyridis individuals were used for each replicate. (t-test: *p< 0.05; ***p< 0.001, NS, not significant).

1-nonene ($t = 41.003$; $df = 10$; $p < 0.01$), acetic acid ($t = 5.921$; $df = 10$; $p < 0.001$), and indole ($t = 8.673$; $df = 10$; $p < 0.001$) were more abundant under HN than under LN. (-)-Aristolene ($t = 2.9$; $df = 10$; $p < 0.05$), azulene ($t = 8.161$; $df = 10$; $p < 0.0001$), and caryophyllene ($t = 7.281$; $df = 10$; $p < 0.0001$) were produced at higher amounts under LN than under HN. The relative amounts of other VOCs were not significantly different (Table 1). PCA of the VOCs showed significant separation between maize infested by aphids in HN and LN conditions. PC1 and PC2 accounted for 82.2% of the variation (Figure 2A). Random forest distribution function analysis showed that 1-nonene had the highest absolute scores (Figure 2B), suggesting that 1-nonene made high contributions to the classification accuracy.

3.3 Induced VOCs from aphid-infested maize under high-nitrogen conditions elicited the EAG responses of *H. axyridis*

Seven VOCs that significant differences between HN and LN conditions were selected for EAG experiments. Of the seven VOCs, four VOCs (benzaldehyde, 1-nonene, indole and acetic acid) elicited the significantly greater EAG responses of *H. axyridis*, the EAG response values of benzaldehyde ($p < 0.0001$), 1-nonene ($p = 0.008$), indole ($p < 0.0001$), and acetic acid ($p < 0.0001$) were significantly higher than the control (paraffin oil) (Figure 3), however, the *H. axyridis* didn't show the significantly greater EAG responses to (-)-aristolene ($p = 1$), caryophyllene ($p =$

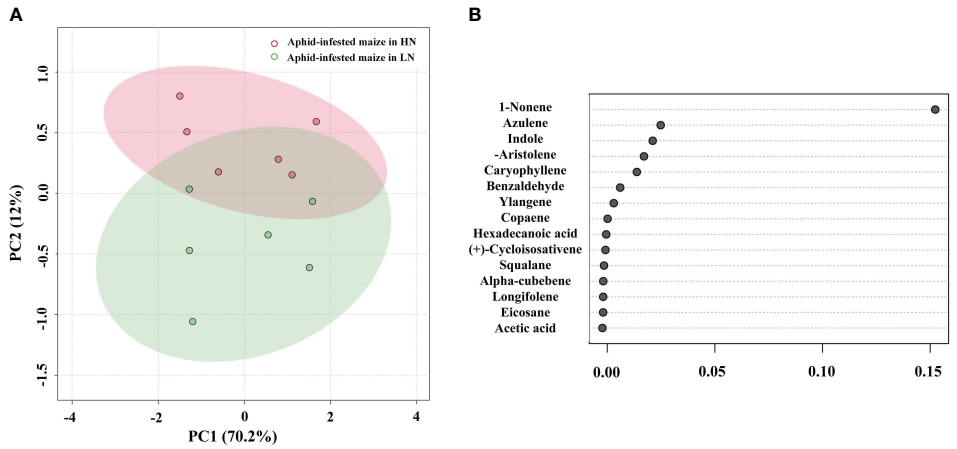

FIGURE 2
(A) Principal component analysis of the volatile organic compounds (VOCs) of the aphid-infested maize under high-nitrogen (HN) and low-nitrogen (LN) conditions. **(B)** Features of VOCs ranked by their contributions to classification accuracy (mean decrease accuracy).

10.3389/fpls.2023.1296915

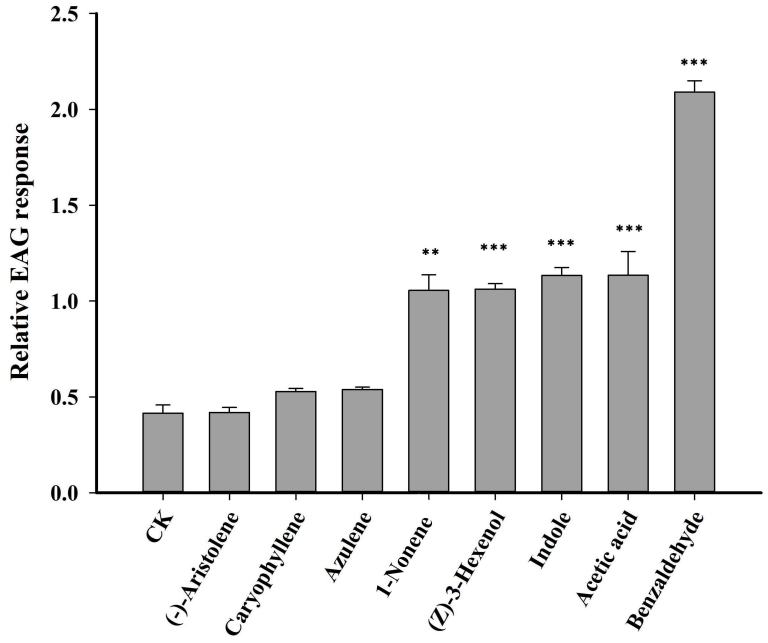

FIGURE 3
An electroantennogram assay was performed to measure the sensitivity of H. axyridis to CK (paraffin oil), benzaldehyde, 1-nonene, acetic acid, azulene, indole, and (-)-aristolene. The EAG multiple comparisons was used Dunnett's test (**p< 0.01; ***p< 0.001).

0.531), and azulene ($p = 0.697$) compared to control (Figure 3). The four HIPVs that were more strongly emitted under high N conditions may have affected *H. axyridis* response.

3.4 Behavioural responses of *H. axyridis* to differential VOCs

Based on the EAG results, four compounds (1-nonene, acetic acid, indole, and benzaldehyde) were selected for behavioral assay. The emissions of these four compounds were quantified from aphid-infested maize under HN condition (Figure 4), and the volatilization rates are as follows: 15.46 ng/g/h 1-nonene, 13.70 ng/g/h acetic acid, 5.43 ng/g/h indole, and 1.88 ng/g/h benzaldehyde. The volatilization rates of 1-nonene ($t = 20.276$; $df = 4$; $p< 0.0001$), acetic acid ($t = 17.08$; $df = 4$; $p< 0.0001$), indole ($t = 92.5$; $df = 4$; $p< 0.0001$), and benzaldehyde ($t = 3.331$; $df = 4$; $p = 0.0291$) were significantly higher than those from aphid-infested maize under LN conditions. Then, we investigated the effects of synthetic standards, which were used at the natural concentrations emitted by HN aphid infested maize, on the behavior of *H. axyridis* using a Y-tube olfactometer. The results indicate that 1-nonene exhibited a significantly attractive effect on *H. axyridis* compared to the control ($t = 3.337$; $df = 10$; $p = 0.008$), however, benzaldehyde

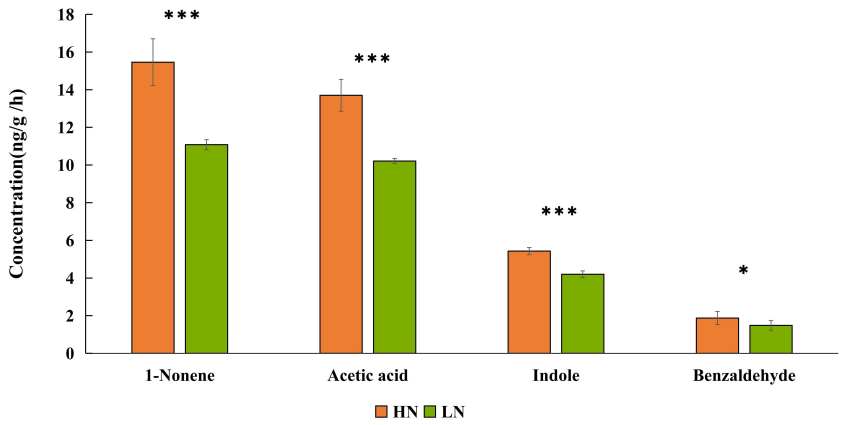

FIGURE 4
Quantitative analysis of 1-nonene, acetic acid, indole, benzaldehyde emitted by aphid-infested maize under high-nitrogen conditions/low-nitrogen conditions. Individual compounds with authentic standards at known concentrations were used for the determination of the absolute amount of each active compound in the headspace volatile sample. The data are shown as the mean ± standard error (SE). Asterisks indicate statistically significant differences between HN and LN (Student's t-test: *p< 0.05 ***p< 0.001).

10.3389/fpls.2023.1296915

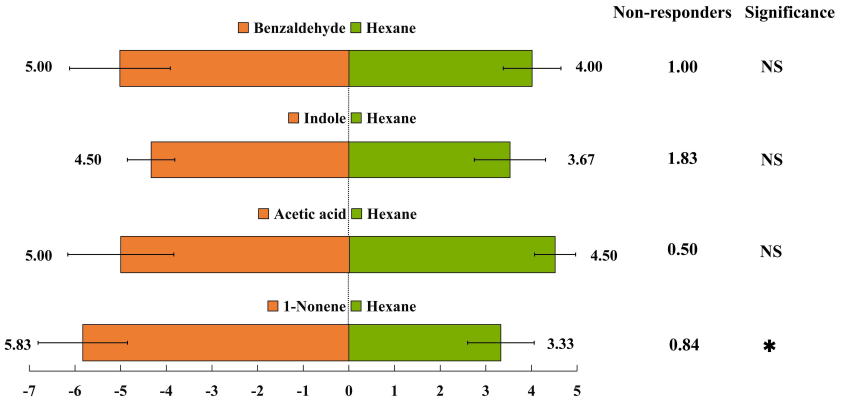

FIGURE 5
Behavioural responses of Harmonia axyridis to synthetic chemicals were determined using a Y-tube olfactometer. Synthetic chemicals, including 1-nonene, acetic acid, indole, and benzaldehyde, correspond to amounts typically emitted by aphid-attacked maize under high-nitrogen conditions. There are six replicates in the Y-tube olfactometer assays, 10 H. axyridis individuals were used for each replicate. (t-test: *p< 0.05, NS, not significant).

(t = 1.936; df = 10; p = 0.082), indole (t = 2.076; df = 10; p = 0.065) and acetic acid (t = 0.275; df = 10; p = 0.789) was not exhibited attraction to *H. axyridis* (Figure 6).

3.5 Regression analysis between VOCs and visits of *H. axyridis*

To further validate that high nitrogen levels enhanced the ability of infected maize to attract *H. axyridis*, the tent bioassays were conducted, the number of *H. axyridis* visiting aphid-infested maize under HN conditions was significant higher than those of *H. axyridis* visiting healthy maize under HN conditions (p = 0.006), aphid-infested maize under the LN conditions (p = 0.006), as well as healthy maize under the LN conditions (p = 0.006). However, there were no significant differences between healthy maize and aphid-infested maize under LN conditions (p = 0.579), between the healthy maize under LN conditions and healthy maize under the HN conditions (p = 1), and between healthy maize under HN conditions and aphid-infested maize under LN (p = 1) (Figure 6A, B), which is consistent with the results of Y tube. In order to evaluate the responses of *H. axyridis* to the four compounds, which

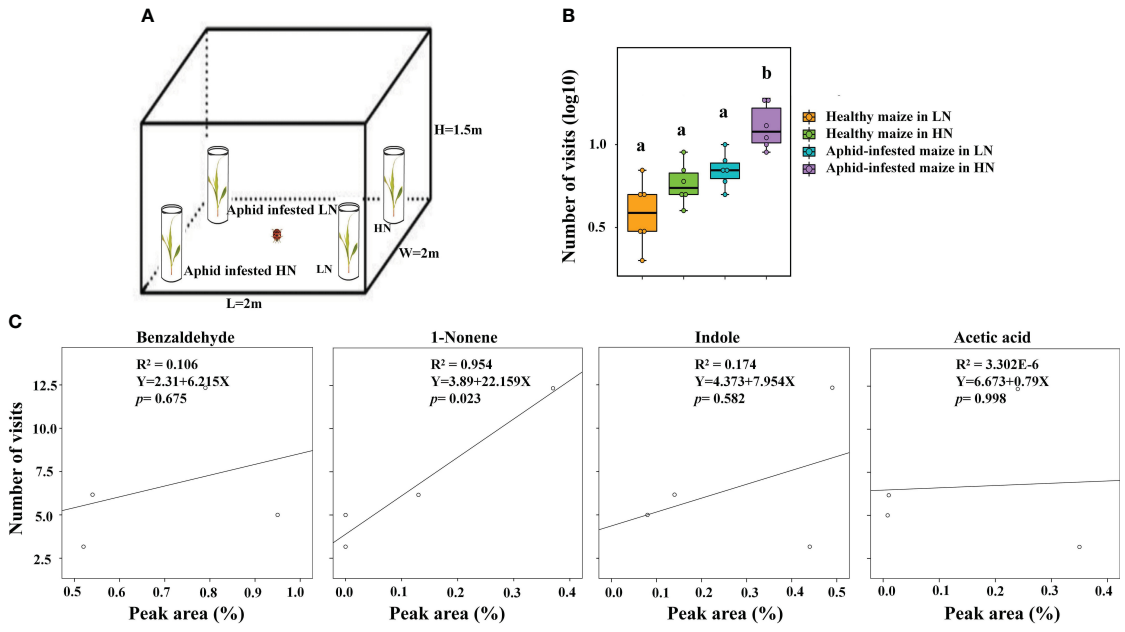

FIGURE 6
The analysis between VOCs and visits of H. axyridis. **(A)** Schematic drawing of the tent assay. **(B)** Number of visits (log10) of H. axyridis in four different treatments, including healthy maize in high nitrogen (HN), healthy maize in low nitrogen (LN), aphid-infested maize in HN, and aphidinfested maize in LN. Different letters above the bars indicate significant differences (The analyzed using a GLMM fitted to a poisson distribution). **(C)** The effect of the amount (Peak area %) of volatiles on attraction (visit number) evaluated using a simple regression analysis.

were identified as potential active compounds and known to be influenced by nitrogen levels, we performed a regression analysis between the peak area of each of the four compounds and the number of *H. axyridis* visits (Figure 6C). The number of *H. axyridis* visits increased along with the increase of peak area of 1-nonene (R^2 = 0.954, F = 41.588, p = 0.023) (Figure 6C). But the number of *H. axyridis* visits were not significantly changed with increase of the peak area of indole(R^2 = 0.174, F = 0.423, p = 0.582), acetic acid (R^2< 0.0001, F< 0.0001, p = 0.998) and benzaldehyde(R^2 = 0.106, F = 0.237, p = 0.675) (Figure 6C).

3.6 Verification of the ecological potential of 1-nonene using repeated bioassays

Four-arm olfactometers and tent assays were used in repeated bioassays to evaluate the ecological potential of 1-nonene. The volatilization of 1-nonene and acetic acid from aphid-infested maize under HN was 4.38 ng/g/h and 3.49 ng/g/h higher, respectively, than that from aphid-infested maize under LN, which are derived from the results in Figure 5. Aphid-infested maize under LN supplemented with the missing portion of 1-nonene and acetic acid was used in the tent assays and four-arm olfactometers. The aphid-infested maize under LN supplemented with 1-nonene significantly attracted more *H. axyridis* than the aphid-infested maize under LN in tent assays (p = 0.006) and in four-arm olfactometers (p = 0.012), and showed similar attractiveness as the aphid-infested maize under HN in tent assays (p = 0.414) and in four-arm olfactometers (p = 1). However, compared to the aphid-infested maize under LN, *H. axyridis* was not attracted by the aphid-infested maize under LN supplemented with acetic acid in tent assays (p = 0.414) and in four-arm olfactometers (p = 0.1) (Figure 7).

3.7 The regulation pathway of 1-nonene

The biosynthetic pathways of 1-nonene are not yet known; however, some biosynthetic enzymes ($OleT_{JE}$/P450 decarboxylase, UndA/nonheme iron decarboxylase, and UndB/membrane-bound desaturase-like decarboxylase) from bacteria can convert free fatty acids to 1-alkenes, providing insights into the biosynthetic pathways of 1-nonene (Liu and Li, 2020). To fill this knowledge gap, we proposed a synthetic pathway for 1-nonene in maize B73 based on the biosynthesis of the fatty acid-derived hydrocarbons described above (Figure 8A). Based on homology analysis by the online program MaizeGDB BLAST (https://staging.maizegdb.org/) using the maize B73 genome, a probable *phospholipid-transporting ATPase 8* (GenBank No: LOC103643332), showing relatively high homology (41.95%) with $OleT_{JE}$, was selected as the candidate gene for 1-nonene biosynthesis in maize B73. Consistent with the amount of 1-nonene emitted, the expression level of the *phospholipid-transporting ATPase 8* in infested maize under high-nitrogen conditions was higher than that in infested maize under low-nitrogen conditions (t test: df=4, t=6.602, p = 0.0027) (Figure 8B). To investigate whether stress-related phytohormones were activated, the concentrations of JA, SA and ABA in maize leaves were determined. The accumulation of SA was significantly increased following aphid infestation under high-nitrogen conditions (Tukey's test, p< 0.001) (Figure 9A), but there is no significant difference for the SA concentration between the healthy maize under HN conditions and LN conditions (Tukey's test, p = 0.996), and there is no significant difference between health maize and aphid-infested maize under LN conditions (Tukey's test, p = 0.646). Similarly, the concentration of ABA in the aphid-infested maize under HN conditions were obviously increased (Tukey's test, p< 0.001), and there is significant difference between health maize and aphid-infested maize under LN conditions (Tukey's test, p = 0.016), but there is no significant difference between HN conditions and LN conditions in the healthy maize (Tukey's test, p = 0.379). However, the concentration of JA in health maize under LN conditions was higher than health maize under HN conditions (Tukey's test, p = 0.003), and also higher than aphid-infested maize under HN conditions (Tukey's test, p = 0.003), but there is no significant difference between aphid-infested maize under LN conditions and aphid-infested maize under HN conditions (Tukey's test, p = 0.319). SA (R^2 = 0.991, F= 232.745, p = 0.004) and ABA (R^2 = 0.964, F= 53.977, p = 0.018) showed significantly

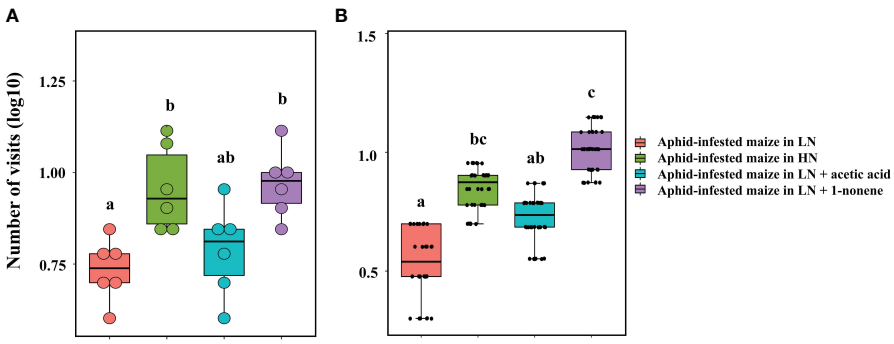

FIGURE 7
Behavioural responses of *H. axyridis* to aphid-infested maize supplied with 1-nonene under low nitrogen conditions in the tent bioassay **(A)** and four-arm olfactometer **(B)**. LN, low nitrogen; HN, high nitrogen. Different letters above the bars indicate significant differences (The analyzed using a GLMM fitted to a poisson distribution).

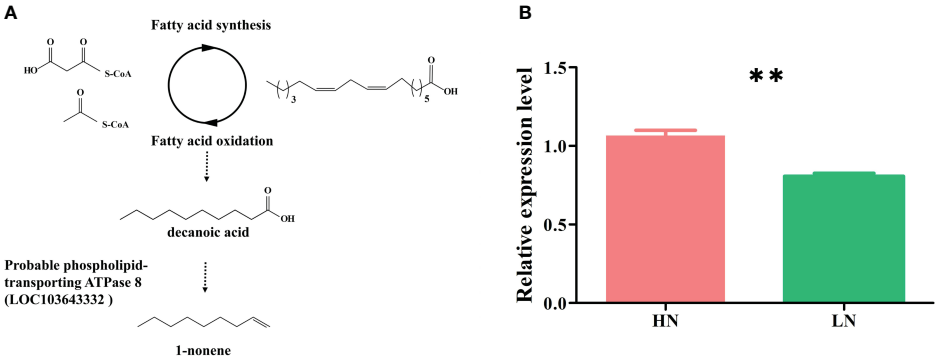

FIGURE 8
(A) Hypothesized pathway for 1-nonene biosynthesis in maize. **(B)** RT-qPCR analysis for the potential biosynthetic genes of the 1-nonene [*probable phospholipid-transporting ATPase* 8 (LOC103643332)]. HN, aphid-infested maize in high nitrogen; LN, aphid-infested maize in low nitrogen.

positive correlation with volatilization of 1-nonene, but, there is no obvious correlation with JA (R^2 = 0.244, F= 0.646, p = 0.280) (Figure 9B).

Discussion

VOCs serve as attractants for predators play an important role in tritrophic interactions (Hiltpold et al., 2011; Aartsma et al., 2017; Turlings and Erb, 2018). The present study reveals that 1-nonene affect tritrophic interactions indirectly via nitrogen changes in the aphid-infested maize. This finding adds a new dimension to the role of HIPVs as mediators of tritrophic interactions.

Herbivore-induced plant volatiles (HIPVs) were usually used to locate the food source for predatory insects in plant-herbivores-natural enemies tritrophic interactions systems. For example, the females of parasitoid (*Cotesia marginiventris*) were attractive by the volatiles from corn seedlings which beet armyworm larvae were feeding in the flight tunnel bioassays. Besides, some researchers found that nitrogen content can mediated plant- herbivores-natural enemies tritrophic interactions systems. Some researchers found that natural enemies preferred plants that growing on a higher nitrogen condition by detected plant volatile

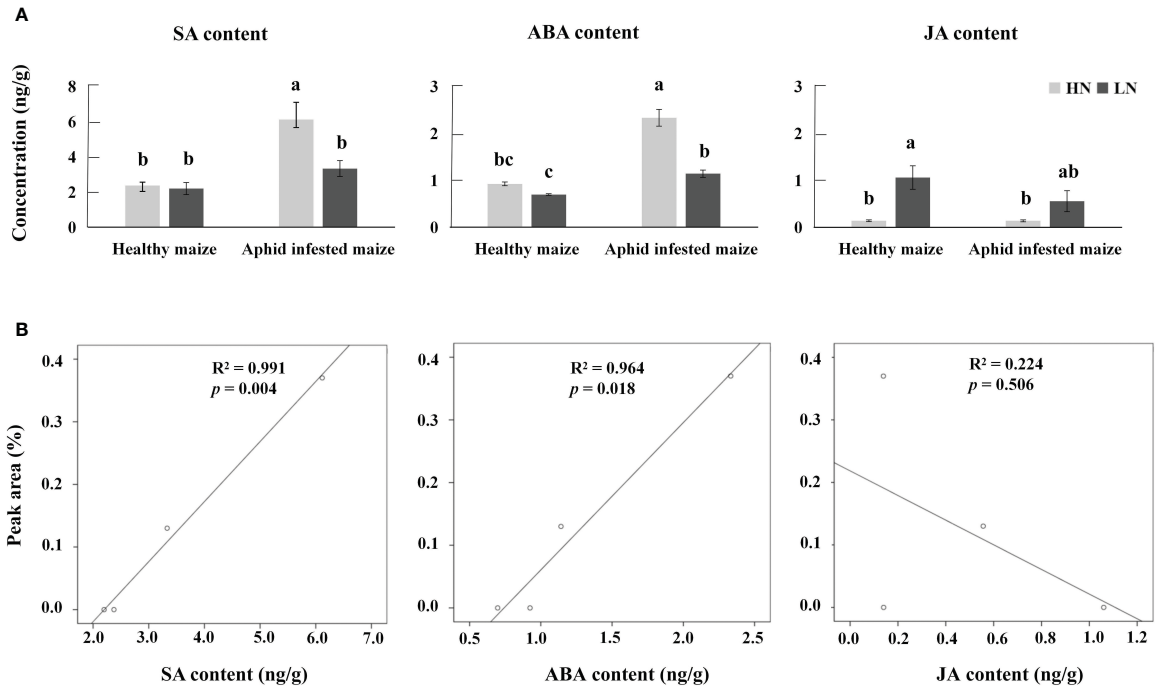

FIGURE 9
(A) Average concentrations of jasmonic acid (JA), salicylic acid (SA), and abscisic acid (ABA) in aphid-infested and healthy maize under high-nitrogen (HN) and low-nitrogen (LN) conditions. Different letters above the bars indicate significant differences (the phytohormone multiple comparisons was used Tukey's test). **(B)** Correlation analysis between SA, ABA, JA, and 1-nonene.

cues (Loader and Damman, 1991; Zhu et al., 2020a). The amount of volatile secondary substances released by the host plant was much greater than the amount of secondary substances released by the pest itself, which provided natural enemies with reliable information about the possible presence of the host plant pest (Turlings et al., 1991). Therefore, we have collected and identified leaf volatiles from host plants in HN/LN conditions. The result showed that the composition of volatiles was significantly altered under different nitrogen levels.

Nitrogen levels affect the levels of plant hormones and the expression of numerous genes involved in metabolite synthesis, which subsequently results in changes in plant volatiles that might be the key signals used by natural enemies to locate pests (Chen et al., 2008; Kutyniok and Müller, 2013). For example, rice plants treated with different nitrogen levels showed changes in the composition of volatiles, thereby regulating the foraging and searching behavior of *Cyrtorhinus lividipennis* (Lou and Cheng, 2003; Zhu et al., 2020b), which consistent with our research. Many studies have shown that higher nitrogen level could enhance capability of parasitism of natural enemies and plant defense (Aqueel et al., 2014; Chesnais et al., 2016; Zhu et al., 2020a). For example, Sun et al. found that rice resistant response to brown rice planthopper (BPH) was obviously affected under different nitrogen condition by regulation of callose content and volatile emission, resulting in BPH preferred rice plants under higher nitrogen levels (Sun et al., 2020).

Our results found that *H. axyridis* was more attracted to volatiles emitted by aphid-infested maize under high-nitrogen conditions than under low-nitrogen conditions. Our study also found differences in the levels of the seven compounds between high- and low-nitrogen conditions. Seven volatile compounds showed significant differences among HN/LN conditions, such as benzaldehyde, 1-nonene, acetic acid, and indole, the levels of which were higher under HN than under LN; (-)-aristolene, azulene, and caryophyllene were produced in higher amounts under LN than under HN. This demonstrated that the same VOCs in different quantities could function as preferred host plant cues, depending upon the context in which they were perceived (Pingyan, 2009). So we quantified the differential volatiles and simulated the volatilities under natural conditions. 1-nonene may affect tritrophic interactions systems. When *H. axyridis* are exposed to mixed volatiles, supplementation with 1-nonene to HN levels can still change *H. axyridis* behavior. Previously reported that herbivory-induced indole increases the recruitment of the solitary endoparasitoid *Microplitis rufiventris* to maize plants that are induced by *Spodoptera littoralis* caterpillars. Indole exposure rendered the body odors of the caterpillars significantly less attractive, an effect that persisted even in the presence of more attractive host plants, which consistent with our research (Ye et al., 2018).

1-Nonene was found in pear, peach trees (Najar-Rodriguez et al., 2013) and *Senecio madagascariensis* (Kashiwagi et al., 2022), it was an attractant for males *Aedes aegypti* (L.) (Diptera: Culicidae). It is found that 1-nonene was the active compound in maize HIPVs that attracted *H. axyridis* that responded to nitrogen. The biosynthesis pathways of 1-nonene are not yet known, however, some biosynthetic enzymes (OleTJE/P450 Decarboxylase, UndA/non-heme iron decarboxylase, UndB/membrane-bound desaturase-like decarboxylase) able to convert free fatty acids to 1-alkenes from Bacteria provided insights into biosynthesis pathways of 1-nonene (Liu and Li, 2020). Based on the results of previous studies (Rude et al., 2011; Zhe et al., 2014; Zhe et al., 2015; Liu and Li, 2020), we predicted the synthesis pathway of 1-nonene. The *in vivo* bioconversion studies along with cell-free *in vitro* olefin biosynthesis studies suggest that *Jeotgalicoccus* utilizes fatty acid intermediates as substrates for olefin biosynthesis and that fatty acid decarboxylation is a primary mechanism of terminal olefin production (Rude et al., 2011). The genes in Maize B73 with high homology to the biosynthesis genes of 1-alkenes above were supposed to possibly participate in biosynthesis of 1-nonene. Finally, the gene probable *phospholipid-transporting ATPase* 8 in maize B73 showing high homolgy with OleTJE/P450 Decarboxylase was selected as potential biosynthesis genes of 1-nonene. Overall, the signaling pathway for the synthesis of 1-nonene is a complex process that includes the interaction of multiple links. By studying these links and their interactions in depth, the mechanisms of 1-nonene synthesis can be better understood and provide strong support for maize tritrophic interactions. The manipulation of 1-nonene biosynthesis allows for precise assessments of HIPV effects in the field and demonstrates that 1-nonene may be beneficial for maize in the context of multitrophic interactions. Interdependence of 1-nonene biosynthesis/action and fatty acyl-CoA reductaseas/oxidative decarbonylase expression is an interesting prospect for future research. How to reconcile the tritrophic interactions with the nitrogen fertilizer and how to make better use of plant volatiles to regulate the behavior of *H. axyridis* to achieve more desirable biological control effects still needs to be studied.

In addition to VOCs and hormones, the nitrogen levels have a significant effect on the growth and development of maize. The root length, root weight, shoot length, shoot weight and crop production increased under high-nitrogen condition (Chen et al., 2008; Schluter et al., 2012; Kutyniok and Müller, 2013; Chesnais et al., 2016), which was in consistant with our previous study as well (Zhao et al., 2022). Similarly, nitrogen levels affect natural enemy insects, it has been reported that improvement in N inputs enhances parasitism, the growth and development of parasites (Kaneshiro et al., 1996; Aqueel et al., 2014). It was also shown high N level positively promotes performances of phytophagous insects in terms of population growth rate and weight increase (Aqueel and Leather, 2011). In this study, aphid-infested maize under high N condition showed stronger attractive to the *H. axyridis* compared to the maize under low N condition. Our previous study showed *Rhopalosiphum padii* preferred the maize grown under the high-nitrogen condition (Zhao et al., 2022). Base on results from the previous and our studies, we proposed that the both of pests and their enemies tend to targets with abundant nutrition, such as the maize under high N condition and more aphids attracted by the maize under high N condition, even though predation risk is high for the aphids (*R. padi*) attracted by the maize under high N condition.

Overall, our study further revealed the key role of 1-nonene when aphids fed on maize in the response of maize-aphid-ladybird tritrophic interactions to nitrogen (Figure 10). These findings may have practical importance for the development of habitat manipulation strategies, given that HIPVs induced by aphid feeding are important signals. Meanwhile, this study also provides a novel perspective and strategy for maize pest resistance research and integrated pest management.

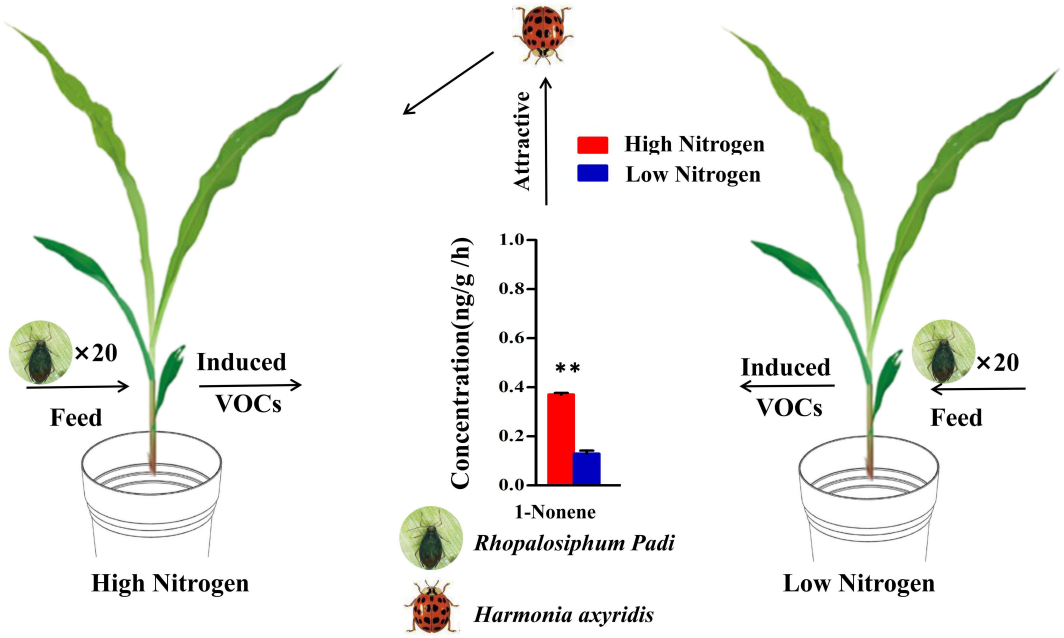

FIGURE 10
Model of the tendency of *H. axyridis* to visit maize under high/low-nitrogen conditions. (Student's *t*-test: $^{**}p < 0.01$).

However, there is also need to comprehend the molecular and biochemical mechanisms in the production and recognition of the key VOCs, which probably offer new insights for molecular breeding and environment-friendly pest control.

Data availability statement

The original contributions presented in the study are included in the article/Supplementary Material. Further inquiries can be directed to the corresponding authors.

Author contributions

S-WZ: Data curation, Methodology, Validation, Writing – original draft, Writing – review & editing. J-HX: Funding acquisition, Project administration, Writing – review & editing. YP: Methodology, Software, Writing – original draft. ZW: Software, Writing – original draft. XW: Writing – original draft. SW: Formal Analysis, Project administration, Validation, Writing – review & editing.

Funding

The author(s) declare financial support was received for the research, authorship, and/or publication of this article. This work was supported by Key Research and Development Program of Jilin Province (20210202073NC), the Project of Disciplinary Crossing and Integration from Jilin University (JLUXKJC2020107), the National Key R&D Program of China (2018YFD0201000, 2017YFD0200600), the National Natural Science Foundation of China (32102196).

Acknowledgments

We are grateful to the National Key R&D Program of China. We also thank Zhiwei Qin (Beijing Normal University, Zhuhai, China) and Benke Hong (Westlake University, Hangzhou, China) for their advice on the synthesis pathway of 1-nonene, and Hui Zhu (Northeast Normal University, Changchun, China) for her help with the statistical analyses.

Conflict of interest

The authors declare that the research was conducted in the absence of any commercial or financial relationships that could be construed as a potential conflict of interest.

Publisher's note

Supplementary material

The Supplementary Material for this article can be found online at: https://www.frontiersin.org/articles/10.3389/fpls.2023.1296915/full#supplementary-material

References

Aartsma, Y., Bianchi, F., van der Werf, W., Poelman, E. H., and Dicke, M. (2017). Herbivore-induced plant volatiles and tritrophic interactions across spatial scales. *New Phytol.* 216 (4), 1054–1063. doi: 10.1111/nph.14475

Ali, M. Y., Naseem, T., Holopainen, J. K., Liu, T., Zhang, J., and Zhang, F. (2023). Tritrophic Interactions among Arthropod Natural Enemies, Herbivores and Plants Considering Volatile Blends at Different Scale Levels. *Cells* 12, 251. doi: 10.3390/cells12020251

Aqueel, M. A., and Leather, S. R. (2011). Effect of nitrogen fertilizer on the growth and survival of *Rhopalosiphum padi* (L.) and Sitobion avenae (F.) (*Homoptera: Aphididae*) on different wheat cultivars. *Crop Prot.* 30, 216–221. doi: 10.1016/j.cropro.2010.09.013

Aqueel, M. A., Raza, A. B., Balal, R. M., Shahid, M. A., Mustafa, I., Javaid, M. M., et al. (2014). Tritrophic interactions between parasitoids and cereal aphids are mediated by nitrogen fertilizer. *Insect Sci.* 22 (6), 813–820. doi: 10.1111/1744-7917.12123

Chen, Y., Schmelz, E. A., Wäckers, F., and Ruberson, J. R. (2008). Cotton plant, Gossypium hirsutum L., defense in response to nitrogen fertilization. *J. Chem. Ecol.* 34 (12), 1553–1564. doi: 10.1007/s10886-008-9560-x

Chesnais, Q., Couty, A., Catterou, M., and Ameline, A. (2016). Cascading effects of n input on tritrophic (plant–aphid–parasitoid) interactions. *Ecol. Evol.* 6 (21), 7882–7891. doi: 10.1002/ece3.2404

Chirgwin, E., Yang, Q., Umina, P. A., Gill, A., Soleimannejad, S., Gu, X. Y., et al. (2022). Fungicides have transgenerational effects on Rhopalosiphum padi but not their endosymbionts. *Pest Manag Sci Undefined* 78(11), 4709–4718. doi: 10.1002/ps.70911

Clavijo, M. ,. A., Unsicker, S. B., and Gershenzon, J. (2012). The specificity of herbivore-induced plant volatiles in attracting herbivore enemies. *Trends Plant Sci.* 17 (5), 303–310. doi: 10.1016/j.tplants.2012.03.012

Erb, M., Veyrat, N., Robert, C. A., Xu, H., Frey, M., Ton, J., et al. (2015). Indole is an essential herbivore-induced volatile priming signal in maize. *Nat. Commun.* 6, 6273. doi: 10.1038/ncomms7273

Gouinguené, S., Pickett, J. A., Wadhams, L. J., Birkett, M. A., and Turlings, T. C. J. (2005). Antennal electrophysiological responses of three parasitic wasps to caterpillar-induced volatiles from maize (Zea mays), cotton (Gossypium herbaceum), and cowpea (Vigna unguiculata). *J. Chem. Ecology 31* pp, 1023–1038. doi: 10.1007/s10886-005-4245-1

He, J., Fandino, R. A., Halitschke, R., Luck, K., Köllner, T. G., Murdock, M. H., et al. (2019). An unbiased approach elucidates variation in (S)-(+)-linalool, a context-specific mediator of a tri-trophic interaction in wild tobacco. *Proc. Natl. Acad. Sci. United States America* 116 (29), 14651–14660. doi: 10.1073/pnas.1818585116

Heil, M. (2008). Indirect defence *via* tritrophic interactions. *New Phytol.* 178 (1), 41–61. doi: 10.1111/j.1469-8137.2007.02330.x

Hiltpold, I., Erb, M., Robert, C. A. M., and Turlings, T. C. J. (2011). Systemic root signalling in a belowground, volatile-mediated tritrophic interaction. *Plant Cell Environ.* 34 (8), 1267–75. doi: 10.1111/j.1365-3040.2011.02327.x

Jagtap, A. B., Vikal, Y., and Johal, G. S. (2020). Genome-wide development and validation of cost-effective KASP marker assays for genetic dissection of heat stress tolerance in maize. *Int. J. Mol. Sci.* 21 (19), 1. doi: 10.3390/ijms21197386

Jamieson, M. A., Trowbridge, A. M., Raffa, K. F., and Lindroth, R. L. (2012). Consequences of climate warming and altered precipitation patterns for plant-insect and multitrophic interactions. *Plant Physiol.* 160 (4), 1719–1727. doi: 10.1104/pp.112.206524

Jing, T., Qian, X., Du, W., Gao, T., Li, D., Guo, D., et al. (2021). Herbivore-induced volatiles influence moth preference by increasing the β-Ocimene emission of neighbouring tea plants. *Plant Cell Environ.* 44 (11), 3667–3680. doi: 10.1111/pce.14174

Kaneshiro, L. N., Johnson, M. W., and Tritrophic, (1996). Effects of leaf nitrogen on liriomyza trifolii (Burgess) and an associated parasitoid chrysocharis oscinidis (Ashmead) on bean. *Biol. Control* 6 (2), 186–192. doi: 10.1006/bcon.1996.0023

Kashiwagi, G., Von Oppen, S., Harburguer, L., and González-Audino, P. (2022). The main component of the scent of Senecio Madagascariensis flowers is an attractant for Aedes aEgypti (L.) (Diptera: Culicidae) mosquitoes. *Bull. Entomological Res.* 112 (6), 837–846. doi: 10.1017/S0007485322000256

Kessler, A., and Baldwin, I. T. (2001). Defensive function of herbivore-induced plant volatile emissions in nature. *Science.* 291 (5511), 2141–2144. doi: 10.1126/science.291.5511.2141

Kontodimas, D. C., and Stathas, G. J. (2005). Phenology, fecundity and life table parameters of the predator hippodamia variegata reared on dysaphis crataegi. *Biocontrol* 50 (2), 223–233. doi: 10.1007/s10526-004-0455-7

Kuramitsu, K., Vicencio, E. J., and Kainoh, Y. (2019). Differences in food plant species of the polyphagous herbivore *Mythimna separata* (*Lepidoptera: Noctuidae*) influence host searching behavior of its larval parasitoid, *Cotesia kariyai* (*Hymenoptera*: Braconidae). *Arthropod-Plant Interact.* 13, 49–55. doi: 10.1007/s11829-018-9659-0

Kutyniok, M., and Müller, C. (2013). Plant-mediated interactions between shoot-feeding aphids and root-feeding nematodes depend on nitrate fertilization. *Oecologia* 173 (4), 1367–1377. doi: 10.1007/s00442-013-2712-x

Liu, K., and Li, S. (2020). Biosynthesis of fatty acid-derived hydrocarbons: perspectives on enzymology and enzyme engineering. *Curr Opin Biotechnol.* 62, 7–14. doi: 10.1016/j.copbio.2019.07.005

Loader, C., and Damman, H. (1991). Nitrogen content of food plants and vulnerability of Pieris rapae to natural enemies. *Ecology* 72, 1586–1590. doi: 10.2307/1940958

Lou, Y. G., and Cheng, J. A. (2003). Role of rice volatiles in the foraging behavior of the predator *Cyrtorhinus lividipennis* for the rice brown planthopper *Nilaparvata lugens*. *BioControl* 48, 73–86. doi: 10.1023/a:1021291427256

Manoli, A., Sturaro, A., Trevisan, S., Quaggiotti, S., and Nonis, A. (2012). Evaluation of candidate reference genes for qPCR in maize. *Plant Physiol.* 169 (8), 807–815. doi: 10.1016/j.jplph.2012.01.019

Meijer, D., van der Vleut, J., Weldegergis, B. T., Costaz, T., Duarte, M. V. A., Pekas, A., et al. (2023). Effects of far-red light on tritrophic interactions between the two-spotted spider mite (Tetranychus urticae) and the predatory mite *Phytoseiulus persimilis* on tomato. *Pest Manage. Sci.* 79, 1820–1828. doi: 10.1002/ps.7358

Najar-Rodriguez, A., Orschel, B., and Dorn, S. (2013). Season-long volatile emissions from peach and pear trees in situ, overlapping profiles, and olfactory attraction of an oligophagous fruit moth in the laboratory. *J. Chem. Ecol.* 39, 418–429. doi: 10.1007/s10886-013-0262-7

Pan, Y., Wang, Z., Zhao, S. W., Wang, X., Li, Y. S., Liu, J. N., et al. (2021). The herbivore-induced plant volatile tetradecane enhances plant resistance to holotrichia parallela larvae in maize roots. *Pest Manage. Sci.* 78(2), 550–560. doi: 10.1002/ps.6660

Pfaffl, M. W. (2001). A new mathematical model for relative quantification in real-time RT-PCR. *Nucleic Acids Res.* 29, e45. doi: 10.1093/nar/29.9.e45

Pingyan, W. (2009). Selectivity of branches from the various apple varieties by Eriosoma lanigerum with volatiles from the branches. *Scientia Silvae Sinicae 45* pp, 91–95. doi: 10.1007/978-1-4020-9623-5_5

Qin, D., Liu, B., Zhang, P., Zheng, Q., and Zhang, Z. (2021). Treating green pea aphids, myzus persicae, with azadirachtin affects the predatory ability and protective enzyme activity of harlequin ladybirds, *harmonia axyridis*. *Ecotoxicology Environ. Saf.* 212 (10), 111984. doi: 10.1016/j.ecoenv.2021.111984

R Core Team. (2022). *R: A Language and Environment for Statistical Computing*. R Foundation for Statistical Computing. https://www.R-project.org

Rude, M. A., Baron, T. S., Brubaker, S., Alibhai, M., Cardayre, S. D., and Schirmer, A. (2011). Terminal olefin (1-alkene) biosynthesis by a novel p450 fatty acid decarboxylase from jeotgalicoccus species. *Appl. Environ. Microbiol.* 77 (5), 1718. doi: 10.1128/AEM.02580-10

Schluter, U., Mascher, M., Colmsee, C., Scholz, U., Brautigam, A., Fahnenstich, H., et al. (2012). Maize source leaf adaptation to nitrogen deficiency affects not only nitrogen and carbon metabolism but also control of phosphate homeostasis. *Plant Physiol. 160* pp, 1384–1406. doi: 10.1104/pp.112.204420

Schnable, P. S., Ware, D., Fulton, R. S., Stein, J. C., Wei, F., Pasternak, S., et al. (2009). The B73 maize genome: complexity, diversity, and dynamics. *Science 326* pp, 1112–1115. doi: 10.1126/science.1178534

Schnee, C., Kllner, T. G., and Degenhardt, G. J. (2002). The maize gene terpene synthase 1 encodes a sesquiterpene synthase catalyzing the formation of (e)-beta-farnesene, (e)-nerolidol, and (e,e)-farnesol after herbivore damage. *Plant Physiol.* 130 (4), 2049–2060. doi: 10.1104/pp.008326

Sun, Z., Shi, J., Fan, T., Wang, C., Liu, L., and Jin, H. (2020). The control of the brown planthopper by the rice bph14 gene is affected by nitrogen. *Pest Manage. Sci.* 76 (11), 3649–3656. doi: 10.1002/ps.59

Turlings, T. C. J., and Erb, M. (2018). Tritrophic interactions mediated by herbivore-induced plant volatiles: mechanisms, ecological relevance, and application potential. *Annu. Rev. Entomol* 63, 433–452. doi: 10.1146/annurev-ento-020117-043507

Turlings, T. C. J., Tumlinson, J. H., Heath, R. R., Proveaux, A. T., and Doolittle, R. E. (1991). Isolation and identification of allelochemicals that attract the larval parasitoid, Cotesia marginiventris (Cresson), to the microhabitat of one of its hosts. *J. Chem. Ecology.* 17, 2235–2251. doi: 10.1007/BF00988004

Turlings, T. C. J., Tumlinson, J. H., and Lewis, W. J. (1990). Exploitation of herbivore-induced plant odors by host-seeking parasitic wasps. *Science 250* pp, 1251–1253. doi: 10.1126/science.250.4985.1251

Yang, F., Shen, H., Huang, T., Yao, Q., Hu, J., Tang, J., et al. (2023). Flavonoid production in tomato mediates both direct and indirect plant defences against whiteflies in tritrophic interactions. *Pest Manage. Sci.* 79, 4644–4654. doi: 10.1002/ps.7667

Ye, M., Veyrat, N., Xu, H., Hu, L., Turlings, T. C. J., and Erb, M. (2018). An herbivore-induced plant volatile reduces parasitoid attraction by changing the smell of caterpillars. *Sci. Adv.* 4 (5), eaar4767. doi: 10.1126/sciadv.aar4767

Zhang, J., Komail Raza, S. A., Wei, Z., Keesey, I. W., Parker, A. L., Feistel, F., et al. (2022). Competing beetles attract egg laying in a hawkmoth. *Curr. Biol. CB* 32 (4), 861–869.e8. doi: 10.1016/j.cub.2021.12.021

Zhao, S. W., Pan, Y., Wang, Z., Wang, X., Liu, J. N., Wang, S., et al. (2022).)."Effects of nitrogen application in maize (*Zea mays* L.) on host selection behaviour of the bird cherry-oat aphid (*Rhopalosiphum padi* L.).". *Allelopathy J.* 55 (2), 1389–1391. doi: 10.26651/allelo.j/2022-56-1-1389

Zhe, R., Nicholas, C., Harris,, and Xuejun, (2015). Discovery of a family of desaturase-like enzymes for 1-alkene biosynthesis. *ACS Catalysis* 5 (12), 7091–7094. doi: 10.1021/acscatal.5b01842

Zhe, R., Xin, L., Xue, j., Zhu,, and Zhang, W. J. (2014). Microbial biosynthesis of medium-chain 1-alkenes by a nonheme iron oxidase. *Proc. Natl. Acad. Sci. United States America* 111 (51), 18237–18242. doi: 10.1073/pnas.1419701112

Zhu, P., Zheng, X., Xu, H., Johnson, A. C., and Lu, Z. (2020a). Nitrogen fertilization of rice plants improves ecological fitness of an entomophagous predator but dampens its impact on prey, the rice brown planthopper, *Nilaparvata lugens*. *J. Pest Sci.* 93, 747–755. doi: 10.1007/s10340-019-01174-w

Zhu, P., Zheng, X., Xu, H., Johnson, A. C., and Lu, Z. (2020b). Nitrogen fertilizer promotes the rice pest *Nilaparvata lugens via* impaired natural enemy, *Anagrus flaveolus*, performance. *J. Pest Sci.* 93, 757–766. doi: 10.1007/s10340-019-01177-7

frontiers | Frontiers in Plant Science

TYPE Original Research
PUBLISHED 08 March 2024
DOI 10.3389/fpls.2024.1341781

OPEN ACCESS

EDITED BY
Shengli Jing,
Xinyang Normal University, China

REVIEWED BY
Saumik Basu,
Washington State University, United States
Quentin Chesnais,
Institut National de recherche pour l'agriculture, l'alimentation et l'environnement (INRAE), France

*CORRESPONDENCE
Rajagopalbabu Srinivasan
babusri@uga.edu

RECEIVED 20 November 2023
ACCEPTED 19 February 2024
PUBLISHED 08 March 2024

CITATION
Pandey S, Catto M, Roberts P, Bag S, Jacobson AL and Srinivasan R (2024) Aphid gene expression following polerovirus acquisition is host species dependent. *Front. Plant Sci.* 15:1341781. doi: 10.3389/fpls.2024.1341781

Aphid gene expression following polerovirus acquisition is host species dependent

Sudeep Pandey[1], Michael Catto[2], Phillip Roberts[3], Sudeep Bag[4], Alana L. Jacobson[5] and Rajagopalbabu Srinivasan[1]*

[1]Department of Entomology, University of Georgia, Griffin, GA, United States, [2]Department of Entomology, University of Georgia, Athens, GA, United States, [3]Department of Entomology, University of Georgia, Tifton, GA, United States, [4]Department of Plant Pathology, University of Georgia, Tifton, GA, United States, [5]Department of Entomology and Plant Pathology, Auburn University, Auburn, AL, United States

Upon acquisition of persistent circulative viruses such as poleroviruses, the virus particles transcytose through membrane barriers of aphids at the midgut and salivary glands via hemolymph. Such intricate interactions can influence aphid behavior and fitness and induce associated gene expression in viruliferous aphids. Differential gene expression can be evaluated by omics approaches such as transcriptomics. Previously conducted aphid transcriptome studies used only one host species as the source of virus inoculum. Viruses typically have alternate hosts. Hence, it is not clear how alternate hosts infected with the same virus isolate alter gene expression in viruliferous vectors. To address the question, this study conducted a transcriptome analysis of viruliferous aphids that acquired the virus from different host species. A polerovirus, cotton leafroll dwarf virus (CLRDV), which induced gene expression in the cotton aphid, *Aphis gossypii* Glover, was assessed using four alternate hosts, viz., cotton, hibiscus, okra, and prickly sida. Among a total of 2,942 differentially expressed genes (DEGs), 750, 310, 1,193, and 689 genes were identified in *A. gossypii* that acquired CLRDV from infected cotton, hibiscus, okra, and prickly sida, respectively, compared with non-viruliferous aphids that developed on non-infected hosts. A higher proportion of aphid genes were overexpressed than underexpressed following CLRDV acquisition from cotton, hibiscus, and prickly sida. In contrast, more aphid genes were underexpressed than overexpressed following CLRDV acquisition from okra plants. Only four common DEGs (*heat shock protein*, *juvenile hormone acid O-methyltransferase*, and two unannotated genes) were identified among viruliferous aphids from four alternate hosts. Gene ontology (GO) enrichment analysis and Kyoto Encyclopedia of Genes and Genomes (KEGG) annotations indicated that the acquisition of CLRDV induced DEGs in aphids associated with virus infection, signal transduction, immune systems, and fitness. However, these induced changes were not consistent across four alternate hosts. These data indicate that alternate hosts could differentially influence gene expression in aphids and presumably aphid behavior and fitness despite being infected with the same virus isolate.

KEYWORDS

***Aphis gossypii*, cotton leafroll dwarf virus, acquisition, alternate hosts, vector-virus interactions**

Introduction

Persistently transmitted single-stranded RNA phytoviruses such as poleroviruses are phloem-limited, and phloem-feeding and colonizing insects such as aphids efficiently transmit such viruses (Harris and Maramorosch, 1977; Ng and Perry, 2004). The vectors and their viruses interact intricately in these pathosystems. Ingestion of viruses occurs when aphids feed on virus-infected plants; once in the midgut, these viruses traverse into the hemocoel and then into the accessory salivary glands through transcytosis (Gray and Gildow, 2003). Also, such viruses are exclusively transmitted by specific vector species, and the specificity seems to be associated with unique receptors in vectors that mediate transcytosis (Ng and Falk, 2006; Hogenhout et al., 2008; Whitfield et al., 2015).

Persistent virus infections are known to modulate the host plant physiology and in turn alter the phenotypical traits such as leaf hue, plant growth, availability of nutrients including free amino acids and soluble carbohydrates, and profiles of volatile organic compounds (VOCs) and metabolites (Eigenbrode et al., 2002; Mauck et al., 2010). These alterations can influence vector behavior (attraction or repulsion) and performance (feeding and colonization) (Fereres and Moreno, 2009; Mauck, 2016). The host–aphid–polerovirus interactions are complex, and previous studies have reported favorable, unfavorable, and/or neutral outcomes on vector fitness (Jiménez-Martínez et al., 2004; Rajabaskar et al., 2013; Srinivasan et al., 2013; Lightle and Lee, 2014; dos Santos et al., 2016; Ghosh et al., 2016; Claudel et al., 2018; Chesnais et al., 2020, 2022; Fingu-Mabola et al., 2020; Bertasello et al., 2021; Fingu-Mabola and Francis, 2021; Jayasinghe et al., 2022). However, the majority of interactions seem to influence vector fitness and behavior positively to enhance virus transmission (Hogenhout et al., 2008).

The magnitude of the effects of virus acquisition could largely depend on virus species, vector species, host species, and their interactions. For example, the green peach aphid (*Myzus persicae* Sulzer) preferred and survived longer on potato leafroll virus (PLRV)-infected plants compared with non-infected plants (Eigenbrode et al., 2002; Srinivasan et al., 2006, 2008). On the contrary, viruliferous bird cherry-oat aphid (*Rhopalosiphum padi* L.) preferred non-infected or sham-inoculated plants compared with barley yellow dwarf virus (BYDV)-infected plants (Ingwell et al., 2012). Also, BYDV infection reduced the population growth of cereal aphids (*Sitobion avenae* F.) compared with non-infected plants (Fiebig et al., 2004). This shift or alteration in vector–virus interactions can be better understood by exploring their genetic and molecular bases (Brault et al., 2010; Li et al., 2019, 2020; Patton et al., 2021; Catto et al., 2022; Marmonier et al., 2022). For example, the underexpression of genes associated with immunity, hormone biosynthesis, and proteolytic pathways has been reported from transcriptome analysis in aphids (*S. avenae*, *Schizaphis graminum* Rondani, and *R. padi*) upon BYDV acquisition (Li et al., 2019, 2020). Similarly, the genes related to receptor activities and/or vesicular transport in *M. persicae* were underexpressed upon acquiring the turnip yellows virus (TuYV). However, the differentially expressed genes (DEGs) identified varied when the vector acquired the virus from an artificial medium compared with the virus-infected plant (Marmonier et al., 2022). Previous transcriptome studies have predominantly used only one host species as a source of virus acquisition. Only one study has been conducted to understand the discrepancies that may occur in vector fitness upon acquiring the same plant virus from different host species (Chesnais et al., 2022). Nonetheless, there remains a knowledge gap in understanding the impact of alternate hosts on virus–vector interactions as well as their fidelity across such hosts.

This study attempted to answer the above-stated question using another persistently transmitted polerovirus–aphid pathosystem. Cotton leafroll dwarf virus (CLRDV) is a phloem-limited, positive-sense, single-stranded RNA virus in the genus *Polerovirus* and belongs to the family *Solemoviridae* (Sõmera et al., 2021). The CLRDV genome is 5.8 kb long with seven open reading frames (ORFs) grouped into two blocks and separated by a non-coding region. The symptoms of CLRDV infection were first observed in cotton in the United States in Alabama in 2017, but the virus was identified in 2019 (Avelar et al., 2019). Subsequently, the virus has been reported in several cotton-producing states including Georgia (Aboughanem-Sabanadzovic et al., 2019; Tabassum et al., 2019; Alabi et al., 2020; Ali and Mokhtari, 2020; Ali et al., 2020; Faske et al., 2020; Iriarte et al., 2020; Price et al., 2020; Thiessen et al., 2020; Wang et al., 2020b). The CLRDV-infection symptoms include stunting; leaf rolling; vein yellowing; dark-green leaves; reddening of leaves, petioles, and stems; leaf puckering, crinkling, and deformation of leaf lamina; wilting; downward leaf drooping with V-shaped lamina folding; and small bolls (Cascardo et al., 2015; Silva et al., 2015; Brown et al., 2019; Sedhain et al., 2021; Pandey et al., 2022). Often, CLRDV also was detected in asymptomatic plants via reverse transcription–PCR (Bag et al., 2021). Further, CLRDV was detected in alternate hosts in the landscape in Georgia (Sedhain et al., 2021; Edula et al., 2023).

The cotton/melon aphid (*Aphis gossypii* Glover) is the only known vector of CLRDV in the United States, and it transmits the virus in a persistent and non-propagative manner (Michelotto and Busoli, 2007; Heilsnis et al., 2022, 2023). In a previous study, the aphid-mediated inoculation of CLRDV led to successful infection of hibiscus (*Hibiscus acetosella* Welw. Ex Hiern.), okra (*Abelmoschus esculentus* L.), prickly sida (*Sida spinosa* L.), Palmer amaranth (*Amaranthus palmeri* S. Wats.), and *Nicotiana benthamiana* Domin plants. Nevertheless, no CLRDV symptoms were observed in any of those host plants. Aphids were able to acquire the virus exclusively from CLRDV-infected hibiscus, okra, and prickly sida plants and subsequently inoculate the virus back to cotton plants. Although cotton, hibiscus, okra, and prickly sida belong to Malvaceae, there was a notable discrepancy in the amount of virus acquired by *A. gossypii* from those CLRDV-infected host species (Pandey et al., 2022). Also, previous studies have reported that the total fecundity and intrinsic rate of increase of *A. gossypii* varied among alternate hosts (Barman et al., 2018; Pandey et al., 2022).

This study explored how the acquisition of CLRDV from different host species affects the gene expression associated with behavior and/or fitness in its vector. Specifically, cotton, hibiscus, okra, and prickly sida were used as host plants to assess differential gene expression in *A. gossypii* post-acquisition of CLRDV by

transcriptome analyses. This study hypothesized that aphid genes will be differentially expressed when they acquire the same virus isolate from different host species, and consequently aphid behavior and fitness could be differentially affected. The cDNA libraries were prepared for viruliferous and non-viruliferous *A. gossypii* after a 72-h acquisition access period (AAP) on CLRDV-infected or non-infected host plants. The specific objectives of this study were to i) assess the differences in gene expression in *A. gossypii* upon virus acquisition from four CLRDV-infected hosts and ii) locate putative hub genes and co-expressed genes (modules) in *A. gossypii* post-acquisition of CLRDV from specific hosts using weighted gene correlation network analysis (WGCNA).

Materials and methods

Plants and insects

The CLRDV host species identified in a previous study, viz., cotton, *Gossypium hirsutum* L. cv. PHY 339 WRF (Corteva, Indianapolis, IN, USA), hibiscus, *H. acetosella* Welw. Ex Hiern. (Johnny's Selected Seeds, Winslow, ME, USA), okra, *A. esculentus* L. cv. 'Clemson spineless 80' (Clemson University, Clemson, SC, USA), and prickly sida, *S. spinosa* L. (Azlin Seed Service, Leland, MS, USA) were used as inoculum sources in this study (Pandey et al., 2022). Two to four seeds of each plant were sown per pot in Sunshine propagation mix (SunGro Horticulture Industries, Bellevue, WA, USA) in 10-cm-diameter plastic pots (depth 8 cm). The pots were kept in insect-proof cages of size 47.5 (l) × 47.5 (w) × 93 (h) cm^3 (Megaview Science Co., Taichung, Taiwan) in the greenhouse. The greenhouse was maintained at 25°C, 60% relative humidity, and 14-h L:10-h D photoperiod. The seedlings were thinned post-germination, and only one plant per pot was used. Water-soluble Miracle-Gro (Scotts Miracle-Gro Products, Inc., Marysville, OH, USA) at 0.5 g/L was used for weekly fertilization. The aphids were originally collected from cotton fields in 2017 at Tifton, Georgia, and thereafter, the population was maintained in the greenhouse at the University of Georgia, Griffin Campus, under the same conditions indicated above.

Maintenance of CLRDV-infected plants

Cotton plants infected with CLRDV were originally collected from cotton fields in September 2020 at the University of Georgia, Tifton Campus, GA, USA, and maintained in the greenhouse at the above-stated conditions. Aphid-mediated CLRDV transmission to cotton seedlings was undertaken to maintain the virus inoculum source. CLRDV-infected cotton, hibiscus, okra, and prickly sida plants were obtained following the protocols described in an earlier study (Pandey et al., 2022). *A. gossypii* adults were provided with a 72-h AAP on CLRDV-infected cotton plants followed by a 72-h inoculation access period (IAP) on the undersurface of leaves of young seedlings at the two-true leaf stage. The CLRDV-inoculated plants were placed in aphid-proof cages under the greenhouse conditions described above. Clip cages and aphids were removed 3 days post-inoculation. The infection status of the plants was evaluated at approximately 3 weeks post-inoculation by reverse transcription–PCR as described earlier (Pandey et al., 2022).

Viruliferous and non-viruliferous aphids for RNA sequencing

The non-viruliferous *A. gossypii* colonies were maintained on all four host species, i.e., non-infected cotton, hibiscus, okra, and prickly sida plants, in separate insect-proof cages. Approximately 1,000 *A. gossypii* were collected from each colony and then introduced to non-infected or CLRDV-infected cotton, hibiscus, okra, and prickly sida plants. The aphids were allowed to feed for an AAP of 72 h. After 72 h of AAP on non-infected or CLRDV-infected plants, approximately 500 adults per treatment were collected, and total RNA was extracted from the collected aphid samples (Figure 1). Each treatment was biologically replicated four times. Another set of aphids (three pools of 10 aphids/per treatment) was used to confirm the acquisition of CLRDV in different treatments. The results indicated that 100% of pools of aphids collected from CLRDV-infected plants were positive for CLRDV, whereas aphids feeding on non-infected plants tested negative for CLRDV.

Total RNA extraction and sequencing

The total RNA was extracted from the collected aphid samples using Qiagen RNA mini-Kit (Valencia, CA, USA) as per the manufacturer's instructions. For each sample, 40 µL of total RNA was shipped to Novogene Corporation Inc. (Sacramento, CA, USA), and the rest of the total RNA was stored at −80°C for validation. Quality control (QC) of RNA samples was accomplished by preliminary quantitation using a NanoDrop and testing for RNA degradation and contamination via agarose gel electrophoresis. Then, RNA integrity (RIN) was assessed using Agilent 2100. Three samples failed the QC test. The samples that passed QC (RIN value >6.8 and concentration of >20 ng/µL) were used for cDNA library preparation. The library preparation began with enriching mRNA using oligo(dT) beads and removing rRNA using the Ribo-Zero kit. Then, the mRNA fragmentation was followed by first- and second-strand cDNA synthesis. Subsequently, adaptor ligation and PCR enrichment were performed for cDNA library generation. Finally, the library quality was assessed using a Qubit 2.0. NovaSeq 6000 Sequencing System (Illumina, San Diego, CA, USA) with the NovaSeq paired-end 150 sequencing platform was used for sequencing the libraries that passed QC.

Transcriptome assembly and analysis

FastQC v0.11.9 and multiQC v1.11 were used to assess the quality of raw reads before and after trimming (Andrews and FastQC, 2010; Ewels et al., 2016). The adapters were removed by

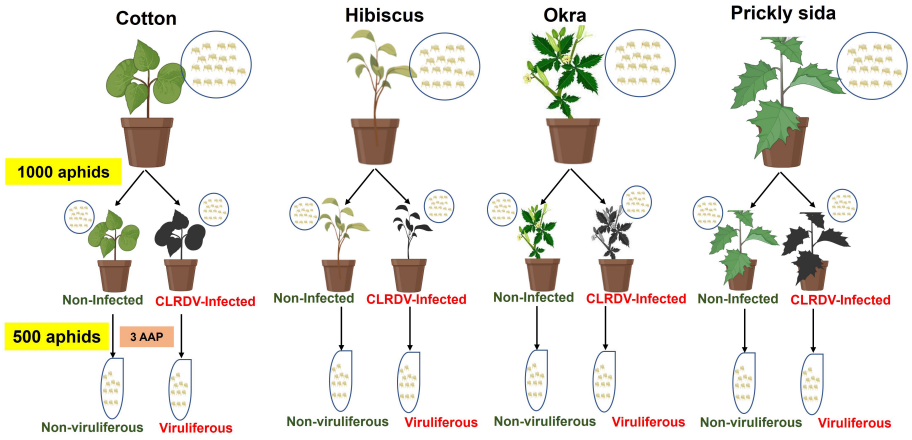

FIGURE 1
Schematic diagram of experimental setup for generating viruliferous and non-viruliferous aphid samples from CLRDV-infected and non-infected cotton, hibiscus, okra, and prickly sida plants. The aphid colonies were maintained on each plant species separately, and 1,000 adult aphids from each colony were collected and attached to the respective CLRDV-infected and non-infected plants. After 3 days of acquisition access period (AAP), 500 aphids from each treatment were collected for total RNA extraction. The experiment was repeated four times to obtain eight aphid samples from each host plant. CLRDV, cotton leafroll dwarf virus.

using Trimmomatic v0.39 with the default setting (Bolger et al., 2014). Bowtie2 v2.4.1 was used with default mapping parameters to map the trimmed reads with the reference *A. gossypii* transcriptome (Langmead and Salzberg, 2012; Quan et al., 2019). RSEM v1.3.3 was used to obtain gene count estimates of the mapped reads (Li and Dewey, 2011). Fragments per kilobase million (FPKM) were determined using a custom R script with the following R libraries: dplyr, tidyverse, and stringr on R v4.1.0 (R Core Team, 2021). DESeq2 compared the gene counts from non-viruliferous aphids with viruliferous aphids to identify DEGs. Genes that had log2fold changes $|LFC| \geq 1$ and a false discovery rate (FDR) ≤ 0.05 were identified as DEGs (Love et al., 2014). The DEGs were annotated and assigned to gene ontology (GO) classes (up to level 3) and Kyoto Encyclopedia of Genes and Genomes (KEGG) pathways (Kanehisa and Goto, 2000) using the annotated *A. gossypii* genome (Quan et al., 2019). TopGO (https://www.bioconductor.org/packages/release/bioc/html/topGO.html) and visualize Gene Ontology (REVIGO) web tool were used for the processing and visualization of the GO terms (Supek et al., 2011).

The WGCNA software v1.70-3 was run to create co-expression modules and identify sets of DEGs expressed in a similar pattern in *A. gossypii* that acquired the CLRDV from alternate hosts using the R software v4.1.0 (Langfelder and Horvath, 2008; R Core Team, 2021). The gradient-independent method with the scale-independent condition of the signed R2 set to 0.90 was used to test the soft-thresholding power modules (1 to 40). The topological overlap matrix (TOM) was constructed using the interaction relationships across the co-expression modules by using correlation expression values. A dendrogram with the parameters mergeCutHeight = 0.15 and detectCutHeight = 0.995 was set to represent the TOM. Each module was represented using randomly assigned colors. The module eigengene was calculated from the first principal component of each module. The labeledHeatmap package in WGCNA software was used to show the topological overlap of co-expression modules based on eigengenes. The network analysis of the top 30 genes from the *A. gossypii* turquoise was visualized using Cytoscape v3.9.0 (Shannon et al., 2003). Also, the hub genes in the most correlated clusters (magenta, pink, brown, and gray) observed in viruliferous *A. gossypii* that acquired the virus from each host species (cotton, hibiscus, okra, and prickly sida) were visualized using Cytoscape v3.9.0.

Validation of RNA-sequencing data by RT-qPCR

To validate transcriptomic data, 10 DEGs of *A. gossypii* were randomly selected for each host species (n = 40). The expression levels of the DEGs were compared between viruliferous and non-viruliferous *A. gossypii* that acquired CLRDV from different hosts (cotton, hibiscus, okra, and prickly sida) by RT–quantitative polymerase chain reaction (qPCR). Primer pairs designed for each DEG using Primer3web version 4.1.0 are listed in Supplementary Table S1. The GoScript™ Reverse Transcription System (Promega, Madison, WI, USA) was used to reverse-transcribe the total RNA for each sample according to the manufacturer's instructions. Then, the cDNA was diluted 20-fold for qPCR. The 2xGoTaq® qPCR Master Mix (7.5 µL) (Promega, Madison, WI, USA), primers (0.3 µM), 1 µL of cDNA, and nuclease-free distilled water for a final volume of 15 µL were mixed. The QuantStudio™ 3 Real-Time PCR System (Applied Biosystems by Thermo Fisher Scientific, Waltham, MA, USA) was used for qPCR. The following qPCR conditions were used: an initial denaturation step at 95°C for 3 minutes followed by 40 cycles at 95°C for 15 s and 60°C for 1 minute. Three technical replicates for each sample were used, and the melting curve analysis was conducted to evaluate the specificity of the fluorescence signal. The expression level of each gene was normalized to the expression level of

elongation factor 1α (EF1α)—an *A. gossypii* reference gene. The $2^{-\Delta\Delta Ct}$ method was used to calculate the relative expression of DEGs (Ma et al., 2016).

Results

Summary of RNA sequencing

Three to four biological replicates were included per treatment on each host, resulting in seven cDNA libraries constructed for *A. gossypii* on each host (cotton, hibiscus, and prickly sida plants), whereas eight libraries were constructed for *A. gossypii* on okra. Hence, a total of 29 libraries were constructed. Raw read pairs for the generated libraries ranged from nearly 19 to 34 million. After trimming and removing the reads that aligned with the ribosomal RNA and the mitochondrial genome, 19 to 33 million reads were retained (Table 1). *A. gossypii* cleaned read pairs from different libraries (63 to 82%) were mapped to the *A. gossypii* transcriptome (Table 1).

The reads obtained from viruliferous and non-viruliferous *A. gossypii* samples from different host species were normalized and

TABLE 1 Summary of RNA-sequencing datasets generated from *Aphis gossypii* adults provided with feeding access for 72 h on cotton leafroll dwarf virus-infected or non-infected cotton, hibiscus, okra, and prickly sida plants.

Host plant	Aphid sample description	Library ID	No. of raw read pairs	No. final cleaned read pairs	No. mapped	% Mapped
Cotton	Viruliferous rep 1	VCA3	21,945,977	21,713,280	15,207,354	71.32
	Viruliferous rep 2	VCA31	22,410,682	22,186,141	15,823,387	72.96
	Viruliferous rep 3	VCA4	23,484,566	21,083,698	16,966,911	82.88
	Non-viruliferous 1	NCA1	21,411,742	21,173,955	14,922,104	70.47
	Non-viruliferous 2	NCA21	20,444,716	20,241,718	14,728,795	72.76
	Non-viruliferous 3	NCA31	25,859,605	25,586,107	18,430,062	72.03
	Non-viruliferous 4	NCA4	21,551,498	21,321,979	15,479,092	72.60
Hibiscus	Viruliferous rep 1	VHA2	21,750,272	21,535,344	14,776,609	68.62
	Viruliferous rep 2	VHA31	21,073,589	20,863,690	15,371,030	73.67
	Viruliferous rep 3	VHA41	22,643,895	22,416,676	16,318,387	72.80
	Non-viruliferous 1	NHA1	19,760,059	19,579,065	14,062,884	71.83
	Non-viruliferous 2	NHA2	22,087,712	21,852,903	15,802,753	72.31
	Non-viruliferous 3	NHA31	22,047,340	21,835,392	15,627,346	71.57
	Non-viruliferous 4	NHA41	29,645,536	29,332,261	20,541,833	70.03
Okra	Viruliferous rep 1	VOA5	29,963,400	29,514,383	20,328,303	68.88
	Viruliferous rep 2	VOA6	26,044,703	25,668,773	18,363,422	71.54
	Viruliferous rep 3	VOA7	31,133,707	30,628,153	20,935,316	68.35
	Viruliferous rep 4	VOA8	28,946,216	28,511,952	20,019,531	70.21
	Non-viruliferous 1	NOA11	21,383,934	21,171,951	14,256,767	67.34
	Non-viruliferous 2	NOA2	21,834,007	21,609,657	15,320,142	70.89
	Non-viruliferous 3	NOA31	20,943,829	20,717,474	14,232,750	68.70
	Non-viruliferous 4	NOA4	22,327,129	22,097,040	15,290,654	69.20
Prickly sida	Viruliferous rep 1	VTA11	30,962,491	30,453,700	19,301,698	63.38
	Viruliferous rep 2	VTA2	32,573,331	32,067,776	21,748,225	67.82
	Viruliferous rep 3	VTA3	26,690,046	26,330,120	17,217,266	65.39
	Viruliferous rep 4	VTA41	31,546,741	31,118,783	20,631,968	66.30
	Non-viruliferous 1	NTA11	26,883,664	26,525,060	18,276,409	68.90
	Non-viruliferous 2	NTA21	34,473,691	33,950,452	22,458,131	66.15
	Non-viruliferous 3	NTA31	27,134,539	26,748,727	18,013,818	67.34

clustered using FPKM and principal component analysis (PCA) for comparison. The PCA clustered viruliferous *A. gossypii* samples separately from the non-viruliferous samples for all four host species (Supplementary Figures S1A–D).

Overview of DEGs

Out of 14,134 annotated genes, a total of 750 (622 overexpressed and 128 underexpressed), 310 (168 overexpressed and 142 underexpressed), 1,193 (548 overexpressed and 645 underexpressed), and 689 genes (432 overexpressed and 257 underexpressed) were differentially expressed in viruliferous aphids that acquired CLRDV from infected cotton, hibiscus, okra, and prickly sida plants, respectively (Figure 2; Supplementary Figure S2).

RT-qPCR with 10 randomly selected DEGs per *A. gossypii* host (n = 40) was performed to validate RNA sequencing-based differential gene expression results (Supplementary Table S1). The expression trends of the randomly selected *A. gossypii* DEGs from

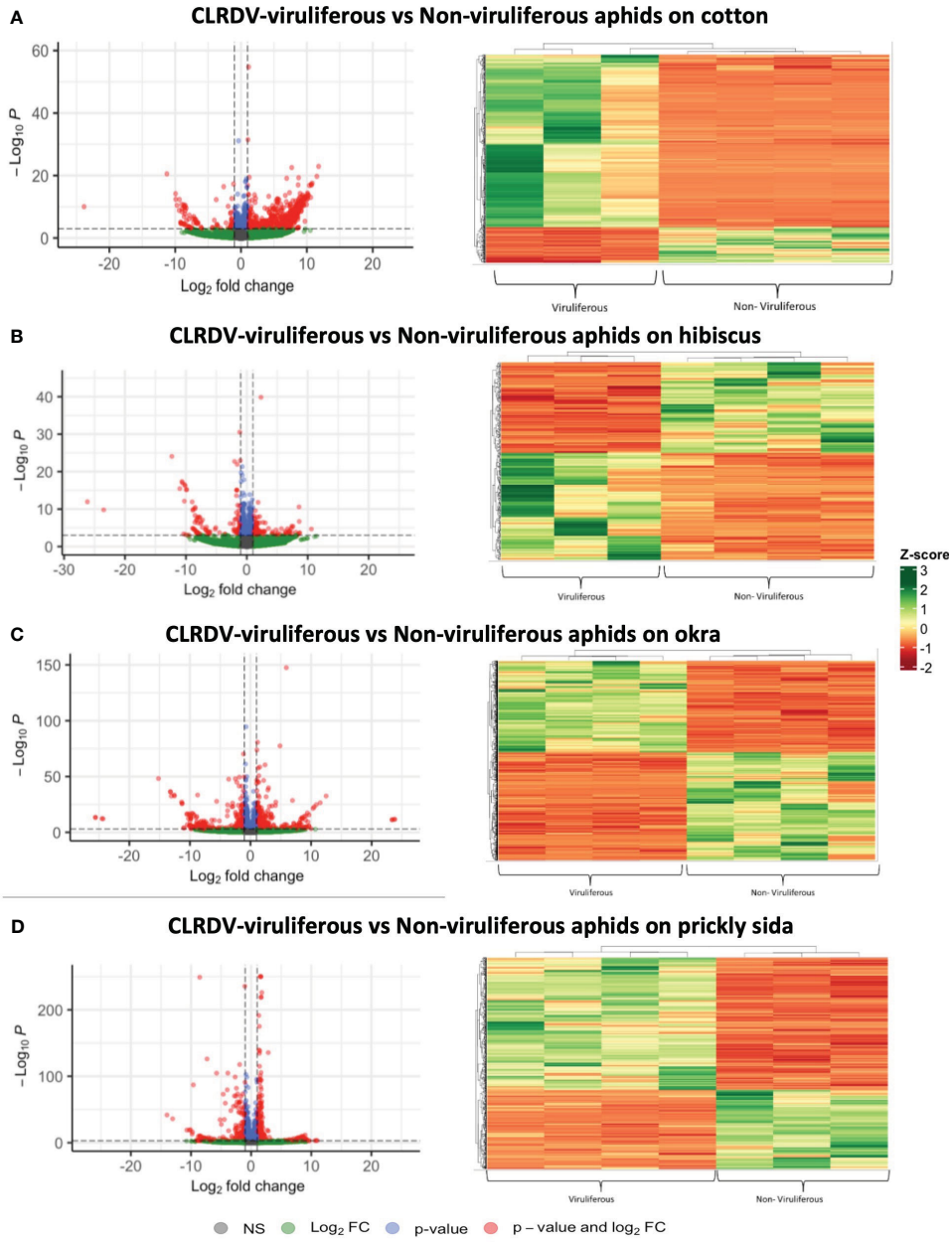

FIGURE 2
Left: Volcano plots detailing the differential expression profiles of CLRDV-viruliferous versus non-viruliferous *Aphis gossypii*. Genes with an |LFC| ≥ 1 and a false discovery rate (FDR) <0.05 are highlighted in red and were differentially expressed. Right: Hierarchical clustering analysis of normalized count data z-scores exhibited by differentially expressed genes: **(A)** 750 DEGs in viruliferous *A. gossypii* adults that acquired CLRDV from infected cotton plants, **(B)** 310 DEGs in viruliferous *A. gossypii* adults that acquired CLRDV from infected hibiscus plants, **(C)** 1,193 DEGs in viruliferous *A. gossypii* adults that acquired CLRDV from infected okra plants, and **(D)** 689 DEGs in viruliferous *A. gossypii* adults that acquired CLRDV from infected prickly sida plants. CLRDV, cotton leafroll dwarf virus; DEGs, differentially expressed genes.

RNA sequencing and RT-qPCR were highly consistent for all four host species (Supplementary Figures S3A–D).

Common DEGs among viruliferous *A. gossypii* adults feeding on different host species

Of the 2,942 DEGs in aphids that acquired CLRDV from different host species, only four genes were found to be differentially expressed in common (Figure 3). Two common DEGs were annotated as uncategorized proteins, whereas the other two were functionally annotated. Both the unknown DEGs were overexpressed in *A. gossypii* on all four hosts, whereas differences in the direction of expression were observed for the annotated common DEGs. The annotated common DEGs were *juvenile hormone acid O-methyltransferase* and *heat shock protein*. They were overexpressed in *A. gossypii* that acquired the virus from CLRDV-infected cotton and okra, whereas they were underexpressed in *A. gossypii* that acquired CLRDV from infected hibiscus and prickly sida (Table 2).

Functional annotation of DEGs

Only 320 of the 750 DEGs in *A. gossypii* that acquired CLRDV from infected cotton were assigned functional groups under three classification systems: biological process (313 genes), molecular function (267 genes), and cellular component (287 genes). Fifty-three GO terms were assigned under the biological process category, of which only two terms (microtubule-based process and ATP metabolic process) were significant (Figure 4A; Supplementary Table S2). Thirty-five GO terms were assigned under the molecular function category, only one (a structural constituent of the cytoskeleton) of which was significant (Figure 4B; Supplementary Table S2). In the cellular component category, 30 GO terms were identified, and only one (cAMP-dependent protein kinase complex) was significant (Figure 4C; Supplementary Table S2). Similarly, the DEGs identified in aphids that acquired CLRDV from hibiscus, okra, and prickly sida were assigned functional groups under three classification systems (Supplementary Figures S4–S6; Supplementary Tables S3-S5). The categorization of these genes was used to identify the DEGs associated with virus–vector interactions.

Co-expression networks from *A. gossypii* on CLRDV hosts

The co-expression of genes from *A. gossypii* adults that acquired CLRDV from cotton, hibiscus, okra, and prickly sida was evaluated. WGCNA, which clusters genes into modules based on weighted gene–gene interactions, was used to evaluate co-expression. For *A. gossypii*, 13 modules with 19 to 180 genes in each module were identified (Figure 5A; Supplementary Table S6), and Pearson's correlation coefficient analysis showed the connections between the four CLRDV hosts. The heatmap visualized overall patterns of co-expression of (viruliferous/non-viruliferous) aphid–host relationships (Figure 5B). *A. gossypii* interactions for the largest module, MEturquoise, were checked for top interacting genes among the 30 identified genes (Figure 5C). The top four most highly connected genes were XM_027993669.1 (*trichohyalin*-like), XM_027997289.1 (uncharacterized protein), XM_027997209.1 (*glucose dehydrogenase* [*FAD, quinone*]-like), and XM_027983368.1 (*neuroendocrine convertase 1*-like) with interconnectivity scores of 58.99, 57.81, 53.87, and 52.58, respectively (Supplementary Table S6).

Hub genes from candidate modules

Four modules (magenta, pink, brown, and gray) were highly correlated with viruliferous *A. gossypii* that acquired CLRDV from infected cotton, hibiscus, okra, and prickly sida plants, respectively.

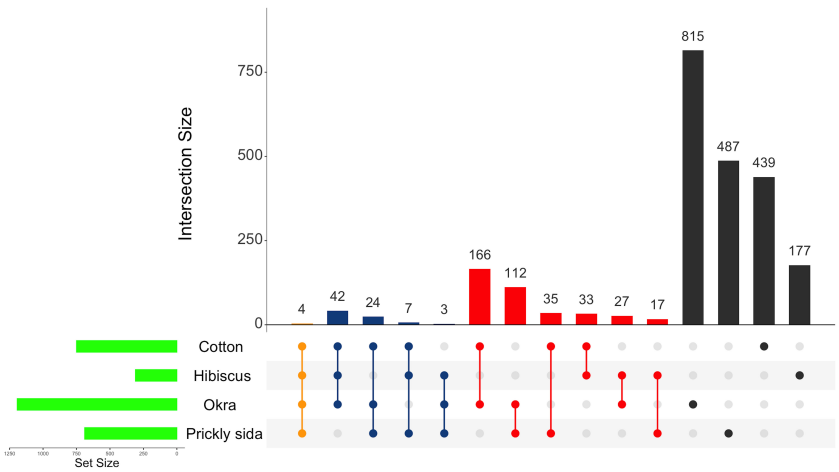

FIGURE 3
Normalized Venn diagram showing unique and common DEGs in viruliferous *Aphis gossypii* adults that acquired CLRDV from infected cotton, hibiscus, okra, and prickly sida plants. DEGs, differentially expressed genes; CLRDV, cotton leafroll dwarf virus.

TABLE 2 List of common DEGs in *Aphis gossypii* adults that acquired CLRDV from the infected cotton, hibiscus, okra, and prickly sida plants.

Common DEGs	Annotation	LFC in *A. gossypii* genes acquiring the virus from			
		Cotton	Hibiscus	Okra	Prickly sida
XM_027995716.1	Uncharacterized protein LOC114130688	1.63	1.72	2.51	2.85
XM_027991388.1	Uncharacterized protein LOC114127180	2.15	1.22	1.14	1.78
XM_027987236.1	Juvenile hormone acid *O*-methyltransferase	2.35	−1.79	2.15	−3.25
XM_027981156.1	Heat shock protein 70	2.04	−1.02	4.18	−2.20

The negative sign indicates the underexpressed DEGs, whereas no negative sign indicates the overexpressed DEGs.
DEGs, differentially expressed genes; CLRDV, cotton leafroll dwarf virus.

The magenta module associated with viruliferous *A. gossypii* that acquired CLRDV from infected cotton plants contained 34 genes. Similarly, pink, brown, and gray modules associated with *A. gossypii* that acquired CLRDV from infected hibiscus, okra, and prickly sida plants included 40, 130, and 129 genes, respectively. The maximum connectivity in magenta, pink, and brown modules were 8.9, 8.8, and 20, respectively. However, the connectivity in the gray module was less than one. Hence, only magenta, pink, and brown modules were considered to identify candidate genes related to virus interactions and transmission (Supplementary Table S6).

Most genes in the magenta module were overexpressed only in viruliferous *A. gossypii* that acquired CLRDV from infected cotton plants, and 10 genes were identified as hub genes based on their high connectivity values (Figure 6A). Some of the hub genes were predicted to encode *tubulin-β* (XM_027988533.1 and XM_027985455.1), *tubulin-α* (XM_027988908.1), *GPI-anchored protein* (XM_027997066.1), *U1 small nuclear ribonucleoprotein* (XM_027985431.1), *mucin-7-like* (XM_027997067.1), and *dynein beta chain* (XM_027985730.1) (Supplementary Table S6). The *tubulin-α* and *tubulin-β* genes were associated with cellular responses following virus acquisition (Table 3).

Similarly, most genes in the pink module were underexpressed in viruliferous *A. gossypii* that acquired CLRDV from infected hibiscus plants, and 10 genes were identified as hub genes based on their high connectivity values (Figure 6B). Some of these hub genes were predicted to encode *proteasome subunit-β* (XM_027980885.1), *trehalose transporter Tret1* (XM_027996416.1), and *M-phase inducer phosphatase* (XM_027998546.1) (Supplementary Table S6).

Most genes in the brown module were underexpressed in viruliferous *A. gossypii* that acquired CLRDV from infected okra plants, and 10 genes were identified as hub genes based on their high connectivity values (Figure 6C). These hub genes were predicted to encode ubiquitin *carboxyl-terminal hydrolase 7* (XM_027983467.1), *dynein heavy chain* (XM_027987391.1), *serine/threonine-protein kinase WNK1* (XM_027980933.1), and *eukaryotic translation initiation factor 4 gamma* (XM_027992697.1) (Supplementary Table S6). The *serine/threonine-protein kinase* genes were associated with signal transduction following virus acquisition (Table 4).

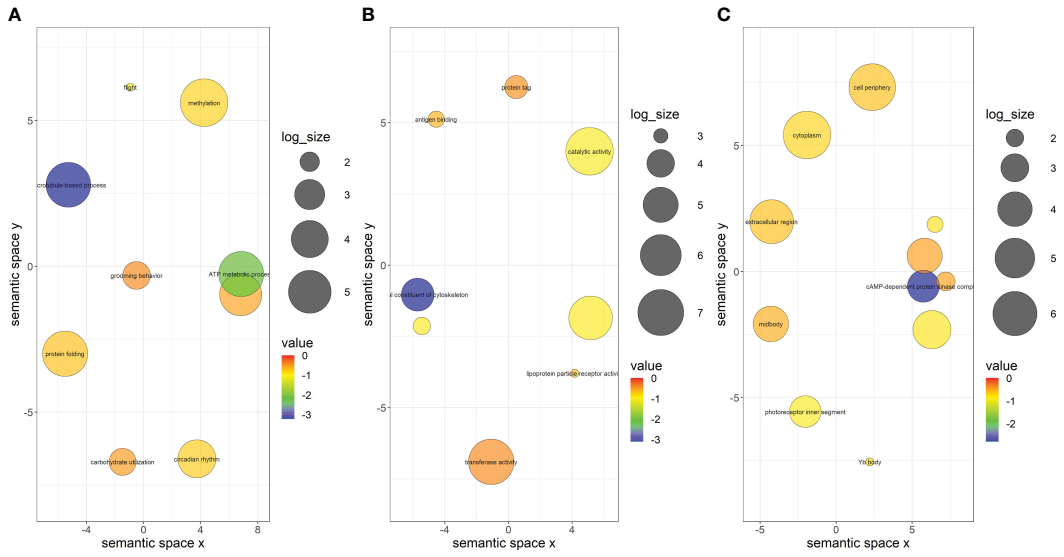

FIGURE 4
Scatterplots showing **(A)** biological process, **(B)** cellular component, and **(C)** molecular function gene ontology terms in viruliferous *Aphis gossypii* adults that acquired CLRDV from infected cotton plant. Cluster representatives in a two-dimensional space were derived by applying multidimensional scaling to a matrix of the semantic similarities of the gene ontology terms. The bubble color indicates the p-value, and the size indicates the frequency of the GO term in the underlying GOA database. CLRDV, cotton leafroll dwarf virus; GO, gene ontology; GOA, Gene Ontology Annotation.

10.3389/fpls.2024.1341781

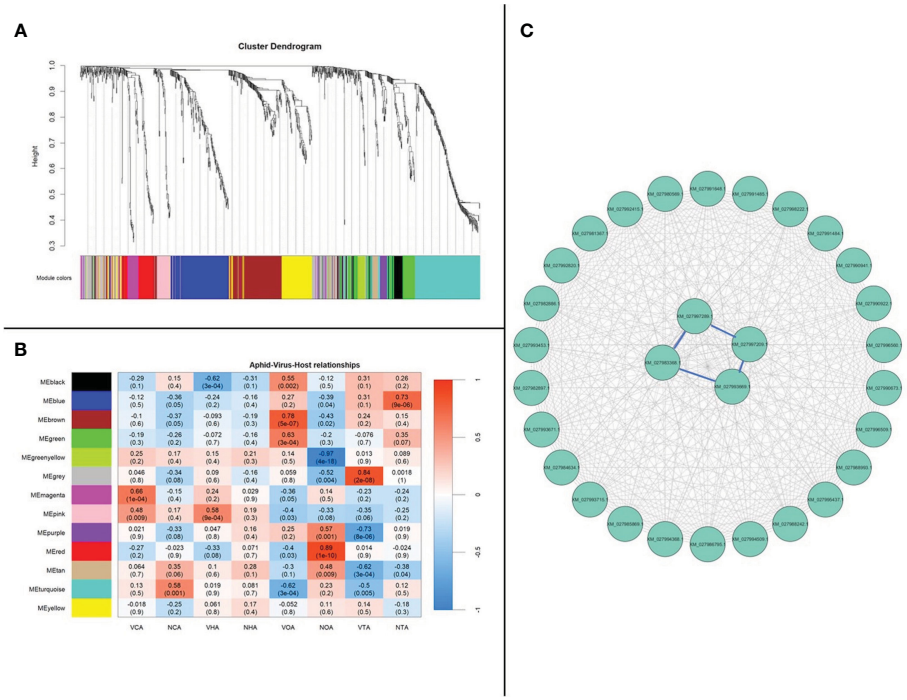

FIGURE 5
Aphis gossypii adults weighted gene co-expression network analysis. **(A)** Dendrogram clustering shows eight modules of co-expressed genes. A total of 981 genes are represented in this network, with 190 genes belonging to MEturquoise. **(B)** Heatmap showing the correlation of module eigengenes in relation to *A. gossypii* that acquired CLRDV from cotton, hibiscus, okra, and prickly sida. **(C)** Top 30 genes from MEturquoise with connectivity lines (blue) associated with the top 5% of the connected genes. NCA, non-viruliferous aphid from cotton; VCA, viruliferous aphid from cotton; NHA, non-viruliferous aphid from hibiscus; VHA, viruliferous aphid from hibiscus; NOA, non-viruliferous aphid from okra; VOA, viruliferous aphid from okra; NTA, non-viruliferous aphid from prickly sida; VTA, viruliferous aphid from prickly sida; CLRDV, cotton leafroll dwarf virus.

DEGs among *A. gossypii* adults associated with virus–vector interactions

Virus infection

In *A. gossypii* adults, DEGs associated with different viruses, including measles virus, coronavirus, human cytomegalovirus, human immunodeficiency virus 1, herpes simplex virus 1, human T-cell leukemia virus 1, human papillomavirus, hepatitis B and C, virus, influenza A virus, and Epstein–Barr virus were identified upon CLRDV acquisition from different host species. Eleven, four, 12, and seven genes associated with virus infection in *A. gossypii* that acquired CLRDV from infected cotton, hibiscus, okra, and prickly sida plants, respectively, were identified. The expression of these DEGs ranged from −26.18- to 7.60-fold (Table 5).

Signal transduction

Twelve DEGs were associated with 14 signal transduction pathways in *A. gossypii* that acquired CLRDV from infected cotton plants. Similarly, eight, 24, and 13 DEGs associated with different signal transduction pathways in *A. gossypii* that acquired

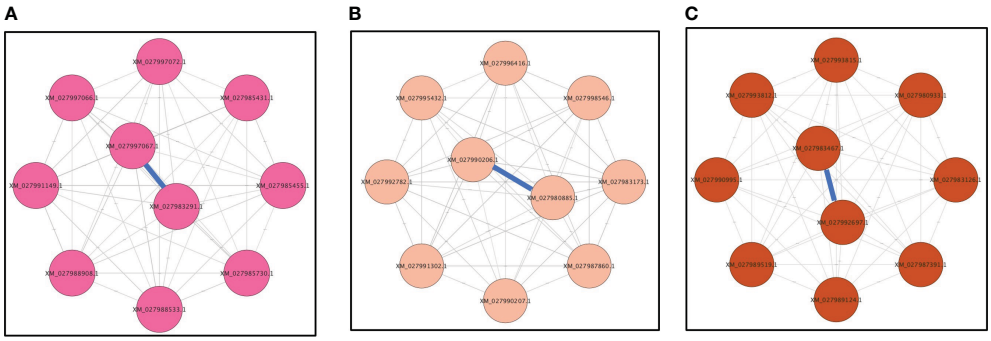

FIGURE 6
Top 10 genes from **(A)** magenta, **(B)** pink, and **(C)** brown modules with connectivity lines (blue) associated with viruliferous *Aphis gossypii* adults that acquired CLRDV from infected cotton, hibiscus, and okra plants, respectively. CLRDV, cotton leafroll dwarf virus.

10.3389/fpls.2024.1341781

TABLE 3 Differential expression of genes associated with cellular responses (endocytosis, apoptosis, lysosome, and phagosome) in viruliferous *Aphis gossypii* adults compared with non-viruliferous adults.

Gene ID	Function	LFC of *A. gossypii* genes acquiring the virus from			
		Cotton	Hibiscus	Okra	Prickly sida
XM_027981156.1	Heat shock protein 70	2.04	−1.02	4.18	−2.20
XM_027981452.1	Formylglycine-generating enzyme			1.10	
XM_027981875.1	Proton-coupled amino acid transporter-like protein CG1139			9.64	
XM_027981872.1	Proton-coupled amino acid transporter-like protein CG1139			−9.21	
XM_027982644.1	Dynamin-1-like protein	6.88			
XM_027985455.1	Tubulin beta chain	5.48		−10.53	
XM_027985527.1	GSK3B-interacting protein-			−6.51	
XM_027985860.1	Tubulin beta-1 chain	7.71			
XM_027986526.1	Proton-coupled amino acid transporter-like protein CG1139			−1.37	
XM_027987245.1	Sialin-like	8.62		−6.68	
XM_027988908.1	Tubulin alpha-4 chain	8.22		−11.06	
XM_027990131.1	Alpha-L-fucosidase		7.38		
XM_027992363.1	ADP-ribosylation factor-binding protein GGA1			−9.79	
XM_027992365.1	ADP-ribosylation factor-binding protein GGA1			1.34	
XM_027992845.1	Phosphatidylinositol 3,4,5-trisphosphate 3-phosphatase and dual-specificity protein phosphatase PTEN			1.17	
XM_027993821.1	Mitochondrial Rho GTPase			1.02	
XM_027994292.1	Lipopolysaccharide-induced tumor necrosis factor-alpha factor homolog				1.41
XM_027994521.1	Phosphatidylinositol 3-kinase regulatory subunit gamma			−8.20	
XM_027995767.1	Proton-coupled amino acid transporter-like protein CG1139			1.03	
XM_027996300.1	Protein transport protein Sec61 subunit gamma			−1.14	
XM_027996848.1	Actin-42A	1.68			−2.55
XM_027997003.1	Heat shock protein 68			4.87	−2.38
XM_027997432.1	Heat shock protein 70	2.04		4.13	
XM_027998191.1	Oxidation resistance protein 1				1.17
XM_027998701.1	Heat shock protein 70	1.90		3.48	−1.02

Genes with the same annotation name but different gene IDs are isoforms. The negative sign indicates the underexpressed DEGs, whereas no negative sign indicates the overexpressed DEGs. DEGs, differentially expressed genes.

CLRDV from infected hibiscus, okra, and prickly sida plants, respectively, were identified (Figure 7). The expression of these DEGs ranged from −8.08- to 8.40-fold (Table 4).

Signaling molecules and virus interaction

Using KEGG annotation, one putative receptor gene was identified in *A. gossypii* that acquired CLRDV from infected cotton (XM_027997734.1, *cardioacceleratory peptide receptor*) and one from prickly sida (XM_027980613.1, *neuropeptide SIFamide receptor*). Putative receptor genes were not identified in *A. gossypii* adults that acquired CLRDV from infected hibiscus and okra plants (Table 6).

Immune systems

A total of nine DEGs were annotated using KEGG analysis and associated with six immune system pathways in *A. gossypii* adults that acquired CLRDV from infected cotton plants. Similarly, 11 DEGs with 15 immune system pathways were identified for *A. gossypii* adults that acquired CLRDV from infected okra plants. Only two DEGs from two immune system pathways and seven DEGs from six immune system pathways were identified in *A. gossypii* that acquired CLRDV from infected hibiscus and prickly sida plants, respectively. The expression of these DEGs ranged from 9.99- to 7.28-fold (Table 6; Supplementary Table S7).

10.3389/fpls.2024.1341781

TABLE 4 Differential expression of genes associated with signal transduction in viruliferous *Aphis gossypii* adults compared with non-viruliferous adults.

Gene ID	Function	LFC of *A. gossypii* genes acquiring the virus from			
		Cotton	Hibiscus	Okra	Prickly sida
XM_027980601.1	Acyl-CoA Delta(11) desaturase			1.35	
XM_027981156.1	Heat shock protein 70	2.04	−1.02	4.18	−2.20
XM_027982467.1	Phosphatidylinositol 4-kinase type 2-beta			1.05	
XM_027982644.1	Dynamin-1-like protein	6.88			
XM_027983386.1	Sodium/potassium-transporting ATPase subunit alpha	−6.52			4.22
XM_027983455.1	ADP, ATP carrier protein 2				−2.55
XM_027983505.1	Probable phosphorylase b kinase regulatory subunit alpha		−8.08		
XM_027983941.1	Serine palmitoyltransferase 2				−1.16
XM_027985527.1	GSK3B-interacting protein			−6.51	
XM_027987983.1	Protein giant-lens-like			1.29	
XM_027988560.1	Guanine nucleotide-binding protein G(o) subunit alpha	−1.33		−1.99	
XM_027989043.1	Plasma membrane calcium-transporting ATPase 2			−1.04	
XM_027989047.1	Plasma membrane calcium-transporting ATPase 2			−1.19	
XM_027989048.1	Plasma membrane calcium-transporting ATPase 2				1.75
XM_027989866.1	Low-molecular-weight phosphotyrosine protein phosphatase		−6.99	−7.91	
XM_027990405.1	Embryonic polarity protein dorsal-like			1.47	
XM_027990451.1	cAMP-dependent protein kinase catalytic subunit beta	7.28			
XM_027990995.1	(11Z)-Hexadec-11-enoyl-CoA conjugase			−1.11	
XM_027991215.1	ATP-dependent 6-phosphofructokinase				−1.14
XM_027991280.1	Serine/threonine-protein kinase PLK1				8.40
XM_027991279.1	Serine/threonine-protein kinase PLK1				−7.89
XM_027991716.1	Multidrug resistance-associated protein 1			−1.37	
XM_027992190.1	Putative phosphatidate phosphatase			1.44	
XM_027992685.1	5′-AMP-activated protein kinase subunit gamma			1.26	
XM_027992684.1	5′-AMP-activated protein kinase subunit gamma			−4.51	
XM_027992845.1	Phosphatidylinositol 3,4,5-trisphosphate 3-phosphatase and dual-specificity protein phosphatase PTEN			1.17	
XM_027993702.1	Ras-related protein Rab-2A			3.08	
XM_027994156.1	cAMP-dependent protein kinase catalytic subunit beta	7.05			
XM_027994521.1	Phosphatidylinositol 3-kinase regulatory subunit gamma			−8.20	
XM_027994620.1	Tyrosine-protein kinase Btk29A				−1.15
XM_027994967.1	Profilin		−2.75		
XM_027995400.1	Glyceraldehyde-3-phosphate dehydrogenase	7.49	8.33	−8.16	
XM_027995849.1	Calcineurin subunit B type 2			−9.99	
XM_027995848.1	Calcineurin subunit B type 2			−1.16	
XM_027996465.1	Hexokinase type 2		1.32		

(Continued)

TABLE 4 Continued

Gene ID	Function	LFC of *A. gossypii* genes acquiring the virus from			
		Cotton	Hibiscus	Okra	Prickly sida
XM_027996848.1	Actin-42A	1.68			−2.55
XM_027996979.1	Interleukin-1 receptor-associated kinase 4-like	−4.39			
XM_027997003.1	Heat shock protein 68			4.87	−2.38
XM_027997371.1	Inositol-trisphosphate 3-kinase homolog				2.00
XM_027997432.1	Heat shock protein 70	2.04		4.13	
XM_027997466.1	Misshapen-like kinase 1		−1.29		
XM_027998688.1	ATP-dependent 6-phosphofructokinase	7.79	6.69		
XM_027998701.1	Heat shock protein 70	1.90		3.48	−1.02

Genes with the same annotation name but different gene IDs are isoforms. The negative sign indicates the underexpressed DEGs, whereas no negative sign indicates the overexpressed DEGs. DEGs, differentially expressed genes.

Cellular processes (apoptosis, lysosome, and phagosome)

A total of six, one, 15, and three DEGs were associated with cellular processes in *A. gossypii* that acquired CLRDV from infected cotton, hibiscus, okra, and prickly sida plants, respectively. The expression of these DEGs ranged from −11.06- to 9.64-fold (Table 3).

In the cellular process category, *heat shock proteins 70* and *68* were identified as genes playing a role in endocytosis. The heat shock proteins were overexpressed in *A. gossypii* acquired CLRDV from infected cotton and okra plants but underexpressed when acquired from infected hibiscus and prickly sida plants. Another gene related to endocytosis was underexpressed in *A. gossypii* that acquired CLRDV from infected okra plants (Table 7).

DEGs among *A. gossypii* adults associated with aphid fitness

Longevity

Based on KEGG pathway annotation, five DEGs were associated with two aging pathways in *A. gossypii* that acquired CLRDV from infected cotton plants (Table 8). Similarly, one, 11, and three DEGs associated with different aging pathways in *A. gossypii* that acquired CLRDV from infected hibiscus, okra, and prickly sida plants, respectively, were identified (Figure 7). The expression of these DEGs ranged from −8.49- to 7.28-fold (Table 8).

Reproduction

Using GO annotation, several genes associated with reproduction were identified in *A. gossypii* adults. The number of DEGs was the highest in *A. gossypii* that acquired CLRDV from infected okra, followed by cotton, prickly sida, and hibiscus plants (Figure 8). Unlike that in *A. gossypii* that acquired CLRDV from infected cotton, hibiscus, and prickly sida plants, the number of underexpressed genes in *A. gossypii* that acquired CLRDV from infected okra plants was higher than the overexpressed genes (Figure 8). One of the common genes identified in this GO annotation was *juvenile hormone acid O-methyltransferase* (Supplementary Table S8).

Discussion

In some rare instances, direct effects of persistent non-propagative viruses on their vectors' behavior and/or fitness have been documented (Bosque-Pérez and Eigenbrode, 2011; Ingwell et al., 2012; Marmonier et al., 2022). However, most effects of persistent and non-propagative phytoviruses on their vectors' behavior and fitness seem to be modulated by the host plants due to their altered phenotypic traits following virus infection (Eigenbrode et al., 2002; Srinivasan et al., 2006; Ngumbi et al., 2007; Hodge and Powell, 2008; Medina-Ortega et al., 2009; Werner et al., 2009; Bosque-Pérez and Eigenbrode, 2011; Legarrea et al., 2020; Fingu-Mabola and Francis, 2021; Safari Murhububa et al., 2021; Hu et al., 2022). The degree of the altered host phenotype would substantially depend upon the virus susceptibility status of the host. While this phenomenon has been researched in many persistent virus pathosystems involving hemipteran vectors, it has been extremely difficult to parse apart the host effect from the direct virus-induced impacts on vectors (Eigenbrode et al., 2002; Ingwell et al., 2012; Marmonier et al., 2022). In addition, generalizations seem to originate from host and virus-modulated effects on vectors based on individual hosts and viruses that at least possess a modest or often a promiscuous host range (Jiménez-Martínez et al., 2004; Lightle and Lee, 2014; dos Santos et al., 2016; Ghosh et al., 2016; Claudel et al., 2018; Chesnais et al., 2020; Moeini et al., 2020; Bertasello et al., 2021; Fingu-Mabola and Francis, 2021; Jayasinghe et al., 2022). This also applies to vectors and their host utilization capacities when they are generalists (Castle et al., 1998; Eigenbrode et al., 2002; Ngumbi et al., 2007; Rajabaskar et al., 2013; Ren et al., 2015; Liu et al., 2019). Host-modulated virus-induced effects on the

10.3389/fpls.2024.1341781

TABLE 5 Differential expression of genes associated with virus infection in viruliferous *Aphis gossypii* adults compared with non-viruliferous adults.

Gene ID	Function	LFC in *A. gossypii* genes acquiring the virus from			
		Cotton	Hibiscus	Okra	Prickly sida
XM_027981070.1	60S ribosomal protein L10		−26.18		
XM_027981156.1	Heat shock protein 70 A1-like	2.04	−1.02	4.18	−2.20
XM_027982887.1	Angiotensin-converting enzyme			−1.02	
XM_027983455.1	ADP, ATP carrier protein 2				−2.55
XM_027988560.1	Guanine nucleotide-binding protein G(o) subunit alpha	−1.33		−1.99	
XM_027990206.1	60S ribosomal protein L31	−11.27	−12.31	−15.19	
XM_027990451.1	cAMP-dependent protein kinase catalytic subunit beta	7.28			
XM_027990946.1	Uncharacterized protein LOC114126902				−1.02
XM_027991760.1	Ubiquitin-protein ligase E3A			1.59	
XM_027992845.1	Phosphatidylinositol 3,4,5-trisphosphate 3-phosphatase and dual-specificity protein phosphatase PTEN			1.17	
XM_027994156.1	cAMP-dependent protein kinase catalytic subunit beta	7.05			
XM_027994521.1	Phosphatidylinositol 3-kinase regulatory subunit gamma			−8.20	
XM_027994543.1	Zinc finger protein 436	7.60			
XM_027995723.1	40S ribosomal protein SA	−5.99			
XM_027995849.1	Calcineurin subunit B type 2			−9.99	
XM_027995848.1	Calcineurin subunit B type 2			−1.16	
XM_027996455.1	Serine/arginine-rich splicing factor 1A				−1.27
XM_027996848.1	Actin-42A	1.68			−2.55
XM_027996937.1	Oxysterol-binding protein-related protein 6		−4.49		
XM_027996979.1	Interleukin-1 receptor-associated kinase	−4.39			
XM_027997003.1	Heat shock protein 68			4.87	−2.38
XM_027997432.1	Heat shock protein 70	2.04		4.13	
XM_027998701.1	Heat shock protein 70	1.90		3.48	−1.02

Genes with the same annotation name but different gene IDs are isoforms. The negative sign indicates the underexpressed DEGs, whereas no negative sign indicates the overexpressed DEGs. DEGs, differentially expressed genes.

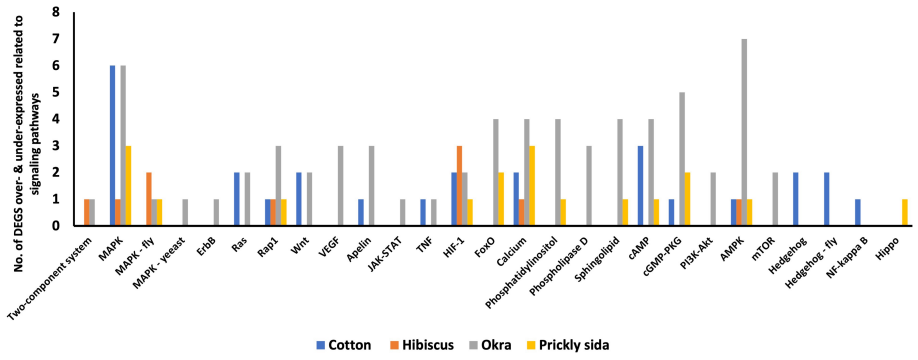

FIGURE 7
Number of differentially expressed genes (DEGs) related to different signaling pathways in viruliferous *Aphis gossypii* adults that acquired CLRDV from infected cotton, hibiscus, okra, and prickly sida plants. CLRDV, cotton leafroll dwarf virus.

10.3389/fpls.2024.1341781

TABLE 6 Differential expression of genes associated with immune systems in viruliferous *Aphis gossypii* adults compared with non-viruliferous adults.

Gene ID	Function	LFC of *A. gossypii* genes acquiring the virus from			
		Cotton	Hibiscus	Okra	Prickly sida
XM_027981156.1	Heat shock protein 70	2.04	−1.02	4.18	−2.20
XM_027982644.1	Dynamin-1-like protein	6.88			
XM_027983455.1	ADP, ATP carrier protein 2				−2.55
XM_027985527.1	GSK3B-interacting protein			−6.51	
XM_027988560.1	Nucleotide-binding protein G(o) subunit alpha	−1.33		−1.99	
XM_027990405.1	Embryonic polarity protein dorsal			1.47	
XM_027990451.1	cAMP-dependent protein kinase catalytic subunit beta	7.28			
XM_027992190.1	Putative phosphatidate phosphatase			1.44	
XM_027994156.1	cAMP-dependent protein kinase catalytic subunit beta	7.05			
XM_027994521.1	Phosphatidylinositol 3-kinase regulatory subunit gamma			−8.20	
XM_027994620.1	Tyrosine-protein kinase Btk29A				−1.15
XM_027994723.1	Histone H3.3		1.41		
XM_027995849.1	Calcineurin subunit B type 2			−9.99	
XM_027995848.1	Calcineurin subunit B type 2			−1.16	
XM_027996455.1	Serine/arginine-rich splicing factor 1A				−1.27
XM_027996848.1	Actin-42A	1.68			−2.55
XM_027996979.1	Interleukin-1 receptor-associated kinase 4-like	−4.39			
XM_027997003.1	Heat shock protein 68			4.87	−2.38
XM_027997432.1	Heat shock protein 70	2.04		4.13	
XM_027998701.1	Heat shock protein 70	1.90		3.48	−1.02

Genes with the same annotation name but different gene IDs are isoforms. The negative sign indicates the underexpressed DEGs, whereas no negative sign indicates the overexpressed DEGs. DEGs, differentially expressed genes.

vector are realized in the form of ecological, behavioral, and fitness patterns. However, advancements in omics techniques that capture associated gene expression patterns provide greater opportunities to explore this paradigm of vector–virus interactions. This study assessed the differences in gene expression in *A. gossypii* adults in response to the acquisition of CLRDV from its primary host plant (cotton) and alternate host plants (hibiscus, okra, and prickly sida). The results show that transcriptional changes observed in viruliferous *A. gossypii* vary substantially between the host species from which it acquired the virus. The results indicate that the host plant could be a major determinant of vector–virus interaction outcomes.

Across all four host species, most transcriptional changes were observed in *A. gossypii* that acquired CLRDV from infected okra

TABLE 7 Differential expression of genes associated with cellular responses (endocytosis) in viruliferous *Aphis gossypii* adults compared with non-viruliferous adults.

Gene ID	Function	LFC of *A. gossypii* genes acquiring the virus from			
		Cotton	Hibiscus	Okra	Prickly sida
XM_027981156.1	Heat shock protein 70	2.04	−1.02	4.18	−2.20
XM_027997432.1	Heat shock protein 70 A1-like	2.04		4.13	
XM_027998701.1	Heat shock protein 70 A1-like	1.89		3.48	−1.0
XM_027985527.1	GSK3B-interacting protein-like			−6.51	
XM_027997003.1	Heat shock protein 68-like			4.87	−2.38

Genes with the same annotation name but different gene IDs are isoforms. The negative sign indicates the underexpressed DEGs, whereas no negative sign indicates the overexpressed DEGs. DEGs, differentially expressed genes.

10.3389/fpls.2024.1341781

TABLE 8 Differential expression of genes associated with aging in viruliferous *Aphis gossypii* adults compared with non-viruliferous adults.

Gene ID	Function	LFC of *A. gossypii* genes acquiring the virus from			
		Cotton	Hibiscus	Okra	Prickly sida
XM_027980601.1	Acyl-CoA Delta(11) desaturase-like			1.35	
XM_027981156.1	Heat shock protein 70 A1-like	2.04	−1.02	4.18	−2.20
XM_027990451.1	cAMP-dependent protein kinase catalytic subunit beta-like	7.28			
XM_027990995.1	(11Z)-Hexadec-11-enoyl-CoA conjugase-like			−1.11	
XM_027990998.1	(11Z)-Hexadec-11-enoyl-CoA conjugase-like			−8.49	
XM_027992685.1	5′-AMP-activated protein kinase subunit gamma isoform X1			1.26	
XM_027992684.1	5′-AMP-activated protein kinase subunit gamma isoform X1			−4.51	
XM_027992845.1	Phosphatidylinositol 3,4,5-trisphosphate 3-phosphatase and dual-specificity protein phosphatase PTEN isoform X3			1.17	
XM_027994156.1	cAMP-dependent protein kinase catalytic subunit beta-like	7.05			
XM_027994521.1	Phosphatidylinositol 3-kinase regulatory subunit gamma-like			−8.20	
XM_027997003.1	Heat shock protein 68-like			4.87	−2.38
XM_027997432.1	Heat shock protein 70 A1-like	2.04		4.13	
XM_027998701.1	Heat shock protein 70 A1-like	1.90		3.48	−1.02

Genes with the same annotation name but different gene IDs are isoforms. The negative sign indicates the underexpressed DEGs, whereas no negative sign indicates the overexpressed DEGs. DEGs, differentially expressed genes.

plants, followed by cotton, prickly sida, and hibiscus, which represented 8.11%, 5.1%, 4.6%, and 2.1% of the overall genes in the aphid genome, respectively. Similarly, the number of unique genes of *A. gossypii* was the highest when the virus was acquired from okra, followed by prickly sida, cotton, and hibiscus plants. These findings indicate that CLRDV-induced transcriptional changes in *A. gossypii* adults upon virus acquisition from different host species vary drastically. This variation in the number of transcriptional responses occurring in *A. gossypii* could be affected by differences in host susceptibility to the virus, host nutrient quality, physiology, and defense mechanisms (Gadhave et al., 2019; Marmonier et al., 2022). In a previous study, the

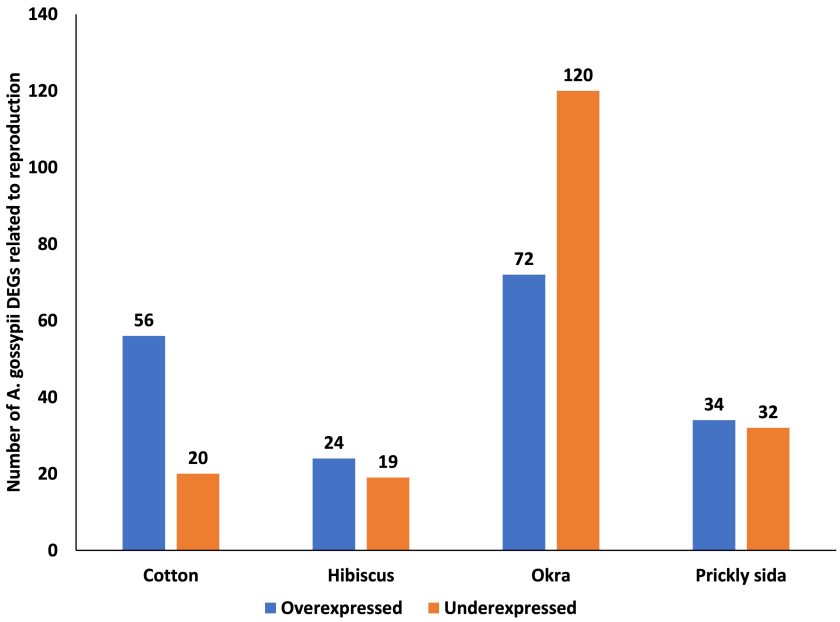

FIGURE 8
Number of differentially expressed genes (DEGs) related to reproduction in viruliferous *Aphis gossypii* adults that acquired CLRDV from infected cotton, hibiscus, okra, and prickly sida plants. CLRDV, cotton leafroll dwarf virus.

percentage of adult aphids that acquired CLRDV, the amount of virus acquired, and the percentage of aphid-mediated back-transmission of the virus varied significantly between the four host plants (Pandey et al., 2022). The transcriptional differences observed when adult *A. gossypii* acquired CLRDV from different hosts observed in this study, in part, could explain some of the observed variations in virus acquisition and inoculation ability of adult aphids (Pandey et al., 2022).

Previous studies also have reported varying transcriptional responses in aphids upon polerovirus acquisition. For instance, 164 DEGs were identified in *M. persicae* adults that acquired TuYV from infected plants compared with non-viruliferous aphids, whereas 201 DEGs were identified when the aphids acquired the virus from an artificial medium compared with non-viruliferous aphids in the same study (Marmonier et al., 2022). Similarly, the number of DEGs was greater in viruliferous aphids that acquired TuYV from *Arabidopsis thaliana* (L.) Heynh (1,073 genes) compared with viruliferous aphids that acquired TuYV from *Camelina sativa* (L.) Crantz (474 genes) (Chesnais et al., 2022). Thus, the variation in the number of DEGs may be influenced by the host species from which it is acquiring the virus. The number of DEGs in the same aphid species (*M. persicae*) upon acquisition of another polerovirus species PLRV from infected potato plants, when compared with their non-viruliferous counterparts, was 134 (Patton et al., 2021). The acquisition of the same virus species (BYDV) from virus-infected wheat plants resulted in significant variation in the number of DEGs of two of its aphid vectors—*S. graminum* (1,525 genes) and *S. avenae* (800 genes)—in comparison with non-viruliferous vectors (Li et al., 2019, 2020). These results reiterate that different viruses and host interactions as well as the same virus–host interactions could differentially induce gene expression in the same vector or different vectors. Also, the experimental design factors such as acquisition period, gut clearing, sequencing platforms, number of libraries sequenced, and bioinformatics tools used for analysis may have contributed to the variation in the number of DEGs across virus–vector–host pathosystems in different studies. What is missing in understanding component interactions within a phytovirus–vector pathosystem is the impact of alternate hosts on virus–vector interactions. In other words, how conserved are vector–virus interactions across host species?

Common DEGs among viruliferous *A. gossypii* adults associated with virus–vector interactions

In this study, the acquisition of CLRDV resulted in transcriptional changes in *A. gossypii*, of which only four DEGs were common between the viruliferous *A. gossypii* adults acquiring the virus from four host species. Among four common DEGs, the direction and/or level of the expression (over or under) of common genes varied between host species. The KEGG annotation and GO enrichment analysis revealed the role of one of the common genes (XM_027981156.1, *heat shock protein 70*) in virus infection, signal transduction, immune responses, longevity, and endocytosis. Heat shock protein 70 was overexpressed in *A. gossypii* upon acquiring the virus from CLRDV-infected cotton and okra plants, whereas it was underexpressed in *A. gossypii* that acquired the virus from CLRDV-infected hibiscus and prickly sida plants. In this study, the expression level of heat shock protein was nearly double in *A. gossypii* that acquired the virus from infected okra compared with cotton. The heat shock proteins are essential chaperone proteins known to be overexpressed in response to stress conditions. One study found that *heat shock protein 70* was overexpressed upon BYDV acquisition in its aphid vector (*R. padi*). The BYDV infection has been reported to increase the plant surface temperature and aphid heat tolerance, suggesting a protective role (Porras et al., 2020). Another study has reported the interaction of tomato yellow leaf curl virus (TYLCV) with *Bemisia tabaci* (Gennadius) *heat shock protein 70* in the midgut using *in vitro* studies. The protein was suggested to play an inhibitory role in virus transmission (Götz et al., 2012). The higher expression level of heat shock protein could be one of the reasons for reduced CLRDV acquisition and inoculation from okra to cotton plants by *A. gossypii* reported in an earlier study (Pandey et al., 2022).

However, the other common gene (XM_027987236.1, *juvenile hormone acid O-methyltransferase*) was overexpressed in aphids that acquired the virus from cotton and okra but underexpressed in aphids that acquired the virus from hibiscus and prickly sida plants. In a previous study, the *JHAMT* (*juvenile hormone-III synthase*) was overexpressed in *S. avenae* that acquired BYDV from wheat plants (Li et al., 2019). This gene is known to play a regulatory role, as a rate-limiting enzyme in insect juvenile hormone biosynthesis, which is essential in the development, metamorphosis, and reproduction of insects (Shinoda and Itoyama, 2003; Minakuchi et al., 2008; Niwa et al., 2008). In contrast, in another study, the underexpression of juvenile hormones in aphids was linked with increased wing development and enhanced virus spread (Quan et al., 2019; Zhang et al., 2019). Variations in the expression levels of *juvenile hormone acid O-methyltransferase* observed in *A. gossypii* suggest that CLRDV acquisition may enhance or reduce the fitness of *A. gossypii* depending on the host species and warrants further examination.

Unique DEGs associated with virus–vector interactions

In addition to the four DEGs in common, many unique DEGs were identified in *A. gossypii* depending on the plant species from which the virus was acquired. The number of DEGs uniquely expressed was the highest in aphids that acquired the virus from okra plants. For example, the *ras-related protein* (*Rab* protein) associated with signaling in the circadian clock cells in *Drosophila melanogaster* Meigen was uniquely identified and underexpressed in aphids that acquired the virus from okra plants (Williams et al., 2001). *Rab* proteins also function as transporters of vesicle cargo, responsible for trafficking among several membrane compartments (Zhang et al., 2007). Hence, the underexpression of this gene could be one of the reasons for the lower virus acquisition and/or retention ability of aphids from okra plants. The *tubulin beta-1 chain* gene encoding a structural constituent of the cytoskeleton was

uniquely overexpressed in *A. gossypii* that acquired CLRDV from infected cotton plants in this study. The overexpression of this gene enhances the insects' development and reproduction (Nielsen et al., 2010). Tubulin is also a major constituent of microtubules, which is an integral part of intracellular transport (Logan and Menko, 2019). This could be one of the reasons for better fitness and acquisition of CLRDV in adult *A. gossypii* that acquired the virus from cotton plants compared with the other three hosts in the previous study (Pandey et al., 2022). In contrast, this gene was underexpressed in *M. persicae* adults that acquired TuYV from virus-infected plants and artificial medium (Marmonier et al., 2022).

The gene coding for *ubiquitin-conjugating enzyme* was overexpressed sixfold in *A. gossypii* that acquired CLRDV from virus-infected cotton plants, whereas it was overexpressed ~1.5-fold when the virus was acquired from okra and prickly sida plants in this study. The gene was not differentially expressed in *A. gossypii* acquiring CLRDV from virus-infected hibiscus plants (Table S3). The overexpression of *ubiquitin-conjugating enzymes* was previously reported in *M. persicae* and *B. tabaci* feeding on BYDV-infected and sida golden mosaic virus (SiGMV)-infected plants, respectively (Li et al., 2020; Mugerwa et al., 2022). The conjugating enzyme can transfer the ubiquitin from E1 to the substrate and is required for *Notch* signaling activation during *Drosophila* wing development (Gonen et al., 1999; Zhang et al., 2021). Since this gene is reported in the endocytic trafficking of the *Notch* protein, it could potentially influence the endocytic traversion of virus particles in *A. gossypii*. The overexpression of this gene may partially be responsible for the efficient retention and inoculation of CLRDV upon acquisition of the virus from cotton than the other three hosts (Pandey et al., 2022). This gene also is vital for insect defense against pathogens (Lemaitre and Hoffmann, 2007).

The immune system of insects helps them defend against pathogens (Wang et al., 2016). The change in the expression level of the genes related to the immune system and different signaling pathways in *A. gossypii* varied between the host species from which the virus was acquired. The genes related to the MAPK signaling pathway were differentially expressed in *A. gossypii* that acquired the virus from all hosts. In contrast, genes related to the JAK–STAT signaling pathway were only differentially expressed in *A. gossypii* that acquired the virus from okra plants. The JAK–STAT signaling pathway triggers insects' innate immunity and antiviral responses (Dostert et al., 2005; Hedges and Johnson, 2008; Kingsolver et al., 2013). One of the genes associated with the immune system in aphids is *Cathepsin B* (Kubo et al., 2012; Quan et al., 2019). *Cathepsin B* is an aphid gut cysteine protease that regulates host protein activity and plays a role in the recognition and movement of viruses at the gut level (Pinheiro et al., 2017; Heck and Brault, 2018). *Cathepsin B* gene transcripts were overexpressed in *A. gossypii* acquiring CLRDV from infected cotton and okra plants alone. It was reported previously that the *cathepsin B* expression in aphids depends significantly on the host species (Pinheiro et al., 2017). This may partially explain the identification of the *cathepsin B* gene only in two host species in this study. The overexpression of the *cathepsin B* gene also was reported from *M. persicae* that acquired TuYV from infected plants (Marmonier et al., 2022). In contrast, *M. persicae* that acquired PLRV from infected plants had reduced expression of *cathepsin B*, which was associated with enhanced PLRV transmission (Pinheiro et al., 2017). The overexpression of the *cathepsin B* gene in *A. gossypii* acquiring the virus from okra plants may be one of the reasons for reduced CLRDV retention and subsequent inoculation in the previous study (Pandey et al., 2022). However, it does not explain the CLRDV retention and inoculation results obtained in *A. gossypii* upon acquisition from cotton despite overexpression of *cathepsin B* genes (Pandey et al., 2022).

For successful aphid-mediated transmission of circulative non-propagative phytoviruses such as poleroviruses, the virus capsid protein must interact with putative receptors at the midgut and accessory salivary glands (Gray and Gildow, 2003). One of the critical gene families identified in this study was *serine/threonine kinase receptors*. These genes were differentially expressed in both directions (over and under) in *A. gossypii* upon virus acquisition from four different host species in this study. This gene also was identified as one of the hub genes in the largest module (turquoise) in WGCNA in this study. The differential expression of these genes also was reported in whiteflies that acquired another group of persistent non-propagative circulative phytoviruses (begomoviruses) compared with their non-viruliferous counterparts (Mugerwa et al., 2022). *Serine/threonine kinase*, in mammalian cells, also has been recorded to play a vital role in clathrin-mediated endocytosis of the rabies virus (Wang et al., 2020a). The identification of these receptors in this study highlights their potential role in the circulative movement of poleroviruses in their aphid vectors. However, the role of host plants in the differential expression of these receptors' genes cannot be explicitly established in this study.

Another important group of DEGs is associated with xenobiotics detoxification. Genes such as *cytochrome P450*, *ATP binding cassette transporters* (*ABCs*), and *UDP-glycosyltransferases* (*UGTs*) were differentially expressed in *A. gossypii* that acquired CLRDV from different host species in this study. These detoxification genes are essential for the adaption of insects to different host plants (Quan et al., 2019). Among them, *cytochrome P450* genes were mainly overexpressed in *A. gossypii* that acquired CLRDV from infected okra and prickly sida plants. However, they were not differentially expressed in *A. gossypii* that acquired CLRDV from other host species. The overexpression of *cytochrome P450* genes also was reported in *M. persicae* upon PLRV acquisition (Patton et al., 2021). Therefore, the overexpression of these genes may assist aphids enhancing the tolerance of non-desirable host plants, which could ultimately help in virus transmission and epidemics (Casteel and Jander, 2013).

Co-expression networks and hub genes from candidate modules

Gene co-expression networks attained through WGCNA also identified modules of highly correlated genes associated with virus transmission and vector performance. Three of the four most interacting hub genes were annotated: XM_027993669.1 (*trichohyalin*-like), XM_027997289.1 (uncharacterized protein), XM_027997209.1 (*glucose dehydrogenase [FAD, quinone]*-like), and XM_027983368.1 (*neuroendocrine convertase 1*-like). A

previous study speculated the role of trichohyalin during immune defense via tissue remodeling and interaction with cuticular binding blocks that facilitate encapsulation (Takase and Hirai, 2012; Simons, 2015; Feng et al., 2022). Similarly, the *FAD glucose dehydrogenase* is a detoxification enzyme, the overexpression of which induces defense by reducing quinone in parasite-infected bumble bees (Stone and Yang, 2006; Giacomini et al., 2023). The *neuroendocrine convertase 1*, also called proprotein convertase (*PC1/3*), is a neuropeptide involved in regulating insect growth and development (Greenlee and Harrison, 2004; Callier and Nijhout, 2011). Another earlier study also has identified the essential role of *PC1/3* in maintaining metabolic balance and nutrient-dependent fertility in adult beetles (Fritzsche and Hunnekuhl, 2021). These highly interacting hub genes could play a significant role in the development and defense mechanisms in *A. gossypii* following CLRDV acquisition and could be important targets for future investigation.

Conclusion

Gene expression profiles varied in substantial magnitude with hosts even within the same family and when interacting with the same virus isolate. Only four common genes were identified between the aphids acquiring the virus from four host species. Several unique genes associated with virus infection, immunity, growth, and development were identified among all DEGs analyzed. In addition, DEG families identified in this study indicate similarity with studies involving other persistent non-propagative viruses (Li et al., 2019, 2020; Patton et al., 2021; Catto et al., 2022; Chesnais et al., 2022; Marmonier et al., 2022; Mugerwa et al., 2022). Despite the same gene families that were identified in aphids from multiple hosts, the directional patterns of these DEGs varied (in some instances overexpressed and in other instances underexpressed) with acquisition hosts. These results reiterate that host plants could have an outsized role in determining vector–virus interaction outcomes. Future studies should examine this phenomenon in other virus pathosystems as well and evaluate the effects of differential gene expression patterns in vectors on their fitness parameters and functionally associate unique gene–fitness as well as gene expression directional pattern–fitness relationships.

Data availability statement

The data for this article can be found in the NCBI GenBank repository at https://www.ncbi.nlm.nih.gov/ under the BioProject PRJNA934319. Raw sequence data for the BioSamples: SAMN31430961-SAMN31430989 are deposited in the SRA accessions: SRR23579709-SRR23579737.

Ethics statement

The manuscript presents research on animals that do not require ethical approval for their study.

Author contributions

SP: Data curation, Formal analysis, Investigation, Methodology, Software, Validation, Writing – original draft, Writing – review & editing. MC: Data curation, Formal analysis, Methodology, Software, Validation, Writing – review & editing. PR: Funding acquisition, Resources, Supervision, Writing – review & editing. SB: Resources, Supervision, Writing – review & editing. AJ: Resources, Supervision, Writing – review & editing. RS: Conceptualization, Funding acquisition, Project administration, Resources, Supervision, Validation, Visualization, Writing – review & editing.

Funding

The author(s) declare financial support was received for the research, authorship, and/or publication of this article. This project was financially supported by the Georgia Commodity Commission for Cotton awarded to Georgia and by Agricultural Research Service, U.S. Department of Agriculture, under Agreement No. 58-6010-0-011 awarded to Alabama.

Acknowledgments

We thank Sarah Bragg for her assistance with aphid colony maintenance in the greenhouse.

Conflict of interest

The authors declare that the research was conducted in the absence of any commercial or financial relationships that could be construed as a potential conflict of interest.

Publisher's note

Supplementary material

The Supplementary Material for this article can be found online at: https://www.frontiersin.org/articles/10.3389/fpls.2024.1341781/full#supplementary-material

SUPPLEMENTARY TABLE 2
List of DEGs associated with significant GO terms in *A. gossypii* that acquired CLRDV from infected cotton plant.

SUPPLEMENTARY TABLE 3
List of DEGs associated with significant GO terms in *A. gossypii* that acquired CLRDV from infected hibiscus plant.

SUPPLEMENTARY TABLE 4
List of DEGs associated with significant GO terms in *A. gossypii* that acquired CLRDV from infected okra plant.

SUPPLEMENTARY TABLE 5
List of DEGs associated with significant GO terms in *A. gossypii* that acquired CLRDV from infected prickly sida plant.

SUPPLEMENTARY TABLE 7
DEGs associated with immune pathways in *A. gossypii* that acquired CLRDV from alternate hosts.

SUPPLEMENTARY TABLE 8
DEGs associated with reproduction in *A. gossypii* that acquired CLRDV from alternate hosts.

References

Aboughanem-Sabanadzovic, N., Allen, T. W., Wilkerson, T. H., Conner, K. N., Sikora, E. J., Nichols, R. L., et al. (2019). First report of cotton leafroll dwarf virus in upland cotton (*Gossypium hirsutum*) in Mississippi. *Plant Dis.* 103, 1798. doi: 10.1094/PDIS-01-19-0017-PDN

Alabi, O. J., Isakeit, T., Vaughn, R., Stelly, D., Conner, K. N., Gaytan, B. C., et al. (2020). First report of cotton leafroll dwarf virus infecting upland cotton (*Gossypium hirsutum* L.) in Texas. *Plant Dis. Notes* 104, 10–11. doi: 10.1094/PDIS-09-19-2008-PDN

Ali, A., and Mokhtari, S. (2020). First report of cotton leafroll dwarf virus infecting cotton (*Gossypium hirsutum*) in Kansas. *Plant Dis.* 104, 1880. doi: 10.1094/PDIS-12-19-2589-PDN

Ali, A., Mokhtari, S., and Ferguson, C. (2020). First report of cotton leafroll dwarf virus from cotton (*Gossypium hirsutum*) in Oklahoma. *Plant Dis. Notes* 104, 2531. doi: 10.1094/PDIS-03-20-0479-PDN

Andrews, S., and FastQC, A. (2010). *A quality control tool for high throughput sequence data*. Available online at: http://www.bioinformatics.bbsrc.ac.uk/projects/fastqc/.

Avelar, S., Schrimsher, D. W., Lawrence, K., and Brown, J. K. (2019). First report of cotton leafroll dwarf virus associated with cotton blue disease symptoms in Alabama. *Plant Dis. Notes* 103, 592. doi: 10.1094/PDIS-09-18-1550-PDN

Bag, S., Roberts, P. M., and Kemerait, R. C. (2021). Cotton leafroll dwarf disease: an emerging virus disease on cotton in the U.S. *Crop Soils* 54, 18–22. doi: 10.1002/crso.20105

Barman, A. K., Gadhave, K. R., Dutta, B., and Srinivasan, R. (2018). Plasticity in host utilization by two host-associated populations of *Aphis gossypii* Glover. *Bull. Entomol. Res.* 108, 360–369. doi: 10.1017/S0007485317000852

Bertasello, L. E. T., Carmo-sousa, M., Prado Maluta, N. K., Rossini Pinto, L., Spotti Lopes, J. R., and Gonçalves, M. C. (2021). Effect of sugarcane cultivars infected with sugarcane yellow leaf virus (Scylv) on feeding behavior and biological performance of *Melanaphis sacchari* (Hemiptera: Aphididae). *Plants* 10, 2122. doi: 10.3390/plants10102122

Bolger, A. M., Lohse, M., and Usadel, B. (2014). Trimmomatic: A flexible trimmer for Illumina sequence data. *Bioinformatics* 30, 2114–2120. doi: 10.1093/bioinformatics/btu170

Bosque-Pérez, N. A., and Eigenbrode, S. D. (2011). The influence of virus-induced changes in plants on aphid vectors: Insights from luteovirus pathosystems. *Virus Res.* 159, 201–205. doi: 10.1016/j.virusres.2011.04.020

Brault, V., Uzest, M., Monsion, B., Jacquot, E., and Blanc, S. (2010). Aphids as transport devices for plant viruses. *Comptes Rendus - Biol.* 333, 524–538. doi: 10.1016/j.crvi.2010.04.001

Brown, S., Conner, K., Hagan, A., Jacobson, A., Koebernick, J., Lawrence, K., et al. (2019) . *Report of a research review and planning meeting on cotton leafroll dwarf virus*. Available at: https://www.cottoninc.com/cotton-production/ag-research/ plant-pathology/cotton-leafroll-dwarf-virus-research/ (Accessed 2023 Oct 21).

Callier, V., and Nijhout, H. F. (2011). Control of body size by oxygen supply reveals size-dependent and size-independent mechanisms of molting and metamorphosis. *Proc. Natl. Acad. Sci. U. S. A.* 108, 14664–14669. doi: 10.1073/pnas.1106556108

Cascardo, R. S., Arantes, I. L. G., Silva, T. F., Sachetto-Martins, G., Vaslin, M. F. S., and Corrêa, R. L. (2015). Function and diversity of P0 proteins among cotton leafroll dwarf virus isolates. *Virol. J.* 12, 1–10. doi: 10.1186/s12985-015-0356-7

Casteel, C. L., and Jander, G. (2013). New synthesis: investigating mutualisms in virus-vector interactions. *J. Chem. Ecol.* 39, 809. doi: 10.1007/s10886-013-0305-0

Castle, S. J., Mowry, T. M., and Berger, P. H. (1998). Differential settling by *Myzus persicae* (Homoptera: Aphididae) on various virus infected host plants. *Ann. Entomol. Soc Am.* 91, 661–667. doi: 10.1093/aesa/91.5.661

Catto, M. A., Mugerwa, H., Myers, B. K., Pandey, S., Dutta, B., and Srinivasan, R. (2022). A Review on Transcriptional responses of interactions between insect vectors and plant viruses. *Cells* 11, 693. doi: 10.3390/cells11040693

Chesnais, Q., Caballero Vidal, G., Coquelle, R., Yvon, M., Mauck, K., Brault, V., et al. (2020). Post-acquisition effects of viruses on vector behavior are important components of manipulation strategies. *Oecologia* 194, 429–440. doi: 10.1007/s00442-020-04763-0

Chesnais, Q., Golyaev, V., Velt, A., Rustenholz, C., Verdier, M., Brault, V., et al. (2022). Transcriptome responses of the aphid vector *Myzus persicae* are shaped by identities of the host plant and the virus. *Peer Community J.* 2, 429–440. doi: 10.24072/pcjournal.208

Claudel, P., Chesnais, Q., Fouché, Q., Krieger, C., Halter, D., Bogaert, F., et al. (2018). The aphid-transmitted turnip yellows virus differentially affects volatiles emission and subsequent vector behavior in two *Brassicaceae* plants. *Int. J. Mol. Sci.* 19, 2316. doi: 10.3390/ijms19082316

dos Santos, R. C., Peñaflor, M. F. G. V., Sanches, P. A., Nardi, C., and Bento, J. M. S. (2016). The effects of *Gibberella zeae*, barley yellow dwarf virus, and co-infection on *Rhopalosiphum padi* olfactory preference and performance. *Phytoparasitica* 44, 47–54. doi: 10.1007/s12600-015-0493-y

Dostert, C., Jouanguy, E., Irving, P., Troxler, L., Galiana-Arnoux, D., Hetru, C., et al. (2005). The Jak-STAT signaling pathway is required but not sufficient for the antiviral response of *Drosophila*. *Nat. Immunol.* 69, 946–953. doi: 10.1038/ni1237

Edula, S. R., Bag, S., Milner, H., Kumar, M., Suassuna, N. D., Chee, P. W., et al. (2023). Cotton leafroll dwarf disease: An enigmatic viral disease in cotton. *Mol. Plant Pathol.* 24, 513–526. doi: 10.1111/mpp.13335

Eigenbrode, S. D., Ding, H., Shiel, P., and Berger, P. H. (2002). Volatiles from potato plants infected with potato leafroll virus attract and arrest the virus vector, *Myzus persicae* (Homoptera: Aphididae). *Proc. R. Soc Lond. B* 269, 455–460. doi: 10.1098/rspb.2001.1909

Ewels, P., Magnusson, M., Lundin, S., and Käller, M. (2016). MultiQC: Summarize analysis results for multiple tools and samples in a single report. *Bioinformatics* 32, 3047–3048. doi: 10.1093/bioinformatics/btw354

Faske, T. R., Stainton, D., Aboughanem-Sabanadzovic, N., and Allen, T. W. (2020). First report of cotton leafroll dwarf virus from upland cotton (*Gossypium hirsutum*) in Arkansas. *Plant Dis. Notes* 104, 2742. doi: 10.1094/PDIS-12-19-2610-PDN

Feng, M., Swevers, L., and Sun, J. (2022). Hemocyte Clusters Defined by scRNA-Seq in *Bombyx mori*: In Silico analysis of predicted marker genes and implications for potential functional roles. *Front. Immunol.* 13. doi: 10.3389/fimmu.2022.852702

Fereres, A., and Moreno, A. (2009). Behavioural aspects influencing plant virus transmission by homopteran insects. *Virus Res.* 141, 158–168. doi: 10.1016/j.virusres.2008.10.020

Fiebig, M., Poehling, H. M., and Borgemeister, C. (2004). Barley yellow dwarf virus, wheat, and *Sitobion avenae*: a case of trilateral interactions. *Entomol. Exp. Appl.* 110, 11–21. doi: 10.1111/j.0013-8703.2004.00115.x

Fingu-Mabola, J. C., and Francis, F. (2021). Aphid–plant–phytovirus pathosystems: Influencing factors from vector behaviour to virus spread. *Agriculture* 11, 502. doi: 10.3390/agriculture11060502

Fingu-Mabola, J. C., Martin, C., Bawin, T., Verheggen, F. J., and Francis, F. (2020). Does the infectious status of aphids influence their preference towards healthy, virus-infected and endophytically colonized plants? *Insects* 11, 1–16. doi: 10.3390/insects11070435

Fritzsche, S., and Hunnekuhl, V. S. (2021). Cell-specific expression and individual function of prohormone convertase PC1/3 in *Tribolium* larval growth highlights major evolutionary changes between beetle and fly neuroendocrine systems. *Evodevo* 12, 1–20. doi: 10.1186/s13227-021-00179-w

Gadhave, K. R., Dutta, B., Coolong, T., and Srinivasan, R. (2019). A non-persistent aphid-transmitted potyvirus differentially alters the vector and non-vector biology through host plant quality manipulation. *Sci. Rep.* 9, 1–12. doi: 10.1038/s41598-019-39256-5

Ghosh, A., Das, A., Vijayanandraj, S., and Mandal, B. (2016). Cardamom bushy dwarf virus infection in large cardamom alters plant selection preference, life stages, and fecundity of aphid vector, *Micromyzus kalimpongensis* (hemiptera: Aphididae). *Environ. Entomol.* 45, 178–184. doi: 10.1093/ee/nvv161

Giacomini, J. J., Adler, L. S., Reading, B. J., and Irwin, R. E. (2023). Differential bumble bee gene expression associated with pathogen infection and pollen diet. *BMC Genomics* 24, 157. doi: 10.1186/s12864-023-09143-5

Gonen, H., Bercovich, B., Orian, A., Carrano, A., Takizawa, C., Yamanaka, K., et al. (1999). Identification of the ubiquitin carrier proteins, E2s, involved in signal-induced conjugation and subsequent degradation of IκBα. *J. Biol. Chem.* 274, 14823–14830. doi: 10.1074/jbc.274.21.14823

Götz, M., Popovski, S., Kollenberg, M., Gorovits, R., Brown, J. K., Cicero, J. M., et al. (2012). Implication of *Bemisia tabaci* heat shock protein 70 in begomovirus-whitefly interactions. *J. Virol.* 86, 13241–13252. doi: 10.1128/JVI.00880-12

Gray, S., and Gildow, F. E. (2003). Luteovirus-aphid interactions. *Annu. Rev. Phytopathol.* 41, 539–566. doi: 10.1146/annurev.phyto.41.012203.105815

Greenlee, K. J., and Harrison, J. F. (2004). Development of respiratory function in the American locust *Schistocerca americana*: II. Within-instar effects. *J. Exp. Biol.* 207, 509–517. doi: 10.1242/jeb.00766

Harris, K. F., and Maramorosch, K. (1977). *Aphids As Virus Vectors.* (Academic Press, Cambridge, MA, USA: Elsevier). doi: 10.1016/c2013-0-10831-8

Heck, M., and Brault, V. (2018). Targeted disruption of aphid transmission: a vision for the management of crop diseases caused by *Luteoviridae* members. *Curr. Opin. Virol.* 33, 24–32. doi: 10.1016/j.coviro.2018.07.007

Hedges, L. M., and Johnson, K. N. (2008). Induction of host defence responses by *Drosophila* C virus. *J. Gen. Virol.* 89, 1497–1501. doi: 10.1099/vir.0.83684-0

Heilsnis, B., Mahas, J. B., Conner, K., Pandey, S., Clark, W., Koebernick, J., et al. (2023). Characterizing the vector competence of *Aphis gossypii*, *Myzus persicae* and *Aphis craccivora* (Hemiptera: Aphididae) to transmit cotton leafroll dwarf virus to cotton in the United States. *J. Econ. Entomol.* 116, 719–725. doi: 10.1093/jee/toad080

Heilsnis, B., McLaughlin, A., Conner, K., Koebernick, J., and Jacobson, A. L. (2022). Vector competency of *A*phis gossypii and *Bemisia tabaci* to transmit cotton leafroll dwarf virus. *J. Cotton Sci.* 26, 23–30. doi: 10.56454/VBZR9427

Hodge, S., and Powell, G. (2008). Do plant viruses facilitate their aphid vectors by inducing symptoms that alter behavior and performance? *Environ. Entomol.* 37, 1573–1581. doi: 10.1603/0046-225X-37.6.1573

Hogenhout, S. A., Ammar, E. D., Whitfield, A. E., and Redinbaugh, M. G. (2008). Insect vector interactions with persistently transmitted viruses. *Annu. Rev. Phytopathol.* 46, 327–359. doi: 10.1146/annurev.phyto.022508.092135

Hu, Z., Chai, R., Liu, X., Dong, Y., Su, D., Desneux, N., et al. (2022). Barley yellow dwarf virus-infected wheat plant modulated selection behavior of vector aphids. *J. Pest Sci. (2004).* 95, 1273–1285. doi: 10.1007/s10340-021-01458-0

Ingwell, L. L., Eigenbrode, S. D., and Bosque-Pérez, N. A. (2012). Plant viruses alter insect behavior to enhance their spread. *Sci. Rep.* 2, 578. doi: 10.1038/srep00578

Iriarte, F., Dey, K. K., Small, I. M., Conner, K., O'Brien, K., Johnson, L., et al. (2020). First report of cotton leafroll dwarf virus (CLRDV) in Florida. *Plant Dis.* 104, 2744. doi: 10.1094/PDIS-10-19-2150-PDN

Jayasinghe, W. H., Akhter, M. S., Nakahara, K., and Maruthi, M. N. (2022). Effect of aphid biology and morphology on plant virus transmission. *Pest Manage. Sci.* 78, 416–427. doi: 10.1002/ps.6629

Jiménez-Martínez, E. S., Bosque-Pérez, N. A., Berger, P. H., Zemetra, R. S., Ding, H., and Eigenbrode, S. D. (2004). Volatile cues influence the response of *Rhopalosiphum padi* (Homoptera: Aphididae) to barley yellow dwarf virus-infected transgenic and untransformed wheat. *Environ. Entomol.* 33, 1207–1216. doi: 10.1603/0046-225X-33.5.1207

Kanehisa, M., and Goto, S. (2000). KEGG: kyoto encyclopedia of genes and genomes. *Nucleic Acids Res.* 28, 27–30. doi: 10.1093/nar/28.1.27

Kingsolver, M. B., Huang, Z., and Hardy, R. W. (2013). Insect antiviral innate immunity: Pathways, effectors, and connections. *J. Mol. Biol.* 425, 4921–4936. doi: 10.1016/j.jmb.2013.10.006

Kubo, Y., Hayashi, H., Matsuyama, T., Sato, H., and Yamamoto, N. (2012). Retrovirus entry by endocytosis and cathepsin proteases. *Adv. Virol.* 2012, 14. doi: 10.1155/2012/640894

Langfelder, P., and Horvath, S. (2008). WGCNA: An R package for weighted correlation network analysis. *BMC Bioinf.* 9, 1–13. doi: 10.1186/1471-2105-9-559

Langmead, B., and Salzberg, S. L. (2012). Fast gapped-read alignment with Bowtie 2. *Nat. Methods* 94, 357–359. doi: 10.1038/nmeth.1923

Legarrea, S., Barman, A., Diffie, S., and Srinivasan, R. (2020). Virus accumulation and whitefly performance modulate the role of alternate host species as inoculum sources of tomato yellow leaf curl virus. *Plant Dis.* 104, 2958–2966. doi: 10.1094/PDIS-09-19-1853-RE

Lemaitre, B., and Hoffmann, J. (2007). The host defense of *Drosophila melanogaster*. *Annu. Rev. Immunol.* 25, 697–743. doi: 10.1146/annurev.immunol.25.022106.141615

Li, B., and Dewey, C. N. (2011). RSEM: accurate transcript quantification from RNA-Seq data with or without a reference genome. *BMC Bioinformatics* 12, 323. doi: 10.1186/1471-2105-12-323

Li, D., Su, D., Tong, Z., Zhang, C., Zhang, G., Zhao, H., et al. (2019). Virus-dependent and -independent responses of *Sitobion avenae* (Homoptera: Aphididae) feeding on wheat infected by transmitted and nontransmitted viruses at transcriptomic level. *J. Econ. Entomol.* 112, 2067–2076. doi: 10.1093/jee/toz162

Li, D., Zhang, C., Tong, Z., Su, D., Zhang, G., Zhang, S., et al. (2020). Transcriptome response comparison between vector and non-vector aphids after feeding on virus-infected wheat plants. *BMC Genomics* 21, 638. doi: 10.1186/s12864-020-07057-0

Lightle, D., and Lee, J. (2014). Raspberry viruses affect the behavior and performance of *Amphorophora agathonica* in single and mixed infections. *Entomol. Exp. Appl.* 151, 57–64. doi: 10.1111/eea.12170

Liu, J., Liu, Y., Donkersley, P., Dong, Y., Chen, X., Zang, Y., et al. (2019). Preference of the aphid *Myzus persicae* (Hemiptera: Aphididae) for tobacco plants at specific stages of potato virus Y infection. *Arch. Virol.* 164, 1567–1573. doi: 10.1007/s00705-019-04231-y

Logan, C. M., and Menko, A. S. (2019). Microtubules: Evolving roles and critical cellular interactions. *Exp. Biol. Med.* 244, 1240–1254. doi: 10.1177/1535370219867296

Love, M. I., Huber, W., and Anders, S. (2014). Moderated estimation of fold change and dispersion for RNA-seq data with DESeq2. *Genome Biol.* 15, 1–21. doi: 10.1186/s13059-014-0550-8

Ma, K. S., Li, F., Liang, P. Z., Chen, X. W., Liu, Y., and Gao, X. W. (2016). Identification and validation of reference genes for the normalization of gene expression data in qRT-PCR Analysis in *Aphis gossypii* (Hemiptera: Aphididae). *J. Insect Sci.* 16, 1–9. doi: 10.1093/jisesa/iew003

Marmonier, A., Velt, A., Villeroy, C., Rustenholz, C., Chesnais, Q., and Brault, V. (2022). Differential gene expression in aphids following virus acquisition from plants or from an artificial medium. *BMC Genomics* 23, 1–15. doi: 10.1186/s12864-022-08545-1

Mauck, K. E. (2016). Variation in virus effects on host plant phenotypes and insect vector behavior: what can it teach us about virus evolution? *Curr. Opin. Virol.* 21, 114–123. doi: 10.1016/j.coviro.2016.09.002

Mauck, K. E., De Moraes, C. M., and Mescher, M. C. (2010). Deceptive chemical signals induced by a plant virus attract insect vectors to inferior hosts. *Proc. Natl. Acad. Sci. U. S. A.* 107, 3600–3605. doi: 10.1073/pnas.0907191107

Medina-Ortega, K. J., Bosque-Perez, N. A., Ngumbi, E., Jiménez-Martínez, E. S., and Eigenbrode, S. D. (2009). *Rhopalosiphum padi* (Hemiptera: Aphididae) responses to volatile cues from barley yellow dwarf virus-infected wheat. *Environ. Entomol.* 38, 836–845. doi: 10.1603/022.038.0337

Michelotto, M. D., and Busoli, A. C. (2007). Characterization of the cotton vein mosaic virus by *Aphis gossypii* transmission with relation to persistence and time necessary for inoculation. *Bragantia* 66, 441–447. doi: 10.1590/S0006-87052007000300010

Minakuchi, C., Namiki, T., Yoshiyama, M., and Shinoda, T. (2008). RNAi-mediated knockdown of juvenile hormone acid O-methyltransferase gene causes precocious metamorphosis in the red flour beetle *Tribolium castaneum*. *FEBS J.* 275, 2919–2931. doi: 10.1111/j.1742-4658.2008.06428.x

Moeini, P., Afsharifar, A., Homayoonzadeh, M., and Hopkins, R. J. (2020). Plant virus infection modifies plant pigment and manipulates the host preference behavior of an insect vector. *Entomol. Exp. Appl.* 168, 599–609. doi: 10.1111/eea.12944

Mugerwa, H., Gautam, S., Catto, M. A., Dutta, B., Brown, J. K., Adkins, S., et al. (2022). Differential transcriptional responses in two old world *Bemisia tabaci* cryptic species post acquisition of old and new world begomoviruses. *Cells* 11, 2060. doi: 10.3390/cells11132060

Ng, J. C. K., and Falk, B. W. (2006). Virus-vector interactions mediating nonpersistent and semipersistent transmission of plant viruses. *Annu. Rev. Phytopathol.* 44, 183–212. doi: 10.1146/annurev.phyto.44.070505.143325

Ng, J. C. K., and Perry, K. L. (2004). Transmission of plant viruses by aphid vectors. *Mol. Plant Pathol.* 5, 505–511. doi: 10.1111/j.1364-3703.2004.00240.x

Ngumbi, E., Eigenbrode, S. D., Bosque-Pérez, N. A., Ding, H., and Rodriguez, A. (2007). *Myzus persicae* is arrested more by blends than by individual compounds elevated in headspace of PLRV-infected potato. *J. Chem. Ecol.* 33, 1733–1747. doi: 10.1007/s10886-007-9340-z

Nielsen, M. G., Gadagkar, S. R., and Gutzwiller, L. (2010). Tubulin evolution in insects: Gene duplication and subfunctionalization provide specialized isoforms in a functionally constrained gene family. *BMC Evol. Biol.* 10, 1–21. doi: 10.1186/1471-2148-10-113

Niwa, R., Niimi, T., Honda, N., Yoshiyama, M., Itoyama, K., Kataoka, H., et al. (2008). Juvenile hormone acid O-methyltransferase in *Drosophila melanogaster*. *Insect Biochem. Mol. Biol.* 38, 714–720. doi: 10.1016/j.ibmb.2008.04.003

Pandey, S., Bag, S., Roberts, P., Conner, K., Balkcom, K. S., Price, A. J., et al. (2022). Prospective alternate hosts of an emerging polerovirus in cotton landscapes in the southeastern United States. *Viruses* 14, 2249. doi: 10.3390/v14102249

Patton, M. K. F., Hansen, A. K., and Casteel, C. L. (2021). Potato leafroll virus reduces *Buchnera aphidocola* titer and alters vector transcriptome responses. *Sci. Rep.* 11, 23931. doi: 10.1038/s41598-021-02673-6

Pinheiro, P. V., Ghanim, M., Alexander, M., Rebelo, A. R., Santos, R. S., Orsburn, B. C., et al. (2017). Host plants indirectly influence plant virus transmission by altering gut

cysteine protease activity of aphid vectors. *Mol. Cell. Proteomics* 16, S230–S243. doi: 10.1074/mcp.M116.063495

Porras, M. F., Navas, C. A., Marden, J. H., Mescher, M. C., De Moraes, C. M., Pincebourde, S., et al. (2020). Enhanced heat tolerance of viral-infected aphids leads to niche expansion and reduced interspecific competition. *Nat. Commun.* 11, 1–9. doi: 10.1038/s41467-020-14953-2

Price, T., Valverde, R., Singh, R., Davis, J., Brown, S., and Jones, H. (2020). First report of cotton leafroll dwarf virus in Louisiana. *Plant Heal. Prog.* 21, 142–143. doi: 10.1094/PHP-03-20-0019-BR

Quan, Q., Hu, X., Pan, B., Zeng, B., Wu, N., Fang, G., et al. (2019). Draft genome of the cotton aphid *Aphis gossypii*. *Insect Biochem. Mol. Biol.* 105, 25–32. doi: 10.1016/j.ibmb.2018.12.007

Rajabaskar, D., Wu, Y., Bosque-Pérez, N. A., and Eigenbrode, S. D. (2013). Dynamics of *Myzus persicae* arrestment by volatiles from potato leafroll virus-infected potato plants during disease progression. *Entomol. Exp. Appl.* 148, 172–181. doi: 10.1111/eea.12087

R Core Team. (2021). "R: A language and environment for statistical computing. r foundation for statistical computing," in *R foundation for statistical computing* (R Found. Stat. Comput, Vienna, Austria). Available at: https://www.r-project.org/.

Ren, G.w., Wang, X.f., Chen, D., Wang, X.w., Fan, X.j., and liu, X.d. (2015). Potato virus Y-infected tobacco affects the growth, reproduction, and feeding behavior of a vector aphid, *Myzus persicae* (Hemiptera: Aphididae). *Appl. Entomol. Zool.* 50, 239–243. doi: 10.1007/s13355-015-0328-9

Safari Murhububa, I., Tougeron, K., Bragard, C., Fauconnier, M. L., Bisimwa Basengere, E., Walangululu Masamba, J., et al. (2021). Banana tree infected with banana bunchy top virus attracts *Pentalonia nigronervosa* aphids through increased volatile organic compounds emission. *J. Chem. Ecol.* 47, 755–767. doi: 10.1007/s10886-021-01298-3

Sedhain, N. P., Bag, S., Morgan, K., Carter, R., Triana, P., Whitaker, J., et al. (2021). Natural host range, incidence on overwintering cotton and diversity of cotton leafroll dwarf virus in Georgia USA. *Crop Prot.* 144, 105604. doi: 10.1016/j.cropro.2021.105604

Shannon, P., Markiel, A., Ozier, O., Baliga, N. S., Wang, J. T., Ramage, D., et al. (2003). Cytoscape: a software environment for integrated models of biomolecular interaction networks. *Genome Res.* 13, 2498–2504. doi: 10.1101/gr.1239303

Shinoda, T., and Itoyama, K. (2003). Juvenile hormone acid methyltransferase: A key regulatory enzyme for insect metamorphosis. *Proc. Natl. Acad. Sci. U. S. A.* 100, 11986–11991. doi: 10.1073/pnas.2134232100

Silva, A. K. F., Romanel, E., Silva, T. F., Castilhos, Y., Schrago, C. G., Galbieri, R., et al. (2015). Complete genome sequences of two new virus isolates associated with cotton blue disease resistance breaking in Brazil. *Arch. Virol.* 160, 1371–1374. doi: 10.1007/s00705-015-2380-8

Simons, M. (2015). Flies with skin blisters. *J. Invest. Dermatol.* 135, 1944–1945. doi: 10.1038/jid.2015.193

Sõmera, M., Fargette, D., Hébrard, E., and Sarmiento, C. (2021). *The ICTV report on virus classification and taxon nomenclature Solemoviridae Chapter Solemoviridae*. Available online at: www.ictv.global/report/solemoviridae (Accessed July 18, 2021).

Srinivasan, R., Alvarez, J. M., Bosque-Pérez, N. A., Eigenbrode, S. D., and Novy, R. G. (2008). Effect of an alternate weed host, hairy nightshade, *Solanum sarrachoides*, on the biology of the two most important potato leafroll virus (Luteoviridae: Polerovirus) vectors, *Myzus persicae* and *Macrosiphum euphorbiae* (Aphididae: Homoptera). *Environ. Entomol.* 37, 592–600. doi: 10.1603/0046-225X(2008)37[592:EOAAWH]2.0.CO;2

Srinivasan, R., Alvarez, J. M., and Cervantes, F. (2013). The effect of an alternate weed host, hairy nightshade, *Solanum sarrachoides* (Sendtner) on green peach aphid distribution and potato leafroll virus incidence in potato fields of the Pacific Northwest. *Crop Prot.* 46, 52–56. doi: 10.1016/j.cropro.2012.12.015

Srinivasan, R., Alvarez, J. M., Eigenbrode, S. D., and Bosque-Pérez, N. A. (2006). Influence of hairy nightshade *Solanum sarrachoides* (Sendtner) and potato leafroll virus (*Luteoviridae: Polerovirus*) on the host preference of *Myzus persicae* (Sulzer) (Homoptera: Aphididae). *Environ. Entomol.* 35, 546–553. doi: 10.1603/0046-225X-35.2.546

Stone, J. R., and Yang, S. (2006). Hydrogen peroxide: A signaling messenger. *Antioxidants Redox Signal.* 8, 243–270. doi: 10.1089/ars.2006.8.243

Supek, F., Bošnjak, M., Škunca, N., and Šmuc, T. (2011). Revigo summarizes and visualizes long lists of gene ontology terms. *PloS One* 6, e21800. doi: 10.1371/journal.pone.0021800

Tabassum, A., Bag, S., Roberts, P., Suassuna, N., Chee, P., Whitaker, J. R., et al. (2019). First report of cotton leafroll dwarf virus infecting cotton in Georgia, U.S.A. *Plant Dis.* 103, 1803. doi: 10.1094/PDIS-12-18-2197-PDN

Takase, T., and Hirai, Y. (2012). Identification of the C-terminal tail domain of AHF/trichohyalin as the critical site for modulation of the keratin filamentous meshwork in the keratinocyte. *J. Dermatol. Sci.* 65, 141–148. doi: 10.1016/j.jdermsci.2011.12.014

Thiessen, L. D., Schappe, T., Zaccaron, M., Connor, K., Kobernick, J., Jacobson, A. L., et al. (2020). First report of Cotton leafroll dwarf virus in cotton plants affected by cotton leafroll dwarf disease in North Carolina. *Plant Dis. Notes* 104, 3275. doi: 10.1094/PDIS-02-20-0335-PDN

Wang, H., Greene, J., Mueller, J., Conner, K., and Jacobson, A. (2020b). First report of cotton leafroll dwarf virus in cotton fields of South Carolina. *Plant Dis. Notes* 104, 2532. doi: 10.1094/PDIS-03-20-0635-PDN

Wang, L., Tang, N., Gao, X., Guo, D., Chang, Z., Fu, Y., et al. (2016). Understanding the immune system architecture and transcriptome responses to southern rice black-streaked dwarf virus in *Sogatella furcifera*. *Sci. Rep.* 61, 1–11. doi: 10.1038/srep36254

Wang, C., Wang, J., Shuai, L., Ma, X., Zhang, H., Liu, R., et al. (2020a). The serine/threonine kinase ap2-associated kinase 1 plays an important role in rabies virus entry. *Viruses* 12, 45. doi: 10.3390/v12010045

Werner, B. J., Mowry, T. M., Bosque-Pérez, N. A., Ding, H., and Eigenbrode, S. D. (2009). Changes in green peach aphid responses to potato leafroll virus–induced volatiles emitted during disease progression. *Environ. Entomol.* 38, 1429–1438. doi: 10.1603/022.038.0511

Whitfield, A. E., Falk, B. W., and Rotenberg, D. (2015). Insect vector-mediated transmission of plant viruses. *Virology* 479–480, 278–289. doi: 10.1016/j.virol.2015.03.026

Williams, J. A., Su, H. S., Bernards, A., Field, J., and Sehgal, A. (2001). A circadian output in *Drosophila* mediated by neurofibromatosis-1 and Ras/MAPK. *Sci. (80-.).* 293, 2251–2256. doi: 10.1126/science.1063097

Zhang, C. X., Brisson, J. A., and Xu, H. J. (2019). Molecular mechanisms of wing polymorphism in insects. *Annu. Rev. Entomol.* 64, 297–314. doi: 10.1146/annurev-ento-011118-112448

Zhang, F., Chen, Y., Shen, J., and Zhang, J. (2021). The ubiquitin conjugating enzyme UbcD1 is required for notch signaling activation during *Drosophila* wing development. *Front. Genet.* 12. doi: 10.3389/fgene.2021.770853

Zhang, J., Schulze, K. L., Robin Hiesinger, P., Suyama, K., Wang, S., Fish, M., et al. (2007). Thirty-one flavors of *Drosophila* Rab proteins. *Genetics* 176, 1307–1322. doi: 10.1534/genetics.106.066761

frontiers | Frontiers in Plant Science

TYPE Original Research
PUBLISHED 18 March 2024
DOI 10.3389/fpls.2024.1366515

OPEN ACCESS

EDITED BY
Lida Zhang,
Shanghai Jiao Tong University, China

REVIEWED BY
Zhenying Shi,
Chinese Academy of Sciences (CAS), China
Zhaohai Wang,
Jiangxi Agricultural University, China

*CORRESPONDENCE
Qingsong Liu
qingsongliu@henu.edu.cn
Shengli Jing
shljing@xynu.edu.cn

RECEIVED 06 January 2024
ACCEPTED 26 February 2024
PUBLISHED 18 March 2024

CITATION
Yu B, Geng M, Xue Y, Yu Q, Lu B, Liu M, Shao Y, Li C, Xu J, Li J, Hu W, Tang H, Li P, Liu Q and Jing S (2024) Combined miRNA and mRNA sequencing reveals the defensive strategies of resistant YHY15 rice against differentially virulent brown planthoppers. *Front. Plant Sci.* 15:1366515. doi: 10.3389/fpls.2024.1366515

Combined miRNA and mRNA sequencing reveals the defensive strategies of resistant YHY15 rice against differentially virulent brown planthoppers

Bin Yu[1], Mengjia Geng[1], Yu Xue[1], Qingqing Yu[1], Bojie Lu[2], Miao Liu[1], Yuhan Shao[1], Chenxi Li[1], Jingang Xu[1], Jintao Li[1], Wei Hu[3], Hengmin Tang[1], Peng Li[1], Qingsong Liu[1,4]* and Shengli Jing[1]*

[1]College of Life Sciences, Xinyang Normal University, Xinyang, China, [2]Hubei Provincial Key Laboratory for Protection and Application of Special Plant Germplasm in Wuling Area of China, College of Life Sciences, South-Central Minzu University, Wuhan, China, [3]Guangdong Provincial Key Laboratory of New Technology in Rice Breeding, Rice Research Institute, Guangdong Academy of Agricultural Sciences, Guangzhou, China, [4]State Key Laboratory of Cotton Bio-breeding and Integrated Utilization, State Key Laboratory of Crop Stress Adaptation and Improvement, Key Laboratory of Plant Stress Biology, School of Life Sciences, Henan University, Kaifeng, China

Introduction: The brown planthopper (BPH) poses a significant threat to rice production in Asia. The use of resistant rice varieties has been effective in managing this pest. However, the adaptability of BPH to resistant rice varieties has led to the emergence of virulent populations, such as biotype Y BPH. YHY15 rice, which carries the BPH resistance gene *Bph15*, exhibits notable resistance to biotype 1 BPH but is susceptible to biotype Y BPH. Limited information exists regarding how resistant rice plants defend against BPH populations with varying levels of virulence.

Methods: In this study, we integrated miRNA and mRNA expression profiling analyses to study the differential responses of YHY15 rice to both avirulent (biotype 1) and virulent (biotype Y) BPH.

Results: YHY15 rice demonstrated a rapid response to biotype Y BPH infestation, with significant transcriptional changes occurring within 6 hours. The biotype Y-responsive genes were notably enriched in photosynthetic processes. Accordingly, biotype Y BPH infestation induced more intense transcriptional responses, affecting miRNA expression, defenserelated metabolic pathways, phytohormone signaling, and multiple transcription factors. Additionally, callose deposition was enhanced in biotype Y BPH-infested rice seedlings.

Discussion: These findings provide comprehensive insights into the defense mechanisms of resistant rice plants against virulent BPH, and may potentially guide the development of insect-resistant rice varieties.

KEYWORDS

rice, *Bph15*, brown planthopper, virulent populations, resistance mechanism

1 Introduction

Rice (*Oryza sativa* L.) was domesticated approximately 10,000 years ago in the lower Yangtze Valley in China. From there, it spreads across Asia, Africa, Europe, and the Americas, and now serves as a staple crop for more than half of the world's population (Cheng et al., 2013; Gutaker et al., 2020). However, rice production suffers from numerous pests and pathogens. Among them, the brown planthopper (BPH; *Nilaparvata lugens* Stål) is considered extremely destructive (Bottrell and Schoenly, 2012; Cheng et al., 2013; Jing et al., 2017). BPH feeds on phloem sap and causes dwarfing, wilting, browning, drying, and ultimately death in severe cases (Wang et al., 2008). In addition, BPH serves as a vector for viral diseases, resulting in significant yield shortfalls and economic losses (Cheng et al., 2013).

Over the course of an evolutionary arms race between these two species, rice has developed sophisticated defensive mechanisms against BPH (Cheng et al., 2013), including both basic defenses and resistance (R) gene-mediated defenses. To date, approximately 40 major BPH resistance genes have been identified in cultivated and wild rice species (Wang et al., 2023). Molecular cloning and functional characterization of BPH resistance genes have clarified the molecular mechanisms of rice resistance to BPH (Zheng et al., 2021). One mechanism involves the occlusion of sieve tubes with callose, which is a common plant defense against sap-sucking insects. This mechanism is the most effective in rice varieties carrying BPH resistance genes such as B5 (carrying *Bph14* and *Bph15*), RI35 (carrying *Bph14*), and YHY15 (carrying *Bph15*) (Hao et al., 2008). In susceptible varieties such as Taichung Native1 (TN1), β-1,3-glucanases (which are only weakly induced in resistant plants) decompose the deposited callose and thereby facilitate continuous feeding by BPH (Hao et al., 2008). *Bph14* encodes a typical CC-NB-LRR protein which interacts with the transcription factors (TFs) OsWRKY46 and OsWRKY72 to increase the expression of the receptor-like cytoplasmic kinase gene *RLCK281* and the callose synthase gene by binding to their promoters (Du et al., 2009; Hu et al., 2017). *Bph15* is located on the short arm of chromosome 4 and is composed of a gene cluster encoding three plant lectin receptor-like kinase proteins (LecRLKs) (Yang et al., 2004; Lv et al., 2014; Xiao et al., 2016). However, the precise mechanism by which *Bph15* confers resistance to BPH is unknown.

Phytohormones are thought to play pivotal roles in the interaction of rice plants and BPH herbivory, including salicylic acid (SA), ethylene (ET), jasmonic acid (JA), cytokinin (CK), brassinosteroid (BR), and abscisic acid (ABA). The SA pathway contributes to the immune response against piercing–sucking insects and is involved in *Bph6*-, *Bph9*-, *Bph14*-, and *Bph29*-mediated resistance in rice (Du et al., 2009; Wang et al., 2015; Zhao et al., 2016; Hu et al., 2017; Guo et al., 2018). Antagonistically, ET negatively regulates BPH resistance in rice (Lu et al., 2011, 2014; Ma et al., 2020). However, the role of JA in rice resistance to BPH remains controversial as the silencing of different genes related to JA biosynthesis and signaling results in diverse impacts on BPH resistance. For example, silencing *9-lipoxygenase* (*OsLOX9*/*OsHI-LOX*, a JA biosynthesis-related gene) enhances BPH resistance, suggesting that JA negatively regulates BPH resistance (Zhou et al., 2009). On the other hand, silencing *coronatine insensitive 1* (*OsCOI1*, a JA receptor gene) has no effect on BPH resistance (Ye et al., 2012). According to studies in allene oxide cyclase (AOC, a JA biosynthesis-related enzyme)- and Myelocytomatosis protein 2 (MYC2, a bHLH TF in the JA pathway)-knockout mutant rice, JA appears to be a positive regulator of BPH resistance (Xu et al., 2021). The exogenous application of JA similarly suggests this (Guo et al., 2018). Recent research also suggests that CK may positively regulate BPH resistance in a JA-dependent manner (Zhang et al., 2022). Conversely, BR promotes BPH susceptibility by modulating SA and JA signaling (Pan et al., 2018). ABA enhances BPH resistance by promoting callose formation (Dinh et al., 2013; Liu et al., 2017) and synergizes with JA to stimulate the expression of TFs in BPH-infested rice (Li et al., 2022). Furthermore, a coordinated CK, SA, and JA signaling network has been found to be activated in *Bph6*-near isogenic lines (NILs) (Guo et al., 2018). Taken together, these findings suggest that the various phytohormones play diverse roles in the BPH defense response, and that there is complex crosstalk between them.

BPH biotypes with increased virulence have emerged in response to pressures imposed by these defense mechanisms, which are capable of overcoming resistance conferred by major resistance genes. Biotype 1 BPH, which exhibits low virulence on resistant rice varieties, is widely distributed across southeast Asia and primarily parasitizes susceptible varieties such as TN1 (Alam & Cohen, 1998). Rearing biotype 1 BPH on resistant rice variety YHY15 (carrying *Bph15*) for several years resulted in the development of highly-virulent biotype Y BPH, which are able to overcome resistance conferred by *Bph15* (Jing et al., 2011). Similarly, after force-feeding 40 generations of local BPH using resistant IR56 rice (carrying *Bph3*), the resulting BPH population (IR56-BPH) was able to overcome *Bph3*-conferred resistance (Zheng et al., 2016). In addition, the Mudgo BPH population has been reported to cause substantial damage to Mudgo rice plants (carrying *Bph1*) (Ji et al., 2013; Wan et al., 2019). In response to selective pressures imposed by these resistance genes, BPH populations accumulate adaptations over generations which eventually allow them to overcome such resistance mechanisms. In effect, this process constitutes a loss of resistance in formerly-resistant rice varieties against them. However, the effectiveness of resistance strategies used by different rice varieties against BPH populations with varying levels of virulence requires further investigation. Such combinations of avirulent/virulent BPH and resistant rice provide ideal models for studying resistance adaptation mechanisms.

Just as plants have evolved intricate defense mechanisms to protect themselves against herbivorous insects, insects have in turn developed strategies to overcome plant defenses (Liu Q. et al., 2021). Interactions between plants and insects involve an array of molecular, biochemical, and physiological processes occurring at multiple levels. Multi-omics analyses integrate genomics, transcriptomics, proteomics, and metabolomics, as well as other "omics" approaches, in order to clarify the intricate signaling pathways, molecular responses, and biochemical processes involved in the dynamic interplay between plants and insects (Wang et al., 2020; Shi et al., 2023). Transcriptional profiling has

aided our understanding of the defense mechanisms utilized by rice against BPH. For example, research suggests that BPH infestation results in the upregulation of genes involved in signaling, oxidative stress, pathogen-related response, and macromolecule degradation, as well as the downregulation of genes associated with flavonoid biosynthesis, photosynthesis, and cell growth (Zhang et al., 2004; Yuan et al., 2005; Wang et al., 2008). In addition, microarray analyses of BPH-infested Rathu Heenati and TN1 rice underscore the importance of TFs and phytohormones in the defense response (Wang et al., 2012; Li et al., 2017).

MicroRNAs (miRNAs) are small (approximately 21 nt in length) regulatory RNAs produced through endonucleolytic processing of hairpin precursors (Axtell and Meyers, 2018). miRNAs regulate gene expression by binding to complementary sequences in mRNA molecules, resulting in degradation and/or translational inhibition (Bartel, 2009). In plants, miRNAs are involved in various processes such as phytohormone signaling; abiotic and biotic stress response (Zhang et al., 2013, 2016; Li et al., 2017; Natarajan et al., 2018; Salvador-Guirao et al., 2018; Zhang et al., 2018; Liu X. et al., 2021); and leaf, flower, shoot, root, and vascular tissue development (Marin et al., 2010; Peng et al., 2014; Mangrauthia et al., 2017). However, only a few miRNAs have been found to play roles in the insect-plant interaction (Jing et al., 2023). For example, in an investigation of resistant and susceptible rice varieties, the BPH-responsive miRNAs miR156 and miR396 were found to negatively regulate BPH resistance by regulating JA and flavonoid biosynthesis, respectively (Wu et al., 2017; Ge et al., 2018; Dai et al., 2019). Studies of BPH-responsive mRNA and miRNA transcriptomes have uncovered certain universal responses of rice to BPH infestation (Li et al., 2017; Wu et al., 2017; Nanda et al., 2020). Additionally, integrated expression profiling of miRNAs and target genes associated with the BPH-rice interaction has been conducted (Tan et al., 2020). Such combined miRNA and mRNA analyses will be key to unraveling the transcriptional responses of rice to BPH infestation.

In this study, we employed high-throughput sequencing to analyze the mRNA and miRNA expression profiles of YHY15 rice seedlings infested with either biotype 1 BPH (avirulent population) or biotype Y BPH (virulent population). Furthermore, we combined sequence analysis and physiological assays to reveal the underlying resistance mechanisms of rice against BPH. The findings presented in this work will provide a valuable resource for further genome-wide investigations of BPH-responsive genes, as well as studies of *Bph15*-mediated resistance. Moreover, these findings improve our understanding of the intricate interactions between rice and BPH, and may be used in the development of effective BPH management strategies.

2 Materials and methods

2.1 Plant and insect materials

In this study, we used two rice varieties (Taichung Native1 [TN1] and YHY15) and two BPH populations (biotype 1 and biotype Y). TN1 is a susceptible rice cultivar, while YHY15 is a recombinant inbred line (RIL) derived from the RI93 × TN1 F2 population carrying resistance gene *Bph15* (Yang et al., 2004). Biotype 1 BPH (avirulent) originated from Wuhan University (China) and are reared on TN1. Biotype Y BPH (virulent) were developed by rearing biotype 1 BPH on YHY15 plants beginning in January 2007 (Jing et al., 2011). All rice plants were grown from seeds sown in sponges (6 cm diameter, 2 cm height), with 8 rice plants per cup. Rice plants were reared in a controlled-environment incubator maintained at 30 ± 2 °C during daytime hours (16 h, 06:00–22:00) and 28 ± 2 °C during nighttime hours (8 h, 22:00–06:00). Rice plants were grown for approximately 2-5 weeks following sowing, depending on experimental needs. The BPH populations were reared at Xinyang Normal University (China) under the following conditions: 26 ± 1 °C, 16 h light/8 h dark cycle. Third instar BPH nymphs were used for the infestation experiments.

2.2 Evaluation of BPH resistance in rice

At the two-leaf (2-week-old) stage, YHY15 rice plants were infested with third instar biotype 1 or biotype Y BPH nymphs at a rate of 15 nymphs per seedling. The growth status of each plant was photographically recorded daily until all biotype Y-infested seedlings died. Each experiment consisted of three biological replicates.

2.3 Measurement of BPH weight gain and honeydew excretion

BPH weight gain and honeydew excretion were measured as described previously (Shi et al., 2021). Briefly, newly-emerged adult female BPH were weighed using an electronic balance (Mettler Toledo, MS105DU, Switzerland) and subsequently separated into pre-weighed parafilm sachets (2 × 2.5 cm) fixed to the leaf sheaths of 4-week-old rice plants. After 48 h, the insects were carefully removed from the sachets, and both the insect and the honeydew in each sachet were separately weighed. Weight gain was calculated by comparing each insect's weight before and after feeding, and the weight gain ratio was calculated by dividing the weight gain by the initial weight. Both the weight gain and honeydew excretion assays were conducted using at least 37 replicates.

2.4 BPH infestation and sample collection

Three-week-old YHY15 rice seedlings were infested with third-instar biotype 1 (RT) and biotype Y (RY) BPH at a rate of 15 nymphs per seedling. Each treatment consisted of three biological replicates, with six seedlings per replicate. For RNA-seq and miRNA-seq analysis, leaf sheaths were collected from non-infested controls (0 h), and during early (6 h) and late (48 h) infestation. According to their time of collection, samples of non-infested rice plants were labeled 'R0', samples of biotype 1-infested rice plants were labeled as 'RT6' or 'RT48', and samples of biotype Y-infested rice plants were labeled as 'RY6' or 'RY48'. Each sampled

leaf sheath blade was excised, frozen in liquid nitrogen, and stored at -80 °C for further use.

2.5 mRNA transcriptome sequencing and analysis

2.5.1 RNA extraction, quantification, and qualification

Total RNA was isolated from rice samples using RNA Trizol reagent (Life Technologies, NY, USA), following the manufacturer's instructions. RNA degradation and contamination were evaluated using 1% agarose gels. RNA purity was quantified using a NanoPhotometer spectrophotometer (Implen, CA, USA). RNA integrity was assessed using an RNA Nano 6000 Assay Kit for the Bioanalyzer 2100 system (Agilent Technologies, CA, USA).

2.5.2 Library construction, quality control, and sequencing

RNA libraries were generated using 1 μg of RNA per sample and the NEBNext Ultra RNA Library Prep Kit for Illumina. Index codes were incorporated to distinguish between samples. Briefly, mRNA was purified using poly-T oligo-attached magnetic beads, followed by fragmentation using divalent cations. First-strand cDNA synthesis was carried out using random hexamer primers and M-MuLV Reverse Transcriptase. The second strand was synthesized using DNA Polymerase I and RNase H. Overhangs were blunted using exonucleases or polymerases and NEBNext adaptors were ligated following adenylation. The library fragments (250~300 bp) were purified using an AMPure XP system. The USER Enzyme was applied to size-selected, adaptor-ligated cDNA prior to PCR. PCR was carried out using Phusion High-Fidelity DNA polymerase, Universal PCR primers, and Index (X) Primer. The PCR products were purified using an AMPure XP system, and library quality was evaluated using an Agilent Bioanalyzer 2100 system. Index-coded samples were clustered with a cBot Cluster Generation System using a TruSeq PE Cluster Kit v3-cBot-HS (Illumina), according to the manufacturer's instructions. After clustering, the libraries were sequenced on an Illumina NovaSeq platform, generating 150 bp paired-end reads.

2.5.3 Data analysis

Raw data (fastq format) were first processed using in-house perl scripts. In this step, low-quality reads, adapter sequences, and poly-Ns were removed. Subsequently, the Q20, Q30, and GC content of the clean reads were calculated. All downstream analyses utilized only clean, high-quality data. Next, the reference genome and gene model annotation files were downloaded. An index of the reference genome was constructed, and clean paired-end reads were aligned to the reference genome, using Hisat2 (v2.0.5). The mapped reads from each sample were assembled with StringTie (v1.3.3b) using a reference-based approach. featureCounts (v1.5.0-p3) was used to count the number of reads mapped to each gene. The Transcripts Per Kilobase Million (TPM) of each gene was quantified based on the gene length and the number of reads mapped to the gene. Differentially expressed genes (DEGs) were identified using the R (v1.16.1) package DESeq2, with three biological replicates per treatment, according to the following criteria: P-value < 0.05, false discovery rate (FDR) < 5, and absolute value of $\log_2$ fold change (FC) ≥ 1. The DEGs underwent additional screening through soft clustering using the Mfuzz package, employing a fuzzy c-means algorithm, as previously reported (Kumar and Futschik, 2007). DEGs exhibiting similar expression patterns were categorized into 20 clusters, and the genes within these clusters were subjected to Gene Ontology (GO) and Kyoto Encyclopedia of Genes and Genomes (KEGG) analyses. GO annotations were downloaded from NCBI (http://www.ncbi.nlm.nih.gov/) and GO (http://www.geneontology.org/). The KEGG database was used to identify BPH-responsive pathways. Fisher's exact tests were applied to identify significant GO and KEGG categories according to the absolute values of $P < 0.05$ and FDR < 0.05.

2.6 miRNA transcriptome sequencing and analysis

2.6.1 RNA extraction, quantification, and qualification

RNA extraction, quantification, and qualification were conducted as described in section 2.5.1.

2.6.2 Library construction, quality control, and sequencing

Briefly, 3' and 5' adaptors were ligated to the 3' and 5' ends of small RNAs, respectively. Next, first strand cDNA was synthesized after hybridization with the reverse transcription primer. The double-stranded cDNA library was generated through PCR enrichment. After purification and size selection, libraries with 18~40 bp insertions were selected for Illumina sequencing with SE50. The library was quantified with Qubit and real-time PCR and the library size distribution was evaluated with a Bioanalyzer. Quantified libraries were pooled and sequenced on an Illumina platform, according to the effective library concentration and amount of data required.

2.6.3 Data analysis

Raw data (fastq format) were first processed using in-house perl and python scripts. In this step, low-quality reads; reads containing poly-Ns, 5' adapter sequences, or poly-As/Ts/Gs/Cs; and reads missing 3' adapter sequences or insert tags were removed. Subsequently, the Q20, Q30, and GC content of the clean reads were calculated. All downstream analyses utilized only clean, high-quality data. Small RNA tags were mapped to the reference sequence using Bowtie (Langmead et al., 2009), either without mismatches or with only one mismatch, to analyze their expression and distribution. Mapped small RNA tags were used to identify known miRNAs, with miRBase (v22.0) used as a reference. miRNAs were identified using a modified version of mirdeep2 (Friedlander et al., 2012) and srna-tools-cli was used to draw the secondary structures. Custom scripts were used to obtain

miRNA counts as well as to determine base bias at the first position of identified miRNAs of a certain length and at each position of all identified miRNAs. To remove tags originating from protein-coding genes, repeat sequences, rRNA, tRNA, snRNA, and snoRNA, small RNA tags were mapped to RepeatMasker, the Rfam database, or species-specific data. DEGs were identified using DESeq2. *P*-values were adjusted using the Benjamini & Hochberg method. A corrected *P*-value of 0.05 was selected as the threshold for determining significantly differential expression.

2.7 Analysis of transcriptional signatures of phytohormone responses

To identify the transcriptional signatures of BPH-responsive phytohormone responses, Hormonometer was used to compare gene expression in rice with gene expression in phytohormone-treated *Arabidopsis thaliana* (Volodarsky et al., 2009; Liu et al., 2016). Specifically, only orthologous genes detected in the RNA-seq analysis which were related to the *Arabidopsis thaliana* probe set identifiers were selected for further analyses.

2.8 qRT–PCR validation of DEGs

First-strand cDNA was synthesized using a PrimeScript RT Reagent Kit with gDNA Eraser (Takara, Japan), according to the manufacturer's instructions. qRT-PCR assays of candidate genes were conducted using a PrimeScript™ RT reagent Kit with gDNA Eraser (Perfect Real Time) (Takara, RR047A, China). qRT-PCR was carried out on a CFX96 Real-Time System (Bio-Rad, CA, USA) according to the following protocol: 95 °C for 5 min, followed by 40 cycles at 95 °C for 5 s, 60 °C for 30 s, and 72 °C for 30 s. Relative gene expression was calculated with the 2−11Ct method, using *PP2A* as the reference gene. All primer sequences are listed in Supplementary Table 1.

2.9 Callose staining and evaluation

Callose staining and evaluation were performed as described in a previous study (Hu et al., 2017). Briefly, fresh sheaths collected from two-leaf stage rice seedlings infested with either biotype 1 or Y BPH for 48 h were fixed in an ethanol:acetic acid (3:1 v/v) solution for 5 h. The fixative was changed frequently to ensure thorough fixing and clearing. The samples were then rehydrated successively in 70% ethanol for 2 h, in 50% ethanol for 2 h, and in water overnight. After rinsing three times with water, the samples were treated with 10% NaOH for 1 h to make the tissues transparent. After rinsing four times with water, the samples were incubated in 150 mM K_2HPO_4 (pH 9.5) containing 0.01% aniline blue for 4 h. Finally, the samples were mounted on a slide and callose deposits were observed with a positive fluorescence microscope (Nikon, Eclipse 80i, Japan) under the UV channel.

2.10 Statistical analysis

Statistical analyses were conducted using R (v4.0.4) and SPSS (v22.0) (IBM SPSS, Somers, NY, USA). Two-sided Student's *t*-tests were used to determine statistically significant differences between groups. All bioinformatics analyses were conducted using R packages.

3 Results

3.1 YHY15 exhibits differential resistance to biotype 1 and biotype Y BPH

YHY15 rice, which contains the BPH resistance gene *Bph15*, exhibits robust resistance against avirulent BPH biotypes (i.e., biotype 1) (Yang et al., 2004). In this study, YHY15 seedlings were subjected to infestation by either biotype 1 or biotype Y BPH. The results suggest that YHY15 exhibited distinct responses under the two infestation scenarios. In response to infestation with biotype Y BPH, YHY15 seedlings exhibited signs of withering at 4 days and eventually wilted completely by 7 days. In contrast, seedlings infested with biotype 1 BPH remained healthy and continued to grow vigorously (Figure 1A). To evaluate the ability of YHY15 rice to affect the biology of BPH insects, we measured the weight gain and amount of honeydew produced by the two BPH populations. As expected, biotype Y exhibited a significantly higher weight gain ratio (mean = 41.4%) than biotype 1 (mean = −2.2%) (Figure 1B). In addition, biotype Y produced significantly more honeydew (mean = 16.49 mg) than biotype 1 (mean = 0.57 mg) (Figure 1C). These findings indicate that YHY15 rice plants are highly resistant to biotype 1 BPH but are susceptible to biotype Y BPH, as previously reported (Yang et al., 2004; Jing et al., 2011; Guan et al., 2022). Overall, these results provide strong evidence for the contrasting responses of YHY15 rice to BPH with different levels of virulence, and highlight the efficacy of the *Bph15* gene in conferring resistance against specific BPH strains.

3.2 Overview of the miRNA- and RNA-seq results

To better understand the mechanisms underlying the differential resistance displayed by YHY15 rice to virulent and avirulent BPH, we performed RNA and miRNA sequencing analyses using leaf sheaths from YHY15 seedlings infested with either biotype 1 (RT) or Y (RY) BPH for either 6 (RT6, RY6) or 48 h (RT48, RY48). Un-infested rice plants were used as controls and named as R0. After constructing and sequencing the mRNA/miRNA libraries, high-quality raw sequence reads were normalized and subjected to further analysis.

Out of the 738 identified miRNAs, miR396, miR167, miR166, miR162, miR159, miR156, miR820, miR408, miR1425, miR1862, miR444, and miR827 exhibited the highest relative abundance

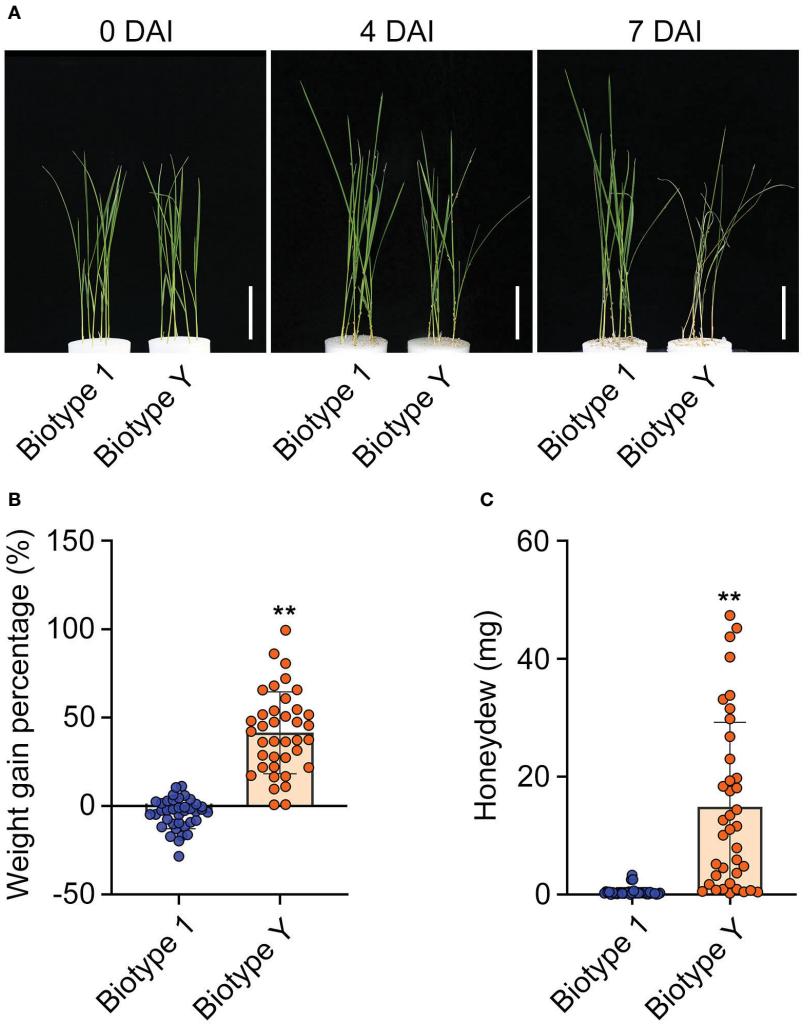

FIGURE 1
Resistance of YHY15 rice plants against biotype 1 and biotype Y BPH. **(A)** YHY15 seedlings infested with biotype 1 or biotype Y BPH. DAI, days after infestation. Scale bar = 5 cm. **(B)** BPH weight gain ratio on YHY15 seedlings. **(C)** BPH honeydew excretion on YHY15 seedlings. Data are shown as means ± SD of 38 biological replicates in **(B)** and **(C)**. Biotype 1, biotype 1 BPH-infested YHY15 seedlings; Biotype Y, biotype Y BPH-infested YHY15 seedlings. Asterisks indicate statistically significant differences between YY and TY (two-tailed Student's *t*-test, $^{**}P < 0.01$).

(Supplementary Table 2). Principal component analysis (PCA) of the miRNA-seq data revealed significant variation between the R0 group and the RY6 or RY48 group, indicating that biotype Y BPH infestation led to distinct fluctuations in the miRNA profiles (Figure 2A). Among the 50 differentially expressed miRNAs (DEMs) detected in R0 *vs* RY6, 13 were upregulated and 37 were downregulated (Figure 2B; Supplementary Table 3). As infection progressed, more DEMs (64) were identified in R0 *vs* RY48, 16 of which were upregulated and 48 were downregulated (Figure 2B; Supplementary Table 3). In total, 38 DEMs were shared between R0 *vs* RY6 and R0 *vs* RY48, with 12 unique DEMs detected at the earlier time point and 26 at the later time point (Figure 2C). These results suggest that many more miRNAs are involved in the interaction between YHY15 and biotype Y BPH than in the interaction between YHY15 and biotype 1 BPH. Among these, miR156, miR5076, miR1856, miR398, miR5072, miR5079, miR408, miR2873, and miR169 exhibited significant variation in amplitude (Table 1). Many of these miRNAs have been reported to play specific roles in plant developmental processes and biotic and abiotic stress responses (Sharma et al., 2015; Zhao et al., 2017; Lin et al., 2018; Liu et al., 2019; Liebsch and Palatnik, 2020; Li et al., 2020; Liu X. et al., 2021; Gao et al., 2022; Pachamuthu and Hari Sundar, 2022; Zhao et al., 2022). Their high abundance and variable expression patterns suggest that they may contribute to BPH resistance in YHY15 seedlings, and therefore subsequent analyses were conducted on these miRNAs.

In comparison, PCA of the RNA-seq data revealed distinct separation among all groups (Figure 2D; Supplementary Table 4). Through comparison of RNA expression levels across different groups, we identified 1027 and 1154 differential expression analysis (DEGs) in R0 *vs* RT6 and R0 *vs* RT48, respectively. Notably, a larger number of DEGs were observed in R0 *vs* RY6 and R0 *vs* RY48 (6817 and 6273, respectively), suggesting that infestation with biotype Y BPH results in more severe effects than infestation with biotype 1 BPH (Figure 2E). A Venn diagram was used to compare the expression patterns of DEGs in avirulent/

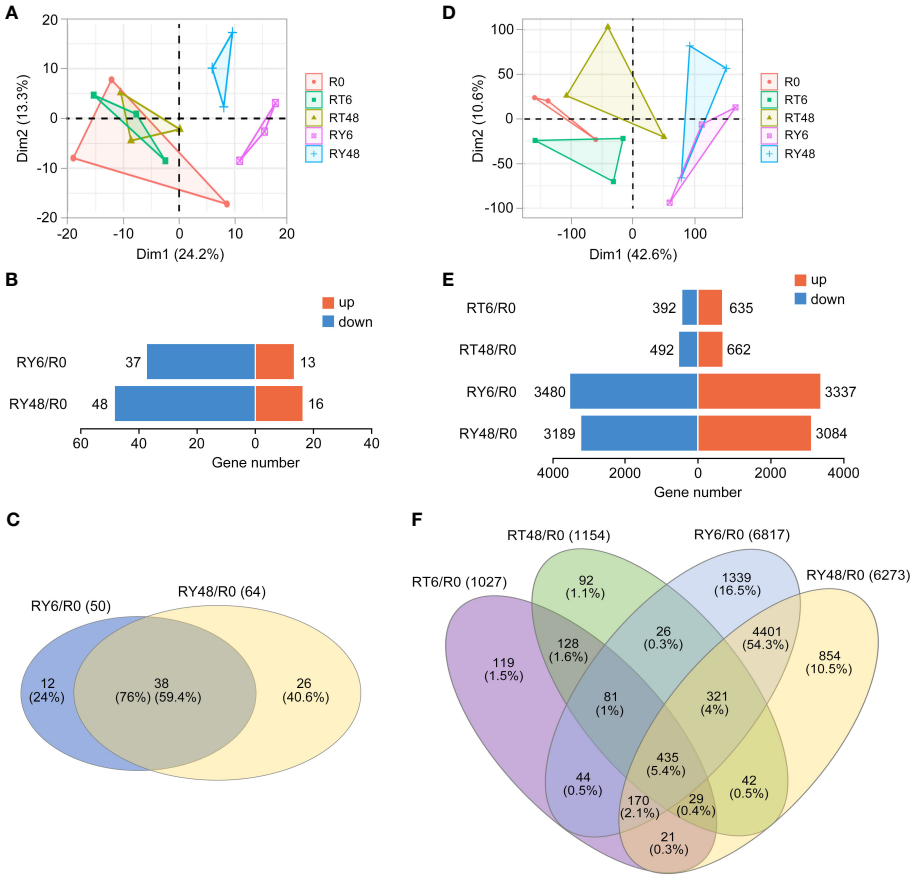

FIGURE 2
Overview of miRNA-seq and RNA-seq results. **(A)** Principal component analysis (PCA) of miRNA-seq data from five comparisons. **(B)** Number of miRNAs up- or downregulated in all comparisons (|$\log_2$ fold change| > 1, $P < 0.05$). **(C)** Venn diagrams of differentially expressed miRNAs in all comparisons. **(D)** PCA of RNA-seq data from five comparisons. **(E)** Number of mRNAs up- or downregulated in all comparisons (|$\log_2$ fold change| > 1, $P < 0.05$). **(F)** Venn diagrams of differentially expressed mRNAs in all comparisons. There are four comparisons: RT6/R0, RT48/R0, RY6/R0, RY48/R0. R0, uninfected controls; RT6, YHY15 seedlings infested with biotype 1 BPH for 6 h; RT48, YHY15 seedlings infested with biotype 1 BPH for 48 h; RY6, YHY15 seedlings infested with biotype Y BPH for 6 h; RY48, YHY15 seedlings infested with biotype Y BPH for 48 h.

virulent BPH-infested rice at the early (6 h) and late (48 h) stages of infestation, and the identified DEGs were subjected to GO and KEGG enrichment analyses (Figure 2F; Supplementary Figure 1; Supplementary Table 5). We identified 730 overlapping DEGs in R0 *vs* RT6 and R0 *vs* RY6 at the early infestation stage, which were enriched in cytochrome P450 (KEGG), protein modification-related biological processes (BP, GO), extracellular region (CC, GO), and monooxygenase activity (MF, GO) (Figure 2F; Supplementary Figures 1A, B). Specifically, genes in R0 *vs* RY6 were enriched in ribosome, photosynthesis proteins, carbon fixation in photosynthetic organisms, and DNA replication proteins (Figure 2F; Supplementary Figures 2A, B). However, genes in R0 *vs* RT6 did not exhibit these enrichments. We identified 827 overlapping DEGs in R0 *vs* RT48 and R0 *vs* RY48 at the late infestation stage, which were enriched in photosynthesis proteins, porphyrin metabolism, zeatin biosynthesis, and cytochrome P450, suggesting disturbance to the photosynthetic system (KEGG) (Figure 2F; Supplementary Figures 3A, B). Additionally, genes in R0 *vs* RY48 were enriched in ribosome-related pathways, DNA replication proteins, photosynthesis proteins, and carbon fixation in photosynthetic organisms (Figure 2F; Supplementary Figures 4A, B). These results indicate that infestation with biotype Y BPH results in damage to the photosynthetic system earlier than infestation with biotype 1 BPH, which is consistent with the phenotypic observations (Figure 1A).

3.3 Transcriptional responses in YHY15 rice to BPH infestation

To elucidate the genome-wide responses of YHY15 rice to BPH infestation, the transcriptome was analyzed over the entire infection time course. According to Mfuzz analysis, distinct temporal patterns were clustered into 20 groups (Figure 3; Supplementary Table 6). Notably, clusters 1 to 4 exhibited significantly lower levels of transcription in RY6/48 compared to R0, whereas this trend was less pronounced in RT6/48 (Figure 3; Supplementary Table 6). The genes in these clusters were subjected to GO and KEGG enrichment analyses to explore their functions. Genes in cluster 1 were enriched in photosynthesis proteins, carbon fixation in photosynthetic organisms, terpenoid backbone biosynthesis, and porphyrin metabolism (Figure 4A; Supplementary Table 7). Accordingly,

10.3389/fpls.2024.1366515

TABLE 1 Candidate BPH resistance-related DEMs.

osa-miRNA	Fold change (log_2)		Target genes
	RY6/R0	RY48/R0	
miR11342-3p	1.22	–	LOC107277366; LOC107278339; LOC9270471; LOC4347355; LOC4327594
miR1320-3p	–	-4.28	LOC4341008; LOC4341009; LOC9272503; LOC107276137; LOC112937314
miR1423-3p	–	1.18	LOC4334792; LOC4334793; LOC4352758; LOC4352759; LOC112936210
miR1425-3p	1.71	–	LOC107277584; LOC4347752; LOC4347753; LOC9267694; LOC9267104
miR1432-5p	-1.59	-1.28	LOC4331372; LOC9270922; LOC107281270; LOC112939644; LOC9269030
miR156a	-1.28	-1.56	LOC4338174; LOC4333935; LOC4333937; LOC4328870; LOC4332289
miR156b-5p	-1.28	-1.56	LOC4338174; LOC4333935; LOC4333937; LOC4328870; LOC4332289
miR156c-3p	–	-4.39	LOC4335110; LOC4335111; LOC9268400; LOC107278252; LOC107279186
miR156c-5p	-1.28	-1.56	LOC4338174; LOC4333935; LOC4333937; LOC4328870; LOC4332289
miR156d	-1.02	-1.08	LOC4338174; LOC4333935; LOC4333937; LOC4328870; LOC4332289
miR156e	-1.28	-1.56	LOC4338174; LOC4333935; LOC4333937; LOC4328870; LOC4332289
miR156f-3p	–	-3.36	LOC9269030; LOC4348312; LOC4332049; LOC9269785; LOC4335110
miR156f-5p	-1.02	-1.08	LOC4338174; LOC4333935; LOC4333937; LOC4328870; LOC4332289
miR156g-3p	–	-4.39	LOC4335110; LOC4335111; LOC9268400; LOC107278252; LOC107279186
miR156g-5p	-1.28	-1.56	LOC4338174; LOC4333935; LOC4333937; LOC4328870; LOC4332289
miR156h-3p	–	-3.36	LOC9269030; LOC4348312; LOC4332049; LOC9269785; LOC4335110
miR156h-5p	-1.02	-1.08	LOC4338174; LOC4333935; LOC4333937; LOC4328870; LOC4332289
miR156i	-1.28	-1.56	LOC4338174; LOC4333935; LOC4333937; LOC4328870; LOC4332289
miR156j-5p	-1.02	-1.08	LOC4338174; LOC4333935; LOC4333937; LOC4328870; LOC4332289
miR156k	–	-2.01	LOC4331703; LOC4338174; LOC4335101; LOC107276848; LOC4341195
miR156l-3p	–	-3.36	LOC9269030; LOC4348312; LOC4332049; LOC9269785; LOC4335110
miR166a-5p	1.53	–	LOC4326513; LOC107277945; LOC107277317; LOC4347823; LOC4343486
miR166c-5p	–	-1.13	LOC4347823; LOC107277945; LOC4326513; LOC112939883; LOC4343038
miR166d-5p	-1.47	-1.97	LOC4326513; LOC4343486; LOC9266571; LOC9268304; LOC4338511
miR166e-5p	1.94	–	LOC4326513; LOC107277945; LOC107277317; LOC4347823; LOC4343486
miR166j-5p	-1.75	-1.81	LOC9269030; LOC107281130; LOC4332497; LOC4325456; LOC4325457
miR166k-3p	–	1.18	LOC107281270; LOC4343122; LOC4328998; LOC107277945; LOC4326262
miR166l-3p	–	1.17	LOC107281270; LOC4343122; LOC4328998; LOC107277945; LOC4326262
miR167h-3p	-1.85	-2.33	LOC107278090; LOC107279103; LOC9267730; LOC4348767; LOC112935985
miR169h	–	-2.37	LOC107277945; LOC107277048; LOC4340902; LOC107277584; LOC4347752
miR169i-3p	–	-1.11	LOC9269693; LOC4352155; LOC4352156; LOC107277945; LOC112938521
miR169i-5p.1	–	-2.37	LOC107277945; LOC107277048; LOC4340902; LOC107277584; LOC4347752
miR169j	–	-2.37	LOC107277945; LOC107277048; LOC4340902; LOC107277584; LOC4347752
miR169k	–	-2.37	LOC107277945; LOC107277048; LOC4340902; LOC107277584; LOC4347752
miR169l	–	-2.37	LOC107277945; LOC107277048; LOC4340902; LOC107277584; LOC4347752
miR169r-3p	–	-2.40	LOC9269030; LOC4330994; LOC4330995; LOC107279587; LOC107277598
miR171a	1.40	1.45	LOC4331702; LOC107276230; LOC107276994; LOC4351951; LOC4349818
miR1851	-1.27	–	LOC4342932; LOC9270958; LOC4342934; LOC4335125; LOC4334367
miR1856	-3.38	-3.56	LOC4345309; LOC4345310; LOC4325535; LOC4325537; LOC107275864
miR1861c	1.22	–	LOC4331658; LOC112938679; LOC107277945; LOC9267779; LOC4330644

TABLE 1 Continued

(Continued)

10.3389/fpls.2024.1366515

TABLE 1 Continued

osa-miRNA	Fold change (log_2)		Target genes
	RY6/R0	RY48/R0	
miR1874-3p	1.34	–	LOC107277945; LOC4346563; LOC4346564; LOC4350472; LOC107276848
miR2121a	–	1.14	LOC112937314; LOC9266659; LOC4340263; LOC112938789; LOC107276637
miR2121b	–	1.14	LOC112937314; LOC9266659; LOC4340263; LOC112938789; LOC107276637
miR2871a-5p	-1.33	-1.39	LOC4331613; LOC4331617; LOC4350261; LOC112936180; LOC4330291
miR2873a	-2.05	-2.58	LOC4326290; LOC107277945; LOC9268610; LOC4347267; LOC9268583
miR319a-3p	5.40	4.59	LOC4347750; LOC107276213; LOC4347751; LOC9271092; LOC4347551
miR319a-3p.2-3p	4.05	4.58	LOC4337861; LOC4337862; LOC4326585; LOC107276637; LOC4335012
miR319b	3.88	4.42	LOC4337861; LOC4337862; LOC4326585; LOC107276637; LOC4335012
miR396a-3p	-1.05	-1.34	LOC4337237; LOC9268610; LOC4331423; LOC4326513; LOC4346184
miR396c-5p	1.01	1.25	LOC112938789; LOC4345308; LOC4331372; LOC9270922; LOC107277366
miR397a	-1.69	-1.89	LOC9267104; LOC4329608; LOC4339828; LOC4326290; LOC107277317
miR397b	-1.73	-1.66	LOC107277945; LOC9270668; LOC107276994; LOC4351951; LOC107277567
miR3980a-5p	-1.09	-1.24	LOC4352509; LOC4337053; LOC4349876; LOC112937650; LOC4352872
miR3980b-5p	-1.09	-1.24	LOC4352509; LOC4337053; LOC4349876; LOC112937650; LOC4352872
miR398a	-4.42	–	LOC4331702; LOC4335368; LOC4349919; LOC9268603; LOC4324333
miR398b	-2.56	-2.33	LOC4331702; LOC4335368; LOC4335110; LOC4335111; LOC4349919
miR399i	-1.30	–	LOC107277584; LOC4347752; LOC4347753; LOC9267694; LOC4348598
miR408-3p	-1.81	-1.57	LOC107276637; LOC4335125; LOC107277770; LOC9267065; LOC112936987
miR408-5p	-2.28	-2.45	LOC4335589; LOC9272252; LOC4334900; LOC4346674; LOC4329468
miR444a-3p.1	–	-1.83	LOC107281435; LOC4335110; LOC4335111; LOC9266659; LOC4340263

(Continued)

TABLE 1 Continued

osa-miRNA	Fold change (log_2)		Target genes
	RY6/R0	RY48/R0	
miR444b.1	-1.04	–	LOC9269785; LOC9272338; LOC107277945; LOC107280439; LOC4331618
miR444c.1	-1.04	–	LOC9269785; LOC9272338; LOC107277945; LOC107280439; LOC4331618
miR444d.1	–	-1.83	LOC107281435; LOC4335110; LOC4335111; LOC9266659; LOC4340263
miR5072	-2.47	-1.86	LOC107277317; LOC9266659; LOC4340263; LOC9272689; LOC112936211
miR5076	-3.33	-2.65	LOC107277945; LOC107279298; LOC4350353; LOC107275975; LOC4351913
miR5079a	-2.38	-2.66	LOC9270668; LOC4326380; LOC4347267; LOC107277945; LOC4332858
miR5079b	-2.38	-2.66	LOC9270668; LOC4326380; LOC4347267; LOC107277945; LOC4332858
miR528-5p	-1.58	-1.31	LOC4347809; LOC4335364; LOC107276241; LOC112936210; LOC107279401
miR535-5p	-1.06	–	LOC4324213; LOC112937314; LOC107277945; LOC107276994; LOC4351951
miR5505	2.48	1.77	LOC4350473; LOC4352601; LOC4352606; LOC4331386; LOC4338511
miR5801b	1.07	1.34	LOC9266659; LOC4340263; LOC107282017; LOC9268610; LOC112936211
miR5816	–	1.41	LOC107279289;LOC107275804; LOC107278811; LOC9269030;LOC112937448
miR818b	–	1.14	LOC4329368; LOC107277317; LOC4335309; LOC4329911; LOC107275634
miR818d	–	1.06	LOC4329368; LOC107277317; LOC4335309; LOC4329911; LOC107275634
miR818e	–	1.14	LOC4329368; LOC107277317; LOC4335309; LOC4329911; LOC107275634
miR827	-1.06	-1.12	LOC4345821; LOC4350156; LOC4352108; LOC4335589; LOC9272252

GO analysis confirmed that many of these genes were related to the photosynthesis biological process, as well as photosynthetic cellular components such as thylakoid, photosynthetic membrane, and photosystem (Supplementary Figure 5A; Supplementary Table 7).

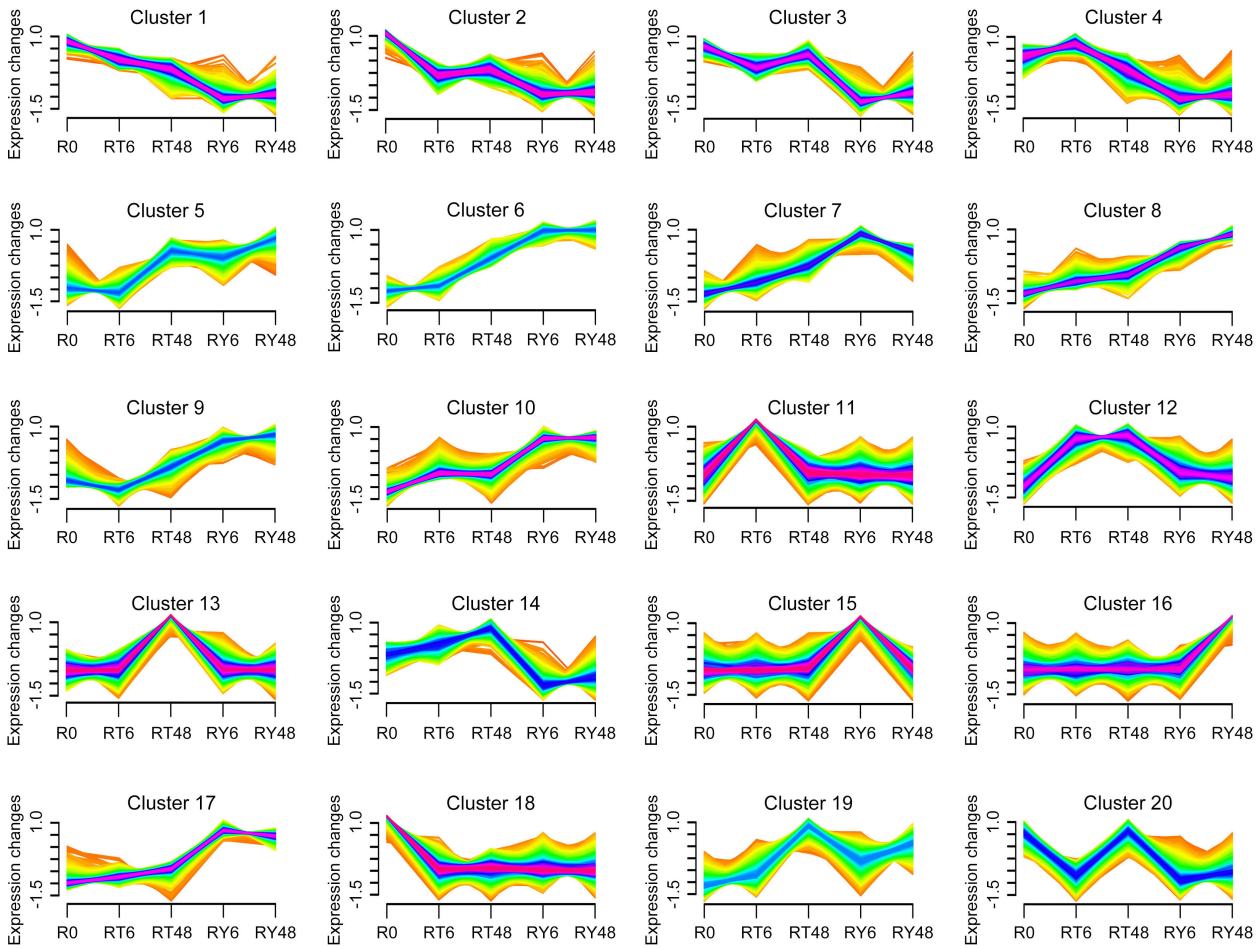

FIGURE 3
Clustering and time-course expression of genes after BPH infestation. The 20 distinct temporal gene expression patterns were computed with Mfuzz. The x axis represents the five treatment groups, and the y axis represents log_2-transformed normalized intensity ratios for each group. R0, uninfected controls; RT6, YHY15 seedlings infested with biotype 1 BPH for 6 h; RT48, YHY15 seedlings infested with biotype 1 BPH for 48 h; RY6, YHY15 seedlings infested with biotype Y BPH for 6 h; RY48, YHY15 seedlings infested with biotype Y BPH for 48 h.

These results suggest that infestation with biotype Y BPH results in significantly greater physical impairment than does infestation with biotype 1 BPH, which was consistent with the growth observations (Figure 1A).

In clusters 5 to 10, gene expression levels increased significantly in the RY groups, but only slightly in the RT groups (Figure 3; Supplementary Table 6). Genes in cluster 6 (Figure 4B; Supplementary Figure 5B; Supplementary Table 7) and cluster 9 (data not shown) were enriched in membrane trafficking (KEGG), cell membrane systems (GO), and protein transporter (GO), suggesting that defense against BPH relies on membrane transport systems and cell secretion. In cluster 7, genes were enriched in glycosyltransferases, GTP-binding proteins, phenylpropanoid biosynthesis, and two-component system (Figure 4C; Supplementary Figure 5C; Supplementary Table 7). The phenylpropanoid pathway is involved in the production of various metabolites, including flavonoids, lignin, lignans, and cinnamic acid amide, among others (Dong and Lin, 2021). Genes in cluster 10 were enriched in ribosomes, DNA replication proteins, translation factors, and other transcriptional activity-related factors (Figure 4D; Supplementary Figure 5D; Supplementary Table 7). Overall, the transcriptional system, transmembrane transport system, exosome, and phenylpropanoid pathway are notably stimulated by BPH infestation, particularly infestation with biotype Y BPH, suggesting that they may be crucial for rice resistance to insects.

The expression patterns of several clusters appeared to be desynchronized, indicative of different responses to infestation by either biotype 1 or biotype Y BPH. In clusters 11 to 14, gene expression was increased at the early (6 h) and late (48 h) stages during infestation with biotype 1 BPH, but remained relatively stable during infestation with biotype Y BPH (Figure 3; Supplementary Table 6). These clusters were mainly enriched in zeatin biosynthesis, nitrogen metabolism, cytochrome P450, and plant hormone signal transduction (Figure 4E; Supplementary Figure 5E; Supplementary Table 7). In plants, cytochrome P450 catalyzes various primary and secondary metabolic reactions and is involved in the synthesis and metabolism of terpenoids, alkaloids, sterols, fatty acids, plant hormones, signaling molecules, pigments, flavonoids, and isoflavones, among others (Hansen et al., 2021).

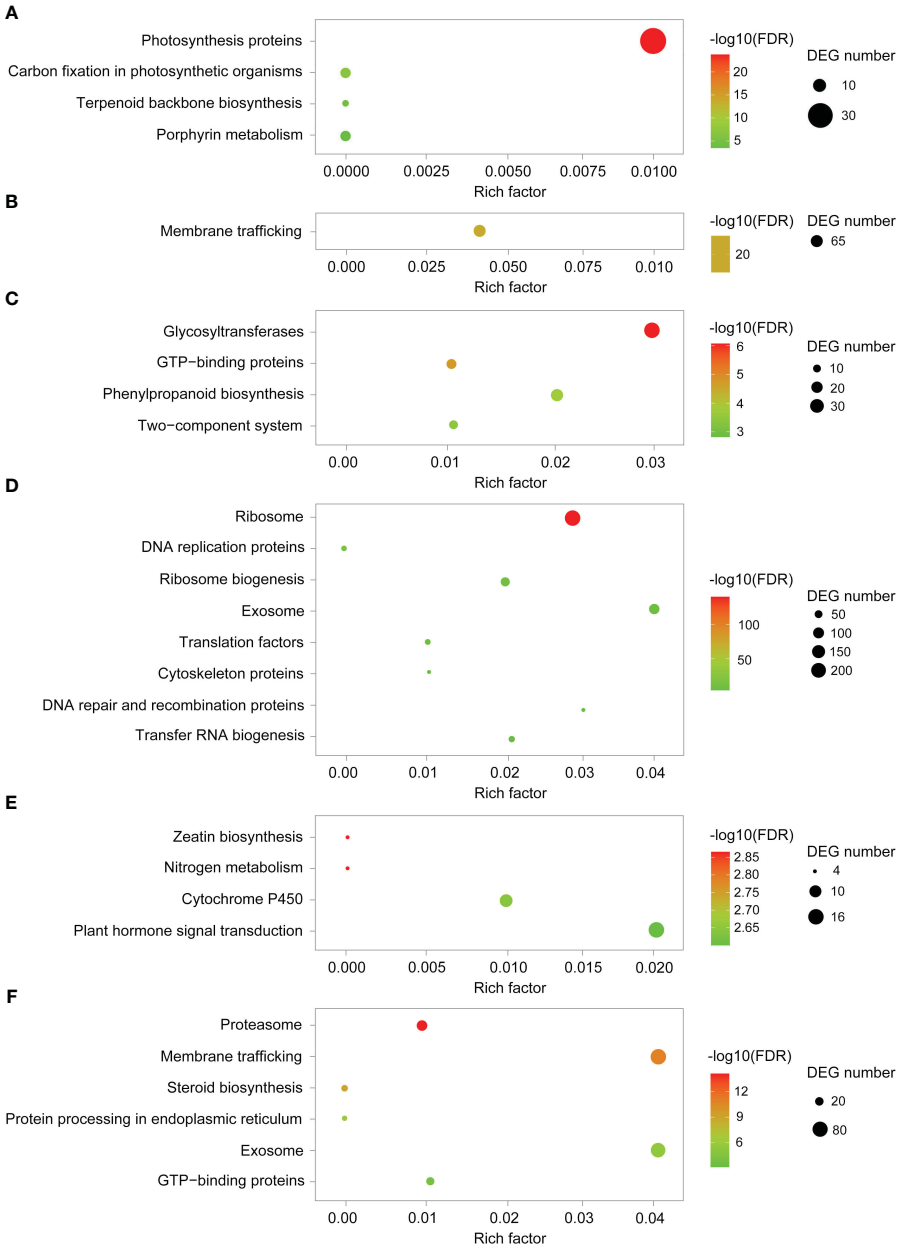

FIGURE 4
KEGG pathway enrichment analyses of representative clusters. **(A–F)** KEGG pathway enrichment analyses of cluster 1, 6, 7, 10, 11, and 17, respectively.

Such multifunctionality makes cytochrome P450 important in the plant defense against pests, diseases, and abiotic stressors. In addition, zeatin is the primary active component of the phytohormone CK. KEGG analysis revealed that the cytochrome P450-phytohormone signal transduction pathway was activated in YHY15 rice under biotype 1 BPH infestation. In contrast, gene expression in clusters 15 to 17 was increased at the early (6 h) and late (48 h) stages during infestation with biotype Y BPH (Figure 3; Supplementary Table 6). These genes were enriched in proteasome, membrane trafficking, steroid biosynthesis, protein processing in endoplasmic reticulum, exosome, and GTP-binding proteins (Figure 4F; Supplementary Figure 5F; Supplementary Table 7). These results suggest that cell secretion and extracellular materials are crucial for defense against insects. Finally, clusters 18 to 20 did not exhibit any notable tendencies (Figure 3).

3.4 Phytohormonal responses in YHY15 rice to BPH infestation

Both the clustering analysis and KEGG/GO enrichment analysis indicated that phytohormone signaling was differentially affected by infestation with either biotype 1 or Y BPH (Figures 3, 4E). Consequently, we compared the expression of BPH-responsive

genes in rice with those induced by exogenous phytohormone application in *A. thaliana*. According to Hormonometer analysis, a total of 15,603 *A. thaliana* orthologs of rice genes were selected for comparison (Supplementary Table 8). The results revealed that genes associated with JA-dependent signaling were significantly altered by infestation with biotype 1 BPH, but only moderately changed by infestation with biotype Y BPH (Figure 5). Genes associated with ABA exhibited a similar pattern, except for being negatively correlated with genes whose expression in *A. thaliana* was elicited 0.5 h after ABA treatment (Figure 5). In contrast, the expression of genes involved in the ET and BR pathways exhibited negative correlations with those responding to phytohormone application in *A. thaliana*, although with more moderate suppression in biotype Y BPH-infested rice (Figure 5). These results show that genes associated with the JA, ABA, ET, and BR pathways are the most responsive to BPH infestation, particularly in the case of biotype 1 BPH, indicating their crucial roles in the rice defense against insects.

Previous research suggests that JA is involved in BPH resistance (Xu et al., 2021). We found that the JA-dependent pathway was differentially induced by infestation with either biotype 1 or Y BPH, implying that JA plays a crucial role in rice defense (Figure 5). We further analyzed the expression of genes involved in the JA pathway, and found that most of the genes involved in the biosynthesis of JA and jasmonoyl-isoleucine (JA-Ile) (e.g., *LOX* and *JAR*) were significantly suppressed by BPH infestation, especially infestation with biotype Y BPH (Figures 6A, B). Accordingly, most JAZs, which inhibit JA signaling, were induced in RT6/48 and RY6/48 (Figures 6A, B). In addition, MYC2 was downregulated in YHY15 rice infested with biotype Y BPH, suggesting that the JA-dependent pathway was inactivated upon infestation with the virulent BPH (Ge et al., 2018). Finally, the expression of many TFs was altered in

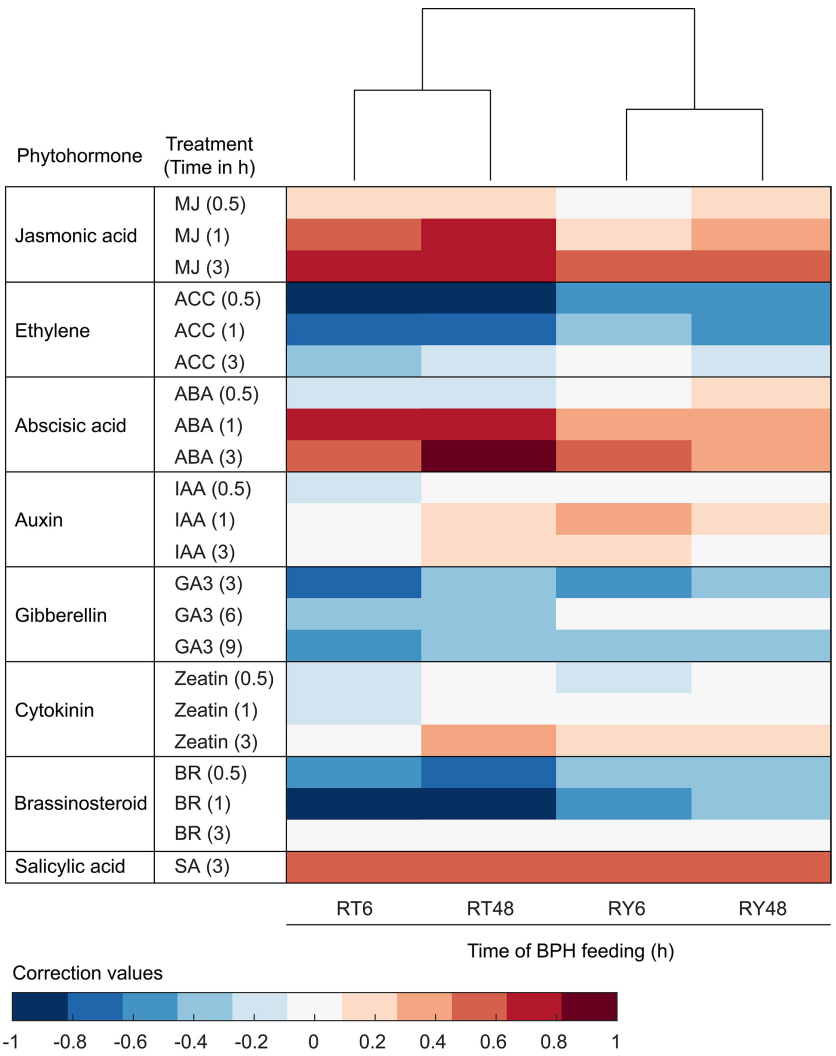

FIGURE 5
Comparison of transcriptomic phytohormone signatures between BPH-infested rice and phytohormone-treated *Arabidopsis thaliana*. Red shading indicates positive correlations and blue shading indicates negative correlations between BPH-infested rice and phytohormone-treated *A. thaliana*. MJ, methyl jasmonate; ACC, 1-aminocyclopropane-1-caroxylic acid (precursor of ethylene); ABA, abscisic acid; IAA, indole-3-acetic acid; GA3, gibberellic acid 3; ZT, zeatin; BR, brassinosteroid; SA, salicylic acid. R0, uninfected controls; RT6, YHY15 seedlings infested with biotype 1 BPH for 6 h; RT48, YHY15 seedlings infested with biotype 1 BPH for 48 h; RY6, YHY15 seedlings infested with biotype Y BPH for 6 h; RY48, YHY15 seedlings infested with biotype Y BPH for 48 h.

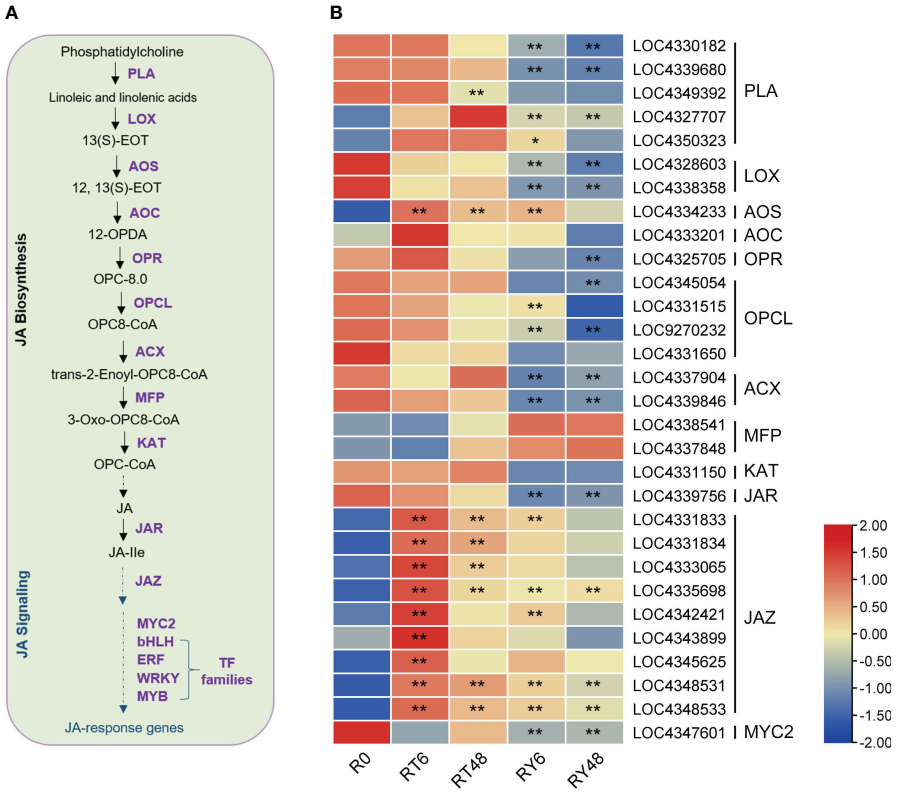

FIGURE 6
BPH-induced responses in the jasmonic acid (JA) pathway. **(A)** Overview of the JA pathway. **(B)** Heat map of the expression of genes associated with the JA pathway. Asterisks indicate statistically significant differences in gene expression at different time points in either biotype 1 or biotype Y BPH-infested rice relative to control (0 h) (*$padj$ < 0.05, **$padj$ < 0.01, via the Benjamini and Hochberg adjustment method). PLA, phospholipase A1; LOX, lipoxygenase; AOS, allene oxide synthase; AOC, allene oxide cyclase; OPR, 12-oxophytodienoate reductase; OPCL, OPC8-CoA ligase; ACX, acyl-CoA oxidase; MFP, multifunctional protein; KAT, 3-ketoacyl-CoA thiolase; JAR, jasmonate resistant; JAZ, jasmonate-ZIM domain. Transcription factor families: myelocytomatosis protein 2 (MYC2), basic helix-loop-helix (bHLH), ethylene responsive factor (ERF), WRKYGOK (WRKY), MYB. R0, uninfected controls; RT6, YHY15 seedlings infested with biotype 1 BPH for 6 h; RT48, YHY15 seedlings infested with biotype 1 BPH for 48 h; RY6, YHY15 seedlings infested with biotype Y BPH for 6 h; RY48, YHY15 seedlings infested with biotype Y BPH for 48 h.

BPH-infested rice, especially rice infested with biotype Y BPH, including those belonging to the JA-responsive bHLH, ERF, WRKY, and MYB families (Supplementary Figure 6). These distinct response patterns imply that these TFs have functions in BPH defense, although further research is required to verify these functions. The expression profiles of the identified TFs can be found in Supplementary Table 9.

3.5 Integrated miRNA and mRNA transcriptional analyses

The functions of the identified miRNAs were initially evaluated by scanning the literature. It has been reported that miR156 negatively regulates BPH resistance in rice by altering the expression of genes related to JA biosynthesis and signaling (Ge et al., 2018). We observed that miR156 expression was significantly decreased in biotype Y BPH-infested rice. Consequently, WRKY53, several MPKs (JA biosynthesis repressors), and several JAZs (negative regulators of JA signaling) were upregulated (Table 2). These transcriptional alterations resulted in low JA expression and improved BPH resistance. According to other research, miR396 suppresses BPH resistance through the miR396b–growth regulating factor 8 (GRF8)–flavanone 3-dioxygenase (F3H)–flavonoid pathway (Dai et al., 2019). Therefore, we examined the expression of *miR396*, *GRF8*, and *F3H*. Mature OsmiR396a and OsmiR396b share the same sequence (Dai et al., 2019), and we observed that miR396a was downregulated by infestation with biotype Y BPH. In contrast, *GRF8* and *F3H-1* expression increased in RY6 and RY48. Notably, *GRF1* and two *flavanone 3-dioxygenase 2-like* genes exhibited the same trend (Table 2). These results suggest that the miR396b–GRF8–F3H–flavonoid pathway was activated in biotype Y BPH- infested rice. Genetic experiments indicate that miR398b negatively regulates pathogen-associated molecular pattern (PAMP)-induced callose deposition (Li et al., 2010). As miR398 expression was significantly downregulated in RY6/48, we further analyzed the transcription of callose deposition-related genes. Surprisingly, a callose synthase gene was activated following biotype Y BPH infestation, while a series of callose degradation genes were suppressed (Table 2). These results suggest that infestation with biotype Y BPH may lead to callose deposition in rice. Taken together, it appears that the expression of these miRNAs and their regulation of target genes may contribute the ability of YHY15 rice to resist infestation with biotype Y BPH.

10.3389/fpls.2024.1366515

TABLE 2 The miRNA-mRNA interactions related to plant resistance.

osa-miRNA	Gene ID	Fold change (log_2)		Discription
		RY6/R0	RY48/R0	
miR156	LOC4338474	1.01	–	Probable WRKY transcription factor 26, WRKY53
	LOC4342017	1.23	1.08	Mitogen-activated protein kinase 12, MAP kinase 12
	LOC4339697	1.03	1.02	Mitogen-activated protein kinase 17 isoform X1, MAP kinase 17
	LOC4331834	2.40	1.64	Jasmonate ZIM domain-containing protein 10, OsJAZ10; protein TIFY 11b
	LOC4331833	2.37	–	Jasmonate ZIM domain-containing protein 11, OsJAZ11; protein TIFY 11c
	LOC4348533	2.76	2.11	Jasmonate ZIM domain-containing protein 12, OsJAZ12; protein TIFY 11d
	LOC4348531	5.83	4.65	Jasmonate ZIM domain-containing protein 13, OsJAZ13; protein TIFY 11e
	LOC4342421	4.59	–	Jasmonate ZIM domain-containing protein 2, OsJAZ2; protein TIFY 5
miR396	LOC4330903	2.99	3.06	Growth-regulating factor 1, OsGRF1
	LOC4350711	1.23	1.35	Growth-regulating factor 8, OsGRF8
	LOC9270463	4.59	4.02	Flavanone 3-dioxygenase 1, OsF3H-1
	LOC4345848	–	1.55	Flavanone 3-dioxygenase 2-like
	LOC4347916	2.56	2.20	Flavanone 3-dioxygenase 3-like
miR398	LOC4345025	-2.62	-2.00	endo-1,3;1,4-beta-D-glucanase
	LOC4338721	-2.84	-3.28	endo-1,3;1,4-beta-D-glucanase
	LOC4350272	-2.44	-1.40	endo-1,3;1,4-beta-D-glucanase
	LOC4350269	-2.48	-1.79	endo-1,3;1,4-beta-D-glucanase
	LOC4350270	-1.23	-1.26	endo-1,3;1,4-beta-D-glucanase
	LOC4345024	-2.17	-1.27	endo-1,3;1,4-beta-D-glucanase
	LOC9268304	–	-1.26	glucan endo-1,3-beta-glucosidase 12, putative beta-1,3-glucanase
	LOC4345052	–	-1.34	glucan endo-1,3-beta-glucosidase 7, putative beta-1,3-glucanase precursor
	LOC4326519	–	-2.13	glucan endo-1,3-beta-glucosidase, putative beta-1,3-glucanase precursor
	LOC4326518	-1.30	-1.59	glucan endo-1,3-beta-glucosidase, beta 1,3-glucanase
	LOC4338611	-1.58	-1.74	putative beta-1,3-glucanase
	LOC4334765	-3.09	–	probable glucan endo-1,3-beta-glucosidase A6, putative beta-1,3-glucanase
	LOC4339201	-1.79	-1.57	putative glucan endo-1,3-beta-glucosidase GVI, putative beta-1,3-glucanase
	LOC4327203	3.03	2.93	glucan endo-1,3-beta-glucosidase 13, putative elicitor inducible beta-1,3-glucanase NtEIG-E76
	LOC4332097	2.84	2.73	glucan endo-1,3-beta-glucosidase 3 isoform X1, Putative beta-1,3-glucanase
	LOC4334391	1.48	1.33	glucan endo-1,3-beta-glucosidase, putative beta-1,3 glucanase
	LOC4346925	–	–	probable endo-1,3(4)-beta-glucanase ARB_01444
	LOC4342136	1.41	1.40	callose synthase 3-like
	LOC4331485	-1.67	-1.36	callose synthase 3

3.6 Callose deposition is activated by BPH infestation

The combined miRNA-seq and RNA-seq analysis indicated that callose deposition might play a vital role in the rice response to BPH infestation. Callose deposition prevents plant hoppers from ingesting phloem sap (Hao et al., 2008; Du et al., 2009). Specifically, callose deposition ensures that the phloem sieve tubes remain occluded. To determine the role of callose in the rice response to BPH infestation, the expression of genes related to callose synthesis and degradation was examined. Consistent with the RNA-seq

results, the transcription of *callose synthase 3-like* (*CAL1*) increased, while several *1,3-beta-glucanase* (*BG*) genes decreased, in RY48 (Figures 7A, B). To confirm this result, callose deposition was measured during BPH infestation. The outermost sheaths of biotype Y BPH-infested seedlings exhibited larger and more numerous callose spots than those from biotype 1 BPH-infested and uninfested seedlings (Figures 7C, D). These results suggest that BPH infestation, particularly infestation with biotype Y BPH, results in the activation of callose synthesis and the suppression of callose degradation.

4 Discussion

The management of rice plant resistance to BPH infestation will be crucial for effective pest management. Understanding the defense strategies employed by resistant rice varieties against both avirulent and virulent BPH populations can provide valuable insights for developing effective pest control strategies. Transcriptomics, which can quantify changes in gene expression and associated regulatory mechanisms, can aid in unraveling these complexities. In plants, miRNAs are involved in various developmental processes and play significant roles in abiotic and biotic stress responses (Zhang et al., 2013; Kumar, 2014; Zhang et al., 2016; Li et al., 2017; Mangrauthia et al., 2017; Natarajan et al., 2018). Specifically, miRNAs regulate targeted gene expression by binding complementary sequences in mRNA molecules, resulting in degradation and/or inhibited translation (Bartel, 2009; Marin et al., 2010; Peng et al., 2014). Integrated mRNA and miRNA transcriptomics analyses have been used to identify miRNA-mRNA networks associated with developmental processes and insect defense (Tan et al., 2020; Li et al., 2021; Mei et al., 2021). However, little attention has been paid to defense strategies employed by resistant rice against differentially virulent BPH populations. In this study, we employed an integrated mRNA and miRNA transcriptomics approach to characterize the defense responses of resistant YHY15 rice (contains *Bph15*) to infestation with avirulent (biotype 1) and virulent (biotype Y) BPH. Our results revealed that YHY15 rice seedlings exhibited distinct responses under the two infestation scenarios (Figure 1). YHY15 rice is highly resistant to biotype 1 BPH and susceptible to biotype Y BPH, which is in accordance with previous reports (Yang et al., 2004; Jing et al., 2011; Guan et al., 2022).

The BPH-resistance gene *Bph15* has been widely applied in rice breeding programs, although the molecular mechanisms underlying *Bph15*-mediated resistance remain unclear (Lv et al., 2014; Zheng et al., 2021). Previous RNA-seq studies of *Bph15* introgression lines and recipient lines before and after BPH infestation have identified key defense mechanisms associated with phytohormone signaling, mitogen-activated protein kinase (MAPK) cascades, receptor kinases, protein post-translational modifications, TFs, Ca^{2+}

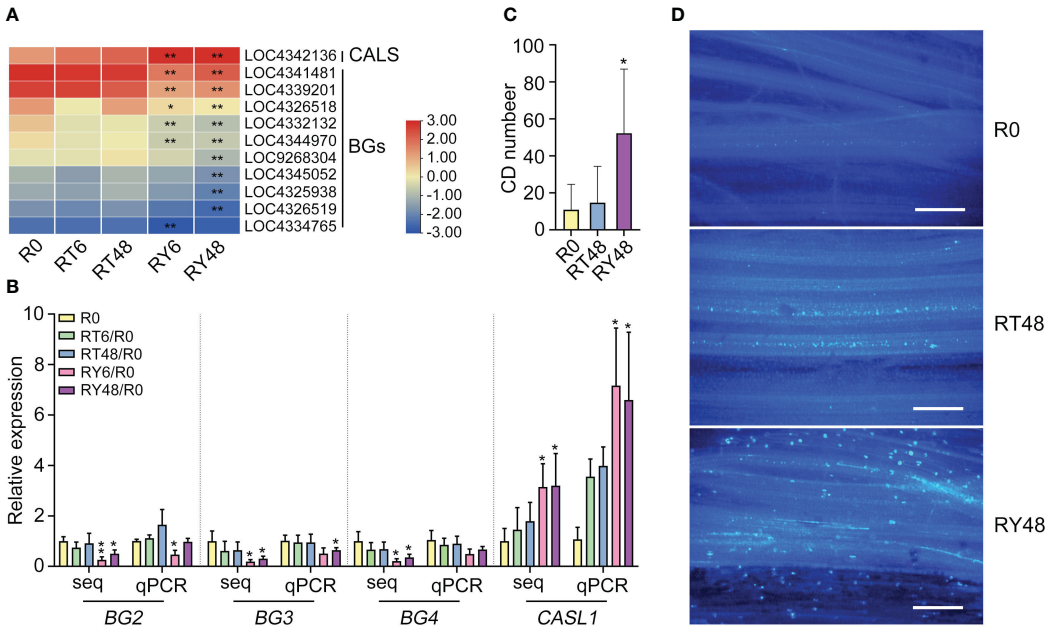

FIGURE 7
Induction of callose deposition in YHY15 rice plants following BPH infestation. **(A)** Heat map of the expression of genes associated with callose deposition and degradation. Asterisks indicate statistically significant differences in gene expression at different time points in either biotype 1 or biotype Y BPH-infested rice relative to control (0 h) (**padj* < 0.05, ***padj* < 0.01, via the Benjamini and Hochberg adjustment method). **(B)** Expression patterns of callose deposition-related genes in BPH-infested rice plants. *UBQ* was used as a control. **(C)** Callose deposition (CD) in BPH-infested YHY15 plants. The images were taken 48 h after BPH infestation. Samples were collected from the outermost sheath. Callose deposition values are the means of 20 biological replicates. Asterisks indicate statistically significant differences between BPH-infested and uninfested rice plants (one-way ANOVA, **P* < 0.05). **(D)** Callose deposition in YHY15 plants infested with either biotype 1 or biotype Y BPH. Scale bar = 20 µm. The images were taken 48 h after BPH infestation. Uninfested YHY15 plants in the same condition served as control. R0, uninfected controls; RT6, YHY15 seedlings infested with biotype 1 BPH for 6 h; RT48, YHY15 seedlings infested with biotype 1 BPH for 48 h; RY6, YHY15 seedlings infested with biotype Y BPH for 6 h; RY48, YHY15 seedlings infested with biotype Y BPH for 48 h.

signaling, and pathogenesis-related proteins (Lv et al., 2014). In addition, 20 upregulated and 3 downregulated miRNAs were identified in resistant rice variety P15 (containing *Bph15*) compared to susceptible rice variety PC (recipient line) (Wu et al., 2017). Combined with the mRNA transcriptome data, the 67 potential targets of these miRNAs were related to resistance responses to avirulent BPH, including abiotic and biotic stimuli, regulation of plant hormones (GA, SA, ET, and CK), cellulose biosynthesis, amino acid biosynthesis, and protein folding (Cheng et al., 2013; Lv et al., 2014; Wu et al., 2017). Here, comprehensive analysis of miRNA-seq and mRNA-seq data shed light on the underlying mechanisms responsible for the contrasting responses of YHY15 rice to BPH biotypes with different virulence.

Plant defense against BPH is a dynamic and sophisticated process which involves many levels of organizational and functional complexity (Barah and Bones, 2015; Erb and Reymond, 2019). During feeding, the BPH stylet transiently punctures the epidermis and then penetrates the plant cell wall. Subsequently, the insect salivates into the cells and ingests the phloem sap (Hao et al., 2008). According to electronic penetration graph (EPG) waveform recordings, BPH begin feeding on phloem sap within 1-3 hours of settling on rice plants (Hao et al., 2008). A greater number of miRNAs were found to be upregulated in biotype 1 BPH-infested resistant P15 rice (a *Bph15* introgression line) than in susceptible PC rice (recipient line) during the early infestation stage (6 h) when the plants had not yet been severely damaged (Wu et al., 2017). In another report, the inducible BPH defense responses (indicated by upregulated DEGs and DEMs) were more robust during the early feeding stages (e.g., 6, 12, and 24 h) in resistant BPH6G rice (*BPH6*-transgenic rice) than in susceptible Nipponbare rice (wild type, WT) (Tan et al., 2020). Moreover, a miRNA profiling was conducted on resistant IR56 rice (carrying *Bph3*) under separate infestations of a virulent IR56-BPH and an avirulent TN1-BPH (Nanda et al., 2020). This study revealed that BPH feeding caused significant alterations in miRNA expression profiles of IR56 rice, with a greater number of miRNAs showing downregulation when IR56 rice was infested with TN1-BPH. However, the distinct mechanisms underlying rice plant responses to BPH of varying levels of virulence remains unclear. Here, resistant YHY15 rice plants were exposed to avirulent (biotype 1) and virulent (biotype Y) BPH. Notably, DEMs were only identified in rice plants infested with biotype Y BPH (Figure 2A). In addition, many more DEGs were identified in rice plants infested with biotype Y BPH, regardless of the infestation time (Figure 2E). Together, these results suggest that biotype Y BPH elicit more intense defense responses in YHY15 rice. DaEGs related with cytochrome P450 (KEGG) were more common at the early infestation stage (6 h) in rice infested with both types of BPH (Figure 2F; Supplementary Figures 1A, B). At the later infestation stage (48 h), overlapping DEGs in R0 *vs* RT48 and R0 *vs* RY48 were enriched in photosynthesis-related pathways (Figure 2F; Supplementary Figures 3A, B). Specifically, DEGs in R0 *vs* RY6 were mainly enriched in photosynthetic organisms and DNA replication proteins (Figure 2F; Supplementary Figures 2A, B), indicating that damage to the photosynthetic system occurs earlier in biotype Y BPH-infested rice. Taken together, compared with biotype 1 BPH, infestation with biotype Y BPH results in more serious damage and induces more intense transcriptional responses in YHY15 rice.

In plants, including rice, phytohormone signaling is widely known to be involved in insect defense and resistance (Liu et al., 2016; Jing et al., 2023; Liu Q. et al., 2021). Among phytohormones, JA is critical to the regulation of plant defenses against insect herbivores (Thaler et al., 2012; Howe et al., 2018). Other phytohormones, such as SA, ET, BR, ABA, and CK are also involved in plant responses to herbivory through cross-talk with JA signaling (Bruessow et al., 2010; Schäfer et al., 2015; Pan et al., 2018; Ma et al., 2020; Li et al., 2022; Zhang et al., 2022). In this study, we found that infestation with differentially virulent BPH populations resulted in noticeable effects on the expression of genes associated with phytohormone signaling in YHY15 rice plants. Specifically, infestation with biotype 1 BPH induced JA- and ABA-related signaling pathways, but suppressed ET- and BR-related signaling (Figure 5). While, infestation with biotype Y BPH induced more moderate expression of JA- and ABA-related pathways. These results suggest that although infestation with virulent biotype Y BPH results in extensive damage to YHY15 rice plants, they exhibit weaker JA- and ABA-mediated defense responses. These findings are in line with previous research suggesting that IR56 BPH can overcome *Bph3*-mediated resistance by suppressing the transcription of defense-responsive MAPK pathways, phytohormone biosynthesis, and secondary metabolite production (Nanda et al., 2018). Previous studies also suggest that oral secretions, digestive and detoxifying enzymes, and endosymbionts can help insect herbivores adapt to host plants (Simon et al., 2015; Yates and Michel, 2018). We therefore speculate that specific BPH effectors may interact with *Bph15* and affect *Bph15*-mediated immunity in rice. However, further studies will be required to test this hypothesis.

The DEMs and their associated mRNAs identified in this study may potentially play roles in the response of rice to BPH infestation. Among the identified DEMs, miR156, miR5076, miR1856, miR398, miR5072, miR5079, miR408, miR2873, and miR169 exhibited significant variation in amplitude (Supplementary Table 3). In addition, many of them have been implicated in various plant developmental processes and stress responses (Li et al., 2017b) (Sharma et al., 2015; Zhao et al., 2017; Lin et al., 2018; Liu et al., 2019; Liebsch and Palatnik, 2020; Li et al., 2020; Liu X. et al., 2021; Gao et al., 2022; Pachamuthu and Hari Sundar, 2022; Zhao et al., 2022). The altered expression of these miRNAs may enhance BPH resistance in YHY15 rice. Combined with mRNA transcriptome data (Table 2), we found that the miR156-JA, miR396b–GRF8–F3H–flavonoid, and miR398b-callose deposition pathways may contribute to the resistance of YHY15 rice to biotype Y BPH. Physiological tests verified the increased deposition of callose in biotype Y BPH-infested rice (Figure 7). Notably, these miRNA-mediated responses only occurred in rice infested with biotype Y BPH, which suggests that they may contribute to the differential resistance of rice against BPH populations with varying levels of virulence.

Finally, research suggests that numerous TFs are involved in the rice response to BPH infestation. For example, OsMYB30 (an R2R3

MYB TF) induces the expression of phenylalanine ammonia-lyase (PAL) enzymes, thereby improving BPH resistance in rice (He et al., 2020). OsMYB22 promotes rice resistance by affecting flavonoid biosynthesis (Sun et al., 2023). The bHLH protein MYC2 is involved in JA-mediated insect resistance (Schweizer et al., 2013; Xu et al., 2021). OsWRKY45, OsWRKY53, OsWRKY70, and OsWRKY89 also mediate herbivore resistance (Chujo et al., 2007; Wang et al., 2007; Hu et al., 2015; Li et al., 2015; Huangfu et al., 2016). A recent study has demonstrated the pivotal involvement of OsWRKY71 in *Bph15*-mediated resistance (Li et al., 2023). Here, we identified several differentially expressed TFs associated with BPH infestation. Notably, several predominant TF families, including bHLH, MYB, ERF, WRKY, bZIP, NAC, C2H2, TALE, G2-like, HD-ZIP, MYB-related, HSF, and NF-Y, were differentially responsive to BPH infestation. The expression of most TFs was altered in biotype Y BPH-infested rice, indicating their specific roles in defense against the virulent biotype. Notably, the expression of certain other TFs was disturbed specifically in response to biotype 1 BPH infestation. These findings highlight the important functions of TFs in BPH defense and warrant further research to uncover their specific roles.

5 Conclusion

In conclusion, our study provides valuable insights into the differential defense strategies employed by resistant YHY15 rice (carrying BPH resistance gene *Bph15*) against avirulent (biotype 1) and virulent (biotype Y) BPH. The BPH defense response was found to involve the modulation of miRNAs, TFs, phytohormone signaling pathways, and the induction of callose deposition. These responses were most noticeable in biotype Y BPH-infested rice plants. These findings contribute to the elucidation of the molecular intricacies underlying rice-BPH interactions and pave the way for further research into the specific genes, pathways, and regulatory elements involved in plant defense against diverse BPH populations. Studying these defense mechanisms will aid our understanding of the intricate interactions between rice and BPH and allow the development of targeted pest control strategies for improved rice cultivation. It is worth noting that the infestation-induced defense responses of YHY15 rice do not appear to alter the survivability of biotype Y BPH, implying the existence of corresponding adaptive responses in the virulent biotype. This result will be the subject of in-depth exploration in future studies.

Data availability statement

All raw RNA sequencing data generated in this study have been deposited under the NCBI SRA database under BioProject PRJNA997052 and PRJNA994598.

Ethics statement

The manuscript presents research on animals that do not require ethical approval for their study.

Author contributions

BY: Writing – original draft, Writing – review & editing. MG: Investigation, Writing – original draft, Writing – review & editing. YX: Investigation, Writing – review & editing. QY: Writing – review & editing. BL: Formal analysis, Writing – review & editing. ML: Writing – review & editing. YS: Writing – review & editing. CL: Writing – review & editing. JX: Writing – review & editing. JL: Writing – review & editing. WH: Writing – review & editing. HT: Writing – review & editing. PL: Writing – review & editing. QL: Investigation, Supervision, Formal analysis, Writing – review & editing. SJ: Supervision, Project administration, Resources, Funding acquisition, Writing – original draft, Writing – review & editing.

Funding

The author(s) declare financial support was received for the research, authorship, and/or publication of this article. This study was supported by grants from the National Natural Science Foundation of China (U1704111, 32372548 and 31401732), ZHONGYUAN YINGCAI JIHUA (ZYYCYU202012165), the Open Project Funding of the State Key Laboratory of Crop Stress Adaptation and Improvement (2023KF10), Young Elite Scientists Sponsorship Program by CAST (2023QNRC001), and the National Key Research and Development Program of China (2022YFD1401600).

Acknowledgments

We thank Prof. Guangcun He (Wuhan University) for kindly providing the insects and plants.

Conflict of interest

The authors declare that the research was conducted in the absence of any commercial or financial relationships that could be construed as a potential conflict of interest.

Publisher's note

Supplementary material

The Supplementary Material for this article can be found online at: https://www.frontiersin.org/articles/10.3389/fpls.2024.1366515/full#supplementary-material

References

Alam, S. N., and Cohen, M. B. (1998). Durability of brown planthopper, *Nilaparvata lugens*, resistance in rice variety IR64 in greenhouse selection studies. *Entomol. Exp. Appl.* 89, 71–78. doi: 10.1046/j.1570-7458.1998.00383.x

Axtell, M. J., and Meyers, B. C. (2018). Revisiting criteria for plant microRNA annotation in the Era of big data. *Plant Cell* 30, 272–284. doi: 10.1105/tpc.17.00851

Barah, P., and Bones, A. M. (2015). Multidimensional approaches for studying plant defence against insects: from ecology to omics and synthetic biology. *J. Exp. Bot.* 66, 479–493. doi: 10.1093/jxb/eru489

Bartel, D. P. (2009). MicroRNAs: target recognition and regulatory functions. *Cell* 136, 215–233. doi: 10.1016/j.cell.2009.01.002

Bottrell, D. G., and Schoenly, K. G. (2012). Resurrecting the ghost of green revolutions past: The brown planthopper as a recurring threat to high-yielding rice production in tropical Asia. *J. Asia Pac. Entomol.* 15, 122–140. doi: 10.1016/j.aspen.2011.09.004

Bruessow, F., Gouhier-Darimont, C., Buchala, A., Metraux, J. P., and Reymond, P. (2010). Insect eggs suppress plant defence against chewing herbivores. *Plant J.* 62, 876–885. doi: 10.1111/tpj.2010.62.issue-5

Cheng, X. Y., Zhu, L. L., and He, G. C. (2013). Towards understanding of molecular interactions between rice and the brown planthopper. *Mol. Plant* 6, 621–634. doi: 10.1093/mp/sst030

Chujo, T., Takai, R., Akimoto-Tomiyama, C., Ando, S., Minami, E., Nagamura, Y., et al. (2007). Involvement of the elicitor-induced gene *OsWRKY53* in the expression of defense-related genes in rice. *Biochim. Biophys. Acta* 1769, 497–505. doi: 10.1016/j.bbaexp.2007.04.006

Dai, Z. Y., Tan, J., Zhou, C., Yang, X. F., Yang, F., Zhang, S. J., et al. (2019). The OsmiR396-OsGRF8-OsF3H-flavonoid pathway mediates resistance to the brown planthopper in rice (*Oryza sativa*). *Plant Biotechnol. J.* 17, 1657–1669. doi: 10.1111/pbi.13091

Dinh, S. T., Baldwin, I. T., and Galis, I. (2013). The HERBIVORE ELICITOR-REGULATED1 gene enhances abscisic acid levels and defenses against herbivores in *Nicotiana attenuata* plants. *Plant Physiol.* 162, 2106–2124. doi: 10.1104/pp.113.221150

Dong, N. Q., and Lin, H. X. (2021). Contribution of phenylpropanoid metabolism to plant development and plant-environment interactions. *J. Integr. Plant Biol.* 63, 180–209. doi: 10.1111/jipb.13054

Du, B., Zhang, W. L., Liu, B. F., Hu, J., Wei, Z., Shi, Z. Y., et al. (2009). Identification and characterization of *Bph14*, a gene conferring resistance to brown planthopper in rice. *Proc. Natl. Acad. Sci.* 106, 22163–22168. doi: 10.1073/pnas.0912139106

Erb, M., and Reymond, P. (2019). Molecular interactions between plants and insect herbivores. *Annu. Rev. Plant Biol.* 70, 527–557. doi: 10.1146/annurev-arplant-050718-095910

Friedlander, M. R., Mackowiak, S. D., Li, N., Chen, W., and Rajewsky, N. (2012). miRDeep2 accurately identifies known and hundreds of novel microRNA genes in seven animal clades. *Nucleic Acids Res.* 40, 37–52. doi: 10.1093/nar/gkr688

Gao, Y., Feng, B. H., Gao, C. X., Zhang, H. Q., Wen, F. T., Tao, L. X., et al. (2022). The evolution and functional roles of miR408 and its targets in plants. *Int. J. Mol. Sci.* 23, 530–530. doi: 10.3390/ijms23010530

Ge, Y. F., Han, J. Y., Zhou, G. X., Xu, Y. M., Ding, Y., Shi, M., et al. (2018). Silencing of miR156 confers enhanced resistance to brown planthopper in rice. *Planta* 248, 813–826. doi: 10.1007/s00425-018-2942-6

Guan, W., Shan, J. H., Gao, M. Y., Guo, J. P., Wu, D., Zhang, Q., et al. (2022). Bulked segregant RNA sequencing revealed difference between virulent and avirulent brown planthoppers. *Front. Plant Sci.* 13. doi: 10.3389/fpls.2022.843227

Guo, J. P., Xu, C. X., Wu, D., Zhao, Y., Qiu, Y. F., Wang, X. X., et al. (2018). *Bph6* encodes an exocyst-localized protein and confers broad resistance to planthoppers in rice. *Nat. Genet.* 50, 297–306. doi: 10.1038/s41588-018-0039-6

Gutaker, R. M., Groen, S. C., Bellis, E. S., Choi, J. Y., Pires, I. S., Bocinsky, R. K., et al. (2020). Genomic history and ecology of the geographic spread of rice. *Nat. Plants* 6, 492–502. doi: 10.1038/s41477-020-0659-6

Hansen, C. C., Nelson, D. R., Møller, B. L., and Werck-Reichhart, D. (2021). Plant cytochrome P450 plasticity and evolution. *Mol. Plant* 14, 1244–1265. doi: 10.1016/j.molp.2021.06.028

Hao, P. Y., Liu, C. X., Wang, Y. Y., Chen, R. Z., Tang, M., Du, B., et al. (2008). Herbivore-induced callose deposition on the sieve plates of rice: an important mechanism for host resistance. *Plant Physiol.* 146, 1810–1820. doi: 10.1104/pp.107.111484

He, J., Liu, Y. Q., Yuan, D. Y., Duan, M. J., Liu, Y. L., Shen, Z. J., et al. (2020). An R2R3 MYB transcription factor confers brown planthopper resistance by regulating the phenylalanine ammonia-lyase pathway in rice. *Proc. Natl. Acad. Sci. U. S. A.* 117, 271–277. doi: 10.1073/pnas.1902771116

Howe, G. A., Major, I. T., and Koo, A. J. (2018). Modularity in jasmonate signaling for multistress resilience. *Annu. Rev. Plant Biol.* 69, 387–415. doi: 10.1146/annurev-arplant-042817-040047

Hu, L., Wu, Y., Wu, D., Rao, W. W., Guo, J. P., Ma, Y. H., et al. (2017). The coiled-coil and nucleotide binding domains of BROWN PLANTHOPPER RESISTANCE14 function in signaling and resistance against planthopper in rice. *Plant Cell.* 29, 3157–3185. doi: 10.1105/tpc.17.00263

Hu, L. F., Ye, M., Li, R., Zhang, T. F., Zhang, G. X., Wang, Q., et al. (2015). The rice transcription factor WRKY53 suppresses herbivore-induced defenses by acting as a negative feedback modulator of mitogen-activated protein kinase activity. *Plant Physiol.* 169, 2907–2921. doi: 10.1104/pp.15.01090

Huangfu, J. Y., Li, J. C., Li, R., Ye, M., Kuai, P., Zhang, T. F., et al. (2016). The transcription factor OsWRKY45 negatively modulates the resistance of rice to the brown planthopper *Nilaparvata lugens*. *Int. J. Mol. Sci.* 17, 697. doi: 10.3390/ijms17060697

Ji, R., Yu, H. X., Fu, Q., Chen, H. D., Ye, W. F., Li, S. H., et al. (2013). Comparative transcriptome analysis of salivary glands of two populations of rice brown planthopper, *Nilaparvata lugens*, that differ in virulence. *PloS One* 8, e79612. doi: 10.1371/journal.pone.0079612

Jing, S. L., Liu, B., Peng, L., Peng, X., Zhu, L., Fu, Q., et al. (2011). Development and use of EST-SSR markers for assessing genetic diversity in the brown planthopper (*Nilaparvata lugens* Stål). *Bull. Entomol. Res.* 102, 113–122. doi: 10.1017/S0007485311000435

Jing, S. L., Xu, J. G., Tang, H. M., Li, P., Yu, B., and Liu, Q. S. (2023). The roles of small RNAs in rice-brown planthopper interactions. *Front. Plant Sci.* 14. doi: 10.3389/fpls.2023.1326726

Jing, S. L., Zhao, Y., Du, B., Chen, R. Z., Zhu, L. L., and He, G. C. (2017). Genomics of interaction between the brown planthopper and rice. *Curr. Opin. Insect Sci.* 19, 82–87. doi: 10.1016/j.cois.2017.03.005

Kumar, R. (2014). Role of microRNAs in biotic and abiotic stress responses in crop plants. *Appl. Biochem. Biotechnol.* 174, 93–115. doi: 10.1007/s12010-014-0914-2

Kumar, L., and Futschik, M. E. (2007). Mfuzz: a software package for soft clustering of microarray data. *Bioinformation* 2, 5–7. doi: 10.6026/bioinformation

Langmead, B., Trapnell, C., Pop, M., and Salzberg, S. L. (2009). Ultrafast and memory-efficient alignment of short DNA sequences to the human genome. *Genome Biol.* 10, R25. doi: 10.1186/gb-2009-10-3-r25

Li, J. T., Chen, L., Ding, X., Fan, W. Y., and Liu, J. L. (2022). Transcriptome Analysis reveals crosstalk between the abscisic acid and jasmonic acid signaling pathways in rice-mediated defense against. *Nilaparvata lugens. Int. J. Mol. Sci.* 23, 6319–6319. doi: 10.3390/ijms23116319

Li, C. Y., Luo, C., Zhou, Z. H., Wang, R., Ling, F., Xiao, L. T., et al. (2017). Gene expression and plant hormone levels in two contrasting rice genotypes responding to brown planthopper infestation. *BMC Plant Biol.* 17, 57. doi: 10.1186/s12870-017-1005-7

Li, X. P., Ma, X. C., Wang, H., Zhu, Y., Liu, X. X., Li, T. T., et al. (2020). Osa-miR162a fine-tunes rice resistance to Magnaporthe oryzae and Yield. *Rice (New York N.Y.).* 13, 38. doi: 10.1186/s12284-020-00396-2

Li, H. Y., Meng, H. L., Sun, X. Q., Deng, J., Shi, T. X., Zhu, L. W., et al. (2021). Integrated microRNA and transcriptome profiling reveal key miRNA-mRNA interaction pairs associated with seed development in Tartary buckwheat (*Fagopyrum tataricum*). *BMC Plant Biol.* 21, 132. doi: 10.1186/s12870-021-02914-w

Li, R., Zhang, J., Li, J. C., Zhou, G. X., Wang, Q., Bian, W. B., et al. (2015). Prioritizing plant defence over growth through WRKY regulation facilitates infestation by non-target herbivores. *eLife* 4, e04805. doi: 10.7554/eLife.04805.021

Li, X. Z., Zhang, J., Shangguan, X. X., Yin, J. J., Zhu, L. L., Hu, J., et al. (2023). Knockout of *OsWRKY71* impairs *Bph15*-mediated resistance against brown planthopper in rice. *Front. Plant Sci.* 14. doi: 10.3389/fpls.2023.1260526

Li, Y., Zhang, Q. Q., Zhang, J. G., Wu, L., Qi, Y. J., and Zhou, J. M. (2010). Identification of MicroRNAs involved in pathogen-associated molecular pattern-triggered plant innate immunity. *Plant Physiol.* 152, 2222–2231. doi: 10.1104/pp.109.151803

Li, Y., Zhao, S. L., Li, J. L., Hu, X. H., Wang, H., Cao, X. L., et al. (2017b). Osa-miR169 negatively regulates rice immunity against the blast fungus *Magnaporthe oryzae*. *Front. Plant Sci.* 8. doi: 10.3389/fpls.2017.00002

Liebsch, D., and Palatnik, J. F. (2020). MicroRNA miR396, GRF transcription factors and GIF co-regulators: a conserved plant growth regulatory module with potential for breeding and biotechnology. *Curr. Opin. Plant Biol.* 53, 31–42. doi: 10.1016/j.pbi.2019.09.008

Lin, W. Y., Lin, Y. Y., Chiang, S. F., Syu, C., Hsieh, L. C., and Chiou, T. J. (2018). Evolution of microRNA827 targeting in the plant kingdom. *New Phytol.* 217, 1712–1725. doi: 10.1111/nph.14938

Liu, J. L., Du, H. T., Ding, X., Zhou, Y. D., Xie, P. F., and Wu, J. C. (2017). Mechanisms of callose deposition in rice regulated by exogenous abscisic acid and its involvement in rice resistance to *Nilaparvata lugens* Stål (Hemiptera: Delphacidae). *Pest Manage. Sci.* 73, 2559–2568. doi: 10.1002/ps.4655

Liu, Q. S., Hu, X. Y., Su, S. L., Ning, Y. S., Peng, Y. F., Ye, G. Y., et al. (2021). Cooperative herbivory between two important pests of rice. *Nat. Commun.* 12, 6772. doi: 10.1038/s41467-021-27021-0

Liu, X., Huang, S., and Xie, H. T. (2021). Advances in the regulation of plant development and stress response by miR167. *Front. Biosci.* 26, 655–665. doi: 10.52586/4974

Liu, M. M., Shi, Z. Y., Zhang, X. H., Wang, M. X., Zhang, K. Z., Liu, J. Y., et al. (2019). Inducible overexpression of Ideal Plant Architecture1 improves both yield and disease resistance in rice. *Nat. plants.* 5, 389–400. doi: 10.1038/s41477-019-0383-2

Liu, Q. S., Wang, X. Y., Tzin, V., Romeis, J., Peng, Y. F., and Li, Y. H. (2016). Combined transcriptome and metabolome analyses to understand the dynamic responses of rice plants to attack by the rice stem borer *Chilo suppressalis* (Lepidoptera: Crambidae). *BMC Plant Biol.* 16, 259. doi: 10.1186/s12870-016-0946-6

Lu, J., Ju, H. P., Zhou, G. X., Zhu, C. S., Erb, M., Wang, X. P., et al. (2011). An EAR-motif-containing ERF transcription factor affects herbivore-induced signaling, defense and resistance in rice. *Plant J.* 68, 583–596. doi: 10.1111/j.1365-313X.2011.04709.x

Lu, J., Li, J. C., Ju, H. P., Liu, X. L., Erb, M., Wang, X., et al. (2014). Contrasting effects of ethylene biosynthesis on induced plant resistance against a chewing and a piercing-sucking herbivore in rice. *Mol. Plant* 7, 1670–1682. doi: 10.1093/mp/ssu085

Lv, W. T., Du, B., Shangguan, X. X., Zhao, Y., Pan, Y. F., Zhu, L. L., et al. (2014). BAC and RNA sequencing reveal the brown planthopper resistance gene *BPH15* in a recombination cold spot that mediates a unique defense mechanism. *BMC Genom.* 15, 674. doi: 10.1186/1471-2164-15-674

Ma, F. L., Yang, X. F., Shi, Z. Y., and Miao, X. X. (2020). Novel crosstalk between ethylene- and jasmonic acid-pathway responses to a piercing-sucking insect in rice. *New Phytol.* 225, 474–487. doi: 10.1111/nph.16111

Mangrauthia, S. K., Bhogireddy, S., Agarwal, S., Prasanth, V. V., Voleti, S. R., Neelamraju, S., et al. (2017). Genome-wide changes in microRNA expression during short and prolonged heat stress and recovery in contrasting rice cultivars. *J. Exp. Bot.* 68, 2399–2412. doi: 10.1093/jxb/erx111

Marin, E., Jouannet, V., Herz, A., Lokerse, A. S., Weijers, D., Vaucheret, H., et al. (2010). miR390, Arabidopsis TAS3 tasiRNAs, and their AUXIN RESPONSE FACTOR targets define an autoregulatory network quantitatively regulating lateral root growth. *Plant Cell.* 22, 1104–1117. doi: 10.1105/tpc.109.072553

Mei, M., Wei, J., Ai, W. F., Zhang, L. J., and Lu, X. J. (2021). Integrated RNA and miRNA sequencing analysis reveals a complex regulatory network of Magnolia sieboldii seed germination. *Sci. Rep.* 11, 10842. doi: 10.1038/s41598-021-90270-y

Nanda, S., Wan, P. J., Yuan, S. Y., Lai, F. X., Wang, W. X., and Fu, Q. (2018). Differential responses of *OsMPKs* in IR56 rice to two BPH populations of different virulence levels. *Int. J. Mol. Sci.* 19, 4030. doi: 10.3390/ijms19124030

Nanda, S., Yuan, S. Y., Lai, F. X., Wang, W. X., Fu, Q., and Wan, P. J. (2020). Identification and analysis of miRNAs in IR56 rice in response to BPH infestations of different virulence levels. *Sci. Rep.* 10, 19093. doi: 10.1038/s41598-020-76198-9

Natarajan, B., Kalsi, H. S., Godbole, P., Malankar, N., Thiagarayaselvam, A., Siddappa, S., et al. (2018). MiRNA160 is associated with local defense and systemic acquired resistance against Phytophthora infestans infection in potato. *J. Exp. Bot.* 69, 2023–2036. doi: 10.1093/jxb/ery025

Pachamuthu, K., and Hari Sundar, V. (2022). Nitrate-dependent regulation of miR444-OsMADS27 signalling cascade controls root development in rice. *J. Exp. Bot.* 73, 3511–3530. doi: 10.1093/jxb/erac083

Pan, G., Liu, Y. Q., Ji, L. S., Zhang, X., He, J., Huang, J., et al. (2018). Brassinosteroids mediate susceptibility to brown planthopper by integrating with the salicylic acid and jasmonic acid pathways in rice. *J. Exp. Bot.* 69, 4433–4442. doi: 10.1093/jxb/ery223

Peng, T., Sun, H. Z., Qiao, M. M., Zhao, Y. F., Du, Y. X., Zhang, J., et al. (2014). Differentially expressed microRNA cohorts in seed development may contribute to poor grain filling of inferior spikelets in rice. *BMC Plant Biol.* 14, 196. doi: 10.1186/s12870-014-0196-4

Salvador-Guirao, R., Hsing, Y., and San Segundo, B. (2018). The polycistronic miR166k-166h positively regulates rice immunity via post-transcriptional control of *EIN2*. *Front. Plant Sci.* 9. doi: 10.3389/fpls.2018.00337

Schäfer, M., Meza-Canales, I. D., Brütting, C., Baldwin, I. T., and Meldau, S. (2015). Cytokinin concentrations and CHASE-DOMAIN CONTAINING HIS KINASE 2 (NaCHK2)- and NaCHK3-mediated perception modulate herbivory-induced defense signaling and defenses in *Nicotiana attenuata*. *New Phytol.* 207, 645–658. doi: 10.1111/nph.13404

Schweizer, F., Fernández-Calvo, P., Zander, M., Diez-Diaz, M., Fonseca, S., Glauser, G., et al. (2013). *Arabidopsis* basic helix-loop-helix transcription factors MYC2, MYC3, and MYC4 regulate glucosinolate biosynthesis, insect performance, and feeding behavior. *Plant Cell.* 25, 3117–3132. doi: 10.1105/tpc.113.115139

Sharma, N., Tripathi, A., and Sanan-Mishra, N. (2015). Profiling the expression domains of a rice-specific microRNA under stress. *Front. Plant Sci.* 6. doi: 10.3389/fpls.2015.00333

Shi, S. J., Wang, H. Y., Nie, L. Y., Tan, D., Zhou, C., Zhang, Q., et al. (2021). *Bph30* confers resistance to brown planthopper by fortifying sclerenchyma in rice leaf sheaths. *Mol. Plant* 14, 1714–1732. doi: 10.1016/j.molp.2021.07.004

Shi, S. J., Zha, W. J., Yu, X.Y., Wu, Y., Li, S. H., Xu, H. S., et al. (2023). Integrated transcriptomics and metabolomics analysis provide insight into the resistance response of rice against brown planthopper. *Front. Plant Sci.* 14. doi: 10.3389/fpls.2023.1213257

Simon, J. C., d'Alencon, E., Guy, E., Jacquin-Joly, E., Jaquiéry, J., Nouhaud, P., et al. (2015). Genomics of adaptation to host-plants in herbivorous insects. *Brief. Funct. Genomics* 14, 413–423. doi: 10.1093/bfgp/elv015

Sun, B., Shen, Y. J., Chen, S., Shi, Z. Y., Li, H. C., and Miao, X. (2023). A novel transcriptional repressor complex MYB22-TOPLESS-HDAC1 promotes rice resistance to brown planthopper by repressing *F3'H* expression. *New Phytol.* 239, 720–738. doi: 10.1111/nph.18958

Tan, J. Y., Wu, Y., Guo, J. P., Li, H. M., Zhu, L. L., Chen, R. Z., et al. (2020). A combined microRNA and transcriptome analyses illuminates the resistance response of rice against brown planthopper. *BMC Genom.* 21, 144. doi: 10.1186/s12864-020-6556-6

Thaler, J., Humphrey, P., and Whiteman, N. (2012). Evolution of jasmonate and salicylate signal crosstalk. *Trends Plant Sci.* 17, 260–270. doi: 10.1016/j.tplants.2012.02.010

Volodarsky, D., Leviatan, N., Otcheretianski, A., and Fluhr, R. (2009). HORMONOMETER: a tool for discerning transcript signatures of hormone action in the Arabidopsis transcriptome. *Plant Physiol.* 150, 1796–1805. doi: 10.1104/pp.109.138289

Wan, P. J., Zhou, R. N., Nanda, S., He, J. C., Yuan, S. Y., Wang, W. X., et al. (2019). Phenotypic and transcriptomic responses of two *Nilaparvata lugens* populations to the Mudgo rice containing. *Bph1. Sci. Rep.* 9, 14049. doi: 10.1038/s41598-019-50632-z

Wang, Y., Cao, L. M., Zhang, Y. X., Cao, C. X., Liu, F., Huang, F. K., et al. (2015). Map-based cloning and characterization of *BPH29*, a B3 domain-containing recessive gene conferring brown planthopper resistance in rice. *J. Exp. Bot.* 66, 6035–6045. doi: 10.1093/jxb/erv318

Wang, Y. B., Guo, H. M., Li, H. C., Zhang, H., and Miao, X. X. (2012). Identification of transcription factors potential related to brown planthopper resistance in rice via microarray expression profiling. *BMC Genom.* 13, 687. doi: 10.1186/1471-2164-13-687

Wang, H. H., Hao, J. J., Chen, X. J., Hao, Z. N., Wang, X., Lou, Y. G., et al. (2007). Overexpression of rice WRKY89 enhances ultraviolet B tolerance and disease resistance in rice plants. *Plant Mol. Biol.* 65, 799–815. doi: 10.1007/s11103-007-9244-x

Wang, Y. Q., Liu, Q. S., Du, L. X., Hallerman, E. M., and Li, Y. H. (2020). Transcriptomic and metabolomic responses of rice plants to *Cnaphalocrocis medinalis* caterpillar infestation. *Insects* 11, 705–705. doi: 10.3390/insects11100705

Wang, H. Y., Shi, S. J., and Hua, W. (2023). Advances of herbivore-secreted elicitors and effectors in plant-insect interactions. *Front. Plant Sci.* 14. doi: 10.3389/fpls.2023.1176048

Wang, Y. Y., Wang, X. L., Yuan, H. Y., Chen, R. Z., Zhu, L. L., He, R. F., et al. (2008). Responses of two contrasting genotypes of rice to brown planthopper. *Mol. Plant Microbe Interact.* 21, 122–132. doi: 10.1094/MPMI-21-1-0122

Wu, Y., Lv, W. T., Hu, L., Rao, W. W., Zeng, Y., Zhu, L. L., et al. (2017). Identification and analysis of brown planthopper-responsive microRNAs in resistant and susceptible rice plants. *Sci. Rep.* 7, 8712. doi: 10.1038/s41598-017-09143-y

Xiao, C., Hu, J., Ao, Y. T., Chen, M. X., Gao, G. J., Zhang, Q. L., et al. (2016). Development and evaluation of near-isogenic lines for brown planthopper resistance in rice cv. 9311. *Sci. Rep.* 6, 38159. doi: 10.1038/srep38159

Xu, J., Wang, X. J., Zu, H. Y., Zeng, X., Baldwin, I. T., Lou, Y. G., et al. (2021). Molecular dissection of rice phytohormone signaling involved in resistance to a piercing-sucking herbivore. *New Phytol.* 230, 1639–1652. doi: 10.1111/nph.17251

Yang, H. Y., You, A. Q., Yang, Z. F., Zhang, F. T., He, R. F., Zhu, L. L., et al. (2004). High-resolution genetic mapping at the *BPH15* locus for brown planthopper resistance in rice (*Oryza sativa* L.). *Theor. Appl. Genet.* 110, 182–191. doi: 10.1007/s00122-004-1844-0

Yates, A. D., and Michel, A. (2018). Mechanisms of aphid adaptation to host plant resistance. *Curr. Opin. Insect Sci.* 26, 41–49. doi: 10.1016/j.cois.2018.01.003

Ye, M., Luo, S. M., Xie, J. F., Li, Y. F., Xu, T., Liu, Y., et al. (2012). Silencing *COI1* in rice increases susceptibility to chewing insects and impairs inducible defense. *PloS One* 7, e36214. doi: 10.1371/journal.pone.0036214

Yuan, H. Y., Chen, X. P., Zhu, L. L., and He, G. C. (2005). Identification of genes responsive to brown planthopper *Nilaparvata lugens* Stål (Homoptera: Delphacidae) feeding in rice. *Planta* 221, 105–112. doi: 10.1007/s00425-004-1422-3

Zhang, X., Bao, Y. L., Shan, D. Q., Wang, Z. H., Song, X. N., Wang, Z. Y., et al. (2018). *Magnaporthe oryzae* induces the expression of a microRNA to suppress the immune response in rice. *Plant Physiol.* 177, 352–368. doi: 10.1104/pp.17.01665

Zhang, C., Ding, Z. M., Wu, K. C., Yang, L., Li, Y., Yang, Z., et al. (2016). Suppression of jasmonic acid-mediated defense by viral-inducible microRNA319 facilitates virus infection in rice. *Mol. Plant* 9, 1302–1314. doi: 10.1016/j.molp.2016.06.014

Zhang, X., Liu, D. M., Gao, D., Zhao, W. N., Du, H. Y., Qiu, Z. Y., et al. (2022). Cytokinin confers brown planthopper resistance by elevating jasmonic acid pathway in rice. *Int. J. Mol. Sci.* 23, 5946–5946. doi: 10.3390/ijms23115946

Zhang, S. H., Yue, Y., Sheng, L., Wu, Y. Z., Fan, G. H., Li, A., et al. (2013). PASmiR: a literature-curated database for miRNA molecular regulation in plant response to abiotic stress. *BMC Plant Biol.* 13, 33. doi: 10.1186/1471-2229-13-33

Zhang, F. T., Zhu, L. L., and He, G. C. (2004). Differential gene expression in response to brown planthopper feeding in rice. *J. Plant Physiol.* 161, 53–62. doi: 10.1078/0176-1617-01179

Zhao, Y., Huang, J., Wang, Z. Z., Jing, S. L., Wang, Y., Ouyang, Y. D., et al. (2016). Allelic diversity in an NLR gene *BPH9* enables rice to combat planthopper variation. *Proc. Natl. Acad. Sci. U. S. A.* 113, 12850–12855. doi: 10.1073/pnas.1614862113

Zhao, C., Ma, J. J., Zhang, Y. H., Yang, S. X., Feng, X. C., and Yan, J. (2022). The miR166 mediated regulatory module controls plant height by regulating gibberellic acid biosynthesis and catabolism in soybean. *J. Integr. Plant Biol.* 64, 995–1006. doi: 10.1111/jipb.13253

Zhao, Y. F., Wen, H. L., Teotia, S., Du, Y. X., Zhang, J., Li, J. Z., et al. (2017). Suppression of microRNA159 impacts multiple agronomic traits in rice (*Oryza sativa* L.). *BMC Plant Biol.* 17, 215. doi: 10.1186/s12870-017-1171-7

Zheng, Y., He, J. C., Wan, P. J., Lai, F. X., Sun, Y. Q., Lin, J. J., et al. (2016). Virulence characteristics of *Nilaparvata lugens* (Stål) reared on resistant rice variety IR56. *Chin. J. Rice Sci.* 30, 552–558. doi: 10.16819/j.1001-7216.2016.6016

Zheng, X. H., Zhu, L. L., and He, G. C. (2021). Genetic and molecular understanding of host rice resistance and *Nilaparvata lugens* adaptation. *Curr. Opin. Insect Sci.* 45, 14–20. doi: 10.1016/j.cois.2020.11.005

Zhou, G. X., Qi, J. F., Ren, N., Cheng, J. A., Erb, M., Mao, B. Z., et al. (2009). Silencing *OsHI-LOX* makes rice more susceptible to chewing herbivores, but enhances resistance to a phloem feeder. *Plant J.* 60, 638–648. doi: 10.1111/j.1365-313X.2009.03988.x

frontiers | Frontiers in Plant Science

TYPE Original Research
PUBLISHED 21 March 2024
DOI 10.3389/fpls.2024.1373081

OPEN ACCESS

EDITED BY
Shengli Jing,
Xinyang Normal University, China

REVIEWED BY
Lilin Yin,
Huazhong University of Science and Technology, China
Guangwei Li,
Henan Agricultural University, China
Tian Qing Zheng,
Chinese Academy of Agricultural Sciences, China

*CORRESPONDENCE
Jin Huang
huang_jin@hbaas.com
Bo Du
bodu@whu.edu.cn

RECEIVED 19 January 2024
ACCEPTED 08 March 2024
PUBLISHED 21 March 2024

CITATION
Zhou C, Jiang W, Guo J, Zhu L, Liu L, Liu S, Chen R, Du B and Huang J (2024) Genome-wide association study and genomic prediction for resistance to brown planthopper in rice.
Front. Plant Sci. 15:1373081.
doi: 10.3389/fpls.2024.1373081

Genome-wide association study and genomic prediction for resistance to brown planthopper in rice

Cong Zhou[1,2], Weihua Jiang[2], Jianping Guo[2], Lili Zhu[2], Lijiang Liu[1], Shengyi Liu[1], Rongzhi Chen[2], Bo Du[2*] and Jin Huang[3*]

[1]Oil Crops Research Institute of the Chinese Academy of Agricultural Sciences/The Key Laboratory of Biology and Genetic Improvement of Oil Crops, The Ministry of Agriculture and Rural Affairs, Wuhan, China, [2]State Key Laboratory of Hybrid Rice, College of Life Sciences, Wuhan University, Wuhan, China, [3]Cash Crops Research Institute, Hubei Academy of Agricultural Sciences, Wuhan, China

The brown planthopper (BPH) is the most destructive insect pest that threatens rice production globally. Developing rice varieties incorporating BPH-resistant genes has proven to be an effective control measure against BPH. In this study, we assessed the resistance of a core collection consisting of 502 rice germplasms by evaluating resistance scores, weight gain rates and honeydew excretions. A total of 117 rice varieties (23.31%) exhibited resistance to BPH. Genome-wide association studies (GWAS) were performed on both the entire panel of 502 rice varieties and its subspecies, and 6 loci were significantly associated with resistance scores (P value < $1.0e^{-8}$). Within these loci, we identified eight candidate genes encoding receptor-like protein kinase (RLK), nucleotide-binding and leucine-rich repeat (NB-LRR), or LRR proteins. Two loci had not been detected in previous study and were entirely novel. Furthermore, we evaluated the predictive ability of genomic selection for resistance to BPH. The results revealed that the highest prediction accuracy for BPH resistance reached 0.633. As expected, the prediction accuracy increased progressively with an increasing number of SNPs, and a total of 6.7K SNPs displayed comparable accuracy to 268K SNPs. Among various statistical models tested, the random forest model exhibited superior predictive accuracy. Moreover, increasing the size of training population improved prediction accuracy; however, there was no significant difference in prediction accuracy between a training population size of 737 and 1179. Additionally, when there existed close genetic relatedness between the training and validation populations, higher prediction accuracies were observed compared to scenarios when they were genetically distant. These findings provide valuable resistance candidate genes and germplasm resources and are crucial for the application of genomic selection for breeding durable BPH-resistant rice varieties.

KEYWORDS

rice, brown planthopper, GWAS, candidate genes, genomic prediction

Introduction

The cultivated rice (*Oryza sativa* L.) is a major staple crop and feeds over half of the global population. Rice is highly diverse, encompassing two major subspecies, *indica* and *japonica*, as well as *circum*-aus and *circum*-basmati (Wang et al., 2018a). The brown planthopper (*Nilaparvata lugens* Stål, BPH) is one of the most devastating insect pests of rice, and widely distributed in South Asia, Southeast Asia, East Asia, Northern Australia and the South Pacific Islands (Jing et al., 2017). BPH, a phloem-feeding insect, causes extensive wilting, yellowing and lethal drying of rice by sucking susceptible rice phloem sap. BPH may also indirectly damage rice plants by transmitting viruses such as grassy stunt and ragged stunt (Zheng et al., 2021). Presently, insecticides are widely used to manage pest infestations. However, this approach has damaged natural enemies and led to insecticide resistance in the insects. The most economical and effective strategy to control BPH pest is to exploit resistance genes and cultivate BPH-resistant rice varieties. Rice varieties carrying resistance genes *Bph1* or *bph2* have been implemented extensively in Southeast Asia (Jairin et al., 2007). Nevertheless, they have lost their resistance to BPH, and new BPH biotypes developed (Kobayashi, 2016). Developing rice varieties with durable resistance to BPH remains a major challenge.

The resistance mechanism of rice to BPH can be divided into antibiosis, tolerance, and antixenosis from the physiological perspective (Qiu et al., 2011). To date, over 49 BPH-resistant genes/quantitative trait loci (QTLs) have been identified and 17 BPH-resistant genes have been isolated in rice (Shi et al., 2023). Among the mapped genes, *Bph14*, *Bph25*, *Bph30* and *Bph32* were reported to confer resistance via antibiosis (Du et al., 2009; Myint et al., 2012; Ren et al., 2016; Wang et al., 2018b); *bph7*, *Bph28* and *Bph37* were considered to confer tolerance to BPH (Qiu et al., 2014; Wu et al., 2014; Yang et al., 2019); *Bph6*, *Bph9*, *Bph18*, *Bph27*, *Bph27 (t)*, *Bph33* and *Bph36* confer resistance through a combination of antibiosis and antixenosis (He et al., 2013; Huang et al., 2013; Ji et al., 2016; Zhao et al., 2016; Guo et al., 2018; Hu et al., 2018; Li et al., 2019); *bph39(t)*, *bph40(t)* through a combination of antibiosis and tolerance (Akanksha et al., 2019); and *Bph31* through a combination of antibiosis, antixenosis and tolerance (Prahalada et al., 2017). The seedling bulk test is extensively used to evaluate resistance scores of rice varieties to BPH. The resistance score obtained from the seedling bulk test was a comprehensive indicator of antibiosis, tolerance and antixenosis (Qiu et al., 2011). Almost all of the BPH resistance genes were detected by the seedling bulk test.

Bi-parental populations had a narrow genetic background, restricting the detection of abundant genes. Genome-wide association study (GWAS) is another strategy to identify genes associated with resistance to BPH in natural population of rice (Zhou et al., 2021). This method take advantage of ancient recombination events to identify genetic loci underlying complex traits at a relatively high resolution (Zhu et al., 2008). Previously, we detected numerous loci associated with antibiosis to BPH from 1,520 rice varieties (Zhou et al., 2021). The antibiosis levels were evaluated by measuring the bodyweight of insects on rice plants. Since the antibiosis level can not fully reflect the resistance of rice. It is essential to utilize an comprehensive method to evaluate the resistance to BPH and identify more resistance loci.

Genomic selection (GS), also known as genomic prediction (GP), uses genome-wide molecular markers to train models for populations with known phenotypes and genotypes. The trained model predicts the phenotype of individuals possessing only known genotypes, subsequently selecting the most performing individual as a parent for the next generation (Crossa et al., 2017). Compared to molecular marker assisted selection (MAS), which use a set of selected markers to track target genes, GS incorporates molecular markers throughout the genome to predict genomic estimated breeding values (GEBVs) to avoid measurement bias and information loss (Spindel et al., 2015). This strategy effectively tracks and selects minor gene effects while maintaining focus on major genes. Consequently, GS is an effective method for incorporating both major and minor genes into new varieties. Prediction ability (accuracy) is quantified via the correlation between observed phenotypes and predicted GEBVs. The benefits of GS are directly proportional to the prediction accuracy. When the prediction accuracy is high enough, GS can shorten breeding time by increasing the proportion of outstanding offspring in the breeding population. Factors influencing prediction accuracy include marker number, training population sample size, genetic relationship between training and testing populations, statistical models, trait heritability and genetic structure, population structure, and so on (Desta and Ortiz, 2014; Wang et al., 2018c; Guo et al., 2019; Voss-Fels et al., 2019; Xu et al., 2021). However, there is no report of GP on BPH resistance, let alone study to explore the effects of these factors on rice resistance to BPH.

In this study, the BPH resistance of 502 rice varieties was comprehensively evaluated, including resistance score, weight gain rate and honeydew excretion, and more BPH-resistant rice varieties were identified. We also analyzed the correlation between different resistance evaluation methods. GWAS were carried out to identify significantly associated loci in the 502 rice panel and subspecies. Eight resistance candidate genes predicted to encode RLK, NB-LRR or LRR protein on chromosome 11 were identified. Furthermore, we evaluated the predictive ability of GS for BPH resistance and explored the effects of marker number, training population sample size, genetic relatedness between training and testing populations, and statistical models on the predictive accuracy of BPH resistance. The results of our study provide novel BPH-resistant candidate genes and germplasm resources. Estimating the predictive accuracy of GS for BPH resistance are of great importance for the application of GS in developing durable BPH-resistant rice varieties.

Materials and methods

Plant materials and BPH insects

The rice materials used in this study comprised of 502 rice varieties randomly selected from 1520 rice varieties (Zhou et al., 2021); taking into account factors, such as the country of origin, eco-cultural type and varietal grouping. The detailed information of these

materials can be found in Supplementary Table 1. The majority of them were *indica* (227), followed by *circum*-aus (146) and *japonica* (102). There were only 8 accession of *circum*-basmati, and the remaining ones belonged to the admixture type. BPH biotype I was employed as the insect for assessing resistance among the 502 varieties, which were reared on Taichung Native1(TN1) within a controlled greenhouse environment. The temperature inside the greenhouse was maintained at 26 ± 2°C, with an alternating dark period of 8 hours and a photoperiod of 16 hours.

BPH resistance scores evaluation

The resistance scores of 502 rice varieties against BPH were determined using a modified bulk seedling test following the method of Pathak et al. (1969). Twenty-five seeds of each variety, including the susceptible control variety TN1, were individually sown separately in a 18-cm row and 2-cm row spacing within a 58×38×9 cm seedbox. At the three-leaf stage, weak seedlings were removed and the remaining seedlings were infested with ten second- to third-instar nymphs per seedling. The damage degree of each seeding was evaluated when more than 90% of the control plants TN1 had died, and assigned a resistance score ranging from 1 to 9 based on criteria described by Huang et al. (2001). Higher resistance score indicate susceptibility and lower score indicate resistance. The average resistance score for approximately twenty seedlings was recorded as the resistance score for each variety.

Evaluation of weight gain rates

Eight seeds of each variety were sown in a 9-cm-diameter plastic cup. At the fifth-leaf stage, newly emerged female BPH adults were weighed using an electronic balance (Shimadzu; Type : AUW120D) and then placed inside a 2×2 cm parafilm bag that had beed securely attached to the leaf sheath of the rice plant. Only insects with initial weight ranging from 1.8 to 2.7 mg were selected for further experimentation. After feeding on the sheath for 48 hours, the insects were removed and reweighted. The weight gain rate was calculated by dividing the insect's weight gain at 48 hours by its initial body weight. The average weight gain rates of approximately 12 insects was used as the final weight gain rate of a rice variety.

Honeydew excretion measurements

The honeydew excretion was simultaneously measured with the insect weight. Firstly, the initial weight of the parafilm bag was obtained using the electronic balance. Subsequently, the parafilm bag was securely attached to the tested rice plant and a selected insect was placed inside. After 48 hours, the parafilm bag was reweighed to determine the change in weight, which represented the amount of honeydew excretion. The amount of honeydew excretion of BPHs on each variety was calculated as an average based on approximately twelve insects.

Statistical analysis

Phenotypic differences among subspecies were performed using the function LSD.test in the R package agricolae (version 1.3-0). The Pearson correlation coefficients (r) between resistance levels and antibiosis levels were calculated in stat_cor function in the R package ggpubr. Kurtosis and skewness analysis were conducted using the R package psych.

Phylogenetic and population structure analysis

The unweighted neighbor-joining tree of 502 rice accessions was constructed based on the identity-by-state (IBS) distance matrix, which was calculated using genome-wide SNPs by PLINK (Chang et al., 2015; version 1.9). and visualized with iTOL software (Letunic and Bork, 2021). The population structure of the 502 varieties was estimated using principal component analysis (PCA) performed by PLINK.

Genome-wide association study

The SNPs of 502 varieties was filtered by PLINK (Chang et al., 2015) with genotype call rate > 0.8 and minor allele frequency (MAF) > 0.01. A total of 4,452,364 SNPs were used for the subsequent analysis. For the 502 varieties (whole panel), the top seven principal components (PCs) explain 80% of the variance and were used as fixed effects, and the Balding-Nichols kinship matrix (Balding and Nichols, 1995) between each individual was used as random effect for population structure correction. Genome wide association studies was performed using the mixed linear model of software EMMAX (Kang et al., 2010). For *indica* or *japonica*, the top five PCs were used as fixed effects. The Bonferroni correction threshold for multiple tests were used for detecting the genome-wide significant SNPs, which defined as α/N ($\alpha = 0.05$ and N is the number of SNPs). The p-value thresholds for significance were 1.0×10^{-8} for whole panel and subspecies. The manhattan plots and QQ plots were visualized with the R package rMVP (Yin et al., 2021).

Identification of candidate genes

The linkage disequilibrium (LD) was analysed using PopLDdecay software. The associated locus was defined as a 200 kbp region centered on each associated SNP. Multiple overlapping associated loci were merged into a single locus. The genes within the associated loci were identified through the MSU Rice Genome Annotation Project database, utilizing the Nipponbare genome release 7 (http://rice.plantbiology.msu.edu/). Based on the gene annotation information, candidate genes were determined as those predicted to encode proteins similar to thoes encoded by cloned BPH-resistant genes, including CC-NB-LRR, CC-NB-NB-LRR, CC-NB, LRR and lectin receptor kinase (Shi et al., 2023).

Selection of marker subsets for genomic prediction

The genotype data utilized the 404K core SNP subset of 3000 Rice Genomes (Wang et al., 2018a). SNPs with a missing rate exceeding 5% and minor allele frequency below 1% were excluded. Following quality control, a total of 268,936 SNPs were obtained. Additionally, the missing SNPs were imputed using Beagle 5.2 with default parameter settings. From the initial set of 268,936 (268K) SNPs set, 12 subsets (0.04K, 0.08K, 0.16K, 0.33K, 0.67K,1.3K, 2.6K, 6.7K, 13K, 26K, 67K, 134K) containing randomly distributed markers were selected utilizing a pseudo-random numbers generator. To minimize the sampling error, the random selections of each subset were repeated 50 times based on the number of SNPs in that particular subset. The numbers of SNPs for the 12 subsets were 42, 84, 168, 336, 672, 1344, 2689, 6723, 13446, 26893, 67234, 134468, respectively.

Estimation of the heritability

The heritability of the 268K SNPs set was estimated by calculating the ratio of additive genetic variance to total phenotypic variance (Wang et al., 2017). Firstly, the genetic marker was utilized to calculate a genetic relationship matrix (G matrix) using the A.mat function in R package rrBLUP. Subsequently, this G matrix was employed as covariance to estimate the additive genetic variance using the kin.blup function in rrBLUP with the default parameters. The heritability of 268K SNPs was calculated by averaging the results of the 50 random selections. The method for estimating heritability for each marker subset was the same as that of 268K SNPs.

Genomic prediction models

A total of eight statistical models with different statistical bases were selected to predict the genomic estimated breeding values (GEBVs) for resistance to BPH. Four linear methods, including genomic best linear unbiased prediction (GBLUP), ridge regression best linear unbiased prediction (rrBLUP), bayesian LASSO (BL) and bayesian sparse linear mixed models (BSLMM), were employed. The GBLUP model utilizes the genomic relationship matrix estimated from SNPs and assumes that all SNPs follow a normal distribution. The rrBLUP model is considered equivalent to the GBLUP model (Habier et al., 2007), except that marker scores were inputed into the model. BL and BSLMM represented Bayesian approaches. The marker effects were assumed to follow a double-exponential distribution in BL, and a mixture of two normal distributions in BSLMM. Linear methods may not fully capture non-linear effects such as epistasis and dominance for complex traits (Monir and Zhu, 2018; Azodi et al., 2019). Therefore, three non-linear machine learning methods were also utilized: support vector machine (SVM), random forest (RF), and artificial neural networks (ANN). Additionally, a kinship-adjusted-multiple-loci (KAML) linear mixed model was used, which selects SNPs with big effects as covariates and simultaneously gives larger weights to SNPs with moderate effects and smaller weights to SNPs with little or no effects in the kinship matrix (Yin et al., 2020). These models are the commonly used methods to estimate GEBVs. BSLMM and KAML have been demonstrated to outperform a range of existing methods; thus, we did not exhaustively include other prediction methods into comparison in our study.

Genomic prediction and cross-validation

The individuals of rice panel was split into a training population that contained 80% of individuals and a validation population that contained the remaining 20%. This produced a training population size of 1179. This procedure was repeated 5 times randomly, and we ensured that the validation populations were the same for all methods. The genomic prediction accuracy was calculated as the average Pearson's correlation between the GEBVs and observed phenotypes of individuals in validation population. Most statistical models was analysed in R packages. GBLUP and BL were implemented in package BGLR (Pérez and De Los Campos, 2004). 100,000 iterations and 10,000 burn-ins were used to fit the GBLUP and BL model. rrBLUP and BSLMM were implemented in package rrBLUP (Endelman, 2011) and software GEMMA (Zhou and Stephens, 2012), respectively. The three machine learning methods RF, ANN and SVM were analysed in package STGS. KAML were analysed in package KAML (Yin et al., 2020). The default parameters were used for all methods.

Sampling methods for genetic relatedness analysis

To determine the impact of the genetic relatedness between training and validation population on prediction accuracy, two sampling methods were created for cross-validation based on known population structure, namely stratified sampling and distant sampling. With stratified sampling, all the individuals within each subspecies (*indica*, *japonica*, circum-*aus* and circum-*basmati*) were partitioned into five datasets W1 to W5 with the similar sample sizes. The individuals that fell into W1 were combined across all the subpopulations to build the validation population. In the similar way, each dataset were combined in turn to act as the validation population, and the remaining datasets were combined to act as the training population to estimate prediction accuracy. In stratified sampling, training and validation population contained similar patterns of population stratification, and the genetic relationship between thetraining and validation population was colse. With distant sampling, one subpopulation acted as the validation population and the other subpopulations were combined and served as the training population. These analyses were performed using the 268K SNPs set.

Selection of training population subsets for genomic prediction

In order to investigate the impact of training population size on prediction accuracy, we select nine subsets from the training population based on proportions of 2%, 5%, 10%, 20%, 30%, 40%, 50%, 60% and 70% of the total training population size. The corresponding individual numbers of the nine training population subsets were 29, 74, 147, 295, 442, 590, 737, 884, and 1032. For each subset, the remaining individuals of 1,520 inbred lines were used as the validation population. Consider the presence of population structure in rice, three training population design methods were also applied in addition to random sampling, including PEVmean and CDmean and stratified sampling (Guo et al., 2019). The selections of subsets by PEVmean and CDmean were implemented in R package STPGA (version 5.2.1) and GenAlgForSubsetSelectionNoTest function. All parameters were set as default. With stratified sampling, the individual number in each subpopulation was determined by the proportion of subpopulation to the whole panel. The sampling process of each sampling method was repeated 50 times. Genomic prediction was conducted using the 268K SNPs set with GBLUP model.

Results

Variations in resistance of rice to BPH

The results of the phenotypic data analysis for resistance scores (RS), weight gain rates (WG) and honeydew excretions (HE) are presented in Table 1. Extensive phenotypic variations were observed among 502 rice varieties in their resistance to BPH. The coefficients of variation (CV) for RS, WG and HE were 0.28, 0.32 and 0.45 respectively, indicating that HE exhibited the highest degree of variation. As indicated by the skewness, RS did not follow a normal distribution but displayed two distinct peaks around values of 6 and 9 on the distribution curve (Figure 1A). Among these varieties, 146 (29.08%) varieties showed moderate resistance at RS level 6, while 140 (27.89%) varieties showed extremely susceptible at RS level 9. Both RS and WG demonstrated a right-skewed distribution; however, WG exhibited a greater degree of right skewness compared to RS (Figures 1A, B). On the other hand, the distribution of HE was close to a normal distribution (Figure 1C).

According to the resistance intervals listed in Table 2, the resistance levels of each rice variety were categorized. There were 28 (5.58%), 28 (5.58%) and 104 (20.72%) rice varieties with resistant (R) levels in RS, WG and HE, respectively. Among these traits, eight varieties showed R level to BPH simultaneously. A total of 117 (23.31%) varieties displayed resistance (R level) to BPH (Figure 1D).

Principal component analysis (PCA) revealed the presence of population structure in the 502 rice varieties (Figures 2A, B). Subsequently, least significant difference tests were conducted to evaluate the resistance differences among the four subspecies. In terms of RS, *indica* exhibited higher resistance compared to *japonica* and *circum*-aus subspecies, and *circum*-basmati displayed the highest susceptibility (Figure 2C). Similarly, for WG, *indica* demonstrated significantly greater resistance than other subspecies (Figure 2D). Regarding HE, both *indica* and *circum*-aus along with *circum*-basmati showed significantly resistant than *japonica* (Figure 2E). To summarize, rice varieties of *indica* subspecies tend to be more resistant to BPH, which was consistent with previous results (Zhou et al., 2021).

TABLE 1 Summary statistics of resistance of 502 rice varieties to BPH.

Trait	Subspecies	Number of individuals	Range	Mean ± SD	Skewness	Kurtosis	CV
RS	Whole	502	1.44-9.00	6.63 ± 1.89	-0.38	2.68	0.28
	indica	227	1.44-9.00	6.20 ± 1.90	-0.18	-0.31	0.31
	japonica	102	3.61-9.00	6.96 ± 1.55	0.27	-1.30	0.22
	circum-*aus*	146	1.70-9.00	6.94 ± 1.98	-0.62	-0.45	0.29
	circum-*basmati*	8	7.00-9.00	8.36 ± 0.92	-0.93	-1.25	0.11
WG	Whole	502	-0.10-1.21	0.78 ± 0.25	-1.04	3.87	0.32
	indica	227	0.01-1.21	0.73 ± 0.25	-0.71	-0.02	0.35
	japonica	102	-0.10-1.19	0.85 ± 0.20	-1.85	6.04	0.24
	circum-*aus*	146	-0.06-1.19	0.80 ± 0.20	-1.22	1.31	0.33
	circum-*basmati*	8	0.39-1.06	0.86 ± 0.22	-1.48	2.10	0.26
HE	Whole	502	0.0003-0.12	0.05 ± 0.02	0.08	-0.51	0.45
	indica	227	0.0003-0.10	0.05 ± 0.02	-0.02	-0.69	0.45
	japonica	102	0.0097-0.12	0.06 ± 0.02	0.14	-0.43	0.39
	circum-*aus*	146	0.0014-0.11	0.05 ± 0.02	0.06	-0.61	0.46
	circum-*basmati*	8	0.0181-0.06	0.04 ± 0.02	-0.19	-1.36	0.38

*SD, standard deviation; CV, coefficient of variation.

10.3389/fpls.2024.1373081

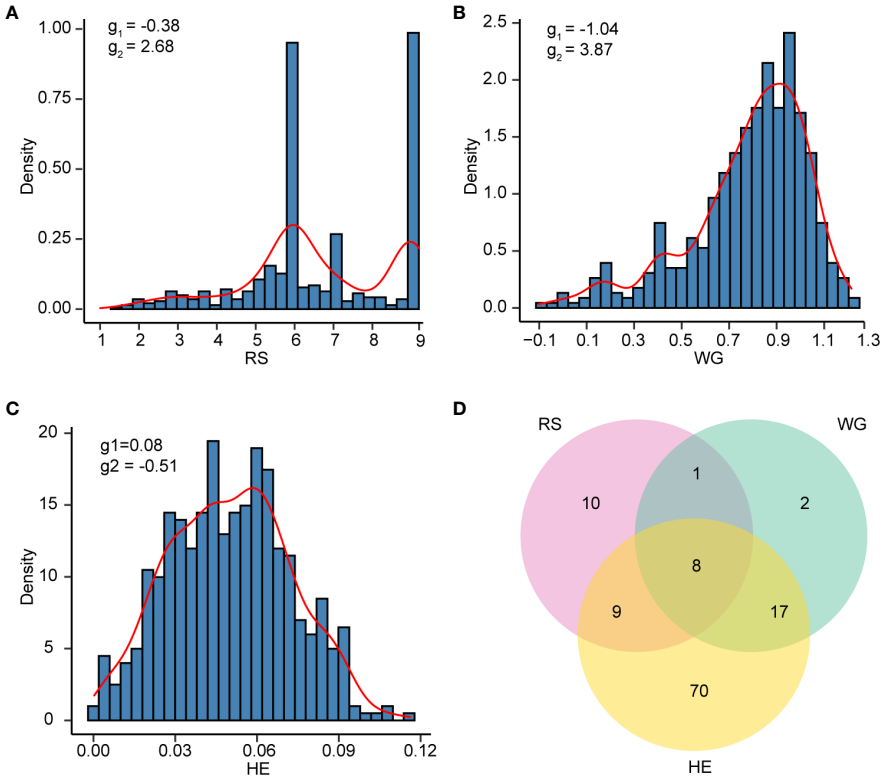

FIGURE 1
The resistance distribution of 502 rice varieties. **(A-C)** Density histogram of RS **(A)**, WG **(B)**, and HE **(C)**. The skewness (g_1) and kurtosis (g_2) are labeled on each plot. **(D)** Venn plot showing the number of varieties with resistant (R) levels in RS, WG and HE.

Correlation analysis between RS, WG and HE

The results of the correlation analysis between different resistance traits are presented in Figure 3. The correlation coefficients between RS, WG, and HE were 0.38, 0.27, and 0.61, respectively (Figure 3A). RS of the 502 rice varieties identified in the seedling bulk test exhibited significant correlations with two antibiosis indicators: WG and HE. Specifically, the correlation between RS and WG (r = 0.38, p < 2.2×10-16) was greater than that between RS and HE (r = 0.27, p = 5.3×10-10). Furthermore, as two indicators of antibiosis to BPH, the pearson correlation coefficient (r) between WG and HE reached 0.61, indicating a strong positive correlation between them (Figure 3A).

TABLE 2 Summary information of resistance levels.

Trait	Resistance interval	Resistance level	Number	Percentage of total
RS	(1,3]	R	28	5.58%
	(3,6]	MR	232	46.22%
	(6,9]	S	242	48.21%
WG	(-0.10,0.30]	R	28	5.58%
	(0.30,0.60]	MR	66	13.15%
	(0.60,0.90]	MS	223	44.42%
	(0.90,1.21]	S	185	36.85%
HE	(0,0.03]	R	104	20.72%
	(0.03,0.06]	MR	231	46.02%
	(0.06,0.09]	MS	147	29.28%
	(0.09,0.12]	S	20	3.98%

*R, Resistant; MR, Moderate resistant; MS, Moderate Susceptible; S, Susceptible.

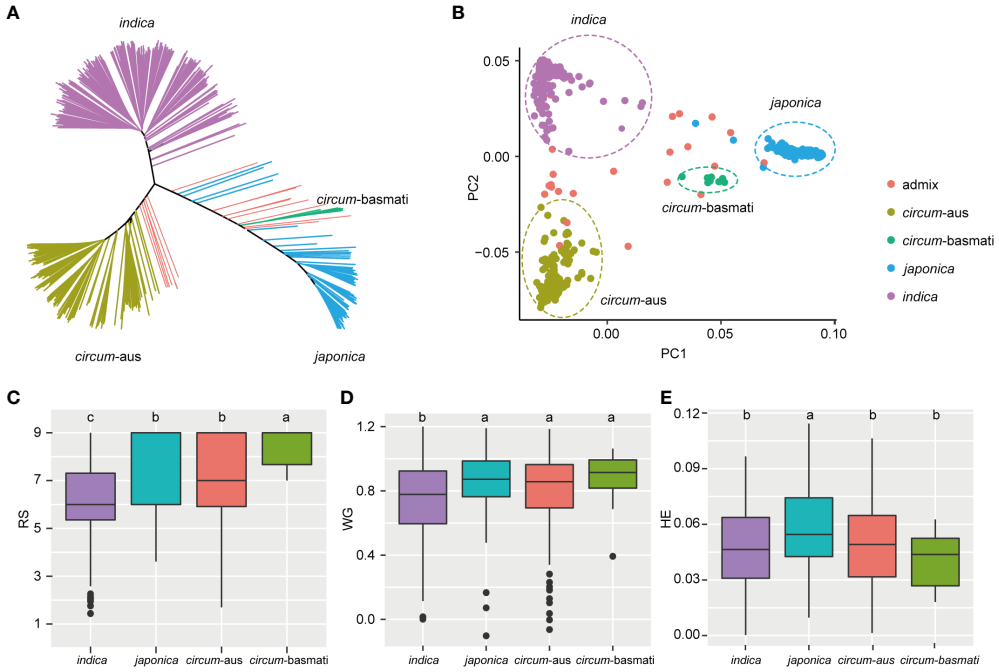

FIGURE 2
Resistance differences among four subspecies. **(A)** Unweighted neighbor-joining tree based on the IBS distance matrix of 502 rice varieties. Samples are colored according to their subspecies. **(B)** The first two principal components are plotted to display the population structure of 502 rice varieties. *indica*, *japonica*, circum-*aus* and circum-*basmati* varieties are clustered separately. **(C-E)** Boxplot of RS, WG, and HE of different subspecies. The significant differences between subspecies are indicated by different lowercase letters ($p < 0.05$, least significant difference test).

The correlation patterns varied among the subspecies. There were significant correlations between RS and WG, as well as RS and HE in *indica* and *circum*-aus; however, no significant correlations were observed in *japonica* and *circum*-basmati (Figures 3B-D). Moreover, significant correlations were identified between the two indicators of antibiosis in *indica*, *circum*-aus and *japonica* but not in *circum*-basmati (Figures 3B-D).

Associated loci identified by GWAS

For RS, a total of 217 significant SNPs ($p<1.0\times10^{-8}$) were detected on chromosome 2, 4, 6, 11, and 12. Notably, 212 (97.7%) significant SNPs were clustered on chromosome 6 (Figure 4A). The genome-wide LD decay rate was estimated at 100 kbp. The associated locus was defined as the 100 kbp region on either side of a significant SNP and multiple overlapping associated loci were merged into a single locus. In total, five loci were associated with RS of 502 varieties. Detailed information regarding these associated loci can be found in Table 3.

Considering the potential influence of population structure, separate GWAS were performed in subspecies. There were three and two loci associated with RS of *indica* and *circum*-aus, respectively (Figures 4B, D, Table 3). It was obvious that the associated loci detected in 502 varieties were contributed by *indica* and *circum*-aus. No associated loci were detected in *japonica* (Figure 4C). Interestingly, one associated locus on chromosome 11 (cA_2) was specific in *circum*-aus but not in 502 varieties. Overall, six unique loci were significantly associated with RS, and two loci (W_4 and cA_2) were novel loci that had not been previously identified (Table 3).

No significant SNP was detected to be associated with WG and HE in 502 varieties, as shown in Figure 5. However, in our previous study with an expanded sample size of 1,520 individuals, we identified 17 loci that were significantly associated with WG. Among the six loci associated with RS, five loci (83.33%) were also associated with WG, and one locus (W_4) is only associated with RS. In addition, separate GWAS were performed in subspecies, and no significant SNP was detected to be associated with WG and HE.

Identification of resistance candidate genes

There were a total of 331 genes annotated in the associated loci according to the Nipponbare reference genome (Supplementary Table S2). These included the known BPH-resistant genes *Bph6*, *Bph32* and *Bph37* on chromosome 4 and 6, confirming the effectiveness of GWAS in identifying BPH-resistant gene. In addition, candidate genes were identified based on their protein domain similarity to the cloned BPH-resistant gene (Shi et al., 2023), resulting in the identification of eight candidate genes (Table 3). On chromosome 11, a significant cluster of SNPs was observed in the region spanning from 16.64 to 16.88 Mbp (Figure 4D). The local manhattan plot and LD heatmap surrounding the peak SNPs showed that three candidate genes

10.3389/fpls.2024.1373081

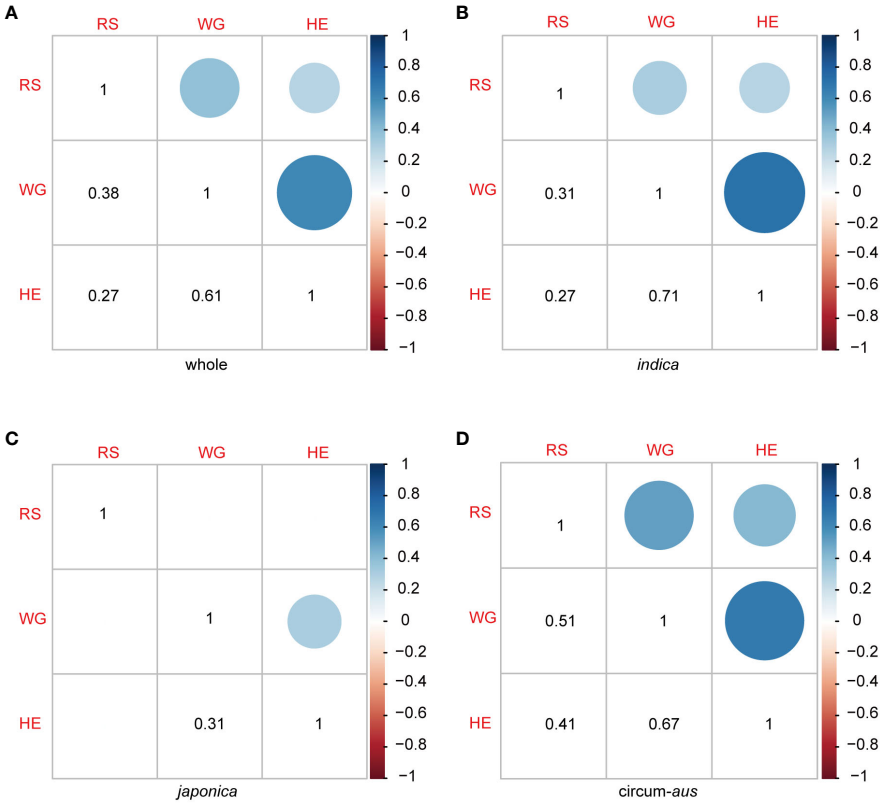

FIGURE 3
Pearson correlation coefcient matrix among RS, WG and HE in 502 rice varieties **(A)**, *indica* **(B)**, *japonica* **(C)** and circum-*aus* **(D)**.The dots (upper triangle) and numbers (lower triangle) denote the correlation coefcients. Blank squares in the matrix indicate that the correlation between the two corresponding traits are not signifcant (P>0.01).

(LOC_Os11g29030, LOC_Os11g29050, LOC_Os11g29110) were localized within a single LD block of approximately 100-kbp size (Figure 6A). Another associated locus on chromosome 11 was located in 20.99-21.19 Mbp, with four candidate genes (LOC_Os11g35890, LOC_Os11g35960, LOC_Os11g35980 and LOC_Os11g36020) localized within a 100-kbp LD block spanning from 21.08 to 21.19 Mbp (Figure 6B). Notably, there was a significant difference in resistance scores between the two haplotypes based on peak SNP (Figures 6C, D). The presence of clustered candidate genes encoding RLK, NBS-LRR or LRR protein on chromosome 11 suggests their potential involvement in BPH resistance.

Effect of marker number and statistical model on GP accuracy

To validate the usefulness of associations identifed by GWAS in molecular improvement programmes, we performed genomic prediction (GP) and evaluated its predictive ability for BPH resistance. Considering that a larger sample size of 1,520 allowed for the detection of more association loci, we used WG data of 1,520 rice varieties for GP.

To investigate the effect of marker number on prediction accuracy and determine the minimum number of markers required for predicting resistance to BPH, we selected 12 subsets with randomly distributed markers from the full set of 268,936 (268K) SNPs. This process was repeated 50 times for each subset. The estimated heritability based on the full set (268K) and subsets ranged from 0.069 to 0.312 (Figure 7A). The heritability value increased as the number of markers increased. Specifically, there was a rapid increase in estimated heritability when the marker number increased from 2.6 K to 6.7 K, and then it tended to stabilize when the marker number increased to 67 K. The average prediction accuracies using eight statistical models under full set and twelve subsets are shown in Figure 7B. The average prediction accuracy ranged from 0.385 to 0.633 and increased as the marker number increased from 0.04K to 26K, subsequently showing minimal improvement. However, there were no significant difference in the prediction accuracy between 6.7K SNPs and 268K SNPs ($p<0.05$, t-test).

To investigate the effect of statistical model on prediction accuracy, we used eight statistical models with different statistical bases. Among these models, RF achieved an average prediction accuracy of 0.633 when the marker number was 26K, while ANN had the lowest prediction accuracy at 0.576. GBLUP, BSLMM and BL showed similar prediction accuracies, as did KAML, rrBLUP and SVM, which were in the middle level between RF and ANN in terms of prediction accuracy. The average prediction accuracies of RF were significant higher than that of other models ($p<0.05$, t-test).

10.3389/fpls.2024.1373081

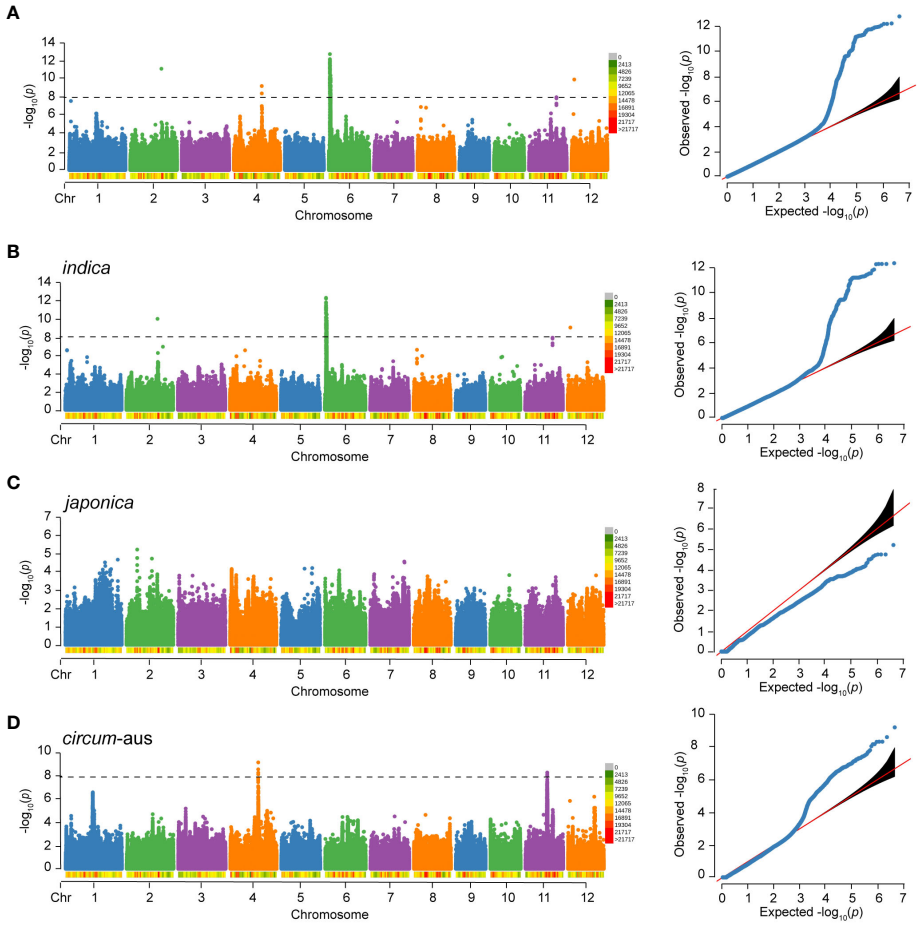

FIGURE 4
Manhattan plot and Quantile-Quantile (QQ) plot of RS to BPH of 502 rice varieties **(A)**, *indica* **(B)**, *japonica* **(C)** and *circum*-aus **(D)**. The density of SNPs are labeled below the chromosomes. The *p*-value threshold for significance is 1.0×10^{-8}.

TABLE 3 Summary information of associated loci obtained by GWAS for RS.

Locus	Population	Chr	Locus region (Mbp)	Number of significant SNPs	Lead SNP	p value	Var (%)	Known R genes	Candidate genes (annotation)
W_1	whole	2	23.86-24.06	1	rs2_23955573	7.26E-12	5.18		
W_2	whole	4	21.27-21.52	2	rs4_21365665	5.78E-10	9.34	*Bph6*	
W_3	whole	6	0.81-1.58	212	rs6_922708	1.78E-13	19.69	*Bph32*/ *Bph37*	LOC_Os06g03970 (receptor-like protein kinase)
W_4	whole	11	20.99-21.19	1	rs11_21088754	9.88E-09	4.14		LOC_Os11g35890 (leucine rich repeat protein), LOC_Os11g35960 (leucine rich repeat protein), LOC_Os11g35980 (leucine rich repeat protein), LOC_Os11g36020 (leucine rich repeat protein)
W_5	whoe	12	1.96-2.16	1	rs12_2060801	1.11E-10	10.03		

(Continued)

10.3389/fpls.2024.1373081

TABLE 3 Continued

Locus	Population	Chr	Locus region (Mbp)	Number of significant SNPs	Lead SNP	p value	Var (%)	Known R genes	Candidate genes (annotation)
I_1	*indica*	2	23.86-24.06	1	rs2_23955573	9.86E-11	4.14		
I_2	*indica*	6	0.81-1.58	256	rs6_922708	4.81E-13	13.65	*Bph32*/ *Bph37*	LOC_Os06g03970 (receptor-like protein kinase)
I_3	*indica*	12	1.96-2.16	1	rs12_2060801	8.89E-10	6.26		
cA_1	*circum*-aus	4	21.27-21.52	4	rs4_21393633	6.58E-10	5.68	Bph6	
cA_2	*circum*-aus	11	16.64-16.88	11	rs11_16777730	4.95E-09	7.02		LOC_Os11g29030 (NBS-LRR disease resistance protein), LOC_Os11g29050 (NBS-LRR type disease resistance protein), LOC_Os11g29110 (Leucine Rich Repeat protein)

Therefore, RF outperformed the other models in predicting rice resistance to BPH.

Effect of training population sizes on GP accuracy

In the studies of phenotypic prediction, the high cost of collecting phenotypic data limits the size of training population. To investigate the influence of training population size on accuracy in predicting resistance to BPH, we successively reduced the size of our training population and evaluated its predictive performance. The prediction accuracies ranged from 0.414 to 0.614 using different training population sizes by four sampling methods, all lower than that achieved by utilizing the entire training population (Figure 7C). Generally, an increase in training population size led to improved accuracy. However, when reducing the sample size to 737, there was no significant difference in prediction accuracy compared to utilizing a larger training population consisting of 1179 varieties ($p<0.05$, t-test).

Among the four different methods employed for selecting the training populations, namely CDmean, PEVmean, stratified sampling and random sampling, comparable levels of prediction accuracies were observed in CDmean, stratified sampling and random sampling. Conversely, PEVmean consistently exhibited lower accuracies.

Effect of genetic relatedness on GP accuracy

The accuracy of genomic prediction can be influenced by the genetic relatedness between the training and validation population (Wang et al., 2017). To assess its effect on the prediction accuracy of

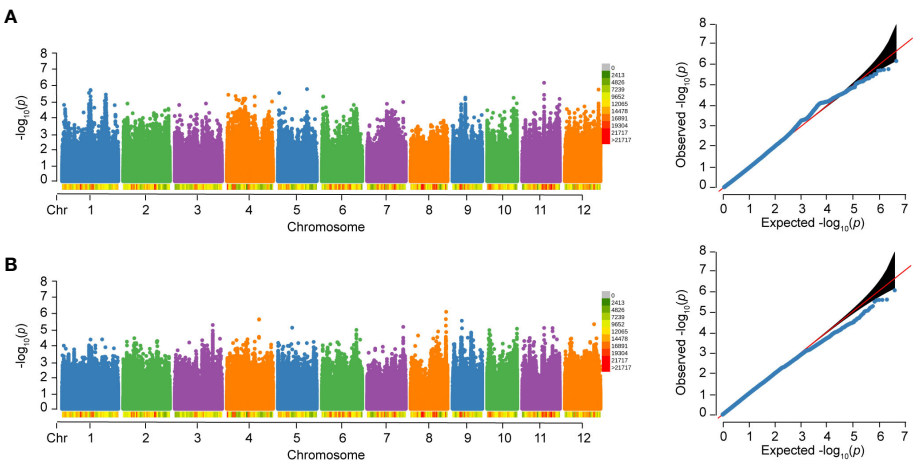

FIGURE 5
Manhattan plots and Quantile-Quantile (QQ) plots of WG and HE of 502 rice varieties to BPH. **(A)** WG. **(B)** HE.

10.3389/fpls.2024.1373081

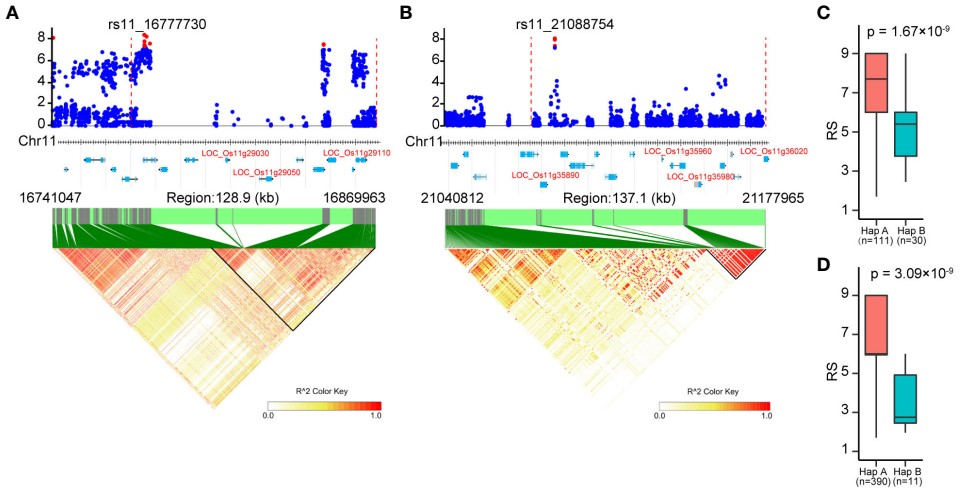

FIGURE 6
Identification of candidate genes for the associated loci on chromosome 11. **(A)**, **(B)** Local manhattan plots (top) and LD heatmaps (bottom) surrounding the peak SNPs of associated loci cA_2 **(A)** and W_4 **(B)**. The vertical dashed lines in the local manhattan plots indicate the LD blocks. Red dots indicate significantly associated SNPs. All genes in the associated loci are marked at the bottom of the manhattan plots, and the candidate genes are represented in red letters. **(C, D)** The resistance of the two haplotypes based on peak SNP of cA_2 **(C)** and W_4 **(D)**. Significant differences between haplotypes were analyzed by student's t-test.

resistance to BPH, we designed stratified sampling and distant sampling based on the known population structure. The prediction accuracies of stratified sampling were significant higher than those achieved with distant sampling ($p<0.05$, t-test). Specifically, GBLUP estimated an average accuracy of 0.605 for stratified sampling, while distant sampling yielded an average accuracy estimate of only 0.056 (Figure 7D). Additionally, We compared the prediction accuracies between stratified and random sampling methods and found no significant differences, suggesting that both training and validation population contained similar patterns of population stratification in random sampling.

Discussion

BPH is the most destructive insect pest that threatens rice production globally (Dyck and Thomas, 1979). BPH biotype II and III with strengthened virulence emerged with the spread of *Bph1* and *bph2*, respectively (Claridge and Den Hollander, 1980; Kobayashi, 2016). In this study, we evaluated the resistance of 502 rice varieties by evaluating the resistance scores (RS), weight gain rates (WG) and honeydew excretions (HE). A wide range of resistance was observed in the 502 rice varieties. A total of 117 (23.31%) of the 502 rice varieties displayed resistance to BPH. The resistance score from the seedling bulk test was a comprehensive indicator of antibiosis, tolerance and antixenosis (Qiu et al., 2011). Our results showed that RS exhibited significant correlations with the two antibiosis indicators:WG and HE. However, ten rice varieties showed resistant (R) level in RS but moderately susceptible (MS) or susceptible (S) level in WG and HE, suggesting their tolerance or antixenosis to BPH. Generally, tolerance has no selection pressure on BPH biotype (Panda and Heinrichs, 1983). These ten varieties are of potential importance to exploit tolerance genes for controlling BPH and slowing down the emergence of new BPH biotypes. Furthermore, there were thirty-six and three rice varieties in the R level in HE and WG respectively, while RS exhibited S level, indicating that RS is not simply a combination of antibiosis, tolerance, and antixenosis.

The seedling bulk test has the advantage of large-scale and rapid identification of resistance. Combined with its ability to comprehensively assess the level of antibiosis, tolerance and antixenosis, it is often employed for evaluating resistance to BPH and maping resistance gene (Qiu et al., 2011). However, it is difficult to differentiate between antibiosis, tolerance, or antixenosis in a seedling bulk test. In addition, in seedling bulk test, rice varieties to be tested are planted in the box with the susceptible control variety and infested with second- to third-instar nymphs. It's challenging to maintain the same insect numbers across varieties, and damage scores detection by human vision is less precise than the insect weight in an antibiosis experiment. In the antibiosis experiments, the insect weight was strictly controlled with a balance to ensure the accuracy of the antibiosis. However, tolerance and antixenosis cannot be simultaneously assessed in antibiosis experiment. Therefore, it is necessary to use multiple methods to comprehensively evaluate rice resistance to find more resistant resources.

GWAS were performed on the panel of 502 rice varieties and its subspecies, and 6 loci were associated with RS. However, no loci were significantly associated with WG and HE in these 502 rice varieties. Notably, when the sample size was expanded to include 1,520 rice varieties in our previous study (Zhou et al., 2021), we detected 17 loci asscated with WG. The limited sample size likely contributed to the lower statistical power for detecting loci associated with WG and HE. Among the six loci associated with RS, five (83.33%) were also found to be associated with WG of 1,520 rice varieties, and one locus was newly discovered. These findings suggest that increasing sample size can enhance detection power for

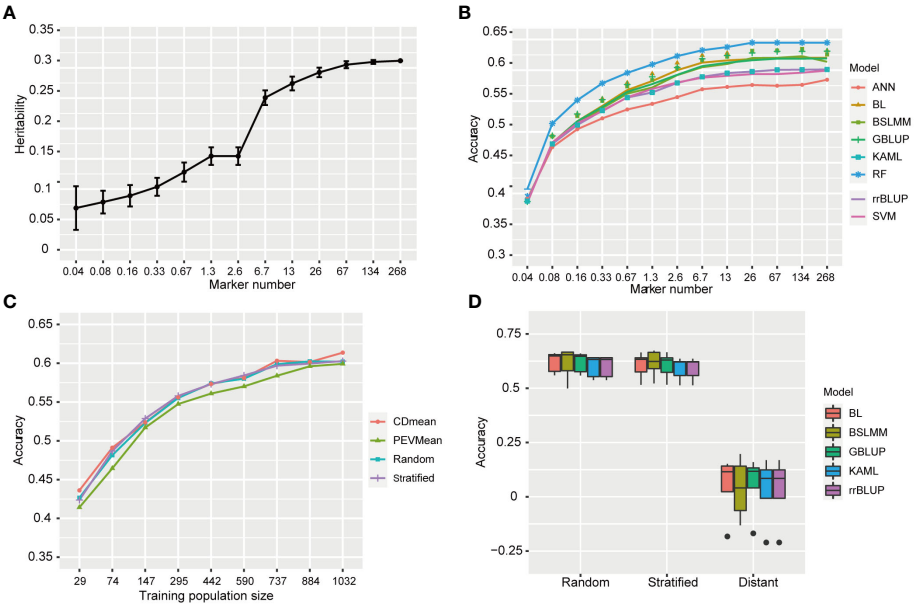

FIGURE 7
Genomic prediction accuracy for resistance to BPH. **(A)** The heritability of resistance to BPH estimated using 12 SNPs subsets. The standard deviation of 50 repetitions is marked with error bar. **(B)** The prediction accuracy for resistance to BPH by eight statistical models under 268K SNPs set and 12 subsets with different SNP numbers. rrBLUP, ridge regression best linear unbiased predictor; GBLUP, genomic best linear unbiased prediction; BL, bayesian LASSO; BSLMM, bayesian sparse linear mixed models; RF, random forest; ANN, artificial neural network; SVM, support vector machine; KAML, kinship-adjusted-multiple-loci linear mixed model. **(C)** The prediction accuracy for resistance to BPH using different training population sizes by four sampling methods. The training sets were selected by CDmean, PEVmean, stratified sampling and random sampling. Nine different training population sizes (29, 74, 147, 295, 442, 590, 737, 884, and 1032) were used. **(D)** The prediction accuracy for resistance to BPH using random, stratified and distant sampling by five statistical models.

identifying BPH-resistant loci; however, it is worth noting that compared to WG and HE traits, RS exhibits higher detection power when a small sample size population was used.

The two associated loci (cA_2 and W_4) on chromosome 11 harbored three and four candidate genes predicted to encode NBS-LRR or LRR proteins. These loci were not mapped before and were completely new loci. It is hypothesized that the two loci may confer tolerance or antixenosis towards BPH infestation based on the fact that they were associated with RS but not WG. The candidate genes were located in close proximity, making it challenging to determine which genes were responsible for BPH resistance. Alternatively, it is possible that these candidate genes function collectively similar to *Bph3*, a cluster of three genes (OsLecRK1-OsLecRK3) to confer resistance (Liu et al., 2015). In conclusion, the identification of these candidate genes within the newly discovered loci provides valuable clues for validating their roles in BPH resistance and facilitating rice breeding for BPH resistance.

We assessed the predictive accuracy of genome selection for BPH resistance using natural populations of 1,520 rice varieties, with the highest predictive accuracy reaching 0.633. The highest prediction accuracy value ranged between 0.31 for rice yield prediction and 0.80 for heading date and plant height prediction, similar to the prediction accuracy of rice flowering time (Onogi et al., 2015; Spindel et al., 2015). Typically, predictive accuracy increases with an increasing number of markers until reaching a platform (Xu et al., 2021). When the SNPs number increased to 26K, the prediction accuracy for BPH resistance remained stable, and there was no significant difference in the prediction accuracy between 6.7K SNPs and 268K SNPs. Therefore, when predicting BPH resistance using a training population consisting of 1179 rice varieties, a minimum of approximately 6.7K SNPs displayed comparable accuracy. Prediction accuracy varied among eight different statistical models tested in this study. Random Forest (RF) achieved the highest prediction accuracy at 0.633; while GBLUP, BSLMM, and BL showed similar accuracies at around 0.618 with only slight differences Despite RF's superior prediction performance, its computational speed was slower compared to others such as GBLUP and BSLMM.

In genome prediction studies, the high costs of phenotyping restrict the size of training population. As we progressively decreased the size of training population, we observed a corresponding decline in its prediction accuracy, indicating that increasing the size could enhance BPH resistance enhance. However, there was negligible difference in prediction accuracy between 737 and 1179 individuals. Therefore, a training population consisting of 737 individuals is sufficient for predicting resistance to BPH. The accuracy of genome prediction is affected by the genetic relatedness between the training and the validation population (Wang et al., 2017). When the genetic proximity is substantial, the prediction accuracy for BPH resistance is considerably higher compared to cases where it is distant. Hence, optimizing the composition of the training population plays a crucial role in achieving superior prediction accuracy even when there is population stratification. Consequently, for high prediction

accuracy, it is important to have a broader genetic diversity within the training population while maintaining close genetic relatedness with the validation population. Additionally, to accurately predict resistance to BPH, one should consider increasing SNP numbers beyond 26K, expanding the training population size beyond 737 individuals, and employing RF models. These findings hold great significance in guiding applications of genome selection towards developing durable BPH-resistant rice.

Data availability statement

The datasets presented in this study can be found in online repositories. The names of the repository/repositories and accession number(s) can be found in the article/Supplementary Material.

Author contributions

CZ: Writing – original draft, Conceptualization, Data curation, Investigation, Formal analysis, Funding acquisition, Visualization. WJ: Writing – original draft, Investigation. JG: Writing – review & editing. LZ: Writing – original draft, Resources. LL: Writing – original draft, Funding acquisition. SL: Writing – review & editing, Funding acquisition. RC: Writing – review & editing, Resources. BD: Writing – review & editing, Conceptualization, Funding acquisition. JH: Writing – review & editing, Data curation, Formal analysis, Investigation.

Funding

The author(s) declare financial support was received for the research, authorship, and/or publication of this article. This work was supported by the Basic research expenses of Oil Crops Research Institute of the Chinese Academy of Agricultural Sciences (1610172022016), the Knowledge Innovation Special Program of Wuhan (2022020801020297), and the Science and Technology Major Program of Hubei Province (2022ABA001).

Acknowledgments

We sincerely thank Prof. Guangcun He (Wuhan University) for kindly providing the 502 rice varieties.

Conflict of interest

The authors declare that the research was conducted in the absence of any commercial or financial relationships that could be construed as a potential conflict of interest.

Publisher's note

Supplementary material

The Supplementary Material for this article can be found online at: https://www.frontiersin.org/articles/10.3389/fpls.2024.1373081/full#supplementary-material

References

Akanksha, S., Lakshmi, J. V., Singh, A. K., Deepthi, Y., Chirutkar, P. M., Ramdeen,, et al. (2019). Genetics of novel brown planthopper Nilaparvata lugens resistance genes in derived introgression lines from the interspecific cross O. sativa var. Swarna×O.nivara. *J. Genet.* 98, 113. doi: 10.1007/s12041-019-1158-2

Azodi, C., Bolger, E., McCarren, A., Roantree, M., Campos, G., Shiu, S., et al. (2019). Benchmarking parametric and machine learning models for genomic prediction of complex traits. *G3-Genes Genomes Genet.* 9, 3691–3702. doi: 10.1534/g3.119.400498

Balding, D. J., and Nichols, R. A. (1995). A method for quantifying differentiation between populations at multi-allelic loci and its implications for investigating identity and paternity. *Genetica* 96, 3–12. doi: 10.1007/BF01441146

Chang, C. C., Chow, C. C., Tellier, L. C., Vattikuti, S., Purcell, S. M., and Lee, J. J. (2015). Second-generation PLINK: rising to the challenge of larger and richer datasets. *Gigascience* 4, 7. doi: 10.1186/s13742-015-0047-8

Claridge, M. F., and Den Hollander, J. (1980). The 'biotypes' of the rice brown planthopper, Nilaparvata lugens. *Entmol. Exp. Appl.* 27, 23–30. doi: 10.1111/j.1570-7458.1980.tb02942.x

Crossa, J., Pérez-Rodríguez, P., Cuevas, J., Montesinos-López, O., Jarquín, D., Campos, G., et al. (2017). Genomic selection in plant breeding: methods, models, and perspectives. *Trends Plant Science.* 22, 961–975. doi: 10.1016/j.tplants.2017.08.011

Desta, Z., and Ortiz, R. (2014). Genomic selection: Genome-wide prediction in plant improvement. *Trends Plant Science.* 19, 592–601. doi: 10.1016/j.tplants.2014.05.006

Du, B., Zhang, W., Liu, B., Hu, J., Wei, Z., Shi, Z., et al. (2009). Identification and characterization of Bph14, a gene conferring resistance to brown planthopper in rice. *Proc. Natl. Acad. Sci. U. S. A.* 106, 22163–22168. doi: 10.1073/pnas.0912139106

Dyck, V., and Thomas, B. (1979). *Brown Planthopper: Threat to Rice Production in Asia*. Ed. N. C. Brady (International Rice Research Institute), 3–17.

Endelman, J. B. (2011). Ridge regression and other kernels for genomic selection with R package rrBLUP. *Plant Genome.* 4, 250–255. doi: 10.3835/plantgenome2011.08.0024

Guo, J., Xu, C., Wu, D., Zhao, Y., Qiu, Y., Wang, X., et al. (2018). Bph6 encodes an exocyst-localized protein and confers broad resistance to planthoppers in rice. *Nat. Genet.* 50, 297–306. doi: 10.1038/s41588-018-0039-6

Guo, T., Yu, X., Li, X., Zhang, H., Zhu, C., Flint-Garcia, S., et al. (2019). Optimal designs for genomic selection in hybrid crops. *Mol. Plant* 12, 390–401. doi: 10.1016/j.molp.2018.12.022

Habier, D., Fernando, R. L., and Dekkers, J. C. M. (2007). The impact of genetic relationship information on genome-assisted breeding values. *Genetics* 177, 2389–2397. doi: 10.1534/genetics.107.081190

He, J., Liu, Y., Liu, Y., Jiang, L., Wu, H., Kang, H., et al. (2013). High-resolution mapping of brown planthopper (BPH) resistance gene Bph27(t) in rice (Oryza sativa L.). *Mol. Breed.* 31, 549–557. doi: 10.1007/s11032-012-9814-8

Hu, J., Chang, X., Zou, L., Tang, W., and Wu, W. (2018). Identification and fine mapping of Bph33, a new brown planthopper resistance gene in rice (Oryza sativa L.). *Rice* 11, 55. doi: 10.1186/s12284-018-0249-7

Huang, Z., He, G., Shu, L., Li, X., and Zhang, Q. (2001). Identification and mapping of two brown planthopper resistance genes in rice. *Theor. Appl. Genet.* 102, 929–934. doi: 10.1007/s001220000455

Huang, D., Qiu, Y., Zhang, Y., Huang, F., Meng, J., Wei, S., et al. (2013). Fine mapping and characterization of BPH27, a brown planthopper resistance gene from wild rice (Oryza rufipogon Griff.). *Theor. Appl. Genet.* 126, 219–229. doi: 10.1007/s00122-012-1975-7

Jairin, J., Phengrat, K., Teangdeerith, S., Vanavichit, A., and Toojinda, T. (2007). Mapping of a broad-spectrum brown planthopper resistance gene, Bph3, on rice chromosome 6. *Mol. Breed.* 19, 35–44. doi: 10.1007/s11032-006-9040-3

Ji, H., Kim, S. R., Kim, Y. H., Suh, J., Park, H., Sreenivasulu, N., et al. (2016). Map-based cloning and characterization of the BPH18 gene from wild rice conferring resistance to brown planthopper (BPH) insect pest. *Sci. Rep.* 6, 34376. doi: 10.1038/srep34376

Jing, S. L., Zhao, Y., Du, B., Chen, R. Z., Zhu, L. L., and He, G. C. (2017). Genomics of interaction between the brown planthopper and rice. *Curr. Opin. Insect Sci.* 19, 82–87. doi: 10.1016/j.cois.2017.03.005

Kang, H. M., Sul, J. H., Service, S. K., Zaitlen, N. A., Kong, S., Freimer, N. B., et al. (2010). Variance component model to account for sample structure in genome-wide association studies. *Nat. Genet.* 42, 348–354. doi: 10.1038/ng.548

Kobayashi, T. (2016). Evolving ideas about genetics underlying insect virulence to plant resistance in rice-brown planthopper interactions. *J. Insect Physiol.* 84, 32–39. doi: 10.1016/j.jinsphys.2015.12.001

Letunic, I., and Bork, P. (2021). Interactive Tree Of Life (iTOL) v5: an online tool for phylogenetic tree display and annotation. *Nucleic Acids Res*. 49, W293–W296. doi: 10.1093/nar/gkab301

Li, Z., Xue, Y., Zhou, H., Li, Y., Usman, B., Jiao, X., et al. (2019). High-resolution mapping and breeding application of a novel brown planthopper resistance gene derived from wild rice (Oryza. rufipogon Griff). *Rice* 12, 41. doi: 10.1186/s12284-019-0289-7

Liu, Y., Wu, H., Chen, H., Liu, Y., He, J., Kang, H., et al. (2015). A gene cluster encoding lectin receptor kinases confers broad spectrum and durable insect resistance in rice. *Nat. Biotechnol.* 33, 301–305. doi: 10.1038/nbt.3069

Monir, M. M., and Zhu, J. (2018). Dominance and epistasis interactions revealed as important variants for leaf traits of maize NAM population. *Front. Plant Sci.* 9. doi: 10.3389/fpls.2018.00627

Myint, K. K. M., Fujita, D., Matsumura, M., Sonoda, T., Yoshimura, A., and Yasui, H. (2012). Mapping and pyramiding of two major genes for resistance to the brown planthopper in the rice cultivar ADR52. *Theor. Appl. Genet.* 124, 495–504. doi: 10.1007/s00122-011-1723-4

Onogi, A., Ideta, O., Inoshita, Y., Ebana, K., Yoshioka, T., Yamasaki, M., et al. (2015). Exploring the areas of applicability of whole-genome prediction methods for asian rice (Oryza sativa L.). *Theor. Appl. Genet.* 128, 41–53. doi: 10.1007/s00122-014-2411-y

Panda, N., and Heinrichs, E. A. (1983). Levels of tolerance and antibiosis in rice varieties having moderate resistance to the brown planthopper, Nilaparvata lugens (Stål) (Hemiptera: Delphacidae). *Environ. Entomol.* 12, 1204–1214. doi: 10.1093/ee/12.4.1204

Pathak, M. D., Cheng, C. H., and Fortuno, M. E. (1969). Resistance to Nephotettix impicticeps and Nilaparvata lugens in varieties of rice. *Nature* 5205, 502–504. doi: 10.1038/223502A0

Pérez, P., and De Los Campos, G. (2004). BGLR: A statistical package for whole genome regression and prediction.

Prahalada, G. D., Shivakumar, N., Lohithaswa, H. C., Gowda, D. K., Ramkumar, G., Kim, S., et al. (2017). Identification and fine mapping of a new gene, BPH31 conferring resistance to brown planthopper biotype 4 of India to improve rice, Oryza sativa L. *Rice* 10, 41. doi: 10.1186/s12284-017-0178-x

Qiu, Y., Guo, J., Jing, S., Tang, M., Zhu, L., and He, G. (2011). Identification of antibiosis and tolerance in rice varieties carrying brown planthopper resistance genes. *Entomol. Experimentalis Applicata* 141, 224–231. doi: 10.1111/j.1570-7458.2011.01192.x

Qiu, Y., Guo, J., Jing, S., Zhu, L., and He, G. (2014). Fine mapping of the rice brown planthopper resistance gene BPH7 and characterization of its resistance in the 93-11 background. *Euphytica* 198, 369–379. doi: 10.1007/s10681-014-1112-6

Ren, J., Gao, F., Wu, X., Lu, X., Zeng, L., Lv, J., et al. (2016). Bph32, a novel gene encoding an unknown SCR domain-containing protein, confers resistance against the brown planthopper in rice. *Sci. Rep.* 6, 37645. doi: 10.1038/srep37645

Shi, S., Wang, H., Zha, W., Wu, Y., Liu, K., Xu, D., et al. (2023). Recent advances in the genetic and biochemical mechanisms of rice resistance to brown planthoppers (Nilaparvata lugens stål). *Int. J. Mol. Sci.* 24, 16959. doi: 10.3390/ijms242316959

Spindel, J., Begum, H., Akdemir, D., Virk, P., Collard, B., Redoña, E., et al. (2015). Genomic selection and association mapping in rice (Oryza sativa): effect of trait genetic architecture, training population composition, marker number and statistical model on accuracy of rice genomic selection in elite, tropical rice breeding lines. *PloS Genet.* 11, e1004982. doi: 10.1371/journal.pgen.1004982

Voss-Fels, K., Cooper, M., and Hayes, B. (2019). Accelerating crop genetic gains with genomic selection. *Theor. Appl. Genet.* 132, 669–686. doi: 10.1007/s00122-018-3270-8

Wang, W., Mauleon, R., Hu, Z., Chebotarov, D., Tai, S., Wu, Z., et al. (2018a). Genomic variation in 3,010 diverse accessions of Asian cultivated rice. *Nature* 557, 43–49. doi: 10.1038/s41586-018-0063-9

Wang, H., Shi, S., Guo, Q., Nie, L., Du, B., Chen, R., et al. (2018b). High-resolution mapping of a gene conferring strong antibiosis to brown planthopper and developing resistant near-isogenic lines in 9311 background. *Mol. Breed.* 38, 107. doi: 10.1007/s11032-018-0859-1

Wang, X., Xu, Y., Hu, Z., and Xu, C. (2018c). Genomic selection methods for crop improvement: current status and prospects. *Crop J.* 6, 330–340. doi: 10.1016/j.cj.2018.03.001

Wang, Q., Yu, Y., Yuan, J., Zhang, X., Huang, H., Li, F., et al. (2017). Effects of marker density and population structure on the genomic prediction accuracy for growth trait in Pacific white shrimp Litopenaeus vannamei. *BMC Genet.* 18, 45. doi: 10.1186/s12863-017-0507-5

Wu, H., Liu, Y., He, J., Liu, Y., Jiang, L., Liu, L., et al. (2014). Fine mapping of brown planthopper (Nilaparvata lugens Stål) resistance gene Bph28(t) in rice (Oryza sativa L.). *Mol. breed.* 33, 909–918. doi: 10.1007/s11032-013-0005-z

Xu, Y., Ma, K., Zhao, Y., Wang, X., Zhou, K., Yu, G., et al. (2021). Genomic selection: A breakthrough technology in rice breeding. *Crop J.* 9, 669–677. doi: 10.1016/j.cj.2021.03.008

Yang, M., Cheng, L., Yan, L., Shu, W., Wang, X., and Qiu, Y. (2019). Mapping and characterization of a quantitative trait locus resistance to the brown planthopper in the rice variety IR64. *Hereditas* 156, 22. doi: 10.1186/s41065-019-0098-4

Yin, L., Zhang, H., Tang, Z., Xu, J., Yin, D., Zhang, Z., et al. (2021). rMVP: A memory-efficient, visualization-enhanced, and parallel-accelerated tool for genome-wide association study. *Genomics Proteomics Bioinf.* 19, 619–628. doi: 10.1016/j.gpb.2020.10.007

Yin, L., Zhang, H., Zhou, X., Yuan, X., Zhao, S., Li, X., et al. (2020). KAML: improving genomic prediction accuracy of complex traits using machine learning determined parameters. *Genome Biol.* 21, 146. doi: 10.1186/s13059-020-02052-w

Zhao, Y., Huang, J., Wang, Z., Jing, S., Wang, Y., Ouyang, Y., et al. (2016). Allelic diversity in an NLR gene BPH9 enables rice to combat planthopper variation. *Proc. Natl. Acad. Sci. U.S.A.* 113, 12850–12855. doi: 10.1073/pnas.1614862113

Zheng, X. H., Zhu, L. L., and He, G. C. (2021). Genetic and molecular understanding of host rice resistance and nilaparvata lugens adaptation. *Curr. Opin. Insect Sci.* 45, 14–20. doi: 10.1016/j.cois.2020.11.005

Zhou, X., and Stephens, M. (2012). Genome-wide efficient mixed-model analysis for association studies. *Nat. Genet.* 44, 821–824. doi: 10.1038/ng.2310

Zhou, C., Zhang, Q., Chen, Y., Huang, J., Guo, Q., Li, Y., et al. (2021). Balancing selection and wild gene pool contribute to resistance in global rice germplasm against planthopper. *J. Integr. Plant Biol.* 63, 169–1711. doi: 10.1111/jipb.13157

Zhu, C., Gore, M., Buckler, E. S., and Yu, J. (2008). Status and prospects of association mapping in plants. *Plant Genome.* 1, 5–20. doi: 10.3835/plantgenome2008.02.0089

frontiers | Frontiers in Plant Science

TYPE Original Research
PUBLISHED 14 May 2024
DOI 10.3389/fpls.2024.1361276

OPEN ACCESS

EDITED BY
Guangcun He,
Wuhan University, China

REVIEWED BY
Anuradha Singh,
Michigan State University, United States
Raghavendra Aminedi,
Indian Council of Agricultural Research (ICAR), India

*CORRESPONDENCE
Jie Li
lijie303@yeah.net

RECEIVED 25 December 2023
ACCEPTED 01 May 2024
PUBLISHED 14 May 2024

CITATION
Sun Z, Shen H, Chen Z, Ma N, Yang Y, Liu H and Li J (2024) Physiological responses and transcriptome analysis of *Hemerocallis citrina* Baroni exposed to *Thrips palmi* feeding stress. *Front. Plant Sci.* 15:1361276. doi: 10.3389/fpls.2024.1361276

Physiological responses and transcriptome analysis of *Hemerocallis citrina* Baroni exposed to *Thrips palmi* feeding stress

Zhuonan Sun[1], Hui Shen[2], Zhongtao Chen[2], Ning Ma[2], Ye Yang[2], Hongxia Liu[2] and Jie Li[2]*

[1]College of Plant Protection, Shanxi Agricultural University, Taigu, China, [2]College of Horticulture, Shanxi Agricultural University, Taigu, China

Thrips are serious pests of *Hemerocallis citrina* Baroni (daylily), affecting crop yield and quality. To defend against pests, daylily has evolved a set of sophisticated defense mechanisms. In the present study, induction of systemic resistance in *Hemerocallis citrina* 'Datong Huanghua' by *Thrips palmi* feeding was investigated at both biochemical and molecular levels. The soluble sugar content of daylily leaves was significantly lower than that in control check (CK) at all time points of feeding by *T. palmi*, whereas the amino acid and free fatty acid contents started to be significantly lower than those in CK after 7 days. Secondary metabolites such as tannins, flavonoids, and total phenols, which are harmful to the growth and reproduction of *T. palmi*, were increased significantly. The activities of defense enzymes such as peroxidase (POD), phenylalanine ammonia lyase (PAL), and polyphenol oxidase (PPO) were significantly increased, and the degree of damage to plants was reduced. The significant increase in protease inhibitor (PI) activity may lead to disrupted digestion and slower growth in *T. palmi*. Using RNA sequencing, 1,894 differentially expressed genes (DEGs) were identified between control and treatment groups at five timepoints. DEGs were mainly enriched in secondary metabolite synthesis, jasmonic acid (JA), salicylic acid (SA), and other defense hormone signal transduction pathways, defense enzyme synthesis, MAPK signaling, cell wall thickening, carbohydrate metabolism, photosynthesis, and other insect resistance pathways. Subsequently, 698 DEGs were predicted to be transcription factors, including bHLH and WRKY members related to biotic stress. WGCNA identified 18 hub genes in four key modules (Purple, Midnight blue, Blue, and Red) including MYB-like DNA-binding domain (TRINITY_DN2391_c0_g1, TRINITY_DN3285_c0_g1), zinc-finger of the FCS-type, C2-C2 (TRINITY_DN21050_c0_g2), and NPR1 (TRINITY_DN13045_c0_g1, TRINITY_DN855_c0_g2). The results indicate that biosynthesis of secondary metabolites, phenylalanine metabolism, PIs, and defense hormones pathways are involved in the induced resistance to *T. palmi* in daylily.

KEYWORDS

***Hemerocallis citrina* Baroni, *Thrips palmi*, physiological responses, biochemical compounds, transcriptome, plant insect resistance**

1 Introduction

Hemerocallis citrina Baroni (daylily) is a perennial herbaceous plant belonging to the Liliaceae family with edible flowers, medicinal properties, and ornamental functions. Daylilies are naturally distributed in East Asia, with the paramount diversity of species originating in Korea, Japan, and China, and have been cultivated for thousands of years (Matand et al., 2020; Misiukevičius et al., 2023). Thrips species such as *Frankliniella intonsa*, *Thrips palmi*, and *Frankliniella occidentalis* are common pests of daylily, causing plant damage. The life cycle of thrips includes five stages: egg, nymph, prepupa, pupa, and adult. Adults lay eggs in young plant tissues; 1st and 2nd instar nymphs are agile, and young plant tissues are their favorite feeding site; 3rd instar nymphs (prepupae) are no longer fed and pupated underground in the uppermost 3–5 cm soil layer; 4th instar nymphs (pupae) do not eat and pass the pupal stage in the soil layer (Cannon et al., 2007). The generational overlap of thrips is extensive, and it takes 15–20 days to complete the first generation, of which the egg duration is 5–7 days, and the adult duration is 7–10 days. The turn of spring and summer is the first peak of thrips infecting daylily (Dhall et al., 2021). The filing-sucking mouthparts of thrips damage the young leaves, tender stems, and flower buds of daylily. Thrips-infested plants exhibit slow growth, shortened internodes, and bent flower buds, which diminishes commercial value. When thrips were present in great numbers, the bud dropping rate of daylily was 31.65% higher than in controls, the actual bud dropping rate was as high as 99.62%, and it is the only insect pest that can lead to a completely failed harvest (Gao et al., 2021). In addition, owing to the small size of thrips, the high degree of concealment, the rapid reproduction, and the high incidence of drug resistance, it is difficult to achieve the desired control effect with a single insecticide (Steenbergen et al., 2018). Therefore, the safest and most effective strategy for thrips prevention and control is to utilize the insect resistance of the host plant. To this end, investigation of the physiological mechanisms of thrips resistance in daylily provides a basis for breeding insect-resistant plants.

Host plant damage by phytophagous insects alters plant nutrient content, production of toxic secondary metabolites, the activities of defense proteins and enzymes, and upregulates the expression of various defense-associated genes (Badenes-Pérez, 2022; Beran and Petschenka, 2022). The redistribution of certain nutrients and rapid synthesis of secondary metabolites in plants after pest infestation affects the feeding, growth, and development of pests, which in turn stimulates insect resistance (Erb and Reymond, 2019; Barbero and Maffei, 2023). Levels of soluble sugars, free amino acids, and soluble proteins in bean leaves decreased with increasing population density and feeding time of *F. occidentalis*, and were lower than those in control levels (Qian et al., 2018). Pest damage induces the accumulation of flavonoids in plants (Ramaroson et al., 2022); *Spodoptera litura* feeding stress has been shown to induce *Glycine max* to synthesize flavonoids (Du et al., 2019). Examples of herbivore-induced defense mechanisms are the accumulation of toxic chemicals such as benzoxazinoids (BXDs; chemical defense), glucosinolates, and alkaloids, which are classes of specialized metabolites that function as deterrents (Batyrshina et al., 2020). Chemical defense by BXDs in wheat showed a complex response at the leaf and phloem level that altered aphid feeding preference, and BXDs act as antifeedants to aphids (Singh et al., 2021a). In response to pest stress, defense-related enzyme systems in plants are activated. The main defense enzymes include peroxidase (POD), polyphenol oxidase (PPO), and phenylalanine ammonia lyase (PAL). Changes in the activities of these enzymes reflects the insect resistance of host plants to a certain extent (War et al., 2018). PAL is the rate-limiting enzyme in the phenylpropanoid metabolic pathway. Pest damage in plants initiates or upregulates phenylpropanoid metabolism, which increases PAL activity in damaged parts, resulting in a substantial accumulation of lignin in the cell wall and cell wall thickening, which prevents the spread of pests. Simultaneously, the increase in PAL activity increases the content of phytoalexins, which are toxic to phytophagous insects, and thereby prevent and control pests (Pant and Huang, 2022). Thrips feeding causes a significant accumulation of reactive oxygen species (ROS) in plants, leading to cell damage; plant PPO and POD remove excessive H_2O_2 and superoxide anions to maintain the dynamic balance of ROS, thus protecting plants against damage (Mouden and Leiss, 2021). Protease inhibitors (PIs) competitively and reversibly bind to intestinal proteases of herbivorous insects and allosterically bind to inhibitor-insensitive proteases to reduce protease hydrolysis activity, ultimately leading to slow growth and dysplasia in insects (Divekar et al., 2023). When herbivorous insects feed, plants are exposed to mechanical challenge in the form of tissue injury and chemical challenge caused by insect salivary secretions entering plant tissues. Subsequently, PI genes are induced at the wound site through transmission of signal molecules and amplification of the signal via a cascade, resulting in PI genes being expressed locally at the wound site and throughout the plant (Ferreira et al., 2023).

Transcriptome sequencing technology (RNA-Seq) has been frequently applied to study the interaction mechanisms between pests and hosts, and has become the main approach to explore gene expression. The transcriptome is a fundamental link between genomic and proteomic information associated with biological functions. Regulation of transcription level is the most studied and most important regulation strategy in organisms (Lowe et al., 2017; Paul et al., 2022). In plants exposed to insect feeding stress, defense signaling pathways are initiated, a series of physiological and biochemical reactions are induced, and expression of defense genes is activated (Whiteman and Tarnopol, 2021). The physiological and biochemical metabolism of plants is altered through signal transduction, transcriptional regulation, and gene expression, which improves the resistance of plants to pest stress (Du et al., 2020; Wani et al., 2022). *Sitobion avenae* feeding induces PAL gene expression in wheat (Van Eck et al., 2010). In cotton, *Helicoverpa armigera* feeding induces changes in the gene expression of lysyl oxidase (LOX), propylene oxide cyclase, and chalcone synthase, and activates plant defenses against pests at the molecular level (Chen et al., 2020). In response to insect feeding, plants initiate multiple hormone signaling pathways such as jasmonic acid (JA), salicylic acid (SA), and ethylene (ET), causing the accumulation of plant defense compounds, stimulating the expression of defense genes, and triggering the release of volatile

substances, which further enhances the resistance of plants to herbivorous insects (Kersch-Becker and Thaler, 2019; Zhao et al., 2021). In maize, *Spodoptera litura* feeding significantly upregulateds defense-related genes, oxidative stress-related genes, transcriptional regulatory genes, protein synthesis genes, plant hormone-related genes, and genes related to primary and secondary metabolism (Singh et al., 2021b). In tobacco exposed to *Bemisia tabaci* stress, defense pathways such as ROS, PI synthesis, hormone metabolism, and WRKY were significantly upregulated, and plant resistance was enhanced (Wang et al., 2023b). Transcription factors play a key regulatory role in the battle between plants and herbivorous insects by regulating cellular activities via gene expression. Members of the WRKY, APETALA2/ethylene response factor (AP2/ERF), basic helix-loop-helix (bHLH), basic leucine zipper (bZIP), myeloblastosis-related (MYB), and NAC (no apical meristem/Arabidopsis transcription activation factor/cup-shaped cotyledon) families are involved in the regulation of plant disease and insect resistance networks (Tsuda and Somssich, 2015).

Herbivorous insect feeding initiates the inducible defense mechanism of plants, triggering a series of signal transduction and gene expression events, and the generation of defense substances. Inducible defense plays an more important role in the self-protection of plants (Maleck and Dietrich, 1999). At present, there are few reports on the physiological responses and omics differences of daylily in response to thrips feeding. In the present study, *H. citrina* 'Datong Huanghua' inoculated with *T. palmi* was used to determine the content of nutrients and secondary metabolites and defense enzyme activities in leaves to elucidate the physiological changes that induce pest defenses. Transcriptome analysis of thrips-infested leaves was performed with healthy leaves as controls. Differentially expressed genes (DEGs) were identified, and the main transcription factors and their expression patterns were analyzed. Key insect resistance genes were identified to elucidate the induced defense mechanism of daylily in response to *T. palmi*.

2 Materials and methods

2.1 Materials

Adults *T. palmi* individuals naturally occurring in daylily fields at the Horticultural Station of Shanxi Agricultural University were used as the source of test insects. The daylily variety used in the study was Datong Huanghua, which was planted at the Horticultural Station of Shanxi Agricultural University.

2.2 Seedling growth

The study was performed from March to June 2023 at the Horticultural Station of Shanxi Agricultural University. To prevent *T. palmi* and other pests, a 60-mesh insect-proof net was used to set up a net room, similar to a vegetable greenhouse, from west to east in the field to establish the experimental plot. After 45 days of seedling growth, the experiment began.

To establish the treatment group with induction of *T. palmi* (*T. palmi*-fed, abbreviated as TF), 1 day before the experiment, sufficient *T. palmi* were collected in the field and brought to the laboratory in a cage (118.7 × 100 × 100 cm) made of 60-mesh insect-proof net. *T. palmi* was starved for 12 h prior to the test, to ensure adequate feeding induction on plants. On the day of the experiment, *T. palmi* were transported to the net room in 50-mL centrifuge tubes, and *T. palmi* from one tube were released onto 3–4 plants such that there were ~90 individuals per plant; at least 15 plants were treated overall to ensure that three biological replicates could be sampled at each point. *T. palmi* concentrated on the upper–middle position of young leaves, and each plant had 6–7 such leaves. Datong Huanghua plants in this treatment group (TF) were individually covered with a 60-mesh insect-proof net to prevent *T. palmi* from escaping. In the control group (control check, abbreviated as CK), no insects were introduced, daylily plants were allowed to grow normally without any treatment in the net room, and each plant was individually covered with insect-proof net. Each treatment group included three biological replicates.

Plant leaves were collected at 1, 3, 5, 7, and 9 days after the introduction of *T. palmi* (named TF1–TF5), and leaves of CK group plants collected at the same time served as controls (named CK1–CK5). Three replicates were included at each stage, yielding five extractions with 30 samples in total, which were frozen in liquid nitrogen and stored at -80°C until future use.

2.3 Determination of plant nutrient content

The content of amino acids, free fatty acids, and soluble sugars in TF1–TF5 and CK1–CK5 was determined. Amino acids content was determined using an amino acids content determination kit (ninhydrin colorimetric method; 50T/48S) and a standard curve obtained using cysteine (Li et al., 2023a). Free fatty acids content was determined using a free fatty acids content determination kit (copper soap colorimetry; 50T/48S) and a standard curve obtained using palmitic acid (Wu and Shen, 2021). Soluble sugars content was determined using a plant soluble sugars content determination kit (anthrone colorimetry; 50T/48S) and a standard curve obtained using anhydrous glucose (Kwon et al., 2015). All kits were purchased from Beijing Solarbio Science & Technology Co., Ltd (Beijing, China). Data were summarized and processed using Microsoft Excel 2010 and statistically analyzed with SPSS software v20.0. The significance of the difference in nutrients between healthy daylily leaves and leaves fed on by *T. palmi* was tested by Tukey's test ($p < 0.05$) and graph plotting using SigmaPlot 14.0 software. Data processing for secondary matter content and defense enzyme activities of daylily leaves before and after feeding by *T. palmi* was done in the same way as data processing for nutrient content determination.

2.4 Determination of plant secondary metabolites content

The content of tannins, flavonoids, and total phenols in TF1–TF5 and CK1–CK5 was determined. Tannins content was determined

using a Tannins content determination kit (Folin-Ciocalteu colorimetric method; 50T/48S) and a standard curve obtained using tannic acid (Sharma et al., 2021). Flavonoids content was determined using a flavonoids content determination kit (AlCl3 colorimetric method; 50T/48S) and a standard curve obtained using rutin (Liu et al., 2022). Total phenols content was determined using a total phenols content determination kit (Folin-Ciocalteu colorimetric method; 50T/48S) and a standard curve obtained using catechol (Palacios et al., 2021). All kits were purchased from Beijing Solarbio Science & Technology Co., Ltd (Beijing, China).

2.5 Determination of plant defense enzyme activities

The activities of POD, PAL, PPO, and PI in TF1–TF5 and CK1–CK5 samples were determined. POD activity was determined using a POD test kit (guaiacol method; 50T/48S) (Li et al., 2019). PAL activity was determined using a PAL test kit (L-phenylalanine method; 50T/48S) (Shang et al., 2023). PPO activity was determined using a PPO test kit (pyrocatechol method; 50T/48S) (Wang et al., 2023a). All kits were purchased from Beijing Solarbio Science & Technology Co., Ltd, Beijing, China. PI activity was measured using a plant PI enzyme-linked immunosorbent assay kit (double-antibody sandwich method; 50T/48S) and a standard curve obtained using serine protease inhibin (Kumar et al., 2018).

2.6 Transcriptome sequencing and analysis

RNA was extracted from TF1–TF5 and CK1–CK5 samples using the TRIzol method (Wang et al., 2022). RNA integrity was assessed using 1% agarose gel electrophoresis, and the RIN value was determined using an Agilent 2100 bioanalyzer (Agilent Technologies Inc., Santa Clara, CA, USA). After RNA quality determination, the cDNA library was constructed and high-throughput sequencing was performed on an Illumina Hiseq platform (Shanghai Majorbio Bio-Pharm Technology Co., Ltd, Shanghai, China) with three biological replicates. Raw data obtained by sequencing were filtered to remove adapters and low-quality reads, and high-quality clean data was obtained. The base quality score (Q30) of clean data was determined. Trinity software was used to assemble the clean data obtained by sequencing to construct the UniGene library.

2.7 Identification and annotation of DEGs

The relative expression levels of each gene were determined using the Transcripts Per Million (TPM) standardization algorithm in FeatureCounts software (Vera Alvarez et al., 2019) and combined with gene transfer format (GTF) files describing genomic features. DESeq 2 (Qi et al., 2023) was used to compare the number of read counts between TF and CK groups, and differential expression analysis was performed on samples between the groups. Genes with p-adjust <0.05 and $|\log2FC| \geq 1$ after p-value correction were considered DEGs. DEGs were functionally annotated using the Gene Ontology (GO) database (http://www.geneontology.org/) and the Kyoto Encyclopedia of Genes and Genomes (KEGG) database (https://www.genome.jp/kegg/). Finally, transcription factors of DEGs were predicted using the Plant Transcription Factor Database (PlantTFDB; http://planttfdb.gao-lab.org/prediction.php/).

2.8 Identification and functional analysis of key modules for defense enzyme activities and secondary metabolites synthesis

We constructed a transcriptome expression matrix of leaves from the TF1-TF5 samples and screened for genes with TPM values <1. Furthermore, we used the WGCNA package (version 1.6.6) in R software (version 3.4.4) to construct a gene co-expression network. We selected $\beta = 16$ as the soft threshold for subsequent analysis and used the 'blockwiseModules' function to construct the gene network, with the following parameter settings: power = 6, TOMType = unsigned, maxBlockSize = 100 000, minModuleSize = 80, mergeCutHeight = 0.25, nThreads = 0; all other parameters were set to default values, and module feature genes for each module were calculated. We used the 'exportNetworkToCytoscape' function in the WGCNA package to export network relationships between genes in relevant modules, and Cytoscape software (version 3.7.1) was used to create graphs.

2.9 Quantitative real-time PCR analysis

Seven genes were selected randomly for qRT-PCR validation. RNA was reverse-transcribed using a PrimeScript RT Reagent Kit (Takara, Beijing, China). All procedures were conducted in accordance with the manufacturer's instructions. The resulting cDNAs were quantified by TB Green Premix Ex Taq II (Takara). Each qRT-PCR experiment (15 µL) consisted of 7.5 µL of 2× SG Fast qPCR Master Mix, 0.6 µL of each primer (10 µM), 40 ng of cDNA template, and ddH_2O to 15 µL. Thermal cycling involved an initial denaturation at 95°C for 3 min, followed by 40 cycles of denaturation at 95°C for 30s, annealing at 56°C for 30s, and extension at 72°C for 40s. Relative expression levels of genes were calculated using the $2^{-\triangle\triangle CT}$ method with the actin gene as an internal control, and the experiment was repeated at least three times. Primer sequences are listed in Supplementary Table 1.

3 Results

3.1 Effect of *T. palmi* feeding on plant nutrient content

Primary metabolites such as amino acids, soluble sugars and free fatty acids play an important role in plant-induced defenses (Prado and Tjallingii, 2007). The amino acid and free fatty acid contents were higher than those in CK at 1 and 3 days, but significantly lower than those in CK at 7 days; they reached the lowest level at 9 days, 0.26 and 0.73 times the content in CK, respectively (Figures 1A, B). The soluble sugars content was significantly lower in the TF group than in the CK group at each

timepoint and reached the lowest level at 9 day, 0.69 times that in CK (Figure 1C).

3.2 Effect of *T. palmi* feeding on plant secondary metabolites content

Insect feeding induces the accumulation of various toxic secondary metabolites such as phenols, alkaloids, and terpenoids in plants, and reduces the digestive capacity of insects and the amount of food and eggs, thereby directly or indirectly enhancing insect resistance (Mipeshwaree et al., 2023). Tannins, flavonoids, and total phenols in plants were increased significantly at each timepoint after *T. palmi* feeding induction. Flavonoids content reached a peak at 3 days, 3.5 times that in CK (Figure 2B). Tannins and total phenols content reached a peak at 5 days, 2 and 1.7 times that in CK, respectively (Figures 2A, C).

3.3 Effect of *T. palmi* feeding on the activities of plant defense enzymes

POD, PAL, PPO, and PI are defense enzymes of plants under biotic stress, and changes in these enzymes activities reflect the insect resistance of host plants to a certain extent (Uemura and Arimura, 2019). The activities of POD, PAL, PPO, and PI in leaves of Datong Huanghua induced by *T. palmi* feeding were significantly higher than in CK at each timepoint. POD, PAL, and PPO were all initially increased then decreased. POD and PAL activities reached a peak at 5 days, at 5 and 2 times those in CK, respectively (Figures 3A, B). PPO activity reached a peak at 3 days, 1.8 times that in CK (Figure 3C). PI activity reached a peak at 1 day, 1.6 times that in CK, and although it showed a downward trend, it was still 1.2-fold higher than in CK at 9 days (Figure 3D).

3.4 Quality assessment of transcriptome sequencing results

To study the changes in transcription levels of daylily under *T. palmi* stress, using Illumina 2× 150 bp paired-end sequencing, 141.58 Gb of clean data was obtained from 10 samples. Clean data from each sample reached >6.03 Gb, the percentage of Q30 bases was >94.18%. The percentage in brackets in the last column of Table 1 is the comparison rate for clean reads; clean reads comparison efficiency ranged between 78.76% and 82.94%. The results showed that the quality of the sequencing output data was good, and the data could be used for further analysis.

3.5 DEGs in plants in response to *T. palmi* feeding

Transient expression of genes was investigated in the leaves of daylily in response to *T. palmi* feeding.The five timepoints after induction of *T. palm* feeding yielded 78,987 DEGs. The highest number of DEGs (20,390) was observed at the TF5 stage, including 13,701 upregulated and 6,689 downregulated genes. The TF1 stage had the lowest number of DEGs (8,010), including 5,956 upregulated and 2,054 downregulated genes. The number of upregulated genes was higher than that of downregulated genes at all stages (Figure 4A). Only 1,894 genes were differentially expressed at all stages (TF1–TF5; Figure 4B).

DEGs were subjected to GO functional annotation analysis to obtain their functions in response to *T. palmi* feeding. GO enrichment analysis showed that DEGs were more enriched in biological process (BP) subcategories, including secondary metabolite biosynthesis (GO:0044550), hormone biosynthesis (GO:0042446), fatty acid biosynthetic process (GO:0006633), jasmonic acid metabolism (GO:0009694), and lignin biosynthesis (GO:0009809). Among cellular component (CC) subcategories, plastids (GO:0009536) and plant-type cell wall (GO:0009505) were significantly enriched. Among molecular function (MF) subcategories, protein phosphatase inhibitor activity (GO:0004864), peroxidase activity (GO:0004601), and phenylalanine 4-monooxygenase activity (GO:0004505) were significantly enriched (Figure 4C).

Pathway analysis of DEGs was performed using the KEGG database to explore the metabolic processes and cell signaling pathways involved in genes associated with resistance to *T. palmi*. According to the KEGG enrichment analysis results for DEGs at the five stages, amino acid metabolic pathways such as α-linolenic acid metabolism, tryptophan metabolism, and phenylalanine metabolism, and plant insect resistance pathways including glutathione metabolism, flavonoid biosynthesis, anthocyanin biosynthesis, cutin, cork, and wax biosynthesis, and

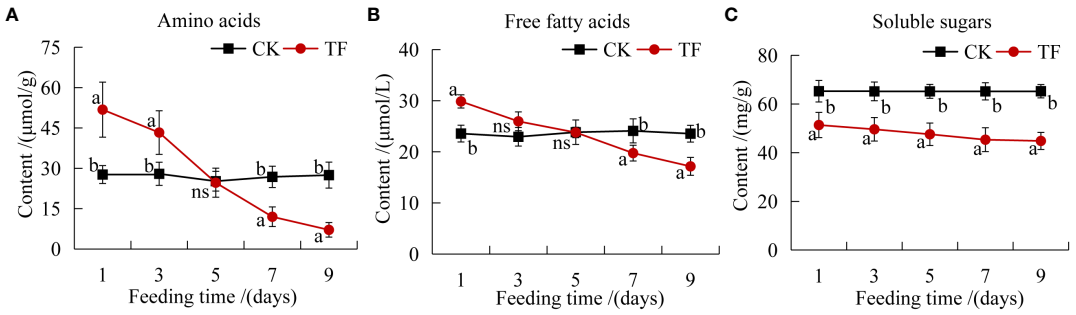

FIGURE 1
Determination of plant nutrients. **(A)** Amino acids content; **(B)** free fatty acids content; **(C)** soluble sugars content. Different letters indicate significant differences in nutrient composition between healthy leaves and leaves after feeding by *T. palmi* (p <0.05).

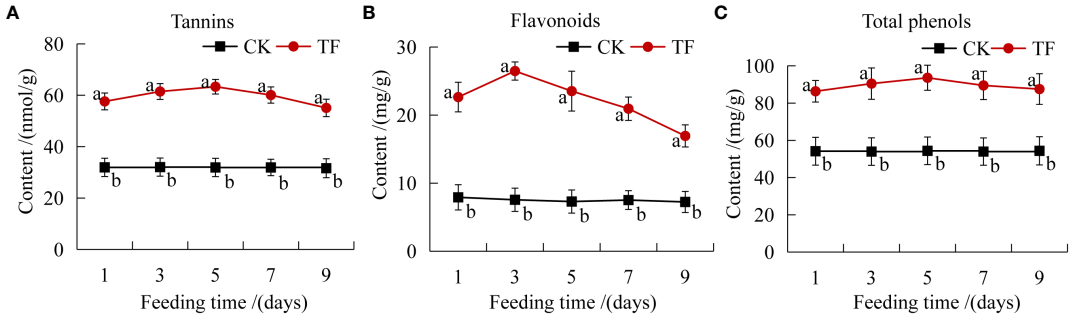

FIGURE 2
Determination of plant secondary metabolites. **(A)** Tannins content; **(B)** flavonoids content; **(C)** total phenols content. Different letters indicate significant differences in the content of secondary metabolites between healthy leaves and leaves after feeding by *T. palmi* ($p < 0.05$).

ascorbic acid and aldehyde acid metabolism, were significantly enriched after *T. palmi* feeding (Figure 4D).

3.6 Analysis of gene expression patterns related to *T. palmi* resistance

Based on the findings from DEGs, and GO enrichment and KEGG pathway analyses, 787 potential candidate genes related to *T. palmi* resistance were subjected to differential expression analysis (Figure 5). These genes could be divided into two expression patterns, among which Cluster 1 contains 679 genes. Its functions include the synthesis of secondary substances such as flavonoids, alkaloids and diterpenes, the synthesis of defense enzymes such as POD, PAL, PPO, PI, and catalase, the signal transduction of defense hormones such as JA and SA, MAPK signaling pathway-plant, wax synthesis, cell wall thickening, and others, which are mainly upregulated after feeding by *T. palmi*, and are more significant in the TF2 period. Cluster 2 contains 108 genes whose functions include amino acid metabolism, starch and sucrose metabolism, nitrogen metabolism, photosynthesis, carbohydrate metabolism, and others, which are mainly downregulated after feeding by *T. palmi*.

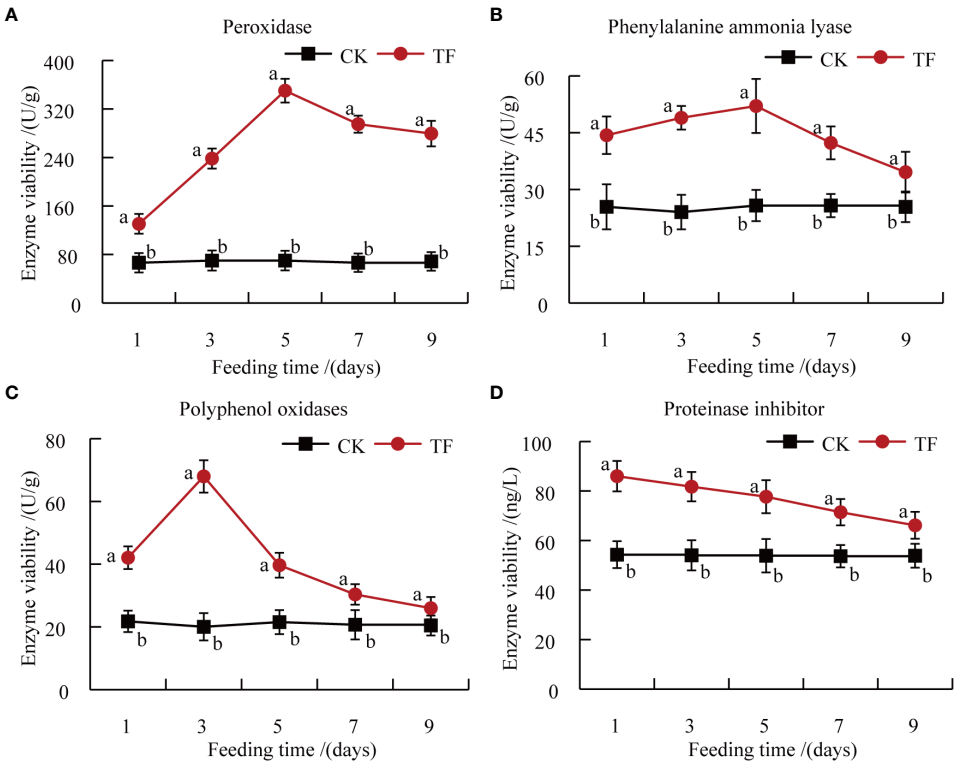

FIGURE 3
Determination of plant defense enzymes. **(A)** Peroxidase (POD) activity; **(B)** phenylalanine ammonia lyase (PAL) activity; **(C)** polyphenol oxidase (PPO) activity; **(D)** protease inhibitor (PI) activity. Different letters indicate significant differences in defense enzymes activities between healthy leaves and leaves after feeding by *T. palmi* ($p < 0.05$).

10.3389/fpls.2024.1361276

TABLE 1 Transcriptome sequencing data statistics.

Sample	Raw reads/bp	Clean reads/bp	Q20 (%)	Q30 (%)	Mapped Reads/bp
CK1	48,597,229	43,722,323	96.95	94.35	17,805,077 (81.45%)
CK2	50,907,231	42,588,800	96.90	94.25	17,268,027 (81.10%)
CK3	46,682,755	41,929,344	96.94	94.36	17,363,380 (82.82%)
CK4	49,858,899	41,816,134	96.91	94.30	17,136,180 (81.96%)
CK5	52,020,018	42,876,465	96.87	94.18	17,551,857 (81.86%)
TF1	48,261,914	43,261,865	97.01	94.40	17,520,186 (81.00%)
TF2	50,083,781	43,001,949	96.92	94.29	16,936,456 (78.76%)
TF3	47,431,502	43,260,224	97.00	94.52	17,586,256 (81.31%)
TF4	44,050,892	42,486,957	97.11	94.72	17,617,214 (82.94%)
TF5	45,904,987	41,947,648	97.51	95.15	17,024,435 (81.18%)

3.7 Prediction of transcription factors and their expression patterns

Transcription factors play a key role in the transcriptional regulatory network related to plant induced defenses. In order to explore the transcription factors related to *T. palmi* resistance in daylily, 698 transcription factors were identified from 78,987 DEGs, which clustered into 31 transcription factors families (Figure 6A, Supplementary Table 2). Approximately half of these genes are closely related to biological and non-biotic stress responses,

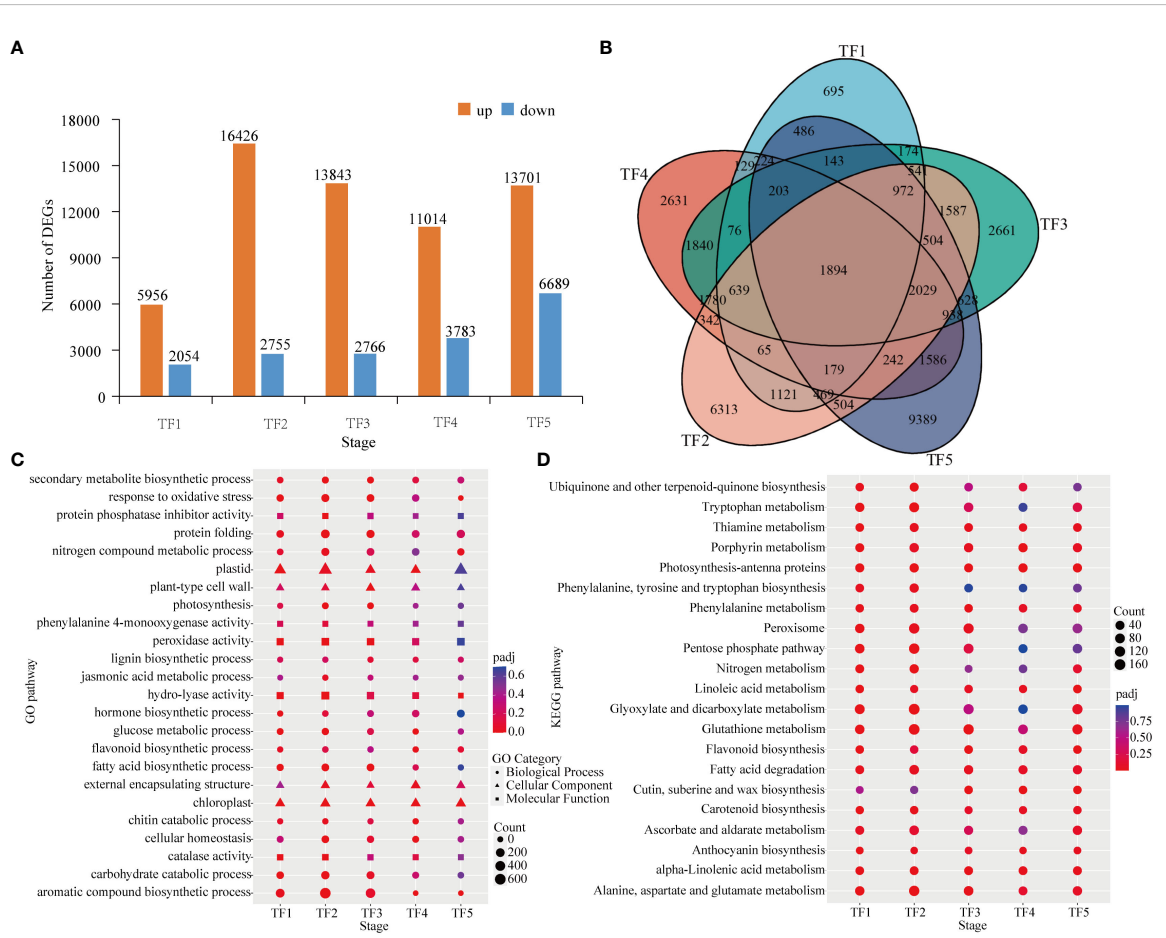

FIGURE 4
Differentially expressed genes (DEGs) in Datong Huanghua exposed to *Thrips palmi* feeding. **(A)** Number of DEGs at different stages; **(B)** venn diagram analysis of DEGs; **(C)** gene ontology (GO) enrichment analysis of DEGs; **(D)** Kyoto Encyclopedia of Genes and Genomes (KEGG) enrichment analysis of DEGs.

including MYB, bHLH, AP2/ERF, WRKY, bZIP, and NAC. On the basis of their expression patterns, these genes were divided into four clusters (Figures 6B, C). The transcription factors in Cluster 1, Cluster 2, and Cluster 3 were upregulated after feeding by *T. palmi*. The transcription factors in Cluster 1 were mainly bHLH and WRKY, and were significantly upregulated at the TF4 stage. The transcription factors in Cluster 2, and Cluster 3 were mainly AP2/ERF and MYB, Cluster 2 was significantly upregulated at the TF5 stage, and Cluster 3 was significantly upregulated at the TF2 stage. The transcription factors in Cluster 4 were mainly bZIP and NAC, which were downregulated compared with CK. Cluster 3 and Cluster 1 included the highest numbers, with 107 and 104 upregulated transcription factors, respectively, indicating that they play an important role in the resistance of daylily to *T. palmi*.

3.8 Co-expression network identification and key module analysis

WGCNA can be used to identify co-expressed gene modules, explore biological correlations between modules and target traits, and mine core genes in the module network. WGCNA was applied to the transcriptomic data to explore the relationships between genes related to the content of amino acids, free fatty acids, soluble sugars, tannins, flavonoids, and total phenols, and the activities of POD, PAL, PPO, and PI in daylily. The soft threshold $\beta = 16$ was determined by calculation (Figure 7A), and 24,665 genes were used to construct a co-expression network with 16 co-expression modules, among which the Turquoise module was the largest with 7,743 genes, whereas the Midnight blue module was the smallest with only 44 genes (Figures 7B, C). The Midnight blue module contained genes strongly linked to flavonoids content, PAL activity, tannins content, PI activity, and PPO activity, with correlation values of 0.572, 0.518, 0.515, 0.443, and 0.407, respectively. The Salmon module included genes strongly linked to soluble sugars content, with a correlation value of 0.647. The Black module contained genes strongly linked to total phenols content, with a correlation value of 0.502. The Blue module included genes strongly linked to POD, with a correlation value of 0.623. The Yellow module contained genes weakly linked to amino acids content and free fatty acids content, with correlation values of 0.221 and 0.205, respectively (Figure 7C). Four key modules (Purple, Midnight blue, Blue, and Red) highly correlated with the 10 phenotypes (amino acids, free fatty acids, soluble sugars, tannins, flavonoids, total phenols, POD, PAL, PPO, and PI) were selected, and key genes in the regulatory network were visualized using Cytoscape 2.0 with weights >0.4 (Figure 7D). A total of 18 network hub genes were identified as key genes and were annotated using *Arabidopsis* and *Asparagus* databases. Examples include natural resistance-associated macrophage protein, cytochrome P450, secondary metabolites biosynthesis, jasmonic/salicylic acid mediated signaling pathway, protein serine/threonine kinase activity, dienelactone biosynthetic, brassinosteroid biosynthetic, endonuclease/exonuclease/phosphatase family, glutamyl endopeptidase, haloacid dehalogenase-like hydrolase, and oxylipin biosynthetic process (Table 2). TRINITY_DN6738_c0_g2 plays a major regulatory role in the secondary material synthesis pathway, which influences pest feeding; TRINITY_DN21120_c0_g1 promotes the synthesis of PIs and hinders the digestive function of pests; TRINITY_DN167_c0_g1 regulates nutrient redistribution by plant amino acid metabolism to reduce the nutrients available to pests while ensuring normal plant growth; TRINITY_DN855_c0_g2 regulates defense hormone signaling, such as JA and SA, to activate plant systemic resistance. In addition, three transcription factors were

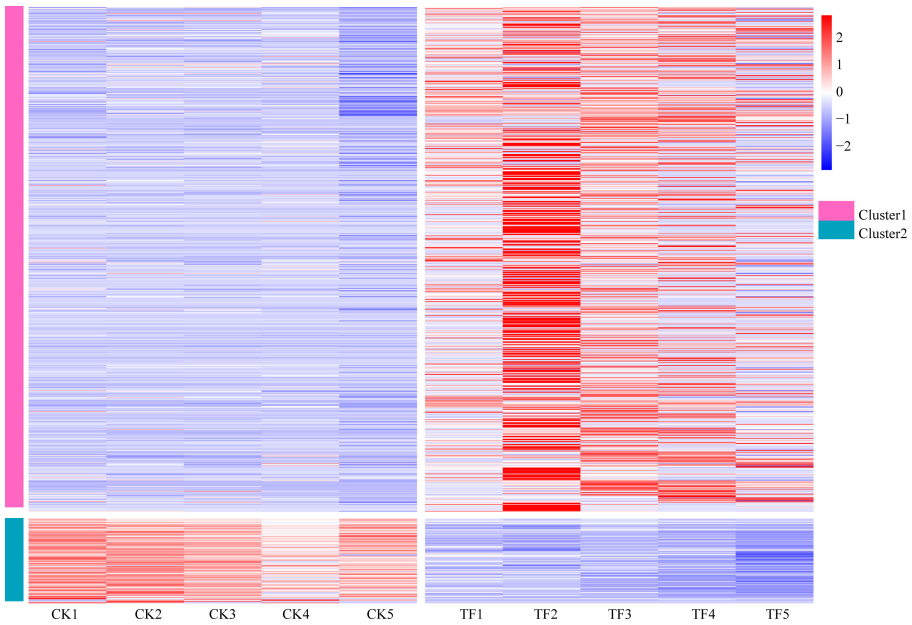

FIGURE 5
Analysis of gene expression patterns related to *T. palmi* resistance.

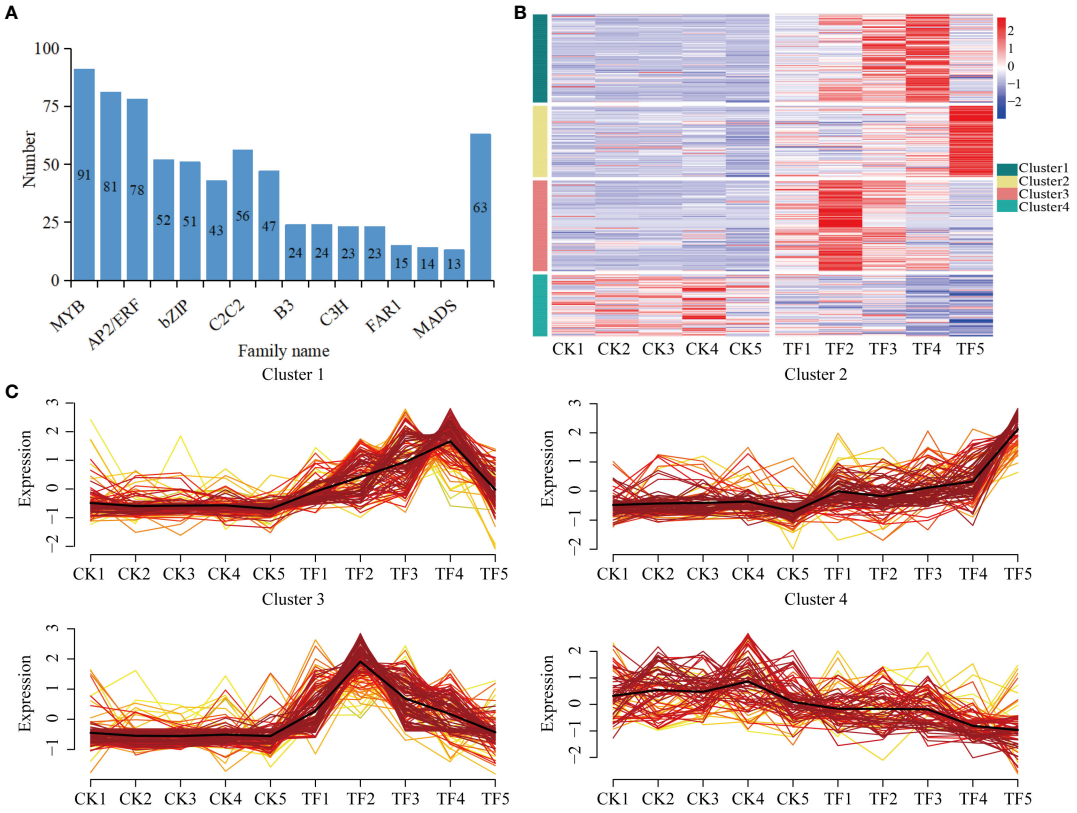

FIGURE 6
Expression of transcription factors. **(A)** Number of transcription factors; **(B)** transcription factors' expression patterns; **(C)** expression pattern clustering results.

annotated, namely MYB-like DNA-binding domain (TRINITY_DN2391_c0_g1, TRINITY_DN3285_c0_g1), zinc-finger of the FCS-type, C2-C2 (TRINITY_DN21050_c0_g2), and regulatory protein NPR1 OS (TRINITY_DN13045_c0_g1, TRINITY_DN855_c0_g2).

3.9 Verification using quantitative real-time PCR

To confirm the reliability of the transcriptome data, seven genes were selected for qRT-PCR verification. Comparison of transcriptome sequencing data and qRT-PCR data indicated very similar expression trends, with a Pearson correlation coefficient (R^2) of 0.838 (Figure 8; Supplementary Figure 1), demonstrating good reliability for the RNA-seq data.

4 Discussion

The defenses initiated by plants after being attacked by herbivorous insects are induced defenses. The process of inducing insect resistance includes the activation of pest stress signals, transmission of internal pest signals, expression of defense compound-associated genes, and synthesis of defense substances, culminating in insect resistance (Stout and Duffey, 1996). Nutrients, secondary metabolites, and defense enzymes play a vital role in the physiological responses of plants to pest stress (War et al., 2013; Li et al., 2022b). Studies have shown that low levels of soluble sugars, amino acids, and other nutrients reduce the desirability for pests, and plant resistance is stronger (Cao et al., 2018). Insect damage induces plants to produce a large number of terpenoids, phenols, nitrogen-containing compounds, and other secondary metabolites, affecting insect feeding, growth, development, and reproduction (Divekar et al., 2022). Changes in the activities of defense-related enzymes occur during the production of secondary metabolites and other anthelmintic-related substances. Plant defense enzymes are upregulated in response to insect stress; they promote the synthesis of quinones, lignin, phytoalexins, and other insect resistance compounds in plants; hinder insect feeding; and maintain plant metabolic balance (Li et al., 2022a). Plant tissues usually contain a small amount of PIs. However, after being damaged by herbivorous insects, the damage site induces a large number of PIs to be rapidly transported throughput the plant, which blocks the protease activity in the intestine of herbivorous insects, thereby inhibiting pest population expansion and protecting the plant (Zhu-Salzman and Zeng, 2015). In previous studies, transcriptome analysis of plants in response to herbivorous insect feeding shown that DEGs were significantly enriched in hormone synthesis pathways such as biosynthesis of secondary metabolites (e.g., quinones and flavonoids), phenylalanine metabolism, POD activity, α-linolenic acid metabolism, and JA synthesis (Li et al., 2020).

10.3389/fpls.2024.1361276

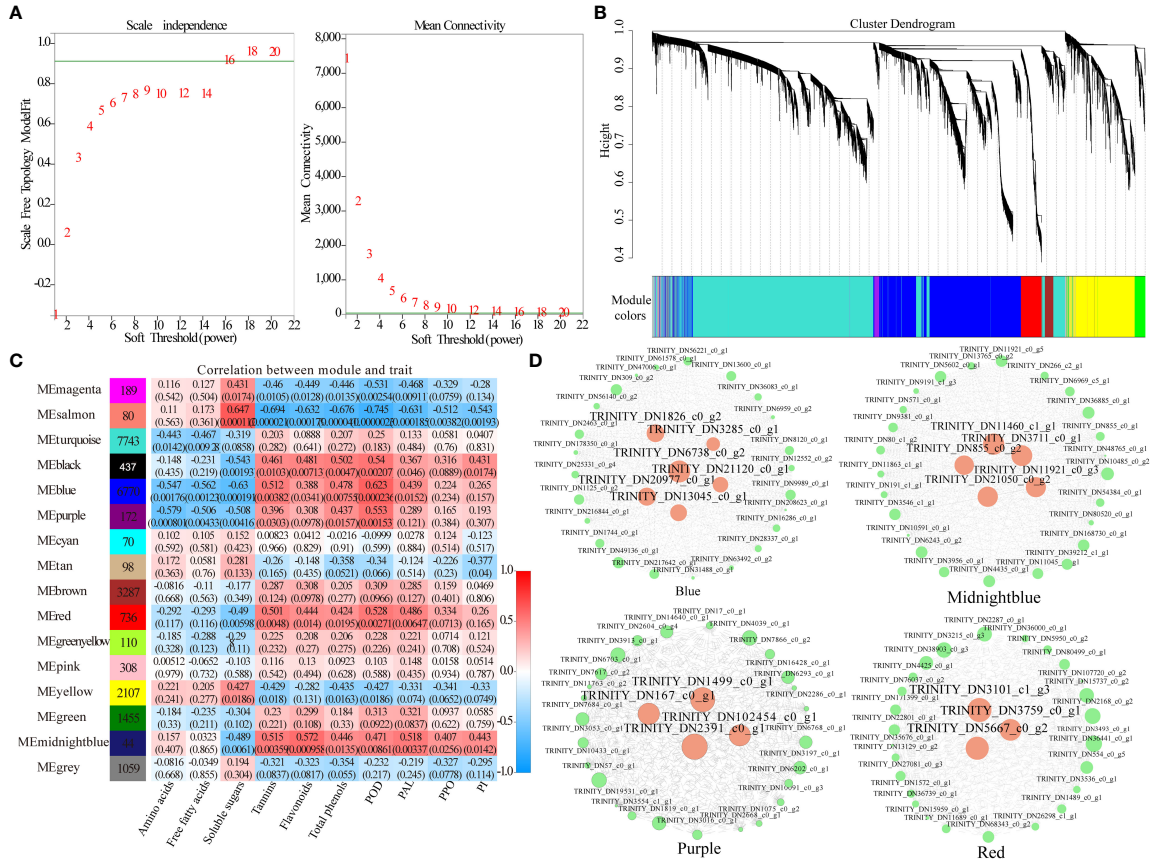

FIGURE 7
Weighted gene co-expression network analysis (WGCNA) of plant defense-related genes. **(A)** Scale-free network model index under different soft thresholds; **(B)** gene clustering tree based on the topological dissimilarity matrix; **(C)** heatmap of correlations between modules and traits; **(D)** gene co-expression network in the plant defense-related gene module; hub genes are colored pink.

Insects feeding on plants induce changes in primary and secondary metabolites, including sugars, amino acids, organic acids, flavonoids, phenols and tannins. In the present study, after feeding by *T. palmi*, the soluble sugars content in the leaves of daylily was significantly lower than that of the CK group at five timepoints. It may be that carbohydrates (mainly soluble sugars) synthesized in the aboveground part may not only meet the needs of plant growth, development, and defenses, but also be more distributed in the root system to ensure its growth activity, thereby improving the tolerance of the plant. Amino acid and fatty acid contents were higher than those in CK after 1 and 3 days of feeding by *T. palmi* and significantly lower than those in CK after 7 days. Amino acid and free fatty acid contents increased in the early stage of infestation, which may be a compensatory resilience of the plant to cope with pest infestation; however, when the infestation increased to a certain degree, the plant's own nutrient supply was insufficient, and then there was a successive decrease in the contents of nutrients, finally lower than those in CK. It suggests that plants can become less attractive to pests through changes in nutrient levels in the body, and that nutrients can also be involved in defense responses to increase plant resistance to pests. Reduction of foliage nutritive quality after herbivory could be an adaptation of plants to insect attack, slowing down larval development and affecting negatively impacting insect fitness (Cornelissen and Stiling, 2006). Analysis of five cotton cultivars revealed that aphid and jassid infestation decreased each cultivar's sugar and protein content (Amin et al., 2016). Notably, a previous study reported that the low sugar and protein content in tomato leaves is not conducive to the growth and development of *Helicoverpa armigera* (Bisht et al., 2022). Insect feeding induction is an important factor triggering the plant defense system. The elicitors in insect oral secretions enable plants to identify harmful signals, then initiate the defense system to induce resistance (Alves-Silva and Del-Claro, 2016). For example, through the catalysis of various defense enzymes such as POD, PAL, PPO, and PI, they induce the accumulation of various toxic secondary metabolites such as phenols, alkaloids, and terpenoids in plants, thereby directly or indirectly improving insect resistance (Appu et al., 2021). *Nilaparvata lugens* feeding increased the activities of POD, PAL, and PPO in rice plants, which not only reduced the damage induced by pest feeding, but also played an important role in the accumulation of toxic metabolites (Li et al., 2023b). *Pieris rapae* feeding causes damage to *Phaseolus vulgaris L.* leaves, which directly induces high expression of PI genes, and plants exhibit induced insect resistance (Xiang et al., 2018). In the present study, the activities of defense enzymes such as POD, PAL, PPO, and PI, and

TABLE 2 Hub genes and predicted functions.

Gene ID	Homologous species/gene	Gene function
TRINITY_DN3285_c0_g1	*Telopea speciosissima* XP_043691361.1	MYB-like DNA-binding domain
TRINITY_DN1826_c0_g2	*Dioscorea alata* KAH7671728.1	Oxidative phosphorylation; Haloacid dehalogenase-like hydrolase
TRINITY_DN6738_c0_g2	*Asparagus officinalis* XP_020261199.1	Cytochrome P450; Secondary metabolites biosynthesis; Brassinosteroid biosynthetic
TRINITY_DN21120_c0_g1	*Asparagus officinalis* XP_020272828.1	Protein serine/threonine kinase activity
TRINITY_DN20977_c0_g1	*Elaeis guineensis* XP_010939670.1	Phosphate-induced protein
TRINITY_DN13045_c0_g1	*Dendrobium catenatum* PKU61926.1	NPR1-interacting
TRINITY_DN11460_c1_g1	*Ananas comosus* XP_020082461.1	AWPM-19-like membrane family protein
TRINITY_DN3711_c0_g1	*Asparagus officinalis* XP_020244100.1	Natural resistance-associated macrophage protein
TRINITY_DN855_c0_g2	*Castanea mollissima* KAF3962412.1	Jasmonic/Salicylic acid-mediated signaling pathway; Regulatory protein NPR1
TRINITY_DN11921_c0_g6	*Dioscorea alata* KAH7666769.1	Endonuclease/Exonuclease/phosphatase family
TRINITY_DN21050_c0_g2	*Asparagus officinalis* XP_020249010.1	Zinc-finger of the FCS-type, C2-C2
TRINITY_DN1499_c0_g1	*Asparagus officinalis* XP_020268739.1	Transcript variant X3, mRNA
TRINITY_DN167_c0_g1	*Asparagus officinalis* ONK67613.1	Glutamyl endopeptidase; Amino acid metabolism; Dienelactone biosynthetic
TRINITY_DN102454_c0_g1	*Dendrobium nobile* KAI0496278.1	Cullin-3A-like
TRINITY_DN2391_c0_g1	*Asparagus officinalis* XP_020250343.1	MYB-like DNA-binding domain
TRINITY_DN3101_c1_g3	*Capsicum annuum* XP_016565577.1	Cysteine-rich receptor-like protein kinase 31;oxylipin biosynthetic process
TRINITY_DN3759_c0_g1	*Dendrobium chrysotoxum* KAH0445920.1	Cytosolic large ribosomal subunit
TRINITY_DN5667_c0_g2	*Quercus suber* XP_023907021.1	EXF-150 Actin

the contents of secondary metabolites such as tannins, flavonoids, and total phenols in leaves of daylily following feeding by *T. palmi* were significantly higher than those of CK. These findings are consistent with previous reports showing that thrips damage significantly increased the flavonoid, tannin, and lignin content in alfalfa leaves (Wu et al., 2021), and *H. armigera* feeding significantly increased the phenol content of pigeon pea (Kaur et al., 2014). In our previous study, PI activity was significantly increased in plants exposed to insect damage, resulting in the obstruction of insect digestion and slow growth, and the tannins, flavonoids, and total phenols content in daylily leaves were significantly higher in plants exposed to insect damage, which were not conducive to colonization by *T. palmi* (unpublished data).

After plants are stressed by insect feeding, defense signaling pathways are initiated, a series of physiological and biochemical reactions are induced, and the expression of defense genes is activated (Wu et al., 2010). In alfalfa damaged by thrips, pathways related to carbohydrate metabolism, lipid metabolism, MAPK signaling, hormone synthesis, and secondary metabolite synthesis are activated to initiate a defense response to thrips damage (Zhang et al., 2021). In the present study, the DEGs identified in daylily exposed to *T. palmi* infestation were mainly enriched in secondary metabolite synthesis, defense hormones signal transduction, defense enzymes synthesis, MAPK signaling pathway-plant, cell wall thickening, carbohydrate metabolism, photosynthesis, and other insect-resistant pathways. The

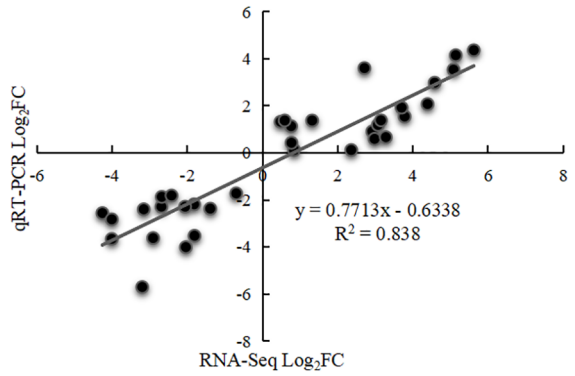

FIGURE 8
Correlation point map between RNA-Seq and qRT-PCR expression patterns.

transcription factors identified on the basis of DEGs were clustered into the MYB, bHLH, AP2/ERF, WRKY, bZIP, and NAC families. Among them, MYB, WRKY, bHLH, and AP2/ERF transcription factors were significantly upregulated after feeding by *T. palmi*, indicating that these four families of transcription factors play an important role in induced resistance to *T. palmi* defense in daylily. The aphid resistance-related transcription factors in alfalfa were consistent with the thrips resistance-associated transcription factors in daylily, but the MYB, NAC, and AP2/ERF families were dominant in alfalfa responses to aphids (Jacques et al., 2020). Furthermore, WGCNA and DEGs analysis demonstrated that MYB-like DNA-binding domain (TRINITY _ DN2391 _ c0 _ g1, TRINITY _ DN3285 _ c0 _ g1), zinc-finger of the FCS-type C2-C2 (TRINITY _ DN21050 _ c0 _ g2), and regulatory protein NPR1 (TRINITY _ DN13045 _ c0 _ g1, TRINITY _ DN855 _ c0 _ g2) are closely related to the synthesis of anti-stress compounds such as antioxidant enzymes, JA, SA and secondary metabolites. These results suggest that these genes play an important role in the defense responses of daylily to *T. palmi*.

In conclusion, the present findings elucidate the potential mechanism and hub genes of the resistance of daylily to *T. palmi*. The synergistic effects of nutrients, secondary metabolites, and defense enzymes increased the resistance of daylily to *T. palmi*. The mechanisms include reducing the nutrients available to *T. palmi*, catalyzing defense enzymes to produce secondary metabolites that are toxic to *T. palmi*, activating JA, SA, and other defense hormones signal transduction pathways, improving the resistance of daylily plants, and reducing the damage caused by *T. palmi*. The results of this study expand our the understanding of the mechanisms of insect resistance in daylily, and inform the development of effective strategies to control *T. palmi* by inducing exogenous factors to enhance insect resistance.

Data availability statement

The data presented in the study are deposited in the NCBI repository, accession number PRJNA1094559.

Author contributions

ZS: Conceptualization, Data curation, Formal analysis, Investigation, Methodology, Visualization, Writing – original draft. HS: Data curation, Visualization, Writing – original draft. ZC: Data curation, Methodology, Writing – original draft, Conceptualization, Formal analysis, Funding acquisition, Investigation, Project administration, Resources, Software, Supervision, Validation, Visualization. NM: Formal analysis, Visualization, Writing – original draft. YY: Data curation, Formal analysis, Writing – original draft. HL: Conceptualization, Methodology, Writing – original draft. JL: Conceptualization, Funding acquisition, Project administration, Resources, Supervision, Writing – review & editing.

Funding

The author(s) declare that financial support was received for the research, authorship, and/or publication of this article. The research was supported by the Development and Promotion of Green Prevention and Control Technology of *Hemerocallis citrina* Baroni Diseases and Insect Pests (2021YFD1600301–5) and Screening of olfactory Attractants for *Frankliniella intonsa* in *Hemerocallis citrina* Baroni (2022–104).

Acknowledgments

The authors would like to thank Prof. Wang Chen Zhu for project discussion and manuscript suggestions.

Conflict of interest

The authors declare that the research was conducted in the absence of any commercial or financial relationships that could be construed as a potential conflict of interest.

Publisher's note

Supplementary material

The Supplementary Material for this article can be found online at: https://www.frontiersin.org/articles/10.3389/fpls.2024.1361276/full#supplementary-material

References

Alves-Silva, E., and Del-Claro, K. (2016). Herbivory-induced stress: leaf developmental instability is caused by herbivore damage in early stages of leaf development. *Ecol. Indicators.* 61, 359–365. doi: 10.1016/j.ecolind.2015.09.036

Amin, R., Afrin, R., Suh, S. J., and Kwon, Y. (2016). Infestation of sucking insect pests on five cotton cultivars and their impacts on varietal agronomic traits, biochemical contents, yield and quality. *SAARC J. Agricult.* 14, 11–23. doi: 10.3329/sja.v14i1.29572

Appu, M., Ramalingam, P., Sathiyanarayanan, A., and Huang, J. (2021). An overview of plant defense-related enzymes responses to biotic stresses. *Plant Gene.* 27, 100302. doi: 10.1016/j.plgene.2021.100302

Badenes-Pérez, F. R. (2022). Plant-insect interactions. *Plants* 11, 1140–1143. doi: 10.3390/plants11091140

Barbero, F., and Maffei, M. E. (2023). Recent advances in plant-insect interactions. *Int. J. Mol. Sci.* 24, 11338–11343. doi: 10.3390/ijms241411338

Batyrshina, Z. S., Yaakov, B., Shavit, R., Singh, A., and Tzin, V. (2020). Comparative transcriptomic and metabolic analysis of wild and domesticated wheat genotypes reveals differences in chemical and physical defense responses against aphids. *BMC Plant Biol.* 20, 19. doi: 10.1186/s12870-019-2214-z

Beran, F., and Petschenka, G. (2022). Sequestration of plant defense compounds by insects: from mechanisms to insect-plant coevolution. *Annu. Rev. Entomol.* 67, 163–180. doi: 10.1146/annurev-ento-062821-062319

Bisht, K., Yadav, S. K., Bhowmik, S., and Singh, N. (2022). Morphological and biochemical resistance to *Helicoverpa armigera* (*Lepidoptera: Noctuidae*) in tomato. *Crop Protect.* 162, 106080. doi: 10.1016/j.cropro.2022.106080

Cannon, R. J. C., Matthews, I., and Collins, D. W. (2007). A review of the pest status and control options for *Thrips palmi*. *Crop Protect.* 26, 1089–1098. doi: 10.1016/j.cropro.2006.10.023

Cao, H. H., Wu, J., Zhang, Z. F., and Liu, T. X. (2018). Phloem nutrition of detached cabbage leaves varies with leaf age and influences performance of the green peach aphid, *Myzus persicae*. *Entomol. experiment. applicata.* 166, 452–459. doi: 10.1111/eea.12676

Chen, D. Y., Chen, Q. Y., Wang, D. D., Mu, Y. P., Wang, M. Y., Huang, J. R., et al. (2020). Differential transcription and alternative splicing in cotton underly specialized defense responses against pests. *Front. Plant Sci.* 11. doi: 10.3389/fpls.2020.573131

Cornelissen, T., and Stiling, P. (2006). Does low nutritional quality act as a plant defence? An experimental test of the slow-growth, high-mortality hypothesis. *Ecol. Entomol.* 31, 32–40. doi: 10.1111/j.0307-6946.2006.00752.x

Dhall, H., Jangra, S., Basavaraj, Y. B., and Ghosh, A. (2021). Host plant influences life cycle, reproduction, feeding, and vector competence of *Thrips palmi* (Thysanoptera: Thripidae), a vector of tospoviruses. *Phytoparasitica* 49, 501–512. doi: 10.1007/s12600-021-00893-0

Divekar, P. A., Narayana, S., Divekar, B. A., Kumar, R., Gadratagi, B. G., Ray, A., et al. (2022). Plant secondary metabolites as defense tools against herbivores for sustainable crop protection. *Int. J. Mol. Sci.* 23, 2690–2713. doi: 10.3390/ijms23052690

Divekar, P. A., Rani, V., Majumder, S., Karkute, S. G., Molla, K. A., Pandey, K. K., et al. (2023). Protease inhibitors: An induced plant defense mechanism against herbivores. *J. Plant Growth Regulat.* 42, 6057–6073. doi: 10.1007/s00344-022-10767-2

Du, B., Chen, R., Guo, J., and He, G. (2020). Current understanding of the genomic, genetic, and molecular control of insect resistance in rice. *Mol. Breed.* 40, 24–48. doi: 10.1007/s11032-020-1103-3

Du, H., Li, X., Ning, L., Qin, R., Du, Q., Wang, Q., et al. (2019). RNA-Seq analysis reveals transcript diversity and active genes after common cutworm (*Spodoptera litura Fabricius*) attack in resistant and susceptible wild soybean lines. *BMC Genomics* 20, 237–253. doi: 10.1186/s12864-019-5599-z

Erb, M., and Reymond, P. (2019). Molecular interactions between plants and insect herbivores. *Annu. Rev. Plant Biol.* 70, 527–557. doi: 10.1146/annurev-arplant-050718-095910

Ferreira, M. M., Santos, A. S., Santos, A. S., Zugaib, M., and Pirovani, C. P. (2023). Plant serpins: potential inhibitors of serine and cysteine proteases with multiple functions. *Plants* 12, 3619–3640. doi: 10.3390/plants12203619

Gao, Y., Huang, W. H., Shuai, N. N., Mu, N. N., Ren, L. J., and Xie, M. C. (2021). Effects of multiple insect pests on squaring of daylily. *China Agric. Abstracts-Agricult. Engineer.* 33, 88–91. doi: 10.19518/j.cnki.cn11–2531/s.2021.0030

Jacques, S., Sperschneider, J., Garg, G., Thatcher, L. F., Gao, L. L., Kamphuis, L. G., et al. (2020). A functional genomics approach to dissect spotted alfalfa aphid resistance in *Medicago truncatula*. *Sci. Rep.* 10, 22159–22176. doi: 10.1038/s41598-020-78904-z

Kaur, R., Gupta, A. K., and Taggar, G. K. (2014). Role of catalase, H_2O_2 and phenolics in resistance of pigeonpea towards *Helicoverpa armigera* (*Hubner*). *Acta Physiol. Plant.* 36, 1513–1527. doi: 10.1007/s11738-014-1528-6

Kersch-Becker, M. F., and Thaler, J. S. (2019). Constitutive and herbivore-induced plant defences regulate herbivore population processes. *J. Anim. Ecol.* 88, 1079–1088. doi: 10.1111/1365–2656.12993

Kumar, V., Rani, A., Shuaib, M., and Mittal, P. (2018). Comparative assessment of trypsin inhibitor vis-à-vis kunitz trypsin inhibitor and bowman-birk inhibitor activities in soybean. *Food Anal. Methods* 11, 2431–2437. doi: 10.1007/s12161-018-1227-9

Kwon, C. W., Park, K. M., Choi, S. J., and Chang, P. S. (2015). A reliable and reproducible method for the lipase assay in an AOT/isooctane reversed micellar system: modification of the copper-soap colorimetric method. *Food Chem.* 182, 236–241. doi: 10.1016/j.foodchem.2015.02.145

Li, A. M., Wang, M., Chen, Z. L., Qin, C. X., Liao, F., Wu, Z., et al. (2022a). Integrated transcriptome and metabolome analysis to identify sugarcane gene defense against fall armyworm (*Spodoptera frugiperda*) herbivory. *Int. J. Mol. Sci.* 23, 13712–13727. doi: 10.3390/ijms232213712

Li, B., Ding, Y., Tang, X., Wang, G., Wu, S., Li, X., et al. (2019). Effect of l-arginine on maintaining storage quality of the white button mushroom (*Agaricus bisporus*). *Food Bioprocess Technol.* 12, 563–574. doi: 10.1007/s11947-018-2232-0

Li, H., Wang, L., Nie, L., Liu, X., and Fu, J. (2023a). Sensitivity intensified ninhydrin-based chromogenic system by ethanol-ethyl acetate: application to relative quantitation of gaba. *Metabolites* 13, 283–294. doi: 10.3390/metabo13020283

Li, H., Zhou, Z., Hua, H., and Ma, W. (2020). Comparative transcriptome analysis of defense response of rice to *Nilaparvata lugens* and *Chilo suppressalis* infestation. *Int. J. Biol. Macromol.* 163, 2270–2285. doi: 10.1016/j.ijbiomac.2020.09.105

Li, S., Qi, L., Tan, X., Li, S., Fang, J., and Ji, R. (2023b). Small brown planthopper nymph infestation regulates plant defenses by affecting secondary metabolite biosynthesis in rice. *Int. J. Mol. Sci.* 24, 4764–4784. doi: 10.3390/ijms24054764

Li, Y., Gao, Y., Van Kleunen, M., and Liu, Y. (2022b). Herbivory may mediate the effects of nutrients on the dominance of alien plants. *Funct. Ecol.* 36, 1292–1302. doi: 10.1111/1365-2435.14019

Liu, W., Zhang, Z., Zhang, T., Qiao, Q., and Hou, X. (2022). Phenolic profiles and antioxidant activity in different organs of *Sinopodophyllum hexandrum*. *Front. Plant Sci.* 13. doi: 10.3389/fpls.2022.1037582

Lowe, R., Shirley, N., Bleackley, M., Dolan, S., and Shafee, T. (2017). Transcriptomics technologies. *PloS Comput. Biol.* 13, e1005457. doi: 10.1371/journal.pcbi.1005457

Maleck, K., and Dietrich, R. A. (1999). Defense on multiple fronts: how do plants cope with diverse enemies? *Trends Plant Sci.* 4, 215–219. doi: 10.1016/s1360–1385(99)01415–6

Matand, K., Shoemake, M., and Li, C. (2020). High frequency in *vitro* regeneration of adventitious shoots in daylilies (*Hemerocallis sp*) stem tissue using thidiazuron. *BMC Plant Biol.* 20, 31–40. doi: 10.1186/s12870-020-2243-7

Mipeshwaree, D. A., Khedashwori, D. K., Premi, D. P., and Lakshmipriyari, D. M. (2023). Metabolic engineering of plant secondary metabolites: prospects and its technological challenges. *Front. Plant Sci.* 14. doi: 10.3389/fpls.2023.1171154

Misiukevičius, E., Frercks, B., Šikšnianienė, J. B., Kącki, Z., Gębala, M., Akulytė, P., et al. (2023). Assessing the genetic diversity of daylily germplasm using ssr markers: implications for daylily breeding. *Plants* 12, 1752–1765. doi: 10.3390/plants12091752

Mouden, S., and Leiss, K. A. (2021). Host plant resistance to thrips (*Thysanoptera: Thripidae*) - current state of art and future research avenues. *Curr. Opin. Insect Sci.* 45, 28–34. doi: 10.1016/j.cois.2020.11.011

Palacios, C. E., Nagai, A., Torres, P., Rodrigues, J. A., and Salatino, A. (2021). Contents of tannins of cultivars of sorghum cultivated in Brazil, as determined by four quantification methods. *Food Chem.* 337, 127970. doi: 10.1016/j.foodchem.2020.127970

Pant, S., and Huang, Y. (2022). Genome-wide studies of PAL genes in *Sorghum* and their responses to aphid infestation. *Sci. Rep.* 12, 22537–22549. doi: 10.1038/s41598-022-25214-1

Paul, S. C., Singh, P., Dennis, A. B., and Müller, C. (2022). Intergenerational effects of early-life starvation on life history, consumption, and transcriptome of a holometabolous insect. *Am. Nat.* 199, E229–E243. doi: 10.1086/719397

Prado, E., and Tjallingii, W. F. (2007). Behavioral evidence for local reduction of aphid-induced resistance. *J. Insect Sci.* 7, 48. doi: 10.1673/031.007.4801

Qi, F., Wang, F., Xiaoyang, C., Wang, Z., Lin, Y., Peng, Z., et al. (2023). Gene expression analysis of different organs and identification of ap2 transcription factors in flax (*linum usitatissimum l.*). *Plants* 12, 3260–3278. doi: 10.3390/plants12183260

Qian, L., He, S., Liu, X., Huang, Z., Chen, F., and Gui, F. (2018). Effect of elevated CO_2 on the interaction between invasive thrips, *Frankliniella occidentalis*, and its host kidney bean, *phaseolus vulgaris*. *Pest Manag. Sci.* 74, 2773–2782. doi: 10.1002/ps.5064

Ramaroson, M. L., Koutouan, C., Helesbeux, J. J., Le Clerc, V., Hamama, L., Geoffriau, E., et al. (2022). Role of phenylpropanoids and flavonoids in plant resistance to pests and diseases. *Molecules* 27, 8371–8393. doi: 10.3390/molecules27238371

Shang, X. C., Zhang, M., Zhang, Y., Li, Y., Hou, X., and Yang, L. (2023). Combinations of waste seaweed liquid fertilizer and biochar on tomato (*Solanum lycopersicum l.*) seedling growth in an acid-affected soil of Jiaodong Peninsula, China. *Ecotoxicol. Environ. Saf.* 260, 115075. doi: 10.1016/j.ecoenv.2023.115075

Sharma, T., Gamit, R., Acharya, R., and Shukla, V. J. (2021). Quantitative estimation of total tannin, alkaloid, phenolic, and flavonoid content of the root, leaf, and whole plant of byttneria herbacea roxb. *Ayu* 42, 143–147. doi: 10.4103/ayu.AYU_25_19

Singh, A., Dilkes, B., Sela, H., and Tzin, V. (2021a). The effectiveness of physical and chemical defense responses of wild emmer wheat against aphids depends on leaf position and genotype. *Front. Plant Sci.* 12. doi: 10.3389/fpls.2021.667820

Singh, A., Singh, S., Singh, R., Kumar, S., Singh, S. K., and Singh, I. K. (2021b). Dynamics of *Zea mays* transcriptome in response to a polyphagous herbivore, *Spodoptera litura*. *Funct. Integr. Genomics* 21, 571–592. doi: 10.1007/s10142-021-00796-7

Steenbergen, M., Abd-El-Haliem, A., Bleeker, P., Dicke, M., Escobar-Bravo, R., Cheng, G., et al. (2018). Thrips advisor: exploiting thrips-induced defences to combat pests on crops. *J. Exp. Bot.* 69, 1837–1848. doi: 10.1093/jxb/ery060

Stout, M. J., and Duffey, S. S. (1996). Characterization of induced resistance in tomato plants. *Entomol. Experiment. Applicata.* 79, 273–283. doi: 10.1111/j.1570-7458.1996.tb00835.x

Tsuda, K., and Somssich, I. E. (2015). Transcriptional networks in plant immunity. *New Phytol.* 206, 932–947. doi: 10.1111/nph.13286

Uemura, T., and Arimura, G. I. (2019). Current opinions about herbivore-associated molecular patterns and plant intracellular signaling. *Plant Signal Behav.* 14, e1633887. doi: 10.1080/15592324.2019.1633887

Van Eck, L., Schultz, T., Leach, J. E., Scofield, S. R., Peairs, F. B., Botha, A. M., et al. (2010). Virus-induced gene silencing of WRKY53 and an inducible phenylalanine ammonia-lyase in wheat reduces aphid resistance. *Plant Biotechnol. J.* 8, 1023–1032. doi: 10.1111/pbi.2010.8.issue-9

Vera Alvarez, R., Pongor, L. S., Mariño-Ramírez, L., and Landsman, D. (2019). TPMcalculator: one-step software to quantify mrna abundance of genomic features. *Bioinformatics* 35, 1960–1962. doi: 10.1093/bioinformatics/bty896

Wang, C., Chen, Y., Chen, S., Min, Y., Tang, Y., Ma, X., et al. (2023a). Spraying chitosan on cassava roots reduces postharvest deterioration by promoting wound healing and inducing disease resistance. *Carbohydr. Polym.* 318, 121133. doi: 10.1016/j.carbpol.2023.121133

Wang, C., Hou, X., Qi, N., Li, C., Luo, Y., Hu, D., et al. (2022). An optimized method to obtain high-quality RNA from different tissues in *Lilium davidii* var. *unicolor*. *Sci. Rep.* 12, 2825–2835. doi: 10.1038/s41598-022-06810-7

Wang, X., Ye, Z. X., Wang, Y. Z., Wang, X. J., Chen, J. P., and Huang, H. J. (2023b). Transcriptomic analysis of tobacco plants in response to whitefly infection. *Genes* 14, 1640–1651. doi: 10.3390/genes14081640

Wani, S. H., Choudhary, M., Barmukh, R., Bagaria, P. K., Samantara, K., Razzaq, A., et al. (2022). Molecular mechanisms, genetic mapping, and genome editing for insect pest resistance in field crops. *Theor. Appl. Genet.* 135, 3875–3895. doi: 10.1007/s00122-022-04060-9

War, A. R., Paulraj, M. G., Ignacimuthu, S., and Sharma, H. C. (2013). Defensive responses in groundnut against chewing and sap-sucking insects. *J. Plant Growth Regulat.* 32, 259–272. doi: 10.1007/s00344-012-9294-4

War, A. R., Taggar, G. K., Hussain, B., Taggar, M. S., Nair, R. M., and Sharma, H. C. (2018). Plant defence against herbivory and insect adaptations. *AoB PLANTS.* 10, 37–55. doi: 10.1093/aobpla/ply037

Whiteman, N. K., and Tarnopol, R. L. (2021). Whiteflies weaponize a plant defense via horizontal gene transfer. *Cell* 184, 1657–1658. doi: 10.1016/j.cell.2021.03.017

Wu, Y., and Shen, Y. (2021). Dormancy in *Tilia miqueliana* is attributable to permeability barriers and mechanical constraints in the endosperm and seed coat. *Braz. J. Bot.* 44, 725–740. doi: 10.1007/s40415-021-00749-1

Wu, F., Shi, S., Li, Y., Miao, J., Kang, W., Zhang, J., et al. (2021). Physiological and biochemical response of different resistant alfalfa cultivars against thrips damage. *Physiol. Mol. Biol. Plants.* 27, 649–663. doi: 10.1007/s12298-021-00961-z

Wu, J., Zhang, Y. L., Zhang, H. Q., Huang, H., Folta, K. M., and Lu, J. (2010). Whole genome wide expression profiles of vitis amurensis grape responding to downy midew by using solexa sequencing technology. *BMC Plant Biol.* 10, 234. doi: 10.1186/1471-2229-10-234

Xiang, M., Zhang, X., Deng, Y., Li, Y., Yu, J., Zhu, J., et al. (2018). Comparative transcriptome analysis provides insights of anti-insect molecular mechanism of *Cassia obtusifolia* trypsin inhibitor against *Pieris rapae*. *Arch. Insect Biochem. Physiol.* 97, e21427. doi: 10.1002/arch.21427

Zhang, Z., Chen, Q., Tan, Y., Shuang, S., Dai, R., Jiang, X., et al. (2021). Combined transcriptome and metabolome analysis of alfalfa response to thrips infection. *Genes* 12, 1967–1980. doi: 10.3390/genes12121967

Zhao, B., Liu, Q., Wang, B., and Yuan, F. (2021). Roles of phytohormones and their signaling pathways in leaf development and stress responses. *J. Agric. Food Chem.* 69, 3566–3584. doi: 10.1021/acs.jafc.0c07908

Zhu-Salzman, K., and Zeng, R. (2015). Insect response to plant defensive protease inhibitors. *Annu. Rev. Entomol.* 60, 233–252. doi: 10.1146/annurev-ento-010814-020816

Frontiers in
Plant Science

Cultivates the science of plant biology and its applications

The most cited plant science journal, which advances our understanding of plant biology for sustainable food security, functional ecosystems and human health.

Discover the latest Research Topics

See more →

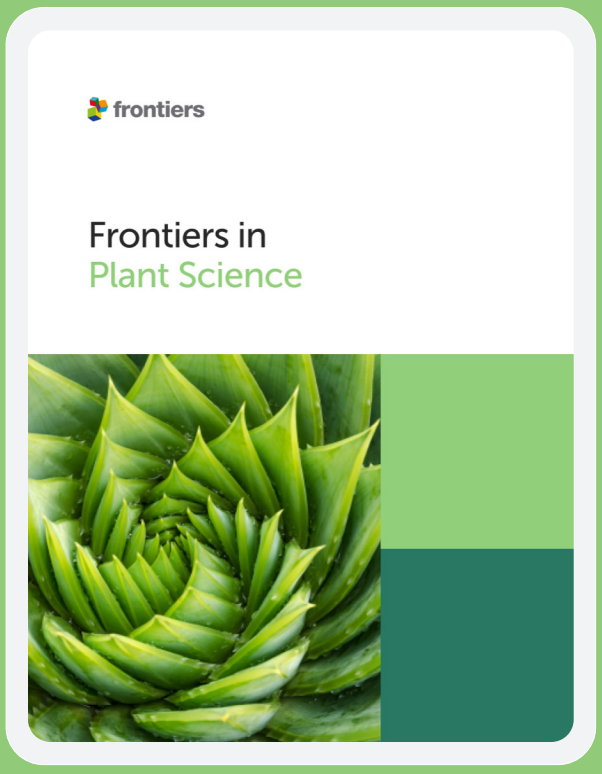

Frontiers

Avenue du Tribunal-Fédéral 34
1005 Lausanne, Switzerland
frontiersin.org

Contact us

+41 (0)21 510 17 00
frontiersin.org/about/contact